

APPLICATIONS OF CHIRAL AMIDINE CATALYSIS TOWARDS THE SYNTHESIS OF
SMALL MOLECULE THERAPEUTICS AND RECENT ADVANCES IN VICINAL
DIAMINE SYNTHESIS

By

Michael W. Danneman

Dissertation

Submitted to the Faculty of the
Graduate School of Vanderbilt University
in partial fulfillment of the requirements

for the degree of

DOCTOR OF PHILOSOPHY

in

CHEMISTRY

May 2016

Nashville, Tennessee

Approved:

Jeffrey N. Johnston (Chair)

Gary A. Sulikowski

Charles M. Lukehart

Brian O. Bachmann

Copyright © 2016 by Michael W. Danneman
All Rights Reserved

Acknowledgements

This document represents more than the conclusions drawn from nearly 2000 chemical reactions. It represents my hard work, dedication, and perseverance during my 5 years and 7 months at Vanderbilt University. As I have matured not only as a chemist, but as a person, during my time at Vanderbilt, I am very grateful to have had this opportunity and to acquire the education that I have. Needless to say, this could not have been done alone. There are numerous people who have contributed to this work and to my success both directly and indirectly. I am very grateful for the contributions of these people during my time in graduate school.

First and foremost, I want to thank God. He is the reason why all of this is possible and why I am where I am today. He has blessed me with the gift of intellect and has given me the dedication and perseverance required in order to maximize my abilities. More importantly, He has blessed me with so many wonderful people in my life who have helped shape me into the young man that I am today. It is with much humility that I can say that I am a very wealthy man in terms of happiness because of His doings.

I want to thank my wonderful parents, Bill and Kathy Danneman. They have given me the best upbringing possible and have taught me how to succeed in every aspect of life, including being a good person. Even as a 27 year old man living on his own, it is important for them to know that they have been, are, and always will be my two main refuges. They have contributed more to this work than they think due to their infinite love and support. The same goes for my brothers Jim, Matt, and Joe as well as my sister Amy. Laughter is very important quality for living a very happy life and my brothers and sister have contributed to that aspect greatly. Whether it be through texts, sports arguments between Matt and Joe (or Matt and Jim), or stories about my mom losing it on my dad (or vice versa), my siblings have always made me smile and I am eternally grateful for them. I also want to thank my sisters-in-law Holly, Amanda, and Lynsey as well as my brother-in-law Patrick for making this the wonderful family it is today. Next, my fifteen (yes...fifteen) beautiful/handsome nieces and nephews. They are more than nieces and nephews to me. Being the youngest child in my family, I treat them as if they're the younger brothers and sisters that I never had. It's so much fun watching them group up and can't imagine life without them. I am so honored to be the godfather of two of my nephews, Jacob and Ryan. To my own in-laws, Monica and Jim Cengia, thank you very much for your unending love and support. You two have been so understanding, unselfish, and generous to me. Although Jim

(Pittsburgh Steelers and Dayton Flyers) and I (Cincinnati Bengals and Xavier Musketeers) couldn't be any more different in terms of our favorite sports teams, I can't imagine a better father-in-law and mother-in-law (Monica) than the ones I have. And of course, I am grateful for all the extended Danneman and Cengia families as well.

I want to thank Dr. Richard J. Mullins for his guidance and his friendship. He is the basis as to why I chose chemistry. He has helped me tremendously and has prepared me well for my time at Vanderbilt. He is also the reason why I made the wise choice of going to Vanderbilt University and working for Jeff Johnston.

Next, I must thank my advisor Dr. Jeffrey N. Johnston. He has been extremely patient with me during the course of these 5 and a half years and I could not imagine a better education than the one he has given me. He has helped me discover brains that I never knew that I had and his concise attention to detail has helped shape me into the chemist that I am today. He has helped me succeed not only intellectually, but practically as well. Because of him, I feel very prepared for the road that lies ahead. It has been a pleasure working with him.

I am very grateful to all of the Johnston group members that I have overlapped with, both past and present. I especially want to thank Dr. Mark Dobish and Dr. Tyler Davis for helping me get situated in the laboratory. Aside from being good friends, they both served as excellent guides and helped push me towards my maximum potential. I especially want to thank Dr. Ki Bum Hong. He is one of the main reasons why I had the success that I had at Vanderbilt. He taught me how to not only engage in new chemistry (diamination chemistry) but to succeed in these areas as well. He was a great friend of mine in Nashville and will miss/have missed him greatly. I also want to thank Sergey for keeping track of my weekly steak consumption as well as singing songs such as "Very Nice White Solid". He always knew how to make me laugh. I am grateful for the numerous intellectual discussions with Matthew Knowe, Thomas Struble, and Zachary Carter. These men have so much potential and I know they will be successful in life. And of course my best friend in Nashville, Brandon Vara. This guy served as my buffer in the lab for 5 years. He is one of those people that can put you in a good mood, no matter what the circumstance. Not only has it been a pleasure working with him, I have been very fortunate to have him as a friend. From late night drinks to intramurals to Las Vegas, Brandon Vara has given me so many great memories that I will cherish for a lifetime.

I want to thank my committee members, Dr. Sulikowski, Dr. Lukehart, and Dr. Bachmann for taking time out their busy schedules and for contributing intellectually during every one of my major milestones. These gentlemen have taught me different ways and have showed me different angles as to how to think about and approach chemistry. They have served as the perfect complement to my advisor chair (Dr. Johnston) and I'm very fortunate to have interacted with them. I would also like to thank Don Stec and Markus Voehler for their exhaustive efforts in making sure that we have state-of-the-art NMR facilities. It is necessary to thank the NSF and NIH for funding and making this science possible. A special thanks goes out to both Dr. Craig W. Lindsley and Dr. Kiplin R. Guy for their collaborations in the GlyT1 and Nutlin-3 work.

I am very grateful to have so many wonderful friends within my life. A special thanks goes out to all of my high school and college friends that I still keep in touch with on a regular basis. I have also made many lifelong friends during my time at Vanderbilt including Kris Hahn, Tim Senter, Matt O'Reilly and Stephen Chau. I enjoyed many fun moments with these guys and will always think of them when I think of Nashville.

Lastly, I want to thank my amazing and beautiful wife, Gail. I can honestly say that none of this would have been possible without here. She is the most selfless person I know as she has gone out of the way to make my life easier and to maximize my time for research. She has made so many sacrifices for me and she has contributed to this work more than she will ever know. No matter how the work day went, she always puts me in a good mood and I am always happy when around her. I'm so incredibly lucky to have her as my wife and I can't imagine my life without her.

Applications of Chiral Amidine Catalysis Towards the Synthesis of Small Molecule Therapeutics and Recent Advances in Vicinal Diamine Synthesis

Table of Contents

ACKNOWLEDGEMENTS	iii
TABLE OF CONTENTS	vi
LIST OF SCHEMES	viii
LIST OF FIGURES	xviii
LIST OF TABLES	xx
Chapter	
Chapter 1. Enantioselective Synthesis of a GlyT1 Inhibitor	1
1.1 Background	1
1.2 Previously Synthesized GlyT1 Inhibitors	2
1.3 PBAM-Catalyzed Asymmetric Synthesis of a GlyT1 Inhibitor	4
1.4 Future Work	10
Chapter 2. PBAM-Catalyzed Additions of Nitromethane into Ketimine Centers – Part I: Sulfonyl Ketimines	11
2.1 Background	11
2.2 Synthesis of Sulfinyl and Sulfonyl Ketimines and Examination of Their Reactivity	16
2.3 PBAM-Catalyzed aza-Henry Additions into Sulfonyl Ketimine Centers	21
2.4 Future Work	26
Chapter 3. The Guided Development of Asymmetric Mono(Amidine) Organocatalysts for the Enantioselective Synthesis of Nutlin Analogs	28
3.1 Background	28
3.2 Synthetic Efforts Towards Amidine-Guanidine Asymmetric Catalysts	31
3.3 Development of Asymmetric Amidine-Amide Organocatalysts and Their Application Towards the aza-Henry Addition en Route to Nutlin-3	34
3.4 Proposed Catalyst Binding Modes	42
3.5 In-Depth Analysis of Catalyst Trends	45
3.6 Application of the Amidine-Amide Organocatalysts	50
Chapter 4. PBAM-Catalyzed Additions of Nitromethane into Ketimine Centers – Part II: Boc-Protected Trifluoromethyl Ketimines	52

4.1	<i>Synthesis of a Trifluoromethyl Ketimine and Examination of Its Reactivity</i>	52
4.2	<i>PBAM-Catalyzed Additions of Nitromethane into Trifluoromethyl Ketimine Centers</i>	54
4.3	<i>Progress Towards the Synthesis of a Trifluoromethyl Ketimine Nutlin Analog</i>	59
4.4	<i>Future Work</i>	67
Chapter 5. Oxidative Inter-/Intermolecular Alkene Diamination of Hydroxy Styrenes with Electron-Rich Amines via Hypervalent Iodine		69
5.1	<i>Background</i>	69
5.2	<i>Known Methods of Alkene Diamination</i>	72
5.3	<i>Reaction Optimization and Substrate Scope</i>	103
5.4	<i>Control Experiments and Mechanistic Hypothesis</i>	115
5.5	<i>Future Work</i>	118
Chapter 6. A Unified Approach to the Four Azaindoline Families by Inter-/Intramolecular Annulative Diamination of Vinylpyridines		120
6.1	<i>Background</i>	120
6.2	<i>Known Methods for the Preparation of Azaindolines</i>	124
6.3	<i>Reaction Optimization and Substrate Scope</i>	140
6.4	<i>Mechanistic Hypothesis</i>	146
6.5	<i>Future Work</i>	147
Chapter 7. Efforts Towards the Enantioselective Synthesis of Sesbanine: A Potential Antileukemic		149
7.1	<i>Background</i>	149
7.2	<i>Previous Syntheses of Sesbanine</i>	154
7.3	<i>Initial Efforts Towards the Enantioselective Synthesis of Sesbanine</i>	159
7.4	<i>Enantioselective Halolactonizations with Z-Alkenes: Model Studies</i>	164
7.5	<i>Future Directions</i>	175
Chapter 8. Experimentals		177

List of Schemes

Scheme 1. Retrosynthetic Analysis of GlyT1 Inhibitor 1	4
Scheme 2. Synthesis of Nitroazetidine 12	5
Scheme 3. Enantioselective 2-Nitropropane Additions.....	5
Scheme 4. Aza-Henry Addition of Nitroazetidine 12 Catalyzed by PBAM•HOTf.....	6
Scheme 5. Optimization of Aza-Henry Addition with Nitroazetidine 12	6
Scheme 6. Stannane-Mediated Denitration to Key Scaffold 21	7
Scheme 7. Synthesis of Dichlorbenzamide 24 from Key Scaffold 21	7
Scheme 8. Saponification Attempts En Route to Amine 25	7
Scheme 9. Isolated By-Products of an Attempted KOH Saponification.....	8
Scheme 10. Azetidine Isomerizations in Literature	8
Scheme 11. Oxazine Isomer Not Observed by HMBC Experimentation	9
Scheme 12. Successful Synthetic Route Towards Desired GlyT1 Target (-)- 1	10
Scheme 13. Aza-Henry Addition en Route to (-)-Nutlin-3	12
Scheme 14. Retrosynthetic Analysis of RG7112	14
Scheme 15. Examples of Nitromethane Additions into Ketimine Centers	15
Scheme 16. aza-Henry Additions into Quinazolinones en Route to DPC 083 by Wang.....	16
Scheme 17. Synthesis of Sulfinyl Ketimine 48 and Tosyl Ketimine 49	17
Scheme 18. Nitromethane Additions into Ketimine 48 with NaOH.....	18
Scheme 19. Attempted Nitroethane Additions into Ketimine 48 with TBAF and TMG.....	19
Scheme 20. Attempted Nitromethane Addition into Ketimine 48 with PBAM.....	19
Scheme 21. Equilibrium Experiment Conducted with PBAM.....	20
Scheme 22. Formation of Double Adduct 56 via Michael Acceptor 57	20

Scheme 23. Attempted Additions of Nitroethane and 1-Nitropropane into Ketimine 49	21
Scheme 24. Synthesis of Electron-Withdrawing and Electron-Donating Ketimine Species	24
Scheme 25. Aza-Henry Additions into Tosyl Ketimine 49	25
Scheme 26. Aza-Henry Additions into Methoxyphenyl Ketimine 60	25
Scheme 27. aza-Henry Additions into Nosyl Ketimine 59	27
Scheme 28. Examples of Nitromethane Additions into Aldehydes and Esters with Nagasawa's Catalyst (65).....	28
Scheme 29. Examples of Mannich and aza-Henry Reactions with Guanidine-Thiourea Organocatalysts.....	30
Scheme 30. Examples of aza-Henry Additions with Other Guanidine and Thiourea Catalysts	30
Scheme 31. Synthesis of Amidine-Amine Intermediate 75	32
Scheme 32. Attempts Towards the Synthesis of an Amidine-Guanidine Organocatalyst	33
Scheme 33. Synthesis of Amidine-Amide Catalyst 78	33
Scheme 34. Comparative Results of the Nutlin-3 aza-Henry System.....	34
Scheme 35. Synthesis of ^{3,5} (CF ₃) ₂ BenzAM (78a).....	35
Scheme 36. Improvements on the Nutlin-3 Aza-Henry System with ^{3,5} (CF ₃) ₂ BenzAM (78a)	35
Scheme 37. Synthesis of Amidine-Amide Catalyst Precursors 80a-80f	36
Scheme 38. Synthesis of Amidine-Amide Catalyst Precursors 80g-80n	36
Scheme 39. S _N Ar Reactions en Route to Amidine-Amide Catalysts 78a-78n	37
Scheme 40. Synthesis of Amidine-Thioamide Catalyst 78o	37
Scheme 41. Synthesis of Amidine-Sulfonamide Catalyst 78p	38
Scheme 42. aza-Henry Results with Amidine-Amide Catalysts 78a-78n	39
Scheme 43. Comparative Results with Thioamide and Sulfonamide Catalysts.....	41
Scheme 44. Steric Trends Observed with Asymmetric Amidine-Amide Catalysts.....	45

Scheme 45. Electronic Trends Observed with Asymmetric Amidine-Amide Catalysts	48
Scheme 46. Acidity Trends Observed with Asymmetric Amidine-Amide Catalysts	49
Scheme 47. Optimization of the (-)-Nutlin-3 System.....	50
Scheme 48. Development of (-)-Nutlin-3 Analogs	51
Scheme 49. Synthesis of Boc-Protected Trifluoromethyl Ketimine 82	53
Scheme 50. Examination of Reactivity with Ketimine 82	53
Scheme 51. Acquisition of Adduct 87 in Isolatable Yield	54
Scheme 52. Effects of Counterions and Asymmetric Catalysts	55
Scheme 53. Application of More Brønsted Basic BAM Catalysts	57
Scheme 54. Examination of Other Counterions	57
Scheme 55. Confirmation of PBAM·HNTf ₂ as the Optimal Catalyst	58
Scheme 56. Scale-Up of the Aza-Henry Addition	59
Scheme 57. Progress Toward the Synthesis of Target 89	60
Scheme 58. Attempts Toward Forming Urea 95 via Isocyanate 96 with DIPEA and DBU.....	61
Scheme 59. The Use of LHMDS and Isolation of a Cyclic By-Product.....	62
Scheme 60. Proposed Mechanism Toward Heterocyclic By-Products	63
Scheme 61. Formation of a Heterocyclic By-Product via Urea 99	64
Scheme 62. Chemoselective Dehydrative Cyclization to Imidazoline 100	65
Scheme 63. Synthesis of Nitrophenyl Urea 102	66
Scheme 64. Chemoselective Dehydrative Cyclization to Imidazoline 103	67
Scheme 65. Proposed Nitrosation Route Towards the Desired Piperazine Urea	68
Scheme 66. Jacobsen's Synthesis of Diamine 130 via Dinitrogen Tetroxide.....	73
Scheme 67. Nitronitrosylations of Alkenes with Nitric Oxide and Dinitrogen Trioxide.....	73

Scheme 68. Alkene Nitronitrosylation via <i>In Situ</i> Generation of N ₂ O ₃ with AgNO ₂ /TMSCl.....	74
Scheme 69. Dinitration of Unsaturated Terpene Achillin (137) with Nitrosyl Chloride and Dinitrogen Tetroxide.....	74
Scheme 70. Photoaddition of <i>N</i> -Nitrosodimethylamine with Cyclohexene (133) en Route to Masked Diamine 141	75
Scheme 71. Nitroamidation of Alkenes with Nitrogen Tetrafluoroborate and Acetonitrile	75
Scheme 72. Vankar's Alkene Nitroamidation Methods.....	76
Scheme 73. Ferrous Sulfate- and Ferric/Ferrous Sulfate-Mediated Diazidations of Alkenes	77
Scheme 74. Mn(III)-Mediated Diazidations of Alkenes	77
Scheme 75. Reaction of [Pb(OAc) _{4-n} (N ₃) _n] with Acyclic and Cyclic Olefins	78
Scheme 76. Zbiral's Reaction of [Tl(OAc) _{3-n} (N ₃) _n] with Cyclohexene and 4-Allylanisole	79
Scheme 77. Barluenga's Addition of Aromatic Amines to Alkenes in the Presence of Thallium(III) Acetate	79
Scheme 78. Barluenga's Addition of Aromatic Amines to Alkenes in the Presence of Mercury(II) Tetrafluoroborate	79
Scheme 79. Diaminations of Alkenes Using Cyclopentadienylnitrosylcobalt Dimer 169	80
Scheme 80. Reaction of Alkenes with Dinitrosyl Complex 175	81
Scheme 81. Stoichiometric Diamination of Alkenes with Imidoosmium(VIII) Complexes	81
Scheme 82. Diastereo- and Enantioselective Diaminations with Imidoosmium 188	82
Scheme 83. Bäckvall's Stoichiometric Pd-Mediated 1,2-Diamination of Alkenes	83
Scheme 84. Pd(II)-Catalyzed Intermolecular and Intramolecular Diaminations of Alkenes.....	83
Scheme 85. Muñiz's Pd(II)-Catalyzed Intramolecular Diamination of Internal Alkenes en Route to Bis(indolines).....	84
Scheme 86. Pd(II)-Catalyzed Intramolecular Cycloguanidation of Alkenes with Copper Chloride as the Oxidant	84
Scheme 87. Doubly Intermolecular Pd(II)-Catalyzed Diamination of Terminal Alkenes.....	84

Scheme 88. NFBS-Promoted Intra/Intermolecular Diamination of Terminal Alkenes	85
Scheme 89. Nickel(II)-Catalyzed Intramolecular Alkene Diamination	85
Scheme 90. Chemler's Intramolecular Diamination of Alkenyl-Substituted Sulfamides with Copper(II) Acetate	86
Scheme 91. Chemler's Copper(II) Neodecanoate-Promoted Intramolecular Diamination of Terminal Alkenes	86
Scheme 92. Copper(II) 2-Ethylhexanoate-Promoted Intra/Intermolecular Alkene Diamination	87
Scheme 93. Enantioselective Copper-Catalyzed Intra/Intermolecular Diamination of Allylaniline 217	87
Scheme 94. Example of Copper-Catalyzed Diamination of Unactivated Alkenes with a Hydroxylamine	87
Scheme 95. Gold-Catalyzed Intramolecular Diamination of <i>N</i> - γ -Alkenyl-Substituted Ureas	88
Scheme 96. Gold-Catalyzed Oxidative Intra/Intermolecular Diamination of <i>N</i> - γ -Alkenyl Tosylated Amines	88
Scheme 97. Symmetric and Asymmetric Pd-Catalyzed Diaminations of Dienes with Di- <i>tert</i> - Butyldiaziridinone	88
Scheme 98. Symmetric and Asymmetric Pd-Catalyzed Dehydrogenative Allylic/Homallylic Diaminations	89
Scheme 99. Phosphine-Ligand-Dependent Regioselective Diaminations of Conjugated Dienes and Trienes	90
Scheme 100. Copper(I)-Catalyzed Diamination of Disubstituted Terminal Alkenes	90
Scheme 101. Copper(I)-Catalyzed Alkene Diaminations with Thiadiaziridine Dioxide 244 and Diaziridine 246	91
Scheme 102. 1,2-Diamination of 1,3-Dienes with Selenium Dioxide Bis(Imide) 249	91
Scheme 103. Imidazolation of α,β -Unsaturated Ketone 257 with a TsNCl ₂ /MeCN/Rh ₂ pbf ₄ •PPh ₃ Reagent	92
Scheme 104. Improved Methods for the Direct Imidazolation of α,β -Unsaturated Ketones	92
Scheme 105. Inter/Intramolecular Aminoazidation of γ -Alkenyl Amines with NCS, NaN ₃ , and NaI	93

Scheme 106. <i>cis</i> -Imidolizidination of Alkenes with <i>N</i> -Chlorosaccharin, CH ₃ CN, and KOEt.....	93
Scheme 107. Diamination of Glucal 270 Using I ₂ and Chloroamine-T.....	94
Scheme 108. Diazidation of a Cyclic Polyene with IN ₃ and NaN ₃	94
Scheme 109. Diazidation of Benzofurans and Indoles with IN ₃	95
Scheme 110. Diazidation of <i>trans</i> -Stilbene 280 Using IN ₃	95
Scheme 111. Hassner's Divergent Reactions of Diene 282 with BrN ₃ and IN ₃	95
Scheme 112. Iodine-Mediated Vicinal Diamination of 1,4-Dihydropyridine 285	96
Scheme 113. Intramolecular <i>anti</i> -Selective Diamination of Alkenes with NIS en Route to 2,2'- Bipyrrolidines.....	96
Scheme 114. Al-Mourabit's Bromine-Mediated Cycloguanidination of Dihydropyridines.....	97
Scheme 115. Tepe's Synthesis of (±)-Dibromophakellin via Alkene Cycloguanidination.....	97
Scheme 116. Cycloguanidination of Dihydropyridines with 2-Aminopyrimidine.....	97
Scheme 117. Zhang's NIS-Mediated Doubly Intramolecular Diamination of <i>N</i> -Alkenyl Thioureas.....	98
Scheme 118. Diazidation of α,β-Unsaturated Esters with PhI(OAc) ₂	98
Scheme 119. Synthesis of Vicinal Diazides Using Iodosobenzene.....	99
Scheme 120. Vicinal Diaminations of Alkenes Employing PhIO/TMSN ₃	99
Scheme 121. Muñiz's Enantioselective, Metal-Free Intermolecular Diamination of Styrenes.....	100
Scheme 122. Muñiz's Enantioselective Synthesis of (<i>S</i>)-Levamisole via Intermolecular Diamination.....	100
Scheme 123. Iodine(III)-Promoted Intermolecular Diaminations of Styrenes and Alkyl- Substituted Alkenes.....	101
Scheme 124. Intermolecular Alkene Diaminations via the Use of Dinuclear Iodine(III).....	101
Scheme 125. Inter/Intramolecular Alkene Diamination with PhI(NTs ₂) ₂ and PhI(NMs ₂) ₂	102
Scheme 126. Inter/Intramolecular Diaminations of Vinylanilines en Route to 3-Aminoindolines..	102

Scheme 127. PhI(OAc) ₂ /KI-Mediated Intramolecular Diamination of Alkenyl Sulfamides.....	102
Scheme 128. PhI(OAc) ₂ /NIS-Mediated Intramolecular Diamination of Formamidines	103
Scheme 129. Wirth's Enantioselective Intramolecular Diaminations en Route to Diamino Bicycles	103
Scheme 130. Hong and Johnston's Iodine(III)-Mediated Inter/Intramolecular Diamination of Terminal Alkenes	104
Scheme 131. Initial Findings of an Iodine(III)-Mediated Doubly Intermolecular Alkene Diamination	104
Scheme 132. Decomposition Experiment with Diamine 338a	106
Scheme 133. Unsuccessful Diamination of 3-Vinyl Phenol with PhI(OAc) ₂ /KI and NIS	109
Scheme 134. Unsuccessful Diamination of 2-Vinylanisole with PhI(OAc) ₂ /KI and NIS	109
Scheme 135. Unsuccessful Diamination of Styrene with PhI(OAc) ₂ /KI and NIS.....	110
Scheme 136. Unsuccessful Diamination of Allylbenzene with PhI(OAc) ₂ /KI and NIS.....	110
Scheme 137. Unsuccessful Diamination of <i>ortho</i> -Nitrostyrene with PhI(OAc) ₂ /KI and NIS	110
Scheme 138. Unsuccessful Diamination of <i>o</i> -Styrylphenol with PhI(OAc) ₂ /KI and NIS	111
Scheme 139. Intermolecular Aminoacetoxylation with Primary Aliphatic Amines.....	113
Scheme 140. Generation of Bis(oxygenation) Product 355	115
Scheme 141. Generation of Iodoacetoxylation Product 356	115
Scheme 142. Other Findings with Bis(oxygenation) and Iodoacetoxylation Products 355 and 356	116
Scheme 143. Acquisition of Monoamination Product 357 via Muñiz's Protocol.....	116
Scheme 144. Proposed Heterodiamination of 2-Vinylphenol.....	119
Scheme 145. Potential Enantioselective Variations of the Doubly Intermolecular Alkene Diamination	119
Scheme 146. Aniline Bioactivation Pathways.....	122
Scheme 147. Synthesis of 7-Azaindolines via an Inverse Electron Demand Diels-Alder Reaction of Pyrimidines	124

Scheme 148. Synthesis of 7-Azaindolines via an Inverse Electron Demand Diels-Alder Reaction of Triazines.....	125
Scheme 149. Sanders's Iodine(III)-Mediated Synthesis of 7-Azaindole 386 via 7-Azaindoline 385	125
Scheme 150. Sumiyoshi's Synthesis of a Key 7-Azaindoline Scaffold.....	126
Scheme 151. Synthesis of Antipsychotic Candidates 392 and 374	127
Scheme 152. Burgos's Synthesis of 7-Azaindoline 400 and Byproducts via Radical Cyclization...	128
Scheme 153. Radical Cyclizations en Route to 7-Azaindolines 405 and 409	128
Scheme 154. Zard's Radical-Mediated Synthesis of 7-Azaindolines Using Xanthate Esters	129
Scheme 155. Johnston's Regioselective Synthesis of 7-Azaindoline 422	130
Scheme 156. Johnston's Radical-Mediated Synthesis of 7-Azaindoline 426 with Complete Stereoretention.....	130
Scheme 157. Johnston's Synthesis of Enantiopure 7-Azaindoline α -Amino Acids	131
Scheme 158. Davies's <i>ortho</i> -Metallation/Transmetallation Approach to 7-Azaindolines	132
Scheme 159. Nguyen's Base-Mediated Synthesis of 7-Azaindolines.....	132
Scheme 160. Méroux's Palladium Heteroannulation en Route to 7-Azaindolines.....	133
Scheme 161. Moss's One-Pot Ring-Opening-Cyclization Sequence en Route to Azaindolines	133
Scheme 162. Synthesis of 6-Azaindolines via an Inverse Electron Demand Diels-Alder Reaction of Pyrazines	134
Scheme 163. Dodd's Synthesis of 6-Azaindoline Scaffolds	134
Scheme 164. Zhu's Three-Component Synthesis of 6-Azaindolines.....	135
Scheme 165. Yakhontov's Synthesis of 5-Azaindolines.....	136
Scheme 166. Kauffmann and Fischer's Synthesis of 5-Azaindoline 473 via a Benzyne Intermediate.....	136
Scheme 167. Synthesis of DMAP Analogs via 5-Azaindoline Intermediates	137

Scheme 168. Titanocene(III)-Catalyzed Formation of 5-Azaindolines	137
Scheme 169. Zard's Synthesis of 5-Azaindolines Using Xanthate Esters	138
Scheme 170. Synthesis of 4-Azaindoline 497 via Photocycloaddition	138
Scheme 171. Ciufolini's Alkoxy-Mediated Radical Synthesis of 4-Azaindolines	139
Scheme 172. Bailey's Unified Approach to All Four Isomeric Azaindoline Families	140
Scheme 173. Hong and Johnston's Iodine(III)-Mediated Inter-/Intramolecular Diamination of Terminal Alkenes	141
Scheme 174. Inter-/Intramolecular Diamination of Vinylpyridines en Route to All Four Azaindoline Families.....	141
Scheme 175. Synthesis of Vinyl Aminopyridine 519	141
Scheme 176. Synthesis of Vinyl Aminopyridine 522	143
Scheme 177. Synthesis of Vinyl Aminopyridine 525	144
Scheme 178. Synthesis of Vinyl Aminopyridine 528	145
Scheme 179. Proposed Synthesis of 3-Alkyl-3-Amino-Azaindolines	147
Scheme 180. Potential Enantioselective Variation of the Annulative Diamination.....	148
Scheme 181. Kende and Demuth's Stereospecific Synthesis of Sesbanine	155
Scheme 182. Tomioka and Koga's Synthesis of Sesbanine.....	155
Scheme 183. Iwao and Kuraishi's Synthesis of Sesbanine	156
Scheme 184. Pandit, Wanner, and Koomen's Synthesis of Sesbanine	157
Scheme 185. Wada, Nishihara, and Akiba's Synthesis of Sesbanine	158
Scheme 186. Bottaro and Berchtold's Synthesis of Sesbanine	159
Scheme 187. Dobish and Johnston's BAM-Catalyzed Enantioselective Iodolactonization	160
Scheme 188. Retrosynthetic Analysis of Sesbanine.....	160
Scheme 189. Synthesis of Cyclopentene Carbonitrile 565	160

Scheme 190. Acquisition of Nicotinate 566 and S _N Ar en Route to Ester 560	161
Scheme 191. Isolation and Confirmation of Imide 571	162
Scheme 192. Acquisition and Confirmation of Imidopiperidinone 574	162
Scheme 193. Repetition of Bottaro and Berchtold's One-Pot Saponification-Iodolactonization	163
Scheme 194. Racemic Synthesis of Iodolactone 577	164
Scheme 195. Iodolactonization Attempt with CH ₂ Cl ₂ as the Solvent.....	166
Scheme 196. Racemic Synthesis of Bromolactone 580	169
Scheme 197. Failed Attempt Towards Chlorolactonization.....	170
Scheme 198. Racemic Synthesis of Selenolactone 582	170
Scheme 199. Racemic Synthesis of [6.5]-Bicyclic Iodolactone 587	171
Scheme 200. Racemic Synthesis of Iodolactone 596	174
Scheme 201. Reaction Optimization and Substrate Scope Development	176
Scheme 202. Revised Proposed Synthesis of Sesbanine.....	176

List of Figures

Figure 1. Structure of GlyT1 Inhibitor 1	2
Figure 2. Previously Published GlyT1 Inhibitors	3
Figure 3. Structure of RG1678 (11).....	4
Figure 4. Structures of Nutlin Compounds 33-35	12
Figure 5. Structural Differences Between (-)-Nutlin-3 and RG7112.....	13
Figure 6. Structure of Cbz-Ketimine 46 and Tautomerization to its Corresponding Enamine 47 ...	17
Figure 7. Proposed Transition State of the Guanidine-Thiourea Catalyzed Henry Reaction	29
Figure 8. Backbone Structure of Desired Amidine-Guanidine Catalyst.....	31
Figure 9. Optimal Catalysts Chosen for Further Studies	41
Figure 10. Proposed Amidine-Amide Activation and Stereochemical Model A	42
Figure 11. Proposed Amidine-Amide Activation and Stereochemical Model B	43
Figure 12. Proposed Amidine-Amide Activation and Stereochemical Model C	43
Figure 13. Proposed Amidine-Amide Activation and Stereochemical Model D	44
Figure 14. Deactivation of the Catalyst via Introduction of a Salt	45
Figure 15. Ring Expansion and its Influence on Enantioselection	46
Figure 16. Steric Interaction and its Influence on Enantioselection	47
Figure 17. Proposed Disruptions of Binding via Unwanted Intramolecular Coordination	48
Figure 18. Intramolecular Interaction Between the Quinoline and Acidic Proton	50
Figure 19. Structure of Boc-Protected Trifluoromethyl Ketimine 82	53
Figure 20. Structural Differences Between (-)-Nutlin-3 and Target 89	59
Figure 21. Naturally Occurring, Non-Proteinogenic <i>vic</i> -Diamino Acids and Their Derivatives	69
Figure 22. Examples of Naturally Occurring Alkaloids That Possess the 1,2-Diamine Framework.....	71

Figure 23. Pharmaceutically Active, Synthetic 1,2-Diamines	72
Figure 24. Mechanistic Hypothesis for $\text{PhI}(\text{OAc})_2/\text{KI}$ -Mediated Intermolecular Diamination.....	117
Figure 25. Relative Comparison of KI Loading and Reactivity	118
Figure 26. Examples of Naturally Bioactive Alkaloids Possessing an Indoline Scaffold	120
Figure 27. Examples of Pharmaceutical Agents Possessing an Indoline Scaffold	121
Figure 28. Phosphodiesterase Inhibition of Aniline and Azaindoline Compounds 370 and 371	123
Figure 29. mAChR Agonist Activity of 7-Azaindoline Compounds 373 and 374	123
Figure 30. Mechanistic Hypothesis for the Inter-/Intramolecular Annulative Diamination.....	147
Figure 31. Chemotherapeutic Agents Used in the Treatment of Acute Lymphocytic Leukemia (ALL)	150
Figure 32. Purines and Other Agents Used in the Treatment of Chronic Lymphocytic Leukemia (CLL)	151
Figure 33. Monoclonal Antibodies Used in the Treatment of Chronic Lymphocytic Leukemia (CLL)	153
Figure 34. Agents Used in the Treatments of Acute and Chronic Myelogenous Leukemias (AML and CML).....	153
Figure 35. Structure of Sesbanine	154
Figure 36. Potential Unwanted Electronic Interaction in the Binding Mode.....	172

List of Tables

Table 1. Nitromethane Additions into Ketimine 48 with TBAF and TMG.....	18
Table 2. Nitromethane Additions into a Tosyl Ketimine to Yield Double Adduct 56	20
Table 3. Catalyst Screen for Nitromethane Additions into Tosyl Ketimine 49	22
Table 4. Reactivity Study with δ (MeO)PBAM	23
Table 5. Reactivity Study with δ (MeO)PBAM•HNTf ₂	23
Table 6. Effects of Concentration and Catalyst Loading	55
Table 7. In-Depth Concentration and Nitromethane Equivalence Studies	56
Table 8. Effects of Temperature.....	58
Table 9. Attempts Toward Forming Urea 95 Using Various Isocyanate Sources	61
Table 10. Synthesis of Urea 99 and Optimization	63
Table 11. Failed Acylation Attempts En Route to Piperazine Urea 95	65
Table 12. Failed Acylation Attempts with Nitrophenyl Urea 102	66
Table 13. Initial Optimization Studies of the Doubly Intermolecular Alkene Diamination	105
Table 14. Solvent Screen of the Doubly Intermolecular Alkene Diamination	106
Table 15. Effects of Temperature on the Doubly Intermolecular Alkene Diamination.....	107
Table 16. Diamination of 2-Vinyl Phenol with PhI(OAc) ₂ /KI and NIS	107
Table 17. Diamination of 4-Vinyl Phenol with PhI(OAc) ₂ /KI and NIS	108
Table 18. Doubly Intermolecular Alkene Diamination: Secondary Amine Scope	112
Table 19. Doubly Intermolecular Alkene Diamination: Primary Amine Scope	113
Table 20. Doubly Intermolecular Alkene Diamination: Amine Scope with <i>para</i> -Hydroxystyrene .	114
Table 21. Doubly Intermolecular Alkene Diamination: Vinylphenol Scope.....	114
Table 22. KI Loading Study.....	117

Table 23. Initial Optimization Studies of the Inter-/Intramolecular Annulative Diamination.....	142
Table 24. 3-Amino-7-Azaindoline Scope	143
Table 25. 3-Amino-6-Azaindoline Scope	144
Table 26. 3-Amino-5-Azaindoline Scope	145
Table 27. 3-Amino-4-Azaindoline Scope	146
Table 28. Initial Investigations of the Enantioselective Saponification-Iodolactonization Reaction.....	163
Table 29. Preliminary Time and Concentration Studies	165
Table 30. Effects of Acid Salts and More Brønsted Basic Organocatalysts	165
Table 31. Application of Different Catalyst Backbones and Reevaluation of Temperature and Iodine Sources	166
Table 32. Reexamination of Acid Salts and Brønsted Basic Catalysts	167
Table 33. Studies with Non-BAM Catalysts	168
Table 34. Brief Investigation of an Enantioselective Bromolactonization	169
Table 35. Brief Investigation of an Enantioselective Selenolactonization.....	170
Table 36. 6-Membered Iodolactonization: Catalyst and Solvent Studies	172
Table 37. 6-Membered Iodolactonization: Examination of Non-Amidine Catalysts	173
Table 38. Initial Iodolactonization Studies with Phenyl-Derived Acid 593	175

Chapter 1. Enantioselective Synthesis of a GlyT1 Inhibitor

1.1 Background

Schizophrenia is among the most mysterious and costly mental disorders in terms of human suffering and social expenditure.¹ This disorder, which is a severe and chronic mental illness, has prevalence estimates ranging from 0.5% to 1% of the world population.² Though schizophrenia has traditionally been associated with mental illness alone, patients diagnosed with this disorder typically die 12 to 15 years earlier than the average population. Studies have also determined that schizophrenia causes more loss of life than most cancers and physical illnesses.¹ Thus, in depth studies and potential treatments for this prevalent disorder remain of high importance.

Today, the leading treatments for this disorder are atypical antipsychotic medicines that belong to the family of dopamine D2 and serotonin 5-HT_{2a} receptor antagonists. Although these drugs are effective in the management of symptoms such as hallucinations, paranoia, delusions, and disorganized speech and thinking, they demonstrate little effect toward improving the more negative symptoms (drowsiness, muscle spasms, blurred vision) or cognitive function. Additionally, these leading medicines have unsatisfactory side effect profiles because of their promiscuous pharmacology.²

Due to this unsatisfactory state of the disease and treatment options, there is a need for the development of improved, safer therapeutic agents for the treatment of schizophrenia. Over the past two decades, clinical research has shown that abnormally low functioning levels of *N*-methyl-D-aspartate (NMDA) receptors may play a key role in the pathophysiology of schizophrenia. Restoration of NMDA receptor activity is considered a potential therapeutic avenue.² Glycine, a common amino acid and coagonist for NMDA activation,³ has been found to potentiate the NMDA response in mouse brain neurons via an allosteric activation of the NMDA receptor.⁴ Though elevation of glycine levels in the brain is a pivotal finding, exogenous administration of glycine is something that must be prevented.

¹ van Os, J.; Kapur, S. *The Lancet* **2009**, *374*, 635-645.

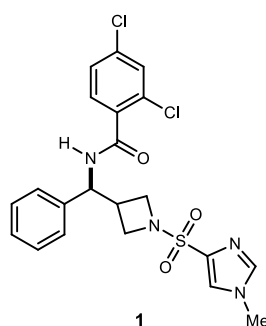
² Pinard, E.; Alanine, A.; Alberati, D.; Bender, M.; Borroni, E.; Bordeaux, P.; Brom, V.; Burner, S.; Fischer, H.; Hainzl, D.; Halm, R.; Hauser, N.; Jolidon, S.; Lengyel, J.; Marty, H.-P.; Meyer, T.; Moreau, J.-L.; Mory, R.; Narquizian, R.; Nettekoven, M.; Norcross, R. D.; Puellmann, B.; Schmid, P.; Schmitt, S.; Stadler, H.; Wermuth, R.; Wettstein, J. G.; Zimmerli, D. *J. Med. Chem.* **2010**, *53*, 4603-4614.

³ Kleckner, N.; Dingledine, R. *Science* **1988**, *241*, 835-837.

⁴ Johnson, J. W.; Ascher, P. *Nature* **1987**, *325*, 529-531.

Of the studies that have been conducted, one of the best preventive methods is through glycine transporter 1 (GlyT1) inhibition. GlyT1 is a type of glycine transporter that is widely expressed in glial cells throughout the nervous system.⁵ Research has shown that GlyT1 transporters can play a variety of roles including serving as a key novel target for the treatment of disorders such as schizophrenia.² It has also been determined that GlyT1 inhibition can reduce allodynia and hyperalgesia in a range of chronic pain models.⁵ Additional studies have further confirmed that GlyT1 is essential for glycine-mediated protection of human intestinal epithelial cells against oxidative damage.⁶ Thus, synthesis of a desired GlyT1 target (**1**) is of high importance due to its potential impact on biological activity (Figure 1).

Figure 1. Structure of GlyT1Inhibitor **1**



1.2 Previously Synthesized GlyT1 Inhibitors

Previous clinical studies have demonstrated that sarcosine (*N*-methylglycine), a prototypical GlyT1 inhibitor, can lead to improved positive, negative, and cognitive symptoms in schizophrenic patients along with standard therapy. However, this compound cannot be classified as an optimal therapeutic agent due to its poor pharmacological profile. Thus, efforts have been made toward the development of improved sarcosine-based GlyT1 inhibitors, such as **2**, **3**, and **4** (Figure 2). Unfortunately, the poor pharmacological profile was sustained as these sarcosine derivatives suffered from undesirable effects including hypoactivity, ataxia (lack of muscle coordination), and reduced respiratory activity.²

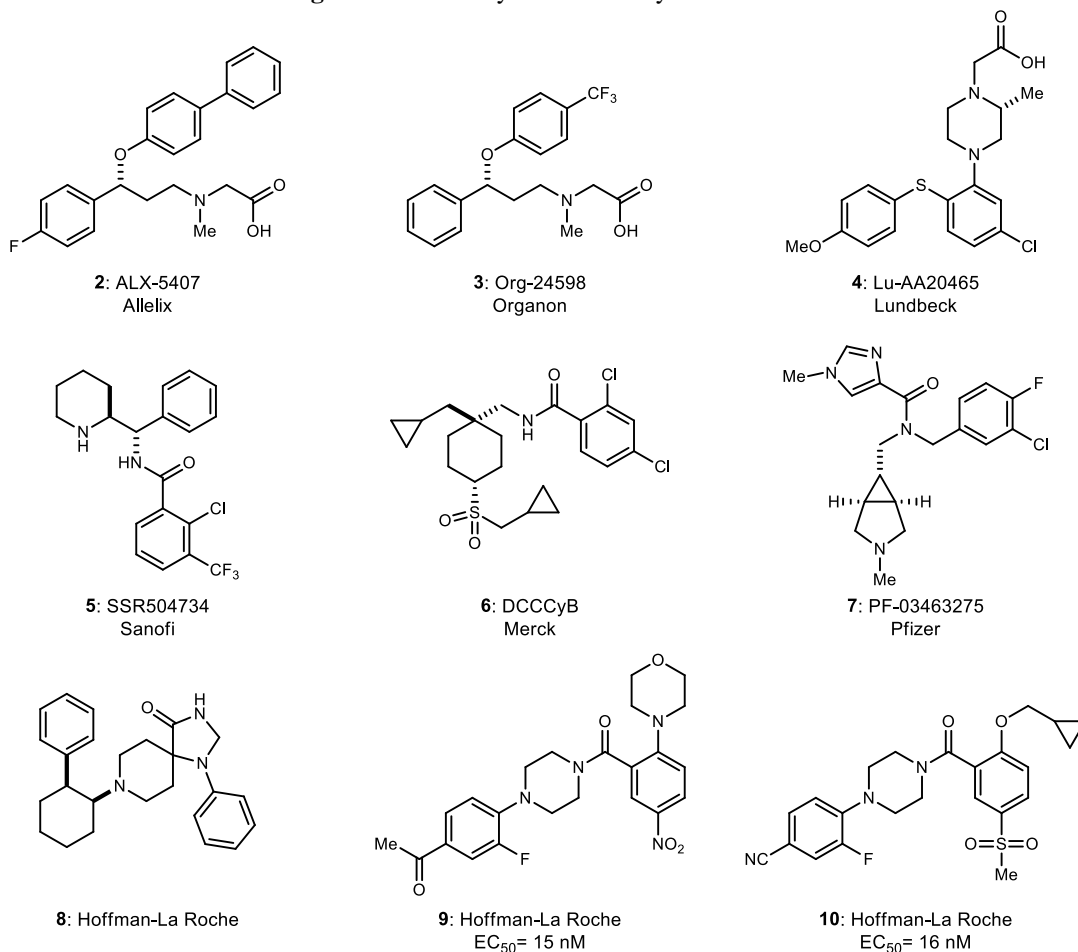
Based on these findings, a variety of pharmaceutical companies shifted their attention toward the identification and development of non-sarcosine-based GlyT1 inhibitors. Some of the successfully synthesized GlyT1 targets include a rich set of highly structurally diverse non-amino-

⁵ Jeong, H.J.; Vandenberg, R. J.; Vaughan, C. W. *Brit. J. Pharmacol.* **2010**, *161*(4), 925-935.

⁶ Howard, A.; Tahir, I.; Javed, S.; Warning, S.; Ford, D.; Hirst, B. *J. Physiol.* **2010**, *588*, 995-1009.

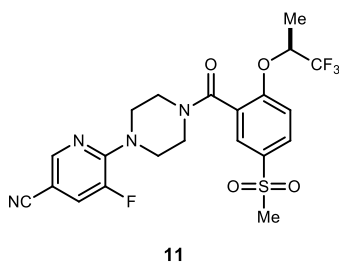
acid chemotypes, **5**, **6**, and **7**, as well as a non-sarcosine-based spiro-piperidine **8**. Furthermore, benzoylpiperazines such as **9** and **10** were shown to be more novel chemotypes as they exhibited EC₅₀ potencies of 15 nM and 16 nM respectively in regards to GlyT1 inhibition via high-throughput screening (Figure 2).² Despite these improvements, the issues of a poor pharmacological profile were not resolved with these specific targets.

Figure 2. Previously Published GlyT1 Inhibitors



Hoffmann-La Roche has successfully synthesized and is continuing to develop a promising benzoylpiperazine chemotype. RG1678 (**11**) has been classified as the first potent and selective GlyT1 inhibitor to have a beneficial effect in schizophrenic patients based on a 2010 phase II clinical trial (Figure 3).²

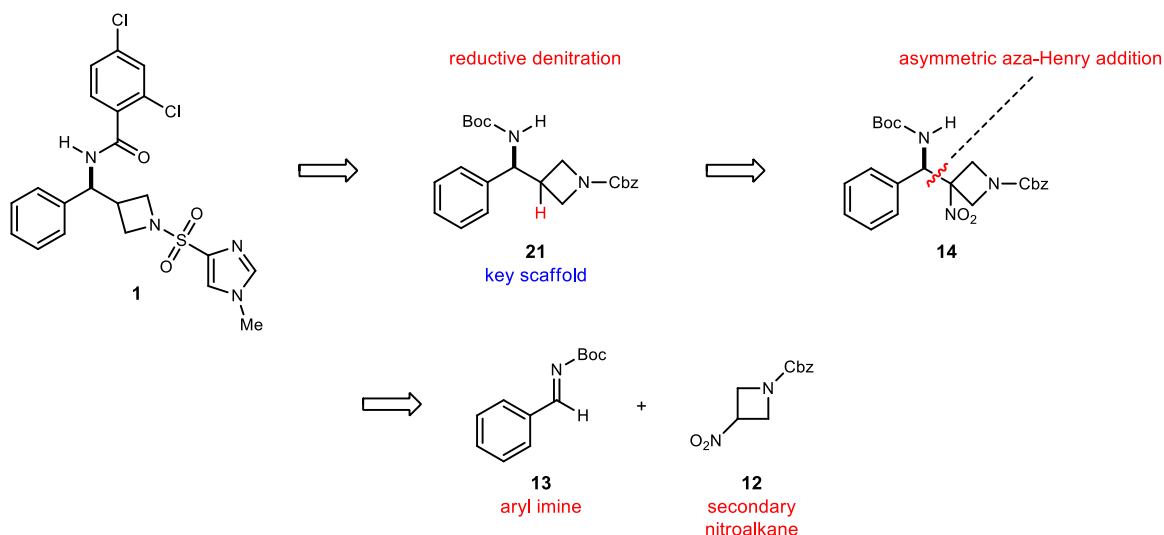
Figure 3. Structure of RG1678 (**11**)



1.3 PBAM-Catalyzed Asymmetric Synthesis of a GlyT1 Inhibitor⁷

A concise synthesis of a desired GlyT1 target has been successfully completed via a collaborative effort between the laboratories of Craig W. Lindsley and Jeffrey N. Johnston at Vanderbilt University. Target molecule **1** has been identified by the Lindsley group as a potent GlyT1 inhibitor and a potential therapeutic for the treatment of schizophrenia.⁸ The more potent enantiomer of this compound was found to bind 10^4 times better than its antipode. When examining the structure of compound **1**, retrosynthetic analysis shows that a key carbon-carbon bond can be made via an asymmetric aza-Henry addition between nitroazetidine **12** and imine **13** through the use of chiral proton catalysis. Successful installation of this key carbon-carbon bond is critical as it will facilitate the development of the more potent enantiomer of GlyT1 inhibitor **1** via functional group manipulation of the scaffold (Scheme 1).

Scheme 1. Retrosynthetic Analysis of GlyT1 Inhibitor **1**

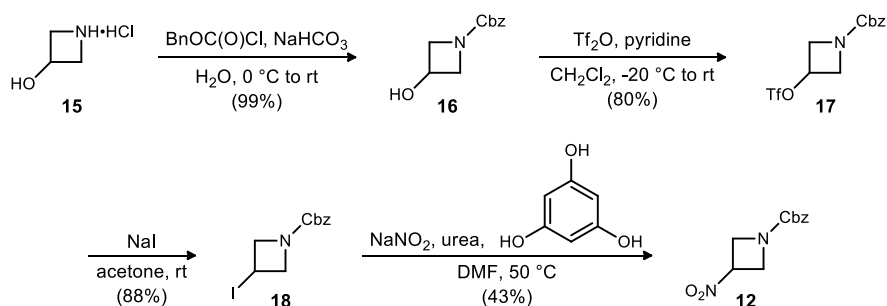


⁷ Davis, T. A.; Danneman, M. W.; Johnston, J. N. *Chem. Commun.* **2012**, 48, 5578-5580.

⁸ Lindsley, C. W.; Conn, J. P.; Williams, R.; Jones, C. K.; Sheffler, D. J., Sulfonyl-azetidin-3-yl-methylamine Amide Analogs As GlyT1 Inhibitors, Methods For Making Same, And Use Of Same In Treating Psychiatric Disorders. U.S. Patent WO 2010/114907 A1, October 7, 2010.

The synthesis of the desired GlyT1 inhibitor was initiated by subjecting commercially available hydroxyazetidine hydrochloride **15** to benzyl chloroformate under basic conditions in order to furnish Cbz-protected hydroxyazetidine **16** in quantitative yield. Compound **16** was then treated with triflic anhydride in the presence of pyridine to yield triflate **17** in 80% yield. Treatment of **17** with sodium iodide resulted in the expected nucleophilic substitution providing iodoazetidine **18** (88% yield), which was then treated with sodium nitrite to afford nitroazetidine **12** in modest yield (43% yield, Scheme 2).

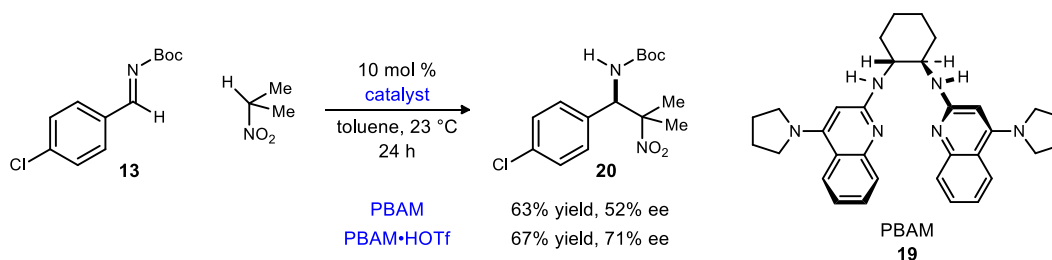
Scheme 2. Synthesis of Nitroazetidine **12**



With the desired nitroazetidine in hand, the stage was now set for the key enantioselective aza-Henry addition. This addition of azetidine **12** into Boc-protected imine **13** was to be carried out using our Brønsted basic Pyrrolidine Bis(AMidine) [PBAM] organocatalysts. Before applying the nitroazetidine motif as the nucleophile however, additions of 2-nitropropane, the simplest secondary nitroalkane, were conducted in order to examine the feasibility of this reaction system.

Additions of 2-nitropropane into imine **13** were carried out by Tyler Davis. He found that when using PBAM free base **19** as the catalyst at ambient temperature, the desired adduct (**20**) was obtained in 63% yield and 52% ee after a 24 hour reaction time (Scheme 3). The triflic acid salt of PBAM (**19**•HOTf) showed improvement as adduct **20** was furnished in comparable yield and

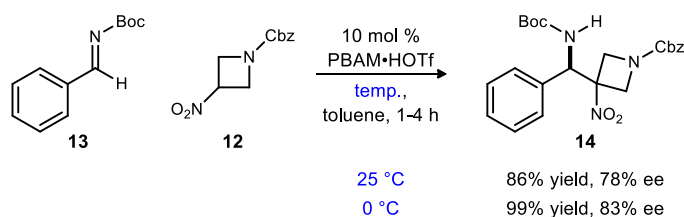
Scheme 3. Enantioselective 2-Nitropropane Additions



enhanced enantioselection. This indicates that use of a polar ionic hydrogen bond is necessary in order to achieve optimal selectivity.

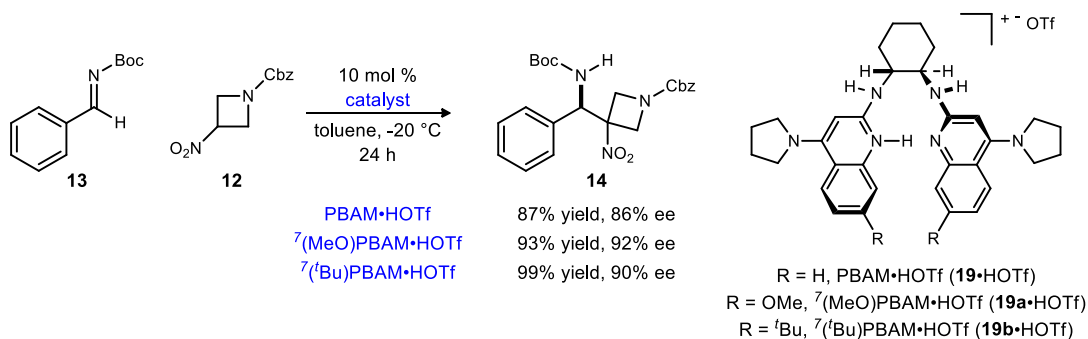
Seeing that reasonable yields and promising levels of enantioselection were achieved with 2-nitropropane, Tyler Davis then submitted nitroazetidine **12** as the donor for this reaction system. When using PBAM•HOTf as the catalyst at room temperature, he found that the desired aza-Henry adduct (**14**) was afforded in 86% yield and 78% ee (Scheme 4). This reaction proved to be surprisingly fast as full conversion was observed after 70 minutes. When lowering the temperature to 0 °C, increased yield and enantioselectivity was observed after a slightly prolonged reaction time of 4 hours.

Scheme 4. Aza-Henry Addition of Nitroazetidine **12** Catalyzed by PBAM•HOTf



Further optimization was achieved upon lowering the temperature to -20 °C. Under these chilled conditions, PBAM•HOTf provided adduct **14** in 87% yield and 86% ee over the course of 24 hours (Scheme 5). Additionally, 7-substituted PBAM catalysts were also tested with ambitions of achieving higher degrees of enantioselectivity. ⁷(MeO)PBAM•HOTf (**19a**•HOTf) proved to be ideal as the desired adduct was furnished in 93% yield and 92% ee. ⁷(^tBu)PBAM•HOTf (**19b**•HOTf) was also successful, affording adduct **14** in 99% yield and 90% ee. Unfortunately when lowering the temperature to -78 °C, minimal conversion was observed after 24 hours.

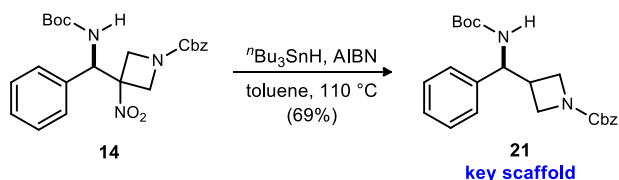
Scheme 5. Optimization of Aza-Henry Addition with Nitroazetidine **12**



With enantiomerically enriched aza-Henry adduct (**14**) in hand, efforts toward the desired GlyT1 target continued through the formation of a key intermediate (**21**) that results from a straightforward denitration. Intermediate **21** was obtained by free radical-mediated reduction by treating **14** with tributyltin hydride (ⁿBu₃SnH) and azobisisobutyronitrile (AIBN) (Scheme 6).

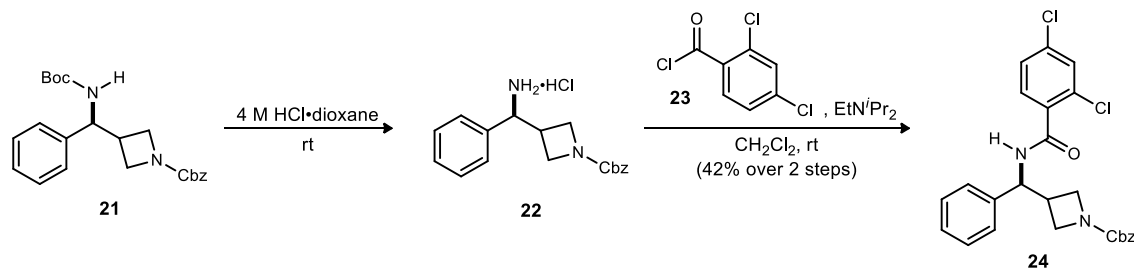
AIBN, which serves as a radical initiator, propagates with ${}^n\text{Bu}_3\text{SnH}$ ultimately cleaving the nitro-carbon bond to yield 1,3-diamine **21**. From this key scaffold, multiple routes could be envisioned to the desired target.

Scheme 6. Stannane-Mediated Denitration to Key Scaffold **21**



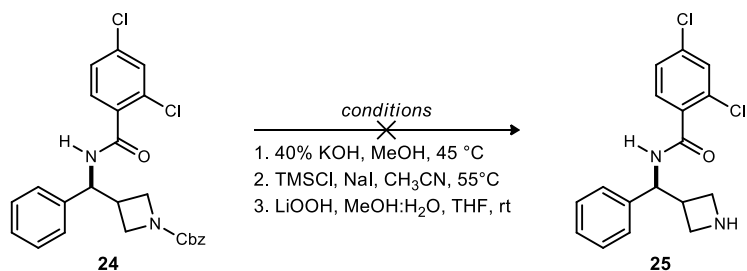
The first route to target **1** began with cleavage of the Boc protecting group. By treating intermediate **21** with an excess of acid, the HCl salt of free amine **22** was acquired. This salt, which was carried on without further purification, was then treated with chloride **23** under basic conditions to provide **24** in 42% yield over two steps (Scheme 7).

Scheme 7. Synthesis of Dichlorobenzamide **24** from Key Scaffold **21**



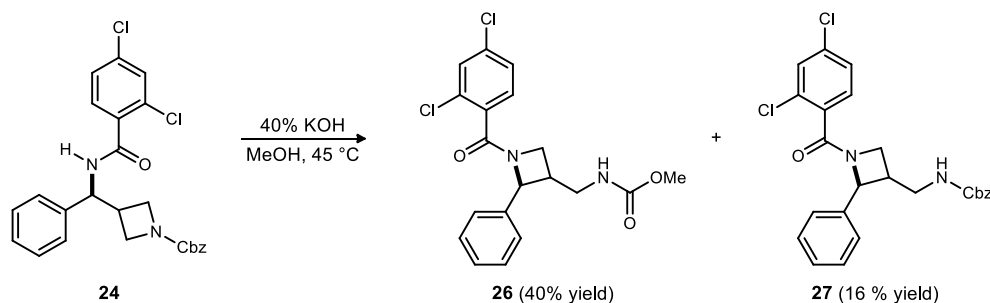
Intermediate **24** was treated with KOH in an attempt to saponify the Cbz group and subsequently decarboxylate to afford secondary amine **25**. Initial attempts of this saponification using 40% KOH with varying methanol to water ratios failed to give the desired amine. Nucleophilic attack on the activated benzyl position of the Cbz group with trimethylsilyl iodide also proved fruitless. Furthermore, the use of stronger nucleophiles, such as LiOOH, did not result in the intended cleavage of the Cbz group via saponification (Scheme 8).

Scheme 8. Saponification Attempts En Route to Amine **25**



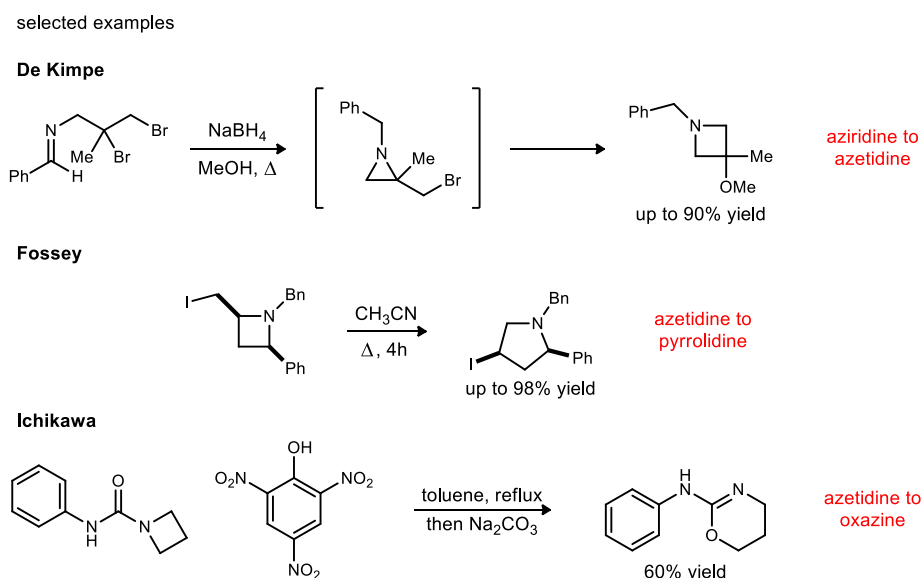
Although these attempts did not result in the formation of the desired secondary amine (**25**), a notable discovery was made. When treating intermediate **24** with 40% KOH in the presence of excess methanol, two products (**26** and **27**) were consistently obtained. Though it was

Scheme 9. Isolated By-Products of an Attempted KOH Saponification



determined for compound **26** that the Cbz group was successfully cleaved, it was also evident that a methyl ester was made in lieu of the intended carbamic acid. Upon chromatographic separation and isolation of ester **26** (40% yield), an azetidine to azetidine isomerization was observed during this saponification attempt as well (Scheme 9). Support of this isomerization was confirmed by observations of desired $^3J_{\text{HC}}$ couplings through an HMBC (600 MHz) experiment (see structure elucidation, Chapter 8).

Scheme 10. Azetidine Isomerizations in Literature

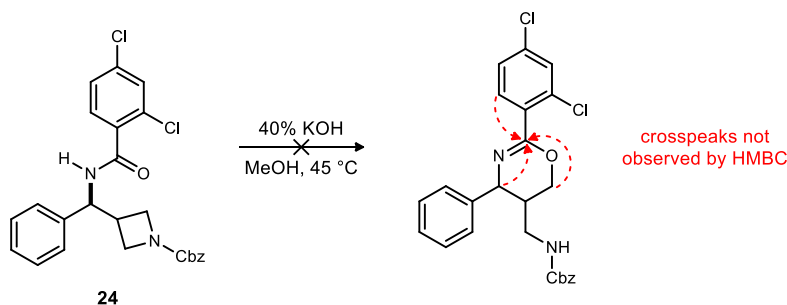


The second product isolated from this reaction, compound **27** (16% yield), also showed azetidine to azetidine isomerization. Unlike methyl ester **26** however, the Cbz group was still intact

(Scheme 9). This isomerization was once again supported by HMBC (600 MHz) experimentation (see structure elucidation, Chapter 8).

Examples of azetidine isomerizations are known in literature. Amongst those reported include an aziridine to azetidine isomerization,⁹ as well as an azetidine to pyrrolidine isomerization.¹⁰ One study in particular has shown the isomerization of an azetidine ring to an oxazine ring via ring expansion¹¹ (Scheme 10). A formation of an oxazine ring can be ruled out in our case as HMBC experimentation would result in 3 crosspeaks associated with the imine carbon of the oxazine ring. From the HMBC experimentation conducted, 3 crosspeaks were never observed for any distinct downfield carbon (Scheme 11). Though acquisition of these isomers proved to be an interesting study, the intended route toward the desired GlyT1 target (**1**) was unsuccessful.

Scheme 11. Oxazine Isomer Not Observed by HMBC Experimentation



An alternative route toward the desired GlyT1 inhibitor was initiated by having intermediate **21** undergo hydrogenolysis in order to afford amine **28** via Cbz-cleavage. Treatment of this secondary amine with sulfonyl chloride **29** under basic conditions furnished the desired sulfonamide (**30**) in 56% isolated yield over 2 steps. Subsequent Boc deprotection and acylation with benzoyl chloride **32** afforded the desired GlyT1 target (**1**) in 27% yield over 2 steps (Scheme 12). HPLC analysis verified that the more potent enantiomer was present in high enantioenrichment. This was verified by observation of comparable HPLC retention times according to a patent belonging to Craig W. Lindsley and co-workers.^{8,12} The synthesized target was then submitted to Lindsley and colleagues to determine the potency of this compound. Tests

⁹ Stankovic, S.; Catak, S.; D'hooghe, M.; Goossens, H.; Tehrani, K. A.; Bogaert, P.; Waroquier, M.; Van Speybroeck, V.; De Kimpe, N. *J. Org. Chem.* **2011**, *76*, 2157-2167.

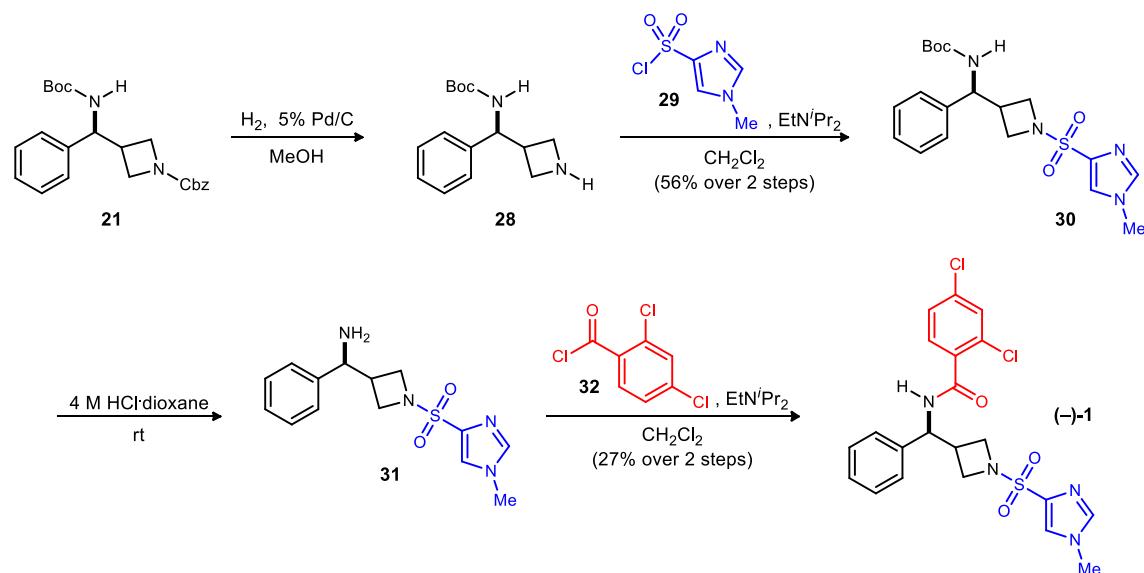
¹⁰ Feula, A.; Male, L.; Fossey, J. S. *Org. Lett.* **2010**, *21*, 5044-5047.

¹¹ Iwakura, Y.; Nabeya, A.; Nishiguchi, T.; Ichikawa, Y. *J. Org. Chem.* **1965**, *30*, 3410-3413.

¹² Observed retention times can be found in the experimental section and compared to the retention times found in U.S. patent document WO 2010/114097 A1 cited above.

indicated good potency as the IC_{50} value for the GlyT1 target was 800 pM. Observations of expected $^1J_{HC}$ couplings through an HSQC (600 MHz) experiment further confirmed the structural assignment (see structure elucidation, Chapter 8).

Scheme 12. Successful Synthetic Route Towards Desired GlyT1 Target (-)-**1**



1.4 Future Work

Future work for the GlyT1 chemistry may include the synthesis of other desired targets (i.e. derivatives) that could possibly show comparable potency to the GlyT1 target that was successfully synthesized. The same key intermediate (**21**) that was used to ultimately synthesize target **1** would also be used in the syntheses of these derivatives. If the syntheses of similar GlyT1 targets are pursued, it is likely that these targets could be successfully synthesized with little or no obstruction as the only major change would be the installation of different acyl groups onto scaffold **21**.

Chapter 2. PBAM-Catalyzed Additions of Nitromethane into Ketimine Centers – Part I: Sulfonyl Ketimines

2.1 Background

The p53 gene is one of the most intensely investigated tumor-suppressor proteins to date. This gene, a transcription factor,¹³ is widely considered the guardian of cell division and plays a critical role in cell cycle control and apoptosis (programmed cell death). Extensive studies have shown that p53 is the most frequently mutated gene in all forms of human cancer.¹⁴ Hollstein and co-workers have reported that a p53 gene mutation is present among cancers of the colon, lung, esophagus, breast, liver, brain, reticuloendothelial tissues, and hemopoietic tissues.¹⁵ Needless to say, it is of vast importance to investigate methods of regulating the mutation of the p53 protein.

MDM2 is a protein that prevents apoptosis of cancer cells by negatively regulating the transcription factor p53.¹⁶ The MDM2 gene can be classified as a cellular proto-oncogene that is amplified in approximately 7% of all human cancers. Over-expression of the MDM2 protein typically occurs by enhanced transcription or translation, and when this proto-oncogene is combined with a p53 mutation, the prognosis can become much more severe.¹⁷ This p53-MDM2 protein–protein interaction arises when MDM2 binds directly to the p53 transactivation domain and targets p53 for proteasomal degradation.¹⁸ Inhibition of this protein–protein interaction can reactivate p53 and be considered as a promising approach to cancer therapy. Furthermore, small molecules could possibly serve as motifs that can sufficiently disrupt the MDM2-p53 interaction.

The Nutlins (short for Nutley inhibitors), which were identified by Vassilev and co-workers, are a class of *cis*-imidazoline compounds that can effectively disrupt the p53-MDM2 protein-protein interaction with median inhibitory concentration values in the 100 to 300 nM range.¹⁹ The development of these Nutlin compounds serves as the first potent and selective small

¹³ Levine, A. J. *Cell* **1997**, *88*, 323-331.

¹⁴ Jaiswal, P. K.; Goel, A.; Mittal, R. D. *BioSci. Trends* **2011**, *5*, 205-210.

¹⁵ Hollstein, M.; Sidransky, D.; Vogelstein, B.; Harris, C. *Science* **1991**, *253*, 49-53.

¹⁶ Doemling, A. US Patent 2011/0313167 A1

¹⁷ Alarcon-Vargas, D.; Ronai, Z. *Carcinogenesis* **2002**, *23*, 541-547.

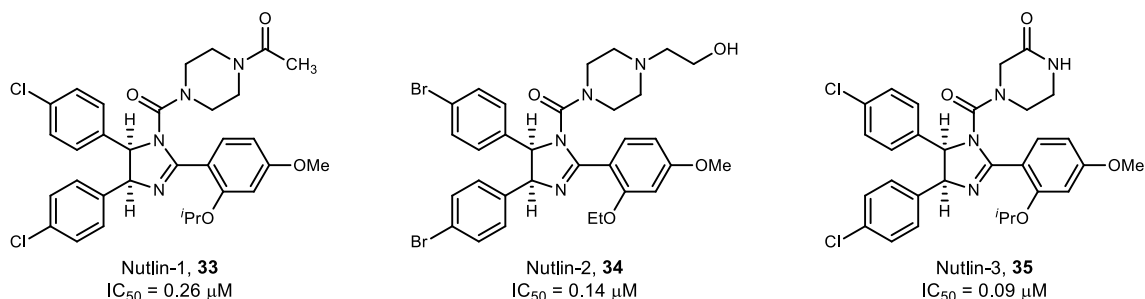
¹⁸ Baek, S.; Kutchukian, P. S.; Verdine, G. L.; Huber, R.; Holak, T. A.; Lee, K. W.; Popowicz, G. M. *J. Am. Chem. Soc.* **2012**, *134*, 103-106.

¹⁹ Vassilev, L. T.; Vu, B. T.; Graves, B.; Carvajal, D.; Podlaski, F.; Filipovic, Z.; Kong, N.; Kammlott, U.; Lukacs, C.; Klein, C.; Fotouhi, N.; Liu, E. A. *Science* **2004**, *303*, 844-848.

molecule inhibitors of the p53-MDM2 interaction. More specifically, the Nutlins selectively activate the p53 pathway in cells only with wild type but not mutant p53.²⁰

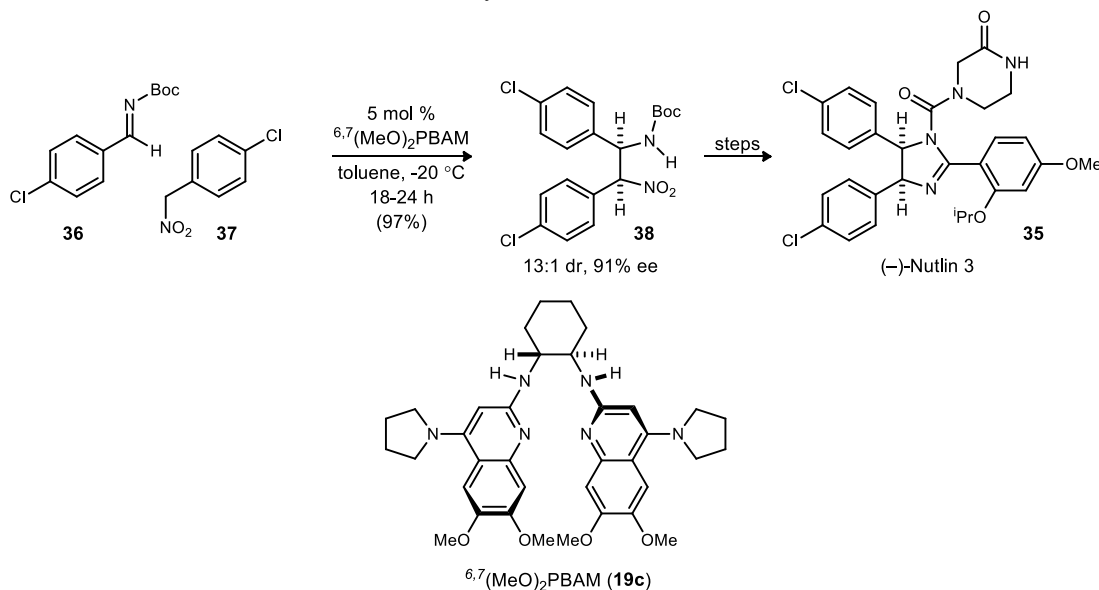
When examining the structures of the three featured Nutlin compounds (**33-35**), various similarities can be seen (Figure 4). Each imidazoline ring core possesses a piperazine-derived urea functionality at the 1-position along with an alkoxy-substituted aromatic ring at the 2-position. Additionally, these potent Nutlins possess halogenated aromatic rings at the 4- and 5-positions of the imidazoline as well.

Figure 4. Structures of Nutlin Compounds **33-35**



Vassilev and colleagues determined that Nutlin-3 was the most potent inhibitor of the p53-MDM2 interaction. They also concluded that one enantiomer was approximately 150 times more potent than its antipode. Additional studies have shown that the more potent enantiomer, (-)-Nutlin-3 (**35**), has been used as a small molecule probe of cell biology and continues to be

Scheme 13. Aza-Henry Addition en Route to (-)-Nutlin-3

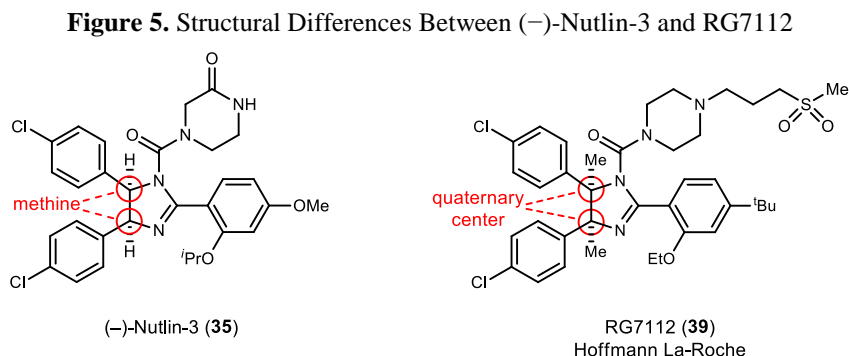


²⁰ Carvajal, D.; Tover, C.; Yang, H.; Vu, B. T.; Heimbrosk, D. C.; Vassilev, L. T. *Cancer Res.* **2005**, *65*, 1918-1924.

developed as a chemotherapeutic.²¹ Hoffmann-La Roche has continued extensive development of this potential anticancer compound, with RG7112 entering clinical trials in 2011.

At Vanderbilt University, an efficient asymmetric synthesis of (-)-Nutlin-3 was developed.²¹ The framework of this synthesis was established upon the formation of a key *cis*-stilbene diamine backbone. This diamine was prepared following a PBAM-catalyzed aza-Henry addition between aryl nitroalkane **37** and aryl imine **36**.^{6,7} (MeO)₂PBAM (**19c**) proved to be the optimal organocatalyst for this system as adduct **38** was afforded in near-quantitative yield with high levels of enantio- and diastereoselection (Scheme 13). The masked *cis*-stilbene diamine was readily converted to (-)-Nutlin-3 through a short synthetic sequence.

Other Nutlin analogs are potent inhibitors of p53-MDM2. RG7112 (**39**) is a dimethyl *cis*-imidazoline Nultin derivative that has been successfully synthesized and is currently being developed by Hoffmann-La Roche. Like Nutlin-3, this compound is a selective inhibitor of p53-MDM2 binding and frees p53 from negative control, activating the p53 pathway in cancer cells leading to cell cycle arrest and apoptosis.²² The enantioselective synthesis of RG7112 is of considerable interest as this molecule has shown promising results in early phases of trials in cancer patients.²³



Structural comparisons can be made between RG7112 and (-)-Nutlin-3 (Figure 5). Both molecules possess an imidazoline ring core with a urea functionality at the 1-position as well as aromatic substituents at the 2-, 4-, and 5-positions. The key difference between these two compounds, however, lies at the 4- and 5-positions of the imidazoline. RG7112 possesses methylated quaternary centers at these two positions while the same positions in Nutlin-3 are

²¹ Davis, T. A.; Johnston, J. N. *Chem. Sci.* **2011**, 2, 1076-1079.

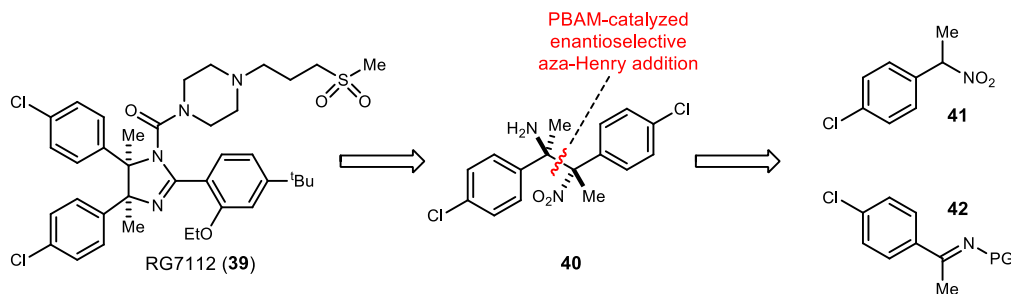
²² Beryozkina, A. *et al. J Clin. Oncol.* 29: **2011** (suppl; abstr 3039) .

²³ Millard, M.; Pathania, D.; Grande, F.; Xu, S.; Neamati, N. *Curr. Pharm. Design* **2011**, 17, 536-559.

methines. The presence of these quaternary centers in RG7112 (**39**) will ultimately change the dynamic as to how this target will be synthesized.

As previously shown, the backbone of the imidazoline entity of Nutlin-3 was readily developed through the PBAM-catalyzed enantioselective aza-Henry addition of a phenyl nitroalkane donor into a Boc-protected aldimine (Scheme 13). Yet as for RG7112, the development of the corresponding dimethyl *cis*-diamine backbone is more challenging. First, the use of a secondary aryl nitroalkane nucleophile is necessary. While secondary nitroalkane donors exhibited considerable success in the GlyT1 chemistry (Chapter 1), their effectiveness has been limited to additions into aldimine centers. The greater challenge of developing the desired backbone, however, is through a ketimine electrophile. While additions into aldimines can be readily achieved, additions into ketimines are more difficult since there is a greater degree of steric bulk about the electrophilic center. The increased sterics can alternate reactivity. Another known problem when handling ketimines is tautomerization into their more stable enamine form. Therefore, the use of a stable ketimine is a necessity as it allows for the possibility of achieving high-yielding aza-Henry additions as a result of minimal tautomerization. Despite these challenges, it is plausible that the dimethyl *cis*-diamine intermediate (**40**) of RG7112 can be acquired through a PBAM-catalyzed aza-Henry addition of a secondary aryl nitroalkane (**41**) into a methyl-derived ketimine (**42**) upon efficient optimization (Scheme 14).

Scheme 14. Retrosynthetic Analysis of RG7112



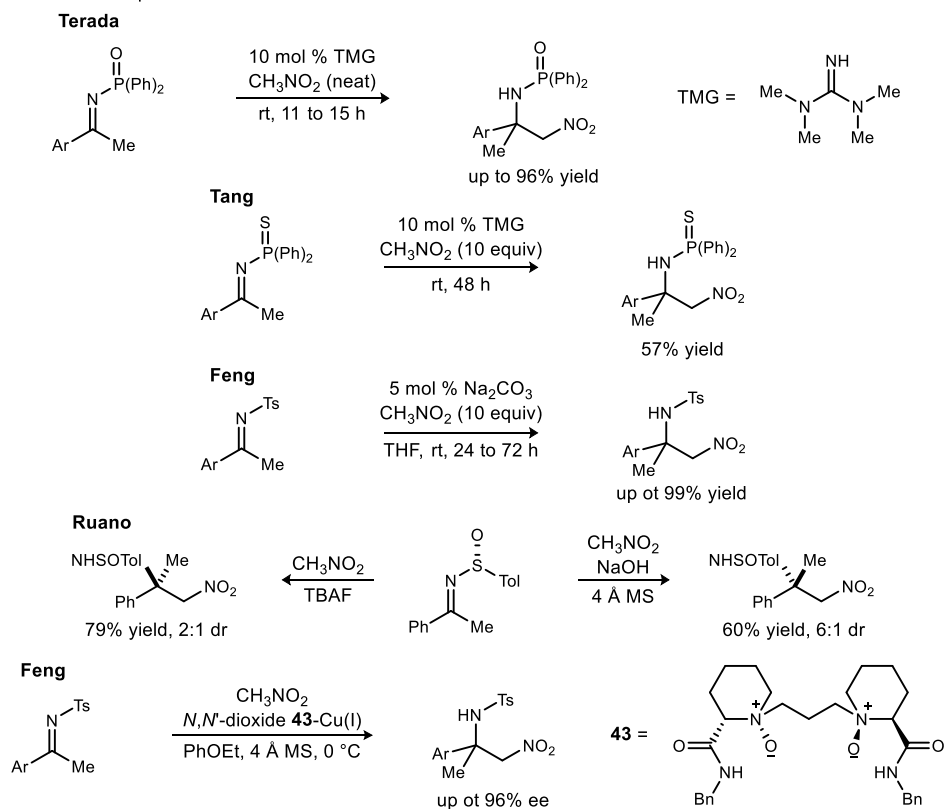
Before applying aryl nitroalkane **41** as the nucleophile, nitromethane was to be used in order to examine the feasibility of ketimine additions. A variety of aza-Henry additions of nitromethane into ketimine centers have been previously reported in literature (Scheme 15). Terada and colleagues demonstrated that simple organic bases, such as 1,1,3,3-tetramethylguanidine (TMG), can facilitate the addition of nitromethane into *N*-diphenylphosphinoyl ketimines.²⁴ TMG

²⁴ Pahadi, N. K.; Ube, H.; Terada, M. *Tetrahedron Lett.* **2007**, *48*, 8700-8703.

can also promote the addition of nitromethane into *N*-thiophosphoryl ketimine centers as described by Tang.²⁵ Despite these successes, these aza-Henry additions were not catalyzed solely by organic bases. Feng illustrated that inorganic bases, such as sodium carbonate, allow for high-yielding additions into tosyl-protected ketimines.²⁶ Asymmetric additions of nitromethane into ketimine centers were also present in literature. Ruano has shown that nitromethane can be incorporated into *N*-sulfinyl ketimines in a diastereoselective manner when catalyzed by tetra-*n*-butylammonium fluoride (TBAF) or sodium hydroxide.²⁷ In this same work, Ruano determined that the direction of diastereoselectivity was dependent upon which base was being used. Highly enantioselective additions into ketimine centers were reported when Feng and colleagues used a chiral *N,N'*-dioxide-copper(I) complex (**43**) as the catalyst.²⁸ Here, they were able to add nitromethane into tosyl ketimines in high yield and up to 96% ee.

Scheme 15. Examples of Nitromethane Additions into Ketimine Centers

selected examples:



²⁵ Hu, K.; Wang, C.; Ma, X.; Wang, Y.; Zhou, Z.; Tang, C. *Tetrahedron Asymmetr.* **2009**, *20*, 2178-2184.

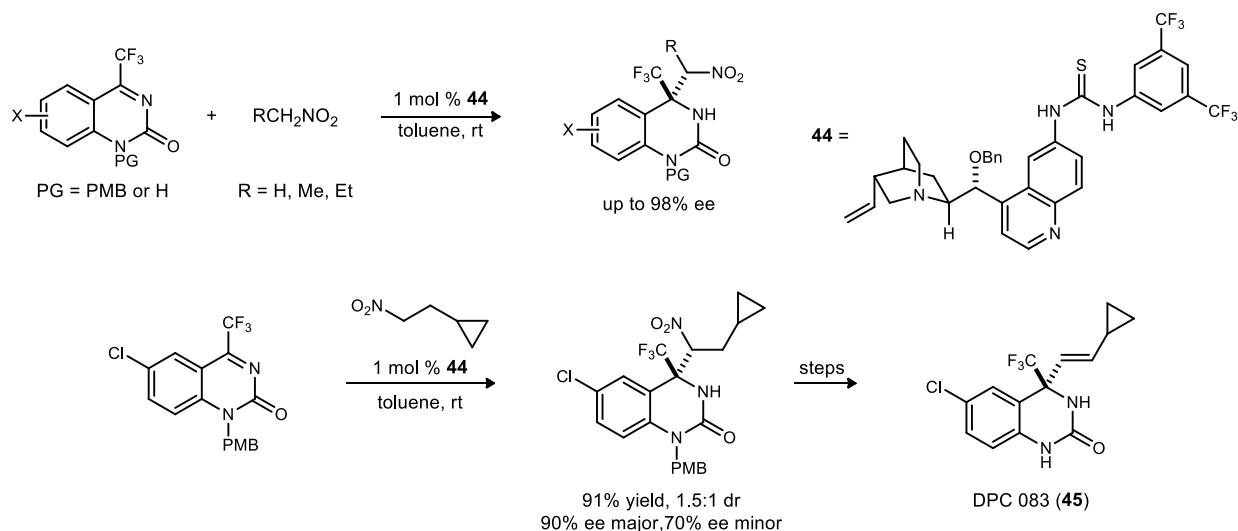
²⁶ Wang, L.; Tan, C.; Liu, X.; Feng, X. *Synlett* **2008**, *13*, 2075.

²⁷ Ruano, J. L. G.; Topp, M.; Lopez-Cantarero, J.; Aleman, J.; Remuinan, M. J.; Cid, M. B. *Org. Lett.* **2005**, *7*, 4407-4410.

²⁸ Tan, C.; Liu, X.; Wang, L.; Wang, J.; Feng, X. *Org. Lett.* **2008**, *10*, 5305-5308.

To the best of our knowledge, there is only one known example of highly enantioselective organocatalyzed aza-Henry additions into ketimines. Wang and colleagues use a simple quinine thiourea motif (**44**) to catalyze the addition of nitromethane as well as nitroethane and 1-nitropropane into trifluoromethyl quinazolinone centers.²⁹ The corresponding dihydroquinazolinones are furnished in high yields and with excellent enantioselection (up to 98% ee). This type of aza-Henry addition is then used as a key step in the asymmetric preparation of anti-HIV drug DPC 083 (**45**) (Scheme 16).

Scheme 16. aza-Henry Additions into Quinazolinones en Route to DPC 083 by Wang



Our goal was then to develop highly enantioselective aza-Henry additions of primary, secondary, and tertiary nucleophiles into ketimine centers via the use of our Brønsted basic Pyrrolidine Bis(AMidine) [PBAM] organocatalysts. If these types of aza-Henry additions are readily achieved, this will lead to a much broader scope of adducts and will facilitate the ultimate goal to synthesize RG7112.

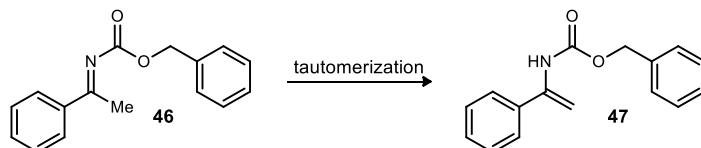
2.2 Synthesis of Sulfinyl and Sulfonyl Ketimines and Examination of Their Reactivity

Initial attempts to prepare an aryl alkyl ketimine proved to be challenging. Acquisition of a TMS-protected ketimine was of particular interest due to the easy manipulation of the silyl group. Unfortunately, multiple attempts toward synthesizing a ketimine of this type were fruitless. Despite these failures, a Cbz-protected ketimine (**46**) was successfully synthesized via literature

²⁹ Xie, H.; Zhang, Y.; Zhang, S.; Chen, X.; Wang, W. *Angew. Chem. Int. Ed.* **2011**, *50*, 11773-11776.

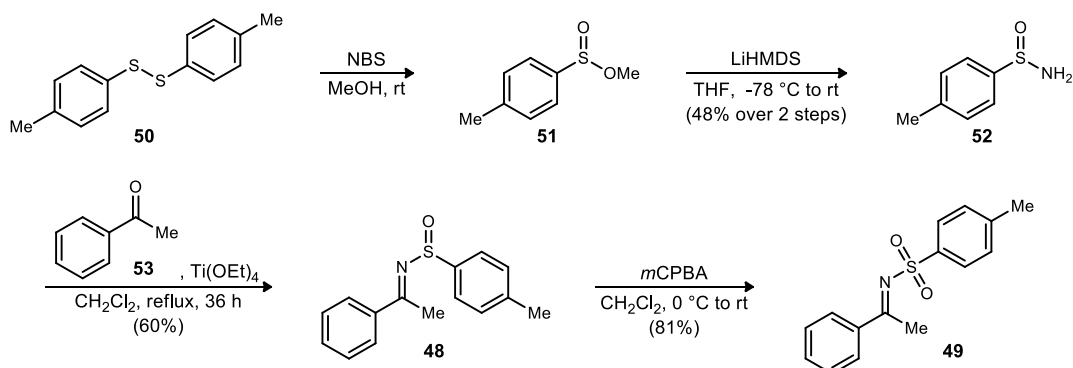
procedure³⁰ in high yields and ketimine to enamine ratios (Figure 6). Attempts toward successfully installing nucleophiles as simple as nitromethane into this specific ketimine via PBAM-catalyzed aza-Henry reactions were unsuccessful as results indicated either tautomerization or hydrolysis. From these findings, it was evident that other ketimines had to be made in order to get a sense of reactivity for these aza-Henry additions.

Figure 6. Structure of Cbz-Ketimine **46** and Tautomerization to its Corresponding Enamine **47**



Two ketimines that were of interest included sulfinyl ketimine **48** and tosyl ketimine **49**. These ketimines, which exhibit a great degree of stability, could be readily synthesized according to the literature protocols of Ruano.^{31,32} Commercially available *p*-tolyl disulfide **50** was subjected to *N*-bromosuccinimide in the presence of methanol to afford sulfinate **51** quantitatively. Treatment of sulfinate **51** with lithium hexamethyldisilazide (LHMDS) gave sulfinamide **52** (48% over 2 steps), which was then condensed with acetophenone (**53**) furnishing sulfinyl ketimine **48** in moderate yield (60%). Subsequent oxidation of **48** with MCPBA afforded the corresponding tosyl ketimine **49** in good yield (81%) (Scheme 17).

Scheme 17. Synthesis of Sulfinyl Ketimine **48** and Tosyl Ketimine **49**



In order to gain a sense of reactivity for aza-Henry additions into ketimines, literature findings were repeated. As previously mentioned, Ruano and Terada have demonstrated successful nitromethane additions via the use of simple bases such as TBAF, TMG, and sodium hydroxide

³⁰ Ahman, J. B.; Boulton, L. T. Patent WO 2006064340

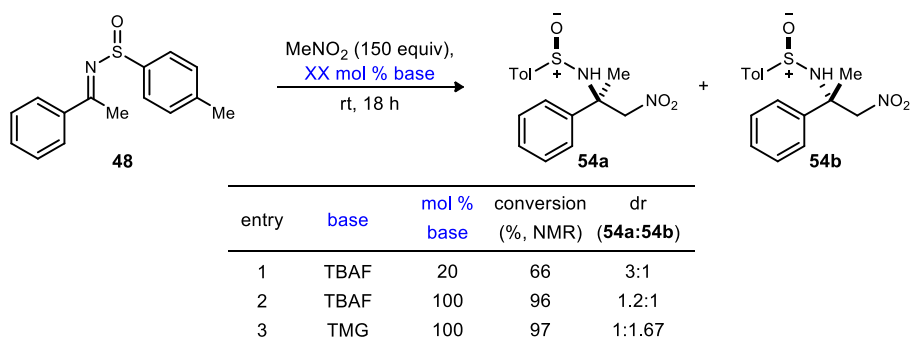
³¹ Ruano, J. L. C.; Aleman, J.; Cid, M. B.; Parra, A. *Org. Lett.* **2005**, *84*, 179-182.

³² Ruano, J. L. C.; Aleman, J.; Parra, A.; Cid, M. B. *Org. Synth.* **2007**, *84*, 129-138.

(NaOH).^{24,27} Additions into sulfinyl ketimine **48**, via Ruano's methods, were repeated using these three bases as catalysts.

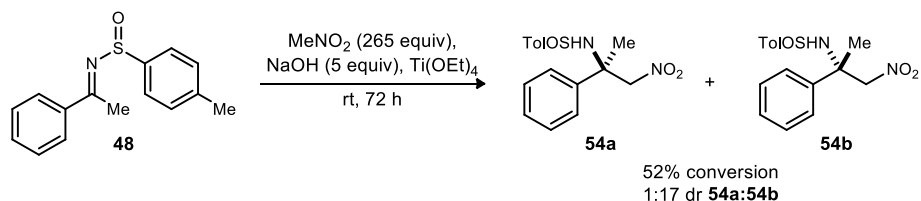
Studies were initiated when sulfinyl ketimine **48** was treated with 20 mol% of TBAF in the presence of neat nitromethane. After an 18 hour reaction period, 66% conversion to adducts **54a** and **54b** was seen by proton NMR in a 3:1 dr (Table 1, entry 1). Raising the amount of TBAF to a full equivalent resulted in 96% conversion to **54a** and **54b** with minimal diastereoselectivity (entry 2). When a full equivalent of TMG was used as the catalyst in the presence of neat nitromethane, 97% conversion to the desired adducts was seen by crude NMR (entry 3). Once again, low degrees of diastereoselection were observed.

Table 1. Nitromethane Additions into Ketimine **48** with TBAF and TMG



When NaOH was used as the catalyst in the presence of neat nitromethane, 4 Å molecular sieves, and a Lewis acid, 52% conversion to adducts **54a** and **54b** was seen in a 1:17 dr (Scheme 18). These findings, which were consistent with Ruano's, show that a Lewis acid-mediated addition with NaOH not only reverses the direction of diastereoselectivity, it also affords the desired products in a much higher degree of selection relative to TBAF or TMG.

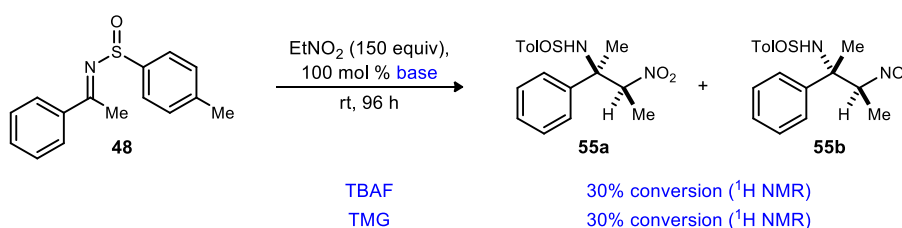
Scheme 18. Nitromethane Additions into Ketimine **48** with NaOH



Ketimine additions with secondary nucleophiles proved to be problematic. Upon treating ketimine **48** with neat nitroethane in the presence of TBAF or TMG, low conversion (30%) was observed over prolonged reaction times (Scheme 19). The aza-Henry adducts **55a** and **55b** were

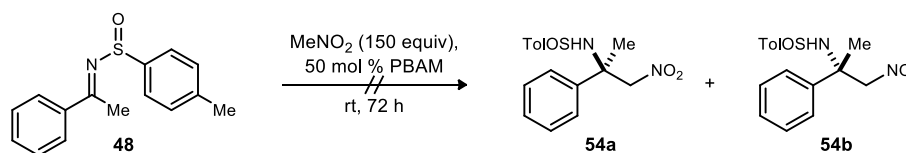
not isolated, nor were their diastereomeric ratios determined, due to low conversion and ambiguities in the crude NMR spectrum. The lack of reactivity may be due to the fact that nitroethane is more sterically hindered relative to nitromethane. This will result in a more congested system about the ketimine center upon attempted addition.

Scheme 19. Attempted Nitroethane Additions into Ketimine **48** with TBAF and TMG



After getting a sense of reactivity with achiral bases, additions of nitromethane into sulfinyl ketimine **48** were attempted with our chiral PBAM organocatalyst. Upon subjecting 50 mol% of PBAM free base (**19**) to 150 equivalents of nitromethane in the presence of THF (co-solvent), no sign of addition could be detected (Scheme 20). This could be due to the fact that PBAM may not be Brønsted basic enough to promote the nucleophilicity needed for nitromethane to effectively add into a sulfinyl ketimine center. Additionally, the catalyst binding mode with this bulkier electrophile may not be ideal as high degrees of congestion may be prevalent, thus inhibiting the desired aza-Henry addition.

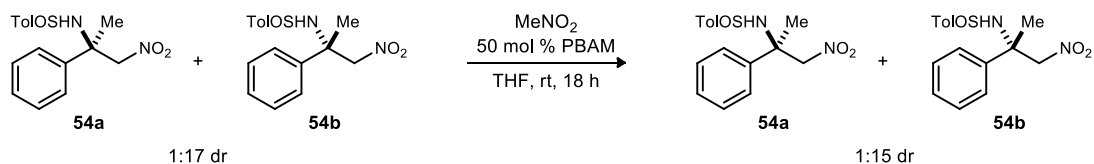
Scheme 20. Attempted Nitromethane Addition into Ketimine **48** with PBAM



As previously seen in Scheme 18, high dr adduct (17:1) was acquired when using NaOH with a Lewis acid. In order to see if PBAM promotes addition into sulfinyl ketimine **48**, an equilibrium experiment was conducted. The high dr adduct was treated with PBAM over the course of 18 hours. If starting material or a significant drop in dr was observed, it can be implied that PBAM is promoting this addition and that the equilibrium is favoring the side of the reactants. Unfortunately, when running this experiment, no drop in dr was seen reaffirming that PBAM is not making nitromethane nucleophilic enough to promote addition into the ketimine (Scheme 21).

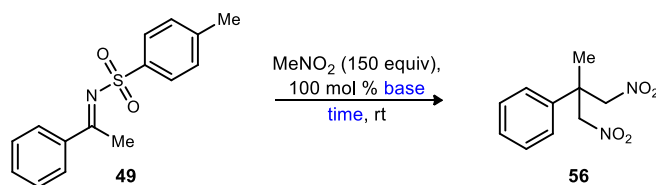
Studies were continued by examining aza-Henry additions into tosyl ketimine **49**. With a higher oxidation state, it was believed that this ketimine would be more reactive relative to sulfinyl

Scheme 21. Equilibrium Experiment Conducted with PBAM



ketimine **48**. This was tested by subjecting the tosyl ketimine to neat nitromethane in the presence of TBAF and TMG. After a 96-hour reaction time, proton NMR indicated complete conversion of starting material, as well as formation of double adduct **56** in both cases (Table 2, entries 1 and 2). When reaction times were decreased to 18 hours, the same results were obtained (entries 3 and 4). Acquisition of double adducts when using tosyl ketimine **49** versus acquisition of single adducts with sulfinyl ketimine **48** clearly indicates that the tosyl ketimine is a more reactive species as expected.

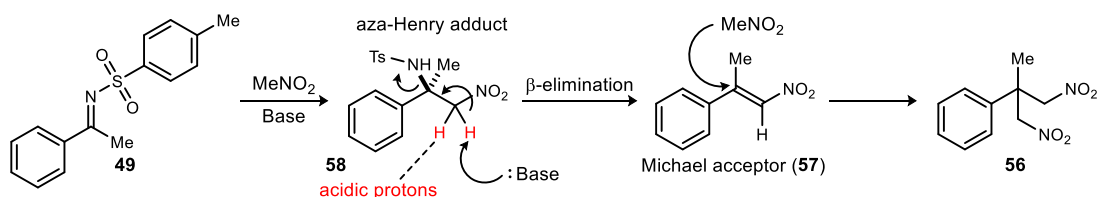
Table 2. Nitromethane Additions into a Tosyl Ketimine to Yield Double Adduct **56**



entry	base	time (h)	conversion (% , NMR)
1	TBAF	96	100
2	TMG	96	100
3	TBAF	18	100
4	TMG	18	100

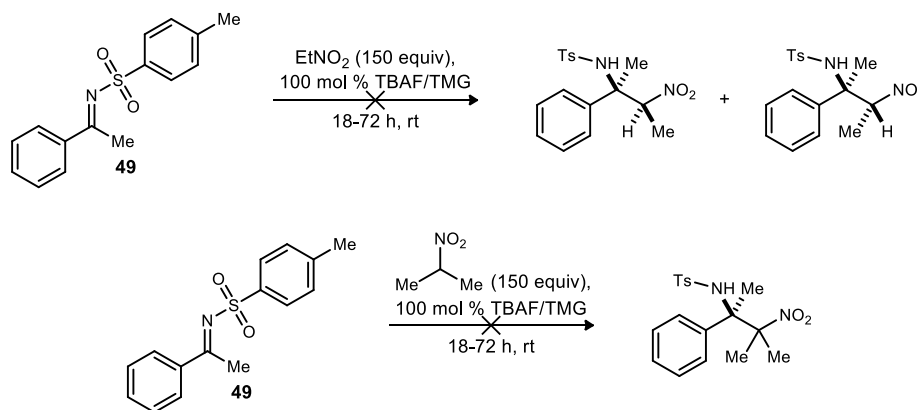
The formation of the double adduct is believed to arise from a Michael acceptor precursor (**57**). When nitromethane adds into the tosyl ketimine center, the desired aza-Henry adduct (**58**) is formed *in situ*. Present in the adduct, however, is a good leaving group in the tosyl amide. The two methylene protons alpha to the tosyl group are considerably acidic and can be readily deprotonated by base to cause β -elimination of the tosyl group resulting in Michael acceptor **57**. This electrophilic acceptor can receive a second equivalent of nitromethane, resulting in the observed double adduct (Scheme 22).

Scheme 22. Formation of Double Adduct **56** via Michael Acceptor **57**



Due to the high reactivity of tosyl ketimine **49**, more hindered nucleophiles were applied in order to determine if sufficient addition could be achieved (Scheme 23). When tosyl ketimine **49** was treated with neat nitroethane in the presence of TBAF and TMG, no adduct could be detected after prolonged reaction times. aza-Henry reactions with a tertiary 2-nitropropane nucleophile were also attempted with the same bases. Once again, neither case yielded the desired adduct.

Scheme 23. Attempted Additions of Nitroethane and 1-Nitropropane into Ketimine **49**



Despite the lack of reactivity with more hindered nitroalkanes, tosyl ketimine **49** appears to be the most reactive ketimine we have encountered up to this point when it comes to additions of nitromethane. Therefore, this ketimine was the electrophile of choice when attempting PBAM-catalyzed aza-Henry additions.

2.3 PBAM-Catalyzed aza-Henry Additions into Sulfonyl Ketimine Centers

With a reactive tosyl ketimine (**49**) in hand, PBAM-catalyzed aza-Henry additions of nitromethane could be conducted. Studies were initiated when ketimine **49** was treated with PBAM free base (**19**) in the presence of neat nitromethane at room temperature. After a three day reaction period, the desired aza-Henry adduct (**58**) was acquired in 65% isolated yield but was determined to be racemic by HPLC analysis (Table 3, entry 1). Using PBAM•HOTf (**19**•HOTf) as the catalyst under the same conditions, a slight increase in yield was observed as well as what appeared to be a low level of enantioselection (entry 2). PBAM•HNTf₂ (**19**•HNTf₂) proved to be a more effective catalyst as adduct **58** was furnished in 78% yield and 13% ee (entry 3). Yet when the more Brønsted basic ^δ(MeO)PBAM (**19d**) motif was applied as the catalyst, only double adduct (**56**) was observed (entry 4). This gives a clear indication that ^δ(MeO)PBAM is the most reactive organocatalyst thus far due to increased Brønsted basicity from electron-donating methoxy

substituents on the quinoline rings. Because of its high reactivity, this catalyst was carried into further studies.

Table 3. Catalyst Screen for Nitromethane Additions into Tosyl Ketimine **49**

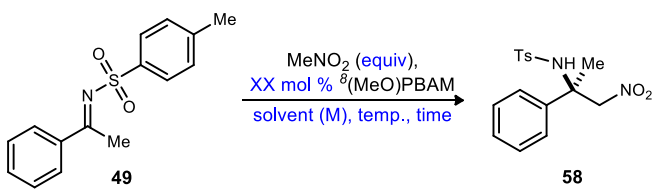
entry	catalyst	conversion (%, NMR)	yield (%)	ee (%)
1	PBAM	77	65	0
2	PBAM•HOTf	88	71	6
3	PBAM•HNTf ₂	89	78	13
4	^δ (MeO)PBAM	100	adduct 56	N/A

R = H, PBAM (**19**)
R = OMe, ^δ(MeO)PBAM (**19d**)

With this highly reactive ^δ(MeO)PBAM catalyst, studies were continued to examine reactivity and possibly develop high levels of enantioselection. As previously shown, double adduct was observed upon treating ketimine **49** with 50 mol% of ^δ(MeO)PBAM in neat nitromethane at ambient temperature over 72 hours (Table 3, entry 4). This indicates that reaction conditions need to be modified in order to reduce the chance of β -elimination (Scheme 22) and promote the possibility of acquiring the desired single adduct (**58**). The most direct way of achieving this would be through reducing the catalyst loading and shortening reaction times. When the catalyst loading was reduced to 20 mol% and the reaction time was shortened to 13 hours, the desired aza-Henry adduct (**58**) was acquired in 47% isolated yield but with no enantioselection (Table 4, entry 1). Further decreasing the reaction time to 3.5 hours resulted in slightly enhanced yield, but no degree of enantioselection could be detected (entry 2). Significantly reducing the quantity of nucleophile to 5 and 2 equivalents in the presence of catalyst **19d** at room temperature resulted in 25% and 29% isolated yields of the adduct as racemates (entries 3 and 4). Temperature studies also proved to be fruitless as lowering the temperature to -20 °C afforded the product in 17% yield and 2% ee (entry 5). When the temperature was lowered even further to -78 °C, reactivity was completely inhibited even after prolonged reaction times (entries 6 and 7). Changing the catalyst loading to 10 mol% did not show much improvement as adduct **58** was furnished in 22% yield and 7% ee over the course of 24 hours (entry 8). Lastly, the use of more dilute conditions slightly diminished yield and selection (entry 9). These studies indicate that ^δ(MeO)PBAM was

not the most ideal catalyst for this reaction system as low to moderate yields of adduct were acquired with very little degree of enantioselectivity.

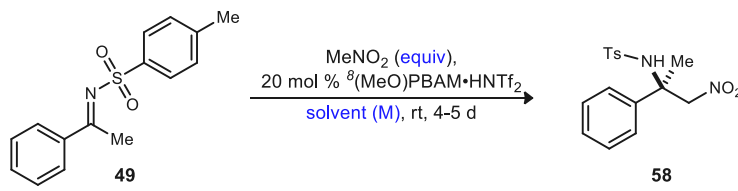
Table 4. Reactivity Study with δ (MeO)PBAM



entry	MeNO ₂ equiv	mol % catalyst	solvent	M	temp (°C)	time (h)	yield (%)	ee (%)
1	150	20	--	--	rt	13	47	0
2	150	20	--	--	rt	3.5	56	0
3	5	20	toluene	1	rt	14-24	25	0
4	2	20	toluene	1	rt	14-24	29	2
5	2	20	toluene	1	-20	14-24	17	2
6	2	20	toluene	1	-78	14-24	N/A	N/A
7	2	20	toluene	1	-78	168	N/A	N/A
8	2	10	toluene	1	rt	14-24	22	7
9	2	10	toluene	0.5	rt	14-24	16	3

The triflimide salt of δ (MeO)PBAM (**19e**•HNTf₂) was briefly examined to see if introduction of a counterion can enhance enantioselection. Upon subjecting 20 mol% of δ (MeO)PBAM•HNTf₂ to ketimine **49** in the presence of neat nitromethane at room temperature, trace amounts of product were detected by NMR after an extensive reaction period (Table 5, entry 1). When the amount of nucleophile was reduced to 20 equivalents, adduct **58** was acquired in 33% isolated yield. Unfortunately, minimal enantioselection was observed once again (entry 2). This indicates that introduction of a salt to the Brønsted basic δ (MeO)PBAM catalyst does not have a significant effect in regards to enantioenrichment.

Table 5. Reactivity Study with δ (MeO)PBAM•HNTf₂



entry	MeNO ₂ equiv	solvent	M	yield (%)	ee (%)
1	150	--	--	N/A	N/A
2	20	toluene	1	33	4

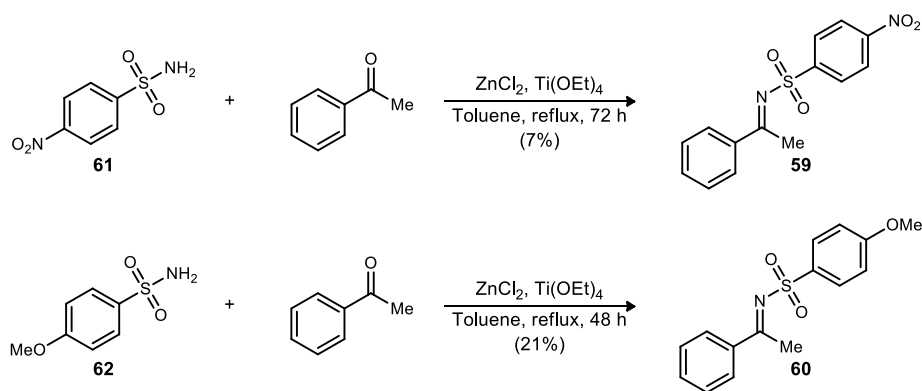
The low to moderate yields of adduct acquired during the course of these runs with δ (MeO)PBAM (**19d**) and δ (MeO)PBAM•HNTf₂ (**19d**•HNTf₂) is mainly owed to the elimination

of the tosyl group (Scheme 22). This, of course, was due to the high Brønsted basicity of this catalyst relative to other PBAM catalysts. Control of reactivity in order to furnish high yields and minimize elimination is an optimization process that must be achieved when using this particular catalyst.

Although it appears that controlling the reactivity of this highly reactive δ (MeO)PBAM catalyst is something that needs to be resolved, enhancement of enantioselection is another area of these aza-Henry additions that needs optimization as the highest ee achieved up to this point is 13% ee (Table 3, entry 3). Since counterion control, as well as concentration, temperature, and equivalents modifications did not result in dramatic increase of enantioselection (Table 4, Table 5), efforts shifted toward making ketimines with different electronic properties in order to see if enantioselectivity is influenced by the nature of the substrate.

Two particular ketimines of interest that were made included an electron-withdrawing nosyl ketimine **59** and an electron-donating methoxy-derived ketimine **60**. Simple condensations of nosyl sulfonamide **61** and *para*-methoxyphenyl sulfonamide **62** in the presence of acetophenone and Ti(OEt)₄ furnished ketimines **59** and **60** in 7% and 21% yields respectively (Scheme 24). With these two ketimines in hand, the stage was now set to examine the difference in selectivity between electron-deficient and electron-rich electrophiles.

Scheme 24. Synthesis of Electron-Withdrawing and Electron-Donating Ketimine Species

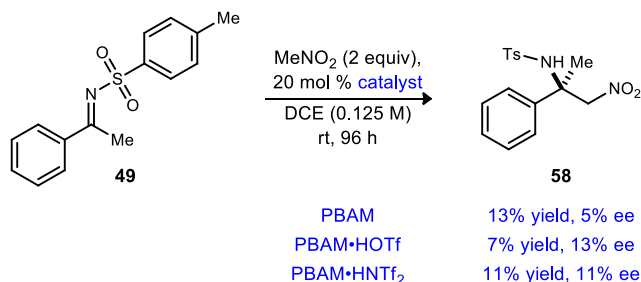


The catalysts to be used in this enantioselective study consisted of PBAM, PBAM•HOTf, and PBAM•HNTf₂. The δ MeOPBAM catalyst could be problematic in this case because of its high reactivity and its ability to readily eliminate, especially with the highly reactive nosyl ketimine. Less reactive catalysts were purposefully chosen in order to minimize elimination so that adduct could be acquired and ee's could be readily determined.

Before additions into more electron-deficient and electron-donating ketimines took place, aza-Henry additions into the tosyl ketimine with only 2 equivalents of nitromethane were conducted. This was to see if using 2 equivalents of nucleophile, versus 150 equivalents (Table 3), would result in a large difference in enantioselection as neat nitromethane may inhibit ideal catalyst binding.

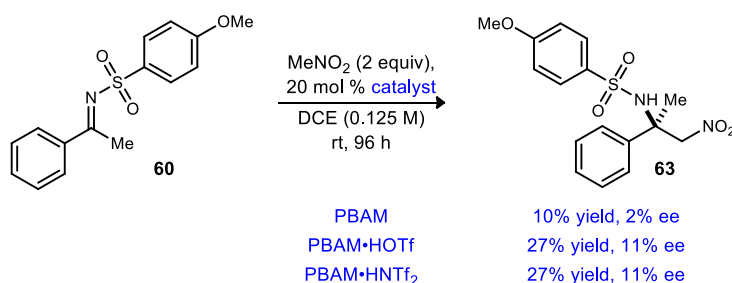
To initiate this study, tosyl ketimine **49** was subjected to 20 mol% of PBAM in the presence of 2 equivalents of nitromethane over 96 hours at room temperature. Upon isolation, aza-Henry adduct **58** was acquired in 13% yield and 5% ee (Scheme 25). PBAM•HOTf, under the same conditions, resulted in slightly diminished yield and slightly enhanced ee. PBAM•HNTf₂ was comparable to PBAM•HOTf as adduct **58** was furnished in 11% yield and 11% ee.

Scheme 25. Aza-Henry Additions into Tosyl Ketimine **49**



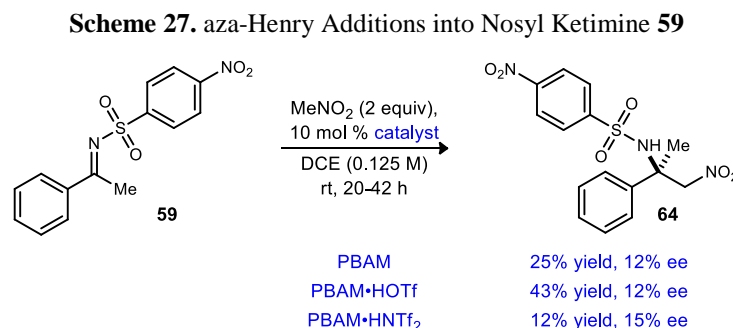
Additions into the less reactive methoxyphenyl ketimine (**60**) were conducted when this electrophile was treated with 20 mol % of PBAM in the presence of 2 equivalents of nitromethane. After 96 hours, aza-Henry adduct **63** was obtained in 10% yield and 2% ee (Scheme 26). PBAM•HOTf and PBAM•HNTf₂ gave identical results as adduct **63** was afforded in 27% yield and 11% ee for both cases.

Scheme 26. Aza-Henry Additions into Methoxyphenyl Ketimine **60**



Additions into the more reactive nosyl ketimine **59** were more challenging since this electron deficient nosyl group is more prone to β -elimination. Thus, extra care had to be taken in order to obtain product so that enantioselectivity could be determined. When treating this nosyl

ketimine with only 10 mol % of PBAM in the presence of 2 equivalents of nitromethane, the desired aza-Henry adduct **64** was obtained in 25% isolated yield and 12% ee after a 24 hour reaction period (Scheme 27). PBAM•HOTf resulted in a minor improvement in yield but no change in ee. Diminished yield but slightly enhanced enantioselectivity was seen with PBAM•HNTf₂ as this catalyst afforded adduct **64** in 12% yield and 15% ee. This was the highest ee observed up to this point.



A variety of conclusions can be drawn from this study. First, enantioselectivity does not appear to be enhanced when using 2 equivalents of the nucleophile versus 150 equivalents. The use of electron-donating substituents on the electrophile does not appear to affect selectivity as the best enantioselectivity achieved with this ketimine was 11% ee. Furthermore, incorporation of an electron-withdrawing moiety on the ketimine electrophile minimally enhances the selectivity of this system as ee values as high as 15% were obtained. Needless to say, altering the electronics of the electrophile at the *para*- position of the aryl ring does not appear to significantly enhance enantioselection.

2.4 Future Work

No promising degrees of enantioselection were seen for this aza-Henry system upon using a variety of PBAM catalysts and changing the electronic nature of the ketimine. Based on this lack of success, efforts now shifted toward the development of a more selective catalyst. Nagasawa and co-workers have developed guanidine-thiourea bifunctional organocatalysts that can facilitate Henry additions,³³ that is the addition of nitro-nucleophiles into aldehydes. It has also been demonstrated that this addition can be done diastereoselectively.³⁴ These catalysts became of considerable interest when Han and colleagues demonstrated that they can be used for the

³³ Sohtome, Y.; Takemura, N.; Iguchi, T.; Hashimoto, Y.; Nagasawa, K. *Synlett* **2006**, *1*, 144-146.

³⁴ Sohtome, Y.; Hashimoto, Y.; Nagasawa, K. *Adv. Synth. Catal.* **2005**, *347*, 1643-1648.

facilitation of aza-Henry addition reactions.³⁵ The combination of these findings along with the findings of Terada in which he used tetramethylguanidine as a base, has prompted us to synthesize guanidine-derived BAM catalysts. These catalysts, when fully developed, can also be applied to aza-Henry reactions into aldimines for comparative studies. It may prove useful to examine their effectiveness in other known aza-Henry systems before applying them to ketimine additions.

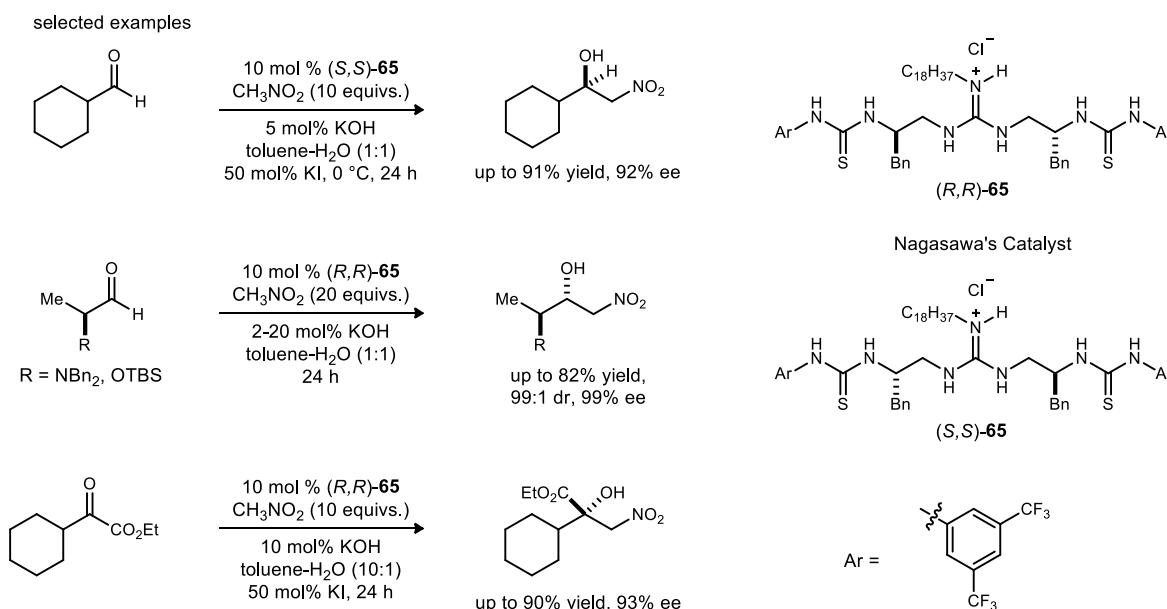
³⁵ Huang, W.; Peng, C.; Guo, L.; Hu, R.; Han, B. *Synlett* **2011**, 20, 2981-2984.

Chapter 3. The Guided Development of Asymmetric Mono(Amidine) Organocatalysts for the Enantioselective Synthesis of Nutlin Analogs

3.1 Background

Previously, PBAM-catalyzed aza-Henry additions into ketimine centers have proven troublesome. After exploring a variety of free-base and protonated versions of symmetric bis(amidine) catalysts for this particular system, no promising degree of enantioselection was achieved, as the highest ee obtained to this point was 15% ee. Various modifications of the ketimine electrophile, including the installation of different protecting groups as well as electronic alterations, were examined in order to improve enantioselection, but to no avail. Therefore, the next course of action to be taken would involve restructuring the current catalysts being used via installation of different functional groups.

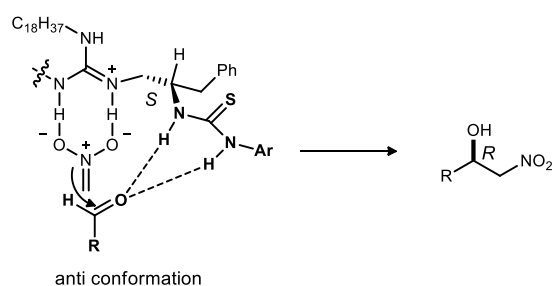
Scheme 28. Examples of Nitromethane Additions into Aldehydes and Esters with Nagasawa's Catalyst (**65**)



After investigating the literature, it was found that organocatalysts bearing guanidine and/or thiourea moieties facilitated the selective addition of nitroalkane nucleophiles into a variety of *sp*²-hybridized centers. More specifically, Nagasawa and colleagues have shown that a guanidine-thiourea bifunctional organocatalyst (**65**) results in the Henry (nitroaldol) addition of nitromethane into aliphatic cyclic aldehydes and branched aliphatic aldehydes with high

enantioselection.³⁶ This guanidine-thiourea catalyst also allows for highly diastereoselective Henry additions into protected α -amino- and α -hydroxy aldehydes as well as α -ketoesters while maintaining high levels of enantioselectivity (Scheme 28).^{37,38} When analyzing the transition states of these reactions with catalyst **65**, it is proposed that the guanidine group coordinates with nitromethane through ionic interactions, while the thiourea group acts as a Brønsted acid and interacts with the aldehyde (or ester), thus lowering the LUMO energy of the carbonyl group (Figure 7). These interactions can then promote the addition of nitromethane in an enantioselective manner.

Figure 7. Proposed Transition State of the Guanidine-Thiourea Catalyzed Henry Reaction



The utility of this bifunctional guanidine-thiourea catalyst backbone was not limited to Henry additions of nitromethane into aldehydes and esters. After slight modifications of the catalyst structure, Nagasawa and colleagues were able to develop bifunctional catalyst **66**, which readily promoted the Mannich-type reaction of aromatic α -amido sulfones with malonates, affording β -amino acid derivatives in high yields and with excellent enantioselectivity.³⁹ Han and co-workers were able to expand on these findings with another derivative of Nagasawa's catalyst. Using guanidine-thiourea motif **67**, they were able to facilitate the aza-Henry (or nitro-Mannich) additions of a wide array of nitroalkanes into *N*-Boc-protected imines, giving the desired 1,2-diamino adducts in sufficient levels of diastereoselection and high degrees of enantioselection (Scheme 29).⁴⁰

³⁶ Sohtome, Y.; Hashimoto, Y.; Nagasawa, K. *Adv. Synth. Catal.* **2005**, *347*, 1643-1648.

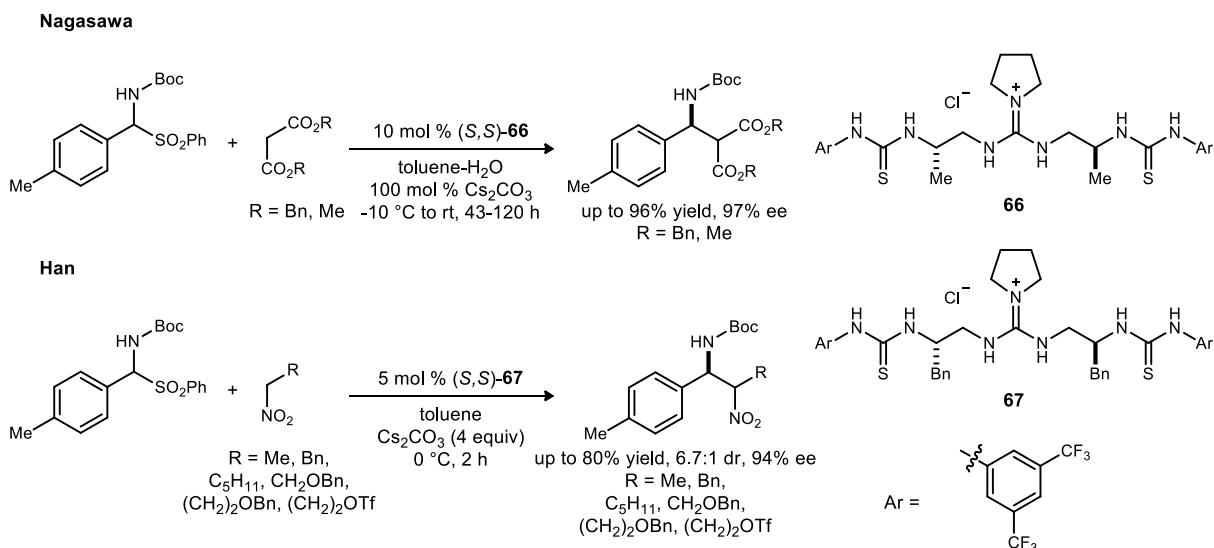
³⁷ Sohtome, Y.; Takemura, N.; Iguchi, T.; Hashimoto, Y.; Nagasawa, K. *Synlett* **2006**, *1*, 144-146.

³⁸ Takada, K.; Takemura, N.; Cho, K.; Sohtome, Y.; Nagasawa, K. *Tetrahedron Lett.* **2008**, *49*, 1623-1626.

³⁹ Takada, K.; Tanaka, S.; Nagasawa, K. *Synlett* **2009**, *10*, 1643-1646.

⁴⁰ Huang, W.; Peng, C.; Guo, L.; Hu, R.; Han, B. *Synlett* **2011**, *20*, 2981-2984.

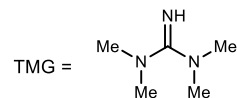
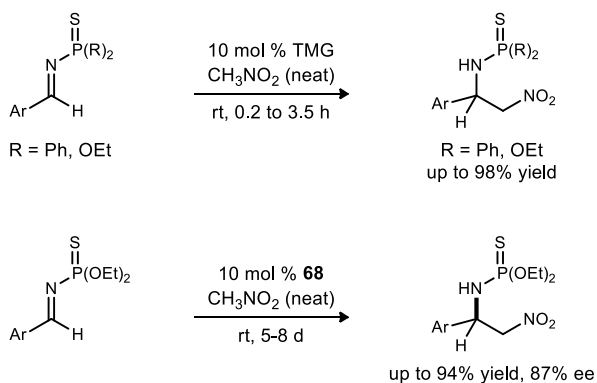
Scheme 29. Examples of Mannich and aza-Henry Reactions with Guanidine-Thiourea Organocatalysts



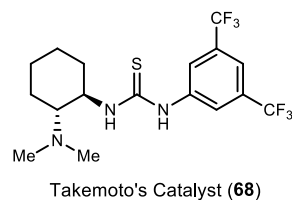
Despite the success with Nagasawa's catalyst backbone, additional studies have shown that a bifunctional guanidine-thiourea system is not entirely necessary in order to achieve aza-Henry additions of nitroalkanes into aldimine or ketimine centers. Instead, catalysts bearing just a thiourea or guanidine entity alone have resulted in considerable success. Tang and colleagues have demonstrated that with commercially available 1,1,3,3-tetramethylguanidine (TMG), the additions of nitromethane into *N*-diethoxythiophosphorylimines and *N*-diphenylthiophosphinoylimines can

Scheme 30. Examples of aza-Henry Additions with Other Guanidine and Thiourea Catalysts

Tang



Terada

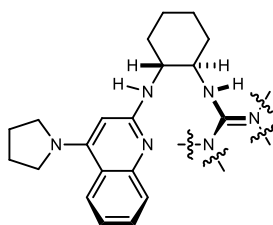


be accomplished in high yields and short reaction times.²⁵ In this same work, they were also able to induce good degrees of stereoselection for the same reaction system using Takemoto's chiral thiourea organocatalyst (**68**). Furthermore, Terada showed that the addition of nitromethane into diphenylphosphinoyl ketimine centers can be achieved in high yields using TMG as the catalyst (Scheme 30).²⁴

3.2 Synthetic Efforts Towards Amidine-Guanidine Asymmetric Catalysts

Based on the success in literature, we sought to restructure our traditional bis(amidine) catalyst framework in such a way that a thiourea or guanidine functionality could be incorporated. Due to the availability of various diimide species and other guanidinating reagents, the synthesis of an asymmetric bifunctional amidine-guanidine organocatalyst was the first priority (Figure 8). It was then necessary to synthesize a free amine intermediate that would readily allow for the installation of various guanidine moieties.

Figure 8. Backbone Structure of Desired Amidine-Guanidine Catalyst

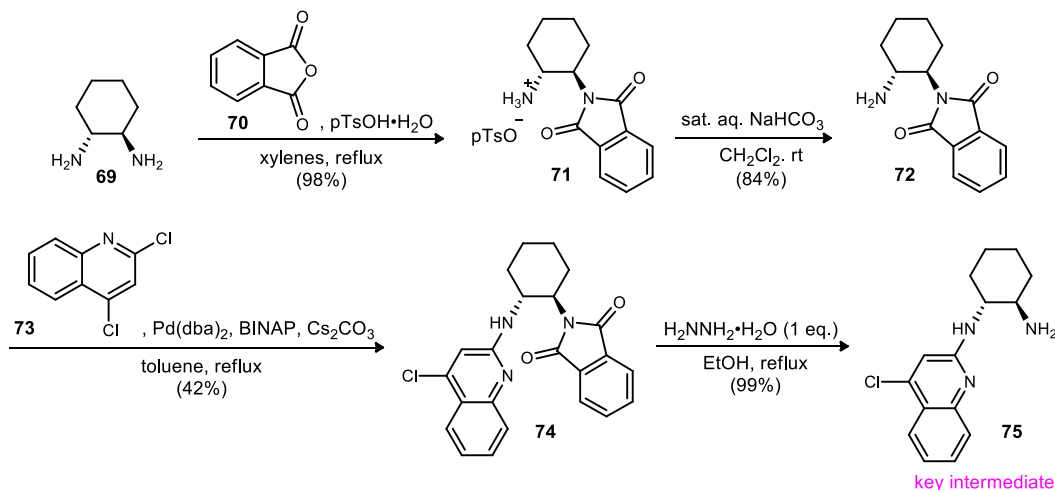


In order to arrive at a key free amine intermediate, it was determined that the amidine portion of the catalyst backbone had to be developed first. This was initiated by treating resolved, enantiopure *R,R*-cyclohexane diamine (**69**) with phthalic anhydride (**70**) in the presence of *para*-toluene sulfonic acid monohydrate according to literature protocol.⁴¹ This resulted in the acid salt of phthalimide **71** in high yield (98%). Aqueous base wash of acid salt **71** would subsequently give the free base of the mono-protected diamine (**72**) in 84% yield. A chloro-substituted quinoline moiety was then installed via a Buchwald-Hartwig amination reaction in which amine **72** was treated with 2,4-dichloroquinoline (**73**) in the presence of cesium carbonate and catalytic amounts of 2,2'-bis(diphenylphosphino)-1,1'-binaphthyl (BINAP) and bis(dibenzylideneacetone)palladium (Pd(dba)₂) in order to furnish amidine **74** in modest yield (42%). Phthalate deprotection with hydrazine monohydrate afforded amidine-amine species **75** in

⁴¹ Kiak, M.; Gawronski, J. *Tetrahedron: Asymmetry* **2003**, *14*, 1559-1563.

99% yield. This amidine-amine, which would serve as the key intermediate, can readily lead to the incorporation of a variety of guanidine derivatives as previously mentioned (Scheme 31).

Scheme 31. Synthesis of Amidine-Amine Intermediate **75**



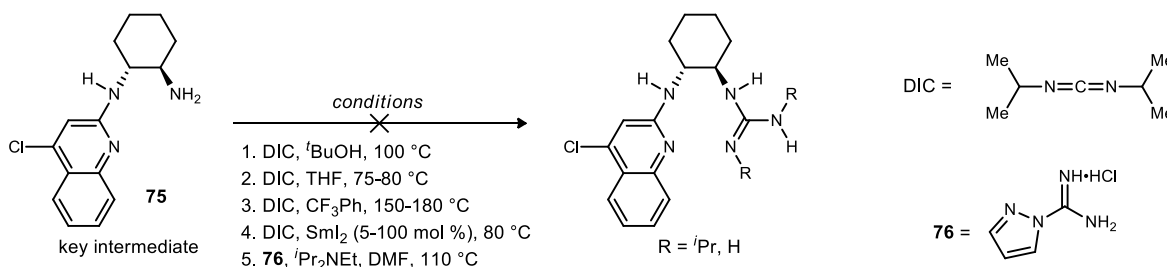
Initial attempts towards the installation of a guanidine entity proved to be fruitless. When key intermediate **75** was subjected to N,N' -diisopropylcarbodiimide under high temperatures in the presence of a variety of solvents, no desired addition product could be isolated. When searching for alternate conditions, it was found that Shen and co-workers were able to add a wide range of aliphatic and aromatic amines into diimide centers in the presence of SmI_2 .^{42,43} In this reaction pathway, it is believed that the samarium species can activate the diimide by forming a $\text{Sm}(\text{III})$ complex, which would promote the insertion of an amine, ultimately resulting in the formation of a desired guanidine. Unfortunately, when applying this SmI_2 approach to our own reaction system, no desired guanidine was obtained. Lastly, an acylation approach was attempted in which the amidine-amine intermediate (**75**) was treated with the HCl salt of pyrazole carboxamide (**76**) in the presence of THF at high temperature. Again, no sign of an amidine-guanidine moiety could be detected (Scheme 32).

Due to the lack of success of forming a guanidine functionality at this stage of the synthesis, an alternate route was proposed. Instead of trying to directly install a guanidine onto intermediate **75**, we sought to subject amidine **74** to $\text{S}_{\text{N}}\text{Ar}$ conditions in order to incorporate a pyrrolidine ring at the 4-chloro position of the quinoline ring. The incorporation of this pyrrolidine motif could possibly facilitate the formation of a guanidine species in subsequent steps. However, when

⁴² Du, Z.; Li, W.; Zhu, X.; Xu, F.; Shen, Q. *J. Org. Chem.* **2008**, *73*, 8966-8972.

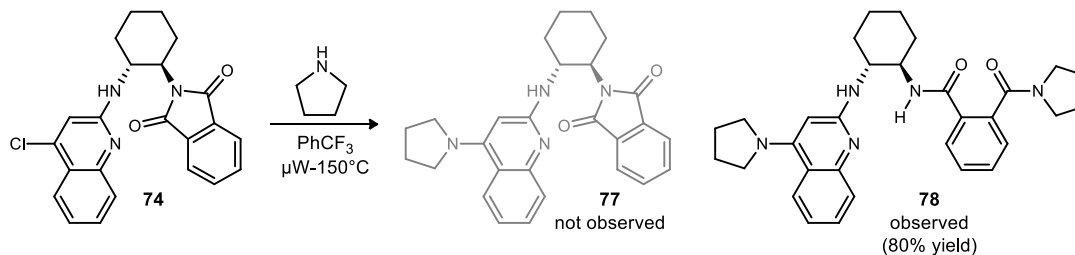
⁴³ Zhu, X.; Xu, F.; Shen, Q. *Chin. J. Chem.* **2009**, *27*, 19-22.

Scheme 32. Attempts Towards the Synthesis of an Amidine-Guanidine Organocatalyst



analyzing the structure of intermediate **74**, a potential problem that could arise is that the phthalate ring would be attacked and opened by pyrrolidine before the aromatic substitution reaction could take place on the quinoline. Keeping in mind this potential problem, amidine **74** was treated with pyrrolidine in the presence of trifluorotoluene under microwave conditions. Upon purification, our desired product, compound **77**, was not observed. Rather, it was determined that both the substitution and the phthalate ring-opening did indeed take place, affording amidine-amide compound **78** in 80% isolated yield (Scheme 33).

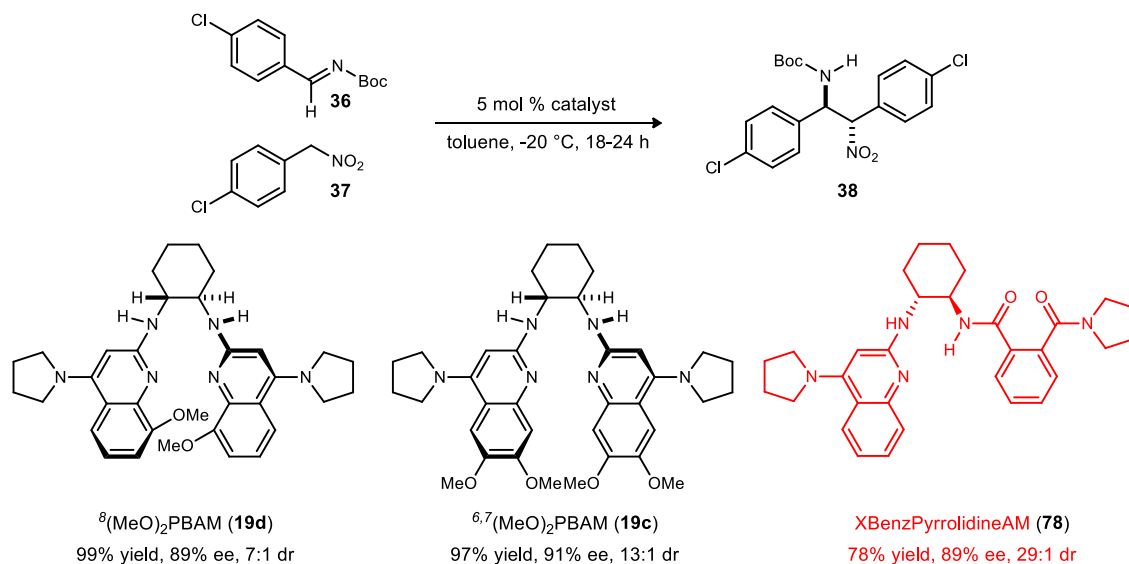
Scheme 33. Synthesis of Amidine-Amide Catalyst **78**



Although acquired amidine-amide product **78** was not initially desired, we saw this compound as a potential enantioselective organocatalyst as a chiral pocket was present within the structure. Before this motif was applied to a ketimine reaction system, however, we wanted to test this potential amidine-amide catalyst on a previously developed aza-Henry system. The system that was chosen was the enantioselective aza-Henry addition en route to Nutlin-3, in which aryl nitroalkane **37** is added into *N*-Boc protected arylimine **36**, resulting in a masked *cis*-stilbene diamine backbone. As seen in previous studies, traditional bis(amidine) catalysts have resulted in a good degree of success for this particular system.²¹ Optimal symmetric bis(amidine) catalysts included ⁸MeOPBAM (**19d**), which furnished the adduct in 99% yield, 89% ee, and 7:1 dr and ^{6,7}(MeO)₂PBAM (**19c**), which gave the adduct in 97% yield, 91% ee, and 13:1 dr. When applying amidine-amide moiety **78**, dubbed XBenzPyrrolidineAM, as the catalyst to this system, the desired adduct was obtained in 78% yield, 89% ee, and 29:1 dr (Scheme 34). In essence, the first

asymmetric amidine-amide catalyst subjected to this system showed comparable results with the most optimal symmetric BAM catalysts. This prompted us to further develop and investigate additional asymmetric amidine-amide organocatalysts in order to determine if this aza-Henry reaction system, en route to Nutlin-3, could be optimized to an even higher degree.

Scheme 34. Comparative Results of the Nutlin-3 aza-Henry System

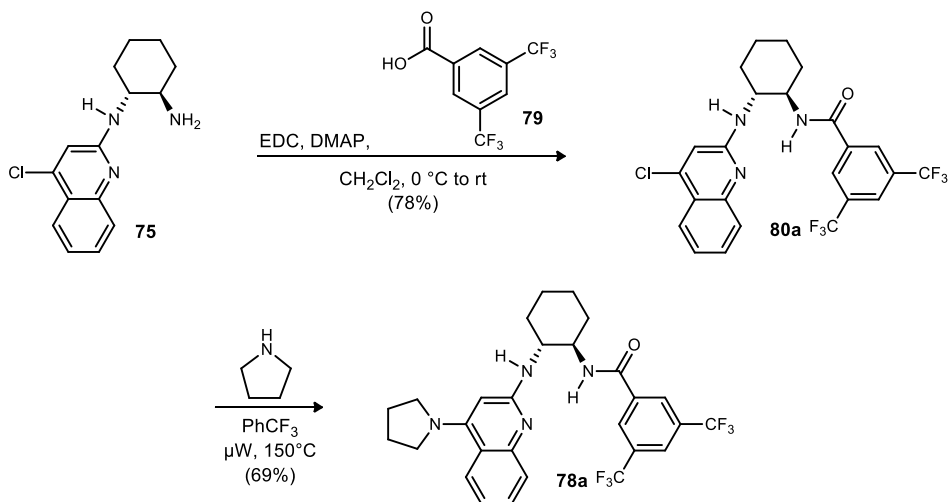


3.3 Development of Asymmetric Amidine-Amide Organocatalysts and Their Application Towards the aza-Henry Addition en Route to Nutlin-3

Seeing that XBenzPyrrolidineAM (**78**) performed well compared to traditional BAM catalysts, we sought a more direct approach for the synthesis of other amidine-amide catalysts. One route to be taken would involve subjecting key amine **75** to standard amide coupling conditions followed by the installation of the pyrrolidine entity via nucleophilic aromatic substitution. An amidine-amide species that was of considerable interest, and could be readily constructed through this pathway, was a 3,5-bis(trifluoromethyl)benzamide-amidine organocatalyst (**78a**). This catalyst, coined $3,5(\text{CF}_3)_2\text{BenzAM}$, can be synthesized by first treating intermediate **75** with 3,5-bis(trifluoromethyl)benzoic acid (**79**), EDC, and a catalytic amount of DMAP in order to afford benzamide **80a** in 78% yield. A subsequent $\text{S}_{\text{N}}\text{Ar}$ reaction of this intermediate with pyrrolidine furnished the desired $3,5(\text{CF}_3)_2\text{BenzAM}$ motif in 69% yield (Scheme 35).

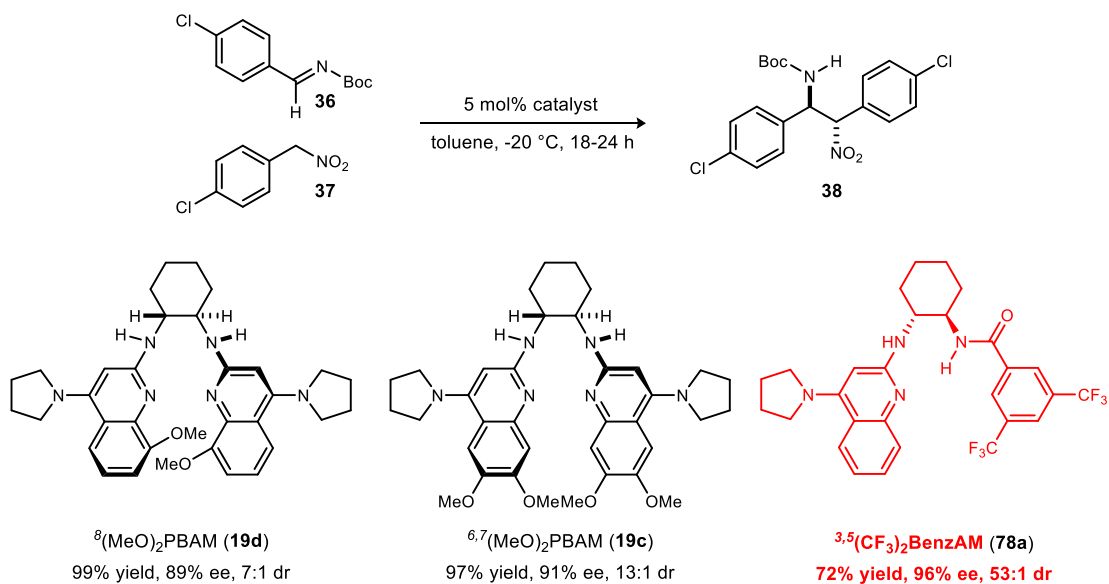
When subjecting $3,5(\text{CF}_3)_2\text{BenzAM}$ catalyst (**78a**) to the benchmark aza-Henry addition, we were delighted to see that higher levels of enantioselection and diastereoselection were

Scheme 35. Synthesis of ^{3,5}(CF₃)₂BenzAM (78a**)**



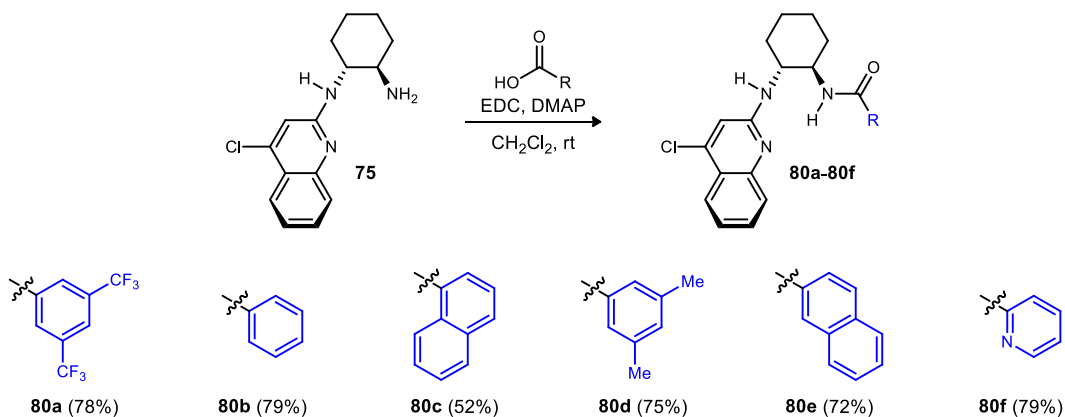
achieved compared to previously reported results. ^{3,5}(CF₃)₂BenzAM gave the desired adduct in 72% yield, 96% ee, and 53:1 dr under standard reaction conditions, making this the most selective and efficient organocatalyst for the Nutlin-3 aza-Henry system up to this point (Scheme 36).

Scheme 36. Improvements on the Nutlin-3 Aza-Henry System with ^{3,5}(CF₃)₂BenzAM (78a**)**



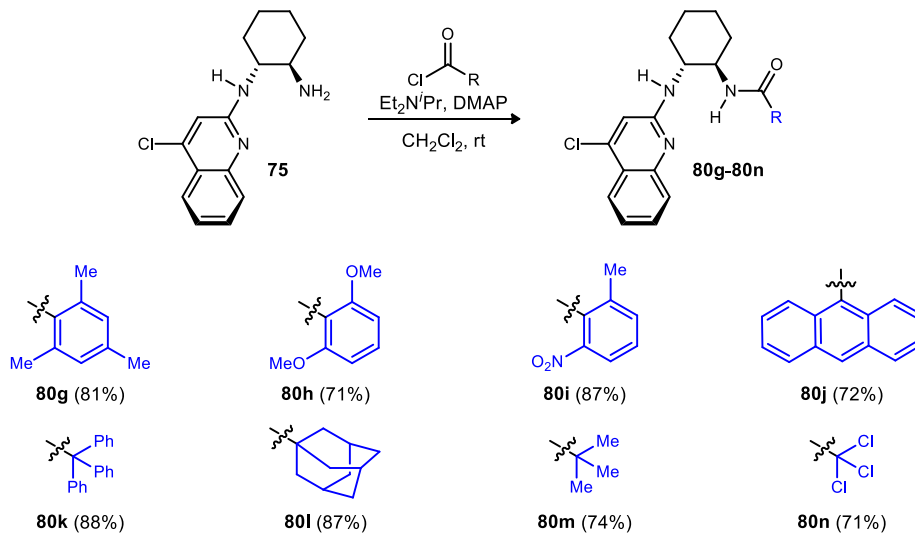
Achieving these degrees of selectivity led to the development of additional amidine-amide catalyst precursors via the amide coupling pathway. Treatment of key intermediate **75** with a series of commercially available carboxylic acids in the presence of EDC furnished a variety of desired amides in modest to good yields (45-79%). Amongst these amides were standard and substituted benzamides, naphthamides, and picolinamides (**80a-80f**) (Scheme 37).

Scheme 37. Synthesis of Amidine-Amide Catalyst Precursors **80a-80f**



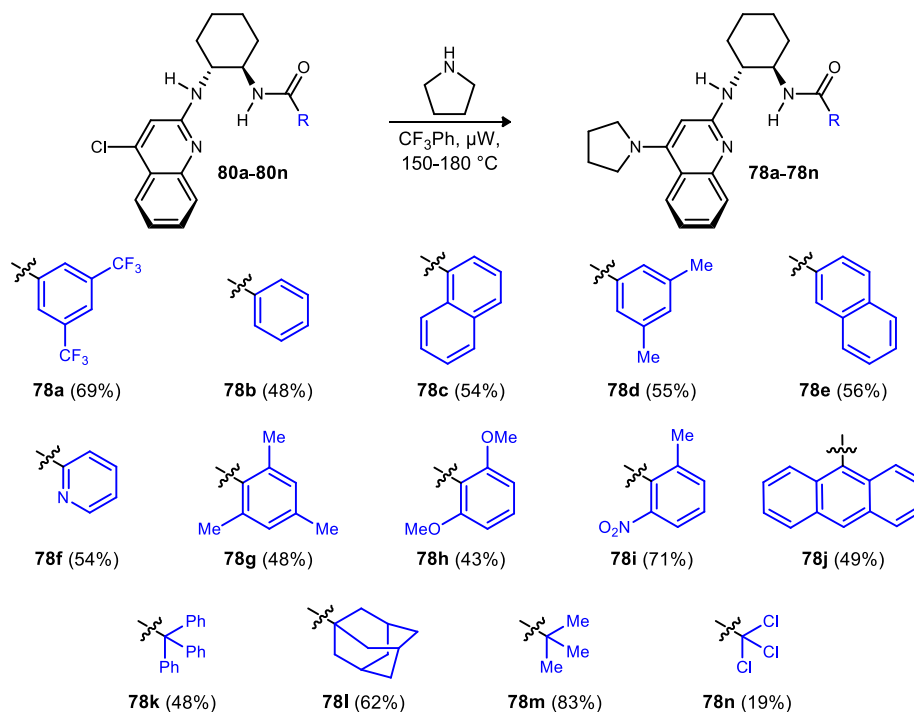
Formation of these amide motifs was not limited to EDC couplings with carboxylic acids. Rather, an acylation pathway was also available with key intermediate **75**. By subjecting this amine to a number of acyl chlorides under basic conditions, additional amidine-amide moieties could be obtained. This acylation approach lead to the installation of adamantyl and anthracenyl amides, pivalamides, acetamides, and other benzamides (**80g-80n**) (Scheme 38). Good yields (71-88%) were typically acquired throughout these acylations.

Scheme 38. Synthesis of Amidine-Amide Catalyst Precursors **80g-80n**



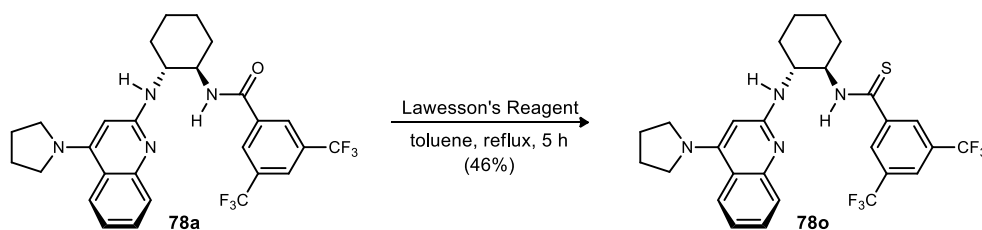
With catalyst precursors **80a-80n** in hand, the stage was now set for the $\text{S}_{\text{N}}\text{Ar}$ reaction en route to the desired catalysts with pyrrolidine as the nucleophile. These reactions were conducted under microwave conditions and were typically completed within 90 minutes. A wide range in yields was observed for these substitutions as yields varied from 19% to 83% (Scheme 39).

Scheme 39. S_NAr Reactions en Route to Amidine-Amide Catalysts **78a-78n**



Before applying these newly developed asymmetric amidine-amide catalysts (**78a-78n**) to the aza-Henry addition en route to Nutlin-3 (**35**), other asymmetric organocatalysts bearing functionalities other than an amide were prepared for comparative purposes. One motif that was prepared was amidine-thioamide **78o**. The thioamide functionality was introduced in a straightforward manner as ^{3,5}(CF₃)₂BenzAM (**78a**) was treated with Lawesson's reagent in order to afford the desired product (**78o**) in 46% yield (Scheme 40).

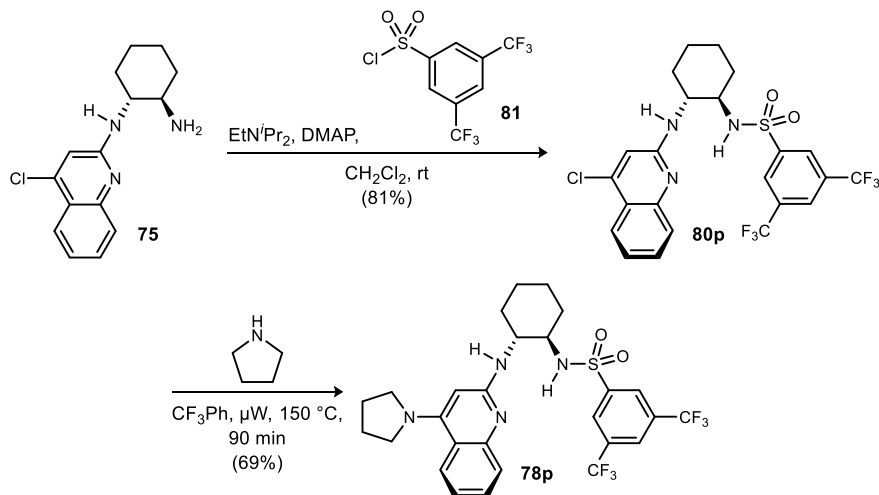
Scheme 40. Synthesis of Amidine-Thioamide Catalyst **78o**



Another functional group that was of interest and could be readily incorporated into our catalyst backbone structure was a sulfonamide species. By treating amine **75** with commercially available ^{3,5}bis(trifluoromethyl)benzenesulfonyl chloride (**81**) under basic conditions, we could arrive at sulfonamide precursor **80p** in good yield (81%). A subsequent nucleophilic aromatic

substitution reaction of this precursor with pyrrolidine afforded the desired amidine-sulfonamide catalyst (**78p**) in 69% yield (Scheme 41).

Scheme 41. Synthesis of Amidine-Sulfonamide Catalyst **78p**

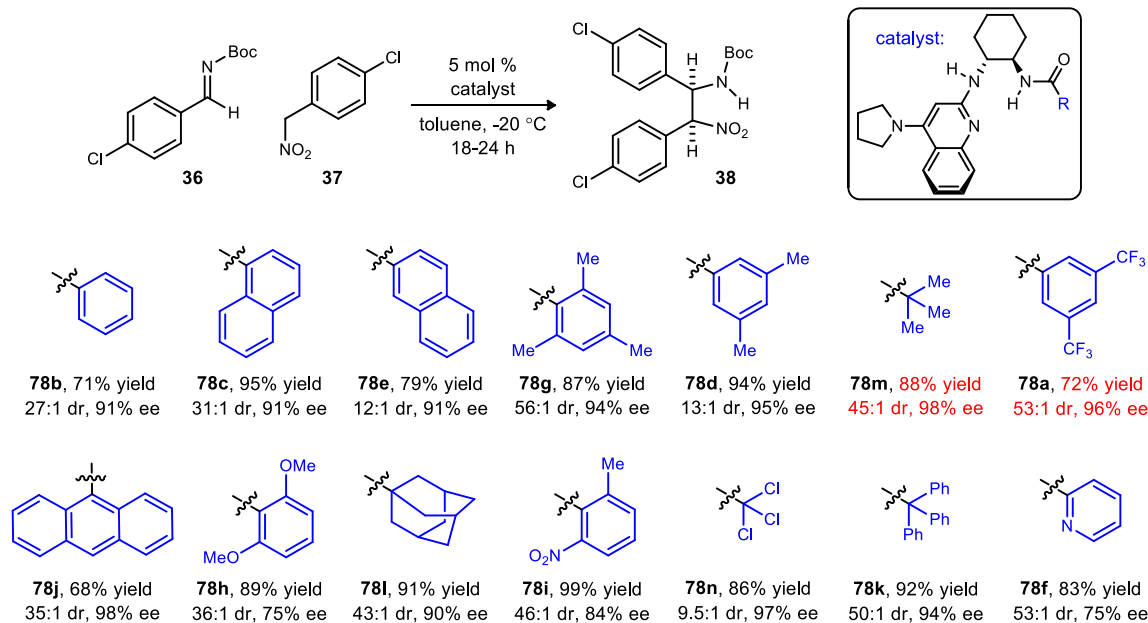


Application of the newly developed amidine-amide catalyst library toward the Nutlin-3 aza-Henry system yielded interesting results in terms of reactivity and selectivity. Steric and electronic modifications of the amide functionality can lead to possible hypotheses as to how the asymmetric chiral pocket behaves for this reaction system. When the amide portion of this catalyst structure is a standard benzamide moiety (**78b**), the desired adduct is obtained in 71% yield, 27:1 dr, and 91% ee (Scheme 42). Although the expansion of the ring system from a benzamide to both 1- and 2-naphthamides (**78c** and **78e**) did result in improved yields, no significant enhancement of diastereo- and enantioselection could be detected. However, when further expanding the amide portion of the catalyst to an anthracenyl amide (**78j**), selection was increased to a considerable degree as the desired product was isolated in 35:1 dr and 98% ee despite a slightly diminished yield (68%). This increase in enantioselection when going from a naphthamide to an anthracenyl amide indicates that sterics are an important component when it comes to creating the most selective chiral pocket for this particular reaction system.

Steric influence of these amidine-amide catalysts was not limited to solely the ring size of the amide. Higher levels of selection were also achieved via introduction of substituents at the *ortho*, *meta*, and *para* positions of the benzamide motif. This was reflected by the results observed with both the ^{2,4,6}(Me)₃benzamide- and the ^{3,5}(Me)₂benzamide-amidine organocatalysts (**78g** and **78d**). These two catalysts afforded the desired aza-Henry adduct in higher yields, comparable dr's,

and improved ee's relative to their standard benzamide counterpart **78b**, reaffirming that better enantioselection can be achieved with proper steric modification (Scheme 42).

Scheme 42. aza-Henry Results with Amidine-Amide Catalysts **78a-78n**



Further comparisons can be made with catalysts **78h** and **78i** via electronic alterations. When introducing an electron-donating methoxy functionality at both *ortho* positions of the benzamide ring (catalyst **78h**), diminishment in enantioselection is seen as the aza-Henry adduct is acquired in only 75% ee relative to ^{2,4,6}(Me)₃benzamide-amide catalyst **78g**, which gave the product in 94% ee. Yet, when an electron-withdrawing nitro group is incorporated at an *ortho* position of the ring (catalyst **78i**), marginal improvement is observed as the product is afforded in 99% yield, 46:1 dr, and 84% ee (Scheme 42). Analysis of the electron-donating and electron-withdrawing benzamides presents the possibility that additional electrons/lone pairs from both the methoxy and the nitro entities may interfere with the catalyst-substrate binding, ultimately resulting in lower levels of selectivity. This possibility was further supported by the results acquired with ^{3,5}(CF₃)₂BenzAM catalyst **78a**, which yielded the adduct in better ee and dr (96% ee and 53:1 dr) compared to methylated counterpart **78d** (95% ee and 13:1 dr). Like nitrobenzamide catalyst **78i**, this catalyst (**78a**) possesses electron-withdrawing substituents in trifluoromethyl groups. In contrast to the nitro group however, these trifluoromethyl groups do not possess a free lone pair that can readily disrupt the catalyst binding pathway and result in less selection. Thus, it

is shown that diastereoselection and enantioselection can be slightly enhanced when electron-withdrawing character is introduced without interruption of catalyst binding.

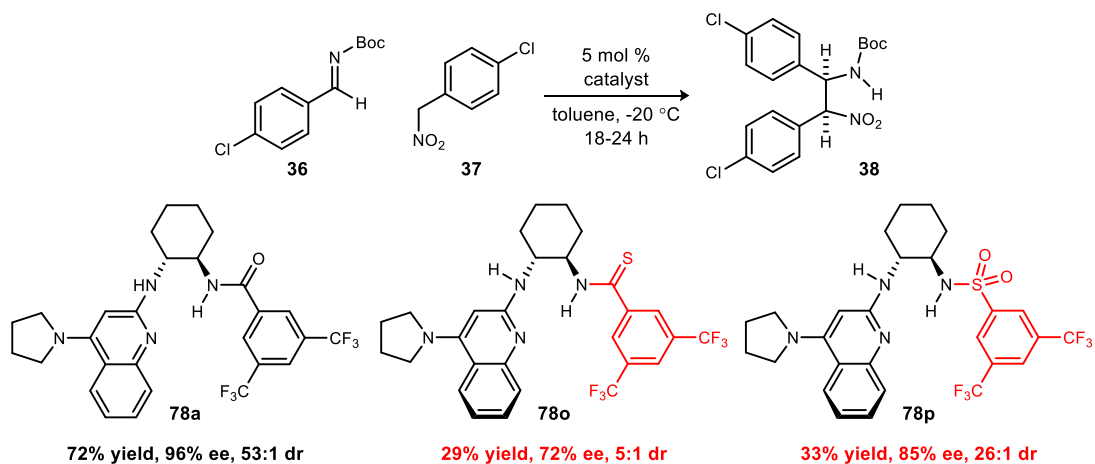
Application of acetamide-derived amidine-amide catalysts to this aza-Henry system also showed high degrees of efficiency (Scheme 42). Pivalamide **78m**, dubbed PivalAM, proved to be the most efficacious amidine-acetamide organocatalyst as this moiety provided the aza-Henry adduct in 88% yield, 45:1 dr, and 98% ee. These results signified the most optimal combination of yield, diastereoselection, and enantioselection for this reaction system up to this point. A change in electronics resulted in a considerable drop in dr and a slightly diminished ee as trichloropivalamide catalyst **78n** gave the desired product in 86% yield, 9.5:1 dr, and 97% ee. Changing the electronics of the pivalamide species will alter the hydrogen bond donor ability of the amide which in turn can affect binding, causing a drop in diastereo- and enantioselection. A bulkier triphenylacetamide-amidine catalyst (**78k**) was also subjected to the benchmark reaction system. This catalyst fared considerably well as the adduct was obtained in 92% yield, 50:1 dr, and 94% ee. The last amidine-acetamide organocatalyst to be tested was adamantyl motif **78l**. This proved to be the least sufficient amidine-acetamide catalyst as the adduct was afforded in only 90% ee despite a high yield and dr (91% yield, 43:1 dr). A drop in enantioselection from PivalAM **78m** (98% ee) to adamantyl amide **78l** (90% ee) reestablished the idea that optimal selectivity, especially enantioselectivity, can be achieved with the correct combination of both sterics and electronics.

A heteroaromatic picolinamide catalyst (**78f**) was the last amidine-amide moiety to be subjected to the Nutlin-3 aza-Henry reaction. Upon completion of addition with **78f** as the catalyst, the product was acquired in 83% yield, 53:1 dr, and 75% ee (Scheme 42). Although a high yield and dr were obtained, this picolinamide-amidine catalyst displayed a lower degree of enantioselectivity relative to its standard phenyl counterpart, amidine-benzamide **78b**, which furnished the adduct in 91% ee. The diminishment in enantiomeric excess when using picolinamide **78f** as the catalyst can once again be attributed to the idea that an extra lone pair of electrons on the pyridine ring is readily interfering with the catalyst's mode of binding, a trend that was observed with the methoxy- and nitrobenzamide-amidine catalysts (**78h** and **78i**).

Two other catalyst types that were tested in this aza-Henry system included amidine-thioamide **78o** and amidine-sulfonamide **78p**. Thioamide catalyst **78o** proved to be inefficient relative to its amide analog, ^{3,5}(CF₃)₂BenzAM (**78a**), as the adduct was obtained in only 29% yield,

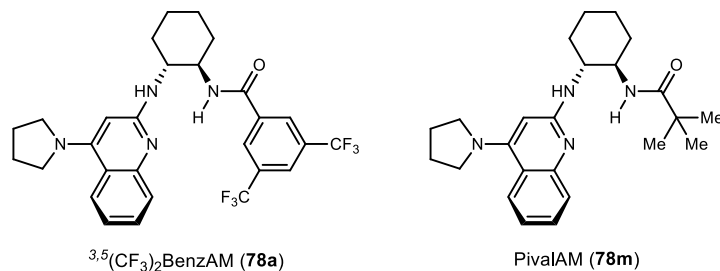
5:1 dr, and 72% ee indicating a significant decrease in yield, and a large drop in selectivity (Scheme 43). Amidine-sulfonamide motif **78p** did not fare much better as this catalyst afforded the desired product in 33% yield, 26:1 dr, and 85% ee. The results obtained by **78o** and **78p** confirm that amidine-amide moieties give far superior degrees of reactivity and selectivity for this particular addition reaction. Changing the amide functionality to a thioamide or sulfonamide will increase the acidity of the proton on the functional group, which can once again disrupt ideal catalyst binding and result in diminished yields and selectivity.

Scheme 43. Comparative Results with Thioamide and Sulfonamide Catalysts



Previously, it was mentioned that the most optimal catalysts for the Nutlin-3 aza-Henry system, prior to the development of the amidine-amide catalyst library, were ⁸MeOPBAM (**19d**) and ^{6,7}(MeO)₂PBAM (**19c**) which gave the desired adduct in up to 13:1 dr and 91% ee. Yet when subjecting these newly developed amidine-amide catalysts to the same system, the desired product was obtained in up to 56:1 dr and 98% ee indicating a significant improvement in diastereo- and enantioselection. The two catalysts that gave the optimal combination of yield and selectivity were ^{3,5}(CF₃)₂BenzAM (**78a**) and PivalAM (**78m**) (Figure 9). These amidine-amide motifs were used in further studies and applications as well.

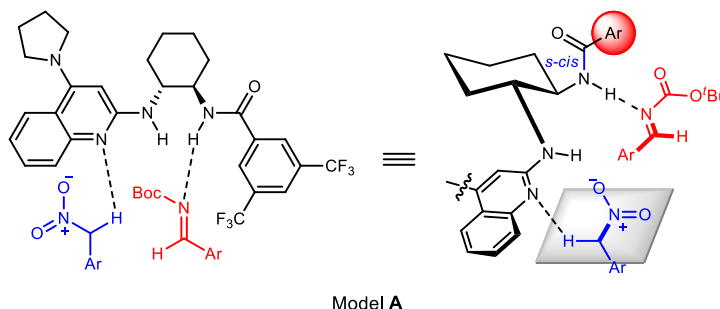
Figure 9. Optimal Catalysts Chosen for Further Studies



3.4 Proposed Catalyst Binding Modes

Although the mechanistic pathway for these catalysts has not been completely studied at this point, it is evident that the combination of amidine and amide motifs allows for a fully bifunctional organocatalyst for this aza-Henry addition en route to Nutlin-3 (**35**). Having both the amidine and amide functionalities in the same chiral pocket can lead to a number of proposed transition states. In model **A**, the hydrogen of the amide can act as hydrogen bond donor to activate the *N*-Boc-protected imine electrophile (Figure 10). Conversely, the nitrogen of the quinoline ring serves as a Brønsted base to deprotonate the nitroalkane to form the nucleophilic nitronate. The simultaneous activation of the electrophile and generation of the nucleophile can allow for the formation of the desired masked *cis*-stilbene diamine adduct in a diastereo- and enantioselective fashion.

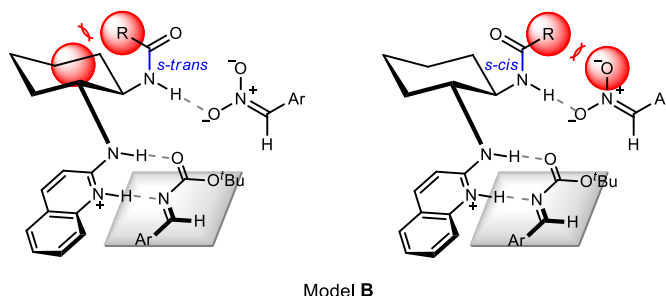
Figure 10. Proposed Amidine-Amide Activation and Stereochemical Model A



In another possible model, model **B**, the quinoline can fully deprotonate the nitroalkane, generating a positively-charged amidinium and a negatively-charged nitronate. The protons of the amidinium species can readily coordinate with the carbonyl of the Boc group and the nitrogen of the imine causing activation of the electrophile. Simultaneously, an oxygen of the nitronate, bearing a negative charge, can coordinate with the proton of the amide (Figure 11). Here, the amide can be oriented in one of two ways relative to the cyclohexyl ring. If the amide is oriented in an *s-trans* fashion, the substituent α to the carbonyl of the amide may be sterically repulsed by the cyclohexyl ring. However, if the amide is arranged in an *s-cis* manner, then the amide substituent may sterically interact with the non-coordinating oxygen of the nitronate. The varying sizes of the amide substituents, as shown in the catalyst library, can have an effect on the degree of steric repulsion. The size of the substituent may dictate if the amide will orient itself *cis* or *trans* relative to the cyclohexane ring, which may ultimately affect selectivity. Furthermore, varying the electronics of the amide entity may inductively influence the amide's hydrogen bond donor ability.

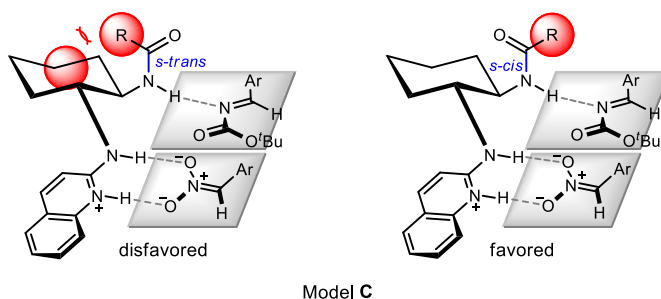
This can affect the strength of coordination with the nitronate, which, in turn, may further influence the degrees of diastereo- and enantioselection of this addition.

Figure 11. Proposed Amidine-Amide Activation and Stereochemical Model **B**



Opposite to model **B**, it is also plausible that coordination between functionalities can be reversed. For a third model, model **C**, the quinoline once again deprotonates the nitroalkane generating an amidinium and a nitronate. Unlike the previous model however, model **C** proposes that the negatively-charged nitronate readily binds to both protons of the positively-charged amidinium, while the nitrogen of the imine binds to the hydrogen of the amide (Figure 12). Again, the amide functionality has the ability to orient itself in an *s-cis* or *s-trans* manner. Yet in this case, it is believed that the lowest-energy transition state will be achieved if the amide is arranged in an *s-cis* fashion as steric interactions should be minimized. An *s-trans* arrangement would be disfavored as there would be a considerable amount of steric repulsion between the amide substituent and the cyclohexyl ring as seen in model **C**. Once again, this model is susceptible to variations in the size and electronics of the amide motif as they can alter steric interaction and amide acidity. These variations can change the levels of selectivity of this reaction system as a consequence.

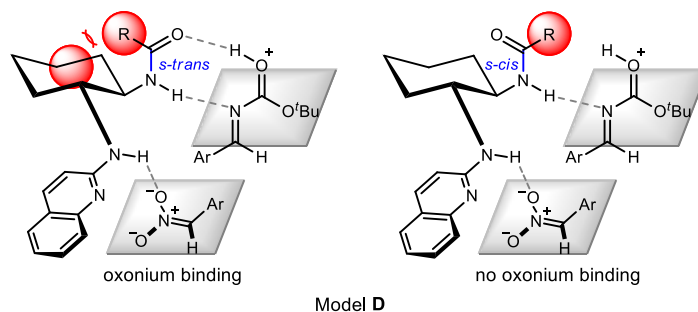
Figure 12. Proposed Amidine-Amide Activation and Stereochemical Model **C**



Lastly, model **D** proposes a binding pattern similar to model **C**, but with different charge coordination. Upon deprotonation of the nitroalkane by the quinoline, the resulting amidinium ion

can be in equilibrium with the carbonyl of the Boc-imine and generate an acidic oxonium ion. Here, the proton of the oxonium can readily coordinate with the carbonyl of the amide while the nitrogen of the imine can bind to the hydrogen of the amide. Conversely, the negatively-charged nitronate can coordinate with the lone proton of the amidine (Figure 13). If the aryl Boc-imine were to bind to the amide moiety in this proposed fashion, then it is believed that the amide would have to be in an *s-trans* orientation for easier accessibility versus an *s-cis* conformation. Forcing the amide to be in an *s-trans* arrangement in this model may once again cause steric repulsion between the amide substituent and the cyclohexyl ring. If the degree of steric repulsion was the only change taking place with varying sizes of the amide, then the ability of the amide substituent to have an effect on selectivity may be significantly reduced as this interaction is occurring outside of the chiral pocket. Furthermore, model **D** also hypothesizes that the aromatic portion of the imine is within the chiral pocket. As a consequence, it is possible that the sterics of the imine can have a critical influence on the selectivity of this addition. This is a potential phenomenon that needs to be examined more closely. Finally, it is also plausible that the acidity of the amide proton can change the degree of activation of the electrophile and ultimately have an effect on reactivity. Data shows that when going from an amide to a thioamide/sulfonamide species, reactivity is significantly diminished. It is feasible through this model that having an amide proton of higher acidity can cause unwanted interactions in this chiral pocket and, consequently, result in less imine activation and reactivity.

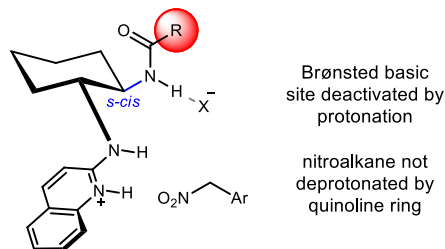
Figure 13. Proposed Amidine-Amide Activation and Stereochemical Model **D**



Based on the proposed transition states, it is reaffirmed that both the amidine and the amide components allow for a completely bifunctional organocatalyst system for the aza-Henry addition en route to Nutlin-3. The binding of these asymmetric catalysts is unique in the sense that unlike the traditional bis(amidine) organocatalysts, introduction of a salt is unnecessary as both Brønsted sites are present in its free base form. If a salt is indeed introduced to these amidine-amide moieties,

the lone Brønsted basic site of the quinoline will be protonated and reactivity will be lost as a result (Figure 14).

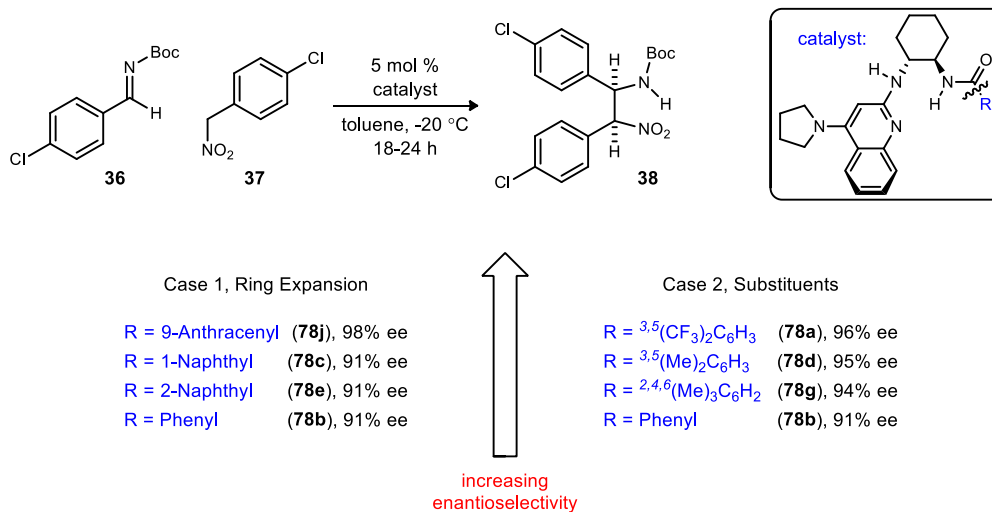
Figure 14. Deactivation of the Catalyst via Introduction of a Salt



3.5. In-Depth Analysis of Catalyst Trends

Subjection of these catalysts to the Nutlin-3 aza-Henry addition yielded data points that could be considered for potential trends. These trends mainly center upon sterics, electronics, and amide acidity.

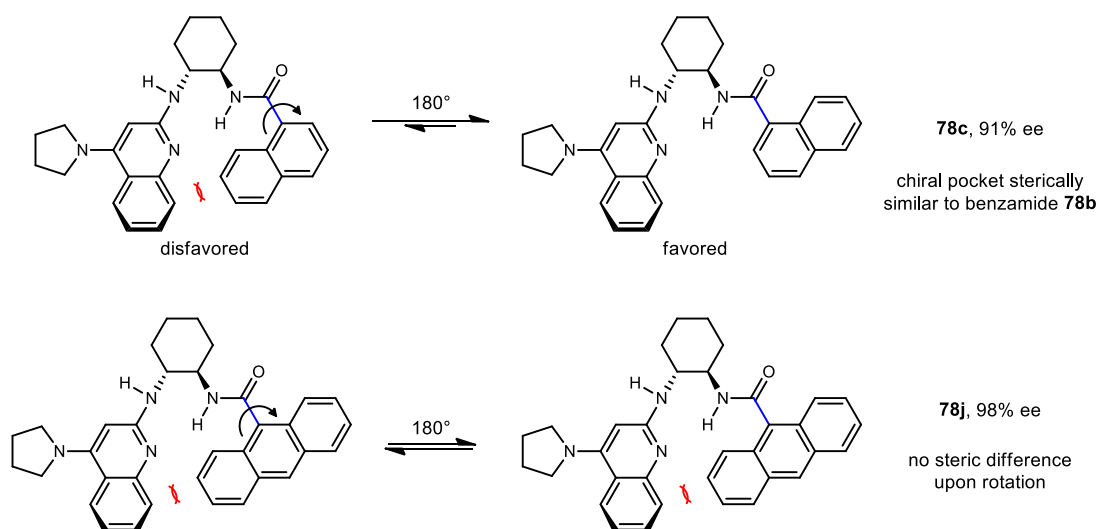
Scheme 44. Steric Trends Observed with Asymmetric Amidine-Amide Catalysts



When examining the effects of sterics, a general trend that was observed was that an increase of amide size results in an enrichment of enantioselection. This trend was consistent among ring expansion of the amide functionality. As previous data indicates (Scheme 44), a change from a benzamide to a naphthamide does not result in an increase of enantioselection as ee is maintained at 91%. Yet when exchanging a naphthamide (**78c** or **78e**) for an anthracenyl amide (**78j**), a substantial jump in selectivity is observed as this catalyst affords adduct **38** in 98% ee. This difference in enantioselectivity may revolve around the ability of the amide substituent to

rotate about the C-C sigma bond attached to the carbonyl of the amide. The rotation about this sigma bond, with asymmetric ring systems, can alter the size and shape of the chiral pocket, ultimately affecting enantioselection. When a 1- or 2-naphthyl ring is introduced as the amide substituent, two different chiral pockets can be acquired upon rotating 180° since they are non-symmetric substituents. It is plausible that the naphthamide moieties arrange themselves in such a way that they minimize their interaction in the chiral pocket as it is the lowest energy conformation (Figure 15). If the naphthamide substituents are arranged in this way, this may create a chiral environment similar to having a benzamide motif present. As a result, the degrees of enantioselection should be very similar. Yet when introducing a bulkier, symmetric anthracenyl functionality, this may change the chiral environment as the same conformation will be achieved upon rotating 180°. In other words, an anthracenyl amide does not have the ability to adapt a lower energy orientation. Part of the anthracenyl ring is forced inside creating a more shallow and narrow chiral pocket. This smaller pocket appears to be preferred for this aza-Henry system as the adduct was acquired in considerably higher ee (98% ee).

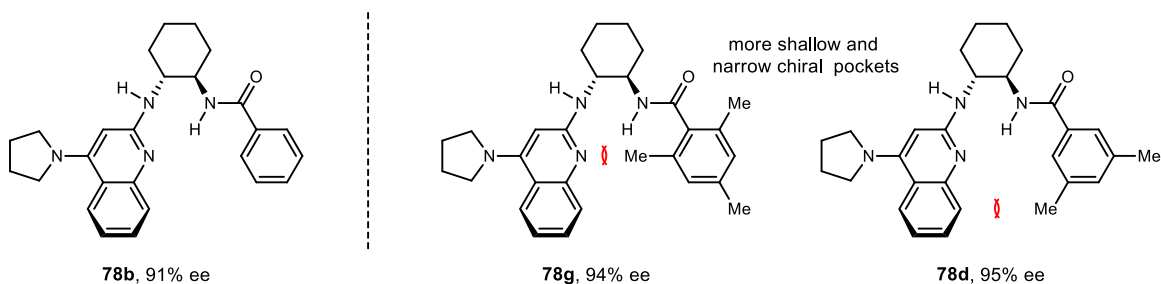
Figure 15. Ring Expansion and its Influence on Enantioselection



This same phenomenon was observed upon incorporation of substituents at the *ortho*, *meta*, and *para* positions of benzamide catalyst **78b**. As previously mentioned, installation of methyl substituents at the *ortho* and *para* positions of the benzamide ring (catalyst **78g**) resulted in higher selectivity as the desired adduct was afforded in 94% ee relative to standard benzamide **78b**, which gave adduct **38** in 91% ee (Scheme 44). Installation of these methyl substituents at both *meta* positions did not seem to make much of a difference as the adduct was acquired in 95% ee. Altering

the electronics of these methyl substituents to electron-withdrawing trifluoromethyl groups also had minimal enhancement in enantioselection as the adduct was obtained in 96% ee. What is consistent throughout these findings is that enantioselection is enhanced as steric bulk is increased via incorporation of neutral or electron-withdrawing substituents on the benzamide ring (Figure 16). The proposal made with the anthracenyl-amide catalyst (**78j**) also applies to the methylated benzamide catalysts. Each of the substituted benzamides are symmetric and larger compared to a standard benzamide. As the bulkier methylated benzamides rotate about the C-C sigma bond attached to the carbonyl of the amide, the same conformation will be achieved upon a 180° rotation. Like the anthracenyl amide, these methylated benzamides do not have the ability to choose a lower energy orientation. As a consequence, these methyl groups (i.e. more steric bulk) are once again forced inside creating a more shallow and narrow chiral pocket. This results in higher degrees of enantioselection relative to benzamide catalyst **78b**, a very similar trend that was seen with ring expansion.

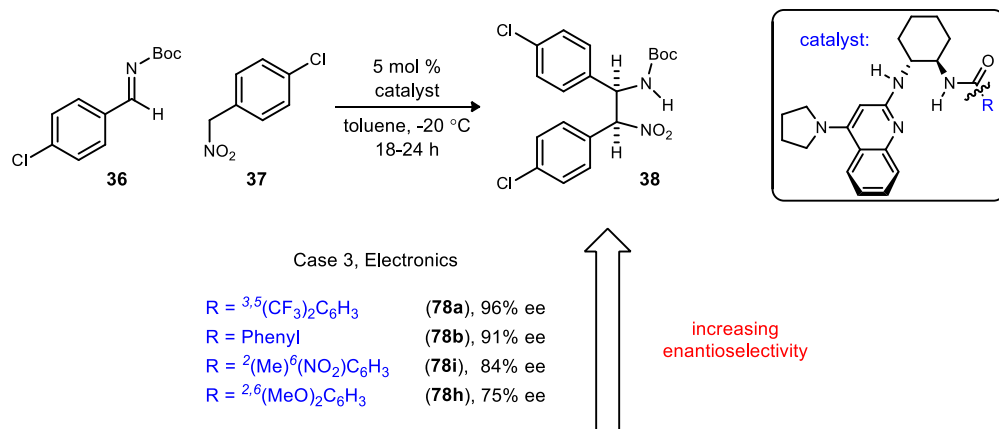
Figure 16. Steric Interaction and its Influence on Enantioselection



Electronic variations of the amide substituent also yielded an interesting trend. As shown in the steric trends, ^{3,5}(CF₃)₂BenzAM (**78a**), furnishes adduct **38** in 96% ee relative to standard benzamide counterpart **78b**, which affords the adduct in 91% ee (Scheme 45). Although it is believed that this increase in enantioselectivity is largely due to increased steric bulk, some of it can be attributed to the electron-withdrawing character of the trifluoromethyl substituents as well. Not all electron-withdrawing motifs resulted in enhanced enantioselection, however. When introducing an electron-withdrawing nitro group at the *ortho* position, as shown in catalyst **78i**, a drop in enantioselection was observed (84% ee). The nitro group is within proximity of the amide proton and depending on how this organocatalyst binds, it is feasible that one of the lone pairs of the nitro group is intramolecularly coordinated to the acidic proton of the amide (Figure 17). This unwanted interaction will disrupt the intended transition state in the sense that the proton of the

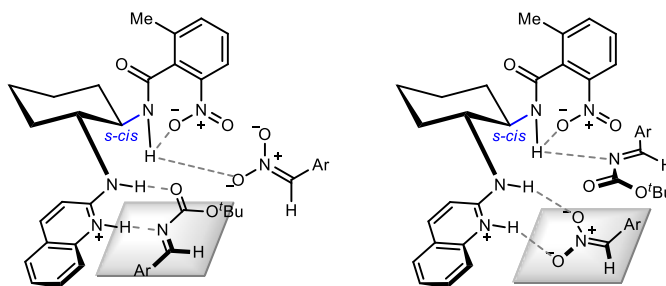
amide will not bind as well to the imine or nitronate. This, in turn, may inhibit activation and reactivity as well as enantioselection. This hypothesis is also supported when two electron-

Scheme 45. Electronic Trends Observed with Asymmetric Amidine-Amide Catalysts



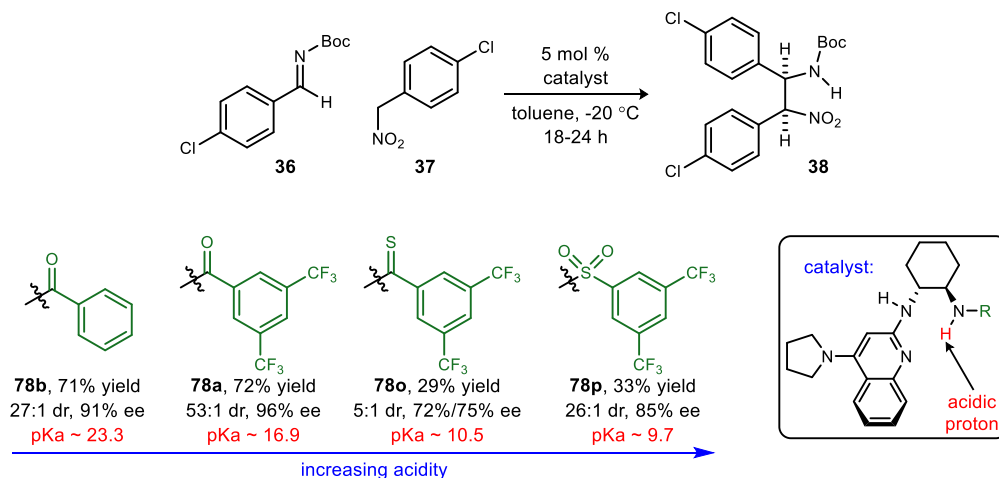
donating methoxy substituents are installed onto the benzamide ring. This particular catalyst (**78h**) gives the intended adduct in only 75% ee. Once again, lone pairs of electrons on these methoxy substituents may interact with the amide proton ultimately causing a diminished ee. When drawing conclusions based on these electronic alterations, it appears that electron-withdrawing groups can enrich enantioselection as long as there is no extra electronic activity (i.e. lone pairs) that can readily disrupt the ideal catalyst binding mode.

Figure 17. Proposed Disruptions of Binding via Unwanted Intramolecular Coordination



Acidity of the amide proton was another variable that led to an interesting trend. The pK_a value of the Brønsted acidic proton can vary by changing the amide substituents to other functionalities. This can lead to different degrees of reactivity and selectivity. Benzamide catalyst **78b** possesses an amide proton with a pK_a value of approximately 23 in DMSO, and when subjected to the benchmark aza-Henry addition, the desired adduct is furnished in 71% yield, 27:1 dr, and 91% ee (Scheme 46). When electron-withdrawing trifluoromethyl substituents are placed at the

Scheme 46. Acidity Trends Observed with Asymmetric Amidine-Amide Catalysts

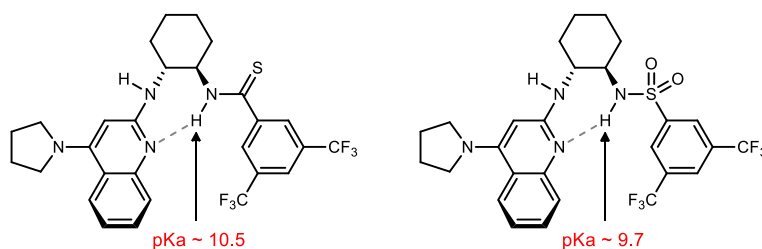


meta positions of the benzamide ring, the amide proton becomes more acidic with a pK_a value of 17. Though this catalyst gives similar reactivity and diastereoselection compared to benzamide **78b**, enantioselection is increased to 96% ee. Once again, this jump in enantioselectivity may be a direct result of increased steric bulk. Yet, it is also possible that the increased acidity plays a role in the acquisition of this higher ee as well. Acidity of this proton was lowered even further upon the installation of thioamide and sulfonamide moieties (**78o** and **78p**). The approximate pK_a values for the thioamide and sulfonamide protons were 10.5 and 9.7 respectively (DMSO scale).^{44,45} When applying these catalysts to the aza-Henry addition however, considerably lower levels of enantioselection as well as diastereoselection and reactivity were observed, indicating that these more acidic thioamide and sulfonamide protons may be inhibiting the catalyst binding mode. In other words, lesser degrees of selection and reactivity may be due to unwanted intramolecular interactions, a phenomenon previously proposed in the electronics trend. In this case however, it is possible that the Brønsted basic quinoline ring can have a high binding affinity for the proton as it becomes more and more acidic (Figure 18). This intramolecular coordination will affect the abilities of the quinoline and amide to properly bind with the imine and nitronate resulting in diminished reactivity and selectivity. In essence, it is believed that increasing the proton acidity to a pK_a of 17 may enhance enantioselection. Yet, if the proton is too acidic ($pK_a \sim 10$), the ideal catalyst transition state may be disrupted and optimal results will not be acquired.

⁴⁴ Ripin, D. H.; Evans, D. A. pK_a Table.1 <evans.rc.fas.harvard.edu/pdf/evans_pka_table.pdf>

⁴⁵ Bordwell pK_a Table (Acidity in DMSO). <www.chem.wisc.edu/areas/reich/pkatable/index.htm>

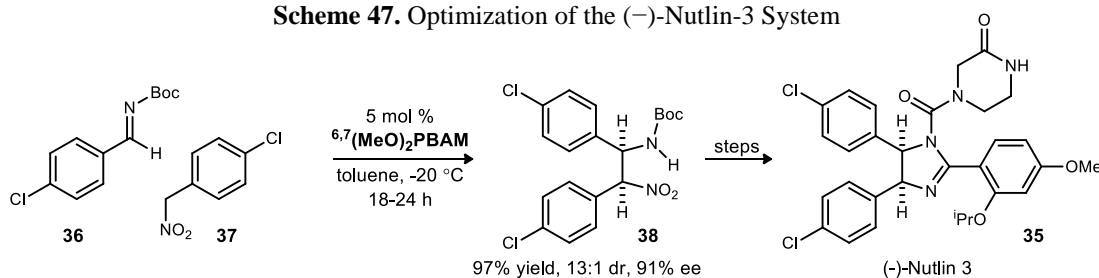
Figure 18. Intramolecular Interaction Between the Quinoline and Acidic Proton



3.6 Application of the Amidine-Amide Organocatalysts

Prior to the development of these asymmetric amidine-amide catalysts, the aza-Henry addition en route to Nutlin-3 was already optimized using symmetric BAM catalysts. According to previous studies,^{6,7}(MeO)₂PBAM afforded adduct **19c** in 97% yield, 13:1 dr, and 91% ee. This enriched adduct could then be converted to (–)-Nutlin-3 (**35**) via a short reaction sequence (Scheme 47).

Scheme 47. Optimization of the (–)-Nutlin-3 System

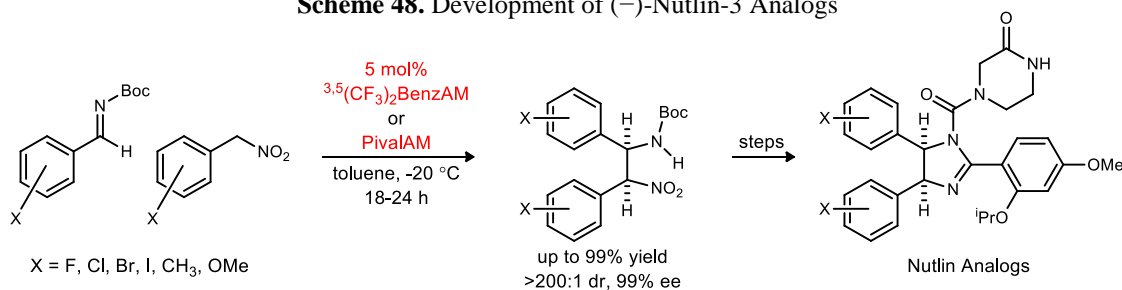


However, when applying optimal BAM catalysts such as ^{6,7}(MeO)₂PBAM (**19c**) and ⁸MeOPBAM (**19d**) to aza-Henry additions en route to Nutlin-3 analogs, diminished enantioselections were observed (60-80% ee). Seeing that the asymmetric catalysts enhanced enantioselectivity for the Nutlin-3 aza-Henry system, we saw this as an opportunity to apply these new amidine-amide catalysts to the synthesis of Nutlin-3 derivatives (Scheme 48). To our delight, we observed that our two most optimal amidine-amide catalysts, ^{3,5}(CF₃)₂BenzAM (**78a**) and PivalAM (**78m**), furnished the new aza-Henry adducts in much higher degrees of enrichment (80-99% ee). With the ^{3,5}(CF₃)₂BenzAM and PivalAM catalysts, a library of over 40 different aza-Henry adducts en route to Nutlin analogs were synthesized with various nitroalkanes and imines in high enantioselection.⁴⁶ These two asymmetric catalysts tolerated aryl imines and aryl nitroalkanes possessing a number of substituents including different halogens, methyl groups, and

⁴⁶ Vara, B. A.; Mayasundari, A.; Tellis, J. C.; Danneman, M. W.; Arredondo, V.; Davis, T. A.; Min, J.; Finch, K.; Guy, R. K.; Johnston, J. N. *J. Org. Chem.* **2014**, *79*, 6913-6938.

methoxy groups. These highly enriched adducts could then be carried onto their corresponding Nutlin derivatives via the same reaction sequence as previously reported. These analogs are then sent to St. Jude's Children's Research Hospital where our collaborator, Dr. Kiplin Guy, analyzes these derivatives in their binding assays. These potency studies will provide findings regarding the binding interaction with the MDM2 protein, and will guide future efforts toward developing more potent analogs.

Scheme 48. Development of (-)-Nutlin-3 Analogs



Chapter 4. PBAM-Catalyzed Additions of Nitromethane into Ketimine Centers – Part II: Boc-Protected Trifluoromethyl Ketimines

4.1 Synthesis of a Trifluoromethyl Ketimine and Examination of its Reactivity

After seeing that electronic modifications of the tosyl protecting group did not result in promising levels of enantioselection, efforts then focused on restructuring the ketimine electrophile. When synthesizing a different ketimine however, the enhancement of reactivity and selectivity must be taken into consideration. One functional group that can readily promote reactivity and ultimately enhance enantioselectivity is a standard electron-withdrawing trifluoromethyl group.

The synthesis of a trifluoromethyl ketimine can have a number of benefits. First, this sort of ketimine will allow for a high degree of imine activation as the electron-withdrawing trifluoromethyl group is within the closest possible proximity of the electrophilic center. Secondly, if a ketimine center possessing both a trifluoromethyl group and aryl group is successfully synthesized, then the issue of tautomerization, as seen with Cbz-ketimine **46** (Figure 6), should not be of concern. In addition, the suppression of the ketimine-to-enamine tautomerization will allow for the introduction of Cbz and *N*-Boc protecting groups, which have, historically, allowed for the highest degrees of selection relative to any other protecting group.^{7,21,47,48,49,50,51,52,53,54} Furthermore, if a Boc-protected aza-Henry adduct is acquired, then β -elimination of the Boc carbamate should be minimized as the Boc carbamate is not as good of a leaving group relative to a tosyl amine. Taking these effects into account, a trifluoromethyl ketimine that was of interest and could be synthesized in a straightforward manner was phenyl Boc-protected trifluoromethyl ketimine **82** (Figure 19).

Desired trifluoromethyl ketimine **82** could be readily synthesized according to literature protocols.^{55,56,57} Acylation of commercially available Boc anhydride (**83**) with hydrazine

⁴⁷ Nugent, B. M.; Yoder, R. A.; Johnston, J. N. *J. Am. Chem. Soc.* **2004**, *126*, 3418-3419.

⁴⁸ Singh, A.; Yoder, R. A.; Shen, B.; Johnston, J. N. *J. Am. Chem. Soc.* **2007**, *129*, 3466-3467.

⁴⁹ Shen, B.; Johnston, J. N. *Org. Lett.* **2008**, *10*, 4397-4400.

⁵⁰ Singh, A.; Johnston, J. N. *J. Am. Chem. Soc.* **2008**, *130*, 5866-5867.

⁵¹ Wilt, J. C.; Pink, M.; Johnston, J. N. *Chem. Commun.* **2008**, *35*, 4177-4179.

⁵² Davis, T. A.; Wilt, J. C.; Johnston, J. N. *J. Am. Chem. Soc.* **2010**, *132*, 2880-2882.

⁵³ Shen, B.; Makley, D. M.; Johnston, J. N. *Nature* **2010**, *465*, 1027-1033.

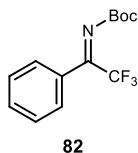
⁵⁴ Dobish, M. C.; Villalta, F.; Waterman, M. R.; Lepesheva, G. I.; Johnston, J. N. *Org. Lett.* **2012**, *14*, 6322-6325.

⁵⁵ Melendez, R. E.; Lubell, W. D. *J. Am. Chem. Soc.* **2004**, *126*, 6759-6754.

⁵⁶ Cali, P.; Begtrup, M. *Synthesis* **2002**, *1*, 63-66.

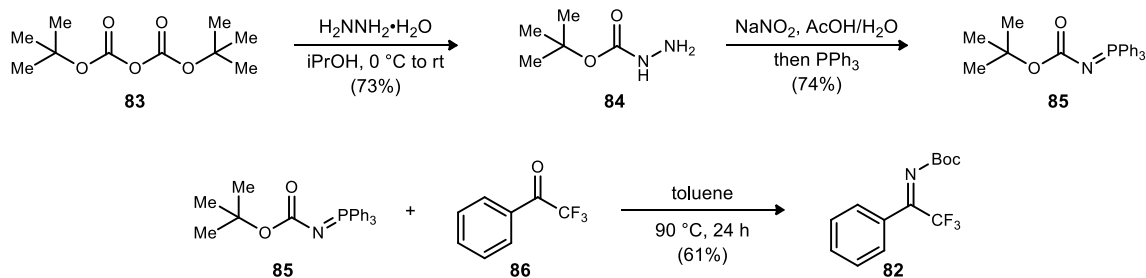
⁵⁷ Sangamesh, B. et al. U.S. Patent WO 2011/009943 A1, January 27, 2011.

Figure 19. Structure of Boc-Protected Trifluoromethyl Ketimine **82**



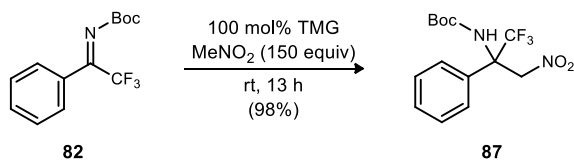
monohydrate resulted in *tert*-butyl carbazate **84** in 73% isolated yield after vacuum distillation. Treatment of this carbazate with sodium nitrite under acidic conditions will result in the corresponding azide *in situ* which, upon treatment with triphenylphosphine, can be converted to iminophosphorane **85** via a Staudinger reduction (74% yield). With iminophosphorane **85** in hand, the stage was now set for an aza-Wittig reaction that would lead to the intended ketimine. When heating iminophosphorane **85** and commercially available 2,2,2-trifluoroacetophenone **86** in the presence of toluene over the course of 24 hours, ketimine **82** was furnished in modest yield upon chromatographic separation (61% yield) (Scheme 49).

Scheme 49. Synthesis of Boc-Protected Trifluoromethyl Ketimine **82**



After successfully synthesizing ketimine **82**, efforts were then shifted toward examining the reactivity of this electrophile. When treating ketimine **82** with a stoichiometric amount of 1,1,3,3-tetramethylguanidine (TMG) in neat nitromethane, we were delighted to see that this aza-Henry addition proceeded cleanly as the desired adduct (**87**) was afforded in 98% yield over the course of 13 hours (Scheme 50). Additionally, observation of only a single adduct indicated that the Boc protecting group was not prone to β -elimination under basic conditions, a phenomenon that was observed with the tosyl protecting group. With a cleaner aza-Henry reaction system and

Scheme 50. Examination of Reactivity with Ketimine **82**

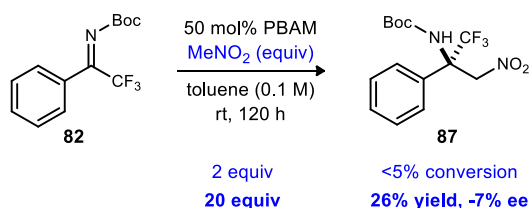


a more stable adduct, studies were now centered upon optimizing an asymmetric version of this addition with our bis(amidine) organocatalysts.

4.2 PBAM-Catalyzed Additions of Nitromethane into Trifluoromethyl Ketimine Centers

Acquisition of a manageable isolated yield was the first objective to be achieved when running this aza-Henry addition in an asymmetric fashion. This was done primarily by prolonging the reaction time and increasing the equivalents of nucleophile. When subjecting ketimine **82** to 2 equivalents of nitromethane and 50 mol% of PBAM (**19**) in toluene (0.1 M) at ambient temperature, minimal conversion to adduct **87** was seen after a 5 day reaction period (Scheme 51). Yet when the amount of nitromethane nucleophile was increased from 2 equivalents to 20 equivalents, the desired product was acquired in 26% isolated yield and -7% ee according to HPLC analysis. Although it is evident that more equivalents of nucleophile leads to product, no promising degree of enantioselection was observed with this new Boc-protected trifluoromethyl ketimine electrophile.

Scheme 51. Acquisition of Adduct **87** in Isolatable Yield

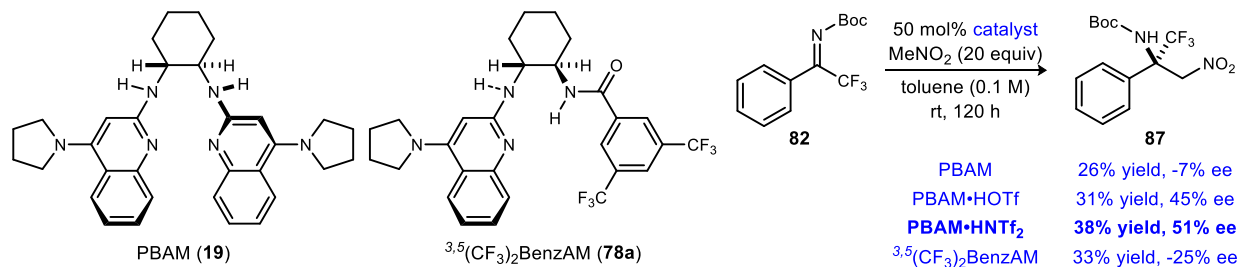


The next variable that was examined for this reaction system was the influence of added Brønsted acid. Previous studies have shown that the introduction of an acid salt to PBAM results in similar or increased levels of selectivity for a number of aza-Henry addition systems. When the triflic acid salt of PBAM (**19**•HOTf) was used as the catalyst for this system, adduct **87** was obtained in 31% yield and 45% ee, a considerably higher degree of enantioselectivity relative to PBAM free base (**19**) (Scheme 52). Upon submission of the triflimidic acid salt (PBAM•HNTf₂), the desired adduct was furnished in 38% yield and 51% ee, the highest enantioselection achieved to this point. These results show that the introduction of an acid not only reverses the direction of selectivity, it also results in a much higher level of enantioselection as well.

Additionally, one of the most optimal asymmetric amidine-amide catalysts, ^{3,5}(CF₃)₂BenzAM (**78a**), was tested in this aza-Henry system. For this particular case however, the catalyst did not fare as well as the traditional bis(amidine) catalysts as adduct **87** was acquired in

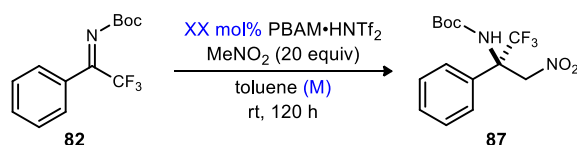
33% yield and -25% ee (Scheme 52). Needless to say, PBAM•HNTf₂ was the catalyst chosen to be carried onto further studies.

Scheme 52. Effects of Counterions and Asymmetric Catalysts



The effects of concentration and catalyst loading were the next two variables that were examined. Up to this point, acquisition of adduct **87** in 38% yield and 51% ee was the optimal result. This was achieved with a 50 mol% catalyst loading of PBAM•HNTf₂ and a 0.1 M concentration of toluene. When the solvent concentration was increased to 0.25 M, adduct **87** was furnished in 64% yield and 48% ee (Table 6, entry 2) indicating that increased concentrations lead to higher yields, but slightly diminished ee. Conversely, lowering the catalyst loading to 20 mol% results in a decrease in yield and a slight enhancement in selectivity as the desired adduct was afforded in 56% yield and 49% ee (entry 3). The reaction conditions used in entry 3 were carried into further studies.

Table 6. Effects of Concentration and Catalyst Loading



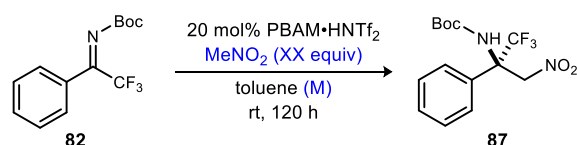
entry	M	mol%	yield (%)	ee (%)
1	0.1	50	38	51
2	0.25	50	64	48
3	0.25	20	56	49

With a 20 mol% catalyst loading of PBAM•HNTf₂, a more in-depth solvent concentration study was conducted. When increasing the concentration of toluene from 0.25 M to 0.5 M, a decrease in both yield and enantioselection was observed (Table 7, entry 2). Further increasing the concentration to 1 M resulted in a considerable increase in yield but a continued diminishment in ee as adduct **87** was acquired in 71% yield and 42% ee (entry 3). Due to the gradual decrease in

enantioselection upon increasing the concentration, 0.25 M was still considered to be the most optimal concentration at this point.

A more in-depth nucleophile equivalence study was also conducted. Although it was previously determined that going from 2 to 20 equivalents of nitromethane resulted in isolatable yields (Scheme 51), there was still the possibility that 20 equivalents of nucleophile may not be optimal as such an excess may result in catalyst deactivation by nitroalkane binding (e.g. solvation). Therefore, lesser amounts of nucleophile were examined to see if both yield and ee could be enhanced. When dropping the amount of nitromethane from 20 equivalents to 10 equivalents, a slight increase of enantioselection was achieved. In this same run however, a considerable drop in yield was also observed (Table 7, entry 5). Dropping the equivalents further to 5 equivalents of nitromethane resulted in lower yield and no change in enantioselection as adduct **87** was furnished in 29% yield and 51% ee (entry 6). Since the minimal increase in ee cannot account for the larger loss in yield, 20 equivalents of nitromethane was still considered to be the optimal amount of nucleophile at this point.

Table 7. In-Depth Concentration and Nitromethane Equivalence Studies



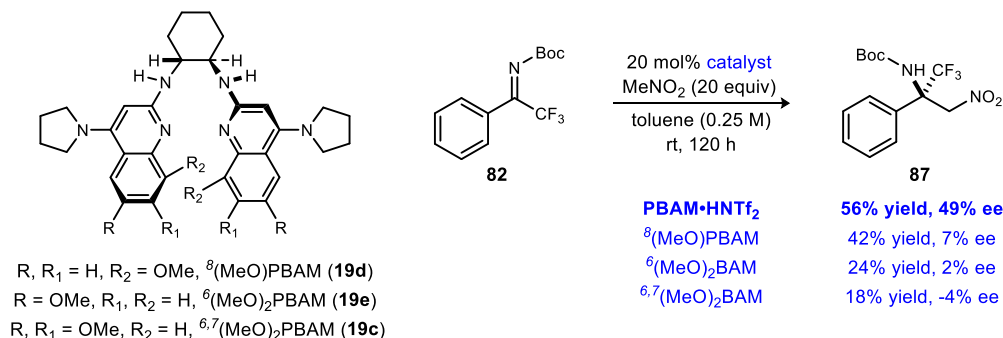
entry	M	MeNO ₂ equiv	yield (%)	ee (%)
1	0.25	20	56	49
2	0.5	20	53	45
3	1	20	71	42
4	0.25	20	56	49
5	0.25	10	47	51
6	0.25	5	29	51

*Entries 1 and 4 are the same data point

Other BAM catalysts with more Brønsted basic character were also tested to see if reactivity and selectivity could be enhanced. As previously mentioned, ⁸(MeO)PBAM was determined to be the most reactive catalyst for the tosyl ketimine aza-Henry system. When ⁸(MeO)PBAM was subjected to the trifluoromethyl ketimine aza-Henry addition, no improvement was seen as the intended product was obtained in only 42% yield and -7% ee (Scheme 53). Other available BAM catalysts of higher Brønsted basicity, such as ⁶(MeO)PBAM and ^{6,7}(MeO)₂PBAM,

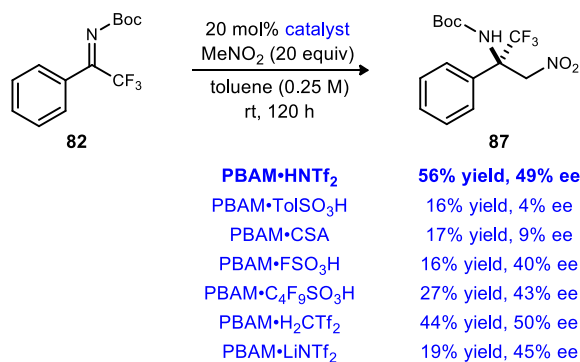
performed worse relative to δ (MeO)PBAM as the adduct was acquired in lower yields and minimal ee.

Scheme 53. Application of More Brønsted Basic BAM Catalysts



Studies continued with the examination of additional counterions. After submitting a number of sulfonic acid salts of PBAM to the aza-Henry system, none gave superior results relative to PBAM•HNTf₂ as the most optimal sulfonic acid salt, nonafluorosulfonic acid, afforded adduct **87** in 27% yield and 43% ee (Scheme 54). The bis(triflyl)methane salt (PBAM•CH₂Tf₂) appeared to be the only salt comparable to PBAM•HNTf₂ as this catalyst furnished the desired product in 44% yield and 50% ee. While the lithium triflimide analog (PBAM•LiNTf₂) gave a comparable ee value relative to the triflimidic acid salt (45% ee), a significant drop in yield was observed as the adduct was obtained in only 19% yield. The bis(triflyl)methane salt, along with PBAM•HNTf₂, was carried onto further studies due to similarity in catalyst behavior.

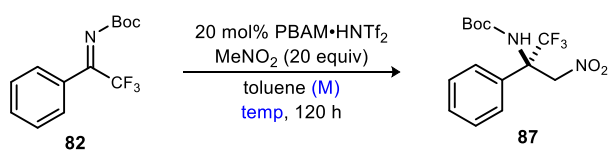
Scheme 54. Examination of Other Counterions



The next variable that was altered was temperature. Traditionally, lowering the temperature results in an increase in enantioselection. This trend held true for this particular reaction system. When the reaction temperature was lowered from room temperature to 0 °C, an increase in enantioselectivity was observed at the expense of decreased yield (Table 8, entry 2). Lowering the

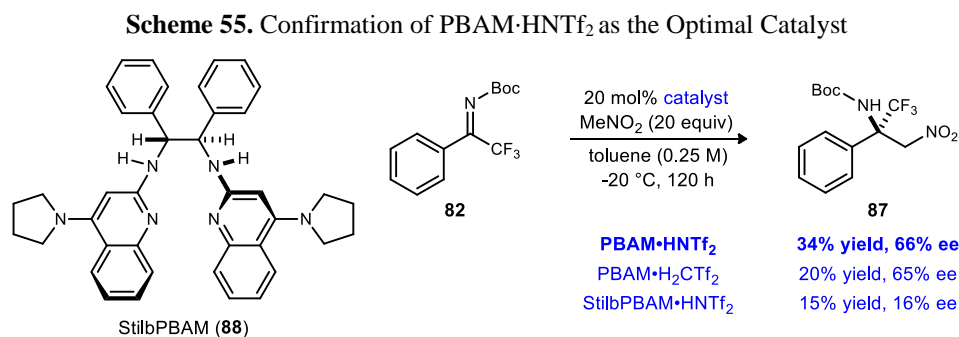
temperature to $-20\text{ }^{\circ}\text{C}$ had little effect on reactivity relative to $0\text{ }^{\circ}\text{C}$, yet higher enantioselection was observed as adduct **87** was afforded in 34% yield and 66% ee (entry 3). Unfortunately, when running this reaction at $-78\text{ }^{\circ}\text{C}$, reactivity was inhibited as minimal conversion was seen over the course of 5 days (entry 4). However, when repeating this run at a higher concentration (0.5 M), the desired product was obtained in 6% isolated yield and 80% ee (entry 5). Although this was the highest degree of selectivity observed for this system, $-20\text{ }^{\circ}\text{C}$ was chosen as this temperature provided a more fruitful and manageable yield. Thus, the most optimal reaction conditions up to date include a 20 mol% catalyst loading of PBAM•HNTf₂, 20 equivalents of nitromethane, a 0.25 M solvent concentration, and a temperature of $-20\text{ }^{\circ}\text{C}$.

Table 8. Effects of Temperature



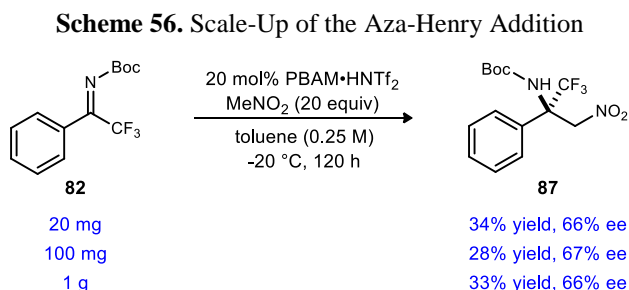
entry	temp. (°C)	M	yield (%)	ee (%)
1	25	0.25	56	49
2	0	0.25	36	59
3	-20	0.25	34	66
4	-78	0.25	<5	N/A
5	-78	0.5	6	80

Before this aza-Henry addition was conducted on a larger scale, it had to be reaffirmed that PBAM•HNTf₂ was the best catalyst under the chosen conditions. As previously shown, PBAM•CH₂Tf₂ showed comparable results at room temperature (Scheme 54). Yet when submitting the same catalyst under more chilled conditions, adduct **87** was afforded in only 20% yield and 65% ee, which proved to be inferior relative to PBAM•HNTf₂ (Scheme 55). Additionally, it had to be verified that the cyclohexane backbone of PBAM•HNTf₂ was indeed ideal. Upon subjecting a catalyst with a stilbene backbone, StilbPBAM•HNTf₂ (**88**•HNTf₂), to the aza-Henry



system, the intended product was furnished in 15% yield and 16% ee. These results confirm that PBAM·HNTf₂ is the best catalyst for this particular reaction.

A great degree of consistency was exhibited upon scaling up this aza-Henry addition. When using 20 mg of substrate, the desired adduct is acquired in 34% yield and 66% ee. The same degree of reactivity and selectivity is seen upon a 50 fold increase of electrophile. When submitting 1 gram of the ketimine, adduct **87** is furnished in 33% yield and 66% ee (Scheme 56). This consistency indicates that the aza-Henry adduct can be taken on to its corresponding Nutlin analog in gram quantities.



4.3 Progress Towards the Synthesis of a Trifluoromethyl Ketimine Nutlin Analog

Now that the asymmetric addition of nitromethane into trifluoromethyl ketimine **82** has been developed to a degree, efforts now shifted toward the synthesis of a trifluoromethyl Nutlin derivative. The desired analog, imidazoline **89**, is modified off of Nutlin-3 (**35**), a previously developed small molecule therapeutic. Target **89** and Nutlin-3 are similar in structure such that they both possess an imidazoline ring core with a urea functionality at the 1-position as well as aromatic substituents at the 2- and 5-positions. Key differences between the two molecules can also be seen. Target **89** possesses a trifluoromethyl quaternary center at the 5-position of the imidazoline where as the same position in Nutlin-3 is a methine. Furthermore, Nutlin-3 possesses an aromatic substituent at the 4-position, while target **89** consists of a fully saturated methylene

Figure 20. Structural Differences Between (-)-Nutlin-3 and Target **89**

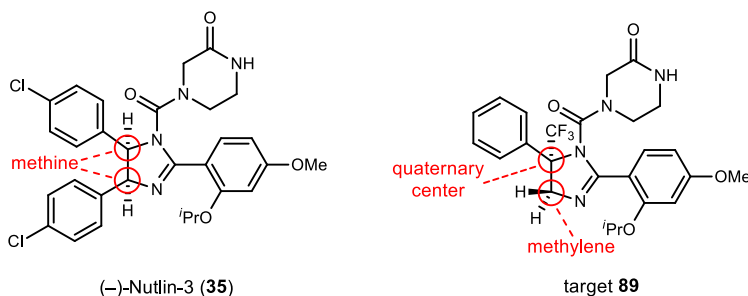
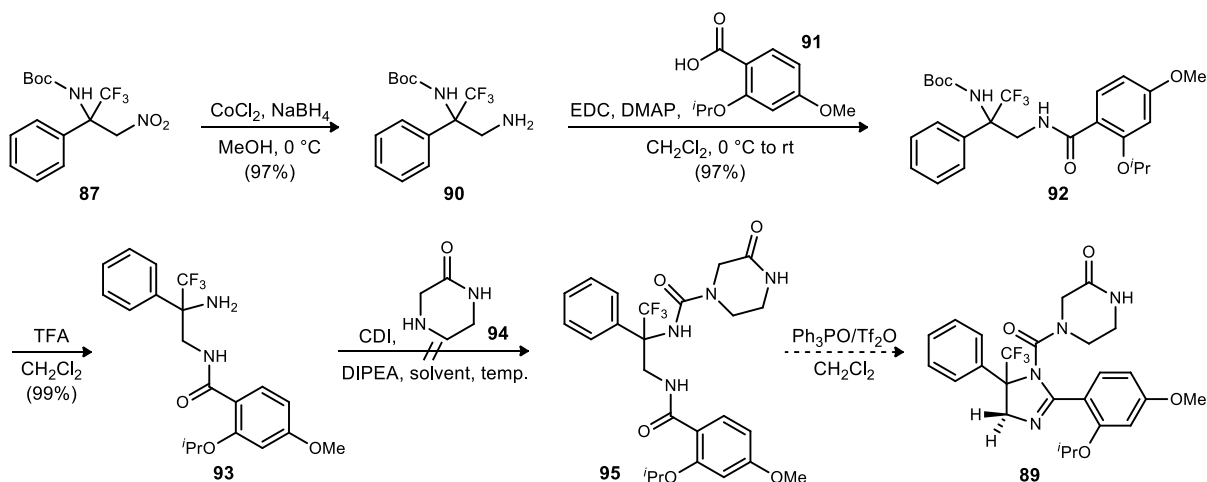


(Figure 20). Before synthesizing compound **89** in enantioenriched form however, a synthesis was to be developed and optimized using racemic material.

It was believed that imidazoline **89** could be readily synthesized via the same reaction sequence that was developed for the synthesis of Nutin-3.²¹ After acquisition of racemic aza-Henry adduct, nitroalkane **87** was reduced to free amine **90** in near quantitative yield upon treatment with CoCl_2 and NaBH_4 in the presence of MeOH (Scheme 57). Amide coupling of amine **90** with carboxylic acid **91** in the presence of EDC and DMAP proceeded smoothly as desired amide **92** was furnished in 97% isolated yield. Treatment of **92** with trifluoroacetic acid resulted in Boc-deprotection giving the intended amine (**93**) in quantitative yield. From here, it was envisioned that amine **93** could be treated with CDI resulting in a reactive isocyanate *in situ*. This isocyanate would then be treated with 2-oxopiperazine **94** affording urea **95**, which could then be taken onto imidazoline **89** via a subsequent chemoselective dehydrative cyclization reaction. Unfortunately, formation of urea **95** from tertiary amine **93** proved to be problematic.

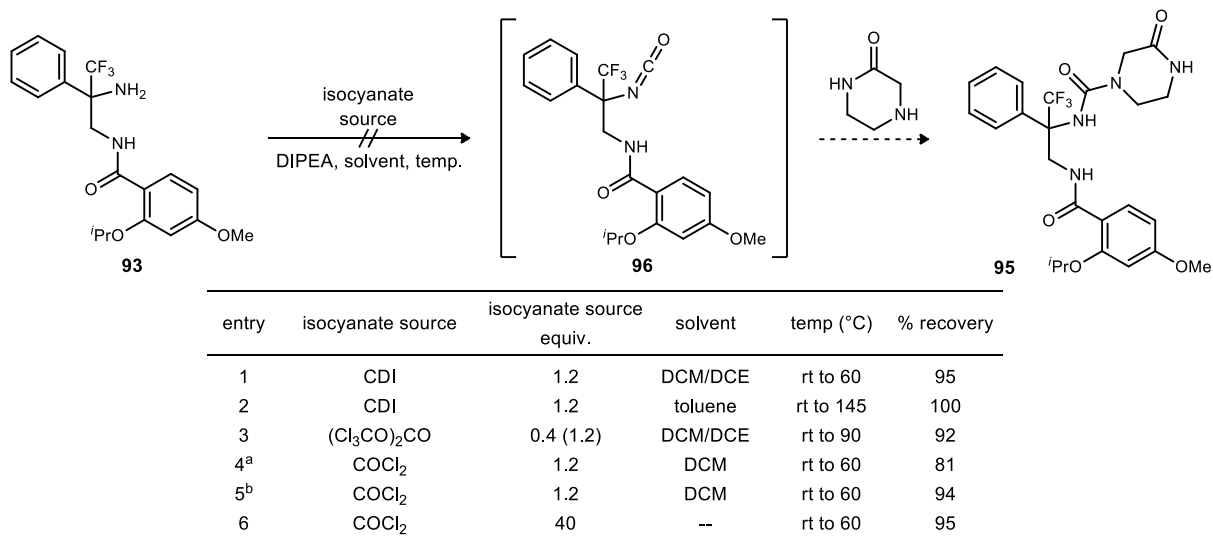
Scheme 57. Progress Toward the Synthesis of Target **89**



Amine **93** was treated with a variety of isocyanate sources under a number of reaction conditions in order to successfully develop the corresponding isocyanate *in situ*. Upon treating amine **93** with CDI, the isocyanate source used in the (-)-Nutlin-3 synthesis, no evidence of isocyanate formation could be detected even when heating to extreme temperatures (Table 9, entries 1 and 2). The use of triphosgene as the isocyanate source proved to be fruitless as no desired urea was formed at ambient as well as elevated temperatures (entry 3). Phosgene, the most reactive source of isocyanate, also yielded no signs of product when used both stoichiometrically and neat

(entries 4-6). Near-quantitative recoveries of starting material throughout these attempts further support the idea that no isocyanate is being formed *in situ*.

Table 9. Attempts Toward Forming Urea **95** Using Various Isocyanate Sources

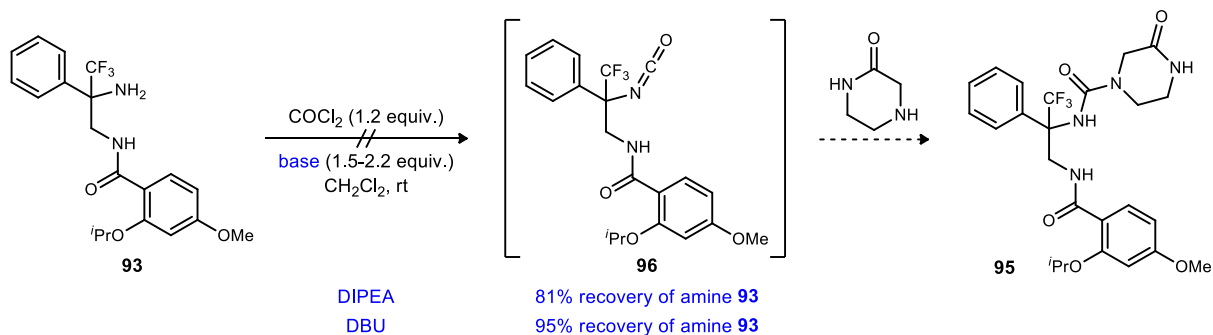


^a Amine, COCl₂, DCM, DIPEA stirred at rt before addition of piperazine

^b Amine, COCl₂, DCM, DIPEA heated to 60 °C before addition of piperazine

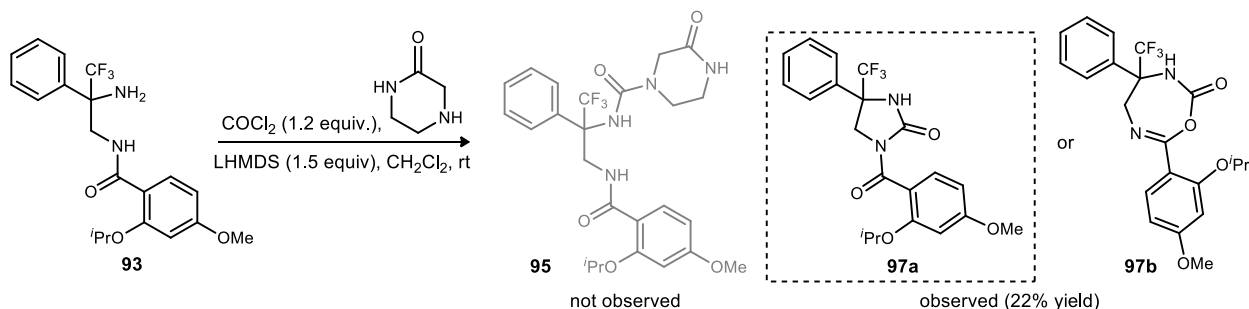
The lack of isocyanate formation with these simple electrophiles may be due to poor reactivity of amine **93**. The reduced reactivity can be a result of steric and electronic factors. When looking at sterics, amine **93** is a tertiary amine, which can create a high degree of congestion even when attacking an electrophile as simple as phosgene. As for electronics, this amine is within close proximity of an electron-withdrawing group. This inductive effect will reduce the basicity of the amine as a result. Therefore, measures had to be taken to increase the nucleophilicity of this amine. One direct approach would be to use bases stronger than *N,N*-diisopropylethylamine (DIPEA), such as DBU and LHMDS.

Scheme 58. Attempts Toward Forming Urea **95** via Isocyanate **96** with DIPEA and DBU



As previously shown, DIPEA was not sufficiently basic to promote the nucleophilicity needed to form the isocyanate *in situ* as starting material was consistently recovered in near-quantitative yields (Table 9). DBU, a stronger base, was also insufficient to initiate the reaction as no change by TLC analysis was detected over an extensive reaction period. In addition, starting amine was obtained in 95% recovery (Scheme 58). Yet when LHMDS was used as the base, a cyclic by-product was observed. Upon chromatographic separation, this heterocyclic by-product, identified either as cyclic urea **97a** or cyclic carbamate **97b**, was acquired in 22% isolated yield (Scheme 59). Although one-dimensional (^1H and ^{13}C) and two-dimensional (HSQC and HMBC) NMR techniques do not indicate a distinguishable difference between urea **97a** and carbamate **97b**, it is believed that the isolated by-product is the cyclic urea simply based on the increased favorability of a 5-membered ring system versus a 7-membered ring system. Furthermore, the chemical shift values observed in the ^{13}C NMR spectrum correspond more directly with reported values of a cyclic urea versus a cyclic carbamate.⁵⁸

Scheme 59. The Use of LHMDS and Isolation of a Cyclic By-Product

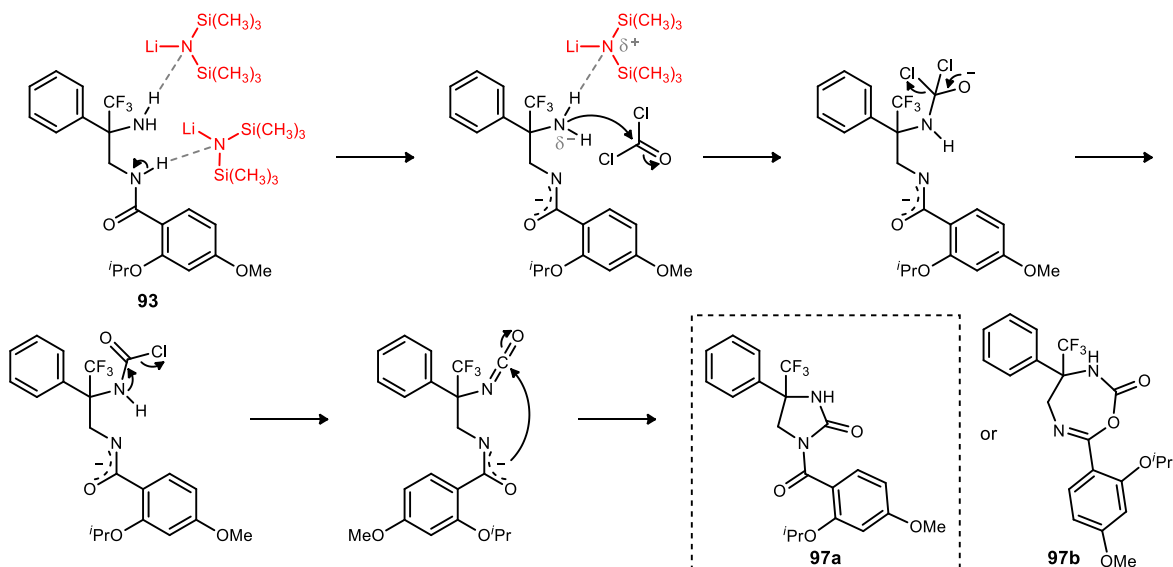


Despite what the correct structure of the cyclic by-product may be, acquisition of this heterocycle is encouraging in the sense that LHMDS is rendering amine **93** nucleophilic to promote reactivity. The proposed pathway toward the heterocyclic by-product begins with LHMDS both deprotonating the amide and activating the amine of **93**. This activated amine can readily react with phosgene generating isocyanate **96** *in situ*. Subsequent intramolecular attack of the amide functionality into isocyanate **96** affords cyclized by-product **97a** or **97b** as a result (Scheme 60). This intramolecular addition will be favored over intermolecular addition of piperazine **94**, hence why acyclic urea **95** was not observed in this case. At this point, conditions have not been found in which a base can promote the formation of isocyanate **96** without

⁵⁸ Pretsch, E.; Buhlmann, P.; Badertscher, M. *Structure Determination of Organic Compounds*; Springer: Berlin, 2009

subsequent intramolecular attack of the amide moiety. With this, efforts now shifted toward treating amine **93** with available isocyanate electrophiles.

Scheme 60. Proposed Mechanism Toward Heterocyclic By-Products



Reacting this amine with accessible isocyanates was seen as a direct way to introduce an acyclic urea functionality. The resulting ureas from these isocyanates could then be converted into desired urea **95** upon subsequent acylation with a 2-oxopiperazine nucleophile. One readily available isocyanate source that was of interest, and may ultimately allow for the synthesis of the desired piperazine urea, was phenyl isocyanate **98**.

Table 10. Synthesis of Urea **99** and Optimization

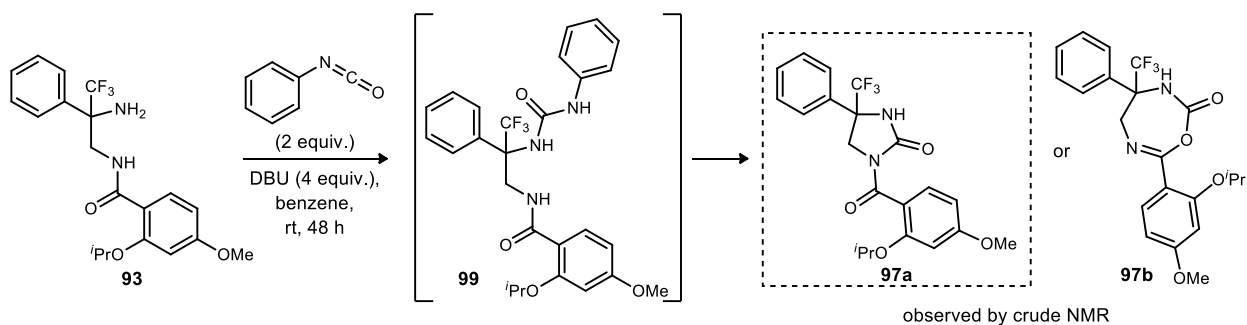
entry	isocyanate equiv.	solvent	conversion (%)	yield (%)
1	1.2	benzene	58	45
2	6	benzene	83	N/A
3	30	—	100	91

Phenyl isocyanate **98** proved to be a highly reactive species as sufficient conversion to urea **99** was achieved without the use of base. Upon treating amine **93** with a stoichiometric amount of

isocyanate according to literature protocol,⁵⁹ 58% conversion was seen by ¹H NMR over the course of 48 hours. This led to a 45% isolated yield of urea **99** upon chromatographic separation (Table 10, entry 1). Increasing the amount of isocyanate to 6 equivalents resulted in 83% conversion under the same reaction conditions (entry 2). No isolated yield was reported for this run, however. Using isocyanate **98** neat (30 equiv.) proved to be most optimal as full conversion to urea **99** was seen, leading to a 91% isolated yield (entry 3).

This addition of amine **93** into phenyl isocyanate was repeated once more with the incorporation of DBU. Here, it was believed that the presence of base will increase the nucleophilicity of the amine, which in turn would facilitate the addition and eliminate the need for excess electrophile. Based on this hypothesis, amine **93** was treated with 2 equivalents of isocyanate and 4 equivalents of DBU in the presence of benzene. Interestingly, after a 48 hour reaction period, the heterocyclic by-product (**97a** or **97b**) was once again observed instead of the intended urea (Scheme 61). Seeing this heterocycle by ¹H NMR indicates that urea **99** was formed *in situ* followed by intramolecular acylation with the amide functionality. The observed acylation also shows that aniline is an efficient leaving group. This finding was beneficial as acylation attempts en route to piperazine urea **95** could be conducted using 2-oxopiperazine as the nucleophile.

Scheme 61. Formation of a Heterocyclic By-Product via Urea **99**

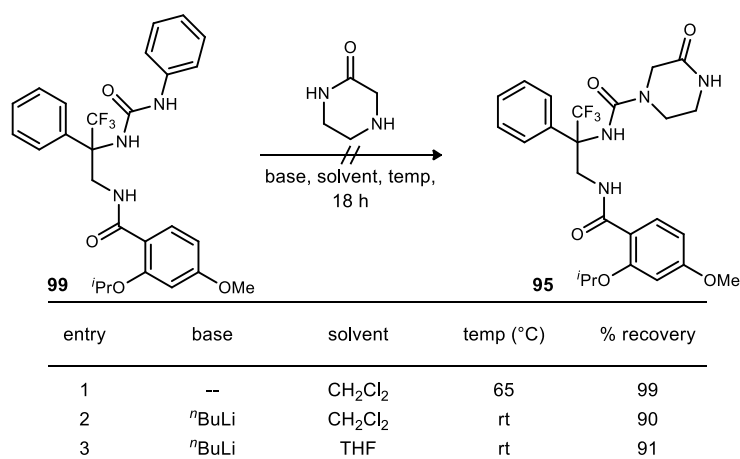


Acylation attempts toward desired urea **95** began when phenyl urea **99** and 2-oxopiperazine were heated to 65 °C in DCM over the course of 18 hours. This attempt proved to be fruitless as starting urea was acquired in 99% recovery (Table 11, entry 1). The lack of conversion prompted the use of a strong base in order to enhance the nucleophilicity of piperazine **94**. Therefore, the next acylation attempt involved treating the piperazine with *n*-butyllithium before introducing

⁵⁹ Ito, A.; Muratake, H.; Shudo, K. *Chem. Pharm. Bull.* **2010**, 58, 82-86.

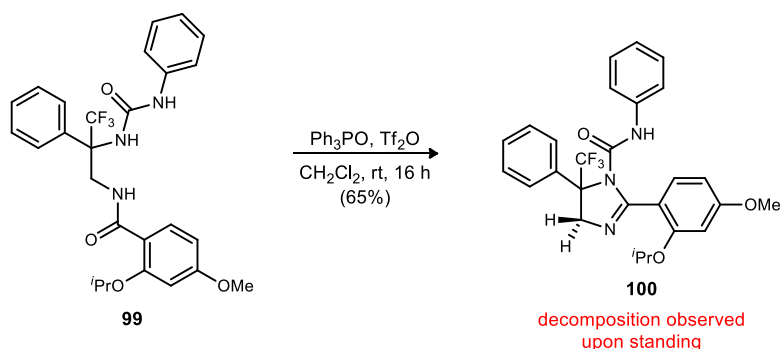
phenyl urea **99**. After an 18 hour reaction period with DCM as the solvent, no conversion was seen by ^1H NMR (entry 2). One potential problem that may be causing the lack of conversion is that the piperazine motif was not readily dissolving. Taking into account that this solubility issue may revolve around the solvent type, the previous reaction was repeated with THF as the solvent. Once again, the piperazine failed to dissolve resulting in no conversion to piperazine urea **95** as starting material was recovered in 91% yield (entry 3). Seeing that piperazine **94** was not soluble in both DCM and THF, it was then hypothesized that the solubility of the piperazine is substrate dependent rather than solvent dependent.

Table 11. Failed Acylation Attempts En Route to Piperazine Urea **95**



Taking into consideration that piperazine solubility may be dependent on the substrate, phenyl urea **99** was carried onto its corresponding imidazoline. The chemoselective dehydrative cyclization proceeded smoothly as treatment of urea **99** with triphenylphosphine oxide and triflic anhydride afforded imidazoline **100** in 65% isolated yield over the course of 16 hours (Scheme 62). One benefit of synthesizing this imidazoline ring core is that there is no competing amide

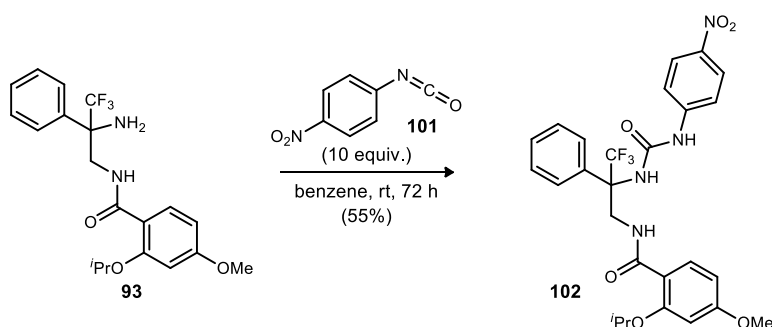
Scheme 62. Chemoselective Dehydrative Cyclization to Imidazoline **100**



functionality when it comes to a subsequent acylation attempt with 2-oxopiperazine **94**. Unfortunately, imidazoline **100** proved to be unstable upon standing as decomposition was observed by ^1H NMR. Thus, no acylations with this substrate could be attempted.

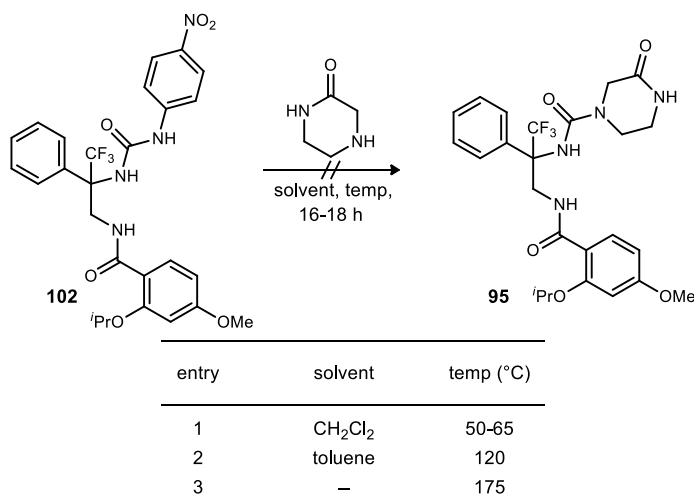
The inability to form desired piperazine urea **95** may be a direct result of insufficient electrophilicity of the phenyl urea precursor. A potential solution would be to form a more activated urea as this would facilitate the acyl substitution with the oxopiperazine nucleophile. One species that would allow for a more electrophilic urea is 4-nitrophenyl isocyanate **101**, as this motif possesses an electron-withdrawing nitro group. Treatment of free amine **93** with 10 equivalents of 4-nitrophenyl isocyanate in the presence of benzene afforded the desired nitrophenyl urea (**102**) in 55% yield after 3 days (Scheme 63). With this more reactive nitrophenyl urea in hand, the stage was now set for subsequent acylation attempts with piperazine **94**.

Scheme 63. Synthesis of Nitrophenyl Urea **102**



The first acylation attempt with this new nitrophenyl urea involved heating urea **102** and piperazine **94** to 65 °C in the presence of DCM. No conversion to the desired piperazine urea was

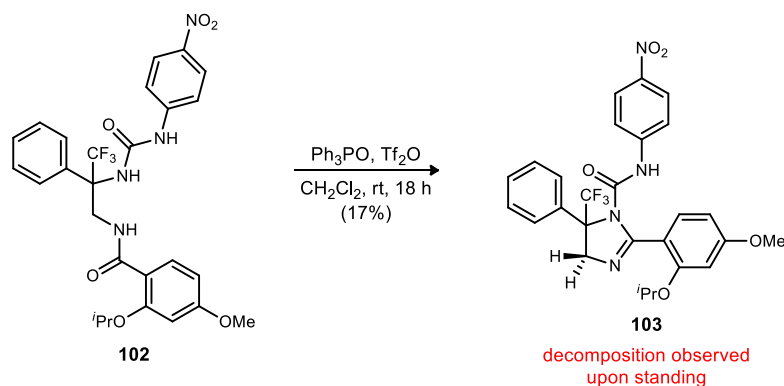
Table 12. Failed Acylation Attempts with Nitrophenyl Urea **102**



seen over an 18 hour reaction period as starting material was recovered in near-quantitative yield (Table 12, entry 1). Heating these reagents to 120 °C in the presence of toluene also resulted in no conversion (entry 2). Another acylation attempt involved heating urea **102** and piperazine **94** to 175 °C without the presence of solvent. Once again, no sign of the desired piperazine urea (**95**) could be detected after 18 hours (entry 3).

These failed acylation attempts with nitrophenyl urea **102** prompted us to convert this substrate to its corresponding imidazoline. Once again, the chemoselective dehydrative cyclization was successful as imidazoline **103** was furnished in 17% isolated yield after 18 hours (Scheme 64). Unfortunately, as seen with imidazoline **100**, this Nutlin derivative was also prone to decomposition upon standing. Again, no acylation attempts with imidazoline **103** could be attempted.

Scheme 64. Chemoselective Dehydrative Cyclization to Imidazoline **103**



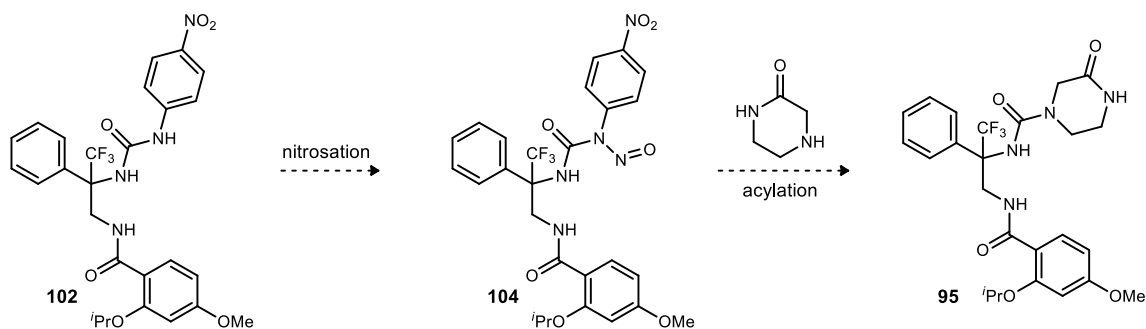
4.4 Future Work

As previously discussed, intramolecular acylation attempts with a 2-oxopiperazine nucleophile proved to be unsuccessful even with a highly electrophilic 4-nitrophenyl urea moiety. Therefore, other measures had to be taken in order to promote the desired acylation en route to piperazine urea **95**. One approach would be to further activate urea **102** via nitrosation. Nitrosations prove to be an effective method of amide activation as they can provide an electrophilic amide for hydrolysis (saponification). Evans demonstrated this in his total synthesis of vancomycin where nitrosation of a methyl amide led to a mild, late stage saponification.⁶⁰ Herein, we are hoping to

⁶⁰ Evans, D. A.; Wood, M. R.; Trotter, B. W.; Richardson, T. I.; Barrow, J. C.; Katz, J. L. *Angew. Chem. Int. Ed.* **1998**, *37*, 2700-2704.

activate the nitroaniline portion of urea **102** so that intramolecular acylation with piperazine **94** can be achieved with this highly reactive electrophile (Scheme 65).

Scheme 65. Proposed Nitrosation Route Towards the Desired Piperazine Urea



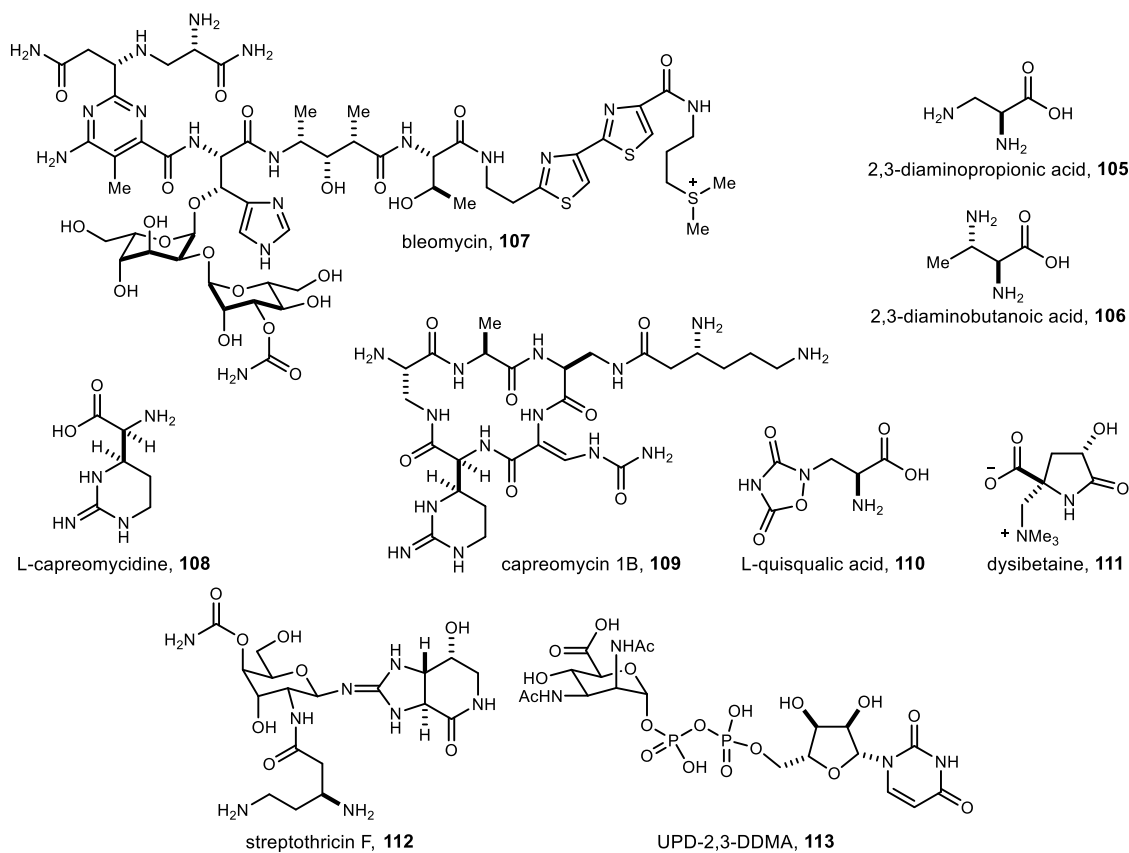
If acylation attempts via this nitrosation method are indeed successful, the resulting urea **95** can be carried onto its corresponding Nutlin derivative (**89**) via a chemoselective dehydrative cyclization. Once the desired Nutlin analog has been successfully synthesized with the racemate, the same synthetic route can be repeated with the enantioenriched material. This will lead us to our ultimate goal, which is to synthesize **89** as a single enantiomer.

Chapter 5. Oxidative Inter-/Intermolecular Alkene Diamination of Hydroxy Styrenes with Electron-Rich Amines via Hypervalent Iodine⁶¹

5.1. Background

1,2-Diamines are ubiquitous among natural products, pharmaceutical agents, chiral ligands and bases, and other organic reagents. The biological activity associated with many of these systems and their synthetic utility has ensured that the development of new methods for the preparation of vicinal diamines is of high importance.⁶² To date, many synthetic strategies for the preparation of 1,2-diamine scaffolds have been established, facilitating access to naturally occurring vicinal diamines and those within pharmaceuticals.

Figure 21. Naturally Occurring, Non-Proteinogenic *vic*-Diamino Acids and Their Derivatives



In the natural world, vicinal diamines are commonly found in the form of non-proteinogenic α,β -diamino carboxylic acids.⁶² The simplest members of this group include 2,3-diaminopropionic acid (**105**) and 2,3-diaminobutanoic acid (**106**), which can be found as

⁶¹ Danneman, M. W.; Hong, K.; Johnston, J. N. *Org. Lett.* **2015**, *17*, 2558-2561.

⁶² De Jong, S.; Nosal, D. G.; Wardrop, D. J. *Tetrahedron* **2012**, *68*, 4067-4105.

components of non-ribosomal peptide antibiotics such as bleomycin (**107**) (Figure 21).⁶³ L-Capreomycin (**108**), a key structural subunit of the tuberculostatic agent capreomycin 1B (**109**), has also been identified as a component of non-ribosomal peptides.⁶⁴ Additionally, certain α,β -diamino acids are of considerable interest due to their biological role as excitatory amino acids (EAA). L-Quisqualic acid (**110**), isolated from the traditional Chinese medicine Shih-chun-tze, is a highly potent agonist of EAA receptors in both mammals and insects.⁶² (-)-Dysibetaine (**111**), isolated from the marine sponge *Dysidea herbacea*, is also a neuroexcitotoxin, which may bind to the glutamate receptors present in the central nervous system of mice.⁶⁵ Other α,β -diamino acids include streptothricin F (**112**), an antibiotic,⁶⁶ and nucleotide sugar UDP-2,3-diacetamido-2,3-dideoxy-D-mannuronic acid (UDP-2,3-DDMA) (**113**), a key building block in the biosynthesis of the lipopolysaccharide of *Pseudomonas aeruginosa*, an opportunistic pathogen.⁶⁷

Numerous alkaloid natural products are known to possess 1,2-diamine scaffolds that are associated with significant biological activity. Loline (**114**), a pyrrolizidine alkaloid, is known for its insecticidal activity,⁶⁸ while the pentacyclic citrinadin A (**115**) exhibits cytotoxicity against murine leukemia L1210 and human epidermoid carcinoma KB cell lines (Figure 22).⁶⁹ The vicinal diamine moiety is also present in tetrahydroisoquinoline-derived alkaloids, such as lemomycin (**116**), an antitumor antibiotic.⁷⁰ Pactamycin (**117**), a terrestrial alkaloid isolated from a fermentation broth of *Streptomyces pactum*, exhibits activity against Gram-positive and Gram-negative bacteria.⁷¹ In addition to terrestrial sources, marine organisms have proven to be a rich source of biologically active 1,2-diamines as well. These marine alkaloids include the antineoplastic agent agelastatin A (**118**),⁷² anti-tuberculosis agent manadomanzamine A (**119**),⁷³

⁶³ Galm, U.; Hager, M. H.; Van Lanen, S. G.; Ju, J.; Thorson, J. S.; Shen, B. *Chem. Rev.* **2005**, *105*, 739-758.

⁶⁴ DeMong, D. E.; Williams, R. M. *J. Am. Chem. Soc.* **2003**, *125*, 8561-8565.

⁶⁵ Sakai, R.; Oiwa, C.; Takaishi, K.; Kamiya, H.; Tagawa, M. *Tetrahedron Lett.* **1999**, *40*, 6941-6944.

⁶⁶ Jackson, M. D.; Gould, S. J.; Zabriskie, M. T. *J. Org. Chem.* **2002**, *67*, 2934-2941.

⁶⁷ (a) Wenzel, C. Q.; Daniels, C.; Keates, R. A. B.; Brewer, D.; Lam, J. S. *Mol. Microbiol.* **2005**, *57*, 1288-1303; (b) Larkin, A.; Imperiali, B. *Biochemistry* **2009**, *48*, 5446-5455.

⁶⁸ Schardl, C. L.; Grossman, R. B.; Nagabhyru, P.; Faulkner, J. R.; Mallik, U. P. *Phytochemistry* **2007**, *68*, 980-996.

⁶⁹ (a) Tsuda, M.; Kasai, Y.; Komatsu, K.; Sone, T.; Tanaka, M.; Mikami, Y.; Kobayashi, J. *Org. Lett.* **2004**, *6*, 3087-3089; (b) Mugishima, T.; Tsuda, M.; Kasai, Y.; Ishiyama, H.; Fukushi, E.; Kawabata, J.; Watanabe, M.; Akao, K.; Kobayashi, J. *J. Org. Chem.* **2005**, *70*, 9430-9435.

⁷⁰ Ashley, E. R.; Cruz, E. G.; Stoltz, B. M. *J. Am. Chem. Soc.* **2003**, *125*, 15000-15001.

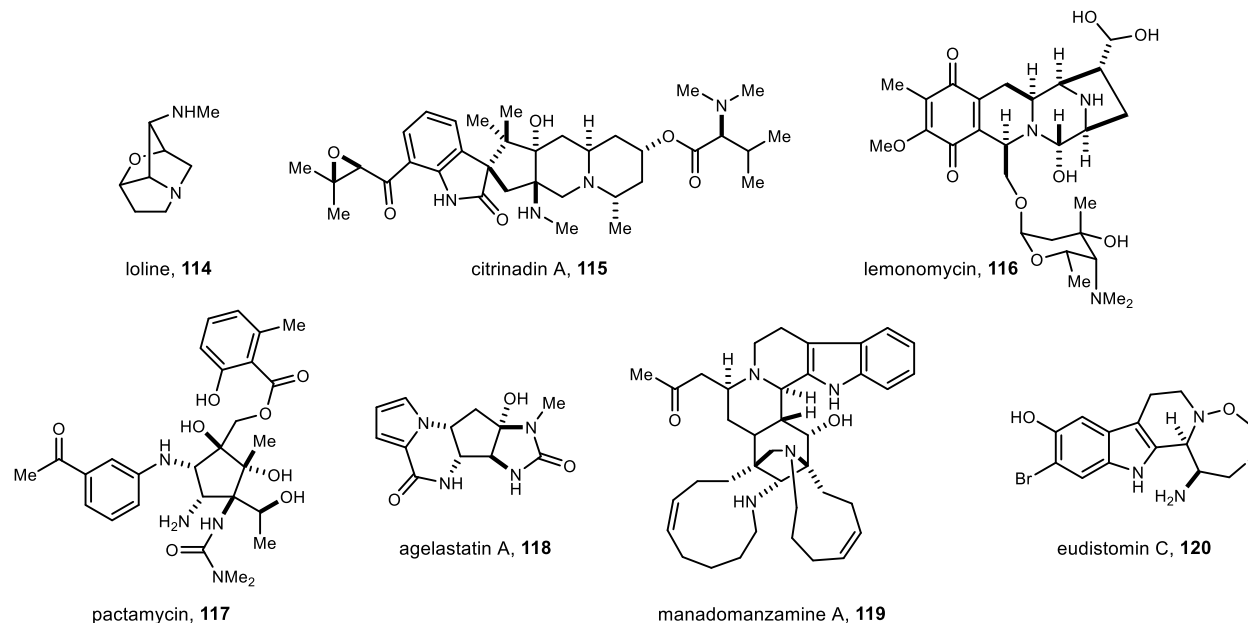
⁷¹ Hanessian, S.; Vakiti, R. R.; Dorich, S.; Banerjee, S.; Lecomte, F.; DelValle, J. R.; Zhang, J.; Deschenes-Simard, B. *Angew. Chem. Int. Ed.* **2011**, *50*, 3497-3500.

⁷² Hama, N.; Matsuda, T.; Sato, T.; Chida, N. *Org. Lett.* **2009**, *11*, 2687-2690.

⁷³ Allin, S. M.; Duffy, L. J.; Towler, J. M. R.; Page, P. C. B. Elsegood, M. R. J.; Saha, B. *Tetrahedron* **2009**, *65*, 10230-10234.

and eudistomin C (**120**), a member of the eudistomin family that displays activity against both RNA and DNA viruses.⁷⁴

Figure 22. Examples of Naturally Occurring Alkaloids That Possess the 1,2-Diamine Framework



Vicinal diamines are also found in a wide array of pharmaceutical agents. For example, fluoroquinolone antibacterial agent moxifloxacin (**121**)⁷⁵ and anticancer agent **122**⁷⁶ both possess a 1,2-diamine functionality within conformationally restricted bicyclononane ring systems (Figure 23). Target compound Sch 425078 (**123**), an anti-emetic agent and NK₁-antagonist, contains a 1,2-diamine framework in the form of a cyclic urea.⁷⁷ α -Galactosylceramide analog HS161 (**124**) is a potent stimulator of invariant natural killer T cells,⁷⁸ while sphingoid analog SG14 (**125**) is a specific inhibitor of human sphingosine kinase, an emerging target for cancer therapeutics.⁷⁹ Furthermore, stilbene diamine derivative **126** has been shown to be a potent inhibitor of hepatitis C virus RNA replication,⁸⁰ whereas *cis*-imidazoline Nutlin-3 (**35**) exhibits anticancer activity via

⁷⁴ Yamashita, T.; Kawai, N.; Tokuyama, H.; Fukuyama, T. *J. Am. Chem. Soc.* **2005**, *127*, 15038-15039.

⁷⁵ De Souza, M. V. N.; Vasconcelos, T. R. A.; De Almeida, M. V.; Cardoso, S. H. *Curr. Med. Chem.* **2006**, *13*, 455-463.

⁷⁶ Geiger, C.; Zelenka, C.; Weigl, M.; Frohlich, R.; Wibbeling, B.; Lehmkühl, K.; Schepmann, D.; Grunert, R.; Bednarski, P. J.; Wunsch, B. *J. Med. Chem.* **2007**, *50*, 6144-6161.

⁷⁷ Reichard, G. A.; Stengone, C.; Paliwal, S.; Mergelsberg, I.; Majmundar, S.; Wang, C.; Tiberi, R.; McPhail, A. T.; Piwinski, J. J.; Shih, N. Y. *Org. Lett.* **2003**, *5*, 4249-4251.

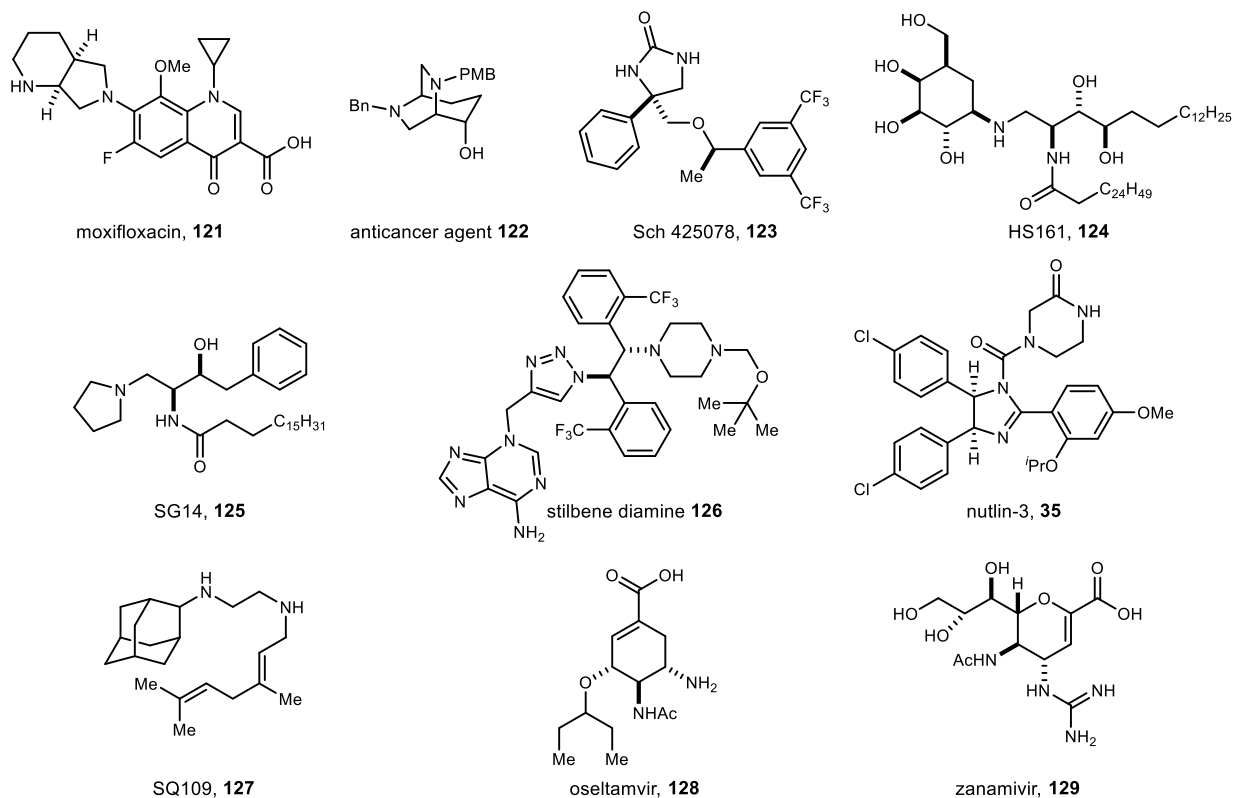
⁷⁸ Harrak, Y.; Barra, C. M.; Delgado, A.; Castano, A. R.; Llebaria, A. *J. Am. Chem. Soc.* **2011**, *133*, 12079-12084.

⁷⁹ Kim, J. W.; Kim, Y. W.; Inagaki, Y.; Hwang, Y. A.; Mitsutake, S.; Ryu, Y. W.; Lee, W. K.; Ha, H. J.; Park, C. S.; Igarashi, Y. *Bioorg. Med. Chem.* **2005**, *13*, 3475-3485.

⁸⁰ Gastaminza, P.; Pitram, S. M.; Dreux, M.; Krasnova, L. B.; Whitten-Bauer, C.; Dong, J.; Chung, J.; Fokin, V. V.; Sharpless, K. B.; Chisari, F. V. *J. Virol.* **2011**, *85*, 5513-5523.

MDM2-p53 protein-protein inhibition.^{81,82} Other small molecule therapeutics bearing vicinal diamines include ethambutol analog SQ109 (**127**), which shows potent activity against multi-drug resistant tuberculosis,⁸³ as well as viral neuraminidase inhibitors oseltamivir (**128**)⁸⁴ and zanamivir (**129**),⁸⁵ which are used for the treatment of influenza A and B.

Figure 23. Pharmaceutically Active, Synthetic 1,2-Diamines



5.2. Known Methods of Alkene Diamination

As previously mentioned, there are many known strategies for the preparation of 1,2-diamine scaffolds. The most direct and efficient means of accessing these systems is through the diamination of alkenes. Alkene diamination is an area that has been explored extensively, and as a result, can be achieved via a variety of methods.

⁸¹ Vassilev, L. T.; Vu, B. T.; Graves, B.; Carvajal, D.; Podlaski, F.; Filipovic, Z.; Kong, N.; Kammlott, U.; Lukacs, C.; Klein, C.; Fotouhi, N.; Liu, E. A. *Science* **2004**, *303*, 844-848.

⁸² Davis, T. A.; Johnston, J. N. *Chem. Sci.* **2011**, *2*, 1076-1079.

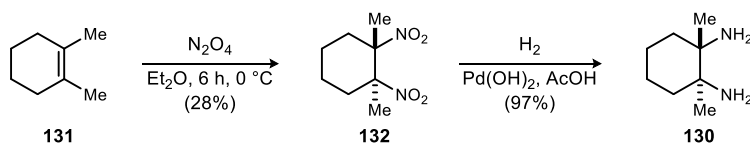
⁸³ Protopopova, M.; Hanrahan, C.; Nikonenko, B.; Samala, R.; Chen, P.; Gearhart, J.; Einck, L.; Nacy, C. A. *J. Antimicrob. Chemother.* **2005**, *56*, 968-974.

⁸⁴ Magano, J. *Tetrahedron* **2011**, *67*, 7875-7899.

⁸⁵ Magano, J. *Chem. Rev.* **2009**, *109*, 4398-4438.

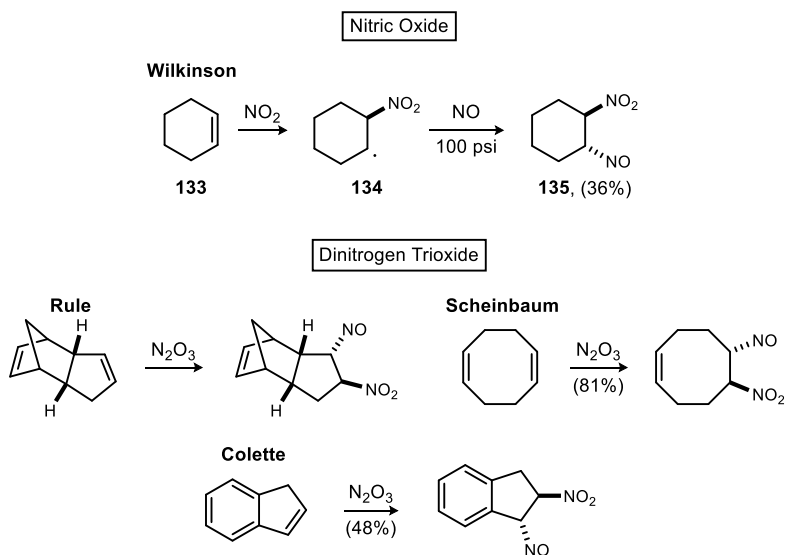
One method of diamination involves the treatment of alkenes with binary nitrogen oxides. Jacobsen demonstrated the efficiency of these nitrogen oxides by using dinitrogen tetroxide (N_2O_4) to ultimately arrive at C_2 -symmetric *trans*-1,2-diamine **130** (Scheme 66).⁸⁶ Here, the reaction of N_2O_4 with dimethylcyclohexene **131** under chilled conditions affords dinitro species **132** as the *trans*-diastereomer. Subsequent palladium-mediated hydrogenation of **132** yielded desired diamine **130**, which was resolved by way of its mandelate salt.

Scheme 66. Jacobsen's Synthesis of Diamine **130** via Dinitrogen Tetroxide



Wilkinson and colleagues have successfully conducted the nitronitrosylation of alkenes under medium pressure (Scheme 67).⁸⁷ This reaction was readily achieved by the disproportionation of nitric oxide (NO) to nitrous oxide (N_2O) and nitrogen dioxide (NO_2). Mechanistically, it is envisioned that this transformation proceeds through a radical pathway in

Scheme 67. Nitronitrosylations of Alkenes with Nitric Oxide and Dinitrogen Trioxide



which NO_2 adds to alkene **133**, generating a β -nitro radical (**134**). This radical can then trap NO at 100 psi to arrive at nitronitrosylation product **135**. To complement these findings, dinitrogen trioxide (N_2O_3) can be effectively employed for nitronitrosylation of alkenes as well (Scheme 67).

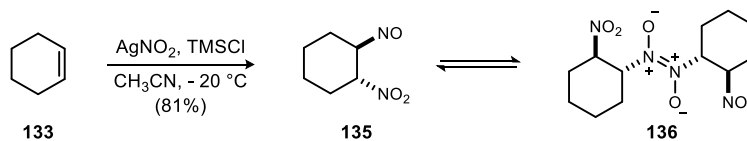
⁸⁶ Zhang, W.; Jacobsen, E. N. *Tetrahedron Lett.* **1991**, 32, 1711-1714.

⁸⁷ Chiu, K. W.; Savage, P. D.; Wilkinson, G.; Williams, D. J. *Polyhedron* **1985**, 4, 1941-1945.

This particular transformation is well documented and is compatible with a range of cyclic alkenes and dienes including dicyclopentadiene,⁸⁸ cyclooctadiene,⁸⁹ and indenes.⁹⁰

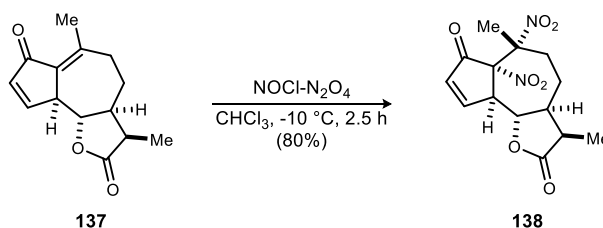
Alkene nitronitrosylation has also been achieved via the *in situ* generation of nitrogen oxides. Demir and Findik have reported a convenient method in which silver nitrite (AgNO₂) and trimethylsilyl chloride (TMSCl) can be used for the generation of N₂O₃.⁹¹ Treatment of alkenes, such as cyclohexene (**133**), with this AgNO₂-TMSCl combination in acetonitrile ultimately affords the desired β-nitroso-nitrite compounds and their corresponding dimers (Scheme 68).

Scheme 68. Alkene Nitronitrosylation via *In Situ* Generation of N₂O₃ with AgNO₂/TMSCl



Adekenov and co-workers made a serendipitous discovery in which alkene dinitration can be promoted via the combination of nitrosyl chloride and N₂O₄. Although it is well known that the treatment of alkenes with nitrosyl chloride almost exclusively leads to β-nitroso chlorides, bisnitration is favored when N₂O₄ is present, even as a minor impurity. Adekenov demonstrated this phenomenon through the dinitration of terpenes. Upon exposure of achillin (**137**) to this nitrosyl chloride-nitrogen oxide system, the corresponding 1,2-dinitro compound (**138**) was afforded in 37% isolated yield. Higher rates and yields (80%) were observed with increasing amounts of N₂O₄ (Scheme 69).⁹²

Scheme 69. Dinitration of Unsaturated Terpene Achillin (**137**) with Nitrosyl Chloride and Dinitrogen Tetroxide



⁸⁸ Rule, A. *J. Chem. Soc. Trans.* **1908**, 93, 1560-1564.

⁸⁹ Scheinbaum, M. L. *J. Org. Chem.* **1970**, 35, 2785-2790.

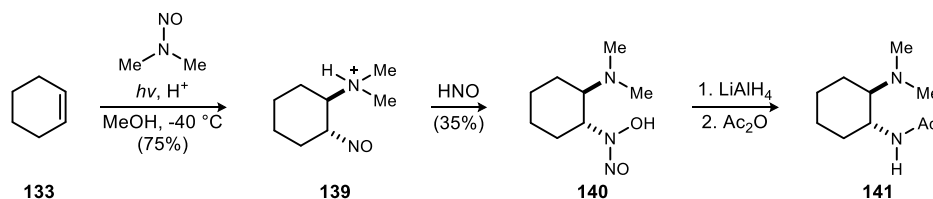
⁹⁰ Colette, M.; Perrot, R. *Helv. Chim. Acta.* **1977**, 60, 2089-2098.

⁹¹ Demir, A. S.; Findik, H. *Lett. Org. Chem.* **2005**, 2, 602-604.

⁹² Adekenov, S. M.; Alebastrov, O. V.; Raldugin, V. A.; Bagryanskaya, I. Y.; Gatilov, Y. V.; Shakirov, M. M.; Kulyyasov, A. T.; Tolstikov, G. A. *Chem. Nat. Compd.* **2001**, 37, 228-233.

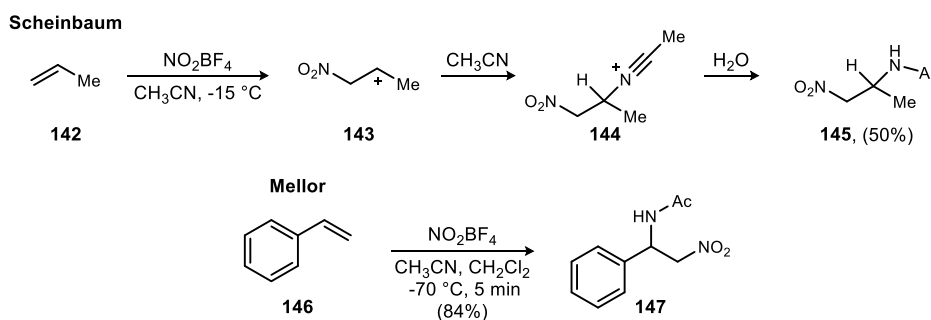
Another synthesis of vicinal diamines from alkenes utilizes photochemistry, as reported by Chow.^{93,94,95,96} Photolysis of cyclohexene (**133**), in the presence of a stoichiometric amount of *N*-nitrosodimethylamine, can generate *trans*-addition product **139** in high yield (Scheme 70). Subsequent treatment of **139** with hyponitrous acid (HNO) furnishes nitrosohydroxylamine **140**, which can then be reduced and acylated to arrive at diamine **141**.

Scheme 70. Photoaddition of *N*-Nitrosodimethylamine with Cyclohexene (**133**) en Route to Masked Diamine **141**



Nitroamidation is also an efficient means for alkene diamination. Scheinbaum illustrates this concept by reacting alkenes with nitronium tetrafluoroborate (NO_2BF_4) in acetonitrile in order to synthesize α -nitro amides.⁹⁷ For example, when propene (**142**) is treated with NO_2BF_4 , carbocation **143** is formed. Acetonitrile traps this intermediate, generating nitrilium ion **144**, which undergoes hydrolysis to give the desired nitroamidation product (**145**), albeit in moderate yield (Scheme 71).⁹⁸ Mellor and colleagues expanded on this nitroamidation method by transforming a wider range of substrates, particularly styrenes, to their corresponding nitroamides with higher yields through the use of CH_2Cl_2 as a co-solvent. Styrene (**146**) itself was readily converted to nitroamide **147** in 84% isolated yield.⁹⁹

Scheme 71. Nitroamidation of Alkenes with Nitrogen Tetrafluoroborate and Acetonitrile



⁹³ Chow, Y. L.; Chen, S. C.; Chang, D. W. L. *Can. J. Chem.* **1970**, *48*, 157-162.

⁹⁴ Chow, Y. L.; Chen, S. C.; Chang, D. W. L. *Can. J. Chem.* **1971**, *49*, 3069-3071.

⁹⁵ Chow, Y. L.; Perry, R. A.; Menon, B. C.; Chen, S. C. *Tetrahedron Lett.* **1971**, *12*, 1545-1548.

⁹⁶ Pillay, K. S.; Chen, S. C.; Mojelsky, T.; Chow, Y. L. *Can. J. Chem.* **1975**, *53*, 3014-3021.

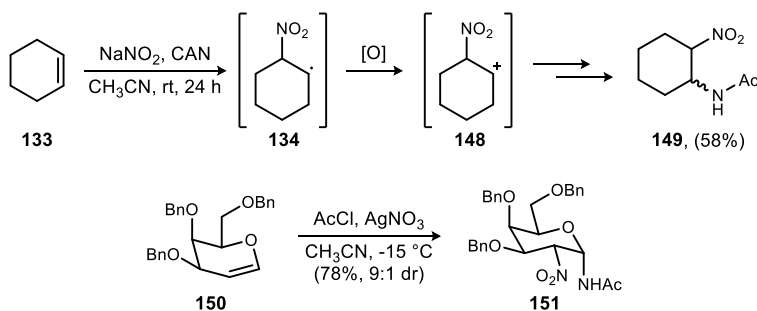
⁹⁷ Scheinbaum, M. L.; Dines, M. *J. Org. Chem.* **1971**, *36*, 3641-3642.

⁹⁸ Bach, R. D.; Holubka, J. W.; Badger, R. C.; Rajan, S. J. *J. Am. Chem. Soc.* **1979**, *101*, 4416-4417.

⁹⁹ Bloom, A. J.; Fleischmann, M.; Mellor, J. M. *J. Chem. Soc., Perkin Trans. 1* **1984**, 2357-2362.

Other reagent combinations are known to promote nitroamidation of alkenes. Vankar and co-workers have developed a nitroamidation method that involves the treatment of alkenes with ceric ammonium nitrate (CAN) and sodium nitrite (NaNO_2) in acetonitrile.¹⁰⁰ Oxidation of nitrite under these conditions generates nitrogen dioxide, which adds to cyclohexene (**133**), forming β -nitroalkyl radical **134**. One-electron oxidation with CAN gives carbocation **148**, which subsequently undergoes a Ritter reaction to give nitroamide **149**. Vankar has also employed an acetyl chloride, silver nitrate (AgNO_3), and acetonitrile reagent combination for the nitroamidation of glycols and other alkenes (Scheme 72). Good yield and d.r. is demonstrated though the conversion of benzylated glycol **150** to nitroamide **151** under these reaction conditions.¹⁰¹

Scheme 72. Vankar's Alkene Nitroamidation Methods



Iron-mediated redox chemistry has proven effective for the synthesis of 1,2-diamines, most notably through the bis-azidation of alkenes. Minisci and colleagues illustrated this phenomenon via a ferrous sulfate-mediated alkene diazidation with hydrogen peroxide (H_2O_2) as the oxidant and sodium azide (NaN_3) as the azide source (Scheme 73).¹⁰² In a closely related approach, Minisci also reported the use of both ferrous sulfate (FeSO_4) and ferric sulfate ($\text{Fe}_2(\text{SO}_4)_3$) to promote the bis-azidation of more complex olefins.¹⁰³ Steroidal compound **152**, for example, was readily converted to its corresponding diazide (**153**) upon exposure to this Fe(II)/Fe(III) system. The efficacy of this system was improved when Galli and co-workers showed that the incorporation of ammonium peroxydisulfate ($(\text{NH}_4)_2\text{S}_2\text{O}_8$) resulted in increased reactivity.¹⁰⁴ When subjected to the ferric/ferrous sulfate system in the presence of ammonium peroxydisulfate, styrene (**146**) was

¹⁰⁰ Reddy, M. V. R.; Mehrotra, B.; Vankar, Y. D. *Tetrahedron Lett.* **1995**, 36, 4861-4864.

¹⁰¹ Kancharla, P. K.; Reddy, Y.; Dharuman, S.; Vankar, Y. D. *J. Org. Chem.* **2011**, 76, 5832-5837.

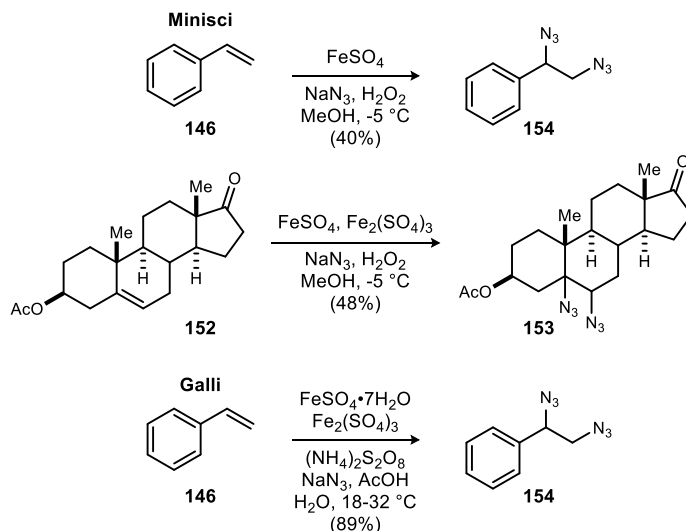
¹⁰² Minisci, F.; Galli, R. *Tetrahedron Lett.* **1962**, 3, 533-538.

¹⁰³ (a) Minisci, F.; Galli, R.; Cecere, M. *Gazz. Chim. Ital.* **1964**, 94, 67-90; (b) Minisci, F.; Galli, R. Procédé de Préparation de Diazides et Produits Obtenus. FR Patent 1,350,360, March 11, 1964.

¹⁰⁴ Galli, R.; Malatesta, V. *Org. Prep. Proced. Int.* **1971**, 3, 231-233.

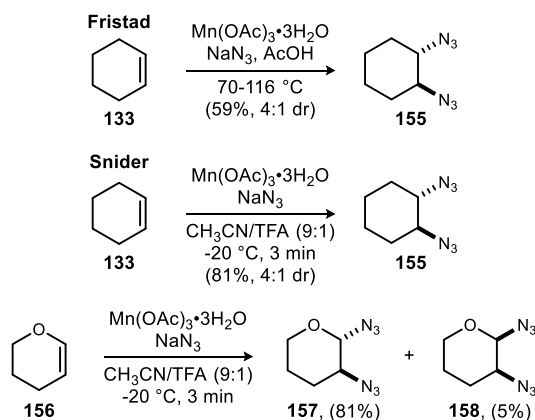
transformed to diazide **154** in 89% yield. This is a vast improvement compared to Minisci's conditions, which affords **154** in only 40% yield.

Scheme 73. Ferrous Sulfate- and Ferric/Ferrous Sulfate-Mediated Diazidations of Alkenes



Alkene diazidation can be achieved through manganese-mediated redox reactions as well. Fristad found that treatment of alkenes with $\text{Mn}(\text{OAc})_3$ and sodium azide in acetic acid at elevated temperatures results in the formation of 1,2-diazides (Scheme 74).¹⁰⁵ Snider subsequently reported a modification of Fristad's protocol in which replacement of acetic acid with trifluoroacetic acid and acetonitrile ultimately affords the desired diazides in improved yield.¹⁰⁶ This revised protocol was further extended to dihydropyran systems as their corresponding diazido compounds were furnished in good yields.

Scheme 74. Mn(III)-Mediated Diazidations of Alkenes

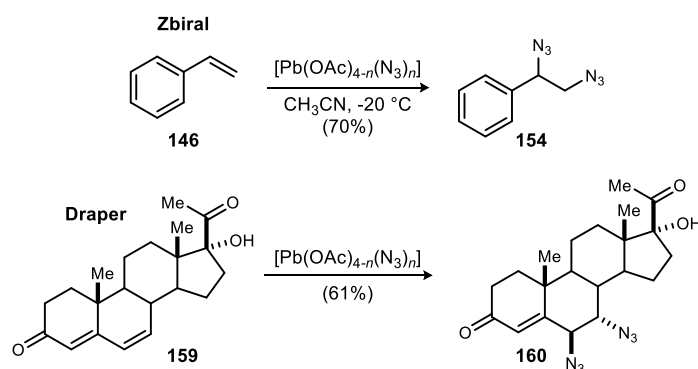


¹⁰⁵ Fristad, W. E.; Brandvold, T. A.; Peterson, J. R.; Thompson, S. R. *J. Org. Chem.* **1985**, *50*, 3647-3649.

¹⁰⁶ Snider, B. B.; Lin, H. *Synth. Commun.* **1998**, *28*, 1913-1922.

Heavy metal-based protocols have also been applied towards the bis-azidation of olefins. Lead(IV) acetate azide ($[\text{Pb}(\text{OAc})_{4-n}(\text{N}_3)_n]$), which is generated by the reaction of lead(IV) acetate and trimethylsilyl azide (TMSN_3), has proven to be an effective azide transfer reagent. Zbiral demonstrates this by reacting lead(IV) acetate azide with alkenes in acetonitrile at 20 °C to arrive at vicinal diazides (Scheme 75).¹⁰⁷ More specifically, $[\text{Pb}(\text{OAc})_{4-n}(\text{N}_3)_n]$ readily converts styrene (**146**) to diazide **154** in 70% isolated yield. While Zbiral has shown the usefulness of lead(IV) acetate azide with acyclic olefins, Draper reported that this same reagent can be used for the transformation of cyclic alkenes to 1,2-diazides as well.¹⁰⁸ For example, when steroidal dienone **159** is treated with lead(IV) acetate azide, diazido compound **160** can be afforded in 61% yield.

Scheme 75. Reaction of $[\text{Pb}(\text{OAc})_{4-n}(\text{N}_3)_n]$ with Acyclic and Cyclic Olefins



Closely related to lead(IV) acetate azide, thallium(III) acetate azide ($[\text{Tl}(\text{OAc})_{3-n}(\text{N}_3)_n]$) can also be employed for alkene bis-azidation. Like its lead analog, thallium(III) acetate azide is prepared by reacting thallium(III) acetate with TMSN_3 . Application of this particular azide transfer reagent by Zbiral was fruitful as both cyclic and acyclic alkenes could be converted to their desired vicinal diazides (Scheme 76).¹⁰⁹ Cyclohexene (**133**) and 4-allylanisole (**161**) were transformed into their corresponding aziridinylazothallium compounds (**162** and **163**), upon exposure to thallium(III) acetate azide. Subsequent thermolysis of **162** and **163** resulted in the formation of diazido compounds **164** and **165** in 38% and 30% yields respectively.

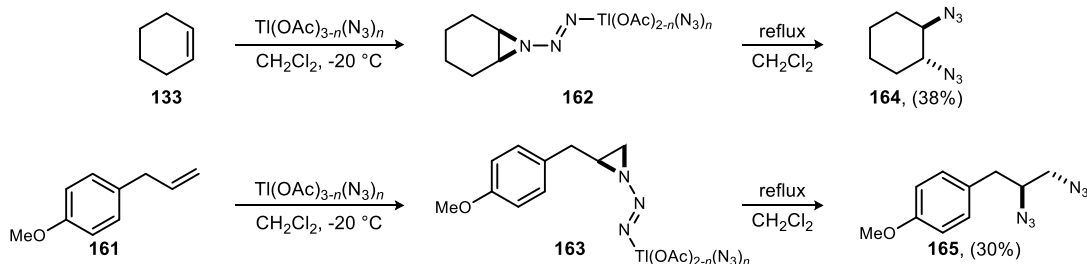
Aside from alkene diazidation, heavy metal protocols have been used for the direct diamination of alkenes as well. Barluenga has reported an efficient method for olefin diamination

¹⁰⁷ (a) Zbiral, E.; Kischka, K. *Tetrahedron Lett.* **1969**, *10*, 1167-1168; (b) Zbiral, E.; Stutz, A. *Monatsh. Chem.* **1973**, *104*, 249-262.

¹⁰⁸ Draper, R. W. *J. Chem. Soc., Perkin Trans 1* **1983**, 2787-2791.

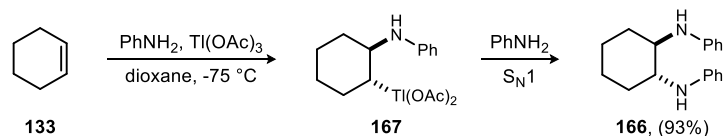
¹⁰⁹ (a) Maxa, E.; Zbiral, E.; Schulz, G.; Haslinger, E. *Liebigs Ann. Chem.* **1975**, *1975*, 1705-1720; (b) Emmer, G.; Zbiral, E.; Brill, G.; Musso, H. *Liebigs Ann. Chem.* **1979**, *1979*, 796-802.

Scheme 76. Zbiral's Reaction of $[\text{Ti}(\text{OAc})_{3-n}(\text{N}_3)_n]$ with Cyclohexene and 4-Allylanisole



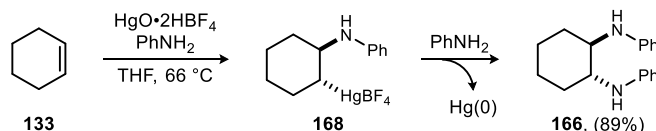
using thallium(III) acetate (Scheme 77).¹¹⁰ This is exemplified through the transformation of cyclohexene (**133**) to diamine (**166**). Cyclohexene, when subjected to aniline and $\text{Ti}(\text{OAc})_3$, is thought to proceed through aminothallation en route to organothallium intermediate **167**. Substitution of the thallium entity via an $\text{S}_{\text{N}}1$ pathway with another equivalent of aniline yields the desired diamine (**166**) in high yield.

Scheme 77. Barluenga's Addition of Aromatic Amines to Alkenes in the Presence of Thallium(III) Acetate



In addition to thallium, mercury(II)-mediated protocols can be used for the synthesis of vicinal diamines. Barluenga has demonstrated that mercury(II) reagents, most notably mercury(II) tetrafluoroborate ($\text{HgO}\cdot 2\text{HBF}_4$), can undergo alkene aminomercuration to form β -amino alkylmercury(II) salts (Scheme 78).¹¹¹ Substitution of the mercury moiety with nucleophilic amine generates the desired diamine. Like thallium-mediated diaminations, primary and secondary amines are tolerated with mercury(II).

Scheme 78. Barluenga's Addition of Aromatic Amines to Alkenes in the Presence of Mercury(II) Tetrafluoroborate



Transition metal catalysis can be classified as the most extensively explored and dominant area of chemistry when it comes to the diamination of olefins. Numerous transition metals have been applied towards the synthesis of vicinal diamines including cobalt, ruthenium, osmium,

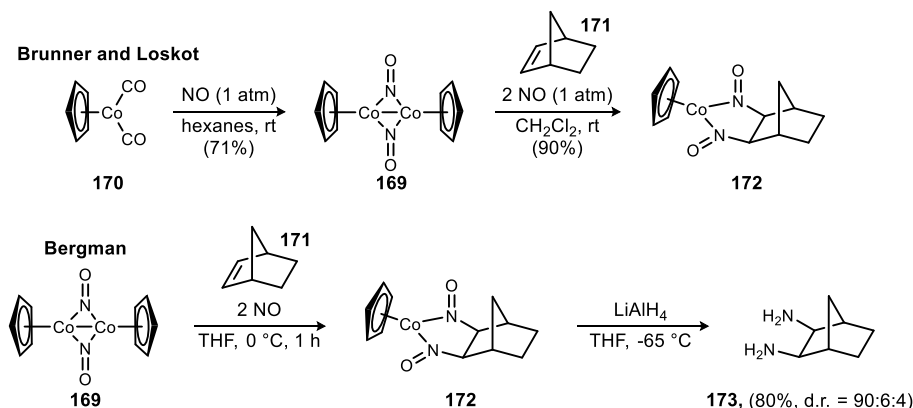
¹¹⁰ Gomez Aranda, V.; Barluenga, J.; Anzar, F. *Synthesis* **1974**, 504-505.

¹¹¹ Barluenga, J.; Alonso-Cires, L.; Asensio, G. *Synthesis* **1979**, 962-964.

palladium, nickel, copper, and gold. With these possibilities, transition metal catalysis can achieve alkene diamination to a high degree of generality.

The use of metal nitrosyl complexes are amongst the earliest applications of transition metals en route to diamination. Brunner and Loskot report a ligand-based reaction of cobalt nitrosyl complex **169** with bicyclo[2.2.1]hep-2-enes.¹¹² This nitrosyl complex, which is generated from the reaction of cyclopentadienylcobalt dicarbonyl (**170**) and nitric oxide, can undergo addition to strained alkenes to form cobalt dinitrosoalkane complexes. Good reactivity is demonstrated as nitrosyl complex **169** readily converts norbornene (**171**) to dinitrosoalkane complex **172** in 90% isolated yield (Scheme 79). This process is diastereoselective as only the *exo* compounds are formed. Bergman improved on Brunner's and Loskot's findings by using cobalt dinitrosoalkane complexes as intermediates in order to access free 1,2-diamines.¹¹³ In this study, *in situ* reduction of dinitrosoalkane ligands with LiAlH₄ affords the corresponding unmasked diamines in good yield and with high levels of diastereoselection.

Scheme 79. Diaminations of Alkenes Using Cyclopentadienylnitrosylcobalt Dimer **169**



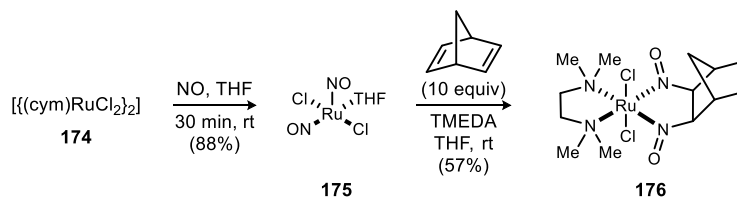
In 2011, Bergman and Toste reported ruthenium-mediated alkene bis-nitrosylations as well.¹¹⁴ Here, treatment of (cymene)ruthenium dichloride dimer (**174**) with nitric oxide in THF generates dinitrosyl complex **175** (Scheme 80). This complex can readily react with strained alkenes in the presence of chelating ligands to arrive at six-coordinate, ruthenium-based dinitrosoalkane complexes.

¹¹² (a) Brunner, H.; Loskot, S. *Angew. Chem., Int. Ed. Engl.* **1971**, *10*, 515-516; (b) Brunner, H.; Loskot, S. *J. Organomet. Chem.* **1973**, *61*, 401-414.

¹¹³ (a) Becker, P. N.; White, M. A.; Bergman, R. G. *J. Am. Chem. Soc.* **1980**, *102*, 5676-5677; (b) Becker, P. N.; Bergman, R. G. *Organometallics* **1983**, *2*, 787-796.

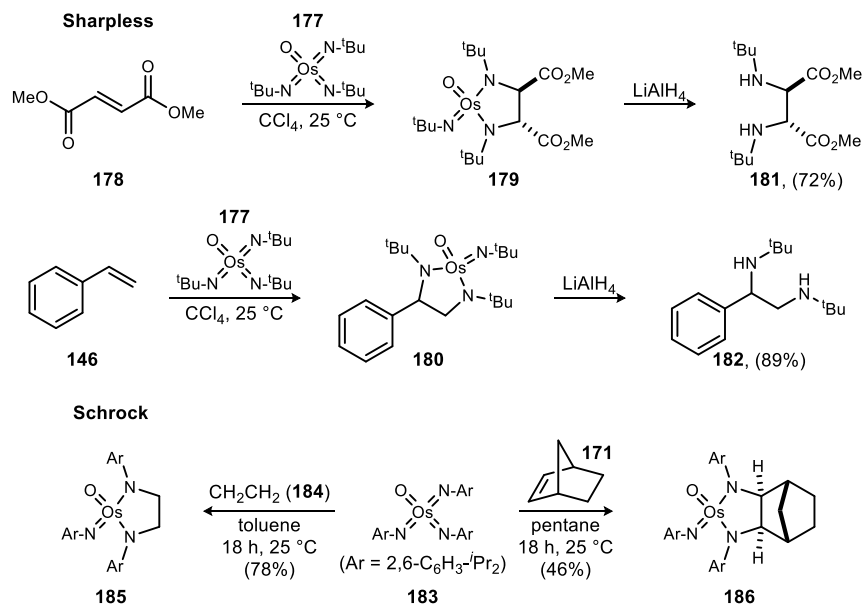
¹¹⁴ Crimmin, M. R.; Bergman, R. G.; Toste, F. D. *Angew. Chem. Int. Ed.* **2011**, *50*, 4484-4487.

Scheme 80. Reaction of Alkenes with Dinitrosyl Complex **175**



Imidoosmium(VIII) reagents have also proven effective in the field of alkene diamination. Sharpless and colleagues were the first to report the use of tris(*tert*-butylimido)osmium (**177**) to promote diaminations of terminal and *trans*-disubstituted alkenes.¹¹⁵ To illustrate, styrene (**146**) and dimethyl fumarate (**178**) were transformed to their osmium-derived diimido complexes (**179** and **180**) upon exposure to imidoosmium **177** (Scheme 81). These complexes can be reduced to their corresponding 1,2-di-*tert*-butylamines (**181** and **182**) when treated with LiAlH₄. Additionally, Schrock and co-workers employed a more sterically encumbered aryl trisimidoosmium complex (**183**) for the synthesis of masked vicinal diamines.¹¹⁶ This complex proved fruitful as simple alkenes such as ethylene (**184**) and norbornene (**171**) were converted to metallaimidazolines **185** and **186** in 78% and 46% yields.

Scheme 81. Stoichiometric Diamination of Alkenes with Imidoosmium(VIII) Complexes

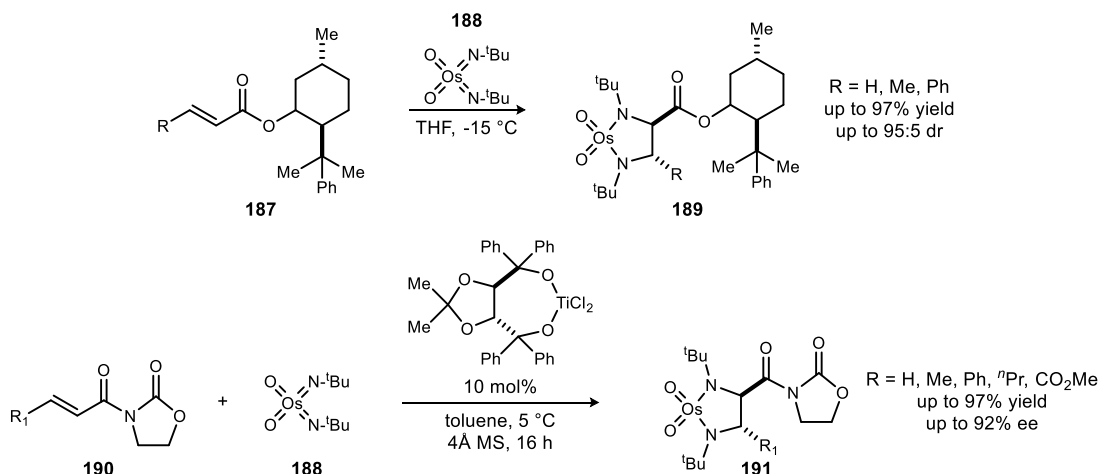


¹¹⁵ Chong, A. O.; Oshima, K.; Sharpless, K. B. *J. Am. Chem. Soc.* **1977**, *99*, 3420-3426.

¹¹⁶ (a) Schofield, M. H.; Kee, T. P.; Anhaus, J. T.; Schrock, R. R.; Johnson, K. H.; Davis, W. M. *Inorg. Chem.* **1991**, *30*, 3595-3604; (b) Anhaus, J. T.; Kee, T. P.; Schofield, M. H. Schrock, R. R. *J. Am. Chem. Soc.* **1990**, *112*, 1642-1643.

Muñiz and colleagues expanded on the studies of Sharpless and Schrock by deploying strategies that effectively control the absolute facial selectivity of imidoosmium(VIII)-mediated diaminations. One approach in particular involves the use of chiral auxiliaries in order to achieve alkene diamination in a diastereoselective fashion.¹¹⁷ This is exemplified as reactions of electron-deficient (–)-8-phenylmenthyl acrylate derivatives (**187**) with imidoosmium **188** proceed through the *Re*-face, furnishing masked diamines (**189**) with high levels of diastereoselection (Scheme 82). An enantioselective catalytic variant has also been developed, which employs a Ti-TADDOLate catalyst and imidoosmium **188** as the stoichiometric nitrogen source.¹¹⁸ Under these conditions, electron-deficient crotonyl oxazolidinones (**190**) are readily converted to their osmium-derived 1,2-diamines (**191**) with good to excellent levels of enantioselection.

Scheme 82. Diastereo- and Enantioselective Diaminations with Imidoosmium **188**



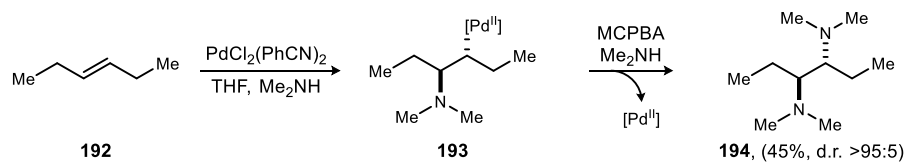
Palladium is one of the more broadly effective transition metals when it comes to the diamination of olefins. The first palladium-assisted alkene diamination was reported in 1978 by Bäckvall.¹¹⁹ Here, stoichiometric quantities of *trans*-bis(benzonitrile)dichloropalladium(II) are used to promote the synthesis of vicinal diamines from simple 1,2-disubstituted alkenes. Hex-3-ene (**192**), for example, undergoes *trans*-aminopalladation to amino alkylpalladium(II) species **193** upon exposure to the stoichiometric palladium and dimethylamine (Scheme 83). Oxidation of **193** with MCPBA gives a palladium(IV) species, which is reductively displaced by another equivalent of dimethylamine, ultimately affording diamine **194** in 45% yield with high *syn*-selectivity.

¹¹⁷ Muñiz, K. *New. J. Chem.* **2005**, 29, 1371-1385.

¹¹⁸ (a) Muñiz, K.; Nieger, M. *Chem. Commun.* **2005**, 2729-2731; (b) Almodovar, I.; Hövelmann, C. H.; Streuff, J.; Nieger, M.; Muñiz, K. *Eur. J. Org. Chem.* **2006**, 704-712.

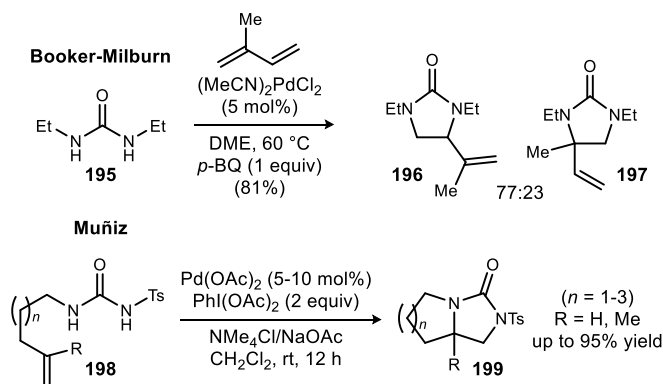
¹¹⁹ (a) Bäckvall, J.-E. *Tetrahedron Lett.* **1978**, 19, 163-166; (b) Bäckvall, J.-E. *Acc. Chem. Res.* **1983**, 16, 335-342.

Scheme 83. Bäckvall's Stoichiometric Pd-Mediated 1,2-Diamination of Alkenes



Although Bäckvall's stoichiometric diamination showed great promise for the advancement of palladium-mediated protocols, catalytic versions of this process were not discovered until 2005 when Booker-Milburn and co-workers reported the first palladium(II)-catalyzed intermolecular diamination of alkenes.¹²⁰ They found that treatment of 1,3-dienes, such as isoprene, with *N,N'*-diethylurea (**195**) in the presence of catalytic bis(acetonitrile)palladium dichloride and benzoquinone led to the formation of cyclic ureas **196** and **197** in 81% yield with a 77:23 regioisomer ratio (Scheme 84). Furthermore, Muñiz and colleagues demonstrated the first palladium(II)-catalyzed intramolecular alkene diamination with alkenyl-substituted ureas (**198**).¹²¹ When subjected to catalytic palladium(II) acetate and stoichiometric quantities of hypervalent iodine oxidant ($\text{PhI}(\text{OAc})_2$) under basic conditions, these terminal alkenes were transformed to their desired cyclic ureas (**199**) with five-, six-, and seven-membered fused rings in excellent yield.

Scheme 84. Pd(II)-Catalyzed Intermolecular and Intramolecular Diaminations of Alkenes



In addition to terminal alkenes, Muñiz has shown that palladium(II)-catalyzed intramolecular diaminations can also be achieved with internal alkenes.¹²² Upon exposure to the palladium(II)acetate-phenyl iodine diacetate ($\text{Pd}(\text{OAc})_2$ - $\text{PhI}(\text{OAc})_2$) combination in the presence of base, homoallylic sulfonamide **200** readily undergoes double annulation to afford bis(indoline)

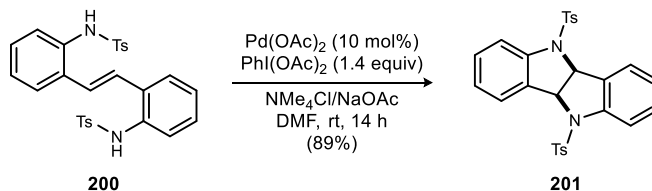
¹²⁰ Bar, G. L. J.; Lloyd-Jones, G. C.; Booker-Milburn, K. I. *J. Am. Chem. Soc.* **2005**, *127*, 7308-7309.

¹²¹ (a) Streuff, J.; Hövelmann, C. H.; Nieger, M.; Muñiz, K. *J. Am. Chem. Soc.* **2005**, *127*, 14586-14587; (b) Muñiz, K.; Hövelmann, C. H.; Streuff, J. *J. Am. Chem. Soc.* **2008**, *130*, 763-773.

¹²² Muñiz, K. *J. Am. Chem. Soc.* **2007**, *129*, 14542-14543.

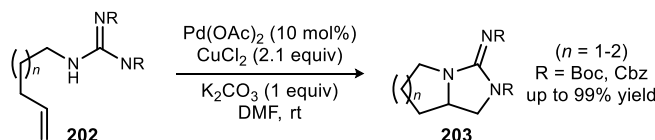
201 in 89% isolated yield (Scheme 85). Aliphatic- and naphthyl-derived homoallylic sulfonamides are tolerated in this reaction as well.

Scheme 85. Muñiz's Pd(II)-Catalyzed Intramolecular Diamination of Internal Alkenes en Route to Bis(indolines)



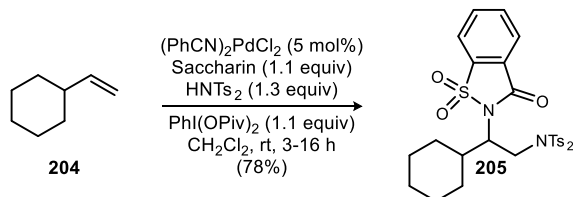
Another notable advancement by Muñiz in the area of palladium-catalyzed alkene diamination is the incorporation of copper(II) salts as terminal oxidants. One system in which this palladium-copper catalyst-oxidant combination can be effectively employed is through the intramolecular cycloguanidation of terminal alkenes (Scheme 86).¹²³ With Pd(OAc)₂ as the catalyst and CuCl₂ as the terminal oxidant, *N*-alkenyl guanidines (**202**) can be converted to their respective Boc- or Cbz- protected bicyclic guanidines (**203**) in up to 99% yield.

Scheme 86. Pd(II)-Catalyzed Intramolecular Cycloguanidation of Alkenes with Copper Chloride as the Oxidant



In an extension of their work on the intramolecular diamination of tethered ureas, Muñiz and colleagues have developed a doubly intermolecular variant of their methodology. This particular method features the regioselective transfer of nitrogen from two distinct sources in bis(tosylimide) and saccharin (Scheme 87).¹²⁴ For example, when using bis(benzonitrile)palladium dichloride as the precatalyst and iodosobenzene dipivalate as the oxidant, vinyl cyclohexane (**204**) can undergo addition to afford heterodiamine **205** in 78% isolated yield with complete regioselectivity.

Scheme 87. Doubly Intermolecular Pd(II)-Catalyzed Diamination of Terminal Alkenes

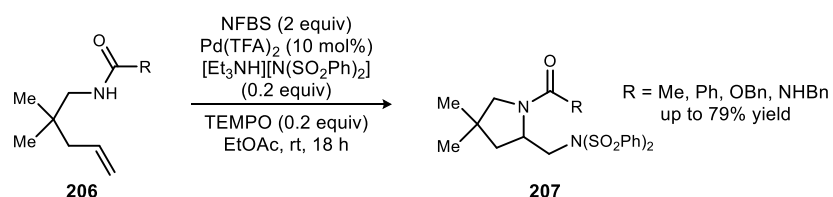


¹²³ Hövelmann, C. H.; Streuff, J.; Berlot, L.; Muñiz, K. *Chem. Commun.* **2008**, 2334-2336.

¹²⁴ Iglesias, A.; Pérez, E. G.; Muñiz, K. *Angew. Chem. Int. Ed.* **2010**, *49*, 8109-8111.

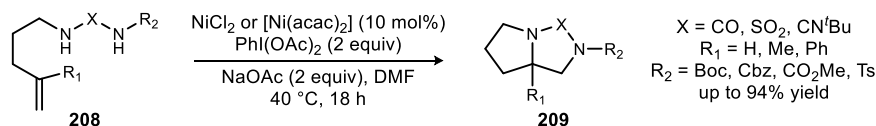
Complementary to Muñiz's doubly intermolecular protocol, Michael and co-workers have reported the intra/intermolecular diamination of terminal alkenyl amides, carbamates, and ureas (Scheme 88).¹²⁵ Here, *N*-fluoro-bis(phenylsulfonyl)imide (NFBS) is used as an external electrophilic aminating agent. When treated with NFBS, catalytic palladium(II) trifluoroacetate and a triethylammonium benzenesulfonamide additive, these terminal alkenes (**206**) readily undergo cyclization en route to their 2-aminomethyl pyrrolidine derivatives (**207**) in moderate to good yield. This methodology by Michael is beneficial not only for its generality and functional/protecting group tolerance, but because these diamination products can be differentially deprotected under mild conditions as well.

Scheme 88. NFBS-Promoted Intra/Intermolecular Diamination of Terminal Alkenes



Nickel catalysis has also been used as a means for alkene diamination. Muñiz and colleagues demonstrate the efficacy of nickel(II) salts in the intramolecular diamination of *N*-alkenyl sulfamides, ureas, and guanidines (Scheme 89).¹²⁶ Upon exposure to catalytic nickel(II) and phenyliodine diacetate (PhI(OAc)₂) in the presence of base, these terminal alkenes (**208**) are transformed to their corresponding diamines (**209**) in up to 94% yield and with a high degree of generality.

Scheme 89. Nickel(II)-Catalyzed Intramolecular Alkene Diamination



Chemler and co-workers have pioneered the use of copper(II) carboxylates for the diamination of olefins. In 2005, this group successfully employed copper(II) acetate to promote the intramolecular diamination of γ -alkenyl and δ -alkenyl-substituted sulfamides (Scheme 90).¹²⁷ To illustrate, alkenyl sulfamide **210** undergoes cyclization to afford its corresponding 5-membered

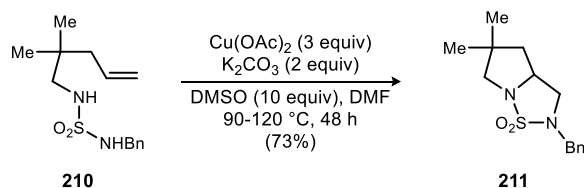
¹²⁵ (a) Sibbald, P. A.; Michael, F. E. *Org. Lett.* **2009**, *11*, 1147-1149; (b) Sibbald, P. A.; Rosewall, C. F.; Swartz, R. D.; Michael, F. E. *J. Am. Chem. Soc.* **2009**, *131*, 15945-15951.

¹²⁶ Muñiz, K.; Streuff, J.; Hövelmann, C.; Nuñez, A. *Angew. Chem. Int. Ed.* **2007**, *46*, 7125-7127.

¹²⁷ Zabawa, T. P.; Kasi, D.; Chemler, S. R. *J. Am. Chem. Soc.* **2005**, *127*, 11250-11251.

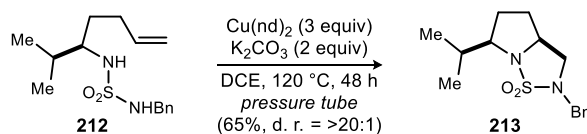
cyclic sulfamide (**211**) when subjected to stoichiometric quantities of copper(II) acetate under basic conditions. Additionally, δ -alkenyl-substituted sulfamides were smoothly converted to their 6-membered cyclic sulfamides under identical reaction parameters.

Scheme 90. Chemler's Intramolecular Diamination of Alkenyl-Substituted Sulfamides with Copper(II) Acetate



Although copper(II) acetate has proven effective for the intramolecular diamination of alkenyl sulfamides, this particular species does suffer from a low degree of solubility, resulting in methodological limitations. As a result, Chemler has introduced copper(II) neodecanoate ($[\text{Cu}(\text{nd})_2]$) as a second-generation mediator for the diamination of alkenes.¹²⁸ When exposing this copper(II) carboxylate to γ -alkenyl-substituted sulfamide **212** in the presence of base at elevated temperatures, the desired cyclic sulfamide (**213**) is furnished in 65% isolated yield as a single diastereomer (Scheme 91). It is also worthy to note that these revised conditions facilitate the generation of a broader ranges of bis(amino) products including ureas, bis(anilines), and α -amido-pyrroles.

Scheme 91. Chemler's Copper(II) Neodecanoate-Promoted Intramolecular Diamination of Terminal Alkenes

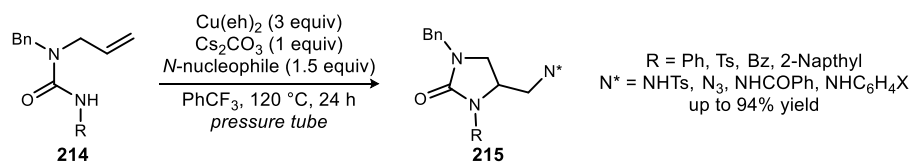


In 2010, Chemler and colleagues expanded on their original diamination methodology by reporting an intra/intermolecular variation that involves external nucleophiles such as azide, sulfonamides, benzamides, and anilines.¹²⁹ This particular study employs copper(II) 2-ethylhexanoate ($[\text{Cu}(\text{eh})_2]$) to facilitate the diamination of 2-substituted 1-allyl-1-benzyl ureas (**214**) (Scheme 92). Once the urea functionality undergoes intramolecular ring closure on the alkene, intermolecular nucleophilic attack by an external amino source generates the second C-N bond ultimately affording 4-substituted imidazolinones (**215**).

¹²⁸ Zabawa, T. P.; Chemler, S. R. *Org. Lett.* **2007**, *9*, 2035-2038.

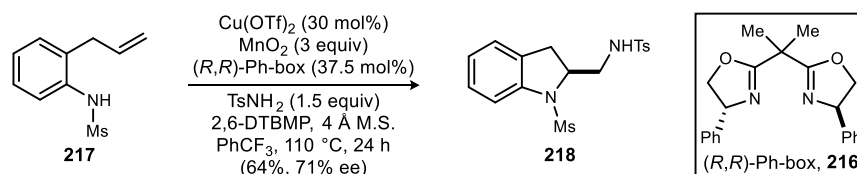
¹²⁹ Sequeira, F. C.; Turnpenny, B. W.; Chemler, S. R. *Angew. Chem. Int. Ed.* **2010**, *49*, 6365-6368.

Scheme 92. Copper(II) 2-Ethylhexanoate-Promoted Intra/Intermolecular Alkene Diamination



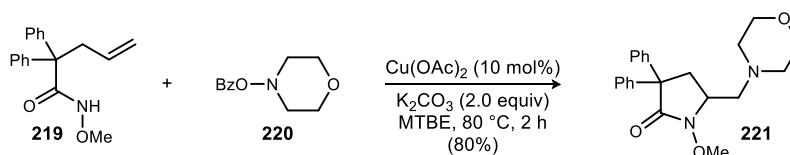
Chemler took this intra/intermolecular approach one step further by achieving a variant with promising levels of enantioselection.¹²⁹ Here, chiral bis(oxazoline) ligand **216** is used in conjunction with catalytic copper(II) triflate and MnO_2 as the terminal oxidant to promote the enantioselective intra/intermolecular diamination of mesyl-protected allylaniline **217** (Scheme 93). With electron-deficient bis(tosylimide) as the external amino source, masked diamine **218** is acquired in 64% yield and 71% ee under these reaction conditions.

Scheme 93. Enantioselective Copper-Catalyzed Intra/Intermolecular Diamination of Allylaniline **217**



Recently, Wang and Shen reported a copper-catalyzed intra/intermolecular diamination of unactivated alkenes with hydroxylamines.¹³⁰ These hydroxyl amines are novel in this study as they serve as a source of electron-rich amines. The efficacy of this system is demonstrated through the direct conversion of alkenyl amides to amino-substituted lactams. For example, when unsaturated amide **219** is treated with *O*-benzoyl hydroxylmorpholine (**220**) in the presence of catalytic copper(II) acetate, morpholine-substituted lactam **221** is furnished in 80% yield (Scheme 94). Other cyclic and aliphatic secondary amines are tolerated in this reaction system as well.

Scheme 94. Example of Copper-Catalyzed Diamination of Unactivated Alkenes with a Hydroxylamine



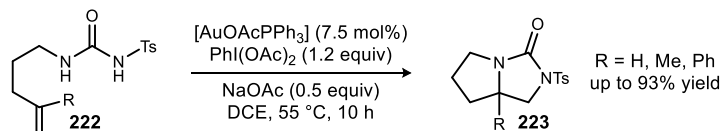
Gold catalysis has also proven to be an effective avenue towards alkene diamination. In 2009, Muñiz and co-workers reported the use of gold(I) to facilitate the doubly intramolecular diamination of alkenyl-derived ureas.¹³¹ When subjecting triphenylphosphine gold(I) acetate as

¹³⁰ Shen, K.; Wang, Q. *Chem. Sci.* **2015**, 6, 4279-4283.

¹³¹ Iglesias, A.; Muñiz, K. *Chem. Eur. J.* **2009**, 15, 10563-10569.

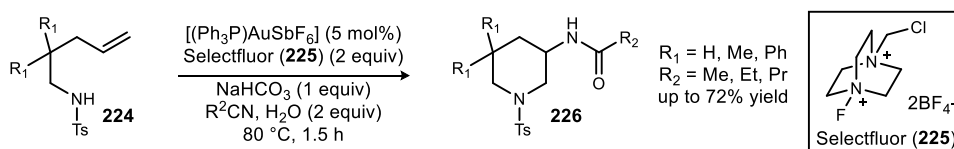
the catalyst and $\text{PhI}(\text{OAc})_2$ as the oxidant, *N*- γ -alkenyl ureas (**222**) can readily convert to their corresponding bicyclic imidazolinones (**223**) in high yield (Scheme 95).

Scheme 95. Gold-Catalyzed Intramolecular Diamination of *N*- γ -Alkenyl-Substituted Ureas



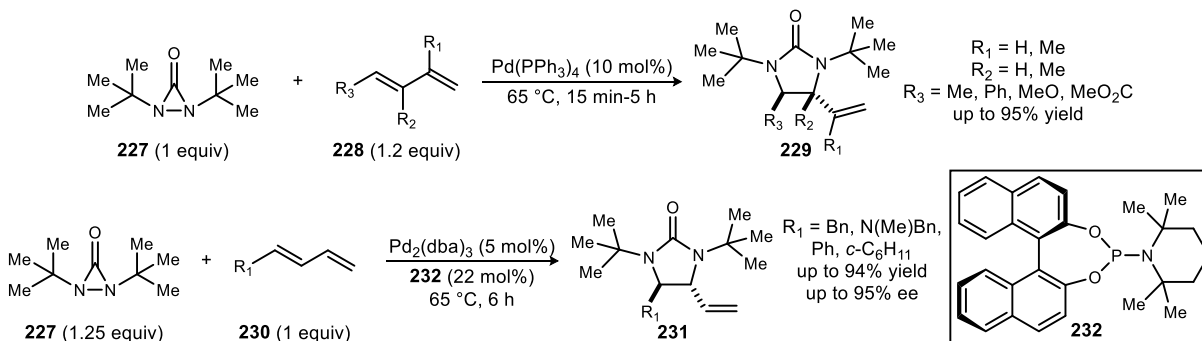
To complement Muñiz's doubly intramolecular protocol, Nevado and de Haro have reported a gold-catalyzed intra/intermolecular diamination of *N*- γ -alkenyl tosylated amines (**224**).¹³² When using cationic complex $[(\text{Ph}_3\text{P})\text{AuSbF}_6]$ as the catalyst and Selectfluor (**225**) as an oxidant, these alkenyl tosylated amines undergo a 6-*endo-trig* cyclization that traps a nitrile solvent. Subsequent *in situ* hydrolysis of the nitrile moiety ultimately results in the generation of *N*-piperidin-3-yl carboxamides (**226**) in moderate to good yield (Scheme 96).

Scheme 96. Gold-Catalyzed Oxidative Intra/Intermolecular Diamination of *N*- γ -Alkenyl Tosylated Amines



Shi and co-workers have extensively explored the use of strained diaziridinones and their analogs as versatile nitrogen sources for metal-mediated alkene diaminations. In 2007, Shi first reported the use of di-*tert*-butyldiaziridinone (**227**) as a nitrogen source in the diamination of conjugated dienes (**228**).¹³³ Treatment of these dienes with **227** and a catalytic amount of tetrakis(triphenylphosphine)palladium(0) at elevated temperatures results in the formation of

Scheme 97. Symmetric and Asymmetric Pd-Catalyzed Diaminations of Dienes with Di-*tert*-Butyldiaziridinone



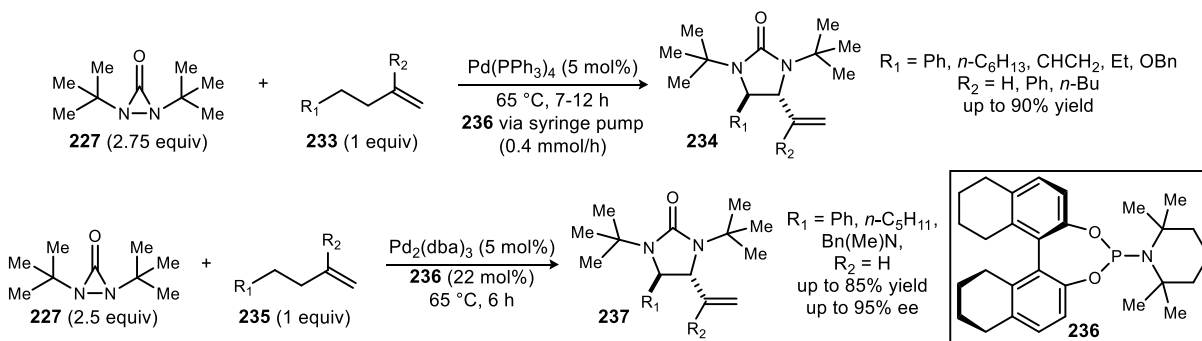
¹³² De Haro, T.; Nevado, C. *Angew. Chem. Int. Ed.* **2011**, *50*, 906-910.

¹³³ Du, H.; Zhao, B.; Shi, Y. *J. Am. Chem. Soc.* **2007**, *129*, 762-763.

imidazolidinones (**229**) in high yield and with excellent regioselectivity (Scheme 97). Shortly thereafter, the same group reported a highly efficacious enantioselective variant of this methodology by employing Pd₂(dba)₃ as the palladium(0) source and BINOL-based phosphorous amidite **232** as the chiral ligand.¹³⁴

In addition to dienes, Shi has also found that monosubstituted and 1,1-disubstituted olefins undergo palladium(0)-catalyzed dehydrogenative diamination at the allylic and homoallylic positions in the presence of excess di-*tert*-butyldiaziridinone (**227**).¹³⁵ Under solvent free conditions, slow addition of **227** to these terminal alkenes (**233**) in the presence of a catalytic tetrakis(triphenylphosphine)palladium(0) at 65 °C leads to the formation of cyclic ureas **234** in good yield with complete regio- and stereoselectivity (Scheme 98). Furthermore, the catalytic asymmetric version of this allylic/homoallylic diamination was readily achieved via the incorporation of a chiral ligand. When subjecting mono- and disubstituted alkenes (**235**) to a catalytic amount of Pd₂(dba)₃ with H₈-BINOL-derived phosphorus amidite **236** as the chiral reagent, the corresponding cyclic ureas (**237**) are furnished in high yield and up to 95% ee.¹³⁶

Scheme 98. Symmetric and Asymmetric Pd-Catalyzed Dehydrogenative Allylic/Homoallylic Diaminations



Another notable discovery made by Shi and colleagues is that the use of copper(I) salts and phosphine ligands can effectively determine the regiochemistry of diamination when using diaziridinone **227** in the presence of conjugated dienes and trienes. One system shows that a combination of copper(I) chloride and triphenyl phosphite (P(OPh)₃) readily promotes the diamination reaction of **227** with dienes and trienes (**238**) exclusively at the terminal position (Scheme 99).¹³⁷ Conversely, when starving the reaction system of phosphine ligands, copper(I)

¹³⁴ Du, H.; Yuan, W.; Zhao, B.; Shi, Y. *J. Am. Chem. Soc.* **2007**, *129*, 11688-11689.

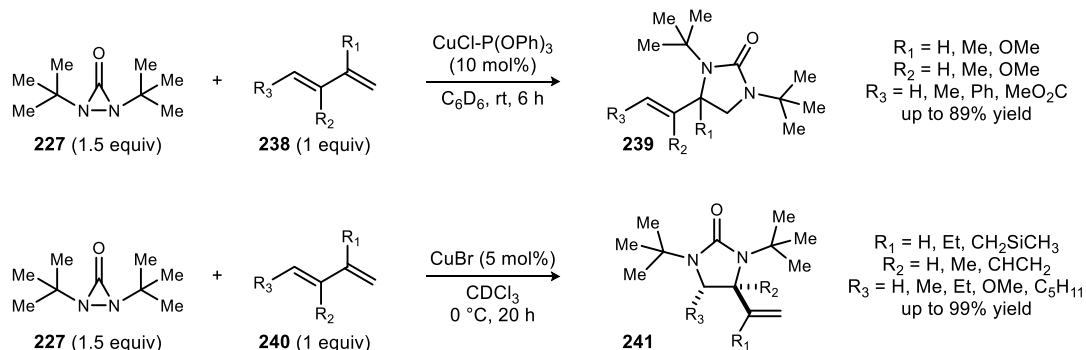
¹³⁵ Du, H.; Yuan, W.; Zhao, B.; Shi, Y. *J. Am. Chem. Soc.* **2007**, *129*, 7496-7497.

¹³⁶ Du, H.; Zhao, B.; Shi, Y. *J. Am. Chem. Soc.* **2008**, *130*, 8590-8591.

¹³⁷ Yuan, W.; Du, H.; Zhao, B.; Shi, Y. *Org. Lett.* **2007**, *9*, 2589-2591.

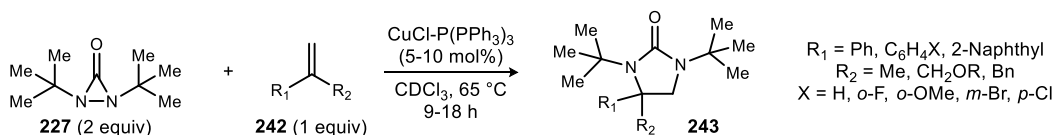
salts, particularly copper(I) bromide, direct diene diamination to the internal alkene position.¹³⁸ Both respective approaches achieve their corresponding diamination in modest to good yield.

Scheme 99. Phosphine-Ligand-Dependent Regioselective Diaminations of Conjugated Dienes and Trienes



Shi has also applied this copper(I)-phosphine ligand combination to the synthesis of 1,2-diamines from aryl-activated 1,1-disubstituted olefins (**242**).¹³⁹ When employing catalytic quantities of copper(I) chloride and triphenylphosphine in a 1:1 ratio, a wide range of styrene derivatives (**242**) can undergo diamination with di-*tert*-butyldiaziridinone at elevated temperatures resulting in the formation of desired imidazolidinones (**243**) in high yield (Scheme 100). Additionally, naphthyl-derived alkenes are tolerated thereby broadening the substrate scope.

Scheme 100. Copper(I)-Catalyzed Diamination of Disubstituted Terminal Alkenes



As for nitrogen sources, Shi has reported that motifs other than di-*tert*-butyldiaziridinone (**227**) have proven effective for alkene diamination. *N,N*-di-*tert*-butylthiadiaziridine 1,1-dioxide (**244**) can undergo addition to a range of activated alkenes to afford cyclic sulfamides.¹⁴⁰ For example, when styrene (**146**) is treated with thiadiaziridine dioxide **244** in the presence of a CuCl-P(*n*-Bu)₃ combination, sulfamide **245** is furnished in 94% isolated yield (Scheme 101). In an analogous manner, di-*tert*-butyldiaziridinimide **246** can be used to promote the diamination of various alkenes en route to their corresponding cyclic *N*-cyano guanidines.¹⁴¹ To illustrate, 4-

¹³⁸ Zhao, B.; Peng, X. G.; Cui, S. L.; Shi, Y. A. *J. Am. Chem. Soc.* **2010**, *132*, 11009-11011.

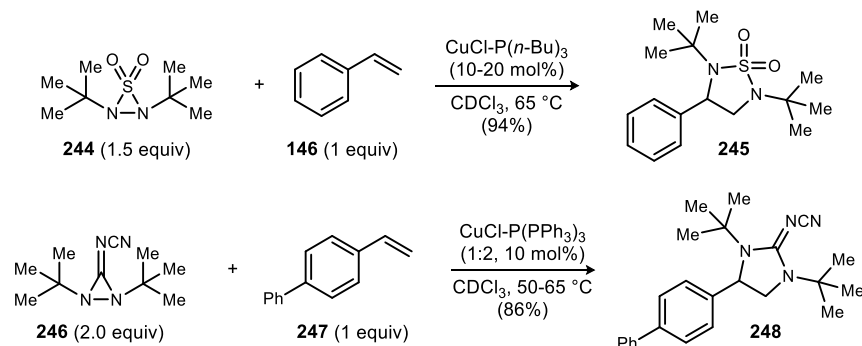
¹³⁹ Wen, Y.; Zhao, B.; Shi, Y. *Org. Lett.* **2009**, *11*, 2365-2368.

¹⁴⁰ Cornwall, R. G.; Zhao, B.; Shi, Y. *Org. Lett.* **2011**, *13*, 434-437.

¹⁴¹ Zhao, B. G.; Du, H.; Shi, Y. A. *Org. Lett.* **2008**, *10*, 1087-1090.

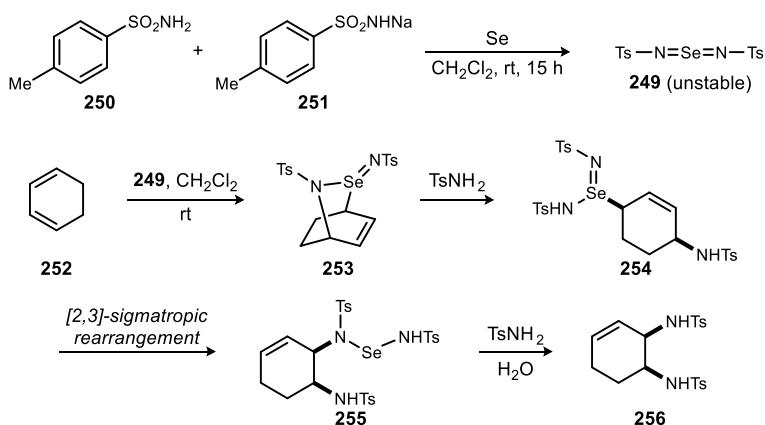
vinylbiphenyl (**247**) is readily transformed to cyano guanidine **248** in 86% yield upon exposure to a CuCl-P(PPh₃)₃ system with diaziridinimide **246** as the nitrogen source.

Scheme 101. Copper(I)-Catalyzed Alkene Diaminations with Thiadiaziridine Dioxide **244** and Diaziridinimide **246**



Pericyclic reactions provide a pathway to 1,2-diamines from alkenes. Among the most notable approaches is that reported by Sharpless and Singer in which they use selenium dioxide bis(amide) **249** to accomplish alkene diamination with exclusive *cis* selectivity.¹⁴² Bis(imide) **249** is generated *in situ* by the oxidation of selenium powder in the presence of *p*-toluenesulfonamide (**250**) and its sodium salt (**251**) (Scheme 102). This compound can then undergo a [4+2] cycloaddition with cyclic 1,3-diene **252** to yield cycloadduct **253**. Subsequent ring-opening with *p*-toluenesulfonamide affords **254**, which undergoes a [2,3]-sigmatropic rearrangement to give **255**. The desired *cis*-diamine product (**256**) is furnished upon desulfurization of selenium(II) amide **255**.

Scheme 102. 1,2-Diamination of 1,3-Dienes with Selenium Dioxide Bis(Imide) **249**

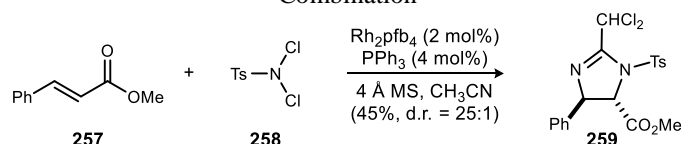


Numerous halogen-mediated approaches have been employed for the synthesis of vicinal diamines from alkenes. One method, in particular, that has proven effective is the use of

¹⁴² Sharpless, K. B.; Singer, S. P. *J. Org. Chem.* **1976**, *41*, 2504-2506.

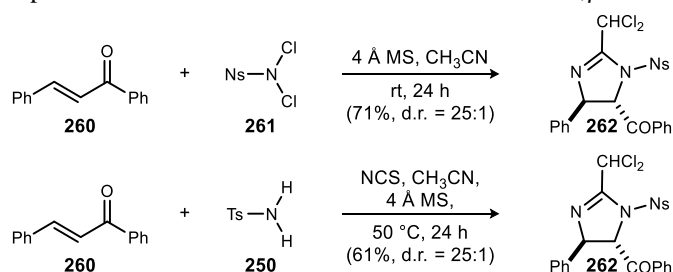
dihaloarylsulfonamide-acetonitrile combinations. This type of reaction system was first reported in 2003 by Li and colleagues in order to promote the imidazolinization of α,β -unsaturated carbonyl compounds.¹⁴³ Treatment of α,β -unsaturated ketones and esters, such as methyl cinnamate (**257**), with *N,N*-dichloro-*p*-toluenesulfonamide (**258**), 4 Å molecular sieves, and the complex generated from Rh₂(pfb)₄ and PPh₃ in the presence of acetonitrile affords the desired *trans*-substituted 2-dichloromethyl-2-imidazolines **259** in moderate to high yield and with excellent diastereoselection (Scheme 103). This type of transformation is thought to proceed through a Ritter-type reaction of an aziridinium ion intermediate.

Scheme 103. Imidazolinization of α,β -Unsaturated Ketone **257** with a TsNCl₂/MeCN/Rh₂pfb₄•PPh₃ Reagent Combination



Subsequent studies by Li and co-workers have revealed that the same imidazolinization of α,β -unsaturated carbonyl compounds can be achieved with a more reactive dihaloarylsulfonamide in the absence of a catalyst.¹⁴⁴ When enone **260** is treated with *N,N*-dichloro-2-nitrobenzenesulfonamide (**261**), 4 Å molecular sieves and acetonitrile, the corresponding dichloromethyl diamine (**262**) is furnished in 71% isolated yield and with high levels of diastereoselectivity (Scheme 104). Li further improved on his findings by developing a protocol that avoids the inconvenience of handling unstable *N,N*-dichlorosulfonamides **258** and **261**.¹⁴⁵ Exposure of enone **260** to *p*-toluenesulfonamide (**250**) and *N*-chlorosuccinimide (NCS) at 50 °C results in the *in situ* generation of dichlorosulfonamide **258**, ultimately yielding the expected imidazoline product **262** in sufficient yield and d.r.

Scheme 104. Improved Methods for the Direct Imidazolinization of α,β -Unsaturated Ketones



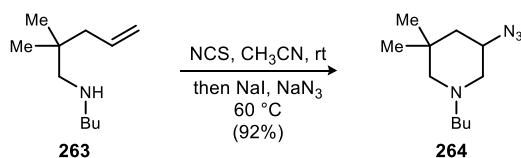
¹⁴³ Li, G.; Wei, H.-X.; Kim, S. H.; Carducci, M. D. *Angew. Chem. Int. Ed.* **2001**, *40*, 4277-4280.

¹⁴⁴ (a) Pei, W.; Wei, H.-X.; Chen, D.; Headley, A. D.; Li, G. *J. Org. Chem.* **2003**, *68*, 8404-8408; (b) Chen, D.; Timmons, C.; Wei, H.-X. *J. Org. Chem.* **2003**, *68*, 5742-5745.

¹⁴⁵ Timmons, C.; Chen, D.; Xu, X.; Li, G. *Eur. J. Org. Chem.* **2003**, 3850-3854.

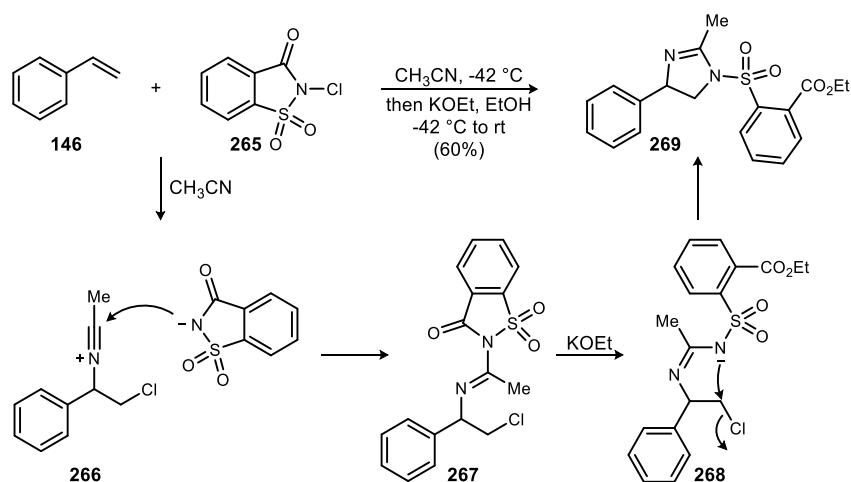
In a related approach, Wang and colleagues reported a system that incorporates NCS, NaN₃, and NaI as the additive, to promote the inter/intramolecular aminoazidation of γ -alkenyl protected amines en route to azidopiperidines.¹⁴⁶ To demonstrate, alkenyl protected amine **263**, when subjected to this NCS, NaN₃, and NaI combination at elevated temperatures, readily converts to azidopiperidine **264** in 92% yield (Scheme 105). It should be noted that this inter/intramolecular aminoazidation displays high favorability towards its 6-*endo*-trig piperidine product relative to its 5-*exo*-trig pyrrolidine regioisomer.

Scheme 105. Inter/Intramolecular Aminoazidation of γ -Alkenyl Amines with NCS, NaN₃, and NaI



Other chloramine-acetonitrile systems have proven sufficient for the diamination of olefins. In 2003, Booker-Milburn and co-workers reported a one-pot method for *cis*-imidazolinization of alkenes via the use of an *N*-chlorosaccharin-acetonitrile-KOEt combination (Scheme 106).¹⁴⁷ Styrene (**146**), when exposed to acetonitrile, can undergo a Ritter-type reaction with the electrophilic chlorinating agent *N*-chlorosaccharin (**265**) to arrive at nitrilium ion **266**. Subsequent capture of **266** with the saccharin anion affords β -chlorosulfonylamidine **267**, which upon treatment with KOEt undergoes an intramolecular cyclization to give imidazoline **269**.

Scheme 106. *cis*-Imidolizidination of Alkenes with *N*-Chlorosaccharin, CH₃CN, and KOEt

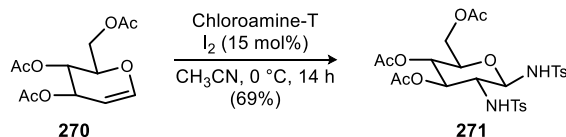


¹⁴⁶ Ortiz Jr., G. X.; Kang, B.; Wang, Q. *J. Org. Chem.* **2014**, 79, 571-581.

¹⁴⁷ Booker-Milburn, K. I.; Guly, D. J.; Cox, B.; Procopiou, P. A. *Org. Lett.* **2003**, 5, 3313-3315.

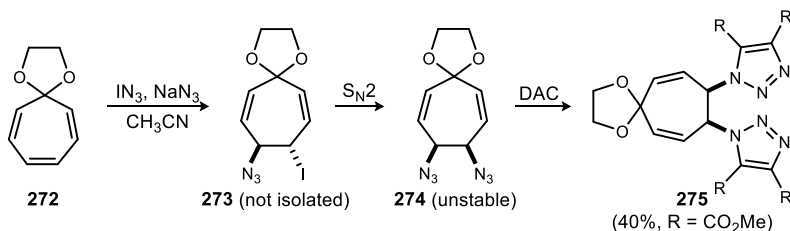
Ramesh and Kumar have also shown that chloramine-T in acetonitrile can be used to facilitate the diamination of enol ethers.¹⁴⁸ To illustrate the efficacy of this one-pot method, treatment of tri-*o*-acetyl-D-glucal (**270**) with stoichiometric amounts of chloramines-T in the presence of catalytic iodine results in the formation of β -D-*gluco* 1,2-disulfonamide **271** in 69% isolated yield (Scheme 107).

Scheme 107. Diamination of Glucal **270** Using I₂ and Chloroamine-T



Iodine azide (IN₃) is another halogen-based reagent that can be used for the diamination, more specifically diazidation, of olefins. Sasaki demonstrates the utility of this substrate through the diazidation of medium-sized cyclic alkenes.¹⁴⁹ For example, when subjecting tropone ethyleneketal (**272**) to both iodine azide and sodium azide in acetonitrile, iodoazide **273** is furnished, although not isolated (Scheme 108). Subsequent displacement of the iodide group with excess azide gives unstable diazide **274**, which is trapped as its respective 1,3-dipolar cycloadduct (**275**) upon treatment with dimethyl acetylenedicarboxylate (DAC).

Scheme 108. Diazidation of a Cyclic Polyene with IN₃ and NaN₃



Tamura has also reported that this iodine azide/sodium azide combination can readily promote the diazidation of benzofurans (Scheme 109).¹⁵⁰ The mechanistic pathway, however, is slightly different. Exposure of benzofuran **276** to IN₃ yields iodoazide **277**. Elimination of the iodide moiety results in the formation of oxonium **278**. A second equivalent of azide can add into the oxonium, affording the desired diazide in 93% yield, but with low levels of diastereoselection.

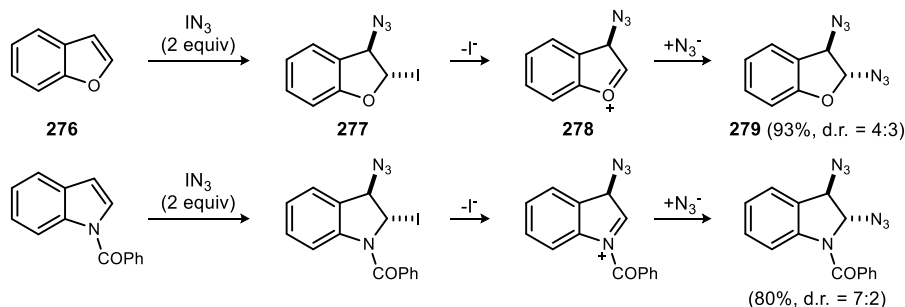
¹⁴⁸ (a) Kumar, V.; Ramesh, N. G. *Chem. Commun.* **2006**, 4952-4954; (b) Kumar, V.; Ramesh, N. G. *Org. Biomol. Chem.* **2007**, *5*, 3847-3858.

¹⁴⁹ Sasaki, T.; Kanematsu, K.; Yukimoto, Y. *J. Org. Chem.* **1972**, *37*, 890-894.

¹⁵⁰ (a) Kwon, S.; Okada, T.; Ikeda, M.; Tamura, Y. *Heterocycles* **1977**, *6*, 33-36; (b) Tamura, Y.; Chun, M. W.; Kwon, S.; Bayomi, S. M.; Okada, T.; Ikeda, M. *Chem. Pharm. Bull.* **1978**, *26*, 3515-3520.

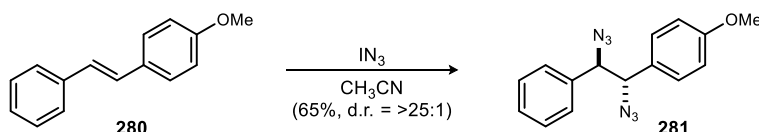
Furthermore, acyl and tosyl indoles can be converted to their corresponding diazides under the same reaction conditions and through an analogous mechanistic pathway.¹⁵¹

Scheme 109. Diazidation of Benzofurans and Indoles with IN_3



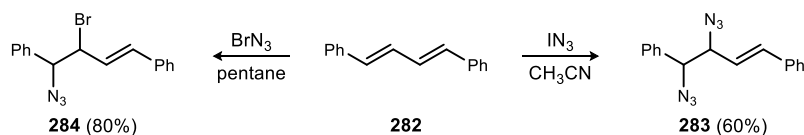
To expand on the versatility of iodine azide, this reagent can be used to transform *trans*-stilbenes to their corresponding 1,2-diaryl-1,2-diazidoethanes (Scheme 110).¹⁵² When *trans*-stilbene **280** is treated with IN_3 in the presence of excess azide, diazidoethane **281** is furnished in 65% yield and with high d.r. The fact that the *anti*-addition product is acquired in such large excess relative to its *syn*-adduct indicates that this transformation may go through a β -azidocarocation intermediate. Trapping of excess azide from the less hindered face would give the *anti*-product of **281**.

Scheme 110. Diazidation of *trans*-Stilbene **280** Using IN_3



Additionally, 1,3-diene systems can undergo 1,2-diazidation as reported by Hassner.¹⁵³ In this particular study, the reaction of *E,E*-diphenylbutadiene (**282**) with IN_3 generates diazide **283** in 60% isolated yield. Hassner also showed that the treatment of the same diene (**282**) with BrN_3 in pentane affords bromoazide analog **284** in 80% yield (Scheme 111).

Scheme 111. Hassner's Divergent Reactions of Diene **282** with BrN_3 and IN_3



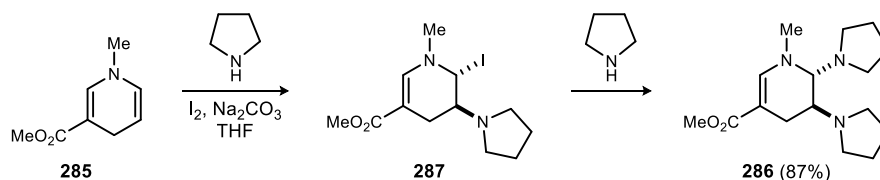
¹⁵¹ Tamura, Y.; Kwon, S.; Tabusa, F.; Ikeda, M. *Tetrahedron Lett.* **1975**, *16*, 3291-3294.

¹⁵² (a) Müller, R.; Gust, R.; Schönenberger, H.; Klement, U. *Chem. Ber.* **1991**, *124*, 2381-2389; (b) Gust, R.; Bernhardt, G.; Spruss, T.; Krauser, R.; Koch, M.; Schönenberger, H.; Bauer, K. H.; Schertl, S.; Lu. *Z. Arch. Pharm.* **1995**, *328*, 645-653.

¹⁵³ Hassner, A.; Keogh, J. *Tetrahedron Lett.* **1975**, *16*, 1575-1578.

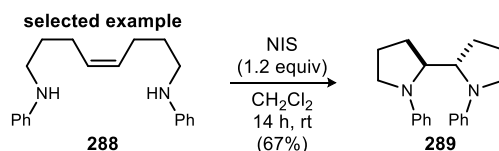
Another pathway that has proven fruitful for the synthesis of vicinal diamines is the intermolecular aminohalogenation of alkenes. Though the competitive oxidation of alkyl and aryl amines may be problematic, Lavilla and colleagues have reported a highly efficient method for the vicinal diamination of 1,4-dihydropyridines in the presence of iodine (Scheme 112).¹⁵⁴ Exposure of *N*-alkyl-1,4-dihydropyridine **285** to I₂ and an excess of pyrrolidine leads to the formation of *trans*-2,3-diaminotetrahydropyridine **286** in high yield. Mechanistically, it is believed that the iodonium intermediate formed from the reaction of the olefin with I₂ is opened with pyrrolidine to arrive at intermediate **287**. Internal displacement of the iodide generates an aziridinium ion which then undergoes ring opening at the 1-position with another equivalent of pyrrolidine to give the desired diamine.

Scheme 112. Iodine-Mediated Vicinal Diamination of 1,4-Dihydropyridine **285**



In 2012, Hennecke and co-workers reported the use of NIS to promote the doubly intramolecular diamination of alkenes en route to 2,2'-bipyrrrolidines.¹⁵⁵ When phenyl-derived alkenyl diamine **288** was subjected to a stoichiometric amount of NIS in dichloromethane, bipyrrrolidine **289** was furnished in 67% yield (Scheme 113). A number of other aryl- and alkyl-substituted alkenyl diamines were also tolerated, and *anti*-selective diamination was consistently observed.

Scheme 113. Intramolecular *anti*-Selective Diamination of Alkenes with NIS en Route to 2,2'-Bipyrrrolidines

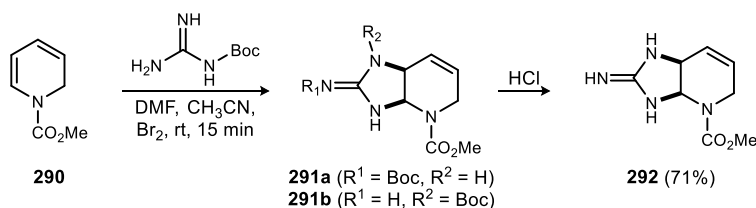


Halogen-mediated cycloguanidinations of alkenes have been explored to a considerable degree. The first reports of this form of alkene diamination were made by Al-Mourabit and colleagues when they demonstrated the bromine-mediated cycloguanidination of *N*-acylated

¹⁵⁴ (a) Lavilla, R.; Kumar, R.; Coll, O.; Masdeu, C.; Bosch, J. *Chem. Commun.* **1998**, 2715-2716; (b) Lavilla, R.; Kumar, R.; Coll, O.; Masdeu, C.; Spada, A.; Bosch, J.; Espinosa, E.; Molins, E. *Chem.-Eur. J.* **2000**, *6*, 1763-1772.

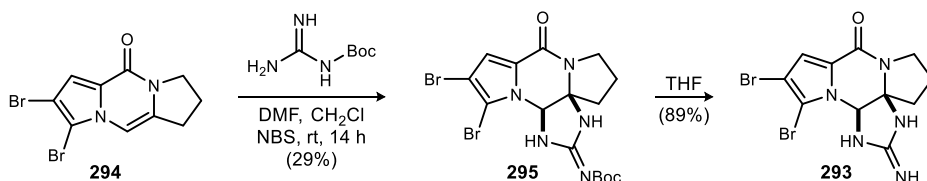
¹⁵⁵ Müller, C. H.; Fröhlich, R.; Daniliuc, C. G.; Hennecke, U. *Org. Lett.* **2012**, *14*, 5944-5947.

Scheme 114. Al-Mourabit's Bromine-Mediated Cycloguanidination of Dihydropyridines



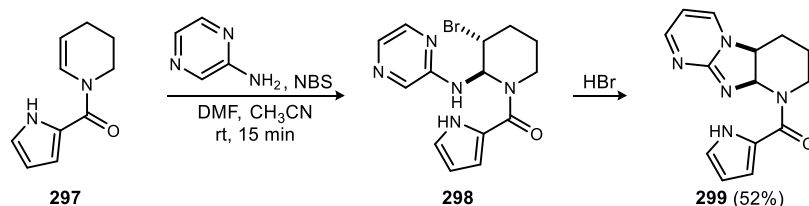
dihydropyridines.¹⁵⁶ Treatment of carbomethoxydihydropyridine (**290**) with bromine or NBS in the presence of excess Boc-guanidine afforded bicycles **291a** and **291b**. Subsequent acid-mediated deprotection of the Boc groups furnished cyclic guanidine **292** in 71% isolated yield (Scheme 114). Tepe and co-workers utilized a closely related cycloguanidination step in their recent synthesis of oroidin-type alkaloid (±)-dibromophakellin (**293**). When dipyrrolopyrazinone **294** was exposed to Boc-guanidine in the presence of NBS, cyclic guanidine **295** could be furnished, albeit in 29% yield. Acid-mediated deprotection of the Boc moiety proceeded more smoothly as dibromophakellin was obtained in high yield (Scheme 115).¹⁵⁷

Scheme 115. Tepe's Synthesis of (±)-Dibromophakellin via Alkene Cycloguanidination



Further studies by Al-Mourabit revealed that 2-aminopyrimidine (**296**) can also be used as a guanidinating agent (Scheme 116). Treatment of *N*-acylpyrrole tetrahydropyridine **297** with NBS in the presence of 2-aminopyrimidine results in the formation of intermediate **298**. Subsequent displacement of the bromide group and generation of HBr gives the desired guanidine (**299**) in 52% isolated yield.¹⁵⁸

Scheme 116. Cycloguanidination of Dihydropyridines with 2-Aminopyrimidine



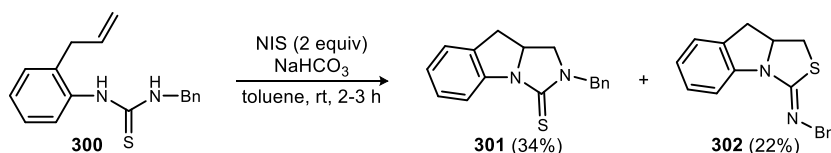
¹⁵⁶ Abou-Jneid, R.; Ghoulami, S.; Martin, M. T.; Dau, E. T.; Travert, N.; Al-Mourabit, A. *Org. Lett.* **2004**, *6*, 3933-3936.

¹⁵⁷ Hewlett, N. M.; Tepe, J. J. *Org. Lett.* **2011**, *13*, 4550-4553.

¹⁵⁸ (a) Picon, S.; Tran, H. D.; Martin, M. T.; Retailleau, P.; Zaparucha, A.; Al-Mourabit, A.; *Org. Lett.* **2009**, *11*, 2523-2526; (b) Schroif-Gregoire, C.; Travert, N.; Zaparucha, A.; Al-Mourabit, A.; *Org. Lett.* **2006**, *8*, 2961-2964.

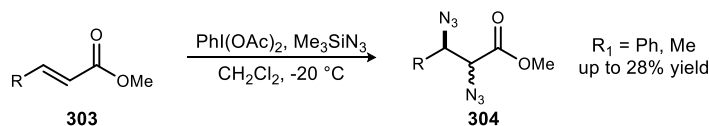
Recently, Zhang and co-workers reported the use of NIS to promote the doubly intramolecular diamination of *N*-alkenyl thioureas.¹⁵⁹ For example, treatment of benzyl-protected alkenyl thiourea **300** with stoichiometric quantities of NIS in the presence of NaHCO₃ afforded diamination product **301** in 34% yield (Scheme 117). Additionally, aminosulfuration was observed as a competitive process as aminosulfuration product **302** was isolated in 22% yield from the same reaction mixture.

Scheme 117. Zhang's NIS-Mediated Doubly Intramolecular Diamination of *N*-Alkenyl Thioureas



Hypervalent iodine reagents display high synthetic utility in the field of alkene diamination. In light of their ready availability, low toxicity, and reduced environmental impact, these iodine(III) species have gradually replaced a number of heavy metal-mediated protocols. Among the earliest methods of using aryl- λ^3 -iodanes en route to diamination is that reported by Zbiral and Ehrenfreund. Here, unsaturated esters (**303**) are subjected to the combination of PhI(OAc)₂ and TMSN₃ to achieve the synthesis of vicinal diazides (**304**). Despite the advance, this approach suffered from low yields and a very limited substrate scope (Scheme 118).¹⁶⁰

Scheme 118. Diazidation of α,β -Unsaturated Esters with PhI(OAc)₂



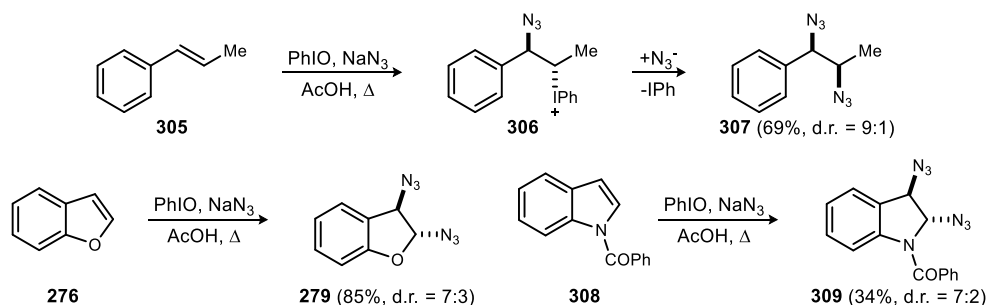
Moriarty and Khosrowshahi later reported a similar, but considerably more effective iodine(III)-mediated alkene diazidation.¹⁶¹ When subjecting alkenes, such as *trans*- β -methylstyrene (**305**) to the combination of sodium azide and iodobenzene in the presence of acid at elevated temperatures, iodonium ion intermediate **306** is formed (Scheme 119). Subsequent displacement of the iodonium species with azide affords diazide **307** in 69% yield and in 9:1 d.r. Further success of this reaction was demonstrated as benzofuran and indole scaffolds are readily converted to their respective diazides as well.

¹⁵⁹ Zhang, J.; Zhang, X.; Wu, W.; Zhang, G.; Xu, S.; Shi, M. *Tetrahedron Lett.* **2015**, *56*, 1505-1509.

¹⁶⁰ Ehrenfreund, J.; Zbiral, E. *Tetrahedron* **1972**, *28*, 1697-1704.

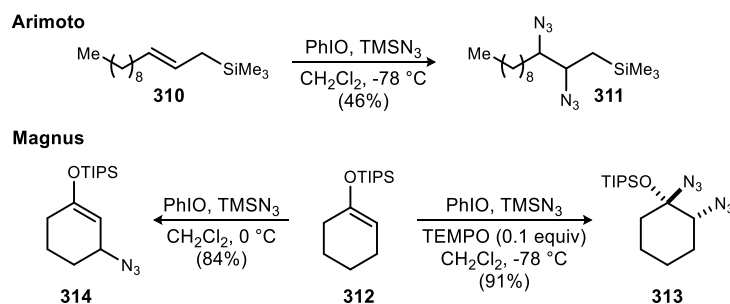
¹⁶¹ Moriarty, R. M.; Khosrowshahi, J. S. *Tetrahedron Lett.* **1986**, *27*, 2809-2812.

Scheme 119. Synthesis of Vicinal Diazides Using Iodosobenzene



Alkene diazidation can also be achieved through the use of iodosobenzene in conjunction with trimethylsilyl azide (TMSN_3). Arimoto and co-workers illustrate the efficacy of this hypervalent iodine/silyl azide combination via the smooth conversion of allylsilanes to their corresponding vicinal diazides (Scheme 120).¹⁶² Additionally, Magnus and colleagues show that this same reagent combination can promote the diazidation of triisopropylsilyl (TIPS) enol ethers under chilled conditions.¹⁶³ For example, reaction of enol ether **312** with iodosobenzene and TMSN_3 in the presence of catalytic amounts of TEMPO at $-78\text{ }^\circ\text{C}$ affords diazide **313** in 91% isolated yield. Yet, if the same reaction is run at $0\text{ }^\circ\text{C}$, β -azidation (**314**) is observed. Thus, diazidation of enol ethers with iodine(III) and azide is highly dependent on temperature.

Scheme 120. Vicinal Diaminations of Alkenes Employing PhIO/TMSN_3



In 2011, Muñiz and co-workers reported a breakthrough method that employs a chiral hypervalent iodine species to promote the doubly intermolecular, enantioselective diamination of styrenes (Scheme 121).¹⁶⁴ Aside from being metal-free and practical, this approach is notable as it is the first example of a doubly intramolecular, enantioselective alkene diamination. When using bis(mesylimide) as the nitrogen source in the presence of Ishihara's C_2 -symmetric

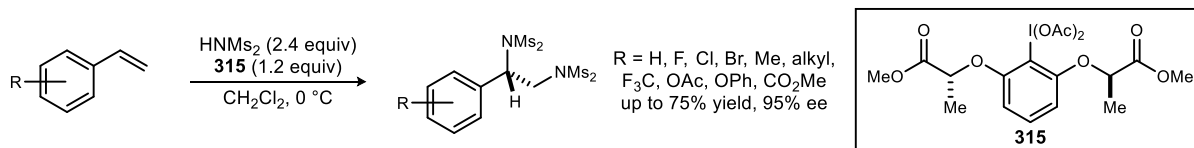
¹⁶² Arimoto, M.; Yamaguchi, H.; Fujita, E.; Nagao, Y.; Ochiai, M. *Chem. Pharm. Bull.* **1989**, *37*, 3221-3224.

¹⁶³ Magnus, P.; Roe, M. B.; Hulme, C. *J. Chem. Soc., Chem. Commun.* **1995**, 263-265.

¹⁶⁴ Roben, C.; Souto, J. A.; González, Y.; Lishchynskiy, A.; Muñiz, K. *Angew. Chem. Int. Ed.* **2011**, *50*, 9478-9482.

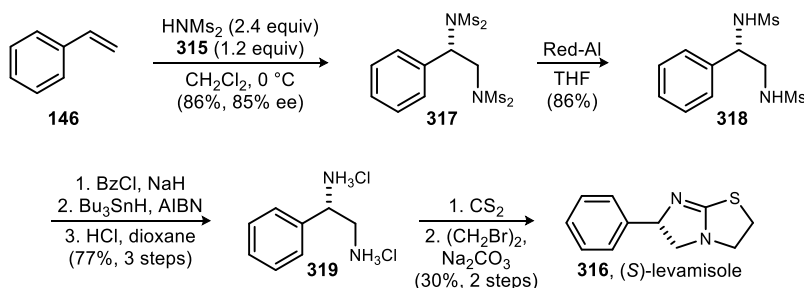
chiral iodane **315**,¹⁶⁵ a variety of styrenes can be converted to their respective diamines in good yields and with high levels of enantioselection.

Scheme 121. Muñiz's Enantioselective, Metal-Free Intermolecular Diamination of Styrenes



Furthermore, Muñiz and colleagues were able to apply this methodology towards the synthesis of the immunomodulator and veterinary anthelmintic (*S*)-levamisole (**316**) (Scheme 122). Styrene (**146**) is converted to masked diamine **317** in good yield and ee via the enantioselective diamination as previously described. Hydride reduction of **317** with Red-Al afforded bis-mono protected diamine **318** in 86% isolated yield. Benzoylation, radical desulfination, and acid hydrolysis afforded the corresponding unmasked diamine as the bis-HCl salt (**319**) in 77% yield over 3 steps. Liberation of **319** to its free base form and subsequent treatment with carbon disulfide results in the formation of the precursor mercaptoimidazoline. This intermediate can then be treated with ethylene dibromide under basic conditions in order to furnish (*S*)-levamisole (**316**) (30% yield over 2 steps).

Scheme 122. Muñiz's Enantioselective Synthesis of (*S*)-Levamisole via Intermolecular Diamination

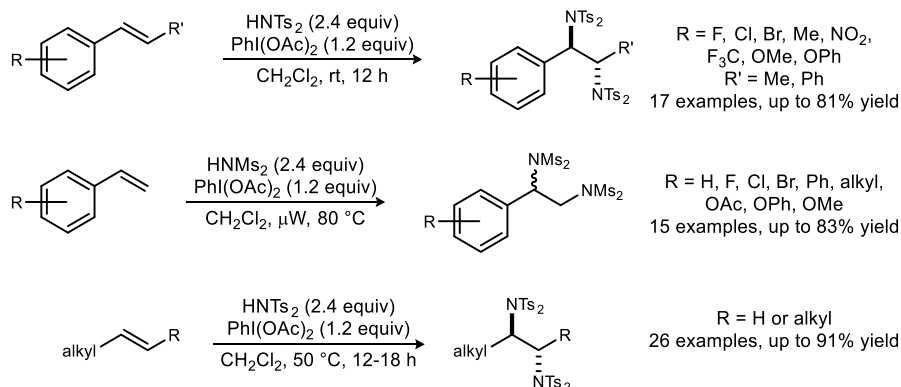


Muñiz continued to demonstrate the efficacy of hypervalent iodine in doubly intermolecular vicinal alkene diaminations by considerable scope expansion (Scheme 123). When using bis(tosylimide) as the nitrogen source in the presence of $\text{PhI}(\text{OAc})_2$, a variety of styrenes were readily transformed to their desired diamines in high yields. The bis(mesyylimide) diamine library was also significantly expanded via microwave irradiation. It is also notable that the diamine library was not limited to just styrene substrates. Numerous alkyl-substituted alkenes were

¹⁶⁵ Uyanik, M.; Yasui, T.; Ishihara, K. *Angew. Chem. Int. Ed.* **2010**, *49*, 2175-2177.

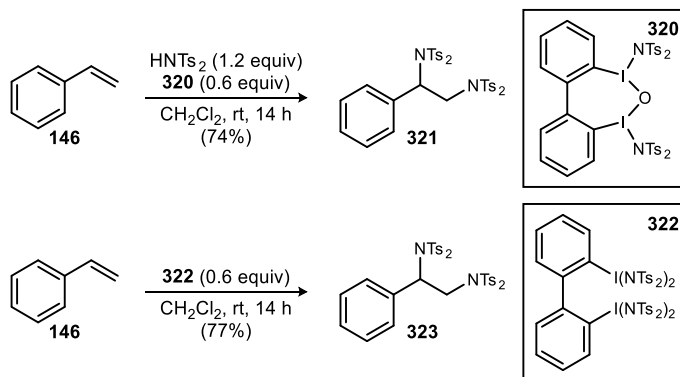
converted to their respective bistosylimide diamine scaffolds upon exposure to $\text{PhI}(\text{OAc})_2$ as well.¹⁶⁶

Scheme 123. Iodine(III)-Promoted Intermolecular Diaminations of Styrenes and Alkyl-Substituted Alkenes



Dinuclear iodine(III) species also proved effective in inter/intermolecular alkene diamination as described by Muñiz and colleagues (Scheme 124).¹⁶⁷ Upon reaction optimization, treatment of styrene (**146**) with substoichiometric quantities of bisimido dinuclear iodine(III) species **320** and stoichiometric quantities of bis(tosylimide) afforded diamine **321** in 74% isolated yield. Additionally, deoxygenated dinuclear iodine(III) compound **322** showed slightly superior reactivity as styrene was converted to **323** without the need for external bistosylimide.

Scheme 124. Intermolecular Alkene Diaminations via the Use of Dinuclear Iodine(III)



To complement iodine(III)-promoted inter/intermolecular alkene diaminations, Chiba and colleagues reported that hypervalent iodine promotes inter/intramolecular vicinal diamination of alkenes (Scheme 125).¹⁶⁸ Here, a variety of amidines are smoothly converted to their desired

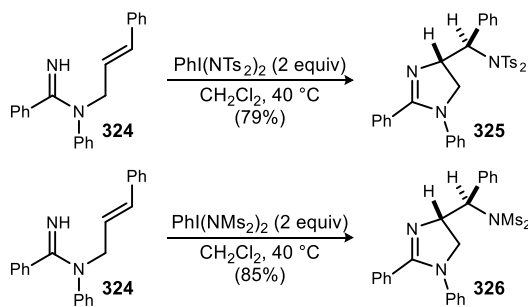
¹⁶⁶ Souto, J. A.; González, Y.; Iglesias, A.; Zian, D.; Lishchynskiy, A.; Muñiz, K. *Chem. Asian. J.* **2012**, *7*, 1103-1111.

¹⁶⁷ Röben, C.; Souto, J. A.; Escudero-Adán, E. C.; Muñiz, K. *Org. Lett.* **2013**, *15*, 1008-1011.

¹⁶⁸ Chen, H.; Kaga, A.; Chiba, S. *Org. Lett.* **2014**, *16*, 6136-6139.

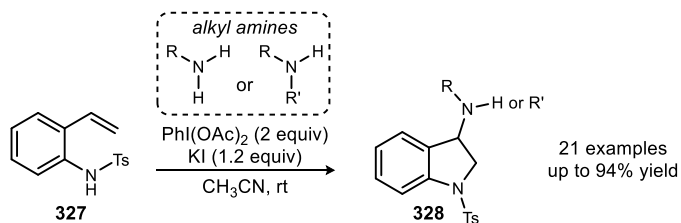
dihydroimidazoles upon exposure to $\text{PhI}(\text{NTs}_2)_2$ or $\text{PhI}(\text{NMs}_2)_2$. For example, when amidine **324** is subjected to $\text{PhI}(\text{NTs}_2)_2$ in dichloromethane at elevated temperatures, dihydroimidazole **325** is provided in 79% yield. The bismesyylimide analog (**326**) can also be furnished when $\text{PhI}(\text{NMs}_2)_2$ is employed as the source of iodine(III).

Scheme 125. Inter/Intramolecular Alkene Diamination with $\text{PhI}(\text{NTs}_2)_2$ and $\text{PhI}(\text{NMs}_2)_2$



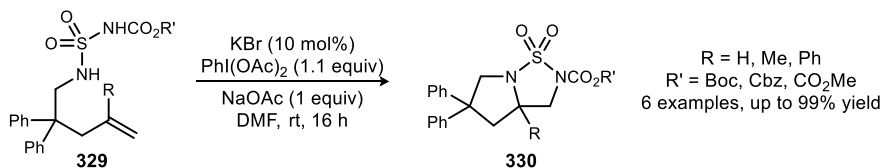
In 2014, Hong and Johnston demonstrated a highly efficacious inter/intramolecular alkene diamination approach that utilizes $\text{PhI}(\text{OAc})_2$ and KI en route to forming 3-aminoindolines (Scheme 126).¹⁶⁹ Here, tosyl-protected vinylaniline **327** can be treated with an array of

Scheme 126. Inter/Intramolecular Diaminations of Vinylanilines en Route to 3-Aminoindolines



commercially available primary and secondary amines in the presence of the aforementioned oxidant/additive combination in order to provide desired indoline compounds (**328**) in moderate to high yields.

Scheme 127. $\text{PhI}(\text{OAc})_2/\text{KI}$ -Mediated Intramolecular Diamination of Alkenyl Sulfamides

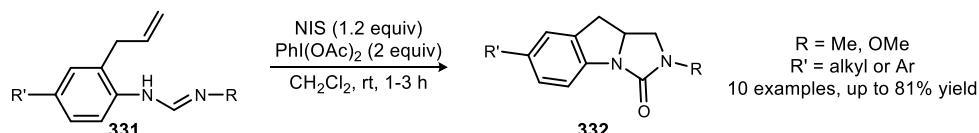


As for iodine(III)-mediated doubly intramolecular vicinal diaminations of alkenes, notable discoveries have been made by both Muñiz and Shi. Muñiz and co-workers reported that a

¹⁶⁹ Hong, K.; Johnston, J. N. *Org. Lett.* **2014**, *16*, 3804-3807.

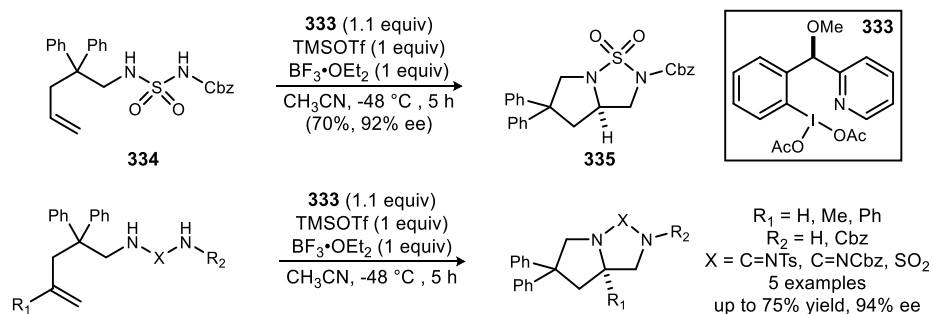
halide/oxidant (KBr/PhI(OAc)₂) combination, similar to that of Hong and Johnston's work, can promote the diamination of alkenyl sulfamides (**329**) to their corresponding cyclic sulfamides (**330**) in practically quantitative yields (Scheme 127).¹⁷⁰ Shi and colleagues reported that a variety of formamidines (**331**) can be converted to their respective tricyclic ureas (**332**) upon treatment with NIS and PhI(OAc)₂ under very mild conditions (Scheme 128).¹⁷¹

Scheme 128. PhI(OAc)₂/NIS-Mediated Intramolecular Diamination of Formamidines



Wirth and co-workers further pioneer intra/intramolecular vicinal diaminations by reporting an enantioselective version of this type of diamination using chiral hypervalent iodine catalyst **333** (Scheme 129).¹⁷² Through reaction optimization, it was found that iodine(III) species **333** in the presence of TMSOTf and BF₃•OEt₂ could readily convert diaminosulfone **334** to cyclic diaminosulfone **335** in good yield and with excellent enantioselection. This highly enantioselective approach was applied to the formation of numerous diamino heterocyclic products as shown in Scheme 129.

Scheme 129. Wirth's Enantioselective Intramolecular Diaminations en Route to Diamino Bicycles



5.3. Reaction Optimization and Substrate Scope

As previously mentioned, Hong and Johnston recently reported a highly efficacious iodine(III)-mediated inter/intramolecular oxidative diamination of terminal alkenes.¹⁶⁹ By employing a PhI(OAc)₂/KI oxidant/additive combination in the presence of electron-rich amines,

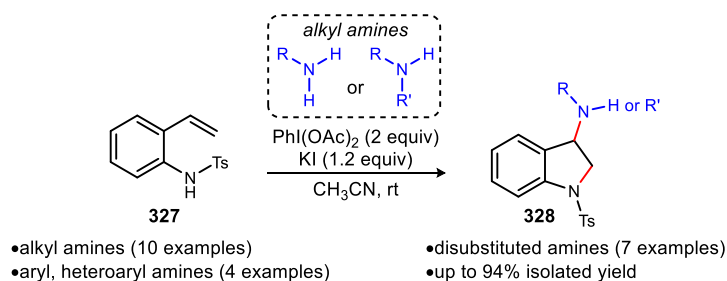
¹⁷⁰ Chávez, P.; Kirsch, J.; Hövelmann, C. H.; Streuff, J.; Martínez-Belmonte, M.; Escudero-Adán, E. C.; Martín, E.; Muñoz, K. *Chem. Sci.* **2012**, *3*, 2375-2382.

¹⁷¹ Zhang, J.; Wu, W.; Zhang, X.; Zhang, G.; Xu, S.; Shi, M. *Chem. Asian. J.* **2015**, *10*, 544-547.

¹⁷² Mizar, P.; Laverny, A.; El-Sherbini, M.; Farid, U.; Brown, M.; Malmedy, F.; Wirth, T. *Chem. Eur. J.* **2014**, *20*, 9910-9913.

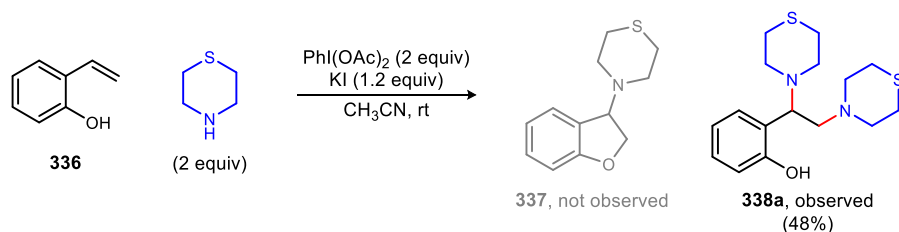
tosylated *ortho*-vinyl aniline **327** was readily converted to a number of 3-aminoindolines (**328**) under mild and metal-free conditions (Scheme 130). Monosubstituted alkyl and aryl amines as well as disubstituted amines were tolerated, ultimately furnishing a library of over 20 aminoindolines. This metal-free approach is unique as it promotes alkene diamination using a combination of electron-rich and electron-deficient (aryl sulfonamide) nitrogen sources without the need for amine preactivation or protection.

Scheme 130. Hong and Johnston's Iodine(III)-Mediated Inter/Intramolecular Diamination of Terminal Alkenes



Inspired by the success of this system, we sought to expand this methodology to vinyl phenol motifs with ambitions of directly accessing 3-aminodihydrobenzofurans via an inter/intramolecular aminohydroxylation reaction. Upon subjecting 2-vinyl phenol (**336**) to stoichiometric quantities of $\text{PhI}(\text{OAc})_2$ and KI in the presence of excess thiomorpholine and CH_3CN , we found that the desired 3-aminodihydrobenzofuran (**337**) was not observed (Scheme 131). Instead, diamine **338a** was acquired in 48% isolated yield under these reaction conditions (Table 13, entry 1). This result garnered immediate interest as the observed diamine can only be afforded via an unexpected doubly intermolecular alkene diamination pathway.

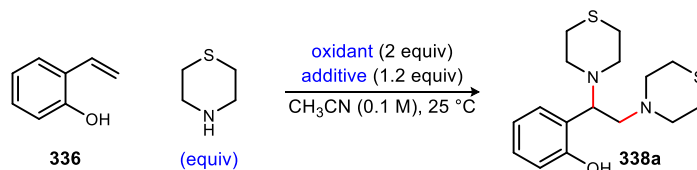
Scheme 131. Initial Findings of an Iodine(III)-Mediated Doubly Intermolecular Alkene Diamination



With this result in hand, optimization studies of this diamination reaction ensued. Previous mechanistic hypotheses indicate that interaction between $\text{PhI}(\text{OAc})_2$ and KI results in the formation of an electrophilic iodinating reagent, which in turn can react with nucleophilic amine to generate an electrophilic *N*-iodamine species.¹⁶⁹ As an alternative to the $\text{PhI}(\text{OAc})_2/\text{KI}$ combination, NIS could be used as the electrophilic iodinating reagent to provide the iodamine

species required for reactivity. When NIS was employed as the iodinating agent in the presence of 2-vinyl phenol and thiomorpholine, diamine **338a** was furnished in 40% yield indicating a slightly inferior reactivity profile compared to the oxidant/additive combination (Table 13, entry 2). Different halide sources in combination with $\text{PhI}(\text{OAc})_2$ were examined next. Use of stoichiometric potassium bromide and ammonium iodide provided diamine **338a** in 36% and 40% yields, respectively (Table 13, entries 3 and 4). The combination of oxidant and additive proved essential as starving the reaction conditions of KI or $\text{PhI}(\text{OAc})_2$ resulted in little or no reactivity (Table 13, entries 5 and 6). Upon increasing the amount of amine to 3 equivalents, full conversion of starting material was observed leading to a 78% isolated yield of **338a** after chromatographic separation (Table 13, entry 7). Interestingly, when 4 equivalents of thiomorpholine were used, inhibition of product formation was observed as **338a** was provided in only 57% yield (Table 13, entry 8). The use of another hypervalent iodine reagent, iodosobenzene, in combination with KI, afforded diamine **338a**, but in depressed yield relative to $\text{PhI}(\text{OAc})_2$ and KI (Table 13, entry 9).

Table 13. Initial Optimization Studies of the Doubly Intermolecular Alkene Diamination

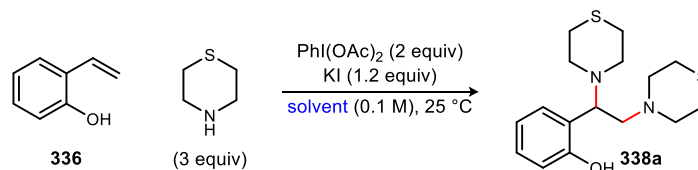


entry	oxidant	additive	amine equiv.	yield (%)
1	$\text{PhI}(\text{OAc})_2$	KI	2	48
2	--	NIS	2	40
3	$\text{PhI}(\text{OAc})_2$	KBr	2	36
4	$\text{PhI}(\text{OAc})_2$	NH_4I	2	40
5	$\text{PhI}(\text{OAc})_2$	--	2	10
6	--	KI	2	N/A
7	$\text{PhI}(\text{OAc})_2$	KI	3	78
8	$\text{PhI}(\text{OAc})_2$	KI	4	57
9	PhIO	KI	3	36

With sufficient reactivity achieved, a variety of solvents were evaluated to see if yield could be further improved. Dichloromethane mitigated product acquisition as **338a** was provided in 21% yield (Table 14, entry 2). Product formation was further inhibited when toluene was employed as the solvent (Table 14, entry 3). Etheral solvents such as THF and 1,4-dioxane proved inferior as the desired diamine was afforded in 6% and 17% yields, respectively (Table 14, entries 4 and 5).

Therefore, it is evident that CH₃CN is necessary in order to achieve maximum conversion to product.

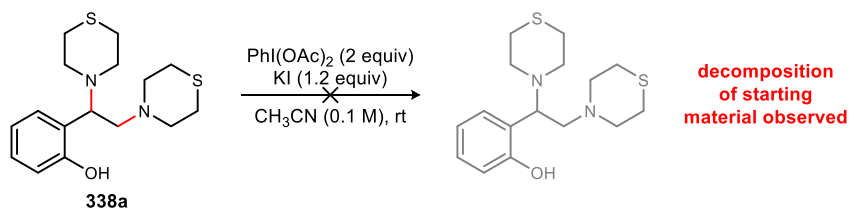
Table 14. Solvent Screen of the Doubly Intermolecular Alkene Diamination



entry	solvent	yield (%)
1	CH ₃ CN	78
2	CH ₂ Cl ₂	21
3	toluene	7
4	THF	6
5	1,4-dioxane	17

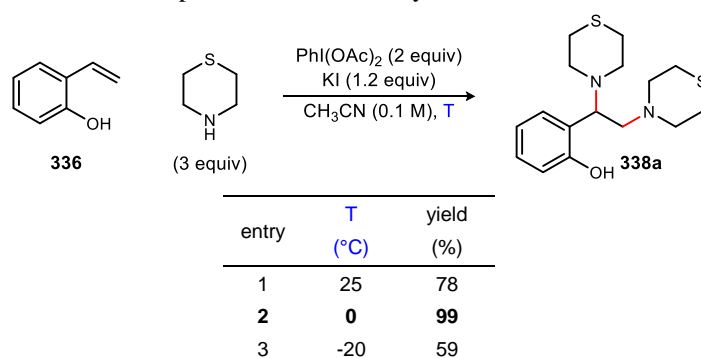
In regards to the most optimal reaction conditions up to this point (Table 13, entry 7), one observation of interest for this particular experiment was the cleanliness of the crude NMR data. First off, there was no sign of starting material (2-vinyl phenol) indicating that this reaction proceeded to full conversion. The only compounds that could be observed by NMR of the crude reaction mixture were iodobenzene (as a result of reaction and subsequent decomposition of PhI(OAc)₂) and the desired diamine. Additionally, there were no discernible side products. Therefore, quantitative or near-quantitative yield of diamine **338a** for this run was expected. Yet after column chromatography, a 78% isolated yield of **338a** indicated that there was indeed room for improved yield. Based on the cleanliness of the reaction and the non-quantitative yield acquired, it was hypothesized that the diamine product may decompose to a degree *in situ*, ultimately owing to a 78% isolated yield rather than a more fruitful and expected yield (>95%). To probe this hypothesis, diamine **338a** was subjected to the optimized reaction conditions, but with no amine, to obtain evidence for product decomposition (Scheme 132). Decomposition was observed as only trace quantities of the submitted diamine were isolated upon chromatographic separation.

Scheme 132. Decomposition Experiment with Diamine **338a**



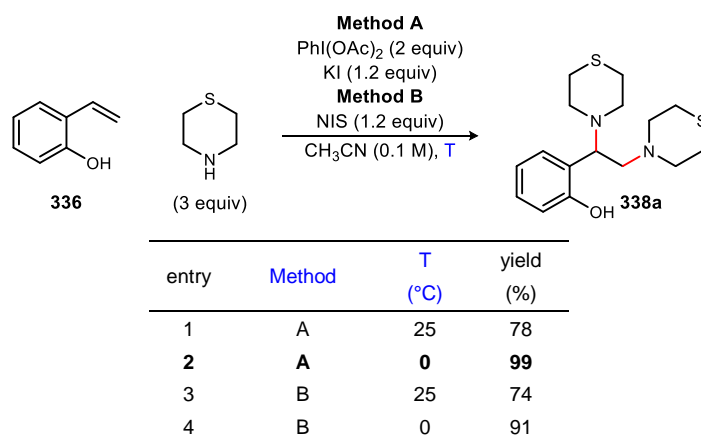
This evidence for decomposition provided a basis for yield optimization. When the temperature was lowered to 0 °C, complete and clean conversion of starting material to product was seen, analogous to that of the run at 25 °C. However, upon chromatographic separation, we were delighted to see that diamine **338a** was acquired in 99% isolated yield (Table 15, entry 2). Further chilling the reaction to -20 °C mitigated product formation as diamine **338a** was afforded in 59% yield after column chromatography (Table 15, entry 3). 0 °C was used as the optimal temperature as desired diamine can be produced while minimizing decomposition or undesired side reactivity.

Table 15. Effects of Temperature on the Doubly Intermolecular Alkene Diamination



Before developing an amine scope, two things needed to be confirmed: 1) that the PhI(OAc)₂/KI combination exhibits superior reactivity relative to NIS, and 2) that the hydroxyl motif of 2-vinyl phenol is essential for reactivity. This involved examining a multitude of alkenes with both sets of reaction conditions. As shown in Table 16, treatment of *ortho*-hydroxystyrene (2-vinyl phenol) with thiomorpholine (3 equivalents) at room temperature and 0 °C led to diamine **338a** in 78% and 99% yields respectively (entries 1 and 2). When NIS was employed as the

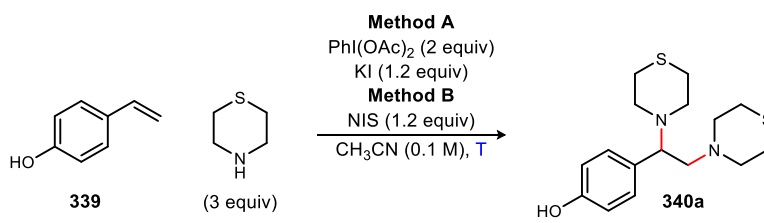
Table 16. Diamination of 2-Vinyl Phenol with PhI(OAc)₂/KI and NIS



electrophilic iodinating reagent at room temperature, the desired diamine was afforded but in slightly lower yield relative to the $\text{PhI}(\text{OAc})_2/\text{KI}$ run (Table 16, entry 3). When the reaction temperature was lowered to 0 °C, NIS once again engaged in diamination, furnishing diamine **338a** in 91% isolated yield (Table 16, entry 4). The results acquired with NIS were analogous to those of $\text{PhI}(\text{OAc})_2/\text{KI}$ in the sense that higher yields were acquired when reaction temperature was lowered. Yet, when directly comparing reaction efficacy between $\text{PhI}(\text{OAc})_2/\text{KI}$ and NIS, it was evident that the iodine(III)/additive combination consistently proves superior yield.

The next alkene that was examined was *para*-hydroxystyrene (4-vinyl phenol). This particular alkene was of interest as the lone pairs of the hydroxyl group should still be in conjugation with the terminal alkene. In other words, because the hydroxyl motifs of both 2-vinyl phenol and 4-vinyl phenol are in conjugation with the terminal olefin, nucleophilicity of 2-vinyl phenol and 4-vinyl phenol should be similar. Consequently, diamination with 4-vinyl phenol (**339**) should be observed. When 4-vinyl phenol was treated with $\text{PhI}(\text{OAc})_2$ and KI in the presence of thiomorpholine at room temperature, we were delighted to see that diamine **340a** was provided in 51% yield, upon chromatographic separation (Table 17, entry 1). Parallel to the 2-vinyl phenol system, lowering the reaction temperature resulted in increased yield of the desired diamine (62% yield) (Table 17, entry 2). NIS also engaged in diamination at both room temperature and 0 °C, furnishing diamine **340a** in 40% and 50% yields, respectively (Table 17, entries 3 and 4). These results once again indicate that better yields are obtained at lower temperature and that the $\text{PhI}(\text{OAc})_2/\text{KI}$ oxidant/additive combination is the superior set of reaction conditions.

Table 17. Diamination of 4-Vinyl Phenol with $\text{PhI}(\text{OAc})_2/\text{KI}$ and NIS

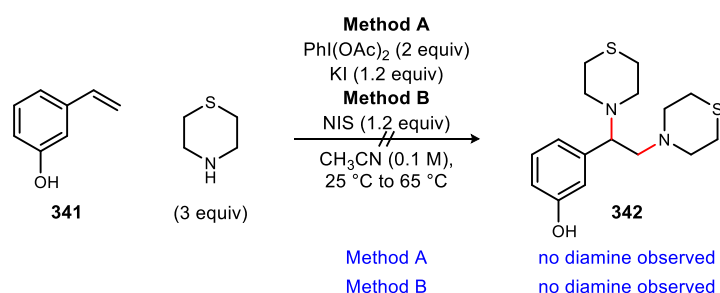


entry	Method	T (°C)	yield (%)
1	A	25	51
2	A	0	62
3	B	25	40
4	B	0	50

3-Vinyl phenol (*meta*-hydroxystyrene) was examined next. Unlike *ortho*-hydroxystyrene and *para*-hydroxystyrene, the lone pairs of the hydroxyl group of *meta*-hydroxystyrene should not

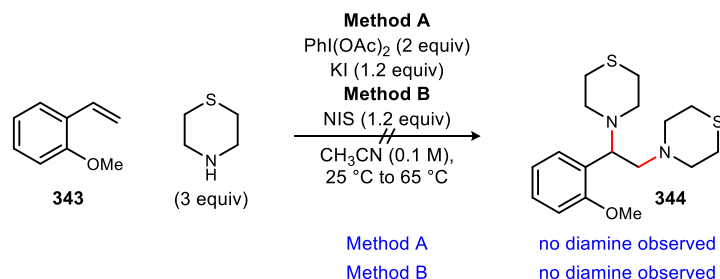
be in conjugation with the terminal alkene. As a result, 3-vinyl phenol (**341**) should have a decreased nucleophilicity compared to its 2-vinyl phenol and 4-vinyl phenol counterparts. When treating 3-vinyl phenol with the $\text{PhI}(\text{OAc})_2/\text{KI}$ combination in the presence of thiomorpholine at room temperature, no conversion of starting material could be seen after an 18 hour reaction period (Scheme 133). The same result was observed even after elevation of reaction temperature. Additionally, NIS proved fruitless as only starting material was observed after prolonged reaction times at both room temperature and 65 °C. These results clearly indicate that having the hydroxyl motif *ortho* or *para* to the terminal alkene is vital for sufficient reactivity.

Scheme 133. Unsuccessful Diamination of 3-Vinyl Phenol with $\text{PhI}(\text{OAc})_2/\text{KI}$ and NIS



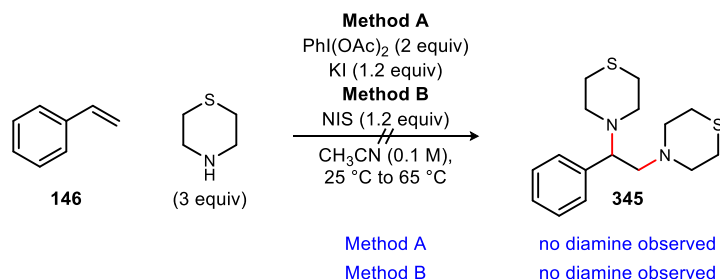
To further probe the necessity of a hydroxyl unit at the *ortho* and/or *para* positions of styrene, 2-vinylanisole (**343**) was submitted to the diamination protocol. This substrate was of interest as it possesses an electron-donating motif *ortho* to the alkene functionality, similar to that of 2-vinyl phenol. Furthermore, the lone pairs of the methoxy motif should be in conjugation with the terminal olefin, giving it a reactivity profile comparable to its *ortho*-hydroxystyrene analog. However, when 2-vinylanisole was treated with $\text{PhI}(\text{OAc})_2/\text{KI}$ or NIS in the presence of thiomorpholine, reactivity was mitigated as no corresponding diamine (**344**) was observed, even with the application of higher temperature (Scheme 134). Based on these findings, it is evident that having a free hydroxyl group as the electron-donating species is critical for the nucleophilicity of the alkene.

Scheme 134. Unsuccessful Diamination of 2-Vinylanisole with $\text{PhI}(\text{OAc})_2/\text{KI}$ and NIS



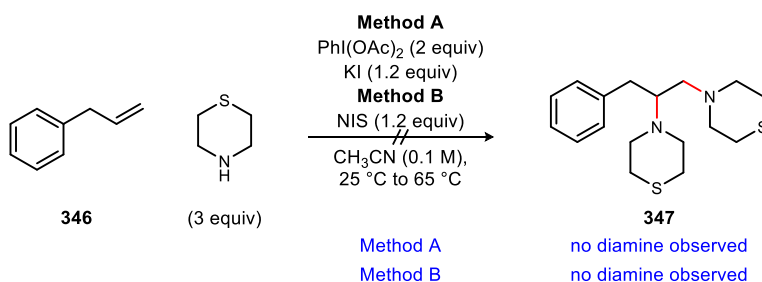
Styrene (**146**) was the next alkene to be evaluated. With decreased nucleophilicity relative to *ortho*-hydroxystyrene and *para*-hydroxystyrene, the expectations for diamination with styrene as the substrate were relatively low. When subjected to the diamination protocol with $\text{PhI}(\text{OAc})_2$ and KI, styrene appeared to be unreactive as predicted (Scheme 135). The same results were observed when NIS was used as the iodinating agent.

Scheme 135. Unsuccessful Diamination of Styrene with $\text{PhI}(\text{OAc})_2/\text{KI}$ and NIS



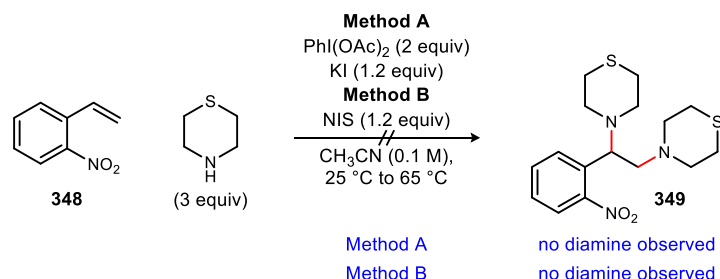
The next alkene that was employed was allylbenzene (**346**). With the terminal alkene out of conjugation with the aromatic ring, it was expected that this substrate would be unreactive. Consequently, no diamination (**347**) was observed when allylbenzene was subjected to either diamination method at ambient or elevated temperatures (Scheme 136).

Scheme 136. Unsuccessful Diamination of Allylbenzene with $\text{PhI}(\text{OAc})_2/\text{KI}$ and NIS



ortho-Nitrostyrene (**348**) was also examined as this was an alkene that benefits from conjugation while being resistant to direct oxidation by $\text{PhI}(\text{OAc})_2$. This, too, failed to convert to

Scheme 137. Unsuccessful Diamination of *ortho*-Nitrostyrene with $\text{PhI}(\text{OAc})_2/\text{KI}$ and NIS

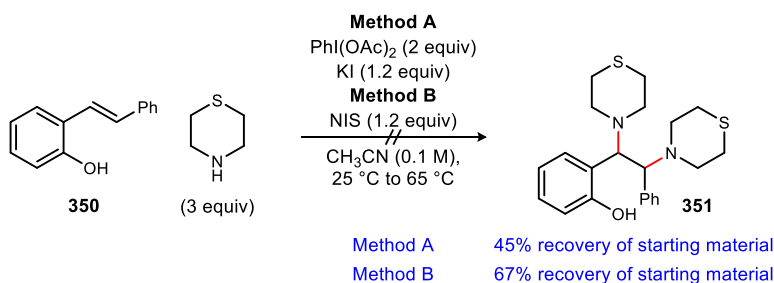


its corresponding diamine (**349**) when treated with either the oxidant/additive combination or NIS (Scheme 137). Additionally, higher temperatures were implemented, but to no avail.

Given that 2-vinyl phenol and 4-vinyl phenol successfully engaged in diamination, whereas 3-vinyl phenol, 2-vinylanisole, styrene, allylbenzene, and *ortho*-nitrostyrene proved fruitless, it is evident that the hydroxyl motif of 2-vinyl phenol and/or 4-vinyl phenol is essential for the promotion of reactivity. Furthermore, the diamination protocol employing the $\text{PhI}(\text{OAc})_2/\text{KI}$ combination consistently gave higher yields, in successful cases, compared to the NIS variation. With these findings in hand, one final parameter was to be examined before developing the amine scope: the necessity of a terminal alkene.

All alkenes subjected to diamination up to this point have been terminal alkenes. Given previous findings, we were interested in seeing if internal alkenes could readily undergo diamination. *ortho*-Styryl phenol (**350**) was the reagent of choice as it was a 2-vinyl phenol analog that possessed an internal alkene. When *ortho*-styryl phenol was treated with $\text{PhI}(\text{OAc})_2$ and KI in the presence of thiomorpholine, no diamination (**351**) was observed, resulting in a 45% recovery of starting material (Scheme 138). NIS also proved ineffective, once again resulting in the reacquisition of *o*-styrylphenol (67% recovery).

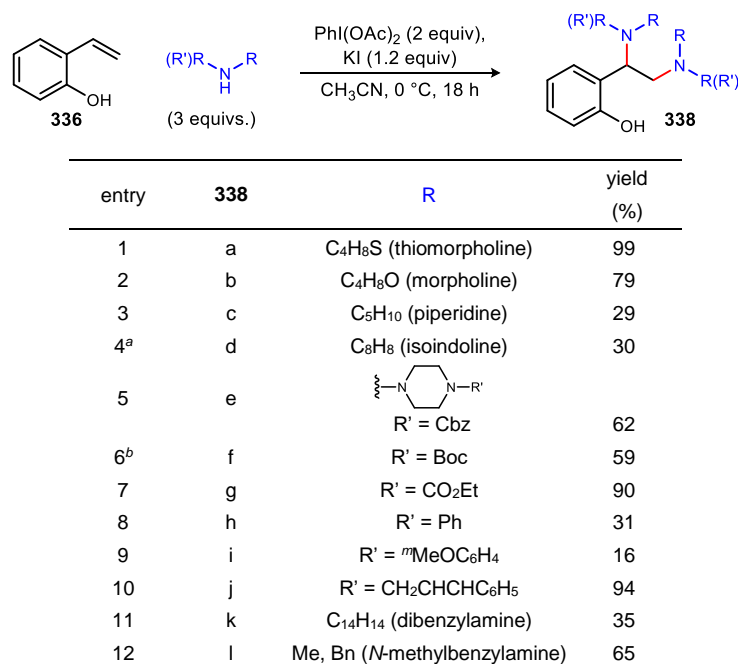
Scheme 138. Unsuccessful Diamination of *o*-Styrylphenol with $\text{PhI}(\text{OAc})_2/\text{KI}$ and NIS



Subsequent studies specifically applied the protocol using $\text{PhI}(\text{OAc})_2/\text{KI}$ and the most reactive styrene (*ortho*-hydroxystyrene) to explore the amine scope of the intermolecular diamination. Beginning with disubstituted amines, diamination with morpholine led to **338b** in 79% yield (Table 18, entry 2). Piperidine and isoindoline, a pyrrolidine derivative, led to vicinal diamines **338c** and **338d**, but with depressed yield (Table 18, entries 3 and 4). Cbz-, Boc-, and ethyl carboxylate-protected piperazines successfully engaged in diamination providing **338e-338g** in moderate (59%) to good (90%) yield (Table 18, entries 5-7). These three diamines are notable as they allow for subsequent unmasking of the piperazine moieties under neutral, acidic, or basic

conditions. *N*-Arylpiperazines, however, proved less reactive under the diamination protocol as 1-phenylpiperazine and 1-(3-methoxyphenyl)piperazine furnished **338h** and **338i** in 31% and 16% yields, respectively (Table 18, entries 8 and 9). *N*-Cinnamylpiperazine displayed high reactivity as vicinal diamine **338j** was acquired in 94% isolated yield upon chromatographic separation (Table 18, entry 10). Acyclic disubstituted amines engaged in diamination as dibenzylamine and *N*-methylbenzylamine led to **338k** and **338l** in 35% and 65% yields, respectively (Table 18, entries 11 and 12).

Table 18. Doubly Intermolecular Alkene Diamination: Secondary Amine Scope

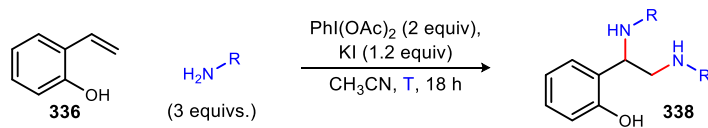


^a3.0 equiv of PhI(OAc)₂ used. ^b2.1 equiv of amine used.

Primary amines were examined next. Subjection of aniline to the diamination protocol at 0 °C led to diamine **338m** in 48% yield (Table 19, entry 1). Interestingly, when the same reaction was repeated at room temperature, an improvement of reactivity was observed (Table 19, entry 2). The same phenomenon proved consistent with 4-*tert*-butylaniline and 3,5-dimethylaniline as diamines **338n** and **338o** were acquired in significantly higher yields at room temperature relative to 0 °C (Table 19, entries 3-6). One exception to this trend, however, was 4-fluoroaniline as vicinal diamine **338p** was isolated in identical yield (47%) at both room temperature at 0 °C (Table 19, entries 7 and 8). Seeing that a number of anilines displayed higher reactivity at room temperature was interesting, since this was opposite the trend observed with disubstituted amines. One hypothesis for explaining these higher yields at room temperature may be the fact that

corresponding aniline diamines (**338m-338p**) are less prone to decomposition compared to their secondary amine counterparts.

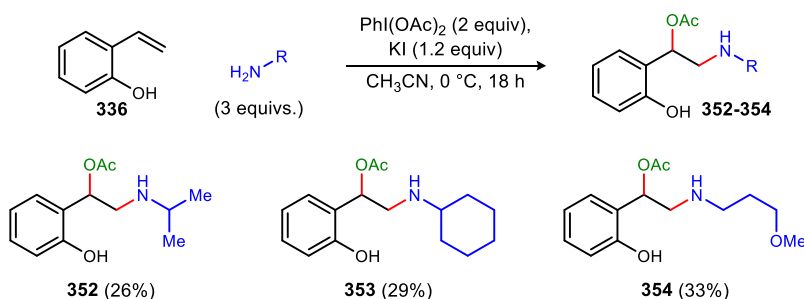
Table 19. Doubly Intermolecular Alkene Diamination: Primary Amine Scope



entry	338	R	T (°C)	yield (%)
1	m	Ph	0	48
2	m	Ph	25	60
3	n	4-Bu-C ₆ H ₄	0	26
4	n	4-Bu-C ₆ H ₄	25	53
5	o	3,5-dimethyl-C ₆ H ₃	0	29
6	o	3,5-dimethyl-C ₆ H ₃	25	60
7	p	4-F-C ₆ H ₄	0	47
8	p	4-F-C ₆ H ₄	25	47

For reasons not clear, one class of amines that proved troublesome in this diamination protocol was primary aliphatic amines. Subjection of these amines to the PhI(OAc)₂/KI combination in the presence of 2-vinyl phenol gave no sign of desired diamination. A common feature among a number of examples, however, was intermolecular aminoacetoxylation (Scheme 139). For example, when isopropylamine, cyclohexylamine, and 3-methoxypropylamine were subjected to standard reaction conditions, aminoacetoxylation products **352-354** were the only products that were cleanly isolated post-column chromatography.

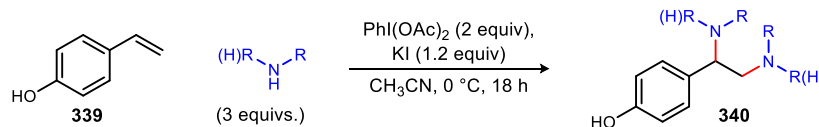
Scheme 139. Intermolecular Aminoacetoxylation with Primary Aliphatic Amines



para-Hydroxystyrene was also an effective precursor for intermolecular vicinal diamination. Although this was previously exemplified with thiomorpholine, successful diamination with morpholine and aniline (**340b** and **340c**) further illustrate that 4-vinyl phenol can

tolerate a number of amine substrates (Table 20, entries 2 and 3). Once again, higher yield was achieved at room temperature for the aniline case.

Table 20. Doubly Intermolecular Alkene Diamination: Amine Scope with *para*-Hydroxystyrene

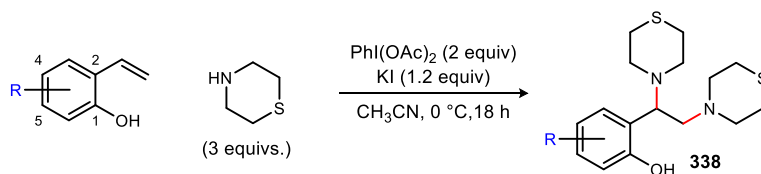


entry	340	R	yield (%)
1	a	C ₄ H ₈ S (thiomorpholine)	62
2	b	C ₄ H ₈ O (morpholine)	59
3 ^a	c	Ph	85

^aReaction run at 25 °C.

Modifications to the vinylphenol precursor were explored, specifically with thiomorpholine, illustrating further generality. Halogen substituents at the 4-position were tolerated as diamination products **338q-338s** were furnished in moderate to good yield (Table 21, entries 2-4). Substrates with electron-withdrawing or electron-donating groups at the 4-position also engaged in diamination as **338t** and **338u** were provided in 50% and 54% yields, respectively (Table 21, entries 5 and 6). Diamination with a hydroquinone species was possible as **338v** was afforded, albeit in low yield (Table 21, entry 7). Lastly, vinylphenol substrates possessing electron-rich methoxy groups at the 5- and 6-positions delivered their diamination products (**338w** and **338x**) in moderate (57%) to good yield (83%) (Table 21, entries 8 and 9).

Table 21. Doubly Intermolecular Alkene Diamination: Vinylphenol Scope



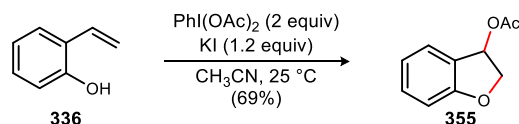
entry	338	R	yield (%)
1	a	H	99
2	q	4-F	83
3 ^a	r	4-Cl	64
4 ^a	s	4-Br	70
5	t	4-NO ₂	50
6	u	4-MeO	54
7	v	4-HO	23
8	w	5-MeO	57
9	x	6-MeO	83

^aIndicates 3 equivalents of PhI(OAc)₂ (PIDA) used.

5.4. Control Experiments and Mechanistic Hypothesis

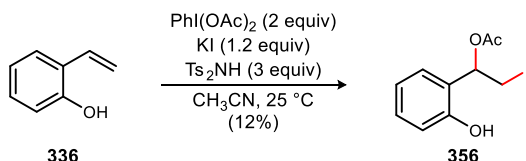
Throughout the course of these exploratory studies for the doubly intermolecular alkene diamination, a number of experiments were directed at the isolation of key intermediates or products along the preferred or competing reaction pathways. Chief among these co-products is bis(oxygenation) product **355**. This particular product arose from a control experiment in which 2-vinyl phenol was treated with $\text{PhI}(\text{OAc})_2$ and KI alone (no amine). ^1H NMR analysis of the crude reaction mixture showed 3-acetoxydihydrobenzofuran (**355**) as the major product, and subsequent chromatographic separation provided compound **355** in 69% isolated yield (Scheme 140).

Scheme 140. Generation of Bis(oxygenation) Product **355**



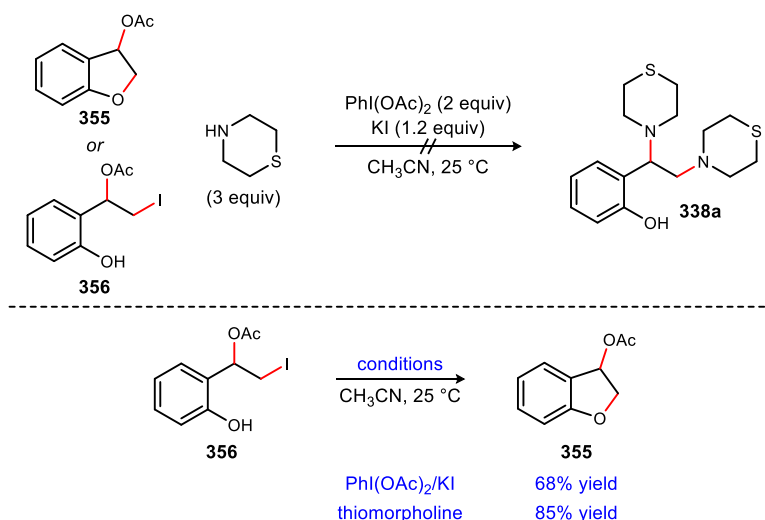
Another key product isolated was that of iodoacetoxylation product **356**. Based on our previous success of alkene diamination with electron-rich amines, we wanted to see if electron-withdrawing amines could also be tolerated. When combining 2-vinyl phenol with the $\text{PhI}(\text{OAc})_2/\text{KI}$ combination in the presence of electron-deficient bistosylimide (Ts_2NH), iodide **356** was furnished, albeit in low yield (12%) (Scheme 141).

Scheme 141. Generation of Iodoacetoxylation Product **356**



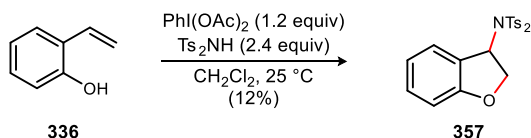
Isolation of bis(oxygenation) and iodoacetoxylation products **355** and **356** enabled further studies that could determine if these compounds indeed serve as intermediates en route to diamination. When **355** and **356** were individually subjected to the standard diamination protocol ($\text{PhI}(\text{OAc})_2$, KI, thiomorpholine, and CH_3CN) at room temperature, no sign of diamine **338a** could be detected (Scheme 142). Furthermore, neither of those intermediates is observed directly during the conversion of 2-vinyl phenol (**336**) to diamination product **338a** under the same reaction conditions. What has been determined, however, is iodide **356** and 3-acetoxydihydrobenzofuran (**355**) are united in a common pathway. This was confirmed as phenol **356** converts to **355** when exposed to $\text{PhI}(\text{OAc})_2/\text{KI}$ in the absence of amine or when treated with amine alone.

Scheme 142. Other Findings with Bis(oxygenation) and Iodoacetoxylation Products **355** and **356**



These intermediates were of interest as they provide useful mechanistic insight. These products appear to collectively arise from electrophile addition to the terminal carbon, followed by nucleophilic addition to the benzylic carbon. It is speculated that carbon-nitrogen bond formation via an electrophilic amine formed *in situ* is a key aspect of the actual mechanism leading to diamination. Additionally, this speculation of electrophilic amine addition (terminal carbon) and subsequent nucleophilic addition (benzylic position) is reflective of the aminoacetoxylation products depicted in Scheme 139. Non-nucleophilic amines such as Ts_2NH did not provide diamination product, even when applying the protocol developed by Muñiz (Scheme 143).¹⁶⁶ Instead, monoamination product **357** was afforded in low yield, perhaps through a pathway analogous to $336 \rightarrow 356 \rightarrow 355$. This result is also consistent with the unique reactivity of an electrophilic amine using the $\text{PhI}(\text{OAc})_2/\text{KI}$ protocol.

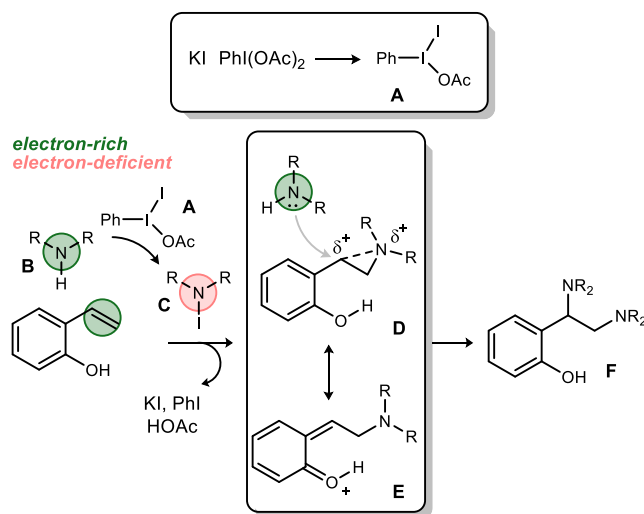
Scheme 143. Acquisition of Monoamination Product **357** via Muñiz's Protocol



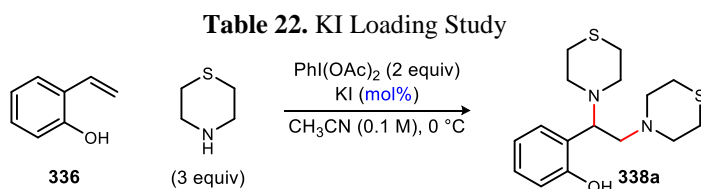
A plausible reaction mechanism is depicted in Figure 24. When KI interacts with $\text{PhI}(\text{OAc})_2$, it is believed that the iodide substitutes for one of the acetoxy groups, generating electrophilic iodinating agent **A**. This particular iodane (**A**) can activate the amine (**B**) through iodamine formation (**C**). The success of NIS in this transformation further suggests that the formation of an iodamine is key in the reaction pathway. Subsequent attack of the halamine by the

alkene moiety of 2-vinylphenol generates intermediate **D**. The lone pairs of electrons on the hydroxyl unit can resonate in order to break open the aziridinium, resulting in *ortho*-quinone methide **E**. This intermediate serves as a suitable electrophile for nucleophilic attack of amine en route to homodiamination (**F**).

Figure 24. Mechanistic Hypothesis for $\text{PhI}(\text{OAc})_2/\text{KI}$ -Mediated Intermolecular Diamination



One of the key features in regard to the mechanistic pathway described above is the regeneration of iodide. Because it is hypothesized that iodide is regenerated *in situ*, it is plausible that diamination can be achieved when employing substoichiometric or catalytic quantities of halide. While previous studies employed a full equivalent of KI in order to apply general conditions

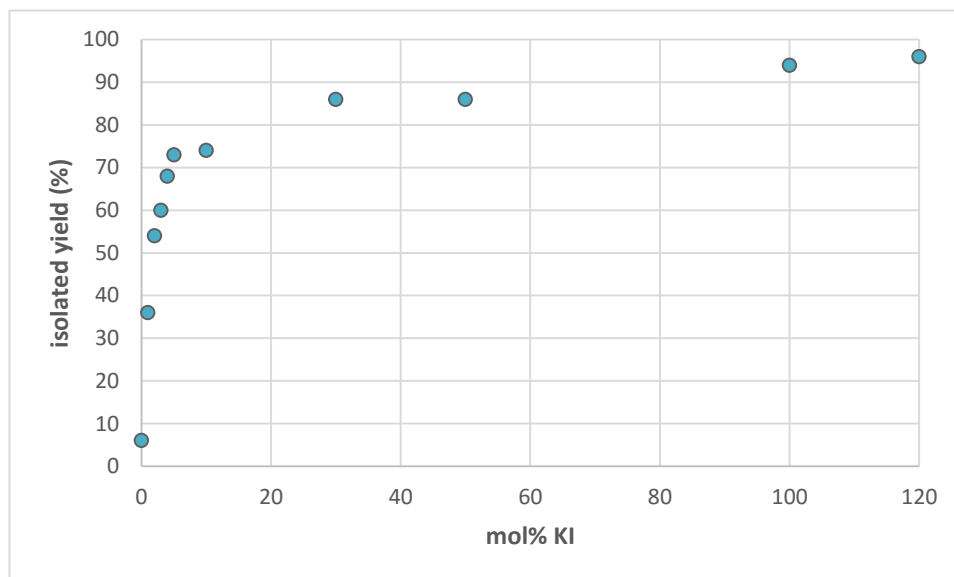


entry	catalyst loading	yield (%)
1	0 mol%	6
2	1 mol%	34
3	2 mol%	54
4	3 mol%	60
5	4 mol%	68
6	5 mol%	73
7	10 mol%	74
8	30 mol%	86
9	50 mol%	86
10	100 mol%	94
11	120 mol%	96

to a broad collection of substrates, a series of experiments were designed to vary KI loading in the diamination of 2-vinyl phenol (**336**) with thiomorpholine.

Starving the reaction conditions of the additive resulted in minimal background reactivity (6% yield) (Table 22, entry 1). Yet, when a 1 mol% loading of KI was used, reactivity increased nearly six-fold as diamination product **338a** was isolated in 34% yield (Table 22, entry 2). Progressively increasing the iodide loading led to higher yield (Table 22, entries 3-6). This was reflected through a 10 mol% loading, which correlated to a 74% yield of **338a** (Table 22, entry 7). Despite observing sufficient reactivity with catalytic halide loadings, further studies confirmed that substoichiometric and even stoichiometric amounts of KI (Table 22, entries 8-11) were necessary in order to achieve optimal yield (Figure 25).

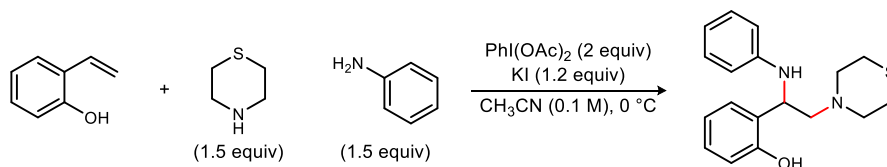
Figure 25. Relative Comparison of KI Loading and Reactivity



5.5. Future Work

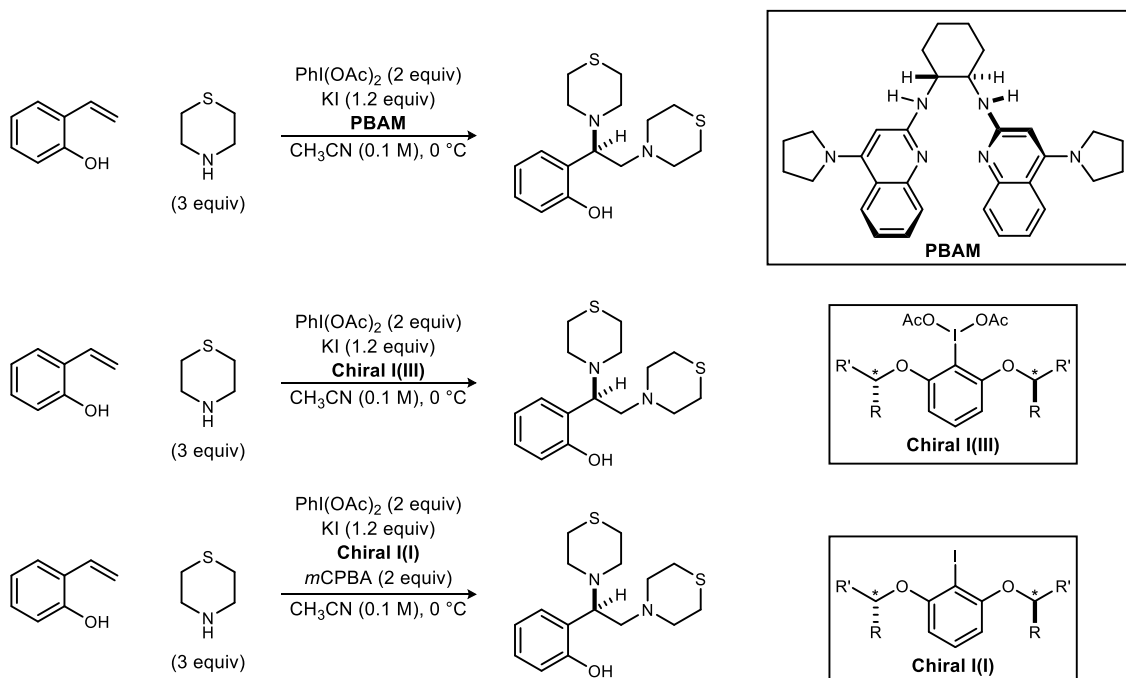
Although this doubly intermolecular diamination with 2-vinylphenol was met with a high degree of success, other avenues can be explored in order to make this system even more efficient. One particular direction to pursue is heterodiamination of 2-vinylphenol. As described previously, this diamination protocol was tolerant to a wide array of amines. One of the main drawbacks, however, is that the amine moieties are identical at both sites of diamination (i.e. homodiamination). If two different amines, such as aniline and thiomorpholine, can be regioselectively installed at these positions through reaction optimization, a much higher level of generality would be achieved for this reaction system (Scheme 144).

Scheme 144. Proposed Heterodiamination of 2-Vinyl Phenol



The enantioselective variation of this system is another route to be taken. This can be probed by subjecting a number of chiral organocatalysts (e.g. PBAM) to the previously developed protocol (Scheme 145). Another plausible approach towards achieving enantioselection would be the use of a chiral hypervalent iodine reagent as employed by Muñiz and Ishihara.^{164,165} If this strategy proves fruitless, *in situ* generation of chiral iodine(III) via incorporation of chiral iodoarenes and MCPBA would be another possibility. These investigations are currently ongoing within our laboratory.

Scheme 145. Potential Enantioselective Variations of the Doubly Intermolecular Alkene Diamination

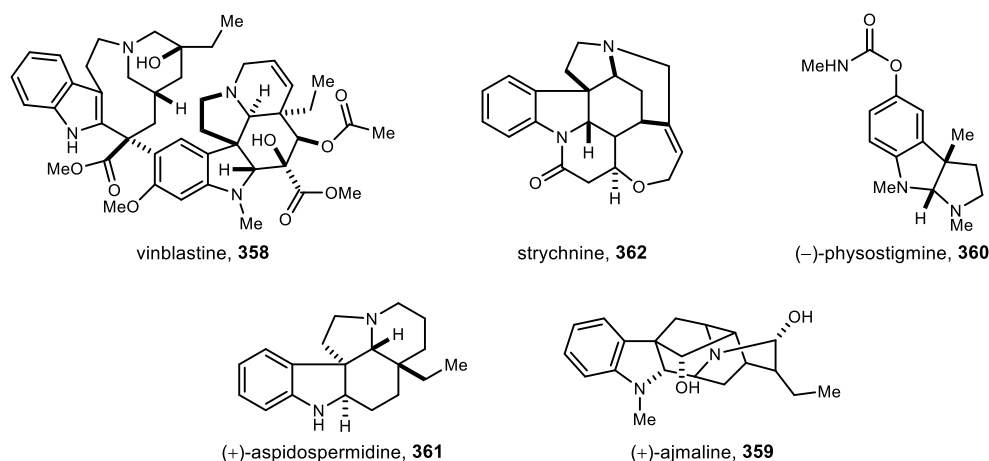


Chapter 6. A Unified Approach to the Four Azaindoline Families by Inter-/Intramolecular Annulative Diamination of Vinylpyridines

6.1. Background

The indoline scaffold is considered to be one of the most privileged structures in nature.¹⁷³ It is found in a variety of naturally bioactive alkaloids and is the structural component of several pharmaceutically active compounds. Because of their strong biological profile, indolines have garnered a high degree of interest and have been synthesized via a number of methodologies as a result.¹⁷⁴

Figure 26. Examples of Naturally Bioactive Alkaloids Possessing an Indoline Scaffold



Vinblastine (**358**) is among the bioactive alkaloids that possess an indoline core (Figure 26). This natural product is of considerable importance as it has been used to treat numerous types of cancer such as Hodgkin's lymphoma,¹⁷⁵ non-small cell lung cancer,¹⁷⁶ bladder cancer,¹⁷⁷ brain cancer,¹⁷⁸ and testicular cancer.¹⁷⁹ Other indoline-containing alkaloids with biological significance

¹⁷³ *Modern Alkaloids: Structure, Isolation, Synthesis and Biology*; Fattorusso, E.; Tagliatela-Scafati, O., Ed.; Wiley-VCH Verlag GmbH & Co. KGaA: Weinheim, Germany, 2008.

¹⁷⁴ For a review of methods that access the indoline scaffold, see Liu, D.; Zhao, G.; Xiang, L. *Eur. J. Org. Chem.* **2010**, 3975-3984.

¹⁷⁵ Eichenauer, D. A.; Bredenfeld, H.; Haverkamp, H.; Müller, H.; Franklin, J.; Fuchs, M.; Borchmann, P.; Müller-Hermelink, H.-K.; Eich, H. T.; Müller, R.-P.; Diehl, V.; Engert, A. *J. Clin. Oncol.* **2009**, *27*, 6079-6085.

¹⁷⁶ Curran Jr., W. J.; Paulus, R.; Langer, C. J.; Komaki, R.; Lee, J. S.; Hauser, L.; Movsas, B.; Wasserman, T.; Rosenthal, S. A.; Gore, E.; Machtay, M.; Sause, W.; Cox, J. D. *J. Natl. Cancer Inst.* **2011**, *103*, 1452-1450.

¹⁷⁷ Petrioli, R.; Roviello, G.; Fiaschi, A. I.; Laera, L.; Miano, S. T.; Bianco, V.; Francini, E. *Colloq. Inse.* **2015**, *26*, 878-883.

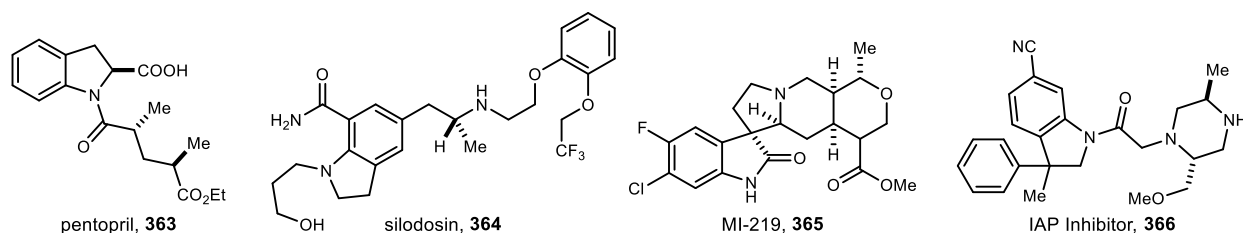
¹⁷⁸ Rebbaa, A.; Chou, P. M.; Vucic, I.; Mirkin, B. L.; Tomita, T.; Bermer, E. G. *Clin. Cancer Res.* **1999**, *5*, 3661-3668.

¹⁷⁹ Hanna, N.; Einhorn, L. H. *J. Clin. Oncol.* **2014**, *32*, 3085-3092.

include ajmaline (**359**), an antiarrhythmic agent,¹⁸⁰ (-)-physostigmine (**360**), a cholinesterase inhibitor,¹⁸¹ and (+)-aspidospermidine (**361**), which shows strong antimalarial activity.¹⁸² Although strychnine (**362**) is classified as an alkaloid that bears an indoline moiety, this particular natural product suffers from a high toxicity profile and is therefore used as a common pesticide.¹⁸³

One of the most notable pharmaceutical agents with an indoline backbone is pentopril (**363**). Previous studies confirm that pentopril displays angiotensin-converting enzyme (ACE) inhibition and is therefore considered an antihypertensive drug (Figure 27).¹⁸⁴ Silodosin (**364**) is another pharmaceutical that possesses an indoline framework. This compound is an α_{1a} -adrenoceptor (AR) antagonist and is used as medication for the treatment of problems associated with the human prostate.¹⁸⁵ Other indoline-bearing pharmaceutical candidates include small-molecule MDM2 inhibitor MI-219 (**365**), a promising anticancer agent,¹⁸⁶ as well as 3-aryl-*N*-acylindoline **366**, which has been recently reported to target inhibitors of apoptosis proteins (IAP).¹⁸⁷ These listed examples constitute only a small portion of the biological impact that these compounds have as SciFinder identifies more than 1300 references where indolines have been described as antibacterials, kinase inhibitors for cancer targets, antidiabetic agents, anti-inflammatory agents, and analgesics.¹⁸⁸

Figure 27. Examples of Pharmaceutical Agents Possessing an Indoline Scaffold



Despite its prominence in natural products and pharmaceutical agents, one of the main limitations of the indoline scaffold from a pharmacological standpoint is that it possesses a

¹⁸⁰ Wang, T.; Xu, Q.; Yu, P.; Liu, X.; Cook, J. M. *Org. Lett.* **2001**, *3*, 345-348.

¹⁸¹ Cho, Y.; Kim, W.-S.; Hur, G.-H.; Ha, Y.-C. *Environ. Toxicol. Phar.* **2012**, *33*, 1-8.

¹⁸² Mitaine-Offer, A.-C.; Sauvain, M.; Valentin, A.; Callapa, J.; Mallié, M.; Zèches-Hanrot, M. *Phytomedicine* **2002**, *9*, 142-145.

¹⁸³ Zhang, H.; Boonsombat, J.; Padwa, A. *Org. Lett.* **2007**, *9*, 279-282.

¹⁸⁴ Rakhit, A.; Hurley, M. E.; Tipnis, V.; Coleman, J.; Rommel, A.; Brunner, H. R. *J. Clin. Pharmacol.* **1986**, *26*, 156-164.

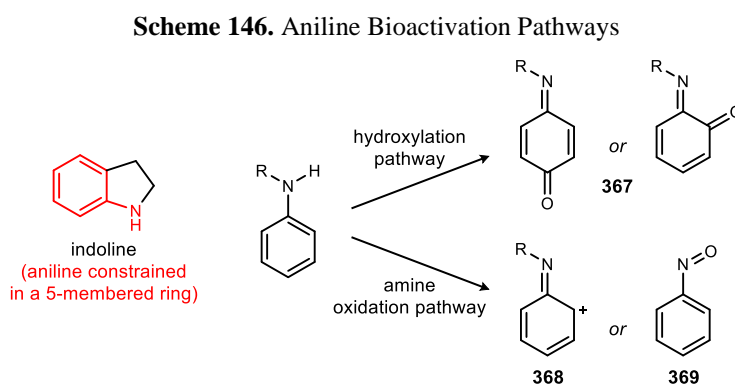
¹⁸⁵ Barve, I. J.; Chen, L.-H.; Wei, P. C. P.; Hung, J.-T.; Sun, C.-M. *Tetrahedron* **2013**, *69*, 2834-2843.

¹⁸⁶ Rajesh, S. M.; Perumal, S.; Menéndez, J. C.; Yogeewari, P.; Sriram, D. *Med. Chem. Commun.* **2011**, *2*, 626-630.

¹⁸⁷ Beaud, R.; Guillot, R.; Kouklovsky, C.; Vincent, G. *Chem. Eur. J.* **2014**, *20*, 7492-7500.

¹⁸⁸ Chekler, E. L. P.; Khan, T. A.; Mamidala, R.; Anderson, J. T.; Tangirala, R. S.; Verhoest, P. R.; Gilbert, A. M. *Tetrahedron Lett.* **2012**, *53*, 377-379.

constrained aniline motif. The aniline moiety is a well-known structural alert, a chemical fragment that is associated with adverse *in vivo* outcomes and/or adverse drug reactions (ADRs).¹⁸⁹ These outcomes include but are not limited to mutagenicity, direct toxicity, carcinogenicity, DNA intercalation, or idiosyncratic toxicity. ADRs (and subsequent toxicity) from anilines are caused by two types of bioactivations: 1) hydroxylation of the aromatic ring resulting in reactive iminoquinones (**367**) and 2) oxidation of the amine which leads to reactive nitrenium (**368**) or nitroso (**369**) derivatives (Scheme 146).¹⁸⁸



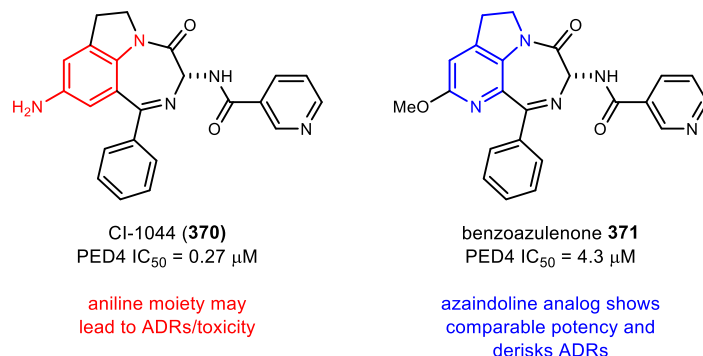
One of the most direct ways to de-risk the aniline structural alert is to incorporate one or more nitrogens into the phenyl ring. These nitrogens will reduce the electron density of the aromatic ring, rendering oxidation to species **367-369** more difficult. Thus, the development of azaindoline pharmaceuticals is seen as novel approach to improve pharmacological profiles. Devillers and colleagues demonstrate this in their respective synthesis of a potent phosphodiesterase-4 (PED4) inhibitor.¹⁹⁰ They report that high throughput screening and initial structure activity relationship (SAR) studies led to the identification of 9-amino-tetrahydrodiazepinoindole compound CI-1044 (**370**). Despite showing high potency for PED4 inhibition, the aniline structural fragment within CI-1044 (**370**) was considered to be a toxicophore. To address for this unwanted toxicity, the aniline moiety was replaced with an azaindoline residue via the synthesis of triaza-benzoazulen-9-one **371** (Figure 28). Other substituents such as a methoxy group at the 9-position and a nicotinic acyl side chain were chosen based on further SAR evaluation. When tested for PDE4 inhibition, compound **371** showed

¹⁸⁹ Kalgutkar, A. S.; Dalvie, D. K.; O'Donnell, J. P.; Taylor, T. J.; Sahakian, D. C. *Curr. Drug Metab.* **2002**, *3*, 379-424.

¹⁹⁰ Devillers, I.; Pevet, I.; Jacobelli, H.; Durand, C.; Fasquelle, V.; Puaud, J.; Gaudillière, B.; Idrissi, M.; Moreau, F.; Wrigglesworth, R. *Bioorg. Med. Chem. Lett.* **2004**, *14*, 3303-3306.

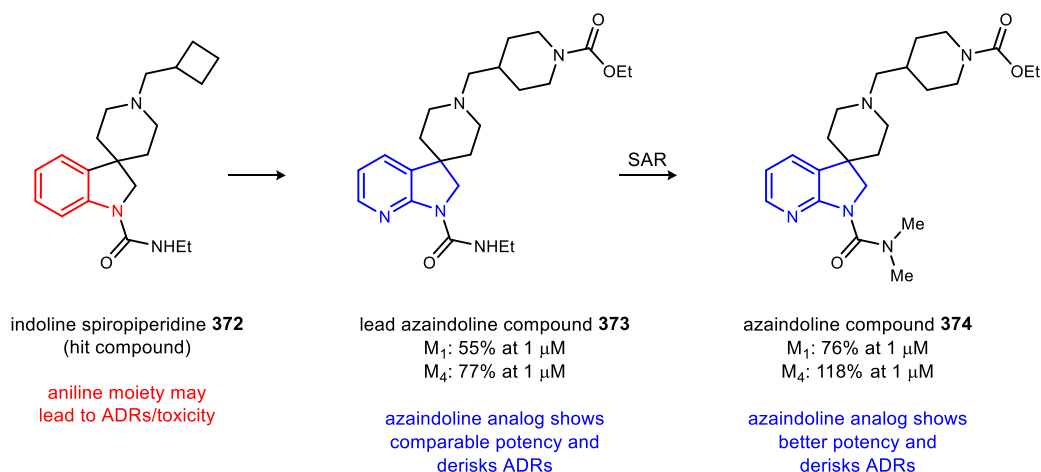
comparable potency relative to **370** indicating that the activity range was conserved with the replacement of the aniline moiety. The difference, however, is that benzoazulenone **371** has a better pharmacological profile since the azaindoline scaffold derisks the aniline structural alert contained within the indoline analog (**370**).

Figure 28. Phosphodiesterase Inhibition of Aniline and Azaindoline Compounds **370** and **371**



Sumiyoshi and co-workers utilized a similar approach in their search for selective M₁ and M₄ muscarinic acetylcholine receptor (mAChRs) agonists.¹⁹¹ High throughput screening led to the identification of indoline spiropiperidine **372** as a hit compound (Figure 29). To account for potential ADRs from the aniline motif within compound **372**, azaindoline analog **373** was synthesized as an initial lead compound. Further SAR studies led to the identification of compound

Figure 29. mAChR Agonist Activity of 7-Azaindoline Compounds **373** and **374**



374, which showed selective M₁ and M₄ mAChRs agonist activity and has good potential as an orally available antipsychotic with a novel mechanism of action.

¹⁹¹ Takai, K.; Inoue, Y.; Konishi, Y.; Suwa, A.; Uruno, Y.; Matsuda, H.; Nakako, T.; Sakai, M.; Nishikawa, H.; Hashimoto, G.; Enomoto, T.; Kitamura, A.; Uematsu, Y.; Kiyoshi, A.; Sumiyoshi, T. *Bioorg. Med. Chem. Lett.* **2014**, *24*, 3189-3193.

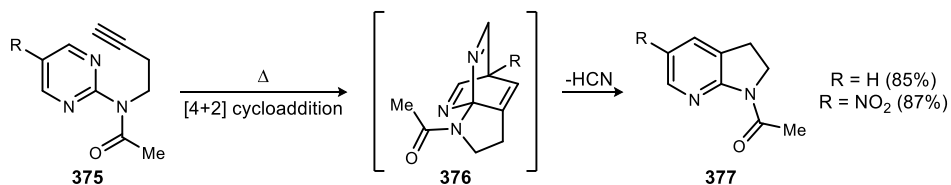
Based on these examples, it is evident that the azaindoline scaffold serves as a nice surrogate for the aniline moiety. Because of their reduced risk of ADRs and minimal effect on promising biological activity, acquisition of azaindoline-containing pharmaceutical candidates is of high importance. The most efficient means of accelerating the syntheses of these types of compounds is through developing new methodologies that readily access azaindoline functionalities.

6.2. Known Methods for the Preparation of Azaindolines

The azaindoline motif has been successfully synthesized via a variety of protocols. Although numerous methods have been employed in order to arrive at each azaindoline ring system, there is only one unified approach that readily accesses all four isomeric azaindolines.¹⁹² Of these four isomeric families, the most accessible azaindoline backbone to date is the 7-azaindoline core.

Among the earliest reports of successfully synthesizing the 7-azaindoline framework is that of van der Plas and colleagues. Here, they utilize an intramolecular inverse electron demand Diels-Alder reaction of pyrimidines with side chain dienophiles in order to furnish the desired bicyclic system.^{193,194} When pyrimidine **375** is subjected to high temperature, the intramolecular [4+2] cycloaddition provides intermediate **376** (Scheme 147). This intermediate is then converted to acetylated 7-azaindoline **377** *in situ* upon the release of hydrogen cyanide (HCN).

Scheme 147. Synthesis of 7-Azaindolines via an Inverse Electron Demand Diels-Alder Reaction of Pyrimidines



In a closely related manner, Taylor and co-workers report the use of an intramolecular inverse electron demand Diels-Alder reaction of 1,2,4-triazines bearing side chain dienophiles to promote the formation of 7-azaindoline motifs.^{195,196} Exposure of these triazine compounds (**378**) to elevated temperatures facilitates the cycloaddition generating the corresponding tricyclic

¹⁹² Bailey, W. F.; Salgaonkar, P. D.; Brubaker, J. D.; Sharma, V. *Org. Lett.* **2008**, *10*, 1071-1074.

¹⁹³ Frissen, A. E.; Marcelis, A. T. M.; van der Plas, H. C. *Tetrahedron Lett.* **1987**, *28*, 1589-1592.

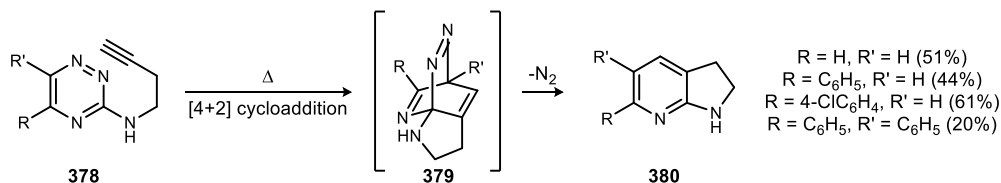
¹⁹⁴ Frissen, A. E.; Marcelis, A. T. M.; van der Plas, H. C. *Tetrahedron* **1989**, *45*, 803-812.

¹⁹⁵ Taylor, E. C.; Macor, J. E.; Pont, J. L. *Tetrahedron* **1987**, *43*, 5145-5158.

¹⁹⁶ Taylor, E. C.; Pont, J. L. *Tetrahedron Lett.* **1987**, *28*, 379-382.

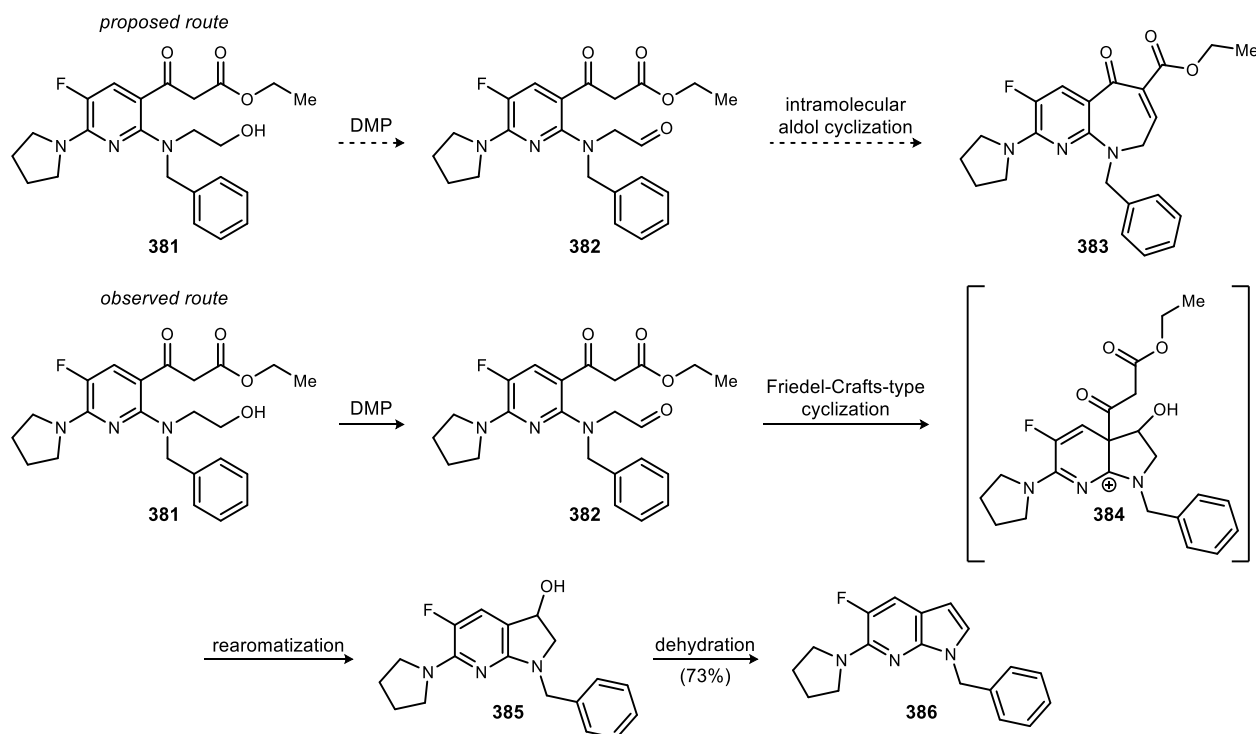
intermediates (**379**) *in situ* (Scheme 148). Conversion of these cycloadducts to their desired azaindolines (**380**) is driven by the expulsion of nitrogen gas, a pathway analogous to that of van der Plas's chemistry.

Scheme 148. Synthesis of 7-Azaindolines via an Inverse Electron Demand Diels-Alder Reaction of Triazines



In 2004, Sanders and colleagues inadvertently discovered that a highly functionalized 2-aminopyridine can be transformed to a 7-azaindole core via a periodinane-mediated formation of a 7-azaindoline scaffold.¹⁹⁷ Their initial goal was to treat advanced aminopyridine **381** with Dess-Martin periodinane in order to arrive at aldehyde **382**, which can then undergo a spontaneous intramolecular aldol cyclization to yield pyrido[2,3-*b*]azepinone **383**. Upon exposure to DMP, the primary alcohol of compound **381** was oxidized as expected (Scheme 149). However, the resultant aldehyde did not react with the enol of the ketoester functionality. Instead, what they observed was

Scheme 149. Sanders's Iodine(III)-Mediated Synthesis of 7-Azaindole **386** via 7-Azaindoline **385**

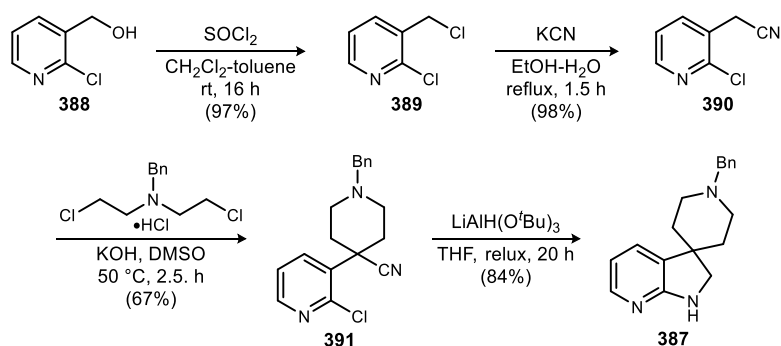


¹⁹⁷ Sanders, W. J.; Zhang, X.; Wagner, R. *Org. Lett.* **2004**, *6*, 4527-4530.

a Friedel-Crafts-type cyclization en route to 7-azaindoline cationic intermediate **384**. Rearomatization via intermolecular transfer of malonate to a reaction byproduct (not shown) affords a 3-hydroxy azaindoline (**385**) that leads to azaindole **386** upon dehydration. The proposed cationic intermediate (**384**) is exceptionally resonance-stabilized by three nitrogen atoms, and this thermodynamic stabilization combined with the kinetic advantage of five-membered ring formation could explain why the azaindoline moiety was generated in this reaction.

Recently, Sumiyoshi and co-workers utilized an intramolecular nucleophilic aromatic substitution reaction to construct a 7-azaindoline scaffold (**387**) en route to synthesizing small molecule therapeutic candidates.^{198,191} Formation of this azaindoline core proceeded in a straightforward manner as commercially available (2-chloro-3-pyridinyl)methanol **388** was converted to chloride **389** in high yield upon treatment with POCl₃ (Scheme 150). Nucleophilic displacement of the chloride with cyanide gave **390** in 98% yield. Treatment of **390** with *N*-benzyl-bis(2-chloroethyl)amine in the presence of base afforded spiropiperidine **391** in modest yield. Reduction of the nitrile functionality in compound **391** and subsequent exposure to heat promoted the desired S_NAr reaction, providing 7-azaindoline **387** in 84% isolated yield. This azaindoline serves as a key scaffold as a multitude of synthetic routes can be pursued in order to arrive at various pharmaceutical candidates.

Scheme 150. Sumiyoshi's Synthesis of a Key 7-Azaindoline Scaffold

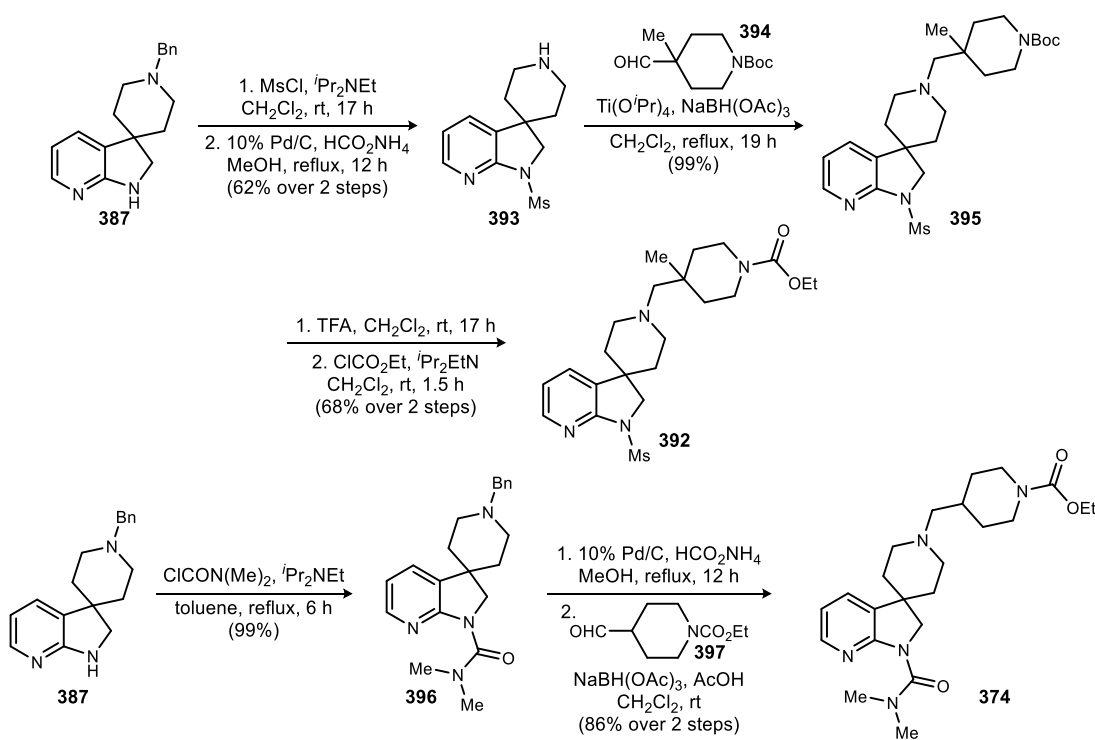


One compound of interest was that of *N*-sulfonyl-7-azaindoline **392**. This compound can be delivered via a five-step synthetic sequence from **387**. Azaindoline **387** was converted to intermediate **393** by mesylation and debenzoylation (Scheme 151). Free amine **393** then underwent reductive amination with *N*-Boc-4-formylpiperidine (**394**) to afford compound **395** in quantitative

¹⁹⁸ Suwa, A.; Konishi, Y.; Uruno, Y.; Takai, K.; Nakako, T.; Sakai, M.; Enomoto, T.; Ochi, Y.; Matsuda, H.; Kitamura, A.; Uematsu, Y.; Kiyoshi, A.; Sumiyoshi, T. *Bioorg. Med. Chem. Lett.* **2014**, *24*, 2909-2912.

yield. Boc-deprotection and subsequent acylation with ethyl chloroformate furnished desired compound **392** in good yield (68% yield over 2 steps).¹⁹⁸ Target compound **374** could also be readily accessed from azaindoline **387** in a highly efficacious manner. Acylation of the free amine moiety with *N,N*-dimethylcarbamoyl chloride delivered urea **396** in quantitative yield. Debenzylation and reductive amination with ethyl 4-formylpiperidine-1-carboxylate **397** led to the desired target (**374**) in 86% yield over two steps.¹⁹¹ These two compounds (**392** and **374**) showed selective M₁ and M₄ mAChRs agonist activity and are promising antipsychotic candidates with novel mechanisms of action.

Scheme 151. Synthesis of Antipsychotic Candidates **392** and **374**

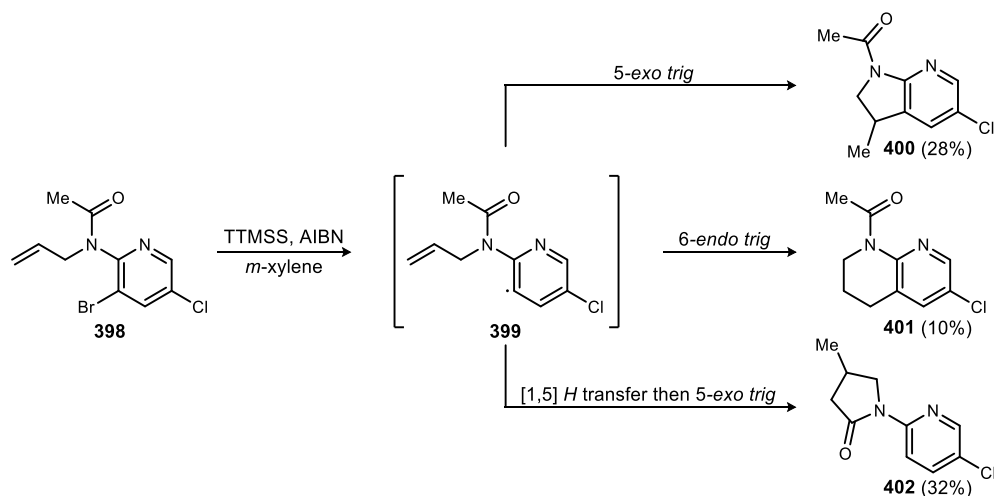


Radical cyclization is another method that can be implemented in order to access the 7-azaindoline backbone. Burgos and colleagues demonstrated this approach when utilizing an intramolecular radical pyridylation en route to synthesizing annulated 2-aminopyridines.¹⁹⁹ Treatment of aminopyridine **398** with AIBN and tris(trimethylsilyl)silane (TTMSS) produced aryl radical **399**, which subsequently engaged in a number of mechanistic pathways ultimately generating a series of products (Scheme 152). Isolation of 7-azaindoline **400** (28% yield), suggests that the aryl radical underwent a 5-*exo trig* cyclization with the terminal alkene. Conversely,

¹⁹⁹ Sánchez, A.; Núñez, A.; Burgos, C.; Alvarez-Builla, J. *Tetrahedron Lett.* **2006**, 47, 8343-8346.

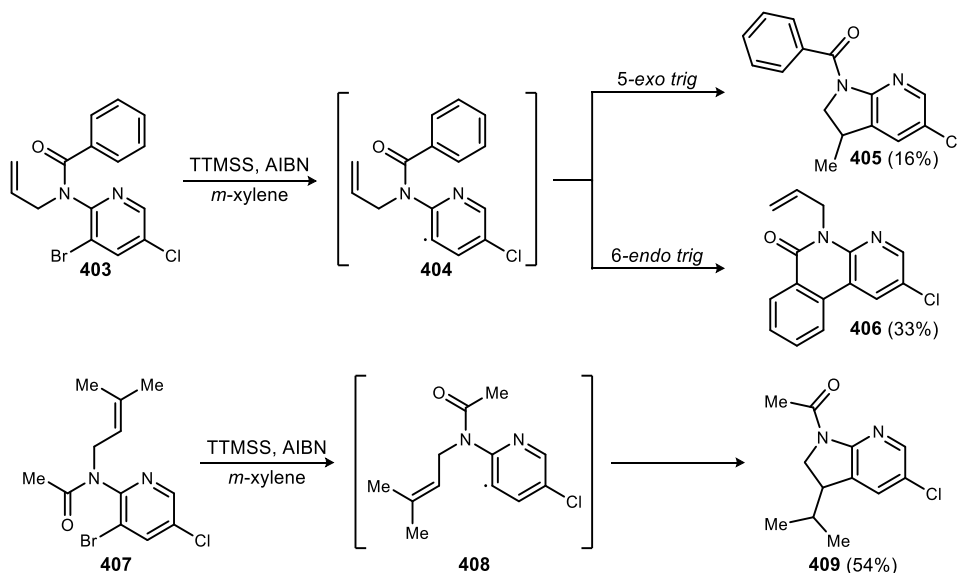
acquisition of tetrahydronaphthyridine **401** (10% yield) indicates that radical **399** proceeded through a 6-*endo trig* cyclization with the olefin. The main product (**402**) however, is thought to result from [1,5]-hydrogen transfer followed by a 5-*exo trig* cyclization (32% yield).

Scheme 152. Burgos's Synthesis of 7-Azaindoline **400** and Byproducts via Radical Cyclization



Consequently, **403** was prepared in order to suppress the unwanted hydrogen atom transfer process. Under similar cyclization conditions, aryl radical **404** was generated, which gave rise to 7-azaindoline **405** and naphthyridinone **406** via the 5-*exo trig* and 6-*endo trig* pathways (Scheme 153). For this particular case, azaindoline **405** was the minor product. Another substrate that was employed in these studies was that of internal alkene **407**. When **407** was treated with AIBN and TTMSS, radical **408** was generated subsequently affording 7-azaindoline **409** in 54% isolated

Scheme 153. Radical Cyclizations en Route to 7-Azaindolines **405** and **409**

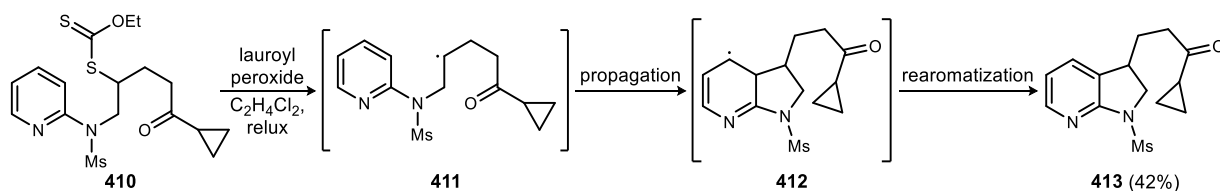


yield. The favorability of the 5-*exo trig* cyclization for this experiment was thought to be driven by the stabilization of the resulting tertiary radical.

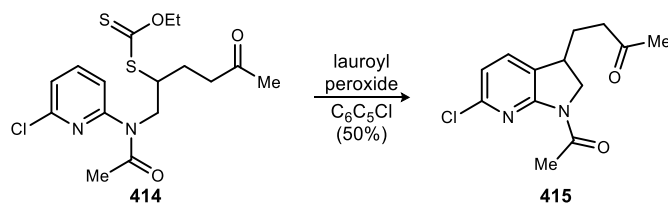
Zard and co-workers were able to effectively synthesize 7-azaindoline cores via radical cyclizations using xanthate esters. As illustrated in their earliest report, treatment of xanthate **410** with stoichiometric quantities of lauroyl peroxide results in the formation of radical **411** (Scheme 154).²⁰⁰ Propagation of this radical with the pyridine ring generates radical species **412** and subsequent rearomatization furnishes the desired azaindoline (**413**) in modest yield (42%). This methodology was later extended to the synthesis of 3-alkyl-7-azaindolines (**415**) as well as fluoro-7-azaindolines (**417**).^{201,202} These advanced azaindoline scaffolds arose through mechanistic pathways analogous to the one previously described.

Scheme 154. Zard's Radical-Mediated Synthesis of 7-Azaindolines Using Xanthate Esters

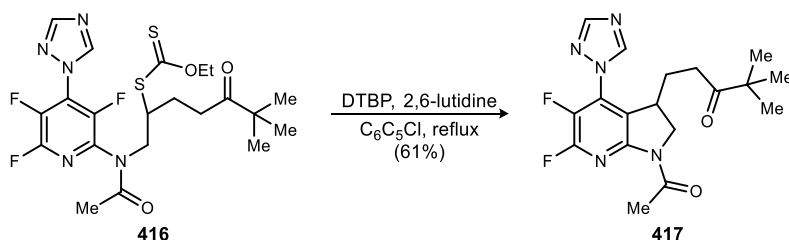
Tetrahedron Lett. **1999**, *40*, 2533-2536



Org. Lett. **2004**, *6*, 3671-3674 (selected example)



Org. Lett. **2014**, *16*, 2704-2707 (selected example)



Radical cyclizations with azomethine have also been employed in order to arrive at the 7-azaindoline framework. In 2001, Johnston and colleagues successfully synthesized this bicyclic

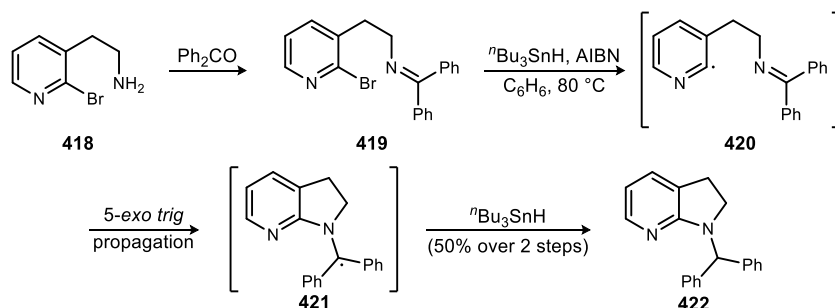
²⁰⁰ Ly, T.-M.; Quiclet-Sire, B.; Sortais, B.; Zard, S. Z. *Tetrahedron Lett.* **1999**, *40*, 2533-2536.

²⁰¹ Bacqué, E.; El Qacemi, M.; Zard, S. Z. *Org. Lett.* **2004**, *6*, 3671-3674.

²⁰² Liu, Z.; Qin, L.; Zard, S. M. *Org. Lett.* **2014**, *16*, 2704-2707.

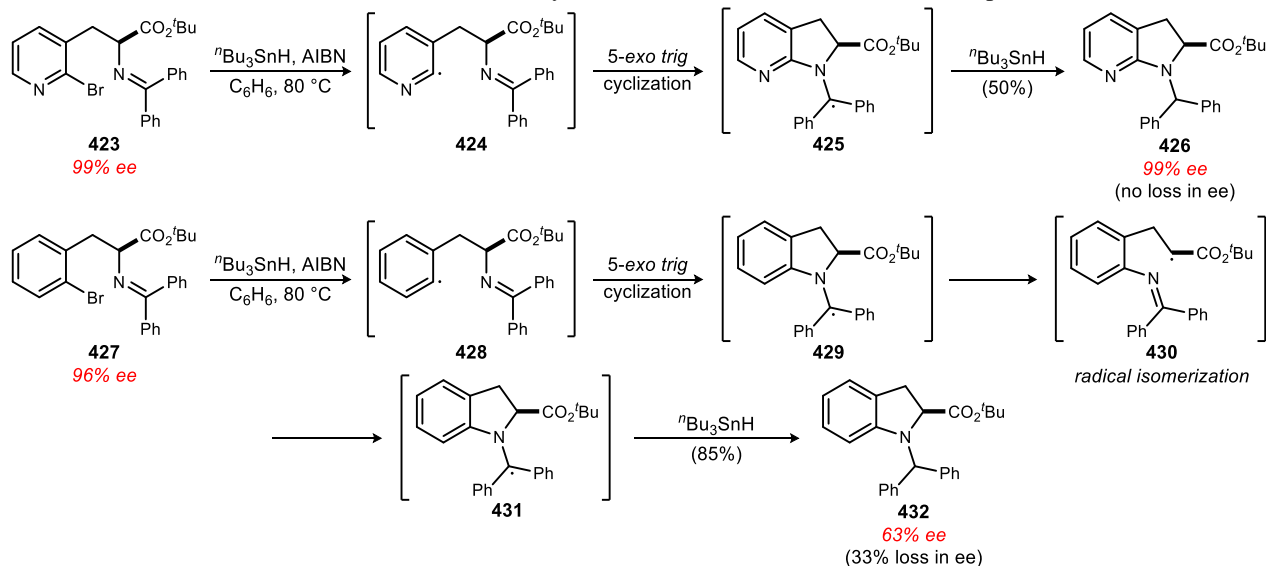
system via an unconventional aryl radical addition to azomethine nitrogen.²⁰³ Herein, amine **418** was condensed with benzophenone to provide azomethine **419** (Scheme 155). Treatment of **419** with AIBN and ⁿBu₃SnH at elevated temperatures results in the formation of radical **420**. This radical then undergoes a regioselective 5-*exo trig* cyclization at the nitrogen position of the azomethine yielding **421**. Termination of **421** with ⁿBu₃SnH affords the desired 7-azaindoline (**422**) in 50% yield over two steps.

Scheme 155. Johnston's Regioselective Synthesis of 7-Azaindoline **422**



Johnston later extended this regioselective aryl radical addition to the synthesis of 7-azaindoline α -amino esters.²⁰⁴ Subjection of enantioenriched α -amino ester **423** to the radical cyclization protocol afforded the desired 7-azaindoline α -amino ester (**426**) in 50% yield upon purification (Scheme 156). What is notable about this cyclization is that no diminishment in enantiopurity was observed. This indicates that ring fragmentation and subsequent radical

Scheme 156. Johnston's Radical-Mediated Synthesis of 7-Azaindoline **426** with Complete Stereoretention



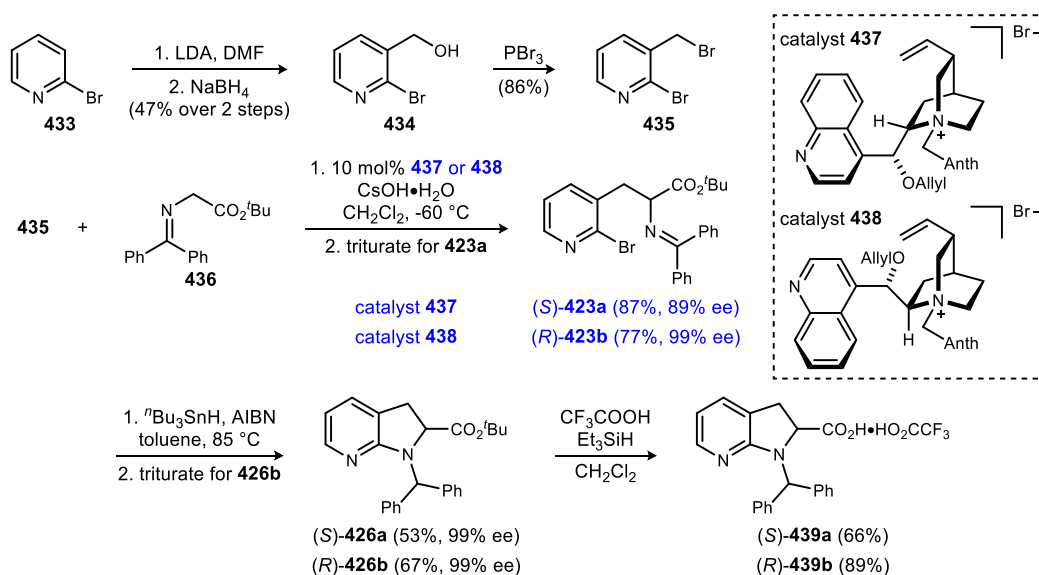
²⁰³ Johnston, J. N.; Plotkin, M. A.; Viswanathan, R.; Prabhakaran, E. N. *Org. Lett.* **2001**, *3*, 1009-1011.

²⁰⁴ Viswanathan, R.; Mutnick, D.; Johnston, J. N. *J. Am. Chem. Soc.* **2003**, *125*, 7266-7271.

isomerization of the stereocenter does not occur en route to making the azaindoline system. This is unique as the phenyl analog (**427**) succumbs to loss of ee during the cyclization process, signifying that ring fragmentation and isomerization occurs for this particular substrate. The loss of stereochemical integrity can ultimately be owed to $A^{1,3}$ -strain.

After seeing the retention of stereochemistry for the azaindoline system, Johnston and co-workers then applied this free radical-mediated aryl amination to the synthesis of enantiopure 7-azaindoline α -amino acids (Scheme 157).^{205,206} Formylation and reduction of commercially available 2-bromopyridine (**433**) affords compound **434** in modest yield (47% over 2 steps). Treatment of primary alcohol **434** with PBr_3 furnishes alkyl bromide **435**, which then undergoes a phase transfer-catalyzed glycine alkylation with azomethine **436** to deliver the *R* and *S* enantiomers (separately) of **423** in high yield and with high enantioselection. Subjection of both enantiomers of **423** to the 5-*exo trig* cyclization provides the respective 7-azaindoline α -amino esters (**426a** and **426b**) in modest yield and with complete stereoretention. Subsequent deprotection of the *tert*-butyl ester moiety under acidic conditions generates acid salts **439a** and **439b** in modest to good yield.

Scheme 157. Johnston's Synthesis of Enantiopure 7-Azaindoline α -Amino Acids



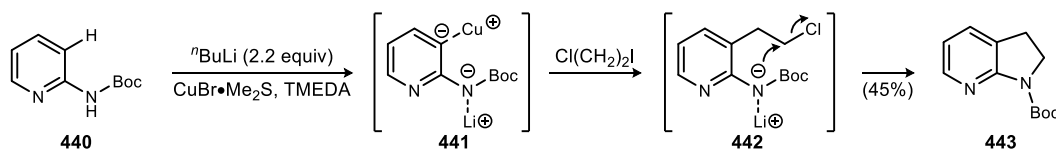
Other methods for the synthesis of 7-azaindoline scaffolds include base- and metal-mediated cyclizations. In 2004, Davies and colleagues utilized a directed *ortho*-

²⁰⁵ Srinivasan, J. M.; Burks, H. E.; Smith, C. R.; Viswanathan, R.; Johnston, J. N. *Synthesis* **2005**, 2, 330-333.

²⁰⁶ Majumdar, K. C.; Basu, P. K.; Mukhopadhyay, P. P. *Tetrahedron* **2005**, 61, 10603-10642.

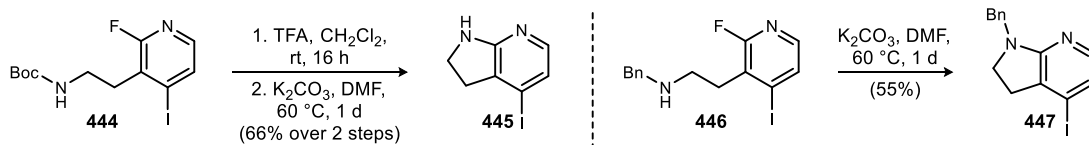
metallation/transmetallation reaction in order to access annulated pyridines.²⁰⁷ For example, when Boc-protected aminopyridine **440** is treated with 2.2 equivalents of ⁿBuLi in the presence of copper(I) bromide dimethyl sulfide (CuBr•Me₂S) and TMEDA, dianion **441** is formed (Scheme 158). The more reactive anion of species **441** undergoes alkylation with 1-chloro-2-iodoethane to deliver intermediate **442**. Subsequent *in situ* cyclization gave the desired 7-azaindoline (**443**) in 45% isolated yield.

Scheme 158. Davies's *ortho*-Metallation/Transmetallation Approach to 7-Azaindolines



Shortly thereafter, Nguyen and Wang were able to promote an intramolecular S_NAr reaction in the presence of potassium carbonate to furnish 7-azaindoline cores (Scheme 159).²⁰⁸ Treatment of Boc-protected 1-fluoro-2-alkylamino-3-iodopyridine **444** with TFA afforded the precursor amine, which then succumbed to S_NAr upon exposure to K₂CO₃ providing 4-iodo-7-azaindoline **445** in good yield (66% yield over 2 steps). Similarly, subsection of benzyl-protected 1-fluoro-2-alkylamino-3-iodopyridine **446** to K₂CO₃ facilitated the intramolecular cyclization delivering *N*-benzyl-4-iodo-7-azaindoline **447** in modest yield (55%).

Scheme 159. Nguyen's Base-Mediated Synthesis of 7-Azaindolines



As for metal-mediated approaches, Desarbre and Mérou reported a palladium heteroannulation process for the synthesis of 7-azaindolines.²⁰⁹ To illustrate, aminopyridine **448** was treated with 1-methoxypropadiene (**449**) and substoichiometric quantities of Pd(PPh₃)₂Cl₂ at elevated temperature to afford 7-azaindoline **450** in 80% yield (Scheme 160). Mechanistically, it is proposed that aminopyridine **448** undergoes palladation followed by π-allylic complexation to arrive at allyl cation **451**. With methoxyallene, the methoxy group stabilizes the carbocation at C₁

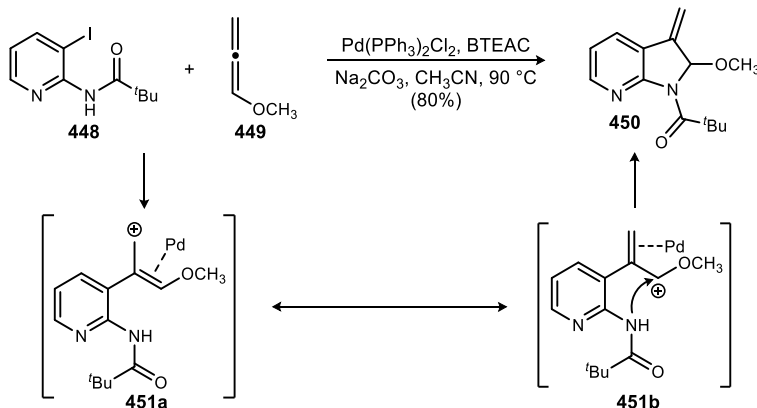
²⁰⁷ Davies, A. J.; Brands, K. M. J.; Cowden, C. J.; Dolling, U.-H.; Lieberman, D. R. *Tetrahedron Lett.* **2004**, 45, 1721-1724.

²⁰⁸ Nguyen, H. N.; Wang, Z. J. *Tetrahedron Lett.* **2007**, 48, 7460-7463.

²⁰⁹ Desarbre, E.; Mérou, J.-Y. *Tetrahedron Lett.* **1996**, 37, 43-46.

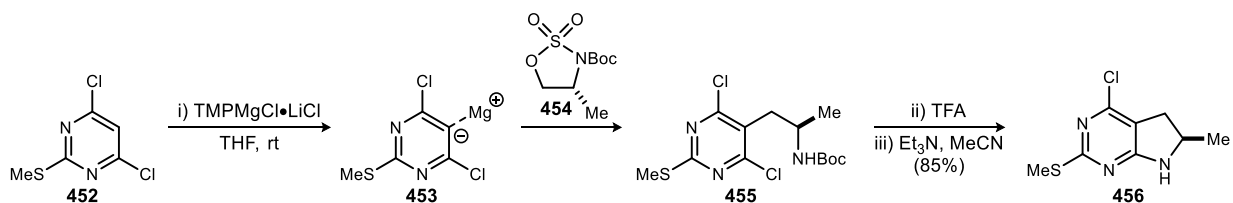
rendering it the most electrophilic position. Regioselective attack by the nitrogen of the amide provides the corresponding azaindoline, consequently.

Scheme 160. Méroux's Palladium Heteroannulation en Route to 7-Azaindolines



In 2012, Moss and co-workers employed a one-pot magnesium-mediated ring-opening-cyclization sequence in order to arrive at azaindoline scaffolds.²¹⁰ To demonstrate the efficacy of this process, pyrimidine **452** was subjected to tetramethylpiperidine magnesium chloride lithium chloride complex (TMPMgCl•LiCl) resulting in the formation of magnesiated chloropyrimidine **453** (Scheme 161). This motif can then undergo a facile ring opening with chiral Boc-protected sulfamidate **454** to furnish intermediate **455** upon loss of SO₃. After an acidic workup (removal of the Boc group), this adduct engages in a rapid intramolecular cyclization upon basicification to give highly functionalized stereodefined azaindoline **456** in 85% isolated yield.

Scheme 161. Moss's One-Pot Ring-Opening-Cyclization Sequence en Route to Azaindolines



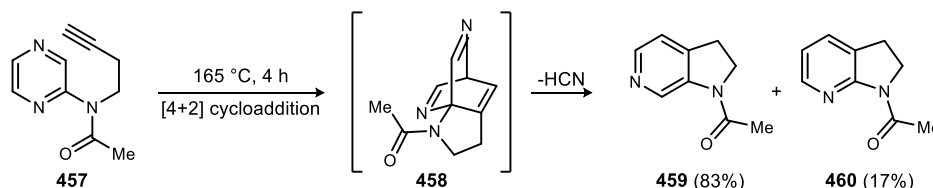
Compared to 7-azaindoline backbones, methods to prepare the 6-azaindoline, 5-azaindoline, and 4-azaindoline congeners are relatively scarce. As for 6-azaindolines, one way to access this bicyclic system is through van der Plas's inverse electron demand Diels-Alder reaction.²¹¹ When pyrazine **457** is subjected to high temperature, the intramolecular 4+2 cycloaddition proceeds to provide tricyclic intermediate **458** *in situ* (Scheme 162). Conversion of

²¹⁰ Moss, T. A.; Hayter, B. R.; Hollingsworth, I. A.; Nowak, T. *Synlett* **2012**, 23, 2408-2412.

²¹¹ de Bie, D. A.; Ostrowicz, A.; Geurtsen, G.; van der Plas, H. C. *Tetrahedron* **1988**, 44, 2977-2983.

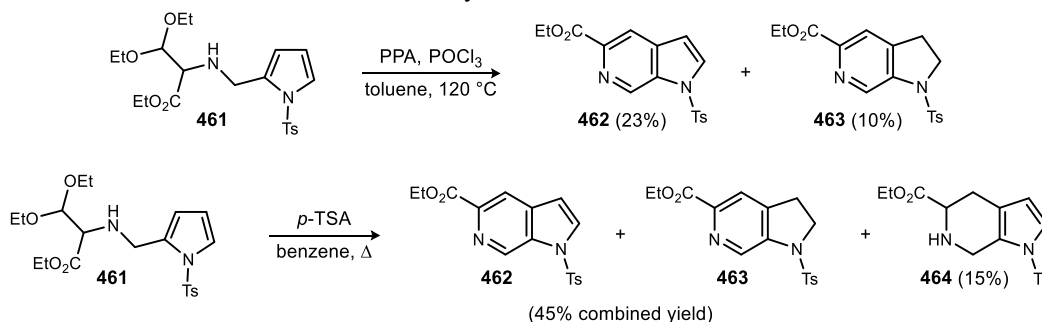
this cycloadduct (**458**) to its corresponding 6-azaindoline (**459**) is driven by the elimination of hydrogen cyanide. The 7-azaindoline analog (**460**) is also furnished via tricycle **458**, but as the minor product.

Scheme 162. Synthesis of 6-Azaindolines via an Inverse Electron Demand Diels-Alder Reaction of Pyrazines



Dodd and colleagues inadvertently accessed a 6-azaindoline moiety en route to making 6-azaindole-5-carboxylates.²¹² After successfully synthesizing acyclic acetal **461**, this intermediate was subjected to a Pomeranz-Fritsch cyclization using polyphosphoric acid (PPA) and phosphorus oxychloride (POCl₃). Aside from furnishing the desired azaindole (**462**) in 23% yield, 6-azaindoline **463** was also acquired, but as the minor product (Scheme 163). Due to the low yields observed under the Pomeranz-Fritsch protocol, other cyclization conditions were investigated. It was found that refluxing **461** in benzene in the presence of *p*-toluene sulfonic acid led to an improved overall yield of **462** and **463** (45%). For this particular case, however, 4,5,6,7-tetrahydro-6-azaindole-5-carboxylate derivative **464** was formed as a minor byproduct.

Scheme 163. Dodd's Synthesis of 6-Azaindoline Scaffolds



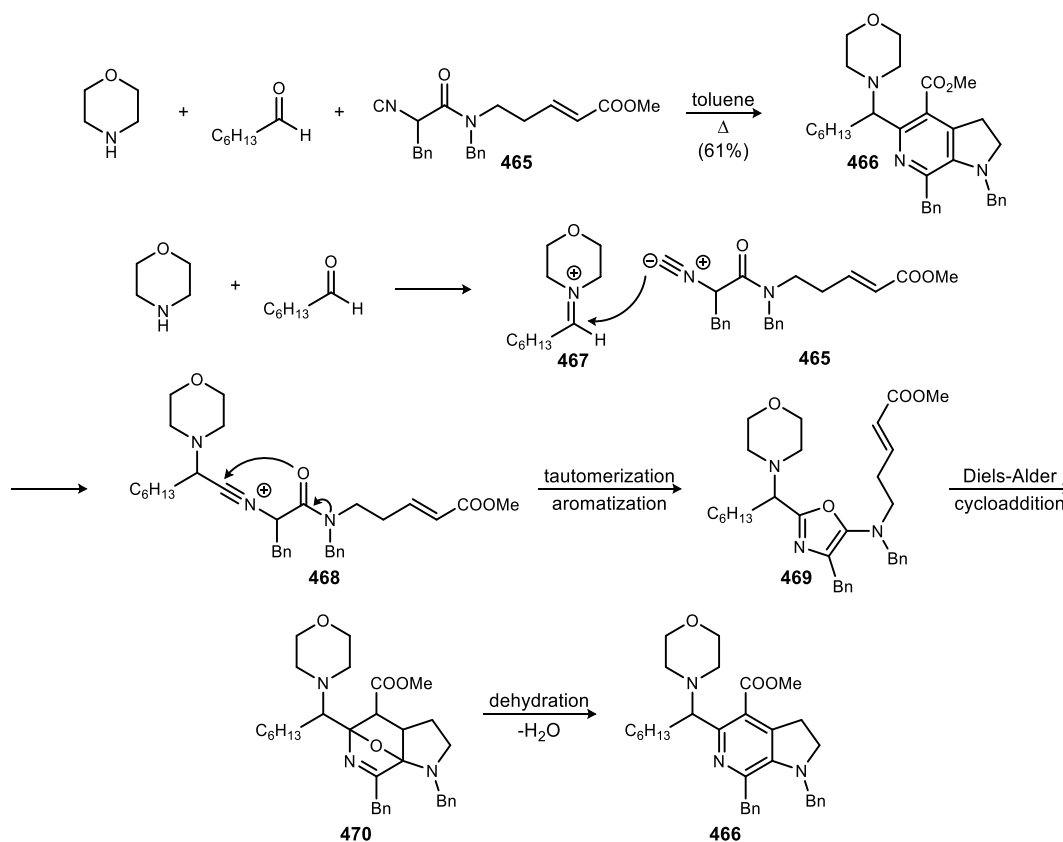
In 2005, Fayol and Zhu reported a highly efficacious three-component synthesis of 6-azaindolines.²¹³ The three substrates employed in this reaction system were that of an isocyanoacetamide, an amine, and an aldehyde. Treatment of morpholine with heptanal and isocyanoacetamide **465** in the presence of toluene at elevated temperature provided polysubstituted 6-azaindoline **466** in modest yield (Scheme 164). Mechanistically, it is envisioned that morpholine

²¹² Dekhane, M.; Potier, P.; Dodd, R. H. *Tetrahedron* **1993**, *49*, 8139-8146.

²¹³ Fayol, A.; Zhu, J. *Org. Lett.* **2005**, *7*, 239-242.

condenses onto heptanal to deliver iminium **467**. Addition of the isocyanoacetamide into the iminium yields nitrilium **468**. Intramolecular attack of the amide to the nitrilium and subsequent tautomerization/aromatization provides oxazole **469**. Interception of the resultant oxazole by the tethered dienophile via an intramolecular Diels-Alder cycloaddition affords oxa-bridge intermediate **470**. Dehydration of the oxa-bridge compound leads to the desired 6-azaindoline (**466**).

Scheme 164. Zhu's Three-Component Synthesis of 6-Azaindolines

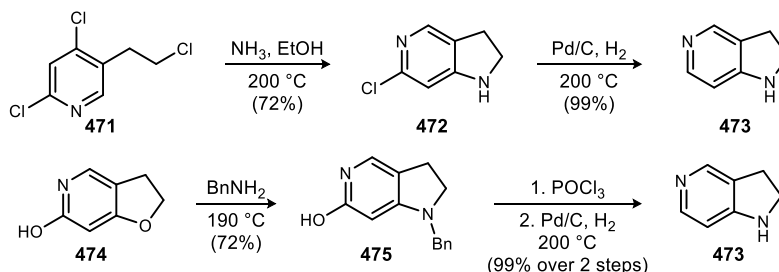


For the 5-azaindoline backbone, earliest reports of successfully constructing this bicyclic system include that of Yakhontov and co-workers.²¹⁴ Herein, treatment of 3-alkyl-4,6-dichloropyridine **471** with ammonia in ethanol at elevated temperature leads to the formation of 5-azaindoline **472** (Scheme 165). This azaindoline is thought to arise via S_N2 displacement of the alkyl chloride with ammonia followed by S_NAr . Reduction of the aryl chloride with Pd/C and H_2 provides 5-azaindoline **473** in 71% yield over 2 steps. Additionally, subjection of 6-hydroxy-5-azabenzofuran **474** to an excess of benzylamine at 190 °C led to benzyl-protected 6-hydroxy-5-

²¹⁴ Yakhontov, L. N.; Azimov, V. A.; Lapan, E. I. *Tetrahedron Lett.* **1969**, 10, 1909-1912.

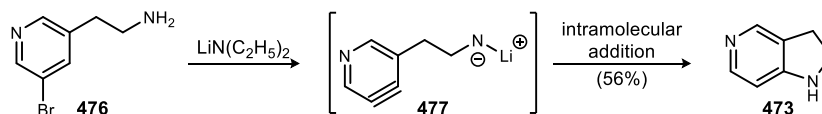
azaindoline **475** in good yield (72%). Treatment of **475** with POCl₃ converts the hydroxyl motif to a chloride and subsequent deprotection/reduction delivers free 5-azaindoline **473** in quantitative yield.

Scheme 165. Yakhontov's Synthesis of 5-Azaindolines



Kauffmann and Fischer later reported that base-mediated side chain cyclizations can also be employed in order to access 5-azaindoline cores.²¹⁵ Exposure of 3-(2-aminoethyl)-5-bromopyridine **476** to lithium diethylamide not only deprotonates the free amine, it also promotes the formation of benzyne intermediate **477** (Scheme 166). Intramolecular addition of the amine to the benzyne affords the desired 5-azaindoline in moderate yield (56%).

Scheme 166. Kauffmann and Fischer's Synthesis of 5-Azaindoline **473** via a Benzyne Intermediate



In 1998, Spivey and colleagues successfully synthesized *N*-methyl-5-azaindoline **478** as a precursor to atropisomeric analogues of DMAP.^{216,217} Beginning with commercially available 4-aminopyridine (**479**), Boc-protection with (Boc)₂O proceeded well as *tert*-butyl carbamate **480** was furnished in excellent yield (95%) (Scheme 167). Base-mediated *ortho*-lithiation of **480** followed by alkylation with ethylene oxide provided alcohol **481** in 75% yield. Mesylation and *in situ* cyclization delivered *N*-Boc azaindoline **482** (not shown). This intermediate was then reduced with DIBAL to give 1-methyl-5-azaindoline **483** in modest yield (52% over 2 steps). *meta*-Bromination with NBS produced bromoarene **484** and the stage was now set for a palladium-mediated Suzuki coupling. Treatment of **484** with 1-naphthylboronic acid (**485**) in the presence of palladium tetrakis and base delivered atropisomeric DMAP analog **478** in 96% yield. Other

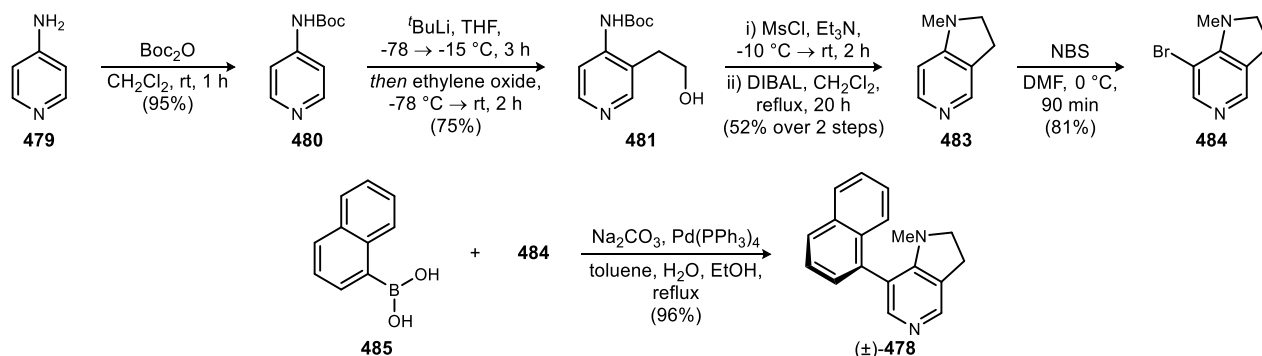
²¹⁵ Kauffmann, T.; Fischer, H. *Chem. Ber.* **1973**, *106*, 220-227.

²¹⁶ Spivey, A. C.; Fekner, T.; Adams, H. *Tetrahedron Lett.* **1998**, *39*, 8919-8922.

²¹⁷ Spivey, A. C.; Fekner, T.; Spey, S. E.; Adams, H. *J. Org. Chem.* **1999**, *64*, 9430-9443.

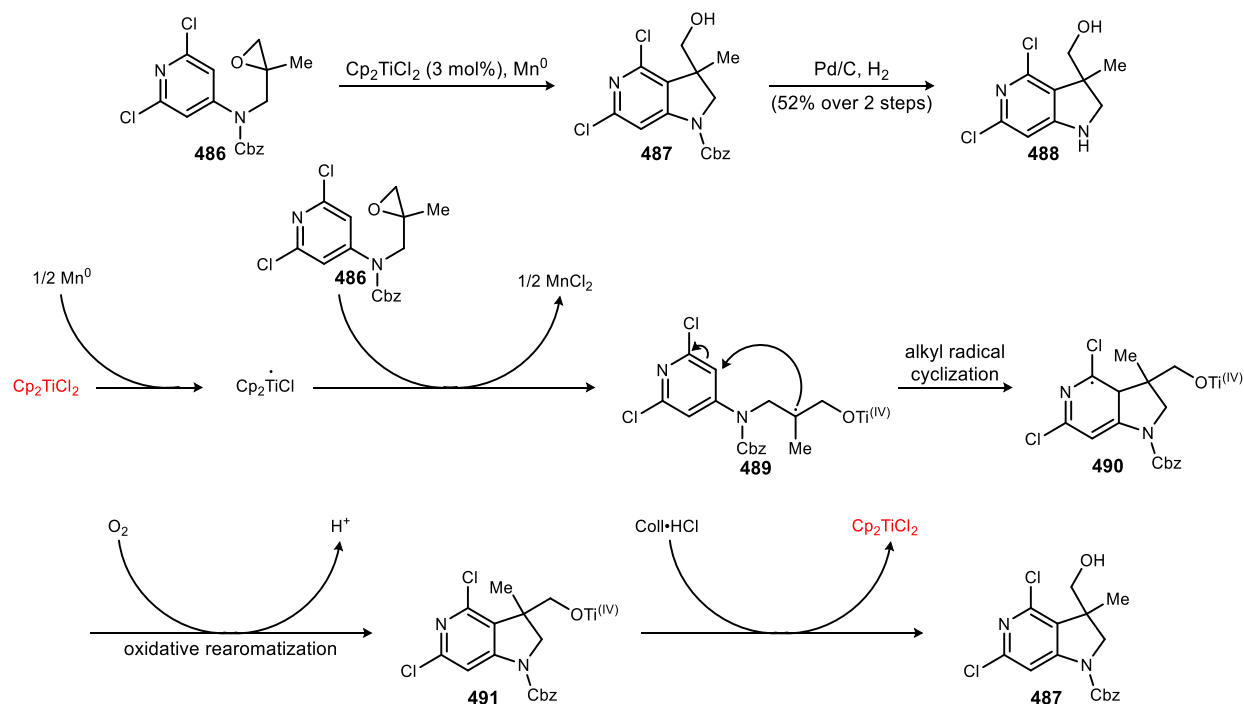
arylboronic acids underwent Suzuki cross couplings with bromoarene **484** to afford a library of DMAP derivatives. These biaryl 5-azaindoline scaffolds were then subjected to acylation reactions in order to test their efficacy as organocatalysts.

Scheme 167. Synthesis of DMAP Analogs via 5-Azaindoline Intermediates



Radical annulations have also been used as a means to access 5-azaindoline cores. In 2008, Wipf and co-workers developed a novel titanocene(III) chloride catalyzed epoxide-opening arene annulation that affords 3,3-disubstituted-5-azaindolines.²¹⁸ To illustrate, when tethered epoxide **486** is subjected to titanocene(III) chloride in the presence of stoichiometric magnesium metal, Cbz-protected 5-azaindoline **487** is produced (Scheme 168). Subsequent debenzoylation delivers

Scheme 168. Titanocene(III)-Catalyzed Formation of 5-Azaindolines

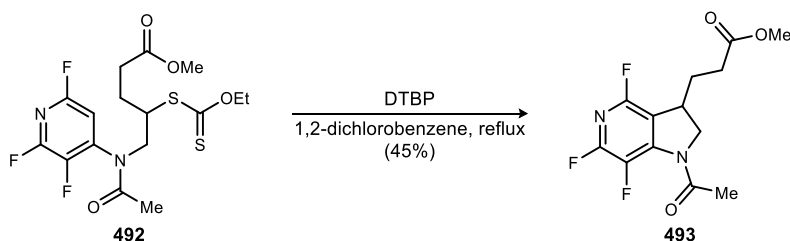


²¹⁸ Wipf, P.; Maciejewski, J. P. *Org. Lett.* **2008**, *10*, 4383-4386.

3,3-disubstituted-5-azaindoline **488** in modest yield (52% over 2 steps). Mechanistically, it is proposed that formation of the β -titanoxy radical **489** is followed by a reversible annulation, which generates aryl radical **490**. Oxidative rearomatization affords **491**, and protodemetalation by collidinium hydrochloride leads to azaindoline **487** upon the regeneration of the precatalyst Cp_2TiCl_2 .

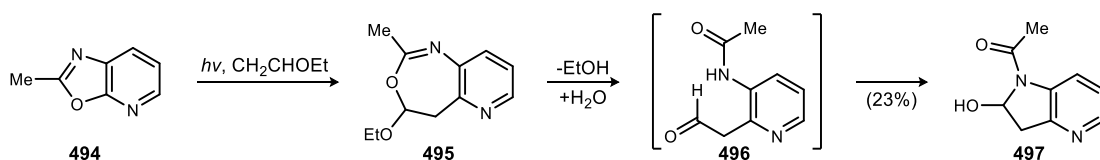
Zard and colleagues utilized xanthate esters in order to promote an unconventional radical-mediated *ipso* substitution en route to generating 5-azaindolines.²¹⁹ For example, treatment of polysubstituted aminopyridine **492** with di-*tert*-butyl peroxide in the presence of 1,2-dichlorobenzene furnished fluorinated 5-azaindoline **493** in 45% isolated yield (Scheme 169). This azaindoline scaffold was acquired through a mechanistic pathway analogous to the previously reported 7-azaindoline studies.^{200,201,202}

Scheme 169. Zard's Synthesis of 5-Azaindolines Using Xanthate Esters



As for 4-azaindoline scaffolds, few approaches have been reported that provide direct access to this bicyclic system. Among these methods is the use of photochemistry as described by Donati and co-workers.²²⁰ For example, 2-methyloxazolo[5,4-*b*]pyridine **494** is treated with ethyl vinyl ether in order to promote a photocycloaddition en route to pyridooxazepine **495** (Scheme 170). This unstable intermediate then undergoes hydrolysis to give amide-aldehyde **496**. Attack of the amide to the aldehyde generates the more stable 2-hydroxy-4-azaindoline (**497**) in low yield (23%).

Scheme 170. Synthesis of 4-Azaindoline **497** via Photocycloaddition

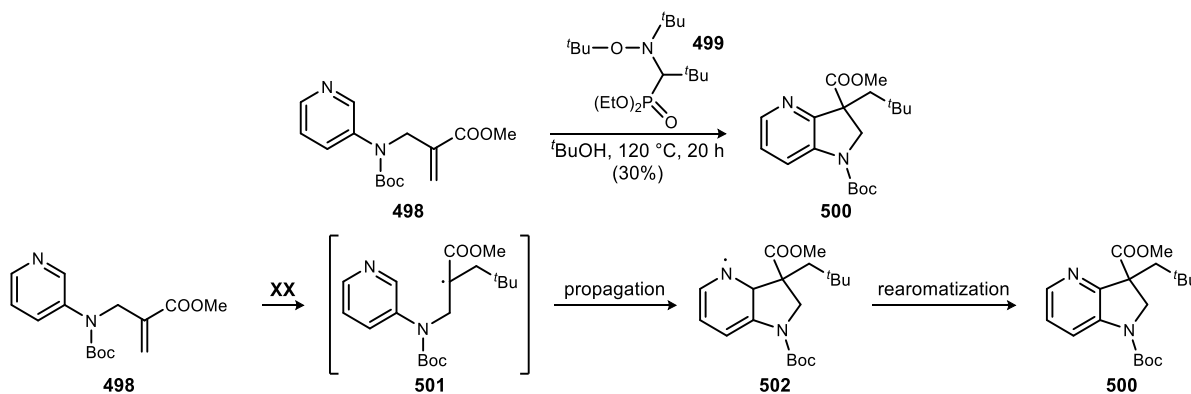


²¹⁹ Laot, Y.; Petit, L.; Zard, S, Z. *Org. Lett.* **2010**, *12*, 3426-3429.

²²⁰ Donati, D.; Fusi, S.; Ponticelli, F. *Eur. J. Org. Chem.* **2002**, 4211-4216.

Ciufolini and colleagues describe an alkoxyamine-mediated radical synthesis of 4-azaindoline backbones.²²¹ Treatment of aminopyridine **498** with alkoxyamine **499** affords 3,3-disubstituted-4-azaindoline **500** in 30% yield upon chromatographic separation (Scheme 171). Mechanistically, it is postulated that alkoxyamine **499** (a *tert*-butyl radical source) propagates with the external alkene of **498** resulting in the formation of tertiary radical **501**. Propagation of this radical with the pyridine moiety generates radical **502**, which later furnishes 4-azaindoline **500** after rearomatization.

Scheme 171. Ciufolini's Alkoxy-Mediated Radical Synthesis of 4-Azaindolines

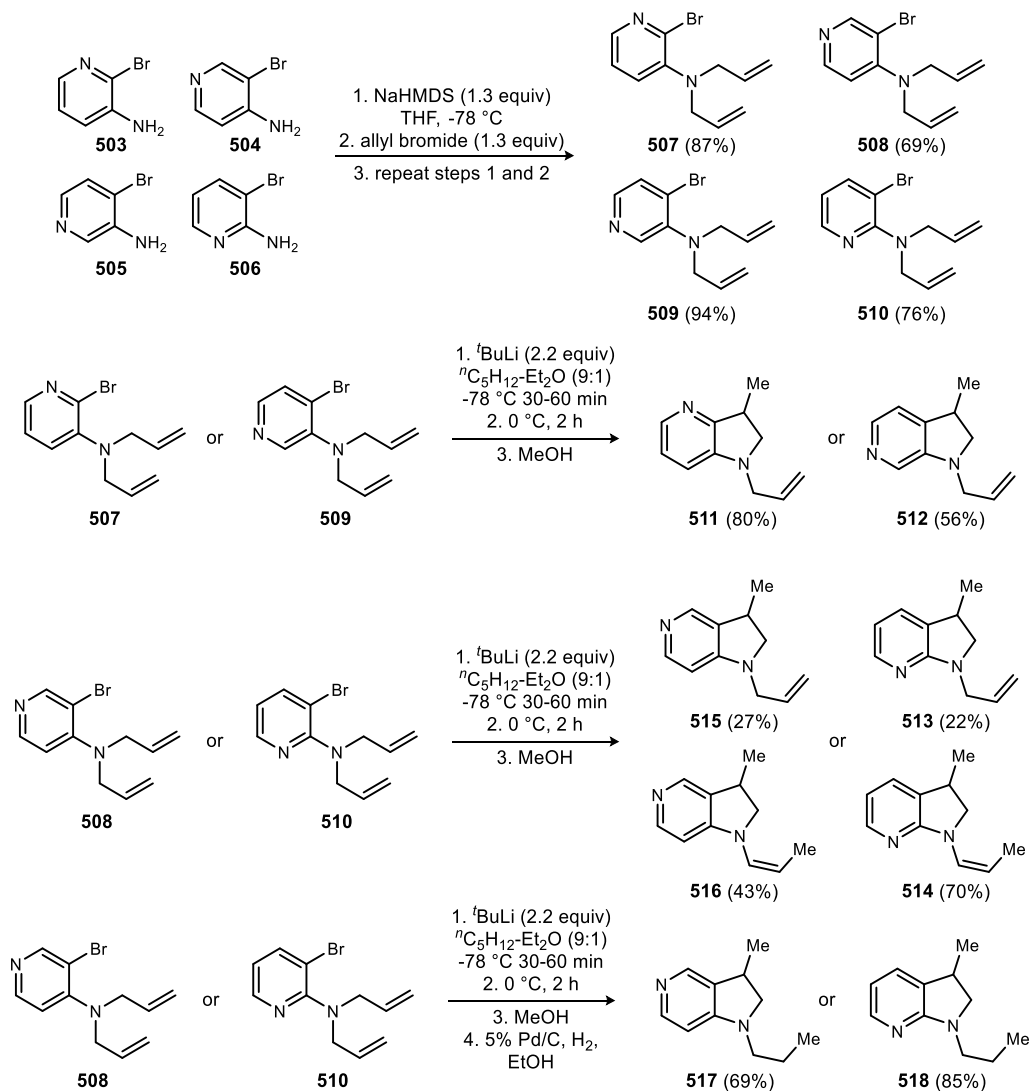


As previously mentioned, there is only one known unified approach that readily accesses all four isomeric azaindoline families. In 2008, Bailey and co-workers introduced an intramolecular carbolithiation sequence as a means of synthesizing 3-alkyl 4-, 5-, 6-, and 7-azaindoline backbones.¹⁹² Precursor substrates were furnished via allylation of aminobromopyridines **503-506** (Scheme 172). The corresponding *N,N*-diallyl compounds (**507-510**) were afforded in reproducible yields of 70-90%. Treatment of substrates **507** and **509** with 2.2 equivalents of *t*-BuLi in the presence of dry *n*-pentane-diethyl ether generates the desired aryllithium intermediates. These aryllithium compounds were allowed to stand under argon atmosphere at $0\text{ }^\circ\text{C}$ for 2 hours before being quenched with MeOH to provide 1-allyl-3-methyl-4-azaindoline **511** and 1-allyl-3-methyl-6-azaindoline **512** in 80% and 56% yields, respectively. When diallyl aminopyridine **510** was subjected to nearly identical reaction conditions, 7-azaindolines **513** and **514** were isolated in 22% and 70% yields. The same phenomenon was observed with precursor substrate **508** as 5-azaindoline products **515** and **516** were furnished in low to modest yield (27% and 43%). Repetition of the cyclization with substrates **508** and **510**

²²¹ Leroi, C.; Bertin, D.; Dufils, P.-E.; Gignes, D.; Marque, S.; Tordo, P.; Couturier, J.-L.; Guerret, O.; Ciufolini, M. A. *Org. Lett.* **2003**, *5*, 4943-4945.

followed by reduction of the crude products delivered 3-methyl-7-azaindoline **518** and 3-methyl-5-azaindoline **517** in 85% and 69% yields, respectively.

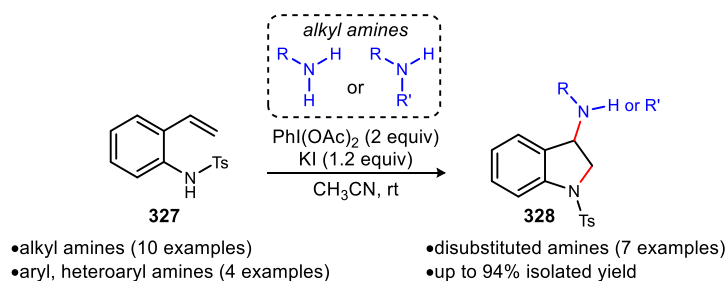
Scheme 172. Bailey's Unified Approach to All Four Isomeric Azaindoline Families



6.3. Reaction Optimization and Substrate Scope

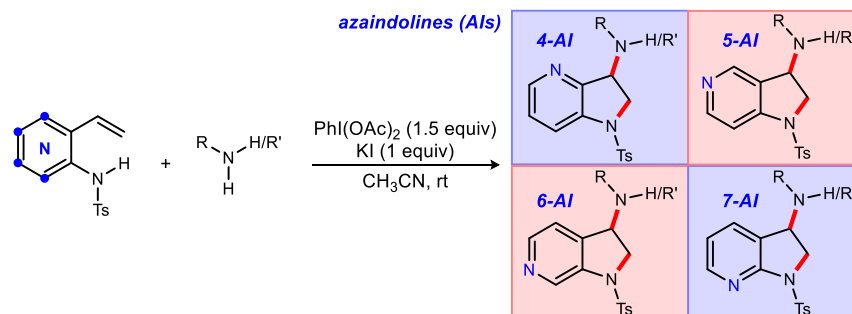
Hong and Johnston recently described a new method for the inter-/intramolecular annulative diamination of terminal alkenes via the use of an oxidant/additive combination (Scheme 173).¹⁶⁹ Treatment of tosylated vinylaniline (**327**) with $\text{PhI}(\text{OAc})_2$, KI, and a broad range of electron-rich amines effectively delivered a library of 3-aminoindolines without the need for amine preactivation and protection. This approach displayed a high degree of generality as both mono- and disubstituted amines were successfully converted to their respective indoline products.

Scheme 173. Hong and Johnston's Iodine(III)-Mediated Inter-/Intramolecular Diamination of Terminal Alkenes



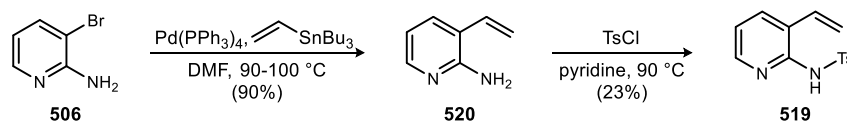
Based on the success of the aforementioned reaction system, we sought to extend this methodology to the synthesis of all four azaindoline heterocycle families. The goal was to convert four isomeric vinylpyridine substrates to their corresponding 3-amino azaindoline scaffolds via a hypervalent iodine-/iodide-mediated inter-/intramolecular annulative diamination, an approach analogous to that of Hong and Johnston's (Scheme 174). Introduction of pyridine-derived starting materials provides an opportunity to evaluate the compatibility of Lewis basic pyridine nitrogens with the oxidative, electrophilic (I^+) conditions.

Scheme 174. Inter-/Intramolecular Diamination of Vinylpyridines en Route to All Four Azaindoline Families



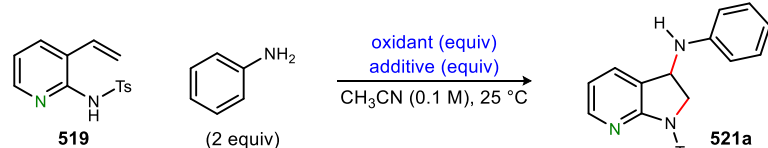
The first substrate to be examined was that of 3-vinyl-2-tosylaminopyridine (**519**). Acquisition of this starting alkene was straightforward as commercially available 2-amino-3-bromopyridine (**506**) was subjected to a Stille coupling with tributyl(vinyl)tin to afford free vinyl aminopyridine **520** in 90% yield upon chromatographic separation (Scheme 175). Subsequent tosylation of **520** under basic conditions and at elevated temperature gave 3-vinyl-2-tosylaminopyridine (**519**) in 23% isolated yield.

Scheme 175. Synthesis of Vinyl Aminopyridine **519**



With vinyl aminopyridine **519** in hand, the stage was now set for reaction optimization. Electrophilic iodinating reagents were the first variant to be examined. When NIS was employed as the iodinating agent in the presence of vinylpyridine **519** and aniline (the amine source), 3-amino-7-azaindoline **521a** was provided but in low yield (Table 23, entry 1). When the iodonium source was generated through $\text{PhI}(\text{OAc})_2$ and KI, the desired azaindoline was furnished in 96% isolated yield, once again proving the superiority of the oxidant/additive combination (Table 23, entry 2). Use of tetrabutylammonium iodide as the halide source proved slightly inferior as azaindoline **521a** was afforded in 80% yield (Table 23, entry 3). Ammonium iodide further mitigated reactivity as **521a** was acquired in only 29% yield (Table 23, entry 4). Use of both components of the oxidant/additive combination proved vital, as no conversion to product was observed when starving the reaction conditions of either the oxidant or the halide additive (Table 23, entries 5-7). Catalytic quantities of iodide proved effective as 30 mol% and 50 mol% loadings of KI led to 63% and 65% isolated yields of azaindoline **521a**, respectively (Table 23, entries 8-9). Despite the success seen with substoichiometric amounts of halide, stoichiometric quantities were necessary as they provided the most fruitful results.

Table 23. Initial Optimization Studies of the Inter-/Intramolecular Annulative Diamination

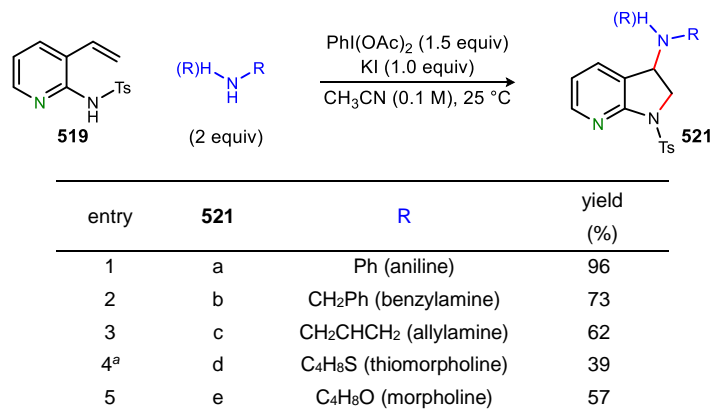


entry	oxidant	oxidant equiv	additive	additive equiv	conversion (%)	yield (%)
1	NIS	1.2	-	-	100	11
2	$\text{PhI}(\text{OAc})_2$	1.5	KI	1.0	100	96
3	$\text{PhI}(\text{OAc})_2$	1.5	$^n\text{Bu}_4\text{NI}$	1.0	100	80
4	$\text{PhI}(\text{OAc})_2$	1.5	NH_4I	1.0	77	29
5	$\text{PhI}(\text{OAc})_2$	1.5	-	-	0	-
6	-	-	$^n\text{Bu}_4\text{NI}$	1.0	0	-
7	-	-	KI	1.0	0	-
8	$\text{PhI}(\text{OAc})_2$	1.5	KI	0.3	75	63
9	$\text{PhI}(\text{OAc})_2$	1.5	KI	0.5	88	65

With optimum reactivity achieved, the next goal was to expand the 3-amino-7-azaindoline library. Monosubstituted aliphatic amines in benzylamine and allylamine successfully engaged in diamination as 3-amino-7-azaindoline products **521b** and **521c** were afforded in 73% and 62% yields, respectively (Table 24, entries 2-3). Heterocyclic disubstituted amines were also tolerated

as thiomorpholine and morpholine delivered their corresponding azaindolines (**521d** and **521e**), albeit in depressed yields (39% and 57%) (Table 24, entries 4-5).

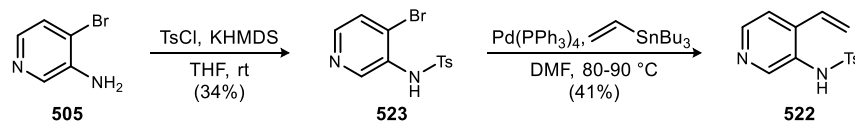
Table 24. 3-Amino-7-Azaindoline Scope



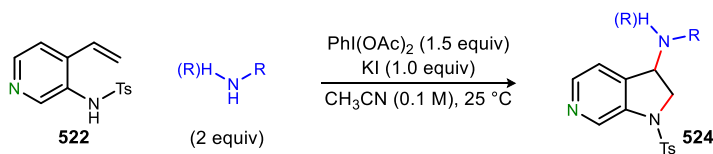
^a2.0 equiv of PhI(OAc)₂, 1.2 equiv of KI, 3.0 equiv of amine used

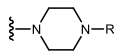
Efforts then shifted towards generating a 3-amino-6-azaindoline library from vinyl aminopyridine **522**. Synthesis of this vinylpyridine substrate was initiated when commercially available 3-amino-4-bromopyridine (**505**) was treated with tosyl chloride in the presence of KHMDS to afford tosylated bromopyridine **523** in 34% yield (Scheme 176). Intermediate **523** was then subjected to a palladium-mediated Stille coupling with tributyl(vinyl)tin at elevated temperature to provide 4-vinyl-3-tosylaminopyridine **522** in modest yield (41%).

Scheme 176. Synthesis of Vinyl Aminopyridine **522**

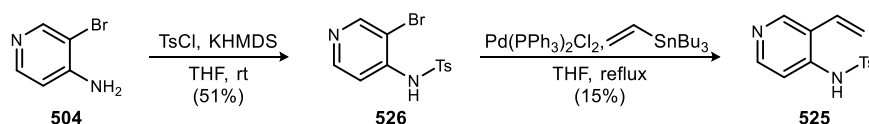


This vinylpyridine substrate (**522**) was then treated with aromatic, primary, and secondary amines in order to generate a series of 6-azaindoline scaffolds. Aniline and benzylamine proved tolerant in this system as the desired 3-amino-6-azaindoline products (**524a** and **524b**) were furnished in 11% and 48% yields, respectively (Table 25, entries 1-2). Furthermore, Cbz-, Boc-, and ethyl carboxylate-protected piperazines were readily converted to their corresponding 6-azaindolines (**524c-524e**) with good yields (Table 25, entries 3-5). These three diamines are notable as they allow for subsequent unmasking of the piperazine moiety under neutral, acidic, or basic conditions.

Table 25. 3-Amino-6-Azaindoline Scope

entry	524	R	yield (%)
1	a	Ph (aniline)	11
2	b	CH ₂ Ph (benzylamine)	48
3	c		63
4	d	R' = CO ₂ Et	66
5	e	R' = Boc	74

Our focus then centered upon successfully generating the 5-azaindoline congener. Vinyl aminopyridine **525**, the precursor to 5-azaindoline diamines, was synthesized via a pathway analogous to those of the 7-azaindoline and 6-azaindoline precursor substrates. 4-Amino-3-bromopyridine (**504**) underwent tosylation with KHMDS, providing intermediate **526** in 51% yield post column chromatography (Scheme 177). This tosylated amino bromopyridine was then subjected to a Stille coupling with tributyl(vinyl)stannane in order to arrive at vinylpyridine **525** in low yield (15%).

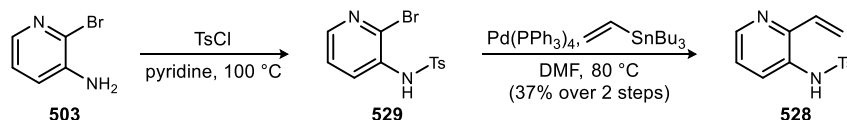
Scheme 177. Synthesis of Vinyl Aminopyridine **525**

This vinyl aminopyridine (**525**) proved to be an effective substrate as it was compatible with a wide array of amines. Aniline performed well under optimal conditions, as 5-azaindoline product **527a** was furnished in 81% yield (Table 26, entry 1). Benzylamine and derivatives were converted to 3-amino-5-azaindolines **527b-527d** in 43-51% yield (Table 26, entries 2-4). Alkyl amines including 3-methoxypropylamine and phenethylamine performed similarly (Table 26, entries 5-6). Other primary amines such as 4-amino tetrahydropyran and 3-picolyamine delivered their corresponding 3-amino-5-azaindolines (**527g** and **527h**) in 33% and 64% yields respectively, when subjected to the reaction protocol (Table 26, entries 7-8). A secondary amine in thiomorpholine also engaged in diamination as 5-azaindoline **527i** was afforded, albeit in lower yield (Table 26, entry 9).

Table 26. 3-Amino-5-Azaindoline Scope

entry	527	R	yield (%)
1	a	Ph (aniline)	81
2	b	CH ₂ Ph (benzylamine)	43
3	c	CH ₃ C ₆ H ₄ CH ₂ (4-methylbenzylamine)	45
4	d	FC ₆ H ₄ CH ₂ (4-fluorobenzylamine)	51
5	e	(CH ₂) ₃ OMe (3-methoxypropylamine)	48
6	f	CH ₂ CH ₂ C ₆ H ₅ (phenethylamine)	48
7	g	C ₅ H ₉ O (4-aminotetrahydropyran)	33
8	h	³ CH ₂ C ₅ H ₄ N (3-picolyamine)	64
9	i	C ₄ H ₈ S (thiomorpholine)	34

The next objective was to apply this inter-/intramolecular annulative diamination protocol towards the synthesis of 3-amino-4-azaindolines and consequently confirm that all four isomeric azaindoline families could be readily accessed. Synthesis of 2-vinyl-3-tosylaminopyridine (**528**) proceeded in a straightforward manner as tosylation of commercially available 3-amino-2-bromopyridine (**503**) delivered tosylated bromopyridine **529** (Scheme 178). This compound, carried on quantitatively, underwent a Stille coupling with tributyl(vinyl)tin in order to generate vinyl aminopyridine **528** in 37% yield over two steps.

Scheme 178. Synthesis of Vinyl Aminopyridine **528**

Development of the 4-azaindoline library was straightforward and suitable with aromatic, primary, and secondary amines. Aniline and 4-*tert*-butyl aniline were successfully converted to their corresponding 3-amino-4-azaindolines (**530a** and **530b**) in 70% and 41% yields, respectively (Table 27, entries 1-2). Benzylamine performed well as its 4-azaindoline (**530c**) was provided in good yield (Table 27, entry 3). Other primary amines in the form of cyclopentylamine and phenethylamine also engaged in diamination as vicinal diamines **530d** and **530e** were afforded in 59% and 68% yields (Table 27, entries 4-5). Disubstituted amines in piperidine and ethyl isonipecotate proved compatible under optimal conditions as 4-azaindoline diamines **530f** and **530g** were isolated in modest to good yields (Table 27, entries 6-7). *N*-Protected piperazines led

to 3-amino-4-azaindolines **530h** and **530i** in good yields, allowing for subsequent unmasking of the piperazine under both basic and acidic conditions (Table 27, entries 8-9). Further success with piperazines was demonstrated when *N*-cinnamyl piperazine delivered 3-amino-4-azaindoline **530j** in 66% isolated yield (Table 27, entry 10). Lastly, the HCl salt of glycine methyl ester underwent annulative diamination as 4-azaindoline **530k** was furnished in moderate yield (Table 27, entry 11). For this particular case, K_2CO_3 was incorporated in the reaction system with the sole purpose of liberating the free base of the glycine methyl ester. This modification had little or no effect on reaction progression as azaindoline **530k** could be cleanly isolated in a straightforward manner. This entry demonstrates that amino acid derivatives can be readily incorporated into azaindoline motifs.

Table 27. 3-Amino-4-Azaindoline Scope

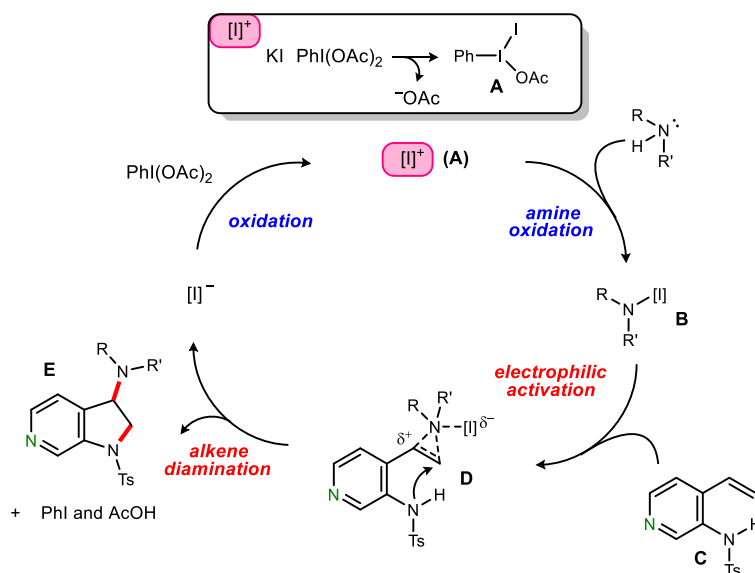
entry	530	R	yield (%)
1	a	Ph (aniline)	70
2	b	4- ^t Bu-C ₆ H ₄	41
3	c	CH ₂ Ph (benzylamine)	88
4	d	C ₅ H ₉ (cyclopentylamine)	59
5	e	CH ₂ CH ₂ C ₆ H ₅ (phenethylamine)	68
6	f	C ₅ H ₁₀ (piperidine)	63
7	g	C ₈ H ₁₄ O ₂ (ethyl isonipecotate)	71
8	h	 R' = CO ₂ Et	86
9	i	R' = Boc	74
10	j	R' = CH ₂ CHCHC ₆ H ₅	66
11 ^a	k	CH ₂ COOCH ₃ •HCl (glycine methyl ester•HCl)	63

^a2.0 equiv of K_2CO_3 used.

6.4. Mechanistic Hypothesis

A mechanistic hypothesis is depicted in Figure 30. It is believed that electrophilic iodinating agent **A** is generated upon the interaction of $PhI(OAc)_2$ with KI. Attack of iodane **A** with nucleophilic amine results in the formation of iodamine **B**. Association of **B** with the alkene moiety of vinylpyridine **C** leads to aziridinium **D**. This intermediate (**D**) then succumbs to intramolecular cyclization via nucleophilic attack of the tosylated amine at the least-hindered position of the aziridinium ring to yield the desired azaindoline product (**E**).

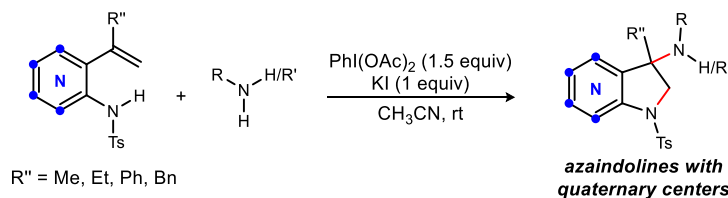
Figure 30. Mechanistic Hypothesis for the Inter-/Intramolecular Annulative Diamination



6.5. Future Work

Based on the high degree of success observed with this annulative diamination, there are several directions that can be pursued in order to make this system more efficacious. One pathway to explore would be the extension of this methodology to the synthesis of 3-alkyl-3-aminoazaindolines (Scheme 179). If α -alkylated vinyl pyridines can successfully engage in the $\text{PhI}(\text{OAc})_2/\text{KI}$ -mediated annulative diamination, this would give rise to azaindoline products bearing tetrasubstituted carbons. Not only would this approach be seen as a novel method to prepare heterocycles with quaternary carbon centers, these scaffolds may also garner interest as they can serve as structural cores for compounds of medicinal importance.

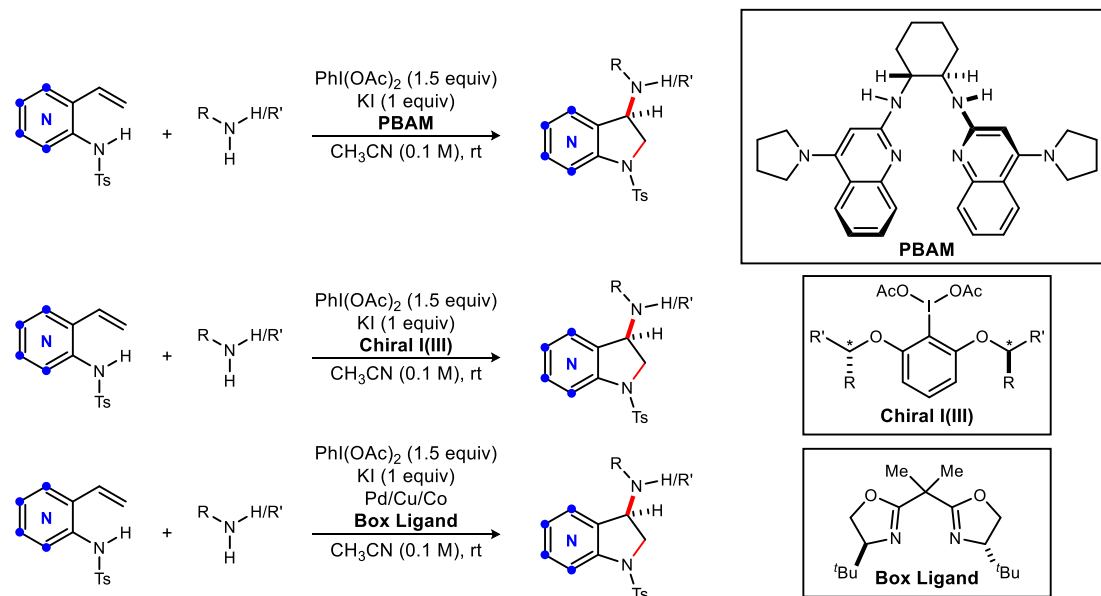
Scheme 179. Proposed Synthesis of 3-Alkyl-3-Amino-Azaindolines



The enantioselective variation of this inter-/intramolecular alkene diamination is another route to be taken. This can be probed by subjecting a number of chiral organocatalysts (e.g. PBAM) to the previously developed protocol (Scheme 180). Application of chiral hypervalent iodine reagents, as described by Muñiz and Ishihara, is another plausible approach that could readily achieve enantioselection. If the use of organocatalysts and/or transition-metal-free methods prove

fruitless, transition-metal catalysis can also be employed in order to induce enantioselectivity. Due to the evidence of halamine formation, it is feasible for a transition metal to oxidatively add between the nitrogen-iodine bond and have a chiral bidentate ligand (e.g. Box ligand) promote enantioselection via coordination to the metal-halamine complex. These investigations are currently ongoing within our laboratory.

Scheme 180. Potential Enantioselective Variation of the Annulative Diamination



Chapter 7. Efforts Towards the Enantioselective Synthesis of Sesbanine: A Potential Antileukemic

7.1. Background

Leukemia is a type of cancer of the blood or bone marrow that is characterized by the uncontrolled proliferation and accumulation of leukocytes (i.e. white blood cells). As there are many different types of leukocytes, there can be many different forms of leukemia. The four most important forms of leukemia, however, are derived from only two types of cells.²²²

Acute and chronic lymphocytic leukemias constitute two of the four important forms of this cancer. Lymphocytic leukemia results from malignancies of lymphocytes, which are cells produced in the lymphoid organs (i.e. the spleen, lymph nodes, and thymus) and in the bone marrow. Acute and chronic myelogenous leukemias make up the other two important forms of this cancer. Myelogenous leukemias (also known as myelocytic leukemias) are disorders of granulocytes. Granulocytes, a category of white blood cells produced by bone marrow, are responsible for engulfing and digesting bacteria as well as other small particles.²²²

Acute leukemias typically appear suddenly, with symptoms like those of a cold, and progress rapidly. Upon progression, the lymph nodes, spleen, and liver may become infiltrated with leukocytes and enlarged. Additional symptoms may include bone pain, paleness, a tendency to bleed easily, and a high susceptibility to infections. Immediate treatment of acute leukemias is necessary as failure to treat these types may result in death in as little as three months after onset.²²²

Chronic leukemias, however, begin much more slowly. Many cases are discovered during routine blood examinations, and several years may pass before significant symptoms appear. Although the symptoms of chronic leukemias are similar to those of acute leukemias, patients with the chronic types can live as long as three years after onset without having to undergo any form of treatment.²²²

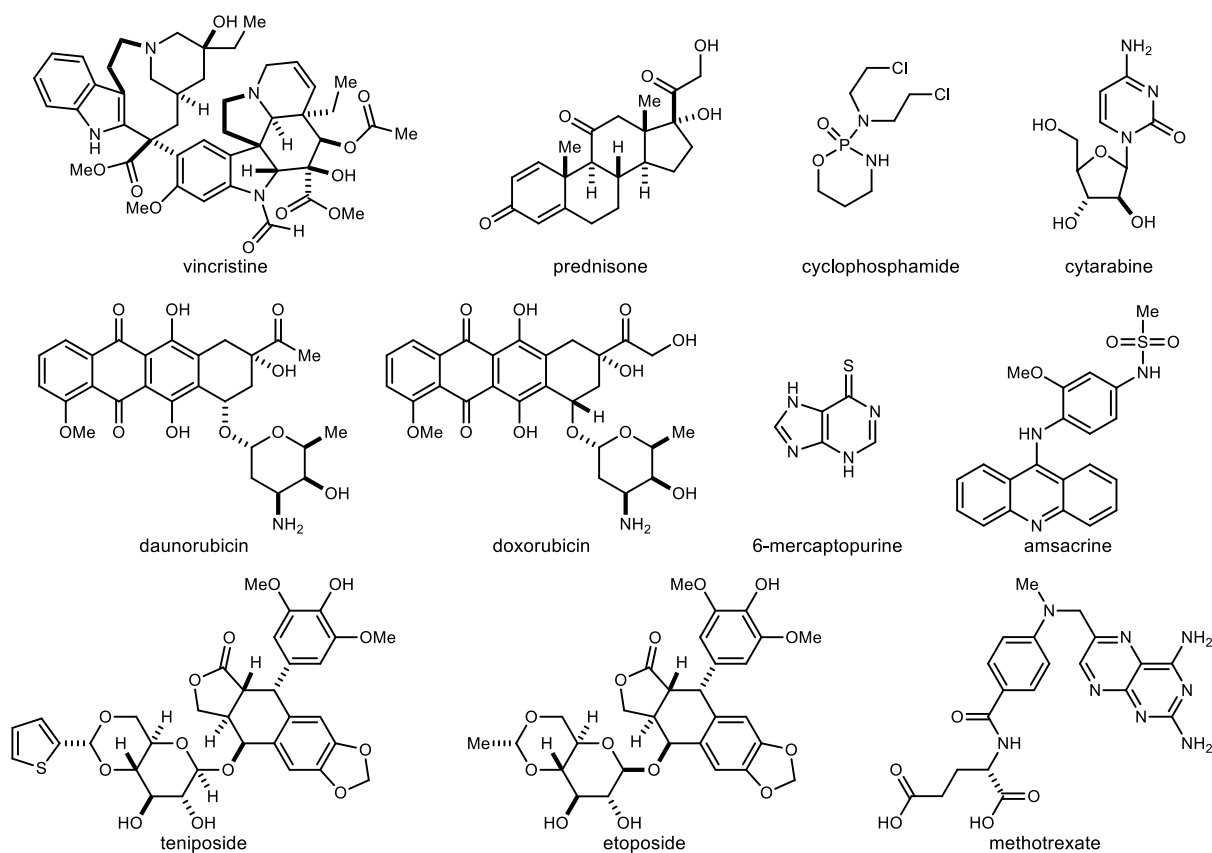
Leukemia can affect people of all ages, and can be a considerably fatal disease if not treated properly. A World Health Organization study conducted in 2000 estimated that 255,932 children and adults around the world had developed some form of leukemia, and 209,328 have died from it indicating an 82% mortality rate.²²³ It is also known that certain types of leukemia are more

²²² Maugh II, T. H. *Science* **1974**, *185*, 48-51.

²²³ Mathers, C. D.; Boschi-Pinto, C.; Lopez, A. D.; Murray, C. J. L.: *Cancer incidence, mortality and survival by site for 14 regions of the world*. Geneva: World Health Organization; **2001**.

prominent in select stages of life. Acute lymphocytic leukemia (ALL), for example, is the most common type of childhood cancer, accounting for approximately one-third of all childhood neoplasms in developed countries.^{224,225} It is estimated that 2,900 children and adolescents under age 20 are diagnosed with ALL each year. It is most common in younger children, especially children ages two and three. The five-year survival rate of children with ALL is 85% for children younger than 15 and 50% for teens aged 15 to 19.²²⁵

Figure 31. Chemotherapeutic Agents Used in the Treatment of Acute Lymphocytic Leukemia (ALL)



Conversely, chronic lymphocytic leukemia (CLL) is the most common type of leukemia among adults in the western world. The incidence of CLL in the United States alone is approximately 3.9 cases per 100,000 inhabitants, and the median age of diagnosis is 72. The clinical course of CLL is heterogeneous and survival times range from a few years to several

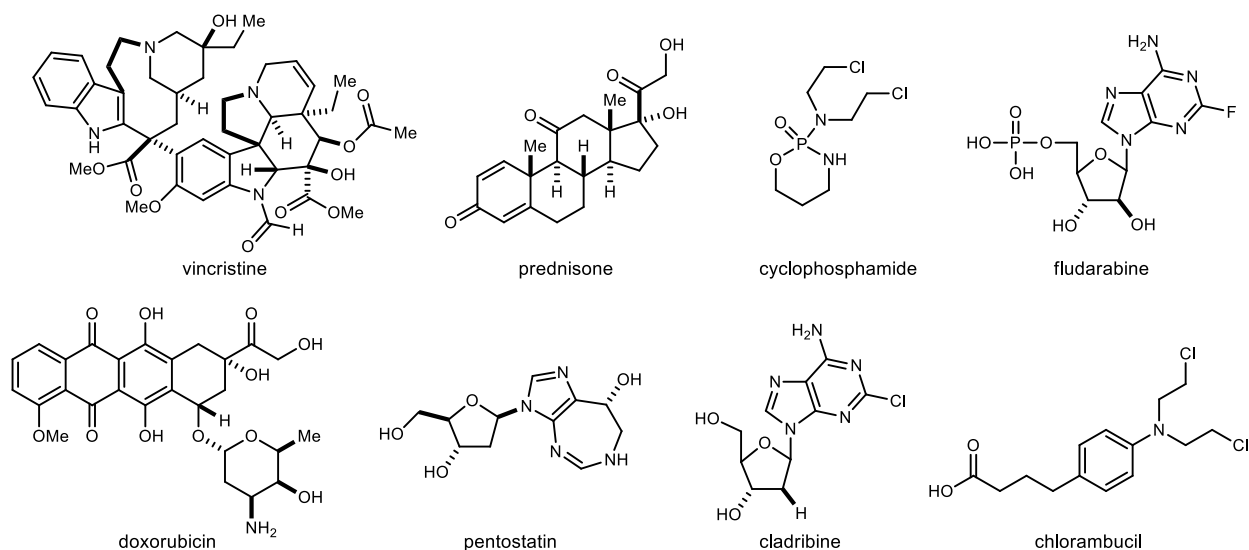
²²⁴ Rudant, J.; Amigou, A.; Orsi, L.; Althaus, T.; Leverger, G.; Baruchel, A.; Bertrand, Y.; Nelken, B.; Plat, G.; Michel, G.; Sirvent, N.; Chastagner, P.; Ducassou, S.; Rialland, X.; Hemon, D.; Clavel, J. *Pediatr. Blood Cancer* **2013**, *60*, 301-308.

²²⁵ Cancer.Net Editorial Board (2015). Leukemia – Acute Lymphoblastic – ALL – Childhood – Statistics. [Online]. Available: <http://www.cancer.net/cancer-types/leukemia-acute-lymphoblastic-all-childhood/statistics> [2016, Jan 18].

decades. However, approximately 5 to 20% of CLL patients develop Richter's syndrome, an aggressive lymphoma, which results in a short survival time.²²⁶

A variety of methods are used to treat leukemia, the most common being chemotherapy. The combinations of drugs used in chemotherapeutic treatments are ultimately dependent upon the type of leukemia present in the patient. For patients diagnosed with ALL, the first combination of drugs to be used successfully for induction chemotherapy included vincristine and corticosteroids, most often prednisone. Forty to sixty percent of patients treated with this combination achieved complete remission, although the median remission duration was only three to seven months. Anthracyclines, such as doxorubicin and daunorubicin, were later incorporated into this combination, and the complete remission rate rose from 47% to 85%. Other chemotherapeutic agents have been incorporated into induction regimens to improve results including cyclophosphamide, L-asparaginase, cytarabine, etoposide, teniposide, and amsacrine (Figure 31). Though these agents proved effective in treating ALL, the overall results seem to be equivalent to those with vincristine, anthracyclines, and corticosteroids.²²⁷

Figure 32. Purines and Other Agents Used in the Treatment of Chronic Lymphocytic Leukemia (CLL)



For consolidation chemotherapy, the use of high dose methotrexate, sometimes in combination with 6-mercaptopurine (6MP) or with teniposide and cytarabine, and asparaginase has significantly contributed to a cure rate of 70-80% among children with ALL (Figure 31). As for adults however, some reviews concluded that consolidation chemotherapy has not improved

²²⁶ Zhou, X.-X.; Wang, X. *Mol. Med. Rep.* **2013**, *8*, 719-725.

²²⁷ Cortes, J. E.; Kantarjian, H. M. *Cancer* **1995**, *76*, 2393-2417.

results, whereas others disagreed. Maintenance chemotherapy has proven valuable, especially in cases of childhood ALL. Similar to consolidation chemotherapy, this therapy is usually given with 6MP and methotrexate and is continued for 2 years.²²⁷

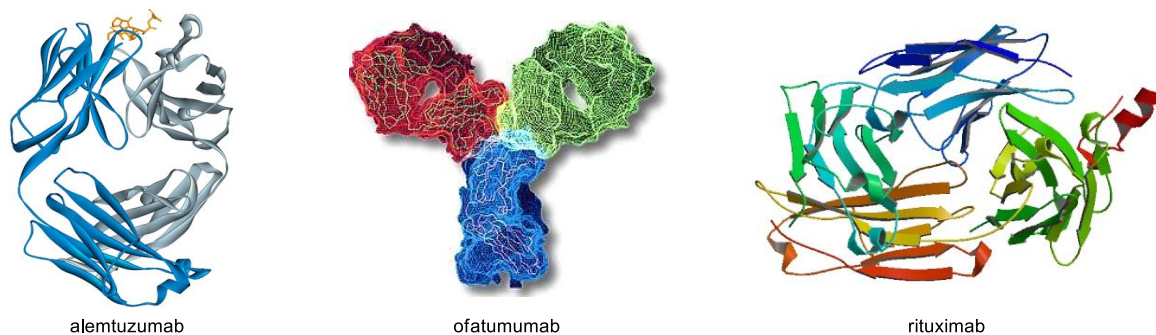
Patients diagnosed with CLL are typically subjected to purine-based chemotherapeutic treatments. Three purine analogues are currently used in CLL chemotherapy: fludarabine, pentostatin, and cladribine. Fludarabine remains by far the best studied compound of the three in CLL, and fludarabine monotherapy produces superior overall response rates compared with other treatment regimens containing alkylating agents or corticosteroids. Additionally, it has been demonstrated that fludarabine induces more remissions and more complete remissions than other conventional chemotherapies, such as CHOP (cyclophosphamide, doxorubicin, vincristine, prednisone), CAP (cyclophosphamide, doxorubicin, prednisone), or chlorambucil (Figure 32). Though fludarabine has proven to be a powerful therapeutic, chemotherapy for CLL is not limited to monotherapy with purine analogues. A number of monoclonal antibodies have been approved and can be used in combination with fludarabine. Some monoclonal antibodies include alemtuzumab, ofatumumab, and rituximab (Figure 33). The most thoroughly studied combination chemotherapy for CLL is fludarabine plus cyclophosphamide (FC). In preliminary, non-comparative trials, the overall response rates did not improve relative to using fludarabine alone. However, the addition of cyclophosphamide appeared to improve the quality of responses.²²⁸ Additional studies have also confirmed that fludarabine and cyclophosphamide (FC) have achieved complete remission in approximately 24% to 39% of patients. Yet when introducing the monoclonal antibody rituximab to fludarabine and cyclophosphamide (FCR), the complete remission rates rose to 70% in chemotherapy-naïve patients. Thus, incorporation of a monoclonal antibody in CLL chemotherapy yields vast improvements.²²⁹

Myelogenous leukemias are treated with a much smaller range of chemotherapeutic agents. Patients diagnosed with acute myelogenous leukemia (AML) are often subjected to a “3+7” induction chemotherapy regimen. This “3+7” therapy consists of treating the patient with an anthracycline (most commonly daunorubicin) for 3 days followed by a 7-day treatment with cytarabine. These “3+7” regimens have proven effective as complete remission is achieved in 60%

²²⁸ Hallek, M. *Hematology* **2005**, *1*, 285-291.

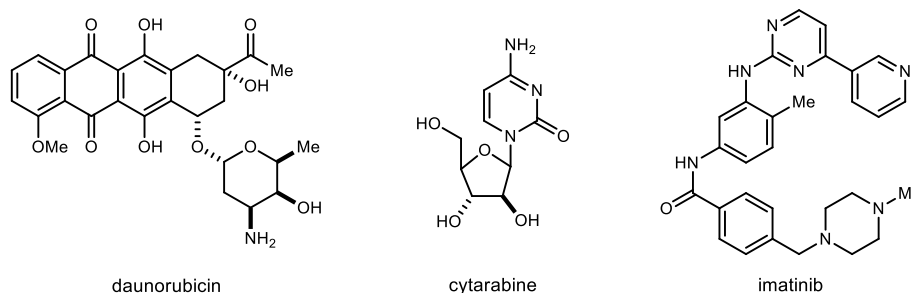
²²⁹ Tam, C. S.; O'Brien, S.; Wierda, W.; Kantarjian, H.; Wen, S.; Do, K.-A.; Thomas, D. A.; Cortes, J.; Lerner, S.; Keating, M. J. *Blood* **2008**, *112*, 975-980.

Figure 33. Monoclonal Antibodies Used in the Treatment of Chronic Lymphocytic Leukemia (CLL)



to 80% of younger adults.²³⁰ Patients diagnosed with chronic myelogenous leukemia (CML) are often treated with imatinib (also known as Gleevec) (Figure 34). Imatinib is effective as a single agent for the treatment of patients in all stages of CML, with the most encouraging results seen in patients in chronic phase disease. Hematologic and cytogenetic responses to imatinib for the treatment of chronic phase CML have permitted imatinib to be registered as the first-line treatment for newly diagnosed CML.²³¹

Figure 34. Agents Used in the Treatments of Acute and Chronic Myelogenous Leukemias (AML and CML)



Although it has been shown that a number of clinically effective drugs can treat leukemia, there are other agents that have shown promising antileukemic activity as well. Amongst these agents is sesbanine, a novel alkaloid compound that has been produced from the tissue of a leguminous plant known as *Sesbania drummondii* (commonly known as coffeebean, rattle bush, or rattle box).^{232,233} First isolated by Powell and colleagues in 1979, sesbanine and other members

²³⁰ Dohner, H.; Estey, E. H.; Amadori, S.; Appelbaum, F. R.; Buchner, T.; Burnett, A. K.; Dombret, H.; Fenaux, P.; Grimwade, D.; Larson, R. A.; Lo-Coco, F.; Naoe, T.; Niederwieser, D.; Ossenkoppele, G. J.; Sanz, M. A.; Sierra, J.; Tallman, M. S.; Lowenberg, B.; Bloomfield, C. D. *Blood* **2010**, *115*, 453-474.

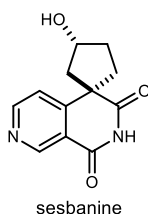
²³¹ Hochhaus, A.; Rosee, P. La. *Leukemia* **2004**, *18*, 1321-1331.

²³² Powell, R. G. Sesbanine and the Use in Treating Leukemic Tumors. U.S. Patent US4200639, April 29, 1980.

²³³ Brossi, A. *The Alkaloids: Chemistry and Pharmacology*, Vol. 25; Academic Press, Inc.: Orlando, 1985.

of *Sesbania drummondii* are significantly active against lymphocytic leukemia P-388 *in vivo*.^{234,235,236} Along with its potential as an antileukemic, sesbanine also possesses a unique structural composition. Structural elucidation shows that this molecule has a previously unreported and highly unusual spirocyclic structure based on the 2,7-naphthyridine framework (Figure 35).²³⁴ With the combination of its potent antileukemic activity and unconventional structure, sesbanine serves as an attractive target for organic synthesis.

Figure 35. Structure of Sesbanine



7.2. Previous Syntheses of Sesbanine

A number of stereospecific and stereoselective syntheses of sesbanine have previously been reported in literature. These approaches are highly efficacious as the desired alkaloid can be successfully furnished within five to eight synthetic steps. Furthermore, these syntheses feature a variety of key reactions that ultimately facilitate the access of sesbanine.

In 1980, Kende and Demuth reported a stereospecific synthesis of sesbanine (**531**) utilizing a key cycloannulation reaction.²³⁷ Beginning with 4-methylnicotinonitrile (**532**), a direct carbethoxylation reaction with diethyl carbonate and NaHMDS provided cyanoester **533** in 40% yield, setting the stage for the key cycloannulation step (Scheme 181). Treatment of **533** with 1,2-epoxy-4-bromobutane in the presence of absolute ethanol and K₂CO₃ afforded cyclopentanol product **534** as a single racemic diastereomer (40-45% yield). Further experimentation and characterization determined that **534** was indeed the undesired *cis*-stereoisomer. To account for the incorrect stereochemistry, the free alcohol of compound **534** was tosylated furnishing tosylate **535** in 67% yield. Nucleophilic displacement of the tosylate with tetraethylammonium acetate and subsequent mild hydrolysis gave cyclopentanol **536** in good yield (83% over 2 steps) and with the

²³⁴ Powell, R. G.; Smith, Jr., C. R.; Weisleder, D.; Muthard, D. A.; Clardy, J. *J. Am. Chem. Soc.* **1979**, *101*, 2784-2785.

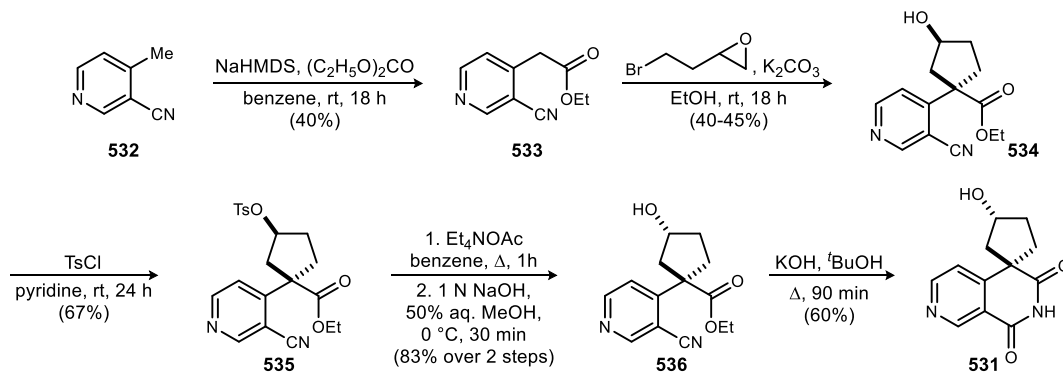
²³⁵ Powell, R. G.; Smith, Jr., C. R.; Madrigal, R. V. *Planta Med.* **1976**, *30*, 1-8.

²³⁶ Powell, R. G.; Smith, Jr., C. R.; Weisleder, D.; Matsumoto, G.; Clardy, J.; Kozlowski, J. *J. Am. Chem. Soc.* **1983**, *105*, 3739-3741.

²³⁷ Kende, A. S.; Demuth, T. P. *Tetrahedron Lett.* **1980**, *21*, 715-718.

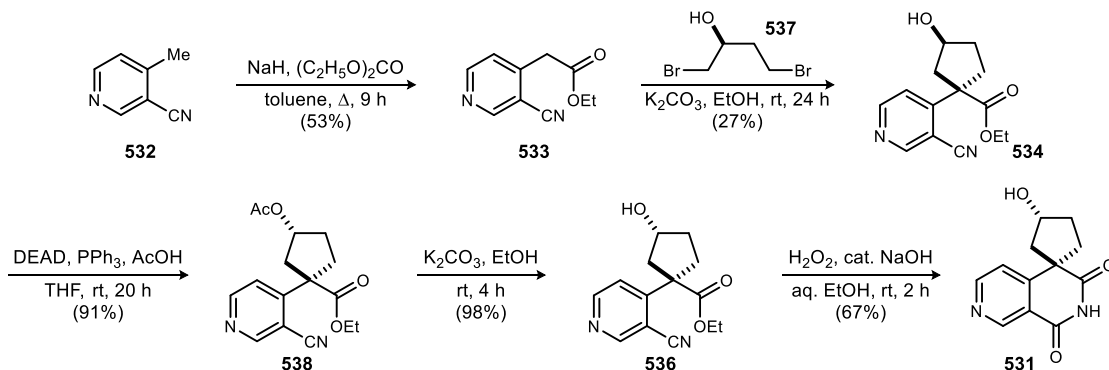
desired stereochemistry. The synthesis was completed when cyclopentanol **536** underwent a mild hydrolytic cyclization to arrive at sesbanine (**531**) in 60% yield.

Scheme 181. Kende and Demuth's Stereospecific Synthesis of Sesbanine



Shortly after the publication of Kende and Demuth's synthesis, Tomioka and Koga described their respective synthesis of sesbanine, which utilized a very similar approach.^{238,239} 4-methylnicotinonitrile was converted to cyanoester **533** via an alkoxyacylation reaction with diethyl carbonate and NaH (Scheme 182). When **533** underwent cycloannulation with racemic 1,4-dibromobutan-2-ol, cyclopentanol **534** was provided, but only as the *cis*-stereoisomer. Because of the selectivity for the *cis*-isomer, optically active 1,4-dibromobutan-2-ol (**537**) was later employed in the key cycloannulation step delivering cyclized product **534** in 27% yield. The stereoinversion of the hydroxyl group in compound **534** was achieved via a Mitsunobu reaction affording acetate **538** in high yield (91%). Cleavage of the acetate moiety under basic conditions furnished desired alcohol in 98% yield. Treatment of **536** with alkaline hydrogen peroxide in aqueous ethanol promoted a cyclic-imide formation to give sesbanine (**531**) in modest yield (67%).

Scheme 182. Tomioka and Koga's Synthesis of Sesbanine

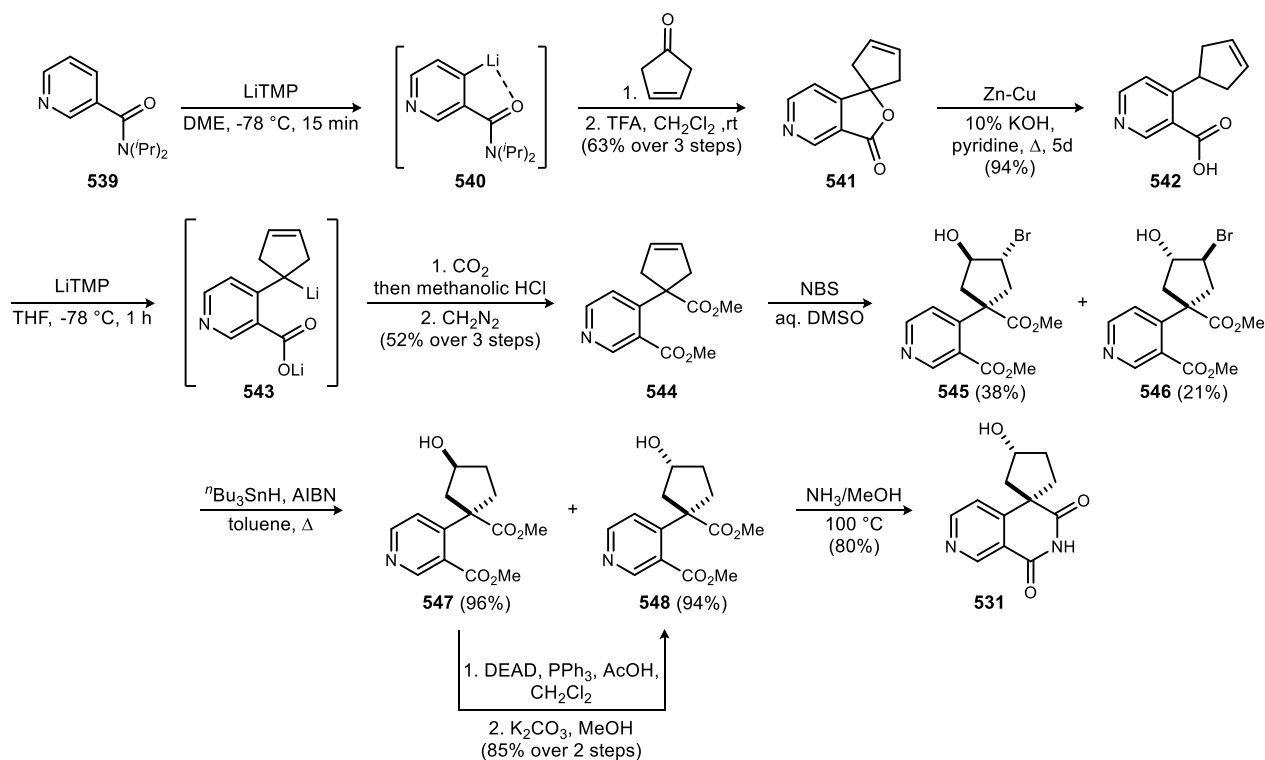


²³⁸ Tomioka, K.; Koga, K. *Tetrahedron Lett.* **1980**, *21*, 2321-2324.

²³⁹ Tomioka, K.; Koga, K. *Tetrahedron* **1988**, *44*, 4351-4355.

In 1983, Iwao and Kuraishi reported the synthesis of sesbanine via the directed metalation of tertiary nicotinamides.²⁴⁰ This synthetic route was initiated when readily available *N,N*-diisopropylnicotinamide (**539**) was selectively lithiated at the 4-position with LiTMP to provide lithiated species **540** (not isolated) (Scheme 183). Condensation of **540** with 3-cyclopentenone and subsequent treatment with TFA afforded spirolactone **541** (63% yield over 3 steps). Lactone **541** was reductively cleaved with zinc-copper couple to give acid **542** in 94% yield. This acid was once again lithiated with LiTMP, generating dianion **543**. This dianionic species was then carboxylated

Scheme 183. Iwao and Kuraishi's Synthesis of Sesbanine



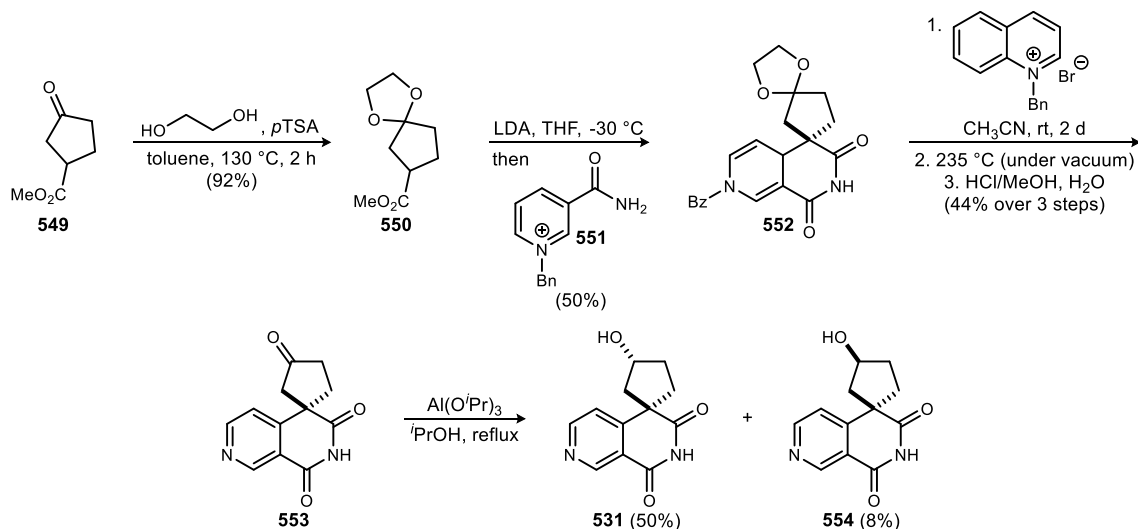
with dry ice, neutralized with methanolic HCl, and subsequently treated with freshly prepared diazomethane to furnish diester **544** in 52% yield over the course of 3 steps. Treatment of **544** with NBS in aqueous DMSO gave bromohydrins **545** and **546** in 38% and 21% yields, respectively. Both bromohydrins were converted to their corresponding alcohols (**547** and **548**) via a reductive dehalogenation with ⁿBu₃SnH and AIBN. The undesired alcohol (**547**) was epimerized to desired alcohol **548** via a Mitsunobu reaction and subsequent hydrolysis of the acetate functionality (85%

²⁴⁰ Iwao, M.; Kuraishi, T. *Tetrahedron Lett.* **1983**, *24*, 2649-2652.

yield over 2 steps). Alcohol **548** was successfully converted to sesbanine in 80% yield upon heating in methanolic NH₃.

Pandit, Wanner, and Koomen demonstrate that the condensation of a carboxylate ester with *N*-benzylnicotinamide can serve as a viable approach in order to arrive at sesbanine.^{241,242} Known methyl 3-oxocyclopentanecarboxylate (**549**) was converted to acetal **550** in 92% yield upon treatment with ethylene glycol under acidic conditions (Scheme 184). **550** was then deprotonated with LDA, and the corresponding anion was allowed to react with *N*-benzylnicotinamide **551** in order to provide tricyclic system **552** after workup. The dihydropyridine ring of **552** was oxidized with *N*-benzylquinolinium bromide in acetonitrile, and the resulting pyridinium salt was debenzylated by heating under vacuum. Subsequent deprotection of the acetal moiety furnished sesbanine precursor **553** in modest yield (44% over 3 steps). Ketone **553** was then subjected to a Meerwein-Ponndorf-Verley reduction with Al(*i*-PrO)₃ affording a mixture of sesbanine (**531**) and epi-sesbanine (**554**) in a 6:1 ratio (58% yield).

Scheme 184. Pandit, Wanner, and Koomen's Synthesis of Sesbanine



Wada, Nishihara, and Akiba later describe a synthesis of sesbanine that utilizes a regioselective γ -addition of a silyl enol ether into a quaternized methyl nicotinate.²⁴³ Treatment of commercially available methyl nicotinate with methyl chloroformate generates a pyridinium salt, which is then condensed *in situ* with the ketene silyl acetal of methyl 3-cyclopentenecarboxylate

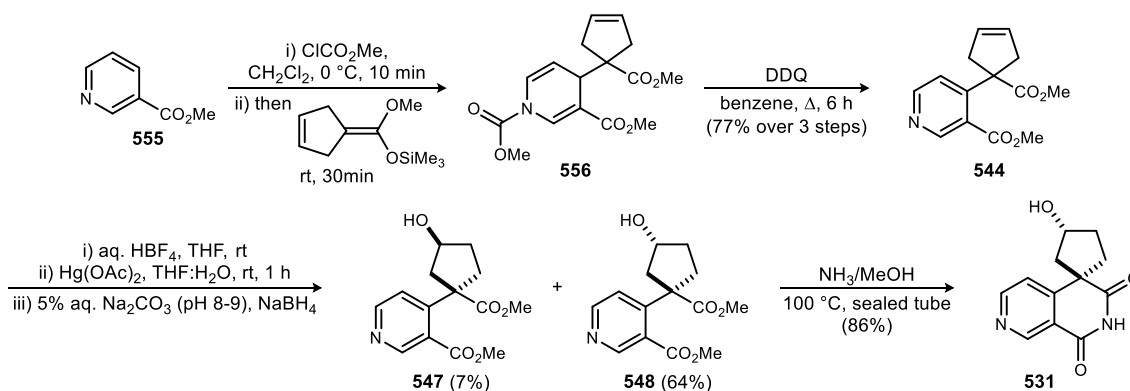
²⁴¹ Wanner, M. J.; Koomen, G.-J.; Pandit, U. K. *Heterocycles* **1981**, *15*, 377-379.

²⁴² Wanner, M. J.; Koomen, G.-J.; Pandit, U. K. *Tetrahedron* **1988**, *38*, 2741-2748.

²⁴³ Wada, M.; Nishihara, Y.; Akiba, K.-Y. *Tetrahedron Lett.* **1985**, *26*, 3267-3270.

to provide compound **556** (Scheme 185). Subsequent oxidation of 1,4-dihydropyridine **556** with DDQ furnished diester **544** in good yield (77% over 3 steps). Subjection of diester **544** to an oxymercuration protocol delivered alcohols **547** and **548** upon careful reduction with NaBH₄. Fortunately, the desired alcohol (**548**) was obtained stereoselectively in 64% yield along with undesired epimeric alcohol **547** (7% yield). Imide formation en route to sesbanine was successfully achieved in 86% yield when **548** was heated in methanolic HCl at 100 °C in a sealed tube.

Scheme 185. Wada, Nishihara, and Akiba's Synthesis of Sesbanine

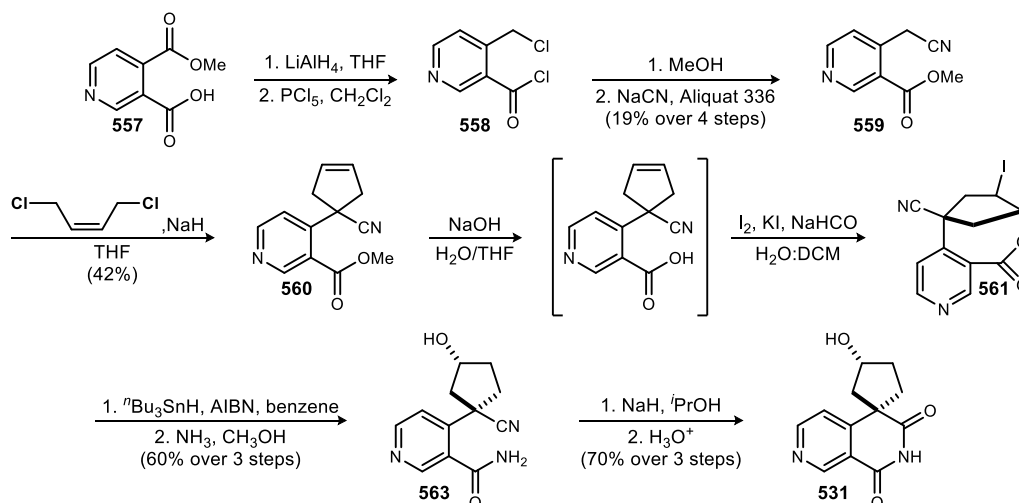


Bottaro and Berchtold employ a key halolactonization reaction in their respective synthesis of racemic sesbanine.²⁴⁴ Beginning with known 4-(methoxycarbonyl)nicotinic acid, reduction with LiAlH₄ and subsequent treatment with PCl₅ led to chloromethyl acyl chloride **558** (Scheme 186). Methanolysis of the acyl chloride and nucleophilic displacement of the alkyl chloride with NaCN delivered cyanoester **559** in 19% yield over the course of 4 steps. Cyanoester **559** then underwent an inter/intramolecular bis-substitution reaction at the benzylic position with (*Z*)-1,4-dichlorobut-2-ene providing intermediate **560** in modest yield (42% yield). With intermediate **560** in hand, the stage was now set for the stereospecific iodolactonization step. Ester **560** was saponified with base generating the precursor acid (not isolated). The resulting saponification mixture was immediately treated with I₂, KI, and NaHCO₃ in order to promote the halolactonization *in situ*. Upon isolation of the desired iodolactone (**561**), this compound underwent reductive dehalogenation with ⁿBu₃SnH and AIBN, furnishing lactone **562** (not shown) in satisfactory yield (60% yield over 3 steps). Aminolysis of lactone **562**, intramolecular addition of the amide anion to the nitrile group,

²⁴⁴ Bottaro, J. C.; Berchtold, G. A. *J. Org. Chem.* **1980**, *45*, 1176.

and hydrolysis to the imide via aqueous workup afforded racemic sesbanine in good yield (70% yield over 3 steps).

Scheme 186. Bottaro and Berchtold's Synthesis of Sesbanine



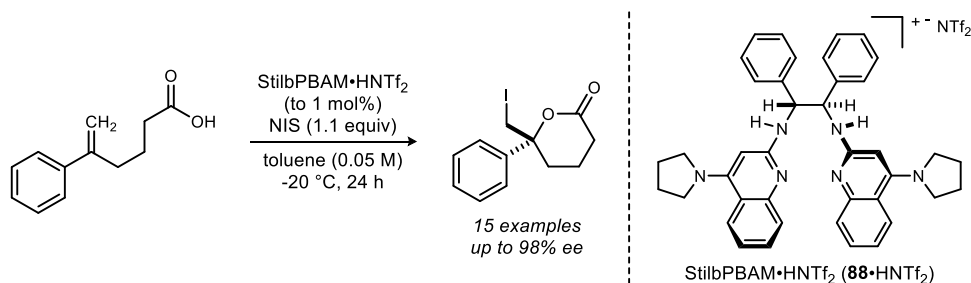
7.3. Initial Efforts Towards the Enantioselective Synthesis of Sesbanine

The use of a halolactonization reaction in Bottaro and Berchtold's synthesis of sesbanine garnered interest as similar chemistry has been pursued within our laboratory. Recently, Dobish and Johnston employed a chiral proton catalyst-*N*-iodosuccinimide (NIS) reagent system to facilitate highly enantioselective iodolactonizations of alkenes.²⁴⁵ Herein, the triflimide salt of a chiral stilbene diamine-derived bis(amidine) organocatalyst (StilbPBAM•HNTf₂, **88**•HNTf₂) promotes the transformation of a broad range of unsaturated carboxylic acids to their corresponding γ -lactones in high yields and with excellent levels of enantioselection (Scheme 187). Based on this success and on Bottaro and Berchtold's synthesis, we saw this as an opportunity to achieve two primary objectives: 1) to extend this methodology to carboxylic acids bearing internal *Z*-alkenes and 2) to apply this system towards an enantioselective synthesis of sesbanine.

Retrosynthetically, the endgame strategy for our respective synthesis will be identical to that of Bottaro and Berchtold's. Sesbanine (**531**) can arise from intermediate **563** through a base-promoted addition of the amide functionality to the nitrile motif followed by acid-mediated hydrolysis (Scheme 188). Amide **563** can be provided via reductive dehalogenation and subsequent aminolysis of iodolactone **561**. We can then arrive at this iodolactone upon subsection

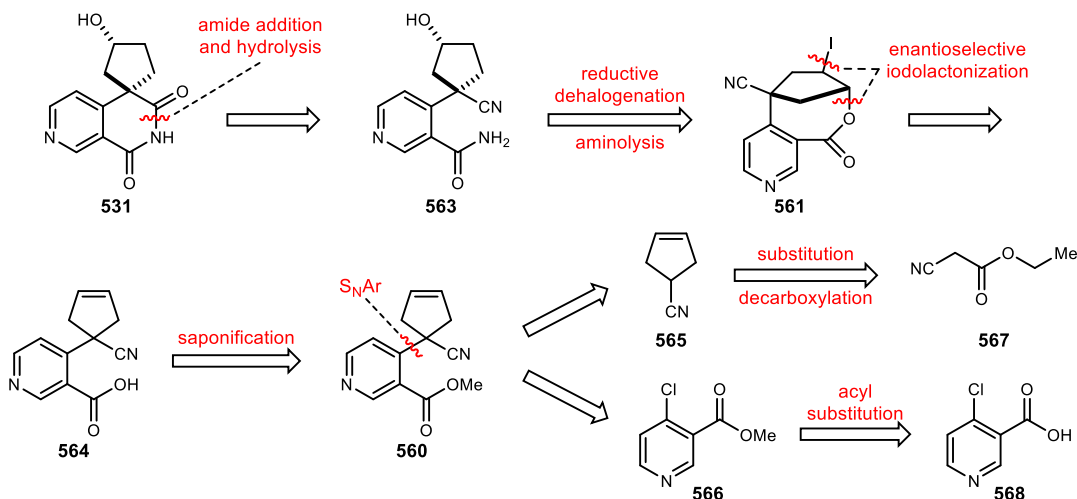
²⁴⁵ Dobish, M. C.; Johnston, J. N. *J. Am. Chem. Soc.* **2012**, *134*, 6068-6071.

Scheme 187. Dobish and Johnston's BAM-Catalyzed Enantioselective Iodolactonization



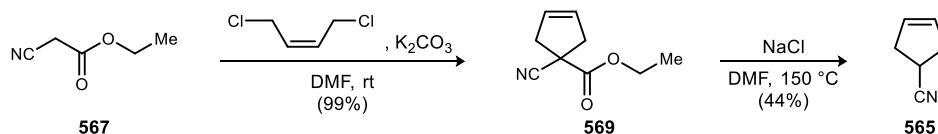
of precursor acid **564** to an enantioselective, BAM-catalyzed halolactonization. Nucleophilic aromatic substitution between cyclopentene carbonitrile **565** and methyl nicotinate **566** will deliver ester **560**, which in turn can be saponified to give acid **564**. Carbonitrile **565** will be afforded from ethyl cyanoacetate (**567**) via substitution and decarboxylation, and nicotinate **566** can be synthesized upon acylation with the acid chloride of nicotinic acid **568**.

Scheme 188. Retrosynthetic Analysis of Sesbanine



In the forward sense, treatment of commercially available ethyl cyanoacetate **567** with (*Z*)-1,4-dichlorobut-2-ene under basic conditions promoted the desired inter/intramolecular bis-substitution reaction as cyclopentene compound **569** was furnished in 99% yield after chromatographic purification (Scheme 189). Subsequent decarboxylation of **569** with sodium

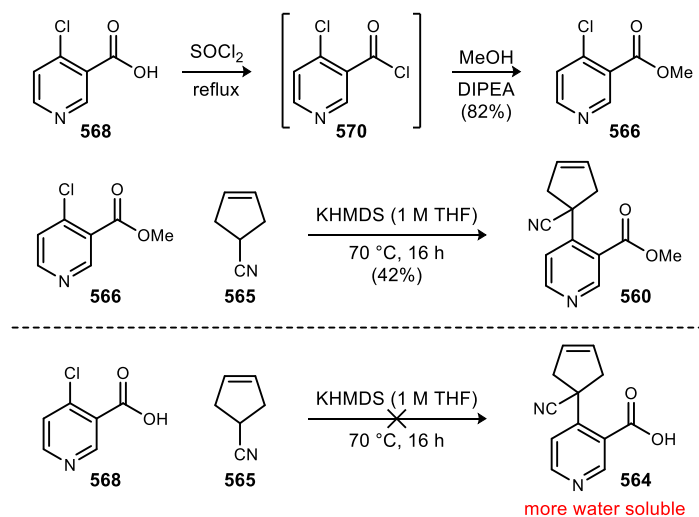
Scheme 189. Synthesis of Cyclopentene Carbonitrile **565**



chloride (NaCl) in DMF at high temperature delivered the cyclopentene carbonitrile nucleophile (**565**) in modest yield upon vacuum distillation (44%).

Synthesis of the electrophilic species for the proposed S_NAr reaction proceeded in a straightforward manner. Treatment of 4-chloronicotinic acid **568** with $SOCl_2$ provided acid chloride **570** quantitatively (Scheme 190). Immediate exposure of **570** to methanol in the presence of base facilitated esterification to give methyl nicotinate **566** in 82% yield.²⁴⁶ With carbonitrile **565** and nicotinate **566** in hand, the stage was now set for nucleophilic aromatic substitution. After several attempts, it was found that subjection of carbonitrile **565** to a solution of KHMDS in THF promoted nucleophilic attack as S_NAr product **560** was cleanly furnished upon incorporation of the nicotinate electrophile. It is worth noting that nicotinate **566** was chosen as the electrophile since S_NAr attempts with nicotinic acid **568** proved fruitless. The inability to isolate carboxylic acid **564** (if formed *in situ*) may be owed to the fact that it is too water soluble to withstand an aqueous work-up. Therefore, it was deemed necessary to use nicotinate **566** since the corresponding substitution product (**560**) will have a lower affinity for the aqueous layer relative to **564**.

Scheme 190. Acquisition of Nicotinate **566** and S_NAr en Route to Ester **560**

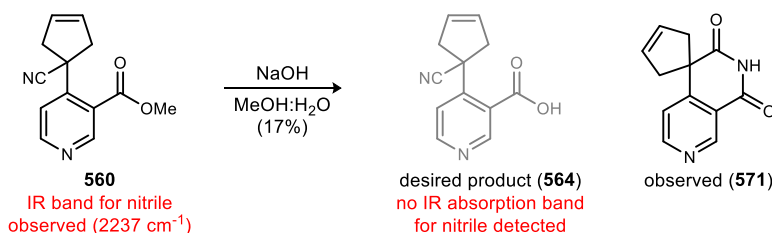


After successfully acquiring ester **560**, the next goal was to isolate acid **564** as its own entity. Ester **560** was subjected to a saponification protocol using sodium hydroxide (NaOH), methanol, and water. Aqueous acidic work-up delivered a compound in which the 1H NMR data

²⁴⁶ Goodacre, S. C.; Williams, K.; Price, S.; Dyke, H. J.; Montana, J. G.; Stanley, M. S.; Bao, L.; Lee, W. Preparation of Aminoazaindolecarboxamides as MEK Kinase Inhibitors. U.S. Patent WO 2008/067481 A1, June 5, 2008.

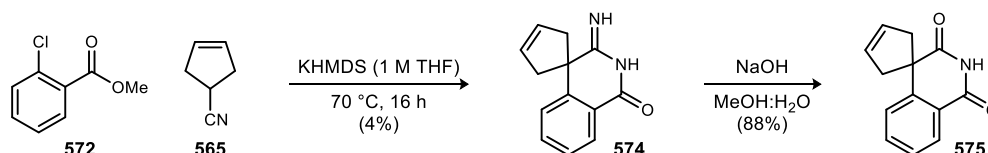
was consistent with that of desired acid **564**. However, when analyzing the IR spectrum for this compound, no absorption band corresponding to a nitrile motif could be found. Further data evaluation determined that the isolated intermediate was that of spirocyclic imide **571** (Scheme 191). Since this imide was obtained in only 17% yield, it is plausible that the desired acid (**564**) was formed *in situ* but resisted isolation since the pyridine and carboxylic acid moieties increase water solubility.

Scheme 191. Isolation and Confirmation of Imide **571**



To account for the potential water solubility of the pyridine ring, carbonitrile **565** and methyl-2-chlorobenzoate (**572**) were subjected to the S_NAr protocol with ambitions of accessing compound **573** (not shown), the phenyl analog of ester **560**. Interestingly, when the cyclopentene carbonitrile was treated with KHMDS (1 M in THF) and benzoate **572**, iminopiperidinone **574** was the only compound that could be cleanly isolated (Scheme 192). Acquisition of this intermediate not only indicated that S_NAr was successful, it also showed that amidation and addition to the nitrile functionality occurred as well. To further confirm that this structure was indeed an imidopiperidinone, **574** was treated with NaOH in the presence of aqueous methanol to provide imide **575** in good yield upon hydrolysis of the imine.

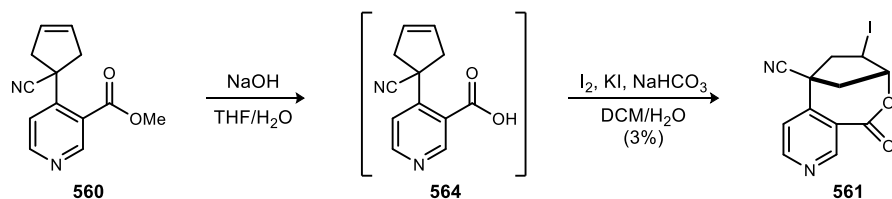
Scheme 192. Acquisition and Confirmation of Imidopiperidinone **574**



Since the isolation of acid **564** and ester **573** proved troublesome, the next avenue that was explored was a one-pot saponification-iodolactonization reaction. Bottaro and Berchtold utilized this approach by treating ester **560** with NaOH in aqueous methanol providing acid **564** *in situ*. Immediate incorporation of iodine, iodide, NaHCO_3 , and DCM in water promoted the biphasic halolactonization reaction, and the desired iodolactone was successfully isolated. When this one-pot reaction was repeated within our laboratory, the desired lactone (**561**) was acquired but in very

low yield (3%) (Scheme 193). Nevertheless, this was an opportunity to see if our Brønsted basic BAM catalysts could promote reactivity and induce enantioselection in this one-pot saponification-lactonization system.

Scheme 193. Repetition of Bottaro and Berchtold's One-Pot Saponification-Iodolactonization



Initial investigations of this enantioselective saponification-iodolactonization reaction consisted of using the same saponification conditions as described by Bottaro and Berchtold. For the halolactonization stage, the same reagents were used with the exception of replacing NaHCO_3 , an achiral base, with PBAM, a Brønsted basic chiral organocatalyst. When substoichiometric amounts of PBAM (**19**) were employed in this reaction system, no desired lactone could be detected as small quantities of the starting ester were recovered (Table 28, entry 1). The reaction conditions were further modified when NIS replaced the I_2 -KI combination as the iodine source. Unfortunately, this variation also proved fruitless (Table 28, entry 2). Substituting the $\text{DCM-H}_2\text{O}$ solvent combination with toluene showed no improvement as no product was seen even at elevated temperatures (Table 28, entries 3 and 4). Additionally, stilbene diamine-derived organocatalyst StilbPBAM (**88**) was subjected in lieu of PBAM, but to no avail (Table 28, entry 5).

Table 28. Initial Investigations of the Enantioselective Saponification-Iodolactonization Reaction

entry	iodine source	additive	catalyst	solvent	T (°C)	result
1	I_2	KI	PBAM	$\text{DCM:H}_2\text{O}$	25	no lactone, SM recovered
2	NIS	--	PBAM	$\text{DCM:H}_2\text{O}$	25	no lactone
3	NIS	--	PBAM	toluene	25	no lactone
4	NIS	--	PBAM	toluene	80	no lactone
5	NIS	--	StilbPBAM	toluene	25	no lactone

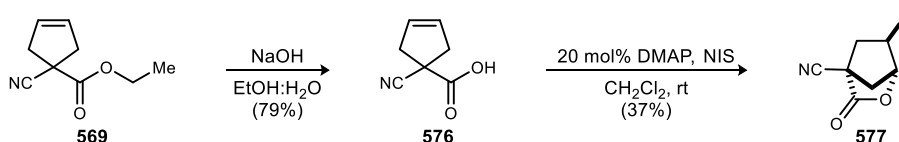
PBAM (**19**)

StilbPBAM (**88**)

7.4. Enantioselective Halolactonizations with *Z*-Alkenes: Model Studies

Due to the lack of success within these initial saponification-halolactonization attempts, it was determined that the next approach to be taken would be the investigation of a model system. Model studies of a smaller, more accessible substrate would provide insight into the feasibility of achieving halolactonizations with unsaturated carboxylic acids bearing *Z*-alkenes. Thus, cyclopentenyl cyanocarboxylic acid **576** was seen as an attractive model substrate due to its ease of availability from previously synthesized material. Saponification of ethyl ester **569** with NaOH in aqueous ethanol furnished cyanoacid **576** in good yield (Scheme 194). To our delight, subsequent treatment of acid **576** with NIS and catalytic quantities of DMAP in the presence of DCM delivered the desired iodolactone (**577**) albeit in modest yield (37%). Acquisition of lactone **577** now set the stage for enantioselective investigations.

Scheme 194. Racemic Synthesis of Iodolactone **577**

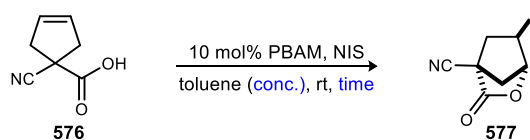


Based on the high degree of success in their respective halolactonization system, reaction conditions described by Dobish and Johnston were used as a template for initial enantioselective studies.²⁴⁵ Herein, PBAM was employed as the chiral organocatalyst, NIS as the iodine source, and toluene (0.05 M) as the solvent. The first variable that was examined was reaction time. When cyanoacid **576** was subjected to the lactonization protocol, iodolactone **577** was afforded in low yield and with minimal levels of enantioselection (12% yield, 5% ee) (Table 29, entry 1). Prolonged reaction times of 12 hours, 24 hours, and 48 hours did not result in any significant change as **577** was acquired in comparable yields and ee's (Table 29, entries 2-4). Yet when this lactonization was run over the course of 72 hours, lactone **577** was furnished in 4% yield and 17% ee (Table 29, entry 5). Despite this minor improvement in enantioselection, subsequent studies utilized a 24 hour reaction time for the sake of acquiring data in a more timely manner.

The next variable that was probed was solvent concentration. Increasing the concentration from 0.05 M to 0.1 M resulted in higher yield, but minimal loss in enantioselection as iodolactone **577** was furnished in 11% yield and 5% ee (Table 29, entry 6). Further concentrated systems (0.5 M and 1.0 M) confirmed the trends of improved yield and diminished ee (Table 29, entries 7 and

8). Due to the gradual decrease in enantioselection upon increased solvent concentration, 0.05 M remained as the optimal concentration up to this point.

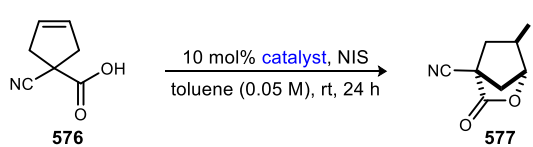
Table 29. Preliminary Time and Concentration Studies



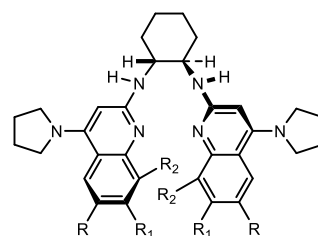
entry	time (h)	conc. (M)	yield (%)	ee (%)
1	6	0.05	12	5
2	12	0.05	8	5
3	24	0.05	6	6
4	48	0.05	8	3
5	72	0.05	4	17
6	24	0.1	11	5
7	24	0.5	13	2
8	24	1.0	12	1

Introduction of counterions ensued as Brønsted acid salts of BAM ligands led to higher selectivity in previous work.²⁴⁵ When the triflic acid salt of PBAM (**19**•HOTf) was used as the catalyst for this system, little change was seen relative to the free base as lactone **577** was afforded in 9% yield and 3% ee (Table 30, entry 2). The triflimide salt of PBAM (**19**•HNTf₂) performed similarly (Table 30, entry 3). Since acid salts proved ineffective in promoting reactivity and/or selectivity, efforts then shifted towards the use of more Brønsted basic organocatalysts.

Table 30. Effects of Acid Salts and More Brønsted Basic Organocatalysts



entry	catalyst	yield (%)	ee (%)
1	PBAM	6	6
2	PBAM•HOTf	9	3
3	PBAM•HNTf ₂	4	6
4	⁸ (MeO)PBAM	11	1
5	⁶ (MeO)PBAM	8	7
6	^{6,7} (MeO) ₂ PBAM	0	N/A
7	--	7	0



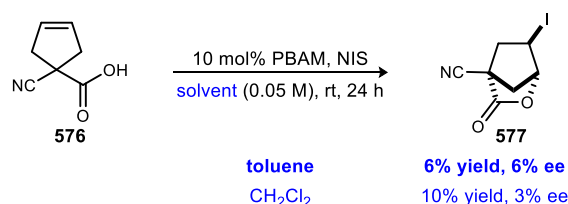
R, R₁ = H, R₂ = OMe, ⁸(MeO)PBAM (**19d**)
 R = OMe, R₁, R₂ = H, ⁶(MeO)PBAM (**19e**)
 R, R₁ = OMe, R₂ = H, ^{6,7}(MeO)₂PBAM (**19c**)

⁸(MeO)PBAM (**19d**) was employed delivering iodolactonization product **577** in increased yield and diminished ee (11% yield, 1% ee) (Table 30, entry 4). ⁶(MeO)PBAM (**19e**) furnished **577** in

8% yield and 7% ee and ^{6,7}(MeO)₂PBAM (**19c**) failed to provide product (Table 30, entries 5 and 6). Furthermore, when this lactonization was run in the absence of catalyst, iodolactone **577** was isolated in 7% yield as a racemate (Table 30, entry 7). This indicates that the use of organocatalysts, thus far, have had little or no effect on reactivity and/or selectivity as previously acquired yields are comparable to that of the background reaction.

When the racemic version of this iodolactonization was run, CH₂Cl₂ was employed as the solvent resulting in the acquisition of lactone **577** in 37% yield (Scheme 194). Since a reasonable yield was observed with CH₂Cl₂, this solvent was used in the enantioselective variant with ambitions of increasing product formation. Unfortunately, CH₂Cl₂ performed poorly in the presence of PBAM as lactone **577** was furnished in only 10% yield and 3% ee (Scheme 195). Toluene, therefore, remained as the solvent of choice.

Scheme 195. Iodolactonization Attempt with CH₂Cl₂ as the Solvent



It should be noted that a 5 mol% loading of PBAM performed similarly relative to when a 10 mol% loading was employed (Table 31, entry 1). Because of these comparable results and for the sake of catalyst economy, 5 mol% catalyst loadings were to be used for subsequent studies.

Table 31. Application of Different Catalyst Backbones and Reevaluation of Temperature and Iodine Sources

entry	catalyst	T (°C)	iodine source	yield (%)	ee (%)
1	PBAM	25	NIS	8	8
2	StilbPBAM	25	NIS	23	19
3	^{3,5} (CF ₃) ₂ BenzAM	25	NIS	8	6
4	PivalAM	25	NIS	1	0
5	StilbPBAM	0	NIS	21	22
6	StilbPBAM	-20	NIS	15	30
7	StilbPBAM	-50	NIS	0	N/A
8	StilbPBAM	-20	DIDMH	19	28

^{3,5}(CF₃)₂BenzAM (78a)

PivalAM (78m)

Amidine catalysts possessing different backbones were submitted to the halolactonization protocol with the hope of introducing different bite angles that can ultimately promote enantioselection. When StilbPBAM (**88**) was used as the catalyst, noticeable improvements in yield and selectivity were seen as iodolactone **577** was furnished in 23% yield and 19% ee (Table 31, entry 2). Amidine-amide catalysts in ^{3,5}(CF₃)₂BenzAM (**78a**) and PivalAM (**78m**) performed poorly, however, as loss in yield and/or enantioselection were observed for both of these cases (Table 31, entries 3-4). Encouraged by these results seen with StilbPBAM, lower temperatures were reevaluated in order to see if selectivity could be further improved. When the reaction was chilled to 0 °C and -20 °C respectively, we were delighted to see consistent improvement in ee albeit the gradual depression in yield (Table 31, entries 5 and 6). Unfortunately, running the reaction at -50 °C completely mitigated product formation as no sign of lactone **577** could be detected (Table 31, entry 7). Nevertheless, these improved degrees of enantioselection clearly indicate that the StilbPBAM catalyst is influential in this iodolactonization reaction. Additionally, DIDMH was also reapplied as the iodo source, but still proved inferior relative to NIS (Table 31, entry 8).

Table 32. Reexamination of Acid Salts and Brønsted Basic Catalysts

576 $\xrightarrow[5 \text{ mol\% catalyst, NIS, solvent (0.05 M), -20 }^\circ\text{C, 24 h}]{}$ 577

R = OMe, R₁ = H, ⁶(MeO)StilbPBAM (**88a**)
R = H, R₁ = OMe, ⁷(MeO)StilbPBAM (**88b**)

entry	catalyst	solvent	yield (%)	ee (%)
1	StilbPBAM	toluene	15	30
2	StilbPBAM•HOTf	toluene	7	19
3	StilbPBAM•HNTf ₂	toluene	9	28
4	⁶(MeO)StilbPBAM	toluene	24	32
5	⁷ (MeO)StilbPBAM	toluene	11	26
6	⁶ (MeO)StilbPBAM	xylenes	0	N/A
7	⁶ (MeO)StilbPBAM	THF	0	N/A
8	⁶ (MeO)StilbPBAM	CH ₃ CN	4	3

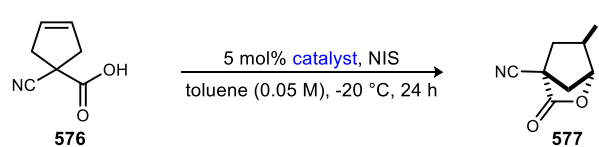
Acid salts were employed once more with the ambition of further enhancing selectivity. Unfortunately, both the triflic acid and triflimide salts of StilbPBAM (**88**•HOTf and **88**•HNTf₂) gave lower yield and diminished enantioselection reaffirming the superiority of the free base catalyst (Table 32, entries 2 and 3). These results led to the examination of more Brønsted basic stilbene diamine-derived ligands. When ⁶(MeO)StilbPBAM (**88a**) was employed as the organocatalyst, mild improvement was observed as lactone **577** was furnished in 24% yield and

32% ee (Table 32, entry 4). ⁷(MeO)StilbPBAM (**88b**) did not fare as well as **577** was acquired in only 11% yield and 26% ee (Table 32, entry 5).

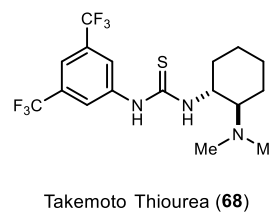
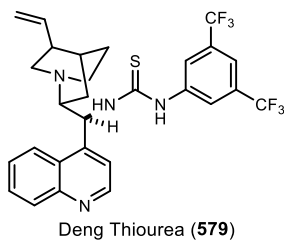
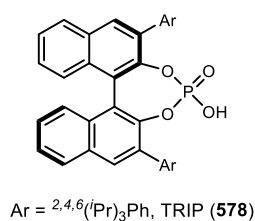
With ⁶(MeO)StilbPBAM (**88b**) chosen as the new optimal catalyst, the effects of different solvents were examined more extensively. Interestingly, xylenes, a solvent similar to that of toluene, failed to yield any product when subjected to the halolactonization protocol (Table 32, entry 6). The same was observed with an ethereal solvent in THF (Table 32, entry 7). CH₃CN was also used, but proved inferior relative to toluene as lactone **577** was afforded in only 4% yield and 3% ee (Table 32, entry 8). Once again, toluene remained the solvent of choice.

Non-BAM catalysts were submitted next in order to see their respective influence on product yield and enantioselection. 2,4,6-Triisopropyl-phenyl-based binaphthol phosphoric acid (TRIP) catalyst **578**²⁴⁷ was ineffective as no product was furnished upon its use (Table 33, entry 2). Deng's²⁴⁸ and Takemoto's²⁴⁹ thiourea organocatalysts (**579** and **68**) were also employed, but to no avail as lactone **577** was isolated in minimal yield and as a racemate in both cases (Table 33, entries 3 and 4).

Table 33. Studies with Non-BAM Catalysts



entry	catalyst	yield (%)	ee (%)
1	⁶ (MeO)StilbPBAM	24	32
2	TRIP	0	N/A
3	Deng Thiourea	1	0
4	Takemoto Thiourea	1	0



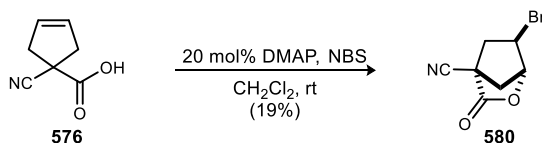
²⁴⁷ Čorić, I.; Vellalath, S.; List, B. *J. Am. Chem. Soc.* **2010**, *132*, 8536-8537.

²⁴⁸ Song, J.; Wang, Y.; Deng, L. *J. Am. Chem. Soc.* **2006**, *128*, 6048-6049.

²⁴⁹ Okino, T.; Nakamura, S.; Furukawa, T.; Takemoto, Y. *Org. Lett.* **2004**, *6*, 625-627.

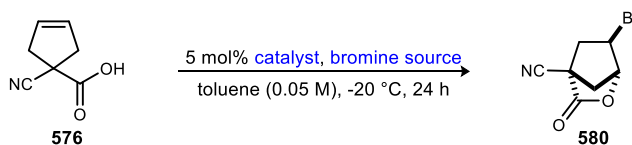
At this point, every variable within this reaction system has been examined to an extent with the optimal result being a 24% isolated yield of lactone **577** with 32% ee. Since modification of these variables did not provide good yields and promising levels of enantioselection, efforts then shifted towards the use of other electrophilic halogen sources (i.e. bromine and chlorine). With aspirations of achieving bromolactonization, cyanoacid **576** was treated with *N*-bromosuccinimide (NBS) and DMAP in the presence of CH₂Cl₂. Gratifyingly, the desired bromolactone **580** was successfully acquired albeit in 19% yield (Scheme 196).

Scheme 196. Racemic Synthesis of Bromolactone **580**



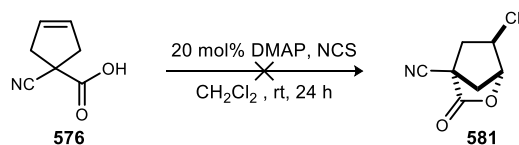
Investigation of the enantioselective variant of this bromolactonization commenced when acid **576** was treated with PBAM (5 mol%) and NBS in the presence of toluene at -20 °C. After a 24 hour reaction period, no sign of bromolactone **580** could be detected (Table 34, entry 1). The same result was seen when StilbPBAM was employed as the catalyst (Table 34, entry 2). The use of a different bromine source in *N*-bromophthalimide (NBP) also proved fruitless as this too failed to provide product (Table 34, entry 3).

Table 34. Brief Investigation of an Enantioselective Bromolactonization

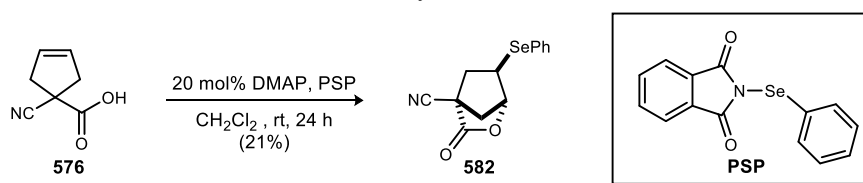


entry	catalyst	bromine source	yield (%)	ee (%)
1	PBAM	NBS	0	N/A
2	StilbPBAM	NBS	0	N/A
3	StilbPBAM	NBP	0	N/A

Due to the limitations of this bromolactonization reaction, efforts shifted towards the development of a chlorolactonization system. This approach was even more problematic as treatment of cyanoacid **576** with *N*-chlorosuccinimide (NCS) and DMAP in the presence of CH₂Cl₂ failed to deliver racemic chlorolactone **581** (Scheme 197). Since chlorolactone **581** could not be isolated as a racemate, no analytical assay could be developed ultimately preventing enantioselective studies.

Scheme 197. Failed Attempt Towards Chlorolactonization

Selenolactonization with acid **576** was the next avenue that was explored. Subjection of acid **576** to *N*-(phenylseleno)phthalimide (PSP) and DMAP in the presence of CH₂Cl₂ provided selenolactone **582** in 21% yield as a racemate (Scheme 198). Acquisition of this selenolactone set the stage for the enantioselective variation of this reaction system.

Scheme 198. Racemic Synthesis of Selenolactone **582**

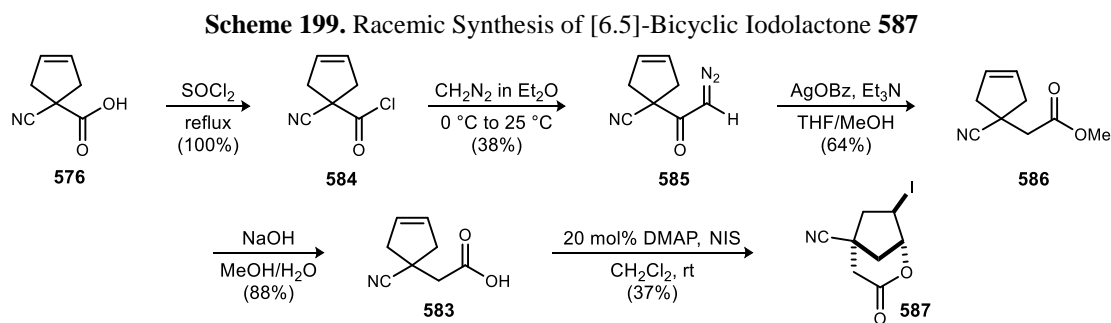
Enantioselective investigations began when cyanoacid **576** was treated with PBAM (5 mol%) and PSP in the presence of toluene at room temperature. After 24 hours, no promising levels of enantioselection were observed as selenolactone **582** was furnished in 26% yield and 2% ee (Table 35, entry 1). Replacing PBAM with StilbPBAM did not show any improvement as a racemic mixture of **582** was delivered in 23% yield (Table 35, entry 2). Both PBAM and StilbPBAM were reemployed in the selenolactonization protocol at -20 °C. Chilled temperatures did not show improvement as selenolactone **582** was isolated but as a racemate in 18% and 21% yields, respectively (Table 35, entries 3 and 4). Furthermore, the triflic acid and triflimide salts of StilbPBAM also proved ineffective as no improvement in yield and/or ee were observed (Table 35, entries 5 and 6).

Table 35. Brief Investigation of an Enantioselective Selenolactonization

Reaction of 576 with 5 mol% catalyst, PSP in toluene (0.05 M) at temperature T for 24 h.

entry	catalyst	T (°C)	yield (%)	ee (%)
1	PBAM	25	26	2
2	StilbPBAM	25	23	0
3	PBAM	-20	18	0
4	StilbPBAM	-20	21	0
5	StilbPBAM•HOTf	-20	13	2
6	StilbPBAM•HNTf ₂	-20	23	0

The focus then centered upon the development of a 6-membered model system as multiple variations of the 5-membered system showed little or no promise. The substrate of choice for these 6-membered model studies was that of cyanoacid **583**, the homologated analog of cyanoacid **576**. Thus, compound **583** could be readily accessed upon subjecting acid **576** to an Arndt-Eistert homologation process.²⁵⁰ Treatment of **576** with SOCl_2 provided acid chloride **584** (Scheme 199). Subsequent exposure of this acyl chloride to diazomethane in diethyl ether furnished diazoketone **585** in modest yield (38% over 2 steps). **585** then underwent homologation when treated with silver benzoate (AgOBz) under basic conditions ultimately delivering methyl ester **586** in 64% yield. Saponification of ester **586** with hydroxide in aqueous methanol afforded the desired precursor acid **583** (88% yield). Acid **583** was successfully converted to [6.5]-bicyclic iodolactone **587** in moderate yield when treated with NIS and DMAP in the presence of CH_2Cl_2 (37%).



Investigation of the enantioselective version of this 6-membered iodolactonization began when acid **583** was treated with PBAM (5 mol%) and NIS in toluene at room temperature. Lactone **587** was acquired in 12% yield and 4% ee after a 24 hour reaction time (Table 36, entry 1). StilbPBAM showed no improvement as lactone **587** was obtained in 14% yield as a racemate (Table 36, entry 2). Triflic acid and triflimide salts of StilbPBAM also proved fruitless as yields and enantioselection remained relatively unchanged (Table 36, entries 3 and 4).

Various solvents were examined next in order to see their respective influence on this lactonization protocol. CH_2Cl_2 resulted in an improvement in yield as lactone **587** was furnished in 25% yield (Table 36, entry 5). However, the enantiopurity was similar to that observed with toluene (3% ee). Nitromethane (MeNO_2) did not show any enhancement as iodolactone **587** was delivered in 19% yield as a racemate (Table 36, entry 6). Alcoholic (MeOH) and nitrile ($\text{CH}_3\text{CH}_2\text{CN}$) solvents performed similarly to that of MeNO_2 , and THF failed to give product

²⁵⁰ Gaucher, A.; Dutot, L.; Barbeau, O.; Hamchaoui, W.; Wakselman, M.; Mazaleyrat, J.-P. *Tetrahedron-Asymmetr.* **2005**, *16*, 857-864.

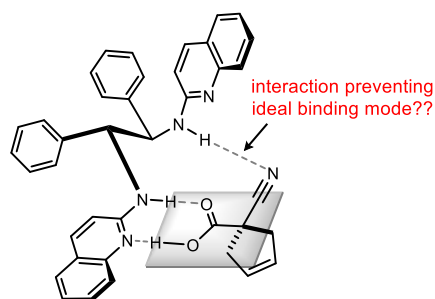
completely (Table 36, entries 7-9). Although CH₂Cl₂ led to improved yield, toluene was taken onto further studies as noticeable levels of enantioselection were achieved with this solvent in the 5-membered lactonization system.

Table 36. 6-Membered Iodolactonization: Catalyst and Solvent Studies

entry	catalyst	solvent	yield (%)	ee (%)
1	PBAM	toluene	12	4
2	StilbPBAM	toluene	14	0
3	StilbPBAM•HOTf	toluene	17	-5
4	StilbPBAM•HNTf ₂	toluene	17	1
5	PBAM	CH ₂ Cl ₂	25	3
6	PBAM	MeNO ₂	19	0
7	PBAM	MeOH	11	1
8	PBAM	CH ₃ CH ₂ CN	8	1
9	PBAM	THF	0	N/A

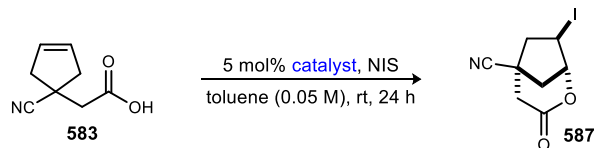
Other non-amidine organocatalysts were also employed with aspirations of increasing yield and selectivity. When 3,5-(bistrifluoromethyl)phenyl-based binaphthol (BINOL) **588** was used as the catalyst, little change was seen relative to PBAM as lactone **587** was isolated in 14% yield and 3% ee (Table 37, entry 2). BINOL phosphoric acid **589** and phenanthrene-derived BINOL phosphoric acid **590** performed similarly (Table 37, entries 3 and 4). Anthracene-derived BINOL phosphoric acid catalyst **591** showed mild improvement as the iodolactone product was isolated in 17% yield and 8% ee (Table 37, entry 5). 2,6-Dimethyl-4-methoxy-phenyl-based BINOL phosphoric acid **592** did not fare as well as this catalyst delivered lactone **587** in 7% yield as a racemate (Table 37, entry 6). TRIP as well as Deng's and Takemoto's thioureas also proved

Figure 36. Potential Unwanted Electronic Interaction in the Binding Mode

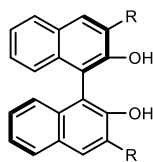


ineffective as diminished yields and selectivities were observed relative to when PBAM was used (Table 37, entries 7-9).

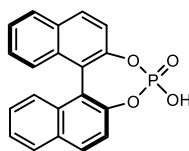
Table 37. 6-Membered Iodolactonization: Examination of Non-Amidine Catalysts



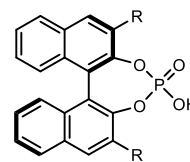
entry	catalyst	yield (%)	ee (%)
1	PBAM	12	4
2	BINOL 588	14	0
3	phosphoric acid 589	17	-5
4	phosphoric acid 590	17	1
5	phosphoric acid 591	25	3
6	phosphoric acid 592	19	0
7	TRIP	11	1
8	Deng Thiourea	8	1
9	Takemoto Thiourea	0	N/A



R = ^{3,5}(CF₃)₂Ph, BINOL **588**



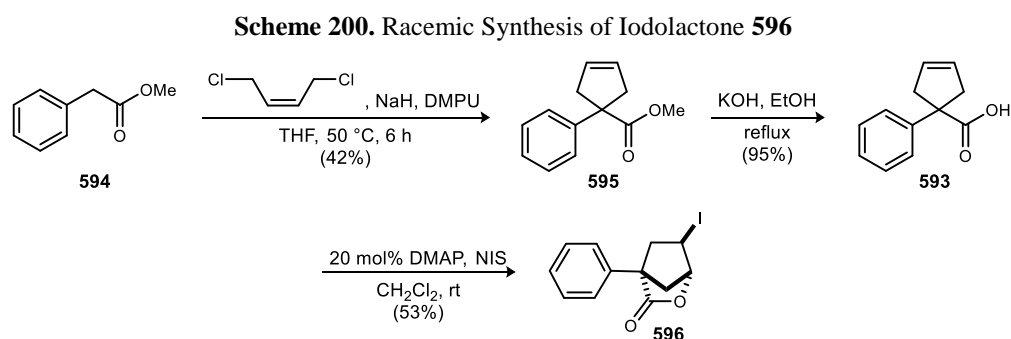
phosphoric acid **589**



R = phenanthrene, phosphoric acid **590**
 R = anthracene, phosphoric acid **591**
 R = ^{2,6}(Me)₂⁴(MeO)Ph, phosphoric acid **592**

The inability to achieve promising levels of enantioselection with a multitude of *Z*-alkene substrates resulted in the analysis of potential problems. One commonality between the starting materials employed throughout the course of these lactonization studies is that they all possess a cyano motif. Also, the fact that 32% ee was observed within the 5-membered iodolactonization system suggests that the starting cyanoacid is indeed binding to the organocatalyst (Table 32, entry 4). With these observations in mind, it is reasonable to infer that the cyano group of the acid may be involved in an unwanted electronic interaction when binding to the organocatalyst (Figure 36). In other words, the cyano motif may be preventing the acid from orienting itself with the catalyst in such a way that favors higher levels of enantioselection. In order to neutralize this potential problem, the cyano functionality should be replaced with a moiety less prone to undesired electronic interaction (i.e. a phenyl group). Therefore, phenyl cyclopentene carboxylic acid **593** was the next substrate of interest.

Acid **593** was synthesized via a known procedure as described by Takacs and colleagues.²⁵¹ Treatment of commercially available methyl phenylacetate (**594**) with NaH and *cis*-1,4-dichloro-2-butene in the presence of *N,N'*-dimethylpropylene urea (DMPU) and THF at elevated temperature provided methyl phenylcyclopentene carboxylate **595** in 42% isolated yield (Scheme 200). Subsequent saponification of **595** with KOH in ethanol furnished known acid **593** in 95% yield. When this acid was treated with NIS and DMAP in CH₂Cl₂, iodolactone **596** was afforded setting the stage for enantioselective studies.



With a phenyl motif in place of the cyano group, we were hopeful that acid **593** would achieve a binding mode that would ultimately increase selectivity. When PBAM was used as the organocatalyst, we were disappointed to see that this substrate was not immediately better behaved as lactone **596** was acquired in 9% yield and 1% ee (Table 38, entry 1). However, when StilbPBAM was employed, increased yield and promising levels of enantioselection were observed as the lactone product was isolated in 25% yield and 48% ee (Table 38, entry 2). This jump in selectivity between the PBAM and StilbPBAM entries indicates that the bite angle of the catalyst is critical for inducing high levels of enantioselection. Encouraged by the StilbPBAM result, the triflic acid and triflimide salts of StilbPBAM were also submitted with aspirations of further enhancing enantioselection. Unfortunately, neither of these fared as well relative to the free base catalyst (Table 38, entries 3 and 4).

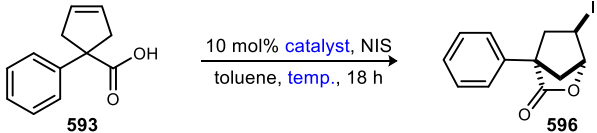
With StilbPBAM taken on as the catalyst, the effects of temperature were examined next. Subjection of StilbPBAM to the reaction protocol at 0 °C led to an increase in both yield and enantioselection as lactone **596** was afforded in 41% yield and 58% ee (Table 38, entry 5). A -20 °C reaction temperature provided the lactone product in 30% yield and 65% ee confirming that

²⁵¹ Hoang, G. L.; Yang, Z.-D.; Smith, S. M.; Pal, R.; Miska, J. L.; Pérez, D. E.; Pelter, L. S. W.; Zheng, X. C.; Takacs, J. M. *Org. Lett.* **2015**, *17*, 940-943.

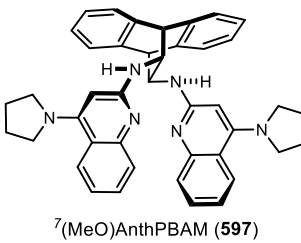
lower temperatures correlate to higher ee (Table 38, entry 6). However, when the lactonization was further chilled to -50 °C and -78 °C, product formation was completely mitigated (Table 38, entries 7 and 8).

After identifying -20 °C as the optimum temperature, organocatalysts with higher Brønsted basicity profiles were studied next. When ⁷(MeO)StilbPBAM was employed as the catalyst, we were disappointed to see a dramatic drop in yield and selectivity as lactone **596** was provided in only 11% yield and 12% ee (Table 38, entry 9). An anthracenyl-bearing analog, dubbed ⁷(MeO)AnthPBAM (**597**), was also examined in the iodolactonization system. Unfortunately, this catalyst also proved fruitless as lactone **596** was delivered in 10% yield and -3% ee (Table 38, entry 10).

Table 38. Initial Iodolactonization Studies with Phenyl-Derived Acid **593**



entry	catalyst	temp. (°C)	yield (%)	ee (%)
1	PBAM	25	9	1
2	StilbPBAM	25	25	48
3	StilbPBAM•HOTf	25	14	41
4	StilbPBAM•HNTf ₂	25	12	16
5	StilbPBAM	0	41	58
6	StilbPBAM	-20	30	65
7	StilbPBAM	-50	0	N/A
8	StilbPBAM	-78	0	N/A
9	⁷ (MeO)StilbPBAM	-20	11	12
10	⁷ (MeO)AnthPBAM	-20	10	-3



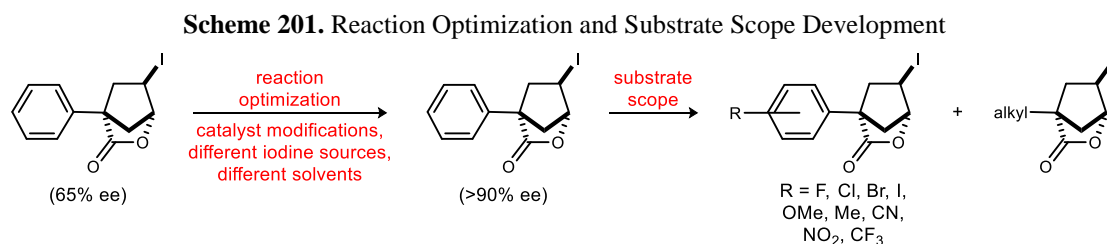
⁷(MeO)AnthPBAM (**597**)

With promising levels of enantioselection achieved, other variables are to be examined in order to further improve this system. These variables include different iodine sources, solvents, and other catalysts modifications. These efforts are currently ongoing within our laboratory by Matthew Knowe and Zachary Carter.

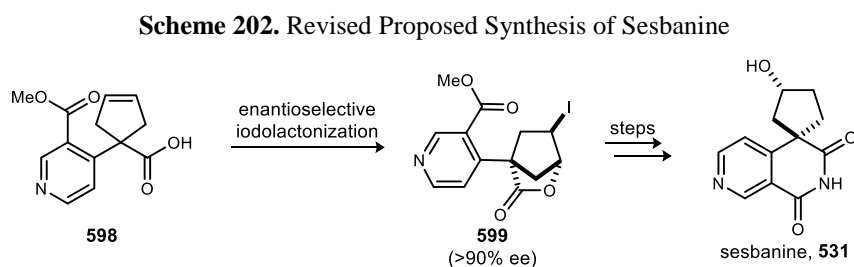
7.5. Future Directions

The immediate objectives are to improve the yield of this iodolactonization and to achieve levels of enantioselection that are high enough for synthetic utility (i.e. >90% ee). The most direct avenues of accomplishing these goals include examining the effects of catalysts modifications as well as different iodine sources and solvents. Additionally, substrates with different steric and

electronic properties can be employed in order to see their respective influence on this reaction system. Once this iodolactonization is achieved in sufficient yield and optimal levels of enantioselection, this protocol can be applied to a multitude of *Z*-alkene bearing carboxylic acids in order to demonstrate the generality of this methodology (Scheme 201).



Another future direction would be to apply this newly developed methodology towards the synthesis of sesbanine (**531**). Pyridyl cyclopentene carboxylic acid **598** can be synthesized as a precursor substrate to the iodolactonization protocol. Subjection of acid **598** to optimal reaction conditions can theoretically deliver iodolactone **599** in good yield and with high levels of enantioselection. This lactone intermediate can then be converted to sesbanine (**531**) via a short synthetic sequence (Scheme 202).

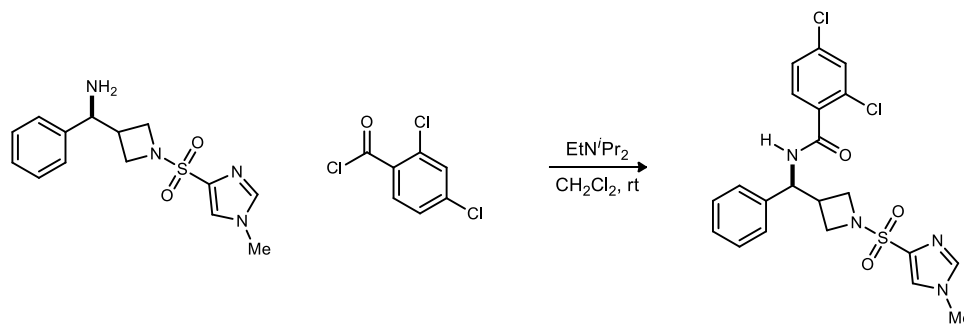


Chapter 8. Experimentals

Glassware was flame-dried under vacuum for all non-aqueous reactions. All reagents and solvents were commercial grade and purified prior to use when necessary. Tetrahydrofuran (THF), dichloromethane (CH_2Cl_2), and toluene was dried by passage through a column of activated alumina as described by Grubbs.²⁵² This was done to accurately quantitate the amount of water in each reaction.

Thin layer chromatography (TLC) was performed using glass-backed silica gel (250 μm) plates and flash chromatography utilized 230-400 mesh silica gel from Sorbent Technologies. UV light and/or the use of potassium permanganate solutions were used to visualize products.

IR spectra were recorded on a Nicolet Avatar 360 spectrophotometer and are reported in wavenumbers (cm^{-1}). All compounds were analyzed as neat films on a NaCl plate (transmission). Nuclear magnetic resonance spectra (NMR) were acquired on a Bruker DRX-500 (500 MHz), Bruker AV-400 (400 MHz) or Bruker AV II-600 (600 MHz) instrument. Chemical shifts are measured relative to residual solvent peaks as an internal standard set to δ 7.26 and δ 77.0 for CDCl_3 . Mass spectra were recorded on a Thermo Electron Corporation MAT 95XP-Trap mass spectrometer by use of electron impact ionization (EI) or electrospray ionization (ESI) by the Indiana University Mass Spectrometry Facility. Optical rotations were measured on a Perkin Elmer-341 polarimeter. Chiral HPLC analysis was conducted on an Agilent 1100 series instrument using the designated ChialPak column.



2,4-Dichloro-N-((1-((1-methyl-1H-imidazol-4-yl) sulfonyl)azetidin-3-yl)(phenyl) methyl) benzamide (1). To a flame dried flask equipped with a stir bar was added the amine (36.1 mg, 118 μmol) and dichloromethane (1 mL), immediately followed by addition of *N,N*-

²⁵² Pangborn, A. B.; Giardello, M. A.; Grubbs, R. K.; Rosen, R. K.; Timmers, F. J. *Organometallics* **1996**, *15*, 1518-1520.

diisopropylethylamine (30.5 mg, 236 μmol) and the benzoyl chloride (42.1 mg, 201 μmol). The reaction was stirred at rt for 16 h, quenched with 1 M HCl and extracted with dichloromethane. The organic extracts were then washed with NaHCO_3 , extracted with dichloromethane, dried (MgSO_4), filtered and concentrated in vacuo. Flash column chromatography of the residue (SiO_2 , 0-10% methanol in dichloromethane) yielded the desired dichlorinated product as an off white viscous oil (15.3 mg, 27% over 2 steps). The major enantiomer was determined to be 87% ee by chiral HPLC analysis. Chiral HPLC analysis (Chiralpak AD, 65% isopropyl alcohol/hexanes, 1.2 mL/min, $t_r(e_1, \text{major}) = 3.65$ min, $t_r(e_2, \text{minor}) = 7.05$ min); $[\alpha]_D^{20} -4.6$ (c 0.41, CHCl_3); $R_f = 0.40$ (5% MeOH/dichloromethane); IR (film) 3262, 3061, 2925, 2855, 1649 cm^{-1} ; ^1H NMR (400 MHz, CDCl_3) δ 7.52 (s, 1H), 7.48 (d, $J = 8.4$ Hz, 1H), 7.40 (d, $J = 2.0$ Hz, 1H), 7.38 (s, 1H), 7.31 (m, 4H), 7.22 (d, $J = 6.8$ Hz, 2H), 6.83 (br d, $J = 8.4$ Hz, 1H), 5.06 (dd, $J = 8.8, 8.8$ Hz, 1H), 4.07 (dd, $J = 8.4, 8.4$ Hz, 1H), 3.96 (dd, $J = 8.4, 8.4$ Hz, 1H), 3.95 (d, $J = 7.2$ Hz, 2H), 3.79 (s, 3H), 3.03 (dddd, $J = 8.8, 8.4, 8.4, 7.2, 7.2$ Hz, 1H); ^{13}C NMR (100 MHz, CDCl_3) ppm 165.3, 138.6, 136.9, 133.4, 131.5, 131.0, 129.9, 129.0, 128.2, 127.5, 126.5, 55.5, 54.0, 53.6, 34.2, 33.3; HRMS (ESI): Exact mass calcd for $\text{C}_{21}\text{H}_{21}\text{Cl}_2\text{N}_4\text{O}_3\text{S}$ $[\text{M}+\text{H}]^+$ 479.0679, found 479.0714. HSQC indicated that the methylene carbons of the azetidine ring are diastereotopic, as would be expected for the assigned structure.

Summary of Structural Elucidation for Azetidine 1.

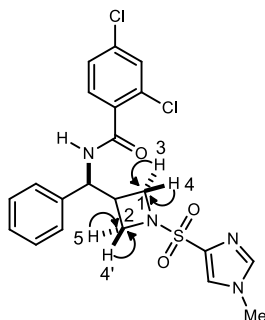
Key Features

The structure was assigned as the desired azetidine using standard 1D and 2D NMR techniques. ^1H NMR indicated the presence of a doublet of doublets integrating to 1H at 4.07 ppm, a doublet of doublets integrating to 1H at 3.96 ppm and a doublet integrating to 2H at 3.95. These 4 hydrogens account for both methylenes of the azetidine ring. The unorthodox splitting of the azetidine methylenes supported the proposal that the hydrogens on the methylenes of the azetidine ring were diastereotopic (all magnetically inequivalent). ^1H NMR also indicated the presence of a doublet of doublets integrating to 1H at 5.06 ppm, assigned as the benzylic methine. A singlet integrating to 3H at 3.79 ppm was assigned as the methyl group of the methyl imidazole ring. A doublet of doublets of doublets of doublets of doublets integrating to 1H at 3.03 ppm was assigned as the methine of the azetidine ring. Also, the presence of 10H in the aromatic region further supports the desired azetidine structure. ^{13}C NMR clearly indicates the presence of an amide at 165 ppm. Peaks at 54.0 ppm and 53.6 ppm indicates that the methylene carbons of the azetidine

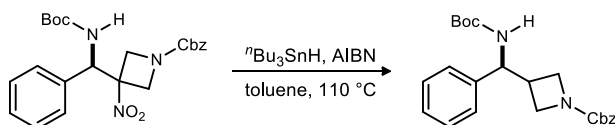
ring are diastereotopic. DEPT 135 experimentation further confirms this finding as the peaks at 54.0 ppm and 53.6 ppm are inverted indicating that they are methylene carbons.

Additional Features

Key HSQC Correlations for **1** (600 MHz)

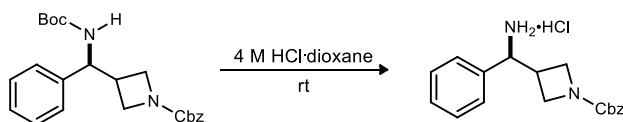


Further evidence supporting the structural assignment includes an HSQC, which clearly showed that the methylene hydrogens and carbons on the azetidine ring were diastereotopic via anticipated $^1J_{\text{HC}}$ couplings. C1 (54.0 ppm) of the azetidine ring showed correlations to methylene hydrogens H3 (4.07 ppm) and H4 (3.95 ppm). C2 (53.6 ppm) of the azetidine ring also showed correlations to methylene hydrogens H5 (3.96 ppm) and H4' (3.95 ppm).

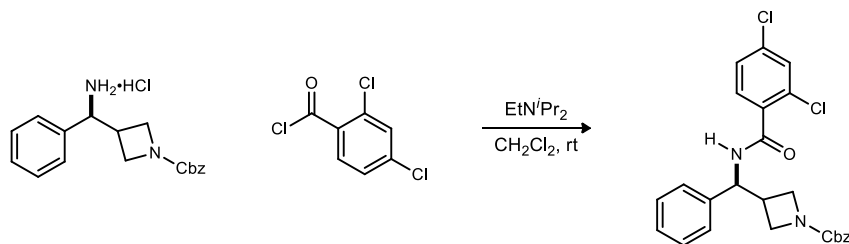


Benzyl 3-(((tert-butoxycarbonyl)amino)(phenyl)methyl)azetidine-1-carboxylate (21). To a solution of the nitro azetidine (75.0 mg, 170 μmol) in toluene (2.1 mL) at room temperature was added $n\text{-Bu}_3\text{SnH}$ (99.0 mg, 340 μmol). The resulting mixture was heated to 110 $^\circ\text{C}$, immediately followed by the addition of azobisisobutyronitrile (AIBN) (6.00 mg, 34.0 μmol). After the reaction mixture stirred for 1 h at 110 $^\circ\text{C}$, additional AIBN (6.00 mg, 34.0 μmol) was added and the mixture was stirred at 110 $^\circ\text{C}$ for an additional 3 h. The reaction was cooled, concentrated, diluted with diethyl ether and washed with satd aq KF. The organic layer was dried (MgSO_4), filtered through a Celite pad with additional diethyl ether and concentrated. Flash column chromatography of the residue (SiO_2 , 20-30% ethyl acetate in hexanes) yielded the desired azetidine as a white solid (45.0 mg, 67%). $[\alpha]_D^{20}$ -26.7 (c 0.69, CHCl_3); mp 110-112 $^\circ\text{C}$; R_f = 0.20 (25% EtOAc/hexanes); IR (film) 3328, 3032, 2973, 2886, 1705 cm^{-1} ; $^1\text{H NMR}$ (400 MHz, CDCl_3) δ 7.31 (m, 8H), 7.21 (d, J

= 7.2 Hz, 2H), 5.09 (s, 2H), 4.89 (br s, 1H), 4.82 (br s, 1H), 4.10 (dd, $J = 8.4, 8.4$ Hz, 1H), 3.98 (br dd, $J = 5.6, 5.6$ Hz, 1H), 3.91 (br dd, $J = 8.8, 8.8$ Hz, 1H), 3.69 (br dd, $J = 6.0, 6.0$ Hz, 1H), 2.94 (br s, 1H), 1.41 (s, 9H); ^{13}C NMR (100 MHz, CDCl_3) ppm 156.3, 155.4, 140.1, 136.5, 128.7, 128.3, 127.9, 127.8, 127.7, 126.5, 79.7, 66.5, 56.8, 51.6, 51.1, 34.1, 28.2; HRMS (ESI): Exact mass calcd for $\text{C}_{23}\text{H}_{28}\text{N}_2\text{NaO}_4$ $[\text{M}+\text{Na}]^+$ 419.1898, found 419.1927.

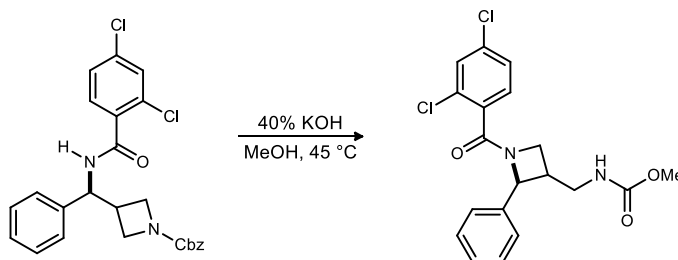


Benzyl 3-(amino(phenyl)methyl)azetidine-1-carboxylate (22). To a flame dried flask equipped with a stir bar was added the carbamate (90.0 mg, 227 μmol) and 4 M HCl·dioxane (426 μL , 1.71 mmol). The resulting mixture was allowed to stir at rt for 16 h prior to TLC analysis. Concentration of the reaction mixture yielded the chloride salt of the desired amine as a light yellow foam. The unpurified material was used in the next step.



Benzyl 3-((2,4-dichlorobenzamido)(phenyl)methyl)azetidine-1-carboxylate (24). To a flame dried flask equipped with a stir bar was added the chloride salt of the amine (76.0 mg, 228 μmol) and dichloromethane (2 mL). The resulting solution was chilled to 0 °C, immediately followed by addition of *N,N*-diisopropylethylamine (70.7 mg, 547 μmol) and the benzoyl chloride (71.8 mg, 343 μmol). The mixture was warmed to room temperature, stirred for 16 h, quenched with 1 M HCl and extracted with dichloromethane. The organic extracts were then washed with NaHCO_3 , extracted with dichloromethane, dried (MgSO_4), filtered and concentrated. Flash column chromatography of the residue (SiO_2 , 10-40% ethyl acetate in hexanes) yielded the desired amide as an off white oil (44.4 mg, 42% over 2 steps). $[\alpha]_D^{20}$ -13.4 (c 0.90, CHCl_3); $R_f = 0.41$ (40% EtOAc/hexanes); IR (film) 3264, 3064, 2925, 2854, 1710, 1643 cm^{-1} , ^1H NMR (400 MHz, CDCl_3) δ 7.64 (d, $J = 8.4$ Hz, 1H), 7.44 (br d, $J = 1.2$ Hz, 1H), 7.35 (m, 11H), 7.17 (br d, $J = 8.4$ Hz, 1H), 5.57 (br t, $J = 8.0, 8.0$ Hz, 1H), 5.41 (br s, 1H), 5.11 (s, 1H), 3.66 (dd, $J = 11.6, 3.6$ Hz, 1H), 3.57

(dd, $J = 11.6, 4.4$ Hz, 1H), 3.43 (m, 1H), 3.36 (m, 1H), 2.63 (br s, 1H); ^{13}C NMR (100 MHz, CDCl_3) ppm 165.2, 156.6, 138.6, 137.2, 131.5, 130.2, 129.1, 128.5, 128.2, 128.1, 128.0, 127.7, 126.5, 66.9, 53.5, 44.8, 43.8, 40.6; HRMS (ESI): Exact mass calcd for $\text{C}_{25}\text{H}_{23}\text{Cl}_2\text{N}_2\text{O}_3$ $[\text{M}+\text{H}]^+$ 469.1079, found 469.1080.



Methyl (((2S)-1-(2,4-dichlorobenzoyl)-2-phenylazetidin-3-yl) methyl)carbamate (26). To a flame dried flask equipped with a stir bar was added the benzamide (37.0 mg, 79.0 μmol), methanol (2 mL) and 40% KOH (301 μL , 3.15 mmol). The reaction mixture was heated to 45 $^\circ\text{C}$, allowed to stir for 16 h, and then concentrated. The resulting residue was diluted with water, extracted with dichloromethane and the organic extracts were dried (MgSO_4), filtered and concentrated. Flash column chromatography of the crude material (SiO_2 , 10-50% ethyl acetate in hexanes) yielded the desired methyl ester as an off white viscous oil (12.4 mg, 40%). $[\alpha]_D^{20} +24.5$ (c 1.24, CHCl_3); $R_f = 0.24$ (40% EtOAc/hexanes); IR (film) 3327, 3062, 3029, 2927, 2361, 1716, 1663 cm^{-1} ; ^1H NMR (600 MHz, CDCl_3) δ 7.55 (d, $J = 7.8$ Hz, 1H), 7.44 (d, $J = 1.8$ Hz, 1H), 7.37 (dd, $J = 7.8, 7.8$ Hz, 2H), 7.28 (m, 4H), 4.82 (br s, 1H), 4.54 (d, $J = 6.0$ Hz, 1H), 4.31 (dd, $J = 11.4, 3.6$ Hz, 1H), 4.16 (dd, $J = 10.8, 6.6$ Hz, 1H), 3.67 (s, 3H), 3.33 (m, 2H), 2.22 (br s, 1H); ^{13}C NMR (150 MHz, CDCl_3) ppm 157.3, 155.7, 142.2, 136.0, 133.3, 132.5, 131.3, 130.0, 128.6, 127.4, 127.2, 127.0, 65.1, 58.9, 52.3, 41.0, 39.2; HRMS (ESI): Exact mass calcd for $\text{C}_{19}\text{H}_{19}\text{Cl}_2\text{N}_2\text{O}_3$ $[\text{M}+\text{H}]^+$ 393.0779, found 393.0766. HMBC (600 MHz) analysis further confirmed the compound structure.

Structural Elucidation for Methyl Ester 26

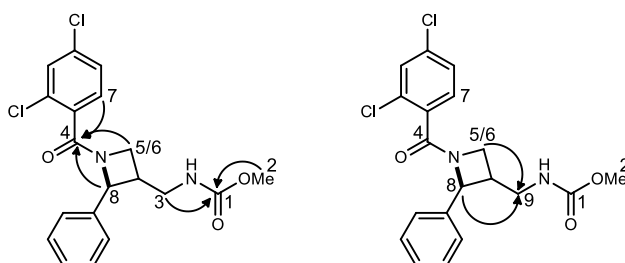
Key Features

The structure was assigned as the methyl ester using standard 1D and 2D NMR techniques. ^1H NMR indicated the presence of a singlet integrating to 3H at 3.67 ppm, assigned as the CH_3O -fragment. The presence of a multiplet integrating to 2H at 3.33 ppm indicates the presence of a methylene group alpha to the nitrogen of the carbamate. The presence of this methylene group also

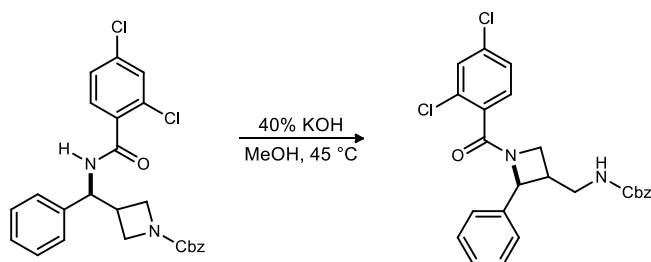
supports the proposal of an azetidine isomerization. The absence of the benzyl peak at 5.1 ppm supports that the Cbz was successfully cleaved. Also, the presence of approximately 8H in the aromatic region is consistent with the cleavage of the Cbz group. ^{13}C NMR clearly indicates the presence of a carbamate at 157.3 ppm and an amide at 155.7 ppm. DEPT 135 experimentation shows the presence of two methylenes, one cyclic at 65.1 ppm, and one acyclic at 41.0 ppm. The presence of these two methylenes with such a large difference in chemical shift further supports the assignment based on azetidine isomerization.

Additional Features

Key HMBC Correlations for Methyl Ester **26** (600 MHz)



Further evidence supporting the structural assignment includes an HMBC, which clearly showed the anticipated $^3J_{\text{HC}}$ couplings for desired methyl ester **26**. C1 (157 ppm) of the carbamate showed correlations to H2/H2'/H2'' (3.67 ppm) and H3/H3' (3.33 ppm). C4 (156 ppm) of the amide showed correlations to diastereotopic methylene hydrogens H5 (4.31 ppm) and H6 (4.16 ppm) as well as to H7 (7.55 ppm) and methine hydrogen H8 (4.54 ppm). Furthermore, methylene C9 (41.0 ppm) showed correlations to diastereotopic methylene hydrogens H5 (4.31 ppm) and H6 (4.16 ppm) and to methine hydrogen H8 (4.54 ppm).



Benzyl (((2*S*)-1-(2,4-dichlorobenzoyl)-2-phenylazetidin-3-yl)methyl)carbamate (27**).** To a flame dried flask equipped with a stir bar was added the benzamide (37.0 mg, 79.0 μmol), methanol (2 mL) and 40% KOH (301 μL , 3.15 mmol). The reaction mixture was heated to 45 $^{\circ}\text{C}$,

allowed to stir for 16 h then concentrated in vacuo. The resulting residue was diluted with water, extracted with dichloromethane and the organic extracts were dried (MgSO₄), filtered and concentrated in vacuo. Flash column chromatography of the crude material (SiO₂, 10-50% ethyl acetate in hexanes) yielded the desired azetidine as a light yellow oil (5.8 mg, 16%). $[\alpha]_D^{20} +13.9$ (*c* 1.24, CHCl₃); *R_f* = 0.37 (40% EtOAc/hexanes); IR (film) 3328, 3031, 2924, 2853, 1713, 1664 cm⁻¹; ¹H NMR (400 MHz, CDCl₃) δ 7.54 (d, *J* = 8.4 Hz, 1H), 7.43 (d, *J* = 2.0 Hz, 1H), 7.35 (m, 8H), 7.28 (m, 3H), 5.10 (m, 2H), 4.88 (br s, 1H), 4.54 (d, *J* = 5.6 Hz, 1H), 4.31 (dd, *J* = 11.2, 3.2 Hz, 1H), 4.16 (dd, *J* = 11.2, 6.8 Hz, 1H), 3.35 (dd, *J* = 10.0, 6.0 Hz, 2H), 2.24 (br d, *J* = 3.2 Hz, 1H); ¹³C NMR (150 MHz, CDCl₃) ppm 156.6, 155.8, 142.2, 136.3, 136.0, 133.3, 132.5, 131.3, 130.0, 128.7, 128.6, 128.3, 128.1, 127.4, 127.2, 127.0, 67.0, 65.0, 58.7, 41.1, 39.1; HRMS (ESI): Exact mass calcd for C₂₅H₂₃Cl₂N₂O₃ [M+H]⁺ 469.1079, found 469.1098. HMBC (600 MHz) analysis further confirmed the compound structure.

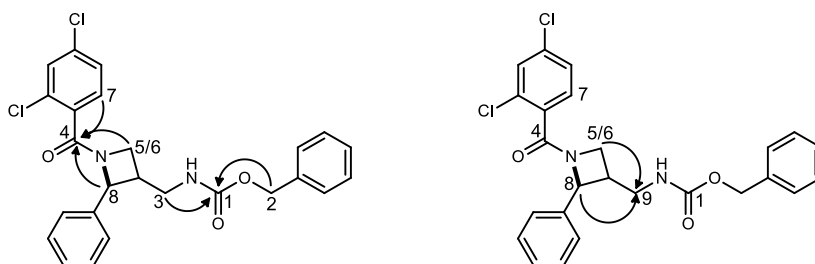
Structural Elucidation for Azetidine Isomer 27

Key Features

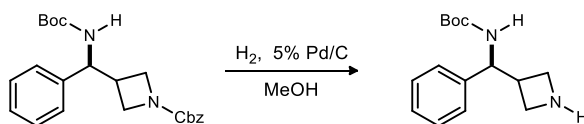
The structure was assigned as the azetidine isomer using standard 1D and 2D NMR techniques. ¹H NMR indicated the presence of a doublet integrating to 2H at 5.10 ppm, assigned as the benzyl methylene of the Cbz protecting group. The presence of a multiplet integrating to 2H at 3.35 ppm indicates the presence of a methylene group alpha to the nitrogen of the carbamate. The presence of this methylene group also supports the proposal of the azetidine isomerization. Also, the presence of approximately 13H in the aromatic region further supports that the Cbz group remained intact. ¹³C NMR clearly indicates the presence of a carbamate at 156.6 ppm and an amide at 155.8 ppm. DEPT 135 experimentation shows the presence of three methylenes, one cyclic at 65.0 ppm, and two acyclic at 67.0 ppm and 41.1 ppm. The methylene at 67.0 ppm is indicative of the benzyl carbon of the Cbz. The presence of the two methylenes with such a large difference in chemical shift (65.0 ppm and 41.1 ppm) further supports the idea that azetidine isomerization did occur.

Additional Features

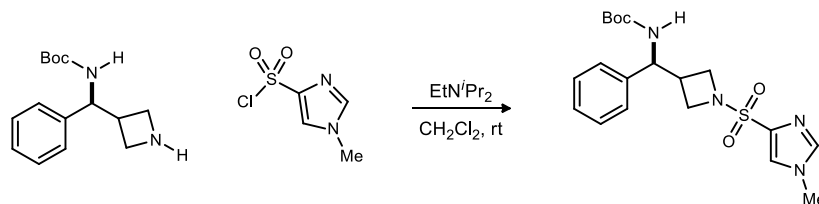
Key HMBC Correlations for Azetidine Isomer **27** (600 MHz)



Further evidence supporting the structural assignment includes an HMBC, which clearly showed the anticipated $^3J_{\text{HC}}$ couplings for desired isomer **27**. C1 (157 ppm) of the carbamate showed correlations to H3/H3' (3.35 ppm) and H2/H2' (5.10 ppm). C4 (156 ppm) of the amide showed correlations to diastereotopic methylene hydrogens H5 (4.31 ppm) and H6 (4.16 ppm) as well as to H7 (7.54 ppm) and methine hydrogen H8 (4.54 ppm). Furthermore, methylene C9 (41.1 ppm) showed correlations to diastereotopic methylene hydrogen H5 (4.31 ppm) and to methine hydrogen H8 (4.54 ppm).

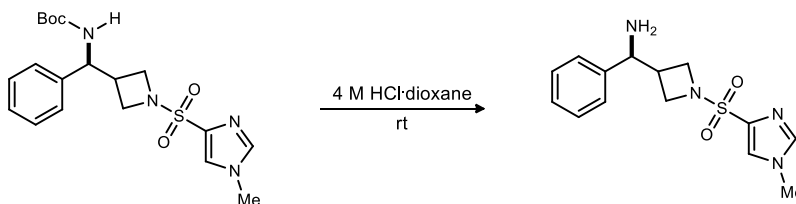


***tert*-Butyl (azetidin-3-yl(phenyl)methyl)carbamate (28)**. To a flame dried flask equipped with a stir bar was added the carbamate (50.0 mg, 126 μmol) followed by the addition of 5% Pd/C (27.0 mg, 130 μmol). Methanol (1 mL) was then added and the resulting suspension was allowed to stir for 5 minutes. The flask and its contents were purged with H₂ gas and left to stir under H₂ atmosphere (balloon) at rt for 3 h. The reaction mixture was filtered through a Celite pad with methanol and dichloromethane and then concentrated in vacuo to afford the desired amine as a colorless oil. The unpurified material was used in the next step.

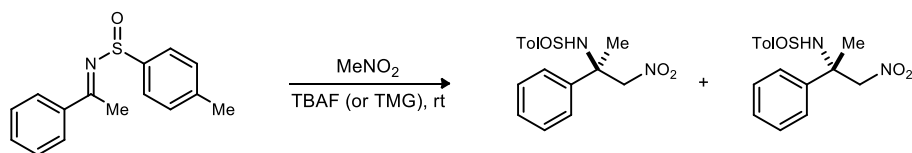


***tert*-Butyl((1-((1-methyl-1*H*-imidazol-4-yl)sulfonyl)azetidin-3-yl)(phenyl)methyl) carbamate**

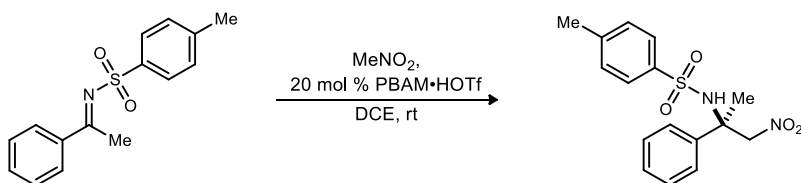
(30). To a flame dried flask equipped with a stir bar was added the azetidine (33.0 mg, 126 μmol) and dichloromethane (3 mL), immediately followed by addition of the sulfonyl chloride (27.0 mg, 151 μmol) and *N,N*-diisopropylethylamine (19.5 mg, 151 μmol). The reaction was stirred at rt for 16 h, diluted with water and extracted with ethyl acetate. The organic extracts were then washed with brine, dried (MgSO_4), filtered and concentrated. Flash column chromatography of the residue (SiO_2 , 0-10% methanol in dichloromethane) yielded the sulfonamide as an off white viscous oil (28.7 mg, 56% over 2 steps). $[\alpha]_D^{20}$ -12.5 (*c* 0.77, CHCl_3); R_f = 0.4 (5% MeOH/dichloromethane); IR (film) 3368, 3134, 2977, 1703, 1526 cm^{-1} ; ^1H NMR (400 MHz, CDCl_3) δ 7.62 (s, 1H), 7.51 (s, 1H), 7.25 (m, 3H), 7.12 (d, *J* = 7.2 Hz, 2H), 5.21 (br d, *J* = 5.2 Hz, 1H), 4.48 (dd, *J* = 8.8, 8.8 Hz, 1H), 3.97 (dd, *J* = 8.4, 8.4 Hz, 1H), 3.85 (dd, *J* = 8.4, 8.4 Hz, 1H), 3.84 (d, *J* = 8.0 Hz, 2H), 3.79 (s, 3H), 2.84 (dddd, *J* = 8.8, 8.4, 8.4, 8.0, 8.0 Hz, 1H), 1.38 (s, 9H); ^{13}C NMR (100 MHz, CDCl_3) ppm 155.3, 139.8, 139.6, 136.2, 128.7, 127.7, 126.2, 125.9, 79.6, 56.3, 53.9, 53.5, 34.1, 33.6, 28.2; HRMS (ESI): Exact mass calcd for $\text{C}_{19}\text{H}_{26}\text{N}_4\text{NaO}_4\text{S}$ [$\text{M}+\text{Na}$] $^+$ 429.1597, found 429.1565.



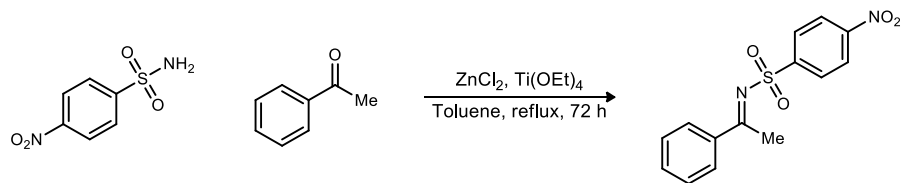
(1-((1-Methyl-1*H*-imidazol-4-yl)sulfonyl)azetidin-3-yl)(phenyl)methanamine (31). To a flame dried flask equipped with a stir bar was added the sulfonamide (48.0 mg, 118 μmol) and 4 M HCl-dioxane (220 μL , 886 μmol). The resulting mixture was allowed to stir at rt for 16 h before it was diluted with dichloromethane and washed with NaHCO_3 . The organic layer was then separated, dried (MgSO_4), filtered, and concentrated to afford the desired amine as a cloudy oil. The unpurified material was used in the next step.



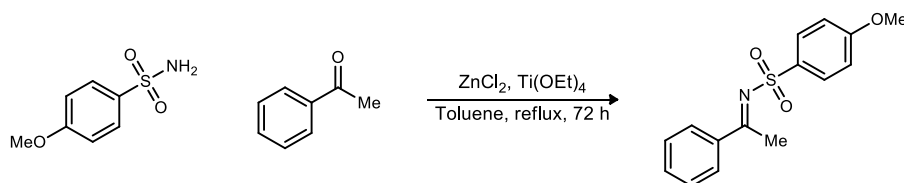
General procedure for (1*S*,(S)S)-*N*-(*p*-Tolylsulfinyl)-2-nitro-1-phenyl-1-methyl-ethanamine (54a) and (1*R*,(S)S)-*N*-(*p*-Tolylsulfinyl)-2-nitro-1-phenyl-1-methyl-ethanamine (54b). This procedure was modified off of a previous protocol found in literature.²⁷ To a flame-dried vial equipped with a stirbar was added the ketimine (31.7 mg, 123 μ mol) and nitromethane (1.00 mL, 18.6 mmol). Tetra-*n*-butylammonium fluoride (6.43 mg, 24.6 μ mol) was then added and the mixture was allowed to stir at rt for 18 h. The reaction mixture was filtered through a silica pad with dichloromethane and ethyl acetate and concentrated in vacuo. Flash column chromatography of the residue (SiO₂, 10-40% ethyl acetate in hexanes) yielded the desired adduct as a colorless oil (23.2 mg, 59%). For characterization data of this compound, refer to the supporting information of the literature reference cited in this experimental.



General Procedure for (S)-4-Methyl-*N*-(1-nitro-2-phenylpropan-2-yl)benzenesulfonamide (58). To a vial equipped with a stir bar was added the ketimine (15.0 mg, 54.9 μ mol), PBAM (5.60 mg, 11.0 μ mol), and dichloroethane (440 μ L). Once the mixture was homogenous, nitromethane (5.90 μ L, 110 μ mol) was added in one portion and the reaction mixture stirred for 96 h. The reaction mixture was filtered through a silica pad with dichloromethane and ethyl acetate and was then concentrated in vacuo. Flash column chromatography of the residue (SiO₂, 15-20% ethyl acetate in hexanes) yielded the desired adduct as a white amorphous solid (2.4 mg, 13%). The characterization data for this compound was found in the literature.²⁸



(E)-4-Nitro-N-(1-phenylethylidene)benzenesulfonamide (59). This procedure was modified off of protocols found in literature.^{32,253} To an oven dried 2-necked round bottom flask equipped with a condenser and a stir bar was added the sulfonamide (937 mg, 4.63 mmol), acetophenone (1.11g, 9.27 mmol), ZnCl₂ (156 mg, 927 μmol), and Ti(OEt)₄ (5.29 mg, 23.2 mmol). The resulting mixture stirred under vacuum for 15 minutes. Toluene (24.0 mL) was then added and the solution was heated to reflux for 72 h. The solution was then cooled to 0 °C followed by the addition of MeOH (15 mL), DCM (15 mL), and sat aq NaHCO₃ (13 mL). The resulting solid was filtered and washed with dichloromethane. Organic extracts were dried (MgSO₄), filtered, and concentrated. Flash column chromatography of the residue (SiO₂, 3%-50% ethyl acetate in hexanes) afforded the desired ketimine as a yellow to orange solid (93 mg, 7%). The characterization data for this compound was found in the literature.²⁵⁴

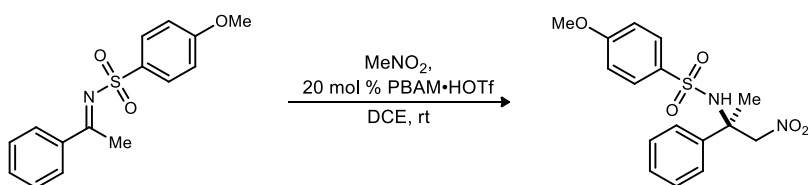


(E)-4-Methoxy-N-(1-phenylethylidene)benzenesulfonamide (60). This procedure was modified off of protocols found in literature.²⁵³ To an oven dried 2-necked round bottom flask equipped with a condenser and a stir bar was added the sulfonamide (810 mg, 4.33 mmol), acetophenone (1.04g, 8.65 mmol), ZnCl₂ (118 mg, 865 μmol), and Ti(OEt)₄ (4.93 mg, 21.6 mmol). The resulting mixture stirred under vacuum for 15 minutes. Toluene (22.0 mL) was then added and the solution was heated to reflux for 48 h. The solution was then cooled to 0 °C followed by the addition of MeOH (13 mL), DCM (13 mL), and sat aq NaHCO₃ (11 mL). The resulting solid was filtered and washed with dichloromethane. Organic extracts were dried (MgSO₄), filtered, and concentrated. Flash column chromatography of the residue (SiO₂, 5%-40% ethyl acetate in

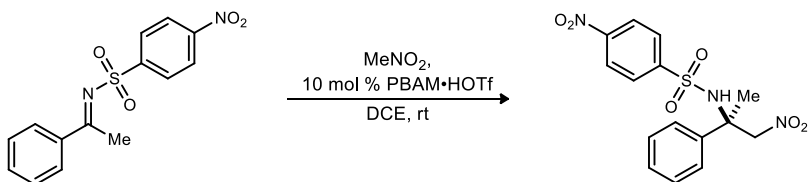
²⁵³ Nakamura, S.; Hayashi, M.; Hiramatsu, Y.; Shibata, N.; Funahashi, Y.; Toru, T. *J. Am. Chem. Soc.* **2009**, *131*, 18240-18241.

²⁵⁴ Shintani, R.; Takeda, M.; Soh, Y.-T.; Ito, T.; Hayashi, T. *Org. Lett.* **2011**, *13*, 2977-2979.

hexanes) afforded the desired ketimine as a white solid (260 mg, 21%). The characterization data for this compound was found in the literature.²⁵³

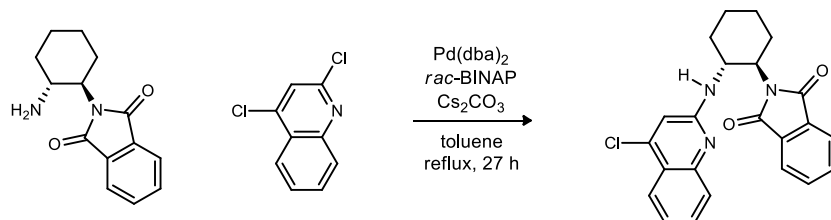


General Procedure for (S)-4-Methoxy-N-(1-nitro-2-phenylpropan-2-yl)benzenesulfonamide (63). To a vial equipped with a stir bar was added the ketimine (15.0 mg, 52.0 μmol), the catalyst (6.80 mg, 10.4 μmol), and dry dichloroethane (416 μL). Nitromethane (6.35 mg, 104 μmol) was then added and the resulting mixture was allowed to stir at rt for 96 h. The reaction mixture was filtered through a silica pad with dichloromethane and ethyl acetate and concentrated in vacuo. Flash column chromatography of the residue (SiO_2 , 25-35% ethyl acetate in hexanes) yielded the desired adduct as a white amorphous solid (4.9 mg, 27%). The major enantiomer was determined to be 11% ee by chiral HPLC analysis. Chiral HPLC analysis (Chiralpak IA, 20% isopropyl alcohol/hexanes, 1.0 mL/min, $t_r(e_1, \text{major}) = 15.2$ min, $t_r(e_2, \text{minor}) = 16.2$ min); $R_f = 0.26$ (33% EtOAc/hexanes); ^1H NMR (600 MHz, CDCl_3) δ 7.67 (dd, $J = 6.6$ Hz, 1.8 Hz, 2 H), 7.29 (m, 5H), 6.89 (dd, $J = 7.2$ Hz, 1.8 Hz, 2H), 5.88 (br s, 1H), 4.88 (AB system, $J = 13.2$ Hz, 2H), 3.86 (s, 3H), 1.70 (s, 3H); ^{13}C NMR (150.9 MHz, CDCl_3) ppm 162.9, 139.7, 133.7, 129.2, 128.9, 128.4, 125.3, 114.1, 82.8, 60.0, 55.6, 24.7; HRMS (ESI): Exact mass calcd for $\text{C}_{16}\text{H}_{18}\text{N}_2\text{NaO}_5\text{S}$ $[\text{M}+\text{Na}]^+$ 373.0834, found 373.0849.

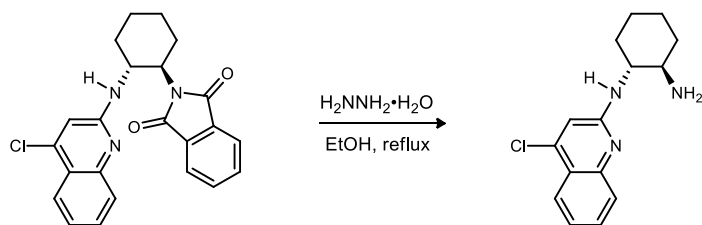


General Procedure for (S)-4-Nitro-N-(1-nitro-2-phenylpropan-2-yl)benzenesulfonamide (64). To a vial equipped with a stir bar was added the ketimine (6.00 mg, 19.7 μmol), the catalyst (1.30 mg, 1.97 μmol), and dry dichloroethane (158 μL). Nitromethane (2.40 mg, 39.4 μmol) was then added and the resulting mixture was allowed to stir at rt for 20 h. The reaction mixture was filtered through a silica pad with dichloromethane and ethyl acetate and concentrated in vacuo. Flash column chromatography of the residue (SiO_2 , 25-50% ethyl acetate in hexanes) yielded the

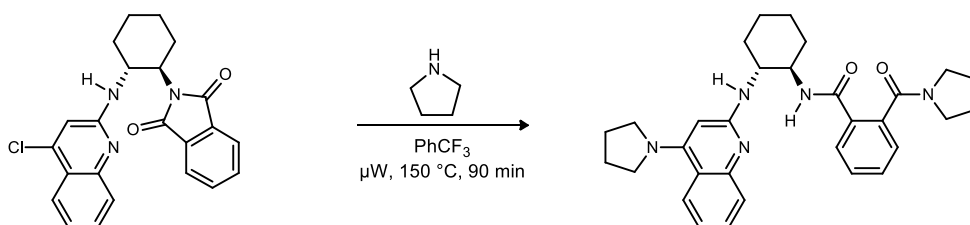
desired adduct as a white amorphous solid (3.1 mg, 43%). The major enantiomer was determined to be 12% ee by chiral HPLC analysis. Chiral HPLC analysis (Chiralpak IA, 20% isopropyl alcohol/hexanes, 1.0 mL/min, $t_r(e_1, \text{major}) = 18.7$ min, $t_r(e_2, \text{minor}) = 19.8$ min); $R_f = 0.32$ (33% EtOAc/hexanes); $^1\text{H NMR}$ (600 MHz, CDCl_3) δ 8.20 (d, $J = 9.0$ Hz, 2H), 7.74 (d, $J = 9.0$ Hz, 2H), 7.27 (m, 1H), 7.22 (m, 4H), 6.12 (br s, 1H), 4.88 (AB system, $J = 12.6$ Hz, 2H), 1.81 (s, 3H); $^{13}\text{C NMR}$ (150.9 MHz, CDCl_3) ppm 147.4, 138.0, 128.9, 128.9, 128.3, 125.8, 124.0, 83.3, 60.1, 24.6.



2-((1R,2R)-2-((4-Chloroquinolin-2-yl)amino)cyclohexyl)isoindoline-1,3-dione (74). A flame dried flask equipped with a stir bar was charged with $\text{Pd}(\text{dba})_2$ (208 mg, 362 μmol), *rac*-BINAP (225 mg, μmol), cesium carbonate (8.84 g, 27.1 mmol), the amine (2.21 g, 9.05 mmol), and 2,4-dichloroquinoline (1.79 g, 9.05 mmol). An oven dried condenser was attached and the apparatus was purged twice with argon. Toluene (45 mL) was added and the resulting solution was stirred under reflux for 27 h. The reaction mixture was then cooled to rt, filtered through a Celite pad with CH_2Cl_2 and EtOAc, and concentrated. Flash column chromatography of the residue afforded the desired product as a light yellow foam (1.53 g, 42%). $[\alpha]_D^{20} +96$ (c 0.68, CHCl_3); $R_f = 0.31$ (20% EtOAc/hexanes); IR (film) 3381, 3060, 2935, 2858, 1767, 1705, 1606, 1567, 1531 cm^{-1} ; $^1\text{H NMR}$ (400 MHz, CDCl_3) δ 7.65 (d, $J = 7.6$ Hz, 1H), 7.49 (m, 3H), 7.38 (ddd, $J = 8.0, 6.8, 1.2$ Hz, 1H), 7.31 (dd, $J = 5.6, 3.2$ Hz, 2H), 7.06 (ddd, $J = 8.0, 8.0, 1.2$ Hz, 1H), 6.59 (s, 1H), 4.84 (dddd, $J = 10.8, 10.8, 10.8, 4.0$ Hz, 1H), 4.74 (d, $J = 10.0$ Hz, 1H), 4.08 (ddd, $J = 10.8, 10.8, 4.0$ Hz, 1H), 2.66 (dddd, $J = 12.8, 12.8, 12.8, 3.6$ Hz, 1H), 2.23 (br m, 1H), 1.85 (m, 3H), 1.66 (dddd, $J = 13.2, 13.2, 3.2, 3.2$ Hz, 1H), 1.42-1.30 (m, 2H); $^{13}\text{C NMR}$ (125.8 MHz, CDCl_3) ppm 168.8, 156.0, 148.1, 142.3, 133.1, 131.3, 129.9, 126.3, 123.3, 122.4, 122.3, 120.9, 111.0, 56.1, 51.3, 33.4, 28.7, 25.5, 24.8; HRMS (ESI) Exact mass calcd for $\text{C}_{23}\text{H}_{21}\text{ClN}_3\text{O}_2$ $[\text{M}+\text{H}]^+$ 406.1322, found 406.1308.

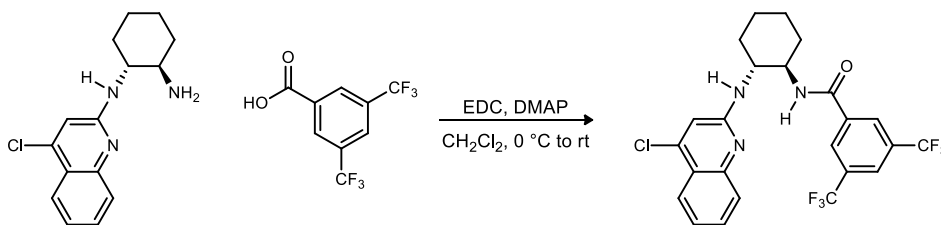


(1R,2R)-N1-(4-Chloroquinolin-2-yl)cyclohexane-1,2-diamine (75). To a flask equipped with a stir bar was added the quinoline (596 mg, 1.47 mmol) and ethanol (3 mL), and the resulting solution was allowed to stir at rt for 5 min. Hydrazine monohydrate (264 μ L, 5.43 mmol) was added and the reaction mixture was stirred under reflux for 3 h whereupon a white solid precipitated out of solution. After cooling the reaction mixture to rt, the solid was washed with ether and filtered. The remaining solid was triturated with ether, filtered once more and the filtrate was concentrated to an orange foam (401 mg, 99%). $[\alpha]_D^{20}$ -3.3 (c 0.61, CHCl_3); $R_f = 0.25$ (10% MeOH/1% AcOH/ CH_2Cl_2); IR (film) 3268, 2930, 2857, 1609, 1538 cm^{-1} ; ^1H NMR (400 MHz, CDCl_3) δ 7.91 (d, $J = 8.0$ Hz, 1H), 7.61 (d, $J = 8.4$ Hz, 1H), 7.49 (ddd, $J = 8.4, 8.4, 1.2$ Hz, 1H), 7.20 (ddd, $J = 8.0, 8.0, 0.8$ Hz, 1H), 6.75 (s, 1H), 5.19 (d, $J = 8.4$ Hz, 1H), 3.64 (m, 1H), 2.44 (ddd $J = 10.0, 10.0, 4.0$ Hz, 1H), 2.07 (br m, 1H), 1.90 (br m, 1H), 1.69-1.64 (br m, 4H), 1.39-1.14 (m, 3H), 1.07 (ddd, $J = 12.8, 12.8, 3.2$ Hz, 1H); ^{13}C NMR (125.8 MHz, CDCl_3) ppm 156.7, 148.5, 142.4, 130.2, 126.1, 123.7, 122.3, 121.3, 111.0, 57.4, 55.8, 35.2, 32.5, 24.9, 24.8; HRMS (ESI) Exact mass calcd for $\text{C}_{15}\text{H}_{19}\text{ClN}_3$ $[\text{M}+\text{H}]^+$ 276.1268, found 276.1260.



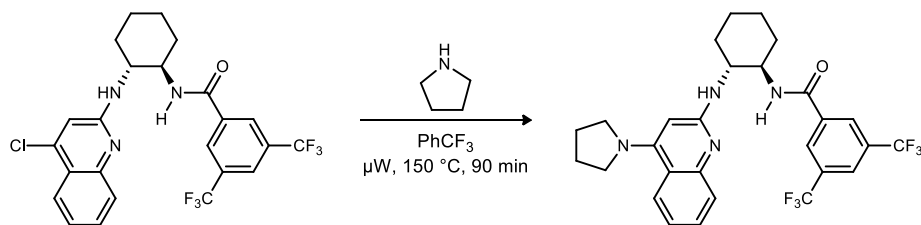
N-((1R,2R)-2-((4-(Pyrrolidin-1-yl)quinolin-2-yl)amino)cyclohexyl)-2-(pyrrolidine-1-carbonyl)benzamide (78). A 0.5-2 mL microwave vial was charged with the 4-chloroquinoline (200 mg, 492 μ mol), pyrrolidine (162 μ L, 1.97 mmol), and trifluorotoluene (2.00 mL). This suspension was heated at 150 $^\circ\text{C}$ and stirred in the microwave for 90 min. The reaction was concentrated and purified by flash column chromatography (1-10% methanol in dichloromethane w/ 1% AcOH) to provide a yellow oil. This material was diluted with dichloromethane and washed with 6 M aq NaOH. The organic layers were combined and washed three times more with 3 M aq

NaOH. The combined organic layers were dried (MgSO₄) and concentrated to afford a yellow foam (201 mg, 80%). $[\alpha]_D^{20} +166$ (*c* 0.90, CHCl₃); *R_f* = 0.18 (5% MeOH/1% AcOH/CH₂Cl₂); IR (film) 3313, 3054, 2932, 2868, 1621, 1590, 1535 cm⁻¹; ¹H NMR (600 MHz, CDCl₃) δ 8.47 (br s, 1H), 7.96 (d, *J* = 8.4 Hz, 1H), 7.55 (br d, *J* = 6.6 Hz, 1H), 7.39 (dd, *J* = 7.2, 7.2 Hz, 1H), 7.23 (dd, *J* = 7.2, 7.2 Hz, 1H), 7.14 (d, *J* = 7.8 Hz, 1H), 7.06 (dd, *J* = 7.2, 7.2 Hz, 2H), 6.78 (br s, 1H), 5.68 (s, 1H), 4.63 (br s, 1H), 4.16 (m, 1H), 3.75 (br s, 1H), 3.62-3.52 (m, 6H), 3.08 (m, 1H), 3.01 (m, 1H), 2.33 (br s, 1H), 2.14 (br d, *J* = 10.2 Hz, 1H), 1.97 (m, 4H), 1.84-1.74 (m, 5H), 1.65 (m, 1H), 1.40 (m, 4H); ¹³C NMR (150.9 MHz, CDCl₃) ppm 169.9, 167.4, 157.9, 153.9, 149.4, 137.5, 132.8, 130.2, 128.7, 128.3, 127.6, 126.7, 126.3, 124.8, 119.8, 118.6, 91.8, 57.4, 53.3, 52.0, 48.5, 45.4, 33.1, 32.0, 25.8, 25.6, 25.1, 24.4; HRMS (ESI): Exact mass calcd for C₃₁H₃₈N₅O₂ [M+H]⁺ 512.3026, found 512.3005.

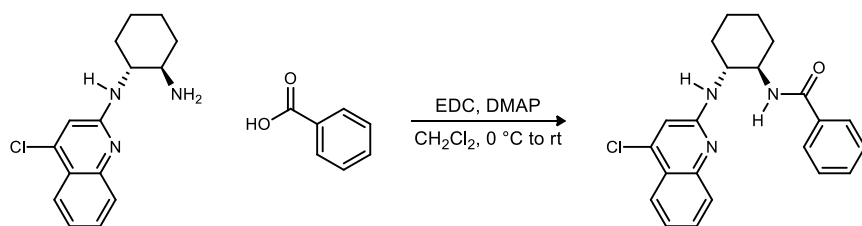


***N*-((1*R*,2*R*)-2-((4-Chloroquinolin-2-yl)amino)cyclohexyl)-3,5-bis(trifluoromethyl)benzamide (80a).** To a flame dried flask equipped with a stir bar was added the amine (200 mg, 725 μmol), the carboxylic acid (187 mg, 725 μmol), and dichloromethane (4 mL). The resulting solution was chilled to 0 °C and EDC (181 mg, 943 μmol) and DMAP (9.00 mg, 72.5 μmol) were added. The reaction mixture was stirred and allowed to gradually warm to room temperature. After 20 h, the reaction mixture was diluted with water and extracted with CH₂Cl₂. The combined organic layers were washed once with water, dried over MgSO₄, and concentrated. Flash column chromatography of the residue (SiO₂, 5-40% ethyl acetate in hexanes) afforded the desired amide as a white amorphous solid (291 mg, 78%). $[\alpha]_D^{20} +291$ (*c* 1.11, CHCl₃); *R_f* = 0.43 (30% EtOAc/hexanes); IR (film) 3335, 2937, 2861, 1654, 1608, 1536 cm⁻¹; ¹H NMR (600 MHz, CDCl₃) δ 8.60 (br d, *J* = 5.4 Hz, 1H), 7.94 (s, 2H), 7.93 (dd, *J* = 9.0, 0.6 Hz, 1H), 7.74 (s, 1H), 7.61 (d, 7.8 Hz, 1H), 7.55 (ddd, *J* = 7.8, 7.8, 0.6 Hz, 1H), 7.29 (ddd, *J* = 7.8, 7.8, 0.6 Hz, 1H), 6.71 (s, 1H), 4.70 (d, *J* = 7.2 Hz, 1H), 4.26 (m, 1H), 3.86 (m, 1H), 2.46 (m, 1H), 2.12 (m, 1H), 1.90 (br dd, *J* = 5.4, 1.8 Hz, 1H), 1.83 (br s, 1H), 1.47 (m, 4H); ¹³C NMR (150.9 MHz, CDCl₃) ppm 164.9, 156.8, 147.6, 143.3, 137.0, 131.7 (q, *J_{FC}* = 34.0 Hz), 131.2, 127.1, 125.7, 124.5 (q, *J_{FC}* = 3.5 Hz), 124.1, 123.4, 122.7

(q, $J_{FC} = 273.0$ Hz), 121.7, 112.1, 58.9, 53.4, 33.2, 32.1, 25.3, 24.3; HRMS (ESI): Exact mass calcd for $C_{24}H_{21}ClF_6N_3O$ $[M+H]^+$ 516.1278, found 516.1254.

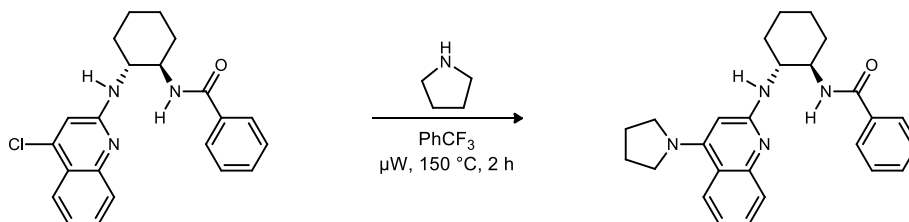


***N*-((1*R*,2*R*)-2-((4-(Pyrrolidin-1-yl)quinolin-2-yl)amino)cyclohexyl)-3,5-bis(trifluoromethyl)benzamide (78a).** A 2-5 mL microwave vial was charged with the 4-chloroquinoline (291 mg, 564 μ mol), pyrrolidine (185 μ L, 2.26 mmol), and trifluorotoluene (3.52 mL). This suspension was heated at 150 °C and stirred in the microwave for 90 min. The reaction was concentrated and purified by flash column chromatography (1-10% methanol in dichloromethane w/ 1% AcOH) to provide a yellow oil. This material was diluted with dichloromethane and washed with 6 M aq NaOH. The organic layers were combined and washed twice more with 3 M aq NaOH. The combined organic layers were dried over $MgSO_4$ and concentrated to afford a white amorphous solid (215 mg, 69%). $[\alpha]_D^{20} +184$ (c 0.93, $CHCl_3$); $R_f = 0.15$ (5% MeOH/1% AcOH/ CH_2Cl_2); IR (film) 3343, 2935, 2861, 1655, 1589, 1531 cm^{-1} ; 1H NMR (600 MHz, $CDCl_3$) δ 9.52 (d, $J = 4.2$ Hz, 1H), 7.98 (s, 2H), 7.96 (dd, $J = 8.4, 0.6$ Hz, 1H), 7.73 (s, 1H), 7.51 (d, $J = 8.4$ Hz, 1H), 7.39 (ddd, $J = 8.4, 8.4, 1.2$ Hz, 1H), 7.07 (ddd, $J = 8.4, 7.2, 1.2$ Hz, 1H), 5.65 (s, 1H), 4.34 (br s, 1H), 4.21 (m, 1H), 3.73 (m, 1H), 3.55 (m, 4H), 2.51 (d, $J = 12.0$ Hz, 1H), 2.07 (m, 1H), 1.98 (m, 4H), 1.87 (d, $J = 4.8$ Hz, 1H), 1.81 (d, $J = 6.0$ Hz, 1H), 1.44 (m, 4H); ^{13}C NMR (150.9 MHz, $CDCl_3$) ppm 165.2, 158.3, 154.0, 149.0, 137.6, 131.5 (q, $J_{FC} = 33.7$ Hz), 129.3, 127.3, 126.1, 124.9, 124.2, 122.8 (q, $J = 273.1$ Hz), 120.3, 118.6, 91.2, 59.6, 53.1, 51.9, 33.3, 31.9, 25.8, 25.5, 24.4; HRMS (ESI) Exact mass calcd for $C_{28}H_{29}F_6N_4O$ $[M+H]^+$ 551.2246, found 551.2237.



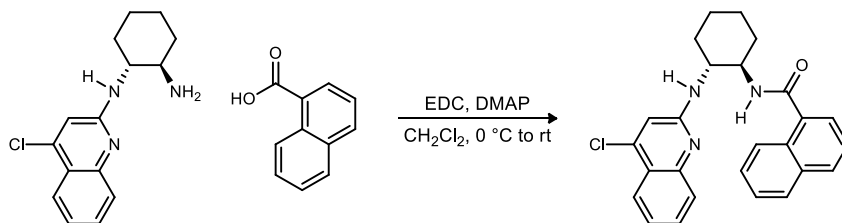
***N*-((1*R*,2*R*)-2-((4-Chloroquinolin-2-yl)amino)cyclohexyl)benzamide (80b).** To a flame dried flask equipped with a stir bar was added the amine (60.0 mg, 218 μ mol), benzoic acid (26.6 mg,

218 μmol), and dichloromethane (2 mL). The resulting solution was chilled to 0 °C and EDC (54.3 mg, 283 μmol) and DMAP (2.70 mg, 22.0 μmol) were added. The reaction mixture was stirred and allowed to gradually warm to room temperature. After 30 h, the reaction mixture was diluted with water and extracted with CH_2Cl_2 . The combined organic layers were washed once with water, dried over MgSO_4 , and concentrated. Flash column chromatography of the residue (SiO_2 , 10-50% ethyl acetate in hexanes) afforded the desired amide as a white amorphous solid (65.2 mg, 79%). $[\alpha]_D^{20} +433$ (c 0.42, CHCl_3); $R_f = 0.23$ (30% EtOAc/hexanes); IR (film) 3305, 3061, 2933, 2857, 1643, 1608, 1574, 1537 cm^{-1} ; ^1H NMR (600 MHz, CDCl_3) δ 8.18 (br d, $J = 5.4$ Hz, 1H), 7.94 (dd, $J = 8.4, 1.2$ Hz, 1H), 7.74 (d, $J = 8.4$ Hz, 1H), 7.62 (ddd, $J = 8.4, 7.2, 1.8$ Hz, 1H), 7.52 (dd, $J = 7.8, 0.6$ Hz, 2H), 7.30 (ddd, $J = 8.4, 6.6, 1.2$ Hz, 1H), 7.25 (dd, $J = 7.2, 7.2$ Hz, 1H), 7.04 (d, $J = 7.8$ Hz, 2H), 6.68 (s, 1H), 5.04 (br d, $J = 7.8$ Hz, 1H), 4.28 (m, 1H), 3.86 (m, 1H), 2.46 (d, $J = 12.0$ Hz, 1H), 2.16 (m, 1H), 1.88 (br dd, $J = 6.0, 1.8$ Hz, 1H), 1.82 (br dd, $J = 4.8, 1.8$ Hz, 1H), 1.48 (m, 4H); ^{13}C NMR (150.9 MHz, CDCl_3) ppm 167.3, 156.9, 148.1, 142.3, 134.2, 130.9, 130.6, 128.1, 126.8, 126.1, 124.2, 122.9, 121.8, 112.5, 58.0, 53.4, 33.1, 32.4, 25.3, 24.5; HRMS (ESI): Exact mass calcd for $\text{C}_{22}\text{H}_{23}\text{ClN}_3\text{O}$ $[\text{M}+\text{H}]^+$ 380.1530, found 380.1543.

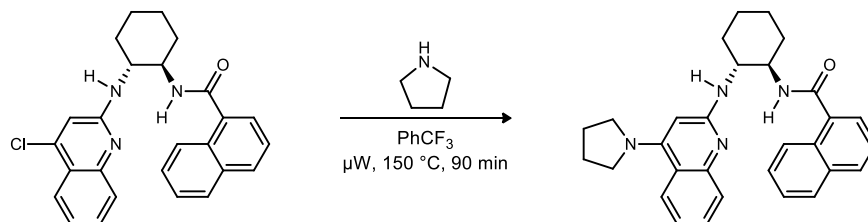


***N*-((1*R*,2*R*)-2-((4-(pyrrolidin-1-yl)quinolin-2-yl)amino)cyclohexyl)benzamide (78b)**. A 0.5-2 mL microwave vial was charged with the 4-chloroquinoline (48.0 mg, 128 μmol), pyrrolidine (42.2 μL , 514 μmol), and trifluorotoluene (1.5 mL). This suspension was heated at 150 °C and stirred in the microwave for 2 h. The reaction was concentrated and purified by flash column chromatography (1-10% methanol in dichloromethane w/ 1% AcOH) to provide a yellow oil. This material was diluted with dichloromethane and washed with 6 M aq NaOH. The organic layers were combined and washed twice more with 3 M aq NaOH. The combined organic layers were dried over MgSO_4 and concentrated to afford a light yellow amorphous solid (25.6 mg, 48%). $[\alpha]_D^{20} +225$ (c 0.47, CHCl_3); $R_f = 0.12$ (5% MeOH/1% AcOH/ CH_2Cl_2); IR (film) 3325, 2930, 2857, 1644, 1588, 1533 cm^{-1} ; ^1H NMR (600 MHz, CDCl_3) δ 8.89 (br s, 1H), 7.98 (d, $J = 7.8$ Hz, 1H), 7.68 (d, $J = 7.8$ Hz, 1H), 7.52 (d, $J = 7.8$ Hz, 2H), 7.48 (ddd, $J = 8.4, 7.2, 1.2$ Hz, 1H), 7.21

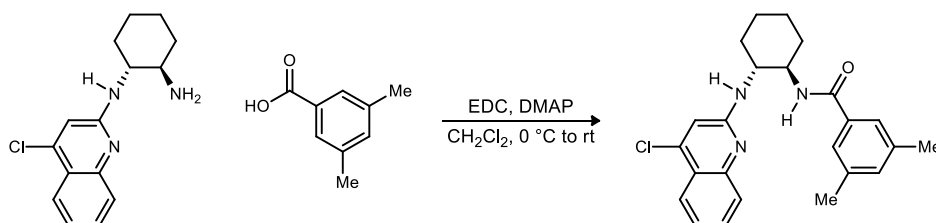
(dd, $J = 7.8, 7.8$ Hz, 1H), 7.10 (ddd, $J = 8.4, 7.2, 1.2$ Hz, 1H), 6.99 (dd, $J = 7.8, 7.8$ Hz, 2H), 5.61 (s, 1H), 4.52 (br s, 1H), 4.30 (m, 1H), 3.74 (m, 1H), 3.48 (m, 4H), 2.51 (d, $J = 12.0$ Hz, 1H), 2.09 (d, $J = 7.2$ Hz, 1H), 1.94 (m, 4H), 1.85 (d, $J = 3.6$ Hz, 1H), 1.78 (d, $J = 8.4$ Hz, 1H), 1.41 (m, 4H); ^{13}C NMR (150.9 MHz, CDCl_3) ppm 167.2, 158.3, 153.8, 149.4, 134.6, 130.5, 128.8, 127.9, 127.0, 126.5, 125.0, 119.9, 118.8, 91.8, 59.0, 52.5, 51.9, 33.3, 32.1, 25.8, 25.5, 24.5; HRMS (ESI): Exact mass calcd for $\text{C}_{26}\text{H}_{31}\text{N}_4\text{O}$ $[\text{M}+\text{H}]^+$ 415.2499, found 415.2480.



***N*-((1*R*,2*R*)-2-((4-Chloroquinolin-2-yl)amino)cyclohexyl)-1-naphthamide (80c).** To a flame dried flask equipped with a stir bar was added the amine (60.0 mg, 218 μmol), the carboxylic acid (37.5 mg, 218 μmol), and dichloromethane (2 mL). The resulting suspension was chilled to 0 $^{\circ}\text{C}$ and EDC (54.3 mg, 283 μmol) and DMAP (2.70 mg, 22.0 μmol) were added. The reaction mixture was stirred and allowed to gradually warm to room temperature. After 30 h, the reaction mixture was diluted with water and extracted with CH_2Cl_2 . The combined organic layers were washed once with water, dried over MgSO_4 , and concentrated. Flash column chromatography of the residue (SiO_2 , 10-40% ethyl acetate in hexanes) afforded the desired amide as a white solid (48.4 mg, 52%). Mp 208.0-210.0 $^{\circ}\text{C}$; $[\alpha]_D^{20} +292$ (c 0.49, CHCl_3); $R_f = 0.40$ (40% EtOAc/hexanes); IR (film) 3296, 3058, 2928, 2855, 2362, 1642, 1607, 1575, 1536 cm^{-1} ; ^1H NMR (600 MHz, CDCl_3) δ 8.17 (d, $J = 8.4$ Hz, 1H), 7.89 (dd, $J = 8.4, 0.6$ Hz, 1H), 7.80 (br d, $J = 6.6$ Hz, 1H), 7.68 (d, $J = 7.8$ Hz, 1H), 7.64 (d, $J = 8.4$ Hz, 1H), 7.36 (dddd, $J = 9.0, 6.6, 4.8, 1.2$ Hz, 2H), 7.32 (ddd, $J = 8.4, 6.6, 1.2$, 1H), 7.21 (m, 2H), 6.97 (dd, $J = 6.6, 0.6$ Hz, 1H), 6.89 (dd, $J = 8.4, 8.4$ Hz, 1H), 6.72 (s, 1H), 5.07 (d, $J = 7.2$ Hz, 1H), 4.22 (m, 1H), 4.02 (m, 1H), 2.50 (br d, $J = 11.4$ Hz, 1H), 2.20 (br m, 1H), 1.87 (m, 2H), 1.48 (m, 4H); ^{13}C NMR (150.9 MHz, CDCl_3) ppm 169.9, 156.5, 147.9, 142.9, 134.4, 133.4, 130.4, 130.0, 129.9, 128.0, 126.6, 125.98, 125.97, 125.2, 124.5, 124.4, 123.8, 122.7, 121.5, 112.2, 57.1, 54.0, 33.0, 32.6, 25.2, 24.6; HRMS (ESI): Exact mass calcd for $\text{C}_{26}\text{H}_{25}\text{ClN}_3\text{O}$ $[\text{M}+\text{H}]^+$ 430.1686, found 430.1673.

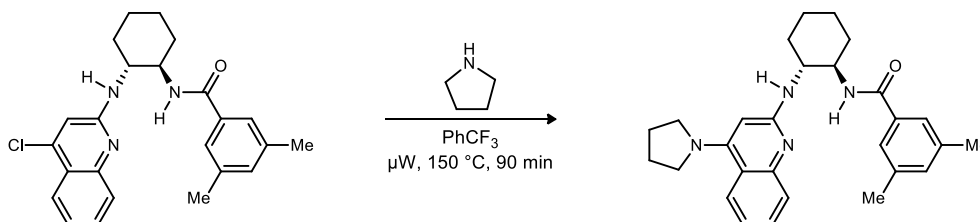


***N*-((1*R*,2*R*)-2-((4-(Pyrrolidin-1-yl)quinolin-2-yl)amino)cyclohexyl)-1-naphthamide (78c).** A 0.5-2 mL microwave vial was charged with the 4-chloroquinoline (30.0 mg, 69.8 μ mol), pyrrolidine (23.0 μ L, 279 μ mol), and trifluorotoluene (446 μ L). This suspension was heated at 150 $^{\circ}$ C and stirred in the microwave for 90 min. The reaction was concentrated and purified by flash column chromatography (1-10% methanol in dichloromethane w/ 1% AcOH) to provide a light yellow oil. This material was diluted with dichloromethane and washed with 6 M aq NaOH. The organic layers were combined and washed three times more with 3 M aq NaOH. The combined organic layers were dried (MgSO_4) and concentrated to afford a tan amorphous solid (17.6 mg, 54%). $[\alpha]_D^{20} +172$ (c 0.79, CHCl_3); $R_f = 0.39$ (5% MeOH/1% AcOH/ CH_2Cl_2); IR (film) 3329, 3047, 2930, 2857, 1643, 1588, 1532 cm^{-1} ; ^1H NMR (600 MHz, CDCl_3) δ 8.65 (br s, 1H), 8.33 (dd, $J = 9.0, 1.8$ Hz, 1H), 7.94 (d, $J = 8.4$ Hz, 1H), 7.69 (dd, $J = 9.0, 1.8$ Hz, 1H), 7.60 (d, $J = 8.4$ Hz, 1H), 7.36 (m, 2H), 7.20 (br dd, $J = 7.2, 7.2$ Hz, 1H), 7.14 (br s, 1H), 7.02 (dd, $J = 7.2, 7.2$ Hz, 1H), 6.81 (br s, 1H), 6.70 (br s, 1H), 5.70 (s, 1H), 4.60 (br s, 1H), 4.26 (br s, 1H), 3.89 (br d, $J = 5.4$ Hz, 1H), 3.51 (br m, 4H), 2.56 (br d, $J = 7.8$ Hz, 1H), 2.14 (br d, $J = 5.4$ Hz, 1H), 1.96 (m, 4H), 1.88 (br s, 1H), 1.82 (br s, 1H), 1.49 (m, 4H); ^{13}C NMR (150.9 MHz, CDCl_3) ppm 169.7, 157.9, 154.0, 149.1, 134.4, 133.5, 130.2, 129.6, 128.6, 127.9, 126.4, 125.8, 125.7, 124.9, 124.7, 124.4, 119.8, 118.5, 91.7, 58.5, 52.7, 51.9, 33.3, 32.4, 25.8, 25.4, 24.6; HRMS (ESI): Exact mass calcd for $\text{C}_{30}\text{H}_{33}\text{N}_4\text{O}$ $[\text{M}+\text{H}]^+$ 465.2654, found 465. 2672.



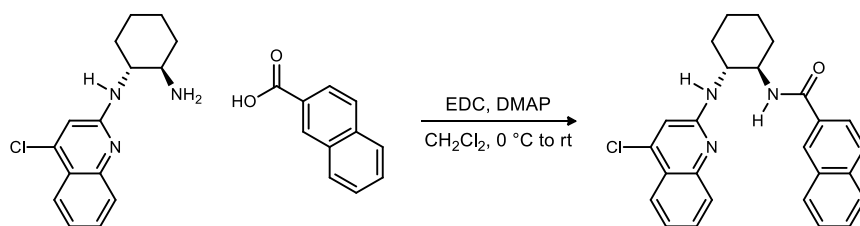
***N*-((1*R*,2*R*)-2-((4-Chloroquinolin-2-yl)amino)cyclohexyl)-3,5-dimethylbenzamide (80d).** To a flame dried flask equipped with a stir bar was added the amine (60.0 mg, 218 μ mol), the carboxylic acid (32.7 mg, 218 μ mol), and dichloromethane (2 mL). The resulting solution was chilled to 0 $^{\circ}$ C

and EDC (54.3 mg, 283 μmol) and DMAP (2.70 mg, 22.0 μmol) were added. The reaction mixture was stirred and allowed to gradually warm to room temperature. After 30 h, the reaction mixture was diluted with water and extracted with CH_2Cl_2 . The combined organic layers were washed once with water, dried over MgSO_4 , and concentrated. Flash column chromatography of the residue (SiO_2 , 10-40% ethyl acetate in hexanes) afforded the desired amide as a white amorphous solid (66.9 mg, 75%). $[\alpha]_D^{20} +387$ (*c* 0.45, CHCl_3); $R_f = 0.34$ (40% EtOAc/hexanes); IR (film) 3303, 3060, 2929, 2857, 2361, 1643, 1605, 1574, 1536 cm^{-1} ; $^1\text{H NMR}$ (600 MHz, CDCl_3) δ 8.00 (br d, $J = 6.6$ Hz, 1H), 7.93 (dd, $J = 7.8, 0.6$ Hz, 1H), 7.72 (d, $J = 8.4$ Hz, 1H), 7.57 (ddd, $J = 8.4, 7.2, 1.2$ Hz, 1H), 7.27 (ddd, $J = 7.8, 7.8, 0.6$ Hz, 1H), 7.02 (s, 2H), 6.87 (s, 1H), 6.69 (s, 1H), 5.22 (d, $J = 7.8$ Hz, 1H), 4.33 (m, 1H), 3.87 (m, 1H), 2.44 (d, $J = 13.2$ Hz, 1H), 2.15 (m, 1H), 1.94 (s, 6H), 1.89 (dd, $J = 6.0, 2.4$ Hz, 1H), 1.83 (m, 1H), 1.57-1.36 (m, 4H); $^{13}\text{C NMR}$ (150.9 MHz, CDCl_3) ppm 167.9, 157.0, 148.2, 142.7, 137.9, 134.3, 132.6, 130.7, 126.2, 124.5, 124.1, 122.8, 121.7, 112.6, 58.0, 53.0, 33.0, 32.4, 25.4, 24.6, 20.8; HRMS (ESI) Exact mass calcd for $\text{C}_{24}\text{H}_{27}\text{N}_3\text{O}$ $[\text{M}+\text{H}]^+$ 408.1843, found 408.1847.

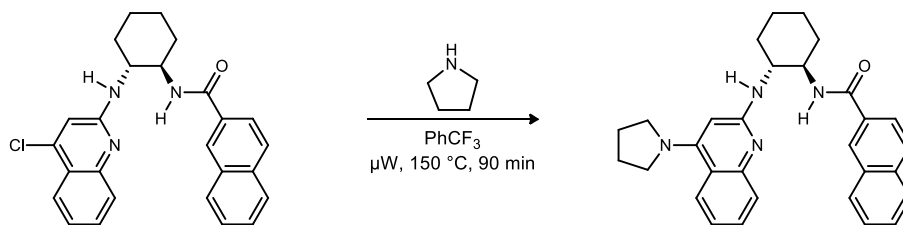


3,5-Dimethyl-N-((1R,2R)-2-((4-(pyrrolidin-1-yl)quinolin-2-yl)amino)cyclohexyl)benzamide (78d). A 0.5-2 mL microwave vial was charged with the 4-chloroquinoline (40.0 mg, 98.1 μmol), pyrrolidine (32.0 μL , 392 μmol), and trifluorotoluene (620 μL). This suspension was heated at 150 $^\circ\text{C}$ and stirred in the microwave for 90 min. The reaction was concentrated and purified by flash column chromatography (1-10% methanol in dichloromethane w/ 1% AcOH) to provide a yellow oil. This material was diluted with dichloromethane and washed with 6 M aq NaOH. The organic layers were combined and washed twice more with 3 M aq NaOH. The combined organic layers were dried over MgSO_4 and concentrated to afford a yellow amorphous solid (23.7 mg, 55%). $[\alpha]_D^{20} +238$ (*c* 0.75, CHCl_3); $R_f = 0.51$ (10% MeOH/1% AcOH/ CH_2Cl_2); IR (film) 3320, 2929, 2858, 2361, 1643, 1590, 1533 cm^{-1} ; $^1\text{H NMR}$ (600 MHz, CDCl_3) δ 8.68 (br s, 1H), 7.98 (d, $J = 8.4$ Hz, 1H), 7.66 (d, $J = 7.8$ Hz, 1H), 7.43 (ddd, $J = 7.8, 7.8, 0.6$ Hz, 1H), 7.08 (ddd, $J = 8.4, 8.4, 1.2$ Hz, 1H), 7.05 (s, 2H), 6.85 (s, 1H), 5.64 (s, 1H), 4.49 (br s, 1H), 4.33 (br m, 1H), 3.74 (m, 1H),

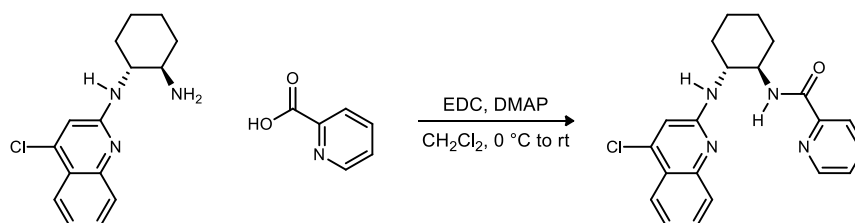
3.50 (br m, 4H), 2.49 (d, $J = 11.4$ Hz, 1H), 2.07 (br d, $J = 2.4$ Hz, 1H), 1.95 (br m, 4H), 1.91 (s, 6H), 1.84 (br d, $J = 3.0$ Hz, 1H), 1.78 (br d, $J = 6.0$ Hz, 1H), 1.46-1.35 (m, 4H); ^{13}C NMR (150.9 MHz, CDCl_3) ppm 167.8, 158.3, 153.9, 149.5, 137.7, 134.8, 132.2, 129.0, 126.7, 125.0, 124.7, 120.0, 118.9, 91.9, 58.9, 52.3, 51.9, 33.4, 32.2, 25.8, 25.6, 24.5, 20.7; HRMS (ESI) Exact mass calcd for $\text{C}_{28}\text{H}_{35}\text{N}_4\text{O}$ $[\text{M}+\text{H}]^+$ 443.2811, found 443.2813.



***N*-((1*R*,2*R*)-2-((4-Chloroquinolin-2-yl)amino)cyclohexyl)-2-naphthamide (80e).** To a flame dried flask equipped with a stir bar was added the amine (61.0 mg, 221 μmol), the carboxylic acid (38.1 mg, 221 μmol), and dichloromethane (2 mL). The resulting suspension was chilled to 0 $^{\circ}\text{C}$ and EDC (55.2 mg, 288 μmol) and DMAP (2.70 mg, 22.0 μmol) were added. The reaction mixture was stirred and allowed to gradually warm to room temperature. After 30 h, the reaction mixture was diluted with water and extracted with CH_2Cl_2 . The combined organic layers were washed once with water, dried (MgSO_4), and concentrated. Flash column chromatography of the residue (SiO_2 , 10-40% ethyl acetate in hexanes) afforded the desired amide as a white solid (68.8 mg, 72%). $[\alpha]_D^{20} +318$ (c 0.42, CHCl_3); $R_f = 0.40$ (40% EtOAc/hexanes); IR (film) 3305, 3058, 2932, 2857, 2361, 1643, 1607, 1572, 1537 cm^{-1} ; ^1H NMR (600 MHz, CDCl_3) δ 8.36 (br d, $J = 6.6$ Hz, 1H), 7.96 (dd, $J = 8.4, 1.2$ Hz, 1H), 7.79 (d, $J = 8.4$ Hz, 1H), 7.76 (s, 1H), 7.69 (dd, $J = 9.0, 2.4$ Hz, 2H), 7.62 (ddd, $J = 8.4, 7.2, 1.8$ Hz, 1H), 7.57 (d, $J = 8.4$ Hz, 1H), 7.41 (ddd, $J = 7.8, 7.2, 1.2$ Hz, 1H), 7.33 (ddd, $J = 8.4, 8.4, 1.2$ Hz, 1H), 7.29 (ddd, $J = 7.8, 7.8, 0.6$ Hz, 1H), 7.05 (d, $J = 8.4$ Hz, 1H), 6.71 (s, 1H), 5.15 (d, $J = 7.8$ Hz, 1H), 4.37 (m, 1H), 3.93 (m, 1H), 2.53 (d, $J = 12.0$ Hz, 1H), 2.17 (br m, 1H), 1.90 (dd, $J = 6.0, 1.8$ Hz, 1H), 1.84 (dd, $J = 5.4, 1.2$ Hz, 1H), 1.58-1.42 (m, 4H); ^{13}C NMR (150.9 MHz, CDCl_3) ppm 167.5, 157.0, 148.1, 142.9, 134.4, 132.2, 131.6, 130.8, 128.8, 128.0, 127.4, 127.2, 126.8, 126.2, 126.1, 124.3, 123.9, 122.9, 121.8, 112.6, 58.4, 53.2, 33.1, 32.5, 25.4, 24.5; HRMS (ESI): Exact mass calcd for $\text{C}_{26}\text{H}_{25}\text{ClN}_3\text{O}$ $[\text{M}+\text{H}]^+$ 430.1686, found 430.1668.

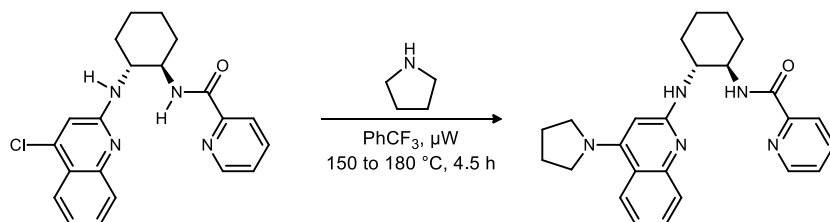


***N*-((1*R*,2*R*)-2-((4-(Pyrrolidin-1-yl)quinolin-2-yl)amino)cyclohexyl)-2-naphthamide (78e).** A 0.5-2 mL microwave vial was charged with the 4-chloroquinoline (35.0 mg, 81.4 μ mol), pyrrolidine (27.0 μ L, 326 μ mol), and trifluorotoluene (520 μ L). This suspension was heated at 150 $^{\circ}$ C and stirred in the microwave for 90 min. The reaction was concentrated and purified by flash column chromatography (1-10% methanol in dichloromethane w/ 1% AcOH) to provide a light yellow oil. This material was diluted with dichloromethane and washed with 6 M aq NaOH. The organic layers were combined and washed three times more with 3 M aq NaOH. The combined organic layers were dried (MgSO_4) and concentrated to afford a light yellow amorphous solid (21.2 mg, 56%). $[\alpha]_D^{20} +150$ (c 0.91, CHCl_3); $R_f = 0.39$ (5% MeOH/1% AcOH/ CH_2Cl_2); IR (film) 3324, 3054, 2930, 2857, 2361, 1644, 1588, 1533, 1502 cm^{-1} ; ^1H NMR (600 MHz, CDCl_3) δ 9.00 (br s, 1H), 8.02 (d, $J = 8.4$ Hz, 1H), 7.76 (s, 1H), 7.73 (m, 2H), 7.68 (d, $J = 8.4$ Hz, 1H), 7.53 (d, $J = 8.4$ Hz, 1H), 7.48 (ddd, $J = 8.4, 7.2, 1.2$ Hz, 1H), 7.39 (ddd, $J = 7.8, 7.8, 1.2$ Hz, 1H), 7.26 (dd, $J = 7.2, 7.2$ Hz, 1H), 7.15 (dd, $J = 7.2, 7.2$ Hz, 1H), 6.95 (d, $J = 7.8$ Hz, 1H), 5.61 (s, 1H), 4.62 (br s, 1H), 4.39 (m, 1H), 3.82 (m, 1H), 3.42 (m, 4H), 2.55 (br d, $J = 12.0$ Hz, 1H), 2.12 (d $J = 10.2$ Hz, 1H), 1.86 (m, 5H), 1.82 (br m, 1H), 1.56-1.41 (m, 4H); ^{13}C NMR (150.9 MHz, CDCl_3) ppm 167.4, 158.5, 153.8, 149.5, 134.3, 132.4, 132.0, 129.1, 129.0, 127.7, 127.2, 126.9, 126.7, 125.8, 125.2, 124.3, 120.0, 118.9, 91.8, 59.3, 52.4, 51.9, 33.3, 32.7, 25.7, 25.6, 24.6; HRMS (ESI): Exact mass calcd for $\text{C}_{30}\text{H}_{33}\text{N}_4\text{O}$ $[\text{M}+\text{H}]^+$ 465.2654, found 465.2646.



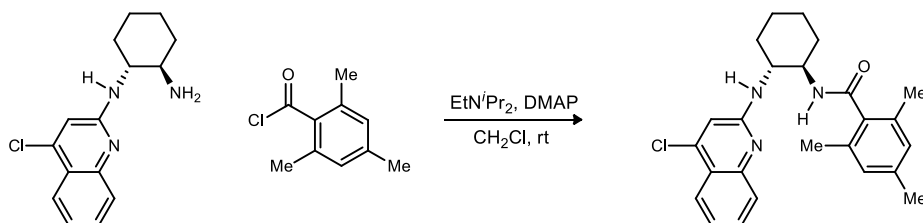
***N*-((1*R*,2*R*)-2-((4-Chloroquinolin-2-yl)amino)cyclohexyl)picolinamide (80f).** To a flame dried flask equipped with a stir bar was added the amine (40.0 mg, 145 μ mol), picolinic acid (17.9 mg, 145 μ mol), and dichloromethane (1 mL). The resulting solution was chilled to 0 $^{\circ}$ C and EDC (36.2

mg, 189 μmol) and DMAP (1.80 mg, 15.0 μmol) were added. The reaction mixture was stirred and allowed to gradually warm to room temperature. After 14 h, the reaction mixture was diluted with water and extracted with CH_2Cl_2 . The combined organic layers were washed once with water, dried (MgSO_4), and concentrated. Flash column chromatography of the residue (SiO_2 , 40-80% ethyl acetate in hexanes) afforded the desired amide as a viscous yellow oil (29.7 mg, 54%). $[\alpha]_D^{20} +158$ (*c* 0.59, CHCl_3); $R_f = 0.14$ (20% EtOAc/hexanes); IR (film) 3319, 2932, 2857, 1658, 1609, 1570, 1534 cm^{-1} ; ^1H NMR (600 MHz, CDCl_3) δ 8.87 (br d, $J = 7.2$ Hz, 1H), 8.04 (dd, $J = 6.6, 0.6$ Hz, 1H), 8.04 (s, 1H), 7.86 (dd, $J = 8.4, 1.2$ Hz, 1H), 7.79 (d, $J = 7.8$ Hz, 1H), 7.68 (ddd, $J = 7.2, 7.2, 1.2$ Hz, 1H), 7.57 (ddd, $J = 8.4, 7.2, 1.2$ Hz, 1H), 7.23 (ddd, $J = 8.4, 7.2, 1.2$ Hz, 1H), 7.17 (m, 1H), 6.64 (s, 1H), 5.17 (d, $J = 7.2$ Hz, 1H), 4.26 (dddd, $J = 11.4, 11.4, 7.8, 4.2$ Hz, 1H), 3.94 (dddd, $J = 10.8, 10.8, 7.8, 3.6$ Hz, 1H), 2.28 (m, 2H), 1.85 (dd, $J = 12.0, 1.8$ Hz, 2H), 1.57-1.44 (m, 3H), 1.43-1.34 (m, 1H); ^{13}C NMR (100.6 MHz, CDCl_3) ppm 165.0, 156.3, 149.7, 148.6, 147.7, 142.2, 136.8, 130.0, 126.8, 125.7, 123.7, 122.4, 121.8, 121.4, 112.1, 55.5, 54.6, 32.7, 32.4, 24.9, 24.8; HRMS (ESI) Exact mass calcd for $\text{C}_{21}\text{H}_{22}\text{ClN}_4\text{O}$ $[\text{M}+\text{H}]^+$ 381.1482, found 381.1495.



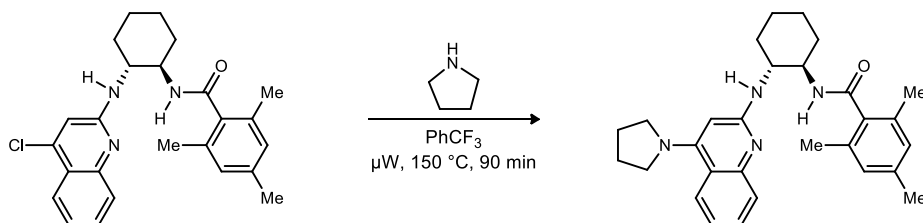
***N*-((1*R*,2*R*)-2-((4-(Pyrrolidin-1-yl)quinolin-2-yl)amino)cyclohexyl)picolinamide (78f).** A 2-5 mL microwave vial was charged with the 4-chloroquinoline (50.0 mg, 131 μmol), pyrrolidine (130 μL , 1.58 mmol), and trifluorotoluene (800 μL). This suspension was heated at 150 $^\circ\text{C}$ and stirred in the microwave for 3 h. More pyrrolidine (65.0 μL , 788 μmol) was added and the reaction mixture was heated to 180 $^\circ\text{C}$ and stirred in the microwave for an additional 1.5 h. The reaction was concentrated and purified by flash column chromatography (1-10% methanol in dichloromethane w/ 1% AcOH) to provide a dark-yellow oil. This material was diluted with dichloromethane and washed twice with 6 M aq NaOH. The organic layers were combined and washed twice more with 3 M aq NaOH. The combined organic layers were dried over MgSO_4 and concentrated to afford an off-white amorphous solid (24.7 mg, 45%). $[\alpha]_D^{20} +144$ (*c* 0.49, CHCl_3); $R_f = 0.49$ (10% MeOH/1% AcOH/ CH_2Cl_2); IR (film) 3337, 2930, 2857, 1657, 1588, 1531 cm^{-1} ; ^1H NMR (400 MHz, CDCl_3) δ 9.36 (br d, $J = 6.8$ Hz, 1H), 8.00 (d, $J = 8.0$ Hz, 1H), 7.97 (br d, J

= 4.4 Hz, 1H), 7.89 (d, $J = 8.4$ Hz, 1H), 7.80 (d, $J = 8.4$ Hz, 1H), 7.63 (ddd, $J = 8.0, 8.0, 1.6$ Hz, 1H), 7.46 (ddd, $J = 8.0, 8.0, 1.2$ Hz, 1H), 7.13 (dd, $J = 6.4, 4.8$ Hz, 1H), 7.04 (br ddd, $J = 8.0, 8.0, 1.2$ Hz, 1H), 5.61 (s, 1H), 4.52 (br d, $J = 6.8$ Hz, 1H), 4.32 (dddd, $J = 11.2, 11.2, 8.0, 4.0$ Hz, 1H), 3.84 (br dddd, $J = 10.8, 10.8, 7.6, 4.4$ Hz, 1H), 3.45 (br m, 4H), 2.33 (m, 1H), 2.22 (d, $J = 12.4$ Hz, 1H), 1.92 (m, 4H), 1.81 (br s, 2H), 1.54-1.33 (m, 4H); ^{13}C NMR (125.8 MHz, CDCl_3) ppm 164.9, 157.8, 153.7, 150.2, 150.0, 147.8, 136.5, 128.2, 127.4, 125.3, 124.6, 121.6, 119.4, 118.6, 92.0, 56.7, 53.3, 51.8, 33.2, 32.2, 25.7, 25.2, 24.7; HRMS (ESI) Exact mass calcd for $\text{C}_{25}\text{H}_{30}\text{N}_5\text{O}$ $[\text{M}+\text{H}]^+$ 416.2450, found 416.2432.



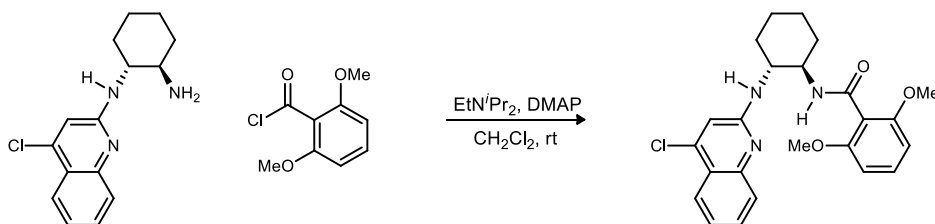
***N*-((1*R*,2*R*)-2-((4-Chloroquinolin-2-yl)amino)cyclohexyl)-2,4,6-trimethylbenzamide (80g).**

To a flame dried flask equipped with a stir bar was added the amine (60.0 mg, 218 μmol) and dichloromethane (3 mL), immediately followed by the addition of *N,N*-diisopropyl ethylamine (45.0 μL , 261 μmol), the acid chloride (43.0 μL , 261 μmol), and DMAP (2.70 mg, 22.0 μmol). The reaction mixture was stirred at rt for 30 h, quenched with 1 M HCl and extracted with dichloromethane. The organic extracts were then washed with satd aq NaHCO_3 , extracted with dichloromethane, dried (MgSO_4), filtered and concentrated. Flash column chromatography of the residue (SiO_2 , 10-80% ethyl acetate in hexanes) afforded the desired amide as an off white solid (74.1 mg, 81%). Mp 261.0-264.0 $^\circ\text{C}$; $[\alpha]_D^{20}$ +193 (c 0.58, CHCl_3); $R_f = 0.46$ (40% EtOAc/hexanes); IR (film) 3250, 3101, 3059, 2930, 2856, 2363, 1642, 1608, 1540 cm^{-1} ; ^1H NMR (600 MHz, CDCl_3) δ 7.93 (dd, $J = 7.8, 1.8$ Hz, 1H), 7.38 (ddd, $J = 7.2, 7.2, 1.2$ Hz, 1H), 7.26 (br s, 1H), 7.22 (m, 2H), 6.71 (s, 1H), 6.56 (s, 2H), 5.25 (br d, $J = 6.0$ Hz, 1H), 4.05 (m, 1H), 3.94 (m, 1H), 2.36 (m, 1H), 2.26 (m, 1H), 2.14 (s, 3H), 1.98 (s, 6H), 1.83 (br m, 2H), 1.48-1.34 (m, 4H); ^{13}C NMR (150.9 MHz, CDCl_3) ppm 171.1, 156.1, 148.0, 142.6, 137.9, 134.9, 133.6, 130.2, 127.8, 126.0, 123.8, 122.6, 121.3, 112.1, 55.5, 54.6, 32.8, 32.5, 24.9, 24.6, 21.0, 18.6; HRMS (ESI): Exact mass calcd for $\text{C}_{25}\text{H}_{29}\text{ClN}_3\text{O}$ $[\text{M}+\text{H}]^+$ 422.1999, found 422.1983.



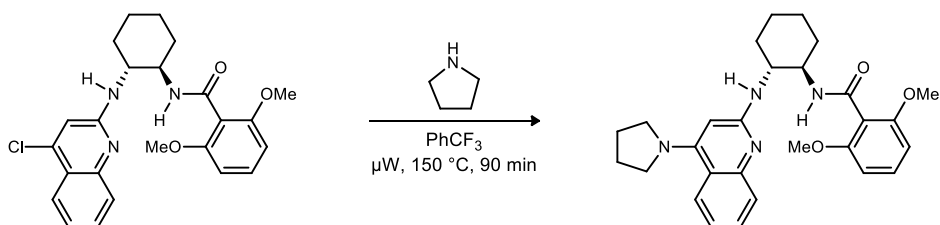
2,4,6-Trimethyl-N-((1R,2R)-2-((4-(pyrrolidin-1-yl)quinolin-2-yl)amino)cyclohexyl)

benzamide (78g). A 0.5-2 mL microwave vial was charged with the 4-chloroquinoline (40.0 mg, 94.8 μmol), pyrrolidine (31.0 μL , 379 μmol), and trifluorotoluene (680 μL). This suspension was heated at 150 $^{\circ}\text{C}$ and stirred in the microwave for 90 min. The reaction was concentrated and purified by flash column chromatography (1-10% methanol in dichloromethane w/ 1% AcOH) to provide a yellow oil. This material was diluted with dichloromethane and washed with 6 M aq NaOH. The organic layers were combined and washed four times more with 3 M aq NaOH. The combined organic layers were dried (MgSO_4) and concentrated to afford a tan foam (20.9 mg, 48%). $[\alpha]_D^{20} +120$ (c 0.43, CHCl_3); $R_f = 0.32$ (5% MeOH/1% AcOH/ CH_2Cl_2); IR (film) 3317, 2926, 2856, 2362, 1644, 1590, 1533 cm^{-1} ; ^1H NMR (600 MHz, CDCl_3) δ 8.55 (br s, 1H), 7.91 (d, $J = 7.8$ Hz, 1H), 7.12 (dd, $J = 6.6, 6.6$ Hz, 1H), 6.99 (dd, $J = 7.2, 7.2$ Hz, 1H), 6.90 (br d, $J = 7.2$ Hz, 1H), 6.47 (s, 2H), 5.68 (s, 1H), 4.57 (br s, 1H), 4.03 (br m, 1H), 3.78 (br m, 1H), 3.55 (br m, 2H), 3.50 (br m, 2H), 2.50 (br d, $J = 10.8$ Hz, 1H), 2.14 (br d, $J = 11.4$ Hz, 1H), 2.12 (s, 3H), 2.05-1.96 (m, 4H), 1.94 (s, 6H), 1.82 (br s, 1H), 1.78 (br s, 1H), 1.48-1.35 (m, 4H); ^{13}C NMR (150.9 MHz, CDCl_3) ppm 170.8, 157.7, 153.9, 149.0, 137.2, 135.4, 133.5, 128.4, 127.6, 126.1, 124.5, 119.6, 118.3, 91.8, 57.2, 53.4, 51.9, 33.2, 32.3, 25.8, 25.2, 24.4, 21.0, 18.6; HRMS (ESI): Exact mass calcd for $\text{C}_{29}\text{H}_{36}\text{N}_4\text{NaO}$ $[\text{M}+\text{Na}]^+$ 479.2787, found 479.2774.



N-((1R,2R)-2-((4-Chloroquinolin-2-yl)amino)cyclohexyl)-2,6-dimethoxybenzamide (80h). To a flame dried flask equipped with a stir bar was added the amine (60.0 mg, 218 μmol) and dichloromethane (3 mL), immediately followed by the addition of *N,N*-diisopropyl ethylamine (45.0 μL , 261 μmol), the acid chloride (52.4 mg, 261 μmol), and DMAP (2.70 mg, 22.0 μmol).

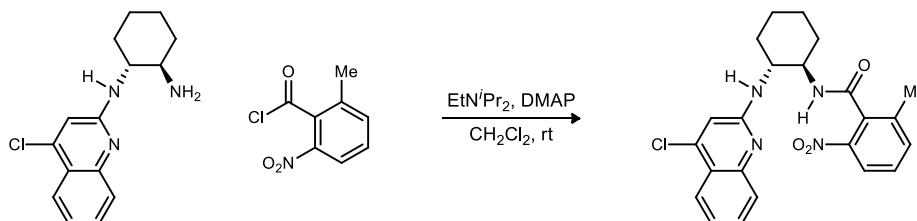
The reaction mixture was stirred at rt for 48 h, quenched with 1 M HCl and extracted with dichloromethane. The organic extracts were then washed with satd aq NaHCO₃, extracted with dichloromethane, dried (MgSO₄), filtered and concentrated. Flash column chromatography of the residue (SiO₂, 10-60% ethyl acetate in hexanes) afforded the desired amide as a white solid (68.3 mg, 71%). Mp 256.0-258.0 °C; $[\alpha]_D^{20} +166$ (*c* 0.56, CHCl₃); *R_f* = 0.16 (40% EtOAc/hexanes); IR (film) 3284, 3060, 2933, 2857, 2361, 1646, 1607, 1538 cm⁻¹; ¹H NMR (600 MHz, CDCl₃) δ 7.92 (d, *J* = 8.4 Hz, 1H), 7.42 (m, 2H), 7.21 (ddd, *J* = 8.4, 6.0, 2.4 Hz, 1H), 7.10 (dd, *J* = 8.4, 8.4 Hz, 1H), 6.78 (br d, *J* = 6.6 Hz, 1H), 6.75 (s, 1H), 6.32 (d, *J* = 8.4 Hz, 2H), 5.50 (d, *J* = 5.4 Hz, 1H), 4.02 (m, 2H), 3.47 (s, 6H), 2.34 (d, *J* = 13.2 Hz, 1H), 2.27 (d, *J* = 10.8 Hz, 1H), 1.82 (dd, *J* = 6.6, 2.4 Hz, 2H), 1.48-1.32 (m, 4H); ¹³C NMR (150.9 MHz, CDCl₃) ppm 166.7, 157.0, 156.5, 148.5, 141.9, 130.3, 130.2, 126.1, 123.7, 122.3, 121.3, 115.7, 112.7, 103.6, 55.6, 55.5, 54.6, 32.7, 32.4, 24.80, 24.75; HRMS (ESI): Exact mass calcd for C₂₄H₂₇ClN₃O₃ [M+H]⁺ 440.1741, found 440.1746.



2,6-Dimethoxy-N-((1R,2R)-2-((4-(pyrrolidin-1-yl)quinolin-2-yl)amino)cyclohexyl)benzamide (78h)

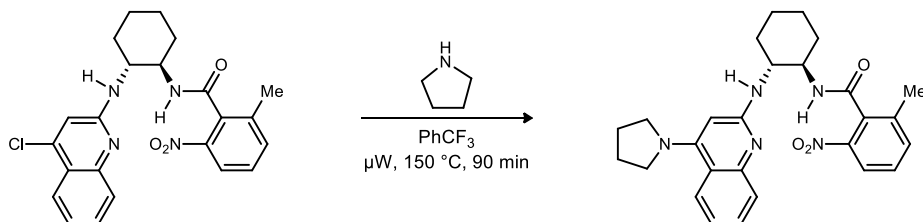
benzamide (78h). A 0.5-2 mL microwave vial was charged with the 4-chloroquinoline (40.0 mg, 90.9 μmol), pyrrolidine (30.0 μL, 364 μmol), and trifluorotoluene (650 μL). This suspension was heated at 150 °C and stirred in the microwave for 90 min. The reaction was concentrated and purified by flash column chromatography (1-10% methanol in dichloromethane w/ 1% AcOH) to provide a yellow oil. This material was diluted with dichloromethane and washed with 6 M aq NaOH. The organic layers were combined and washed twice more with 3 M aq NaOH. The combined organic layers were dried (MgSO₄) and concentrated to afford a tan amorphous solid (18.4 mg, 43%). Mp 238.0-242.0 °C; $[\alpha]_D^{20} +98.6$ (*c* 0.76, CHCl₃); *R_f* = 0.30 (5% MeOH/1% AcOH/CH₂Cl₂); IR (film) 3287, 2931, 2857, 2361, 1645, 1593, 1533 cm⁻¹; ¹H NMR (600 MHz, CDCl₃) δ 8.01 (br s, 1H), 7.90 (d, *J* = 7.8 Hz, 1H), 7.20 (br dd, *J* = 7.2, 7.2 Hz, 1H), 7.14 (br d, *J* = 7.2 Hz, 1H), 7.04 (dd, *J* = 8.4, 8.4 Hz, 1H), 7.00 (dd, *J* = 6.6 Hz, 1H), 6.23 (d, *J* = 7.8 Hz, 2H),

5.75 (s, 1H), 4.70 (br s, 1H), 4.03 (br m, 1H), 3.87 (br m, 1H), 3.57 (br s, 2H), 3.49 (br s, 2H), 3.39 (s, 6H), 2.44 (br d, $J = 7.2$ Hz, 1H), 2.20 (br d, $J = 11.4$ Hz, 1H), 2.04-1.95 (m, 4H), 1.80 (br s, 1H), 1.76 (br s, 1H), 1.43-1.36 (br m, 4H); ^{13}C NMR (150.9 MHz, CDCl_3) ppm 166.1, 157.8, 157.0, 153.8, 149.4, 129.7, 128.5, 126.2, 124.4, 119.5, 118.5, 116.5, 103.6, 92.4, 56.4, 55.5, 53.7, 52.0, 33.2, 32.2, 25.7, 25.1, 24.5; HRMS (ESI): Exact mass calcd for $\text{C}_{28}\text{H}_{35}\text{N}_4\text{O}_3$ $[\text{M}+\text{H}]^+$ 475.2709, found 475.2726.



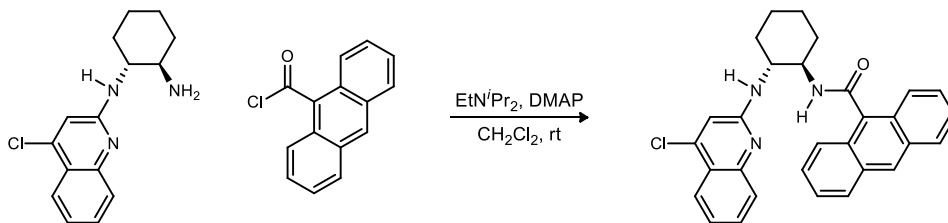
***N*-((1*R*,2*R*)-2-((4-Chloroquinolin-2-yl)amino)cyclohexyl)-2-methyl-6-nitrobenzamide (80i).**

To a flame dried flask equipped with a stir bar was added the amine (70.0 mg, 254 μmol) and dichloromethane (3 mL), immediately followed by the addition of *N,N*-diisopropyl ethylamine (53.0 μL , 305 μmol), the acid chloride (66.0 mg, 330 μmol), and DMAP (3.10 mg, 25.4 μmol). The reaction mixture was stirred at rt for 30 h, quenched with 1 M HCl and extracted with dichloromethane. The organic extracts were then washed with satd aq NaHCO_3 , extracted with dichloromethane, dried (MgSO_4), filtered and concentrated. Flash column chromatography of the residue (SiO_2 , 10-40% ethyl acetate in hexanes) afforded the desired amide as a light yellow amorphous solid (98.7 mg, 89%). Mp 200.0-202.0 $^\circ\text{C}$; $[\alpha]_D^{20} +302$ (c 0.62, CHCl_3); $R_f = 0.23$ (40% EtOAc/hexanes); IR (film) 3299, 3059, 2933, 2858, 2361, 1653, 1608, 1533 cm^{-1} ; ^1H NMR (600 MHz, CDCl_3) δ 8.75 (br d, $J = 3.0$ Hz, 1H), 7.89 (dd, $J = 7.8, 1.2$ Hz, 1H), 7.57 (d, $J = 7.8$ Hz, 1H), 7.23 (ddd, 8.4, 7.2, 1.2 Hz, 1H), 7.17 (dddd, $J = 8.4, 7.2, 1.2$ Hz, 1H), 7.14 (m, 2H), 6.89 (d, $J = 8.4$ Hz, 1H), 6.71 (s, 1H), 5.21 (br d, $J = 6.6$ Hz, 1H), 4.03 (dddd, $J = 10.2, 10.2, 6.6, 3.6$ Hz, 1H), 3.85 (m, 1H), 2.56 (br m, 1H), 2.13 (br dd, $J = 12.0, 2.4$ Hz, 1H), 2.08 (s, 3H), 1.84 (m, 2H), 1.45 (m, 4H); ^{13}C NMR (150.9 MHz, CDCl_3) ppm 166.3, 156.7, 147.2, 145.2, 142.7, 137.3, 135.5, 132.7, 130.3, 128.6, 124.9, 123.8, 122.6, 121.5, 121.3, 112.4, 58.1, 53.6, 32.7, 32.0, 25.1, 24.2, 18.4; HRMS (ESI) Exact mass calcd for $\text{C}_{23}\text{H}_{23}\text{ClN}_4\text{NaO}_3$ $[\text{M}+\text{Na}]^+$ 461.1356, found 461.1357.



2-Methyl-6-nitro-*N*-((1*R*,2*R*)-2-((4-(pyrrolidin-1-yl)quinolin-2-yl)amino)cyclohexyl)benzamide (78i).

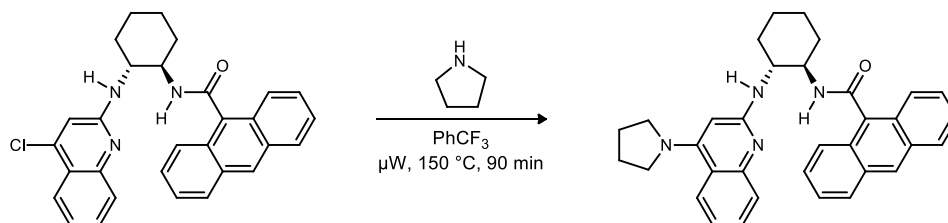
A 0.5-2 mL microwave vial was charged with the 4-chloroquinoline (50.0 mg, 114 μ mol), pyrrolidine (38.0 μ L, 456 μ mol), and trifluorotoluene (820 μ L). This suspension was heated at 150 $^{\circ}$ C and stirred in the microwave for 90 min. The reaction was concentrated and purified by flash column chromatography (1-10% methanol in dichloromethane w/ 1% AcOH) to provide a yellow oil. This material was diluted with dichloromethane and washed with 6 M aq NaOH. The organic layers were combined and washed three times more with 3 M aq NaOH. The combined organic layers were dried (MgSO_4) and concentrated to afford a dark yellow amorphous solid (38.3 mg, 71%). Mp 217.0-223.0 $^{\circ}$ C; $[\alpha]_D^{20} +193$ (c 0.63, CHCl_3); $R_f = 0.37$ (5% MeOH/1% AcOH/ CH_2Cl_2); IR (film) 3329, 2929, 2858, 1653, 1588, 1532 cm^{-1} ; ^1H NMR (600 MHz, CDCl_3) δ 9.82 (br s, 1H), 7.88 (dd, $J = 8.4, 0.6$ Hz, 1H), 7.55 (d, $J = 7.8$ Hz, 1H), 7.09 (m, 2H), 7.00 (br ddd, $J = 7.8, 7.8$ Hz, 1H), 6.93 (br ddd, $J = 7.2, 7.2$ Hz, 1H), 6.66 (d, $J = 8.4$ Hz, 1H), 5.66 (s, 1H), 4.48 (br s, 1H), 4.00 (m, 1H), 3.72 (m, 1H), 3.54 (m, 4H), 2.63 (br dd, $J = 8.4, 1.8$ Hz, 1H), 2.10 (s, 3H), 2.08-1.94 (m, 5H), 1.84 (br m, 1H), 1.78 (br m, 1H), 1.42 (m, 4H); ^{13}C NMR (150.9 MHz, CDCl_3) ppm 166.2, 158.0, 154.0, 148.3, 145.2, 137.3, 135.3, 133.2, 128.5, 128.2, 125.0, 124.7, 121.4, 119.6, 118.3, 91.6, 59.2, 53.1, 51.9, 33.0, 31.7, 25.8, 25.3, 24.1, 18.4; HRMS (ESI): Exact mass calcd for $\text{C}_{27}\text{H}_{31}\text{N}_5\text{NaO}_3$ $[\text{M}+\text{Na}]^+$ 496.2325, found 496.2315.



***N*-((1*R*,2*R*)-2-((4-Chloroquinolin-2-yl)amino)cyclohexyl)anthracene-9-carboxamide (80j).**

To a flame dried flask equipped with a stir bar was added the amine (70.0 mg, 254 μ mol) and dichloromethane (3 mL), immediately followed by the addition of *N,N*-diisopropyl ethylamine (53.0 μ L, 305 μ mol), the acid chloride (79.4 mg, 330 μ mol), and DMAP (3.10 mg, 25.4 μ mol).

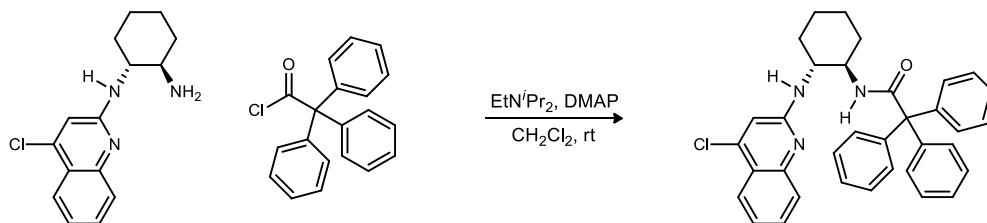
The reaction mixture was stirred at rt for 48 h, quenched with 1 M HCl and extracted with dichloromethane. The organic extracts were then washed with satd aq NaHCO₃, extracted with dichloromethane, dried (MgSO₄), filtered and concentrated. Flash column chromatography of the residue (SiO₂, 10-40% ethyl acetate in hexanes) afforded the desired amide as a light yellow foam (87.5 mg, 72%). $[\alpha]_D^{20} +169$ (c 0.66, CHCl₃); $R_f = 0.38$ (40% EtOAc/hexanes); IR (film) 3288, 3055, 2932, 2857, 1642, 1607, 1535 cm⁻¹; ¹H NMR (600 MHz, CDCl₃) δ 8.44 (br s, 1H), 8.20 (s, 1H), 8.13 (br d, $J = 6.0$ Hz, 1H), 7.95 (br d, $J = 7.2$ Hz, 1H), 7.71 (dd, $J = 8.4, 0.6$ Hz, 1H), 7.53 (br s, 2H), 7.45 (br m, 2H), 7.03 (dd, $J = 6.6, 6.6$ Hz, 1H), 6.98 (dd, $J = 6.6, 6.6$ Hz, 1H), 6.95 (br m, 1H), 6.72 (s, 1H), 6.68 (br m, 1H), 6.45 (d, $J = 7.8$ Hz, 1H), 5.23 (d, $J = 5.4$ Hz, 1H), 4.1 (m, 2H), 2.65 (br m, 1H), 2.15 (br m, 1H), 1.86 (br m, 2H), 1.54-1.39 (m, 4H); ¹³C NMR (150.9 MHz, CDCl₃) ppm 169.7, 156.2, 147.3, 142.8, 132.1, 130.8, 130.7, 129.9, 128.4, 127.8, 127.6, 127.2, 126.3, 125.6, 125.5, 125.1, 125.0, 124.7, 124.0, 123.5, 122.4, 121.2, 111.9, 57.6, 53.8, 32.8, 32.7, 25.1, 24.4; HRMS (ESI) Exact mass calcd for C₃₀H₂₆ClN₃NaO [M+Na]⁺ 502.1662, found 502.1653.



***N*-((1*R*,2*R*)-2-((4-(Pyrrolidin-1-yl)quinolin-2-yl)amino)cyclohexyl)anthracene-9-**

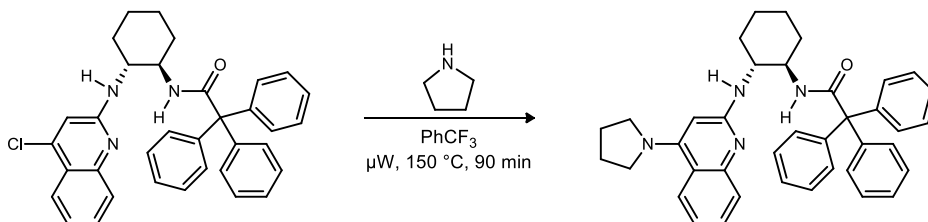
carboxamide (78j). A 0.5-2 mL microwave vial was charged with the 4-chloroquinoline (50.0 mg, 104 μ mol), pyrrolidine (34.0 μ L, 417 μ mol), and trifluorotoluene (750 μ L). This suspension was heated at 150 °C and stirred in the microwave for 90 min. The reaction was concentrated and purified by flash column chromatography (1-10% methanol in dichloromethane w/ 1% AcOH) to provide a yellow oil. This material was diluted with dichloromethane and washed with 6 M aq NaOH. The organic layers were combined and washed three times more with 3 M aq NaOH. The combined organic layers were dried (MgSO₄) and concentrated to afford a tan amorphous solid (26.3 mg, 49%). Mp 273.0-278.0 °C; $[\alpha]_D^{20} +145$ (c 0.43, CHCl₃); $R_f = 0.35$ (5% MeOH/1% AcOH/CH₂Cl₂); IR (film) 3331, 3052, 2929, 2856, 1640, 1588, 1531 cm⁻¹; ¹H NMR (600 MHz, CDCl₃) δ 9.35 (br s, 1H), 8.19 (s, 1H), 8.19 (br s, 1H), 7.95 (br d, $J = 6.0$ Hz, 1H), 7.67 (d, $J = 7.8$ Hz, 1H), 7.52 (br m, 4H), 6.89 (br s, 1H), 6.76 (m, 2H), 6.62 (br s, 1H), 6.21 (br d, $J = 7.8$ Hz,

1H), 5.69 (s, 1H), 4.68 (br s, 1H), 4.09 (br s, 2H), 3.48 (m, 4H), 2.76 (br d, $J = 6.0$ Hz, 1H), 2.15 (br d, $J = 12.0$ Hz, 1H), 1.98 (m, 4H), 1.88 (br d, $J = 10.2$ Hz, 2H), 1.59-1.46 (m, 4H); ^{13}C NMR (150.9 MHz, CDCl_3) ppm 169.6, 157.5, 154.0, 148.4, 132.7, 130.9, 130.8, 128.3, 128.0, 127.4, 127.3, 126.1, 125.5, 125.2, 125.0, 124.8, 124.4, 124.2, 119.4, 118.2, 91.5, 58.5, 53.4, 51.9, 33.3, 32.5, 25.8, 25.3, 24.5; HRMS (ESI) Exact mass calcd for $\text{C}_{34}\text{H}_{34}\text{N}_4\text{NaO}$ $[\text{M}+\text{Na}]^+$ 537.2630, found 537.2607.



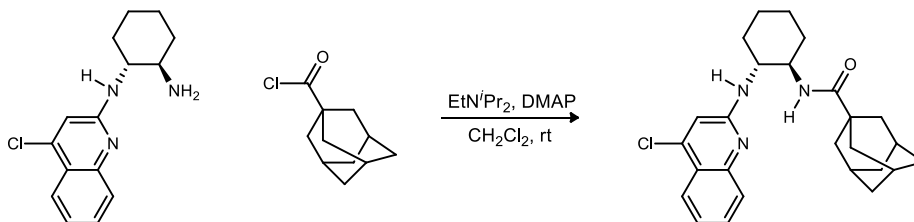
***N*-((1*R*,2*R*)-2-((4-Chloroquinolin-2-yl)amino)cyclohexyl)-2,2,2-triphenylacetamide (80k).** To

a flame dried flask equipped with a stir bar was added the amine (60.0 mg, 218 μmol) and dichloromethane (3 mL), immediately followed by the addition of *N,N*-diisopropyl ethylamine (46.0 μL , 261 μmol), the acid chloride (86.8 mg, 283 μmol), and DMAP (2.70 mg, 21.8 μmol). The reaction mixture was stirred at rt for 18 h, quenched with 1 M HCl and extracted with dichloromethane. The organic extracts were then washed with satd aq NaHCO_3 , extracted with dichloromethane, dried (MgSO_4), filtered and concentrated. Flash column chromatography of the residue (SiO_2 , 5-40% ethyl acetate in hexanes) afforded the desired amide an off white solid (105 mg, 88%). Mp 185.0-188.0 $^\circ\text{C}$; $[\alpha]_D^{20} +72.8$ (c 0.43, CHCl_3); $R_f = 0.47$ (40% EtOAc/hexanes); IR (film) 3334, 3059, 2931, 2361, 1652, 1607, 1533 cm^{-1} ; ^1H NMR (600 MHz, CDCl_3) δ 7.95 (dd, $J = 7.8, 0.6$ Hz, 1H), 7.48 (ddd, $J = 7.8, 7.8, 0.6$ Hz, 1H), 7.34 (d, $J = 8.4$ Hz, 1H), 7.25 (ddd, $J = 7.8, 7.8, 0.6$ Hz, 1H), 7.14-7.07 (m, 15H), 6.55 (s, 1H), 6.46 (d, $J = 7.2$ Hz, 1H), 5.21 (br d, $J = 6.6$ Hz, 1H), 4.00 (dddd, $J = 10.8, 10.8, 7.2, 3.6$ Hz, 1H), 3.93 (dddd, $J = 11.4, 11.4, 7.8, 4.2$, 1H), 2.23 (br d, $J = 13.2$ Hz, 1H), 2.15 (br d, $J = 13.2$ Hz, 1H), 1.77 (br m, 2H), 1.39 (m, 2H), 1.30-1.22 (m, 2H); ^{13}C NMR (150.9 MHz, CDCl_3) ppm 174.1, 155.9, 148.4, 143.2, 142.3, 130.2, 130.1, 127.7, 126.7, 126.5, 123.8, 122.4, 121.5, 112.3, 67.8, 55.1, 54.5, 32.9, 32.1, 24.7 (2C); HRMS (ESI): Exact mass calcd for $\text{C}_{35}\text{H}_{33}\text{ClN}_3\text{O}$ $[\text{M}+\text{H}]^+$ 546.2312, found 546.2285.



2,2,2-Triphenyl-*N*-((1*R*,2*R*)-2-((4-(pyrrolidin-1-yl)quinolin-2-yl)amino)cyclohexyl)

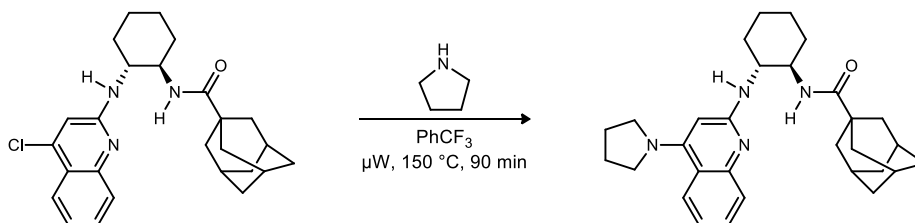
acetamide (78k). A 0.2-0.5 mL microwave vial was charged with the 4-chloroquinoline (20.0 mg, 36.6 μmol), pyrrolidine (12.0 μL , 146 μmol), and trifluorotoluene (270 μL). This suspension was heated at 150 $^{\circ}\text{C}$ and stirred in the microwave for 90 min. The reaction was concentrated and purified by flash column chromatography (1-10% methanol in dichloromethane w/ 1% AcOH) to provide a yellow oil. This material was diluted with dichloromethane and washed with 6 M aq NaOH. The organic layers were combined and washed three times more with 3 M aq NaOH. The combined organic layers were dried (MgSO_4) and concentrated to afford a light yellow amorphous solid (18.1 mg, 85%). Mp 168.0-173.0 $^{\circ}\text{C}$; $[\alpha]_D^{20} +10.2$ (c 0.55, CHCl_3); $R_f = 0.44$ (5% MeOH/1% AcOH/ CH_2Cl_2); IR (film) 3353, 3057, 2927, 2856, 1653, 1589, 1528, 1496 cm^{-1} ; ^1H NMR (400 MHz, CDCl_3) δ 7.93 (d, $J = 8.4, 0.8$ Hz, 1H), 7.32 (ddd, $J = 7.6, 7.6, 0.8$ Hz, 1H), 7.17 (br d, $J = 8.0$ Hz, 1H), 7.18-7.01 (m, 15H), 6.73 (br d, $J = 6.8$ Hz, 1H), 5.61 (s, 1H), 4.65 (br s, 1H), 4.02 (dddd, $J = 11.2, 11.2, 7.6, 4.0$ Hz, 1H), 3.84 (dddd, $J = 11.2, 11.2, 7.6, 3.6$ Hz, 1H), 3.52 (m, 4H), 2.16 (br m, 2H), 2.01 (m, 4H), 1.73 (br d, $J = 7.6$ Hz, 3H), 1.37 (br m, 2H), 1.26 (br m, 2H); ^{13}C NMR (100 MHz, CDCl_3) ppm 173.7, 157.3, 153.8, 149.7, 143.4, 130.4, 128.3, 127.6, 127.0, 126.4, 124.6, 119.5, 118.8, 92.3, 67.7, 56.0, 53.4, 52.0, 33.4, 32.0, 25.8, 24.9, 24.8; HRMS (ESI): Exact mass calcd for $\text{C}_{39}\text{H}_{41}\text{N}_4\text{O}$ $[\text{M}+\text{H}]^+$ 581.3280, found 581.3264.



(3*R*,5*R*,7*R*)-*N*-((1*R*,2*R*)-2-((4-Chloroquinolin-2-yl)amino)cyclohexyl)adamantane-1-

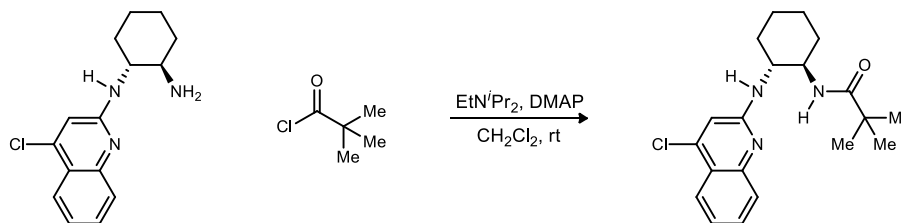
carboxamide (80l). To a flame dried flask equipped with a stir bar was added the amine (70.0 mg, 254 μmol) and dichloromethane (3 mL), immediately followed by the addition of *N,N*-diisopropyl ethylamine (53.0 μL , 305 μmol), the acid chloride (65.6 mg, 330 μmol), and DMAP (3.10 mg,

25.4 μmol). The reaction mixture was stirred at rt for 20 h, quenched with 1 M HCl and extracted with dichloromethane. The organic extracts were then washed with satd aq NaHCO_3 , extracted with dichloromethane, dried (MgSO_4), filtered and concentrated. Flash column chromatography of the residue (SiO_2 , 10-40% ethyl acetate in hexanes) afforded the desired amide as an off white amorphous solid (96.5 mg, 87%). Mp 195.0-199.0 $^\circ\text{C}$; $[\alpha]_D^{20} +234$ (c 0.65, CHCl_3); $R_f = 0.33$ (40% EtOAc/hexanes); IR (film) 3310, 3101, 3062, 2909, 2853, 1638, 1608, 1573, 1535 cm^{-1} ; ^1H NMR (600 MHz, CDCl_3) δ 7.93 (dd, $J = 8.4, 1.2$ Hz, 1H), 7.66 (d, $J = 8.4$ Hz, 1H), 7.54 (ddd, $J = 8.4, 7.2, 1.2$ Hz, 1H), 7.24 (ddd, $J = 7.8, 7.8, 0.6$ Hz, 1H), 6.94 (d, $J = 7.2$ Hz, 1H), 6.84 (s, 1H), 5.49 (d, $J = 8.4$ Hz, 1H), 4.26 (m, 1H), 3.72 (dddd, $J = 10.8, 10.8, 7.2, 4.2$ Hz, 1H), 2.15 (m, 2H), 1.84 (dd, $J = 6.0, 2.4$ Hz, 1H), 1.79 (dd, $J = 12.6, 2.4$ Hz, 1H), 1.67 (br s, 3H), 1.45 (m, 12 H), 1.32 (dq, $J = 12.0, 3.0$ Hz, 1H), 1.21 (br d, $J = 12.0$ Hz, 3H); ^{13}C NMR (150.9 MHz, CDCl_3) ppm 178.5, 157.0, 148.4, 142.5, 130.4, 126.1, 124.0, 122.5, 121.6, 112.6, 56.5, 52.8, 40.3, 38.8, 36.1, 32.9, 32.8, 27.9, 25.2, 24.7; HRMS (ESI) Exact mass calcd for $\text{C}_{26}\text{H}_{32}\text{ClN}_3\text{NaO}$ $[\text{M}+\text{Na}]^+$ 460.2132, found 460.2119.

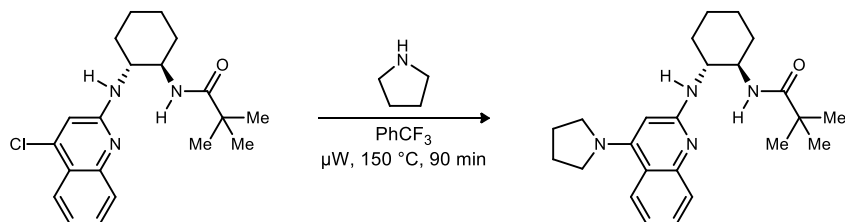


(3R,5R,7R)-N-((1R,2R)-2-((4-(Pyrrolidin-1-yl)quinolin-2-yl)amino)cyclohexyl)adamantane-1-carboxamide (781). A 0.5-2 mL microwave vial was charged with the 4-chloroquinoline (50.0 mg, 114 μmol), pyrrolidine (37.5 μL , 457 μmol), and trifluorotoluene (820 μL). This suspension was heated at 150 $^\circ\text{C}$ and stirred in the microwave for 90 min. The reaction was concentrated and purified by flash column chromatography (1-10% methanol in dichloromethane w/ 1% AcOH) to provide a yellow oil. This material was diluted with dichloromethane and washed with 6 M aq NaOH. The organic layers were combined and washed three times more with 3 M aq NaOH. The combined organic layers were dried (MgSO_4) and concentrated to afford a tan solid (33.6 mg, 62%). Mp 239.0-243.0 $^\circ\text{C}$; $[\alpha]_D^{20} +139$ (c 0.56, CHCl_3); $R_f = 0.38$ (5% MeOH/1% AcOH/ CH_2Cl_2); IR (film) 3324, 2908, 2852, 1637, 1589, 1531 cm^{-1} ; ^1H NMR (600 MHz, CDCl_3) δ 7.94 (dd, $J = 8.4, 0.6$ Hz, 1H), 7.60 (d, $J = 7.8$ Hz, 1H), 7.41 (ddd, $J = 7.8, 7.8, 0.6$ Hz, 1H), 7.34 (br d, $J = 5.4$ Hz, 1H), 7.04 (ddd, $J = 8.4, 8.4, 1.2$ Hz, 1H), 5.63 (s, 1H), 4.34 (br s, 1H), 4.26 (m, 1H), 3.57

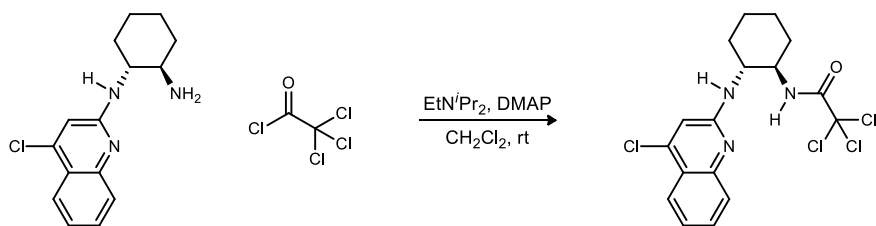
(dddd, $J = 10.8, 10.8, 6.6, 4.2$ Hz, 1H), 3.51 (br s, 4H), 2.17 (d, $J = 11.4$ Hz, 1H), 2.05 (dd, $J = 12.0, 1.8$ Hz, 1H), 1.98 (m, 4H), 1.79 (dd, $J = 13.2, 1.8$ Hz, 1H), 1.73 (d, $J = 12.0$ Hz, 1H), 1.62 (s, 3H), 1.43 (m, 10H), 1.35(m, 3H), 1.20 (d, $J = 12.0$ Hz, 3H); ^{13}C NMR (150.9 MHz, CDCl_3) ppm 178.4, 158.2, 154.1, 149.6, 128.7, 126.6, 124.8, 119.8, 118.8, 92.1, 57.5, 52.0, 51.9, 40.2, 38.6, 36.2, 33.3, 32.7, 28.0, 25.7, 25.4, 24.6; HRMS (ESI): Exact mass calcd for $\text{C}_{30}\text{H}_{40}\text{N}_4\text{NaO}$ $[\text{M}+\text{Na}]^+$ 495.3100, found 495.3089.



***N*-((1*R*,2*R*)-2-((4-Chloroquinolin-2-yl)amino)cyclohexyl)pivalamide (80m).** To a flame dried flask equipped with a stir bar was added the amine (60.0 mg, 218 μmol) and dichloromethane (3 mL), immediately followed by the addition of *N,N*-diisopropyl ethylamine (46.0 μL , 261 μmol), the acid chloride (32.0 μL , 261 μmol), and DMAP (2.70 mg, 22.0 μmol). The reaction mixture was stirred at rt for 24 h, quenched with 1 M HCl and extracted with dichloromethane. The organic extracts were then washed with satd aq NaHCO_3 , extracted with dichloromethane, dried (MgSO_4), filtered and concentrated. Flash column chromatography of the residue (SiO_2 , 20-50% ethyl acetate in hexanes) afforded the desired amide as a white solid (57.9 mg, 74%). Mp 213.0-216.0 $^\circ\text{C}$; $[\alpha]_D^{20} +281$ (c 0.45, CHCl_3); $R_f = 0.38$ (40% EtOAc/hexanes); IR (film) 3313, 2932, 2858, 1607, 1576, 1535 cm^{-1} ; ^1H NMR (600 MHz, CDCl_3) δ 7.96 (dd, $J = 7.8, 0.6$ Hz, 1H), 7.64 (d, $J = 7.8$ Hz, 1H), 7.56 (ddd, $J = 8.4, 6.6, 1.2$ Hz, 1H), 7.27 (ddd, $J = 7.8, 7.8, 1.2$ Hz, 1H), 6.84 (d, $J = 6.0$ Hz, 1H), 6.71 (s, 1H), 5.03 (br d, $J = 7.8$ Hz, 1H), 4.18 (m, 1H), 3.71 (m, 1H), 2.16 (m, 2H), 1.82 (m, 1H), 1.78 (d, $J = 10.8$ Hz, 1H), 1.47-1.28 (m, 4H), 0.87 (s, 9H); ^{13}C NMR (150.9 MHz, CDCl_3) ppm 179.1, 156.7, 148.3, 142.6, 130.5, 126.2, 124.0, 122.6, 121.6, 112.2, 56.1, 53.5, 38.4, 33.1, 32.5, 27.3, 25.1, 24.7; HRMS (ESI) Exact mass calcd for $\text{C}_{20}\text{H}_{26}\text{ClN}_3\text{NaO}$ $[\text{M}+\text{Na}]^+$ 382.1662, found 382.1658.

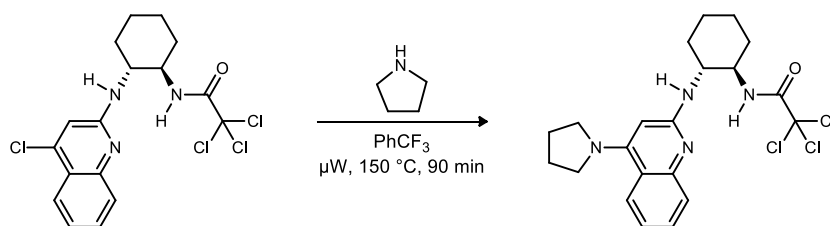


***N*-((1*R*,2*R*)-2-((4-(Pyrrolidin-1-yl)quinolin-2-yl)amino)cyclohexyl)acetamide (78m).** A 0.5-2 mL microwave vial was charged with the 4-chloroquinoline (40.0 mg, 111 μ mol), pyrrolidine (37.0 μ L, 445 μ mol), and trifluorotoluene (800 μ L). This suspension was heated at 150 $^{\circ}$ C and stirred in the microwave for 90 min. The reaction was concentrated and purified by flash column chromatography (1-10% methanol in dichloromethane w/ 1% AcOH) to provide a yellow oil. This material was diluted with dichloromethane and washed with 6 M aq NaOH. The organic layers were combined and washed three times more with 3 M aq NaOH. The combined organic layers were dried (MgSO₄) and concentrated to afford a tan amorphous solid (23.5 mg, 54%). Mp 251.0-256.0 $^{\circ}$ C; $[\alpha]_D^{20}$ +143 (*c* 0.69, CHCl₃); R_f = 0.35 (5% MeOH/1% AcOH/CH₂Cl₂); IR (film) 3299, 2929, 2856, 2361, 1630, 1588, 1534 cm^{-1} ; ¹H NMR (600 MHz, CDCl₃) δ 7.97 (d, *J* = 7.8 Hz, 1H), 7.58 (br d, *J* = 7.8 Hz, 1H), 7.47 (br s, 1H), 7.42 (dd, *J* = 7.8, 7.8 Hz, 1H), 7.06 (dd, *J* = 7.8, 7.8 Hz, 1H), 5.64 (s, 1H), 4.34 (br s, 1H), 4.21 (m, 1H), 3.60-3.54 (m, 5H), 2.22 (br d, *J* = 11.4 Hz, 1H), 2.06 (br m, 1H), 1.99 (m, 4H), 1.80 (br d, *J* = 10.8 Hz, 1H), 1.73 (br d, *J* = 12.0 Hz, 1H), 1.46-1.28 (m, 4H), 0.84 (s, 9H); ¹³C NMR (150.9 MHz, CDCl₃) ppm 178.9, 158.1, 153.9, 149.6, 128.7, 126.6, 124.9, 119.8, 118.8, 92.0, 57.5, 52.3, 52.0, 38.3, 33.5, 32.4, 27.3, 25.8, 25.4, 24.6; HRMS (ESI) Exact mass calcd for C₂₄H₃₄N₄NaO [M+Na]⁺ 417.2630, found 417.2630.



2,2,2-Trichloro-*N*-((1*R*,2*R*)-2-((4-chloroquinolin-2-yl)amino)cyclohexyl)acetamide (80n). To a flame dried flask equipped with a stir bar was added the amine (70.0 mg, 254 μ mol) and dichloromethane (3 mL), immediately followed by the addition of *N,N*-diisopropyl ethylamine (53.0 μ L, 305 μ mol), the acid chloride (846 mg, 4.65 mmol), and DMAP (3.10 mg, 25.4 μ mol). The reaction mixture was stirred at rt for 48 h, quenched with 1 M HCl and extracted with

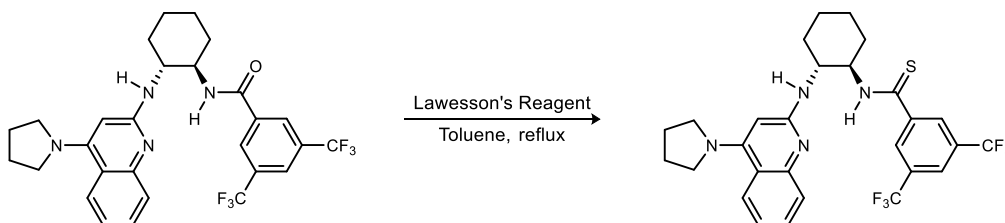
dichloromethane. The organic extracts were then washed with satd aq NaHCO₃, extracted with dichloromethane, dried (MgSO₄), filtered and concentrated. Flash column chromatography of the residue (SiO₂, 5-40% ethyl acetate in hexanes) afforded the desired amide as a tan solid (76.3 mg, 71%). Mp 197.0-201.0 °C; $[\alpha]_D^{20} +287$ (*c* 0.47, CHCl₃); *R_f* = 0.27 (20% EtOAc/hexanes); IR (film) 3363, 2936, 2859, 1697, 1608, 1570, 1532 cm⁻¹; ¹H NMR (600 MHz, CDCl₃) δ 8.85 (br s, 1H), 7.97 (dd, *J* = 8.4, 1.2 Hz, 1H), 7.65 (d, *J* = 8.4 Hz, 1H), 7.57 (ddd, *J* = 8.4, 7.8, 1.2 Hz, 1H), 7.30 (ddd, *J* = 7.8, 6.6, 0.6 Hz, 1H), 6.72 (s, 1H), 4.66 (br d, *J* = 7.2 Hz, 1H), 4.31 (dddd, *J* = 11.4, 11.4, 7.8, 4.2 Hz, 1H), 3.61 (m, 1H), 2.38 (br dd, *J* = 9.0, 5.4 Hz, 1H), 2.10 (m, 1H), 1.88 (m, 1H), 1.83 (m, 1H), 1.48-1.41 (m, 4H), ¹³C NMR (150.9 MHz, CDCl₃) ppm 162.3, 156.5, 147.9, 143.2, 130.7, 126.4, 124.1, 123.2, 121.8, 112.0, 92.7, 60.2, 52.6, 33.0, 31.2, 25.2, 24.2; HRMS (ESI) Exact mass calcd for C₁₇H₁₈Cl₄N₃O [M+H]⁺ 420.0204, found 420.0222.



2,2,2-Trichloro-*N*-((1*R*,2*R*)-2-((4-(pyrrolidin-1-yl)quinolin-2-yl)amino)cyclohexyl)

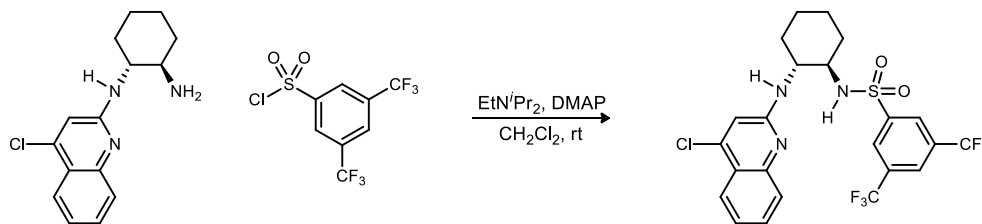
acetamide (78n). A 0.5-2 mL microwave vial was charged with the 4-chloroquinoline (30.0 mg, 71.0 μmol), pyrrolidine (24.0 μL, 285 μmol), and trifluorotoluene (525 μL). This suspension was heated at 150 °C and stirred in the microwave for 90 min. The reaction was concentrated and purified by flash column chromatography (1-10% methanol in dichloromethane w/ 1% AcOH) to provide a yellow oil. This material was diluted with dichloromethane and washed with 6 M aq NaOH. The organic layers were combined and washed three times more with 3 M aq NaOH. The combined organic layers were dried (MgSO₄) and concentrated to afford a yellow solid (9.3 mg, 29%). Mp 189.0-194.0 °C; $[\alpha]_D^{20} +144$ (*c* 0.64, CHCl₃); *R_f* = 0.42 (5% MeOH/1% AcOH/CH₂Cl₂); IR (film) 3374, 2930, 1700, 1588, 1528 cm⁻¹; ¹H NMR (600 MHz, CDCl₃) δ 9.57 (br s, 1H), 7.98 (d, *J* = 8.4 Hz, 1H), 7.58 (br d, *J* = 7.2 Hz, 1H), 7.42 (dd, *J* = 7.8, 7.8 Hz, 1H), 7.08 (dd, *J* = 7.8, 7.8 Hz, 1H), 5.65 (s, 1H), 4.28 (br s, 2H), 3.57 (br m, 4H), 3.51 (br s, 1H), 2.39 (br s, 1H), 2.06 (br d, *J* = 9.6 Hz, 1H), 2.00 (m, 4H), 1.85 (br d, *J* = 9.6 Hz, 1H), 1.80 (br d, *J* = 4.8 Hz, 1H), 1.47-1.37 (br m, 4H); ¹³C NMR (150.9 MHz, CDCl₃) ppm 162.4, 157.9, 154.0, 149.2, 128.8, 126.8,

124.9, 120.1, 118.7, 92.9, 91.4, 60.8, 52.1, 52.0, 33.2, 30.8, 25.8, 25.3, 24.3; HRMS (ESI) Exact mass calcd for C₂₁H₂₆Cl₃N₄O [M+H]⁺ 455.1172, found 455.1160.

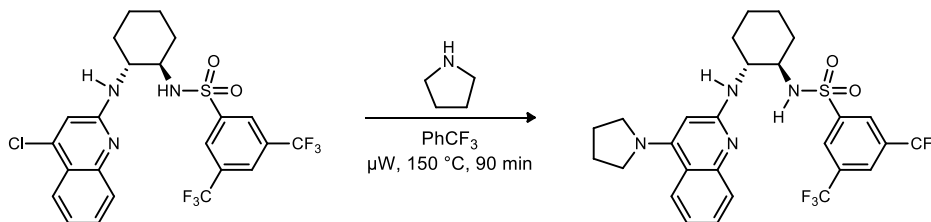


N-((1R,2R)-2-((4-(Pyrrolidin-1-yl)quinolin-2-yl)amino)cyclohexyl)-3,5-bis(trifluoromethyl)benzothioamide (78o).²⁵⁵ A flame dried flask equipped with a stir bar was charged with the amide (68.0 mg, 124 μ mol) and toluene (3 mL) at room temperature. To the resulting solution was added Lawesson's reagent (45.0 mg, 111 μ mol) and the reaction mixture was heated to reflux and stirred. The reaction mixture was monitored by TLC; after 5 h, complete conversion was observed and the reaction mixture was concentrated. Flash column chromatography of the residue (SiO₂, 0.5-10% methanol in dichloromethane w/ 1% AcOH) afforded a yellow oil. This material was diluted with dichloromethane and washed with 6 M aq NaOH. The organic layers were combined and washed twice more with 3 M aq NaOH. The combined organic layers were dried over MgSO₄ and concentrated to yield the desired thioamide as a yellow amorphous solid (32.0 mg, 46%). $[\alpha]_D^{20} +304$ (*c* 0.53, CHCl₃); *R*_f = 0.19 (5% MeOH/1% AcOH/CH₂Cl₂); IR (film) 2930, 1588, 1527 cm⁻¹; ¹H NMR (600 MHz, CDCl₃) δ 7.93 (d, *J* = 7.8 Hz, 1H), 7.80 (s, 2H), 7.61 (s, 1H), 7.23 (dd, *J* = 7.2, 7.2 Hz, 1H), 7.15 (d, *J* = 7.8 Hz, 1H), 7.01 (ddd, *J* = 8.4, 8.4, 1.2 Hz, 1H), 5.66 (s, 1H), 4.38 (d, *J* = 5.4 Hz, 1H), 4.30 (m, 1H), 4.16 (ddd, *J* = 14.4, 10.8, 3.6 Hz, 1H), 3.57 (m, 4H), 2.89 (d, *J* = 12.6 Hz, 1H), 2.08 (d, *J* = 13.2 Hz, 1H), 2.00 (m, 4H), 1.90 (br s, 1H), 1.85 (d, *J* = 9.0 Hz, 1H), 1.58-1.38 (m, 4H); ¹³C NMR (150.9 MHz, CDCl₃) ppm 195.3, 158.0, 154.1, 148.2, 144.6, 131.1 (q, *J* = 33.3 Hz, 1C), 129.0, 126.8, 125.6, 124.9, 123.1 (q, *J* = 3.6 Hz), 122.8 (q, *J* = 273.0 Hz), 120.3, 118.5, 90.9, 65.7, 53.6, 52.0, 33.1, 29.1, 25.9, 25.5, 24.1; HRMS (ESI) Exact mass calcd for C₂₈H₂₉F₆N₄S [M+H]⁺ 567.2018, found 567.2029.

²⁵⁵ Modification of: Raucher, S.; Klein, P. *Tetrahedron Lett.* **1980**, 21, 4061-4064.

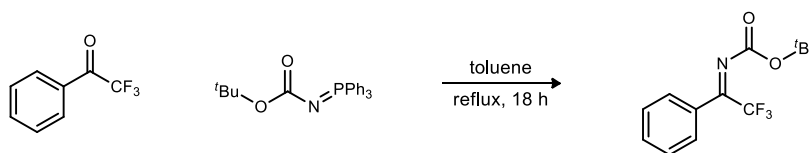


***N*-((1*R*,2*R*)-2-((4-Chloroquinolin-2-yl)amino)cyclohexyl)-3,5-bis(trifluoromethyl) benzenesulfonamide (80p).** To a flame dried flask equipped with a stir bar was added the amine (60.0 mg, 218 μmol) and dichloromethane (3 mL), immediately followed by the addition of *N,N*-diisopropyl ethylamine (45.0 μL , 261 μmol), the sulfonyl chloride (82.0 mg, 261 μmol), and DMAP (2.70 mg, 22.0 μmol). The reaction mixture was stirred at rt for 25 h, quenched with 1 M HCl and extracted with dichloromethane. The organic extracts were then washed with NaHCO_3 , extracted with dichloromethane, dried (MgSO_4), filtered and concentrated. Flash column chromatography of the residue (SiO_2 , 5-30% ethyl acetate in hexanes) afforded the desired amide as a white solid (97.5 mg, 81%). Mp 206.0-208.0 $^\circ\text{C}$; $[\alpha]_D^{20} +198$ (*c* 0.58, CHCl_3); $R_f = 0.64$ (40% EtOAc/hexanes); IR (film) 3379, 3065, 2937, 2862, 2361, 1609, 1535 cm^{-1} ; ^1H NMR (600 MHz, CDCl_3) δ 9.31 (br s, 1H), 7.99 (dd, $J = 8.4, 1.2$ Hz, 1H), 7.85 (s, 1H), 7.84 (s, 2H), 7.75 (d, $J = 8.4$ Hz, 1H), 7.66 (ddd, $J = 8.4, 7.2, 1.8$ Hz, 1H), 7.38 (ddd, $J = 8.4, 7.2, 1.2$ Hz, 1H), 6.37 (s, 1H), 4.18 (br d, $J = 4.8$ Hz, 1H), 3.81 (m, 1H), 2.99 (dt, $J = 10.8, 4.2$ Hz, 1H), 2.37 (d, $J = 10.2$ Hz, 1H), 1.98 (m, 1H), 1.78 (m, 2H), 1.59 (m, 1H), 1.38-1.30 (m, 3H); ^{13}C NMR (150.9 MHz, CDCl_3) ppm 156.0, 146.7, 144.0, 143.7, 132.0 (q, $J_{\text{FC}} = 34.3$ Hz), 131.6, 126.7, 125.8, 125.2 (q, $J_{\text{FC}} = 3.5$ Hz), 124.2, 124.0, 122.3 (q, $J_{\text{FC}} = 273.3$ Hz), 121.7, 111.3, 62.4, 54.9, 35.2, 33.2, 24.7, 24.0; HRMS (ESI): Exact mass calcd for $\text{C}_{23}\text{H}_{21}\text{ClF}_6\text{N}_3\text{O}_2\text{S}$ $[\text{M}+\text{H}]^+$ 552.0947, found 552.0938.



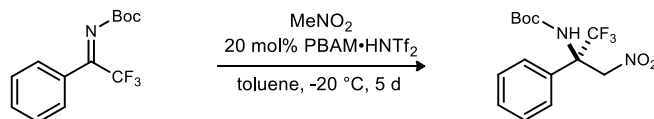
***N*-((1*R*,2*R*)-2-((4-(Pyrrolidin-1-yl)quinolin-2-yl)amino)cyclohexyl)-3,5-bis(trifluoromethyl) benzenesulfonamide (78p).** A 0.5-2 mL microwave vial was charged with 4-chloroquinoline (50.0 mg, 90.6 μmol), pyrrolidine (30.0 μL , 362 μmol), and trifluorotoluene (650 μL). This suspension was heated at 150 $^\circ\text{C}$ and stirred in the microwave for 90 min. The reaction was

concentrated and purified by flash column chromatography (1-10% methanol in dichloromethane w/ 1% AcOH) to provide a light yellow oil. This material was diluted with dichloromethane and washed with 6 M aq NaOH. The organic layers were combined and washed twice more with 3 M aq NaOH. The combined organic layers were dried (MgSO₄) and concentrated to afford an off-white solid (36.5 mg, 69%). Mp 238.0-240.0 °C; $[\alpha]_D^{20} +177$ (*c* 0.72, CHCl₃); *R_f* = 0.53 (10% MeOH/1% AcOH/CH₂Cl₂); IR (film) 3378, 2931, 2361, 1586, 1534 cm⁻¹; ¹H NMR (600 MHz, CDCl₃) δ 8.03 (dd, *J* = 8.4, 0.6 Hz, 1H), 7.86 (s, 2H), 7.79 (s, 1H), 7.72 (d, *J* = 7.8 Hz, 1H), 7.50 (ddd, *J* = 8.4, 8.4, 1.2 Hz, 1H), 7.14 (ddd, *J* = 8.4, 8.4, 1.2 Hz, 1H), 5.32 (s, 1H), 3.81 (br s, 1H), 3.69 (m, 1H), 3.56 (m, 4H), 2.77 (dt, *J* = 10.8, 4.2 Hz, 1H), 2.40 (br d, *J* = 13.2 Hz, 1H), 2.02 (m, 4H), 1.93 (br d, *J* = 11.4 Hz, 1H), 1.76 (m, 2H), 1.58 (m, 1H), 1.35-1.23 (m, 4H); ¹³C NMR (150.9 MHz, CDCl₃) ppm 157.4, 154.1, 148.0, 143.8, 131.7 (q, *J_{FC}* = 34.0 Hz), 129.6, 127.1, 126.2, 125.0, 124.9 (q, *J* = 3.5 Hz), 122.5 (q, *J* = 273.3 Hz), 120.8, 118.3, 90.0, 62.3, 55.2, 51.9, 34.9, 33.3, 25.9, 24.9, 24.1; HRMS (ESI): Exact mass calcd for C₂₇H₂₉F₆N₄O₂S [M+H]⁺ 587.1915, found 587.1893.

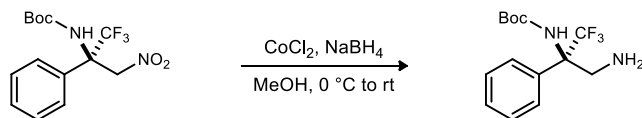


(*Z*)-tert-Butyl (2,2,2-trifluoro-1-phenylethylidene)carbamate (82).²⁵⁶ To a flame dried flask equipped with a stir bar was added trifluoroacetophenone (1.22 mL, 8.69 mmol) and the iminophosphorane (3.61 g, 9.56 mmol). Toluene (35 mL) was added and the resulting solution was heated to reflux for 18 h. The reaction mixture was then cooled to room temperature, diluted with hexanes, and allowed to stir at rt for an additional 2 h whereupon a white solid precipitated out of solution. The mixture was then filtered with hexanes and the filtrate was concentrated. Flash column chromatography of the residue (SiO₂, 2-10% ethyl acetate in hexanes) afforded the desired ketimine as a clear colorless oil (1.46 g, 61%). *R_f* = 0.54 (20% EtOAc/hexanes); IR (film) 3067, 2983, 2938, 1738, 1684 cm⁻¹; ¹H NMR (600 MHz, CDCl₃) δ 7.60 (br s, 2H), 7.54 (t, *J* = 7.2 Hz, 1H), 7.46 (t, *J* = 7.8 Hz, 2H), 1.39 (s, 9H); ¹³C NMR (150.9 MHz, CDCl₃) ppm 158.3, 131.9, 130.0, 128.7, 127.9, 119.1 (q, *J* = 284.4 Hz), 84.1, 27.8; HRMS (ESI) Exact mass calcd for C₁₃H₁₅F₃NO₂ [M+H]⁺ 274.1055, found decomposition upon submission.

²⁵⁶ Modification of: Sangamesh, B. *et al.*, Oxazine Derivatives and Their Use as BACE Inhibitors for the Treatment of Neurological Disorders. U.S. Patent WO 2011/009943 A1, January 27, 2011.

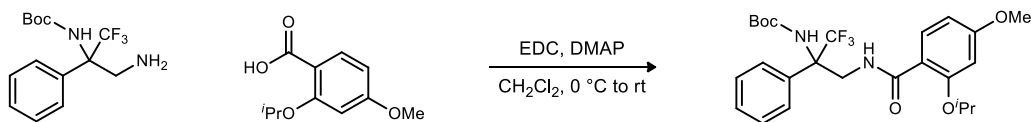


(R)-tert-Butyl (1,1,1-trifluoro-3-nitro-2-phenylpropan-2-yl)carbamate (87). To a flame dried vial equipped with a stir bar was added PBAM·HNTf₂ (11.5 mg, 14.6 μmol), toluene (293 μL) and nitromethane (79.0 μL, 1.46 mmol). The resulting mixture was chilled to -20 °C before addition of the ketimine (20.0 mg, 73.2 μmol). The reaction stirred at -20 °C for 5 days. The reaction was directly filtered through a pad of silica gel with CH₂Cl₂ and EtOAc and the filtrate was concentrated. Flash column chromatography of the residue (SiO₂, 1-10% ethyl acetate in hexanes) afforded the desired adduct as a white crystalline solid (8.40 mg, 34%) that was found to be 66% ee by chiral HPLC; (Chiralpak AD, 5% *i*PrOH/hexanes, 1 mL/min, *t*_r(major) 12.7 min, *t*_r(minor) 11.2 min); Mp 80.0-82.0 °C; [α]_D²⁰ +13.9 (*c* 0.49, CHCl₃); R_f = 0.43 (20% EtOAc/hexanes); IR (film) 3259, 3159, 2979, 2361, 1717, 1563, 1502 cm⁻¹; ¹H NMR (600 MHz, CDCl₃) δ 7.44 (s, 5H), 5.55 (br d, *J* = 12.0 Hz, 1H), 5.48 (br d, *J* = 12.0 Hz, 1H), 5.42 (s, 1H), 1.46 (s, 9H); ¹³C NMR (150.9 MHz, CDCl₃) ppm 153.6, 132.6, 129.7, 129.0, 126.1, 123.9 (q, *J*_{CF} = 286.0 Hz), 81.8, 73.1, 63.9 (q, *J*_{CF} = 28.1 Hz), 28.1; HRMS (ESI): Exact mass calcd for C₁₄H₁₇F₃N₂NaO₄ [M+Na]⁺ 357.1038, found 357.1040.

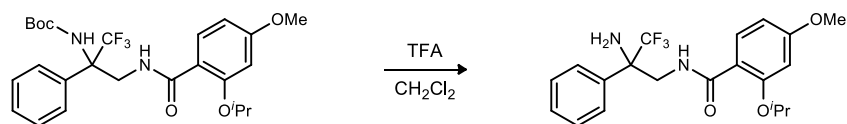


(R)-tert-Butyl (3-amino-1,1,1-trifluoro-2-phenylpropan-2-yl)carbamate (90). The nitroalkane (192 mg, 574 μmol) was dissolved in MeOH (2.3 mL) at rt. CoCl₂ (74.5 mg, 574 μmol) was added and the reaction mixture was chilled to 0 °C before NaBH₄ (327 mg, 8.62 mmol) was added in three portions over 40 min. The reaction mixture was warmed to rt and allowed to stir for an additional 2 h before being quenched with 1 M HCl. The reaction mixture was adjusted to pH 10 with conc aq NH₄OH. The solution was then filtered through a glass frit with water and CH₂Cl₂ and the layers were separated. The organic layer was dried (MgSO₄) and concentrated to afford the amine as an off-white crystalline solid (150 mg, 86%) which was determined to be 69% ee by chiral HPLC analysis (Chiralcel OJ, 10% *i*PrOH/hexanes, 1 mL/min *t*_r(major) = 10.8 min, *t*_r(minor) = 6.2 min). Mp 77.0-79.0 °C; R_f = 0.47 (5% MeOH/1% AcOH/CH₂Cl₂); IR (film) 3328, 2978, 1719 cm⁻¹; ¹H NMR (600 MHz, CDCl₃) δ 7.44 (d, *J* = 8.4 Hz, 2H), 7.38 (dd, *J* = 7.2, 7.2 Hz, 2H),

7.34 (m, 1H), 5.67 (br s, 1H), 3.65 (br d, $J = 11.4$ Hz, 1H), 3.26 (br d, $J = 8.4$ Hz, 1H), 1.39 (br s, 9H), 1.26 (br s, 2H); ^{13}C NMR (150.9 MHz, CDCl_3) ppm 154.0, 128.5, 128.3, 126.3, 126.0 (q, $J = 287$ Hz), 80.5, 65.1 (q, $J = 25.7$ Hz), 46.7, 29.7, 28.1; HRMS (EI) Exact mass calcd for $\text{C}_{15}\text{H}_{19}\text{ClN}_3$ $[\text{M}^+]$ 304.1399, found 304.1393.

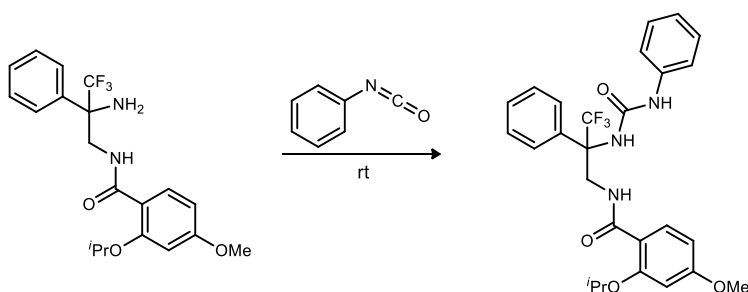


tert-Butyl (1,1,1-trifluoro-3-(2-isopropoxy-4-methoxybenzamido)-2-phenylpropan-2-yl)carbamate (92). To a flame dried flask equipped with a stir bar was added the amine (231 mg, 759 μmol), the carboxylic acid (159 mg, 759 μmol), and dichloromethane (4 mL). The resulting solution was chilled to 0 °C and EDC (189 mg, 987 μmol) and DMAP (9.30 mg, 76.0 μmol) were added. The reaction mixture was stirred and allowed to gradually warm to room temperature. After 16 h, the reaction mixture was diluted with water and extracted with CH_2Cl_2 . The combined organic layers were washed once with water, dried (MgSO_4), and concentrated. Flash column chromatography of the residue (SiO_2 , 10-40% ethyl acetate in hexanes) afforded the desired amide as a white foam (367 mg, 97%). $R_f = 0.77$ (5% MeOH/1% AcOH/ CH_2Cl_2); IR (film) 3388, 3281, 2979, 1734, 1643, 1605, 1532 cm^{-1} ; ^1H NMR (600 MHz, CDCl_3) δ 8.39 (dd, $J = 6.0, 6.0$ Hz, 1H), 8.19 (d, $J = 9.0$ Hz, 1H), 7.50 (d, $J = 7.8$ Hz, 2H), 7.38 (dd, $J = 7.2, 7.2$ Hz, 2H), 7.33 (dd, $J = 7.2, 7.2$ Hz, 1H), 6.58 (dd, $J = 9.0, 2.4$ Hz, 1H), 6.45 (d, $J = 1.8$ Hz, 1H), 6.42 (br s, 1H), 4.65 (qq, $J = 6.0, 6.0$ Hz, 1H), 4.21 (br dd, $J = 12.6, 5.4$ Hz, 1H), 4.03 (dd, $J = 14.4, 5.6$ Hz, 1H), 3.83 (s, 3H), 1.39 (br s, 9H), 1.33 (d, $J = 6.6$ Hz, 3H), 1.27-1.24 (m, 3H); ^{13}C NMR (150.9 MHz, CDCl_3) ppm 166.9, 163.6, 157.3, 153.9, 135.2, 134.3, 128.4, 128.2, 126.3, 125.7 (q, $J = 288$ Hz), 114.3, 105.2, 100.2, 80.3, 71.6, 66.4 (q, $J = 25.8$ Hz), 55.5, 45.5, 28.1, 21.7, 21.6; HRMS (ESI) Exact mass calcd for $\text{C}_{25}\text{H}_{31}\text{F}_3\text{N}_2\text{NaO}_5$ $[\text{M}+\text{Na}]^+$ 519.2083, found 519.2067.



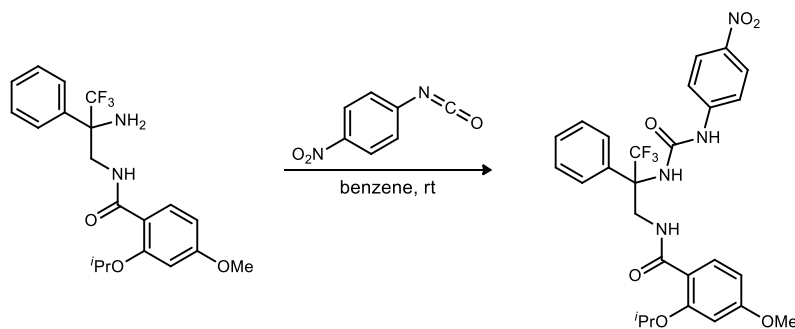
***N*-(2-Amino-3,3,3-trifluoro-2-phenylpropyl)-2-isopropoxy-4-methoxybenzamide (93).** The amide (367 mg, 739 μmol) was dissolved in CH_2Cl_2 (8 mL), treated with TFA (2.27 mL, 29.6 mmol), and stirred at rt for 16 h. The reaction mixture was poured into satd aq NaHCO_3 and extracted with CH_2Cl_2 . The combined organic layers were dried (MgSO_4), filtered, and

concentrated to afford the amine as a light orange solid (293 mg, 100%). Mp 87.0-90.0 °C; $R_f = 0.65$ (5% MeOH/1% AcOH/CH₂Cl₂); IR (film) 3384, 2980, 1645, 1605, 1531 cm⁻¹; ¹H NMR (600 MHz, CDCl₃) δ 8.16 (d, $J = 9.0$ Hz, 1H), 8.11 (dd, $J = 5.4$ Hz, 1H), 7.64 (d, $J = 7.8$ Hz, 2H), 7.40 (m, 2H), 7.35 (dt, $J = 5.4, 1.2$ Hz, 1H), 6.54 (dd, $J = 8.4, 2.4$ Hz, 1H), 6.38 (d, $J = 2.4$ Hz, 1H), 4.55 (qq, $J = 6.0, 6.0$ Hz, 1H), 4.20 (dd, $J = 13.8, 6.0$ Hz, 1H), 4.14 (dd, $J = 13.8, 6.0$ Hz, 1H), 3.80 (s, 3H), 1.97 (br s, 2H), 1.14 (d, $J = 6.0$ Hz, 3H), 1.13 (d, $J = 6.0$ Hz, 3H); ¹³C NMR (150.9 MHz, CDCl₃) ppm 166.1, 163.3, 157.2, 136.1, 134.2, 128.6, 128.5, 127.0, 126.5 (q, $J = 286$ Hz), 114.5, 105.1, 100.2, 71.4, 62.1 (q, $J = 24.1$ Hz), 55.4, 43.8, 21.59, 21.55; HRMS (ESI) Exact mass calcd for C₂₀H₂₄F₃N₂O₃ [M+H]⁺ 397.1715, found 397.1725.



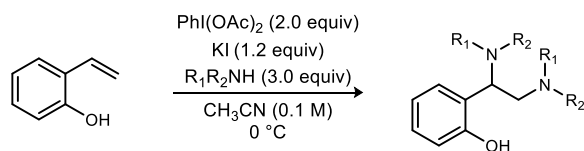
2-Isopropoxy-4-methoxy-N-(3,3,3-trifluoro-2-phenyl-2-(3-phenylureido)propyl)benzamide

(99). To a vial equipped with a stir bar was added the amine (40.0 mg, 101 μ mol) and isocyanate (331 μ L, 3.03 mmol). The resulting mixture was stirred at rt 24 h, diluted with dichloromethane and washed with satd aq NaHCO₃. The aqueous layer was extracted with dichloromethane and the organic extracts were dried (MgSO₄), filtered and concentrated. Flash column chromatography of the residue (SiO₂, 5-100% diethyl ether in hexanes) afforded the desired urea as an off-white viscous oil (47.4 mg, 91%). $R_f = 0.46$ (40% EtOAc/hexanes); IR (film) 3349, 3062, 2980, 2361, 1712, 1626, 1603, 1553 cm⁻¹; ¹H NMR (400 MHz, CDCl₃) δ 8.61 (dd, $J = 6.4, 6.4$ Hz, 1H), 8.11 (d, $J = 8.8$ Hz, 1H), 7.54 (d, $J = 7.6$ Hz, 2H), 7.38-7.31 (m, 3H), 7.26 (dd, $J = 8.4, 8.4$ Hz, 3H), 7.18 (dd, $J = 7.6, 7.6$ Hz, 2H), 7.07 (br s, 1H), 6.96 (dd, $J = 7.2, 7.2$ Hz, 1H), 6.53 (dd, $J = 8.8, 2.0$ Hz, 1H), 6.42 (br d, $J = 2.0$ Hz, 1H), 4.63 (qq, $J = 6.4, 6.4$ Hz, 1H), 4.18 (br dd, $J = 14.0, 6.8$ Hz, 1H), 4.04 (dd, $J = 14.4, 6.0$ Hz, 1H), 3.83 (s, 3H), 1.30 (d, $J = 6.0$ Hz, 3H), 1.26 (d, $J = 6.0$ Hz, 3H); ¹³C NMR (125.8 MHz, CDCl₃) ppm 167.8, 163.8, 157.6, 153.7, 138.7, 135.4, 134.1, 128.8, 128.6, 128.3, 126.2, 125.9 (q, $J = 288.6$ Hz), 123.0, 119.7, 113.7, 105.3, 100.3, 71.9, 67.2 (q, $J = 25.9$ Hz), 55.5, 46.8, 21.63, 21.61; HRMS (ESI) Exact mass calcd for C₂₇H₂₉F₃N₃O₄ [M+H]⁺ 516.2110, found 516.2094.



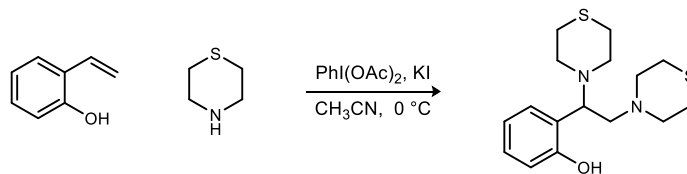
2-Isopropoxy-4-methoxy-N-(3,3,3-trifluoro-2-(3-(4-nitrophenyl)ureido)-2-phenylpropyl)

benzamide (102). To a vial equipped with a stir bar was added the amine (40.0 mg, 101 μmol) and isocyanate (166 mg, 1.01 mmol). Benzene (1 mL) was added and the resulting mixture was stirred at rt 72 h. The solution was then diluted with dichloromethane and washed with satd aq NaHCO_3 . The aqueous layer was extracted with dichloromethane and the organic extracts were dried (MgSO_4), filtered and concentrated. Flash column chromatography of the residue (SiO_2 , 50-100% diethyl ether in hexanes) afforded the desired urea as a light yellow viscous oil (30.4 mg, 55%). $R_f = 0.23$ (100% diethyl ether); IR (film) 3352, 3094, 2928, 1722, 1626, 1603, 1555, 1501 cm^{-1} ; ^1H NMR (600 MHz, CDCl_3) δ 8.72 (dd, $J = 6.0, 6.0$ Hz, 1H), 8.09 (d, $J = 9.0$ Hz, 1H), 8.04 (d, $J = 9.0$ Hz, 2H), 7.84 (br s, 1H), 7.77 (s, 1H), 7.56 (d, $J = 7.8$ Hz, 2H), 7.46-7.41 (m, 4H), 7.37 (m, 1H), 6.52 (dd, $J = 8.4, 1.8$ Hz, 1H), 6.42 (d, $J = 1.8$ Hz, 1H), 4.67 (qq, $J = 6.0, 6.0$ Hz, 1H), 4.10 (dd, $J = 14.4, 7.2$ Hz, 1H), 3.94 (dd, $J = 15.0, 6.0$ Hz, 1H), 3.83 (s, 3H), 1.33 (d, $J = 6.0$ Hz, 3H), 1.31 (d, $J = 6.0$ Hz, 3H); ^{13}C NMR (150.9 MHz, CDCl_3) ppm 168.7, 164.2, 157.7, 152.5, 145.3, 142.2, 134.8, 133.9, 128.9, 128.6, 125.8, 125.8 (q, $J = 289.3$ Hz), 125.0, 117.8, 112.9, 105.6, 100.2, 72.0, 67.7 (q, $J = 26.4$ Hz), 55.6, 48.0, 21.72, 21.69; HRMS (ESI) Exact mass calcd for $\text{C}_{27}\text{H}_{28}\text{F}_3\text{N}_4\text{O}_6$ $[\text{M}+\text{H}]^+$ 561.1961, found 561.1944.

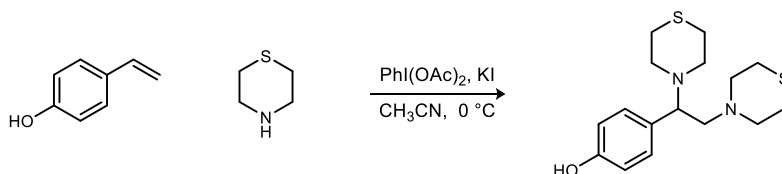


General procedure for Hypervalent Iodine-Mediated Intermolecular Diamination: A vial equipped with a stir bar was charged with potassium iodide (60.0 mg, 360 μmol), iodobenzene diacetate (193 mg, 600 μmol), and acetonitrile (3 mL) and was chilled to 0 $^\circ\text{C}$. The amine (900 μmol) and vinylphenol (300 μmol) were added and the resulting mixture was stirred at 0 $^\circ\text{C}$ for 18

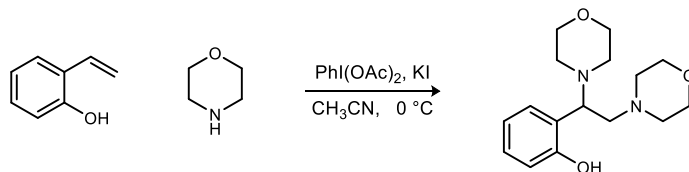
h. The reaction mixture was then diluted with ethyl acetate and concentrated. No reductive workup was used in these studies, but is recommended for a larger scale.



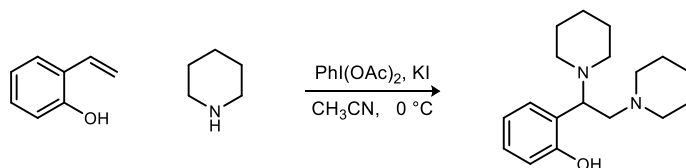
2-(1,2-Dithiomorpholinoethyl)phenol (338a). Prepared according to the general procedure using thiomorpholine (91.0 μL , 900 μmol) and 2-vinylphenol (36.0 mg, 300 μmol). Flash column chromatography of the residue (SiO_2 , 5-60% diethyl ether in hexanes) afforded the desired product as a light orange amorphous solid (97.0 mg, 99%). Mp 82.0-86.0 $^\circ\text{C}$; $R_f = 0.06$ (10% EtOAc/hexanes); IR (film) 3040 (br), 2910, 2810, 1607, 1587 cm^{-1} ; ^1H NMR (600 MHz, CDCl_3) δ 11.18 (br s, 1H), 7.15 (ddd, $J = 8.4, 8.4, 1.2$ Hz, 1H), 7.02 (dd, $J = 7.8, 0.6$ Hz, 1H), 6.80 (d, $J = 7.8$ Hz, 1H), 6.79 (ddd, $J = 7.2, 7.2, 1.2$ Hz, 1H), 3.77 (dd, $J = 6.6, 6.6$ Hz, 1H), 3.10 (dd, $J = 7.2, 3.0$ Hz, 1H), 3.08 (dd, $J = 6.6, 3.0$ Hz, 1H), 2.92-2.88 (m, 3H), 2.77-2.65 (m, 9H), 2.64-2.61 (m, 4H); ^{13}C NMR (150 MHz, CDCl_3) ppm 157.3, 128.7, 128.4, 124.8, 119.1, 116.7, 65.6, 59.2, 55.6, 52.2, 28.04, 27.97; HRMS (ESI): Exact mass calcd for $\text{C}_{16}\text{H}_{25}\text{N}_2\text{OS}_2$ $[\text{M}+\text{H}]^+$ 325.1408, found 325.1395.



4-(1,2-Dithiomorpholinoethyl)phenol (340a). Prepared according to the general procedure using thiomorpholine (91.0 μL , 900 μmol) and 4-vinylphenol (36.0 mg, 300 μmol). Flash column chromatography of the residue (SiO_2 , 25-50-75-100% diethyl ether in hexanes) afforded the desired product as a light brown solid (60.4 mg, 62%). Mp 139.0-143.0 $^\circ\text{C}$; $R_f = 0.21$ (80% EtOAc/hexanes); IR (film) 3200 (br), 2916, 2815, 1611, 1513 cm^{-1} ; ^1H NMR (400 MHz, CDCl_3) δ 7.74 (br s, 1H), 6.99 (d, $J = 8.4$ Hz, 2H), 6.67 (d, $J = 8.4$ Hz, 2H), 3.69 (dd, $J = 6.4, 6.4$ Hz, 1H), 2.97 (dd, $J = 13.2, 6.4$ Hz, 1H), 2.91-2.86 (m, 2H), 2.80-2.71 (m, 7H), 2.66-2.58 (m, 8H); ^{13}C NMR (125 MHz, CDCl_3) ppm 155.6, 129.7, 129.1, 115.1, 66.6, 60.6, 55.3, 52.1, 27.9, 27.4; HRMS (ESI): Exact mass calcd for $\text{C}_{16}\text{H}_{25}\text{N}_2\text{OS}_2$ $[\text{M}+\text{H}]^+$ 325.1408, found 325.1411.

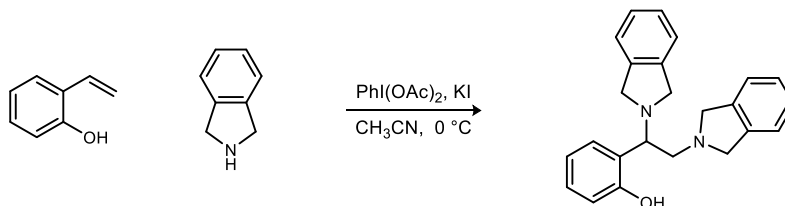


2-(1,2-Dimorpholinoethyl)phenol (338b). Prepared according to the general procedure using morpholine (78.0 μL , 900 μmol) and 2-vinylphenol (36.0 mg, 300 μmol). Flash column chromatography of the residue (SiO_2 , 10-100% diethyl ether in hexanes) afforded the desired product as an off-white solid (69.2 mg, 79%). Mp 86.0-89.0 $^\circ\text{C}$; $R_f = 0.27$ (100% Et_2O); IR (film) 3040 (br), 2958, 2851, 1588 cm^{-1} ; ^1H NMR (400 MHz, CDCl_3) δ 10.60 (br s, 1H), 7.15 (dd, $J = 7.6, 7.6$ Hz, 1H), 6.99 (d, $J = 7.6$ Hz, 1H), 6.79 (d, $J = 8.0$ Hz, 1H), 6.78 (dd, $J = 8.0, 8.0$ Hz, 1H), 3.79-3.69 (m, 4H), 3.64 (dd, $J = 4.0$ Hz, 4H), 3.54 (dd, $J = 5.6, 5.6$ Hz, 1H); 2.94 (dd, $J = 13.6, 6.4$ Hz, 1H), 2.81-2.74 (br m, 2H), 2.63-2.56 (m, 3H), 2.49-2.36 (m, 4H); ^{13}C NMR (125 MHz, CDCl_3) ppm 156.7, 129.1, 128.7, 124.8, 119.2, 116.6, 67.3, 67.0, 66.9, 60.4, 54.2, 51.6; HRMS (ESI): Exact mass calcd for $\text{C}_{16}\text{H}_{25}\text{N}_2\text{O}_3$ $[\text{M}+\text{H}]^+$ 293.1865, found 293.1852.

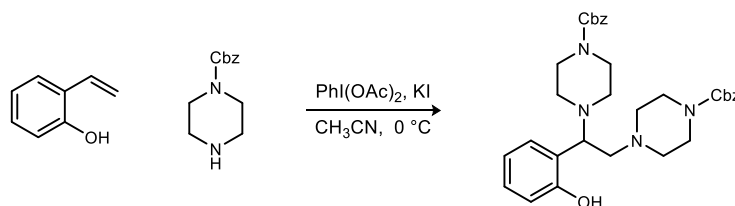


2-(1,2-Di(piperidin-1-yl)ethyl)phenol (338c). A vial equipped with a stir bar was charged with potassium iodide (60.0 mg, 360 μmol), iodobenzene diacetate (290 mg, 900 μmol), and acetonitrile (3 mL) and was chilled to 0 $^\circ\text{C}$. Piperidine (89.0 μL , 900 μmol) and 2-vinylphenol (36.0 mg, 300 μmol) were added and the resulting mixture was stirred at 0 $^\circ\text{C}$ for 18 h. The reaction mixture was then diluted with ethyl acetate and concentrated. Flash column chromatography of the residue (SiO_2 , 50-100% diethyl ether in hexanes) afforded the desired product as a light brown solid (25.4 mg, 29%). Mp 59.0-62.0 $^\circ\text{C}$; $R_f = 0.11$ (20% EtOAc /hexanes); IR (film) 3050 (br), 2933, 2851, 1588 cm^{-1} ; ^1H NMR (400 MHz, CDCl_3) δ 10.17 (br s, 1H), 7.13 (ddd, $J = 7.6, 7.6, 1.6$ Hz, 1H), 7.08 (dd, $J = 7.6, 1.2$ Hz, 1H), 6.80 (dd, $J = 8.0, 1.2$ Hz, 1H), 6.76 (ddd, $J = 7.6, 7.6, 1.2$ Hz, 1H), 3.77 (dd, $J = 6.0, 6.0$ Hz, 1H), 2.93 (dd, $J = 13.6, 5.6$ Hz, 1H), 2.79-2.72 (m, 2H), 2.62 (dd, $J = 13.2, 6.0$ Hz, 1H), 2.61-2.54 (m, 2H), 2.51-2.39 (m, 4H), 1.70-1.52 (m, 8H), 1.51-1.45 (m, 2H), 1.45-1.36 (m, 2H); ^{13}C NMR (125 MHz, CDCl_3) ppm 157.9, 128.4, 128.2, 126.2, 118.6, 116.6,

65.6, 59.6, 55.1, 51.1, 26.2, 25.9, 24.3, 24.2; HRMS (ESI): Exact mass calcd for C₁₈H₂₉N₂O [M+H]⁺ 289.2280, found 289.2294.

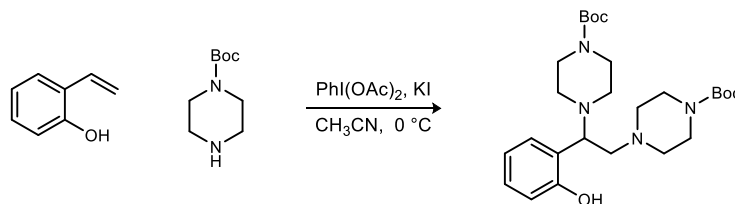


2-(1,2-Di(isoindolin-2-yl)ethyl)phenol (338d). Prepared according to the general procedure using isoindoline (102 μ L, 900 μ mol) and 2-vinylphenol (36.0 mg, 300 μ mol). Flash column chromatography of the residue (SiO₂, 5-100% diethyl ether in hexanes) afforded the desired product as a dark-brown viscous oil (31.9 mg, 30%). $R_f = 0.68$ (40% EtOAc/hexanes); IR (film) 3047, 2937, 2797, 1690, 1588 cm⁻¹; ¹H NMR (400 MHz, CDCl₃) δ 7.25-7.15 (m, 9H), 7.12 (dd, $J = 7.6, 1.6$ Hz, 1H), 6.88 (dd, $J = 8.0, 0.8$ Hz, 1H), 6.83 (ddd, $J = 7.2, 7.2, 0.8$ Hz, 1H), 4.11 (s, 4H), 4.03-3.94 (m, 4H), 3.91 (dd, $J = 6.0, 6.0$ Hz, 1H), 3.47 (dd, $J = 13.2, 6.0$ Hz, 1H), 3.16 (dd, $J = 13.2, 6.4$ Hz, 1H); ¹³C NMR (125 MHz, CDCl₃) ppm 156.9, 139.7, 139.0, 129.0, 128.9, 127.0, 126.8, 125.9, 122.3, 122.2, 119.3, 116.7, 69.3, 60.2, 60.1, 57.9; HRMS (ESI): Exact mass calcd for C₂₄H₂₅N₂O [M+H]⁺ 357.1967, found 357.1968.



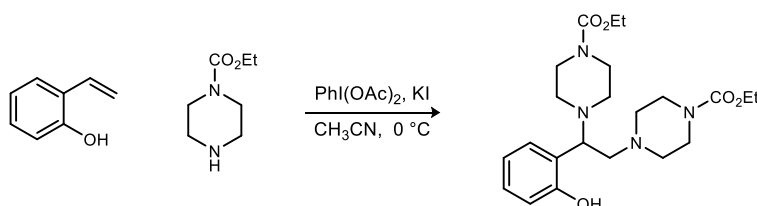
Dibenzyl 4,4'-(1-(2-hydroxyphenyl)ethane-1,2-diyl)bis(piperazine-1-carboxylate) (338e). Prepared according to the general procedure using benzyl piperazine-1-carboxylate (174 μ L, 900 μ mol) and 2-vinylphenol (36.0 mg, 300 μ mol). Flash column chromatography of the residue (SiO₂, 5-80% ethyl acetate in hexanes) afforded the desired product as a yellow viscous oil (105 mg, 62%). $R_f = 0.04$ (20% EtOAc/hexanes); IR (film) 3033, 2940, 2897, 2859, 2823, 1702, 1588 cm⁻¹; ¹H NMR (400 MHz, CDCl₃) δ 10.79 (br s, 1H); 7.39-7.28 (m, 10H), 7.16 (ddd, $J = 8.4, 8.4, 1.6$ Hz, 1H), 6.97 (dd, $J = 7.6, 1.6$ Hz, 1H), 6.80 (d, $J = 8.4$ Hz, 1H), 6.78 (ddd, $J = 7.2, 7.2, 1.2$ Hz, 1H), 5.13 (s, 2H), 5.12 (s, 2H), 3.62-3.42 (m, 9H), 2.95 (dd, $J = 13.6, 6.4$ Hz, 1H), 2.75 (br s, 2H), 2.59 (dd, $J = 13.6, 5.2$ Hz, 1H), 2.63-2.52 (m, 2H), 2.50-2.27 (m, 4H); ¹³C NMR (125 MHz, CDCl₃) ppm 156.7, 155.1, 155.0, 136.6, 136.5, 128.83, 128.81, 128.5, 128.4, 128.1, 128.0, 127.9, 127.8, ,

124.7, 119.3, 116.7, 67.2, 67.1, 66.8, 59.9, 53.4, 50.6, 43.7; HRMS (ESI): Exact mass calcd for $C_{32}H_{39}N_4O_5$ $[M+H]^+$ 559.2920, found 559.2897.



Di-tert-butyl 4,4'-(1-(2-hydroxyphenyl)ethane-1,2-diyl)bis(piperazine-1-carboxylate) (338f).

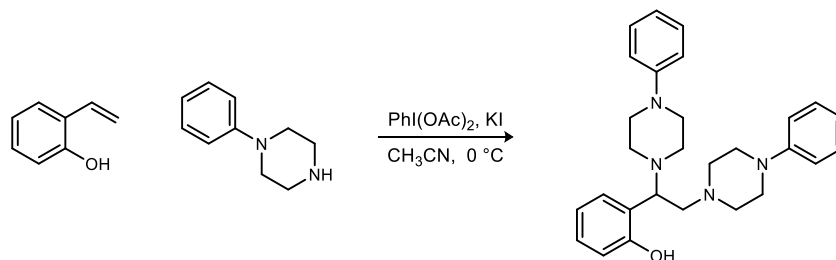
Prepared according to the general procedure using *tert*-butyl piperazine-1-carboxylate (117 mg, 630 μ mol) and 2-vinylphenol (36.0 mg, 300 μ mol). Flash column chromatography of the residue (SiO_2 , 20-80% ethyl acetate in hexanes) afforded the desired product as a light-yellow non-viscous oil (86.4 mg, 59%). R_f = 0.10 (20% EtOAc/hexanes); IR (film) 3040 (br), 2975, 2929, 2857, 1697, 1589 cm^{-1} ; 1H NMR (400 MHz, $CDCl_3$) δ 11.00 (br s, 1H), 7.14 (ddd, J = 8.4, 8.4, 1.2 Hz, 1H), 6.98 (dd, J = 7.6, 0.8 Hz, 1H), 6.79 (d, J = 8.0 Hz, 1H), 6.77 (dd, J = 8.0, 8.0 Hz, 1H), 3.57 (dd, J = 6.0, 6.0 Hz, 1H), 3.53-3.40 (m, 4H), 3.39-3.32 (m, 4H), 2.95 (dd, J = 13.6, 6.4 Hz, 1H), 2.78-2.68 (br m, 2H), 2.57 (dd, J = 13.2, 5.2 Hz, 1H), 2.61-2.51 (m, 2H), 2.48-2.28 (m, 4H), 1.45 (s, 9H), 1.44 (s, 9H); ^{13}C NMR (125 MHz, $CDCl_3$) ppm 156.8, 154.7, 154.5, 128.8, 128.7, 125.0, 119.3, 116.7, 79.9, 79.6, 66.9, 60.0, 53.5, 50.7, 44.0, 43.2, 28.4; HRMS (ESI): Exact mass calcd for $C_{26}H_{43}N_4O_5$ $[M+H]^+$ 491.3234, found 491.3233.



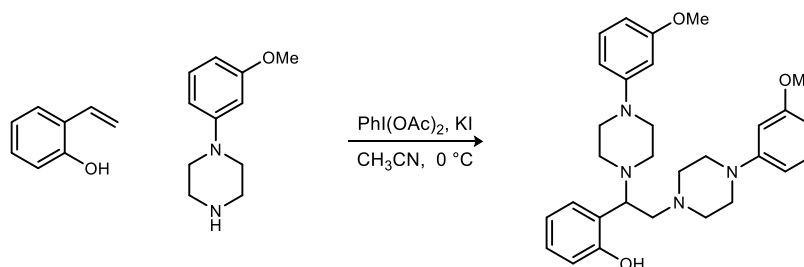
Diethyl 4,4'-(1-(2-hydroxyphenyl)ethane-1,2-diyl)bis(piperazine-1-carboxylate) (338g).

Prepared according to the general procedure using ethyl 1-piperazinecarboxylate (132 μ L, 900 μ mol) and 2-vinylphenol (36.0 mg, 300 μ mol). Flash column chromatography of the residue (SiO_2 , 10-80% ethyl acetate in hexanes) afforded the desired product as a viscous transparent yellow oil (117 mg, 90%). R_f = 0.22 (40% EtOAc/hexanes); IR (film) 3000 (br), 2982, 2860, 1699, 1589 cm^{-1} ; 1H NMR (400 MHz, $CDCl_3$) δ 10.39 (br s, 1H), 7.13 (ddd, J = 8.8, 1.6 Hz, 1H), 6.97 (dd, J = 7.2, 1.2 Hz, 1H), 6.78 (d, J = 8.4 Hz, 1H), 6.77 (ddd, J = 8.4, 0.8 Hz, 1H), 4.11 (dq, J = 6.8, 6.8 Hz, 4H), 3.57 (dd, J = 5.6, 5.6 Hz, 1H), 3.54-3.43 (m, 4H), 3.42-3.35 (m, 4H), 2.94 (dd, J = 13.6, 6.4 Hz, 1H), 2.78-2.69 (m, 2H), 2.60-2.52 (m, 3H), 2.45-2.30 (m, 4H), 1.25-1.21 (m, 6H); ^{13}C

NMR (125 MHz, CDCl₃) ppm 156.7, 155.4, 155.2, 128.8, 124.8, 119.3, 116.7, 66.8, 61.5, 61.3, 60.0, 53.4, 50.6, 43.6, 14.6; HRMS (ESI): Exact mass calcd for C₂₂H₃₅N₄O₅ [M+H]⁺ 435.2607 found 435.2599.

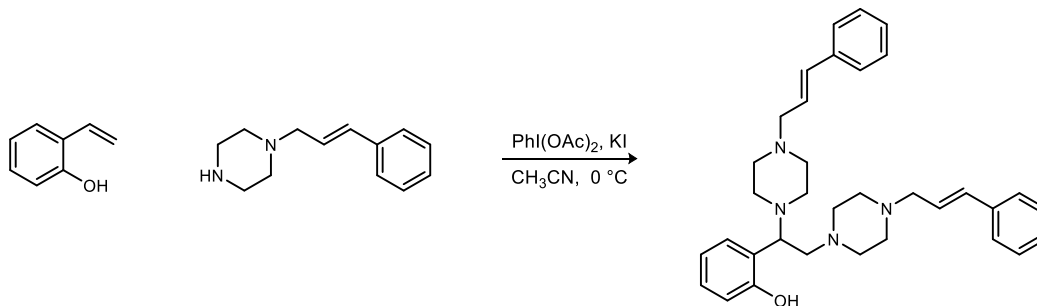


2-(1,2-Bis(4-phenylpiperazin-1-yl)ethyl)phenol (338h). Prepared according to the general procedure using 1-phenylpiperazine (137 μ L, 900 μ mol) and 2-vinylphenol (36.0 mg, 300 μ mol). Flash column chromatography of the residue (SiO₂, 5-100% diethyl ether in hexanes) afforded the desired product as an off-white solid (41.7 mg, 31%). Mp 179.0-182.0 $^{\circ}$ C; R_f = 0.57 (100% Et₂O); IR (film) 3038, 2946, 2881, 2823, 1600 cm^{-1} ; ¹H NMR (400 MHz, CDCl₃) δ 11.29 (br s, 1H), 7.32-7.27 (m, 4H), 7.20 (ddd, J = 9.2, 9.2, 1.6 Hz, 1H), 7.09 (dd, J = 7.6, 1.2 Hz, 1H), 6.94 (dd, J = 7.6, 3.6 Hz, 4H), 6.91-6.82 (m, 4H), 3.68 (dd, J = 6.0, 6.0 Hz, 1H), 3.34-3.28 (m, 2H), 3.26-3.22 (m, 2H), 3.19 (dd, J = 5.2, 5.2 Hz, 4H), 3.10 (dd, J = 13.6, 6.4 Hz, 1H), 3.04-2.99 (m, 2H), 2.83 (ddd, J = 10.4, 6.4, 2.8 Hz, 2H), 2.72-2.68 (m, 3H), 2.65-2.60 (m, 2H); ¹³C NMR (100 MHz, CDCl₃) ppm 157.0, 151.2, 150.9, 129.2, 129.1, 129.0, 128.7, 125.3, 120.1, 119.7, 119.2, 116.7, 116.2, 116.0, 66.9, 60.1, 53.8, 50.9, 49.4, 49.2; HRMS (ESI): Exact mass calcd for C₂₈H₃₅N₄O [M+H]⁺ 443.2811, found 443.2802.

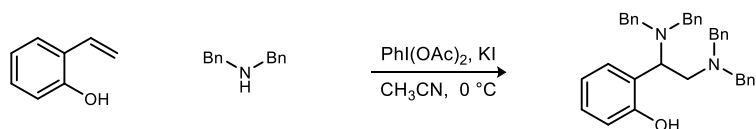


2-(1,2-Bis(4-(3-methoxyphenyl)piperazin-1-yl)ethyl)phenol (338i). Prepared according to the general procedure using 1-(3-methoxyphenyl)piperazine (155 μ L, 900 μ mol) and 2-vinylphenol (36.0 mg, 300 μ mol). Flash column chromatography of the residue (SiO₂, 20% ethyl acetate in hexanes) afforded the desired product as a light-brown viscous oil (23.4 mg, 16%). R_f = 0.15 (20% EtOAc/hexanes); IR (film) 2938, 2829, 1602, 1494 cm^{-1} ; ¹H NMR (600 MHz, CDCl₃) δ 11.15 (br s, 1H), 7.19-7.15 (m, 3H), 7.05 (dd, J = 7.2, 1.2 Hz, 1H), 6.83 (d, J = 8.4 Hz, 1H), 6.81 (ddd, J =

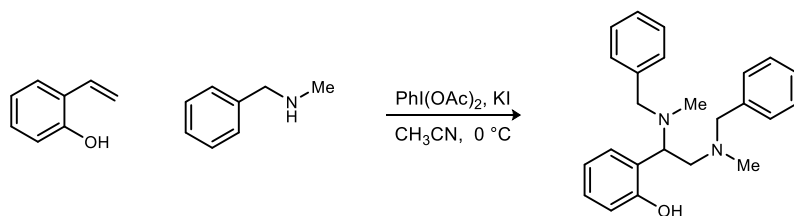
7.8, 7.8, 1.2 Hz, 1H), 6.52 (ddd, $J = 7.2, 4.2, 1.8$ Hz, 2H), 6.47-6.40 (m, 4H), 3.79 (s, 3H), 3.79 (s, 3H), 3.66 (dd, $J = 6.0, 6.0$ Hz, 1H), 3.30-3.24 (m, 2H), 3.22-3.12 (m, 6H), 3.06 (dd, $J = 13.2, 6.6$ Hz, 1H), 3.00-2.94 (m, 2H), 2.81-2.76 (m, 2H), 2.68-2.62 (m, 3H), 2.61-2.55 (m, 2H); ^{13}C NMR (150 MHz, CDCl_3) ppm 160.6, 160.5, 156.9, 152.6, 152.3, 129.8, 129.7, 129.0, 128.7, 125.2, 119.2, 116.7, 108.9, 108.8, 104.8, 104.5, 102.6, 102.5, 66.9, 60.1, 55.2, 53.7, 50.9, 49.3, 49.1; HRMS (ESI): Exact mass calcd for $\text{C}_{30}\text{H}_{39}\text{N}_4\text{O}_3$ $[\text{M}+\text{H}]^+$ 503.3022, found 503.3006.



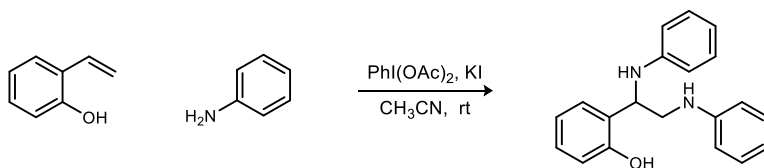
2-(1,2-bis(4-cinnamylpiperazin-1-yl)ethyl)phenol (338j). Prepared according to the general procedure using *trans*-1-cinnamylpiperazine (182 mg, 900 μmol) and 2-vinylphenol (36.0 mg, 300 μmol). Flash column chromatography of the residue (SiO_2 , 0.5-1-2-5-10% methanol in dichloromethane) afforded the desired product as a light-brown viscous oil (146.8 mg, 94%). $R_f = 0.29$ (5% MeOH/DCM); IR (film) 3385 (br), 3026, 2937, 2811, 1588 cm^{-1} ; ^1H NMR (600 MHz, CDCl_3) δ 7.92 (br s, 1H), 7.38-7.36 (m, 4H), 7.31 (dd, $J = 7.2$ Hz, 4H), 7.26-7.23 (m, 2H), 7.14 (ddd, $J = 8.4, 8.4, 1.2$ Hz, 1H), 6.99 (dd, $J = 7.8, 1.2$ Hz, 1H), 6.79 (d, $J = 8.4$ Hz, 1H), 6.77 (dd, $J = 7.2, 7.2$ Hz, 1H), 6.54 (dd, $J = 16.2, 8.4$ Hz, 2H), 6.23-6.24 (m, 2H), 3.59 (dd, $J = 5.4, 5.4$ Hz, 1H), 3.27 (d, $J = 6.6$ Hz, 2H), 3.22 (dddd, $J = 6.6, 6.6, 6.6, 6.6$ Hz, 2H), 2.95 (dd, $J = 13.8, 6.0$ Hz, 1H), 3.10-2.40 (m, 17H); ^{13}C NMR (150 MHz, CDCl_3) ppm 157.0, 136.5, 136.3, 134.9, 134.2, 128.9, 128.7, 128.59, 128.57, 127.9, 127.7, 126.5, 126.4, 125.0, 124.9, 123.8, 119.1, 116.6, 66.7, 60.6, 60.4, 59.3, 53.0, 52.7, 52.6, 50.0; HRMS (ESI): Exact mass calcd for $\text{C}_{34}\text{H}_{43}\text{N}_4\text{O}$ $[\text{M}+\text{H}]^+$ 523.3437, found 523.3416.



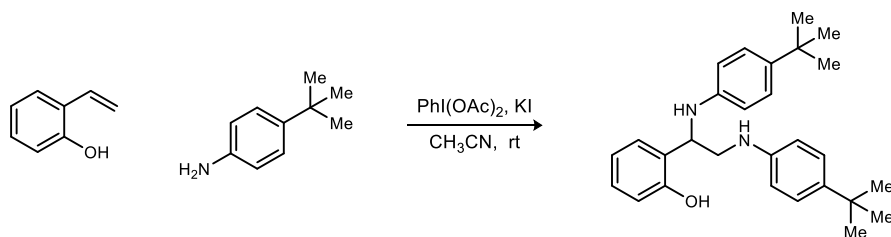
2-(1,2-Bis(dibenzylamino)ethyl)phenol (338k). Prepared according to the general procedure using dibenzylamine (173 μL , 900 μmol) and 2-vinylphenol (36.0 mg, 300 μmol). Flash column chromatography of the residue (SiO_2 , 0.25-0.5-1-2% ethyl acetate in hexanes) afforded the desired product as a light-yellow viscous oil (53.1 mg, 35%). $R_f = 0.84$ (40% EtOAc/hexanes); IR (film) 3061, 3028, 2835, 1585, 1493 cm^{-1} ; ^1H NMR (400 MHz, CDCl_3) δ 10.77 (br s, 1H), 7.30-7.18 (m, 16H), 7.17-7.12 (m, 6H), 6.82 (dd, $J = 8.4, 1.2$ Hz, 1H), 6.76 (ddd, $J = 7.6, 1.2$ Hz, 1H), 4.10 (dd, $J = 8.8, 4.0$ Hz, 1H), 3.62 (s, 2H), 3.62 (s, 2H), 3.52 (d, $J = 13.2$ Hz, 2H), 3.41 (d, $J = 13.2$ Hz, 2H), 3.11 (dd, $J = 13.2, 4.0$ Hz, 1H), 2.97 (dd, $J = 13.2, 8.8$ Hz, 1H); ^{13}C NMR (100 MHz, CDCl_3) ppm 157.0, 138.6, 137.7, 129.29, 129.27, 129.2, 128.6, 128.5, 128.2, 127.4, 127.1, 125.6, 119.0, 116.6, 61.3, 59.1, 54.1, 52.5; HRMS (ESI): Exact mass calcd for $\text{C}_{36}\text{H}_{37}\text{N}_2\text{O}$ $[\text{M}+\text{H}]^+$ 513.2906, found 513.2894.



2-(1,2-Bis(benzyl(methyl)amino)ethyl)phenol (338l). Prepared according to the general procedure using *N*-benzylmethylamine (116 μL , 900 μmol) and 2-vinylphenol (36.0 mg, 300 μmol). Flash column chromatography of the residue (SiO_2 , 5-10-20-40% ethyl acetate in hexanes) afforded the desired product as a light-yellow transparent viscous oil (70.0 mg, 65%). $R_f = 0.43$ (30% EtOAc/hexanes); IR (film) 3061, 3028, 2948, 2844, 2791, 1587 cm^{-1} ; ^1H NMR (600 MHz, CDCl_3) δ 7.35-7.23 (m, 10H), 7.19 (ddd, $J = 9.0, 9.0, 1.2$ Hz, 1H), 7.16 (d, $J = 7.8$ Hz, 1H), 6.87 (d, $J = 7.8$ Hz, 1H), 6.83 (dd, $J = 7.2, 7.2$ Hz, 1H), 3.89 (dd, $J = 6.0, 6.0$ Hz, 1H), 3.78 (d, $J = 13.2$ Hz, 1H), 3.69 (d, $J = 12.6$ Hz, 1H), 3.59 (d, $J = 13.2$ Hz, 1H), 3.52 (d, $J = 13.2$ Hz, 1H), 3.11 (dd, $J = 13.2, 5.4$ Hz, 1H), 2.83 (dd, $J = 13.2, 6.0$ Hz, 1H), 2.24 (s, 3H), 2.22 (s, 3H); ^{13}C NMR (150.9 MHz, CDCl_3) ppm 157.3, 138.6, 137.6, 129.2, 129.0, 128.6, 128.51, 128.45, 128.3, 127.4, 127.1, 126.0, 119.0, 116.7, 65.9, 63.1, 59.0, 58.2, 42.6, 38.0; HRMS (ESI): Exact mass calcd for $\text{C}_{24}\text{H}_{29}\text{N}_2\text{O}$ $[\text{M}+\text{H}]^+$ 361.2280, found 361.2288.

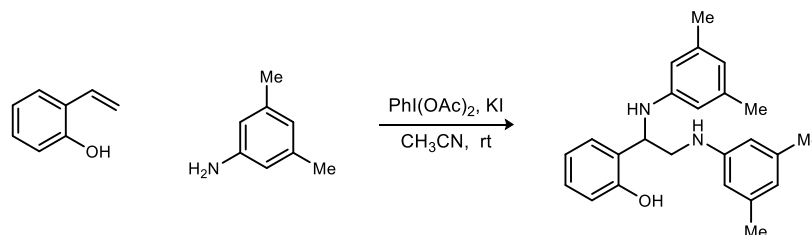


2-(1,2-Bis(phenylamino)ethyl)phenol (338m). A vial equipped with a stir bar was charged with potassium iodide (60.0 mg, 360 μmol), iodobenzene diacetate (193 mg, 600 μmol), and acetonitrile (3 mL). Aniline (82.0 μL , 900 μmol) and 2-vinylphenol (36.0 mg, 300 μmol) were added and the resulting mixture was stirred at rt for 18 h. The reaction mixture was then diluted with ethyl acetate and concentrated. Flash column chromatography of the residue (SiO_2 , 2-5-10-20% ethyl acetate in hexanes) afforded the desired product as a brown viscous oil (54.6 mg, 60%). $R_f = 0.26$ (10% EtOAc/hexanes); IR (film) 3391, 3050, 1602, 1499 cm^{-1} ; ^1H NMR (400 MHz, CDCl_3) δ 9.69 (br s, 1H), 7.25-7.20 (m, 4H), 7.16 (dd, $J = 8.4, 7.6$ Hz, 2H), 6.94 (ddd, $J = 7.2, 7.2, 0.8$ Hz, 1H), 6.91-6.78 (m, 5H), 6.74 (d, $J = 7.6$ Hz, 2H), 4.70 (br s, 1H), 4.53 (dd, $J = 9.6, 4.8$ Hz, 1H), 3.91 (br s, 1H), 3.63 (dd, $J = 13.2, 9.6$ Hz, 1H), 3.51 (dd, $J = 13.2, 4.4$ Hz, 1H); ^{13}C NMR (125 MHz, CDCl_3) ppm 156.7, 147.4, 146.7, 129.5, 129.3, 129.1, 128.0, 124.2, 121.2, 120.3, 118.9, 117.3, 116.7, 113.7, 60.2, 49.1; HRMS (ESI): Exact mass calcd for $\text{C}_{20}\text{H}_{21}\text{N}_2\text{O}$ $[\text{M}+\text{H}]^+$ 305.1648, found 305.1643.

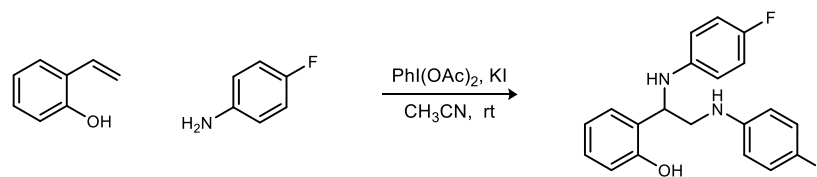


2-(1,2-Bis((4-*tert*-butyl)phenyl)amino)ethyl)phenol (338n). A vial equipped with a stir bar was charged with potassium iodide (60.0 mg, 360 μmol), iodobenzene diacetate (193 mg, 600 μmol), and acetonitrile (3 mL). The aniline (143 μL , 900 μmol) and 2-vinylphenol (36.0 mg, 300 μmol) were added and the resulting mixture was stirred at rt for 18 h. The reaction mixture was then diluted with ethyl acetate and concentrated. Flash column chromatography of the residue (SiO_2 , 0.5-1-2-5-10% ethyl acetate in hexanes) afforded the desired product as a brown viscous oil (66.5 mg, 53%). $R_f = 0.49$ (20% EtOAc/hexanes); IR (film) 3307, 3049, 2961, 2903, 2866, 1614, 1588, 1518 cm^{-1} ; ^1H NMR (400 MHz, CDCl_3) δ 10.06 (br s, 1H), 7.26-7.16 (m, 6H), 6.92 (ddd, $J = 7.2, 7.2, 1.2$ Hz, 1H), 6.84 (d, $J = 8.0$ Hz, 1H), 6.74 (d, $J = 8.4$ Hz, 2H), 6.69 (d, $J = 8.8$ Hz, 2H), 4.69 (br s, 1H), 4.47 (dd, $J = 9.6, 4.4$ Hz, 1H), 3.81 (br s, 1H), 3.61 (dd, $J = 13.2, 10.8$ Hz, 1H), 3.47

(dd, $J = 13.2, 4.4$ Hz, 1H); 1.29 (s, 9H), 1.24 (s, 9H); ^{13}C NMR (125 MHz, CDCl_3) ppm 157.1, 144.9, 144.2, 141.9, 129.01, 128.03, 126.3, 126.1, 124.3, 120.1, 117.3, 116.5, 113.5, 60.8, 49.4, 34.0, 33.9, 31.5, 31.4; HRMS (ESI): Exact mass calcd for $\text{C}_{28}\text{H}_{37}\text{N}_2\text{O}$ $[\text{M}+\text{H}]^+$ 417.2906, found 417.2917.

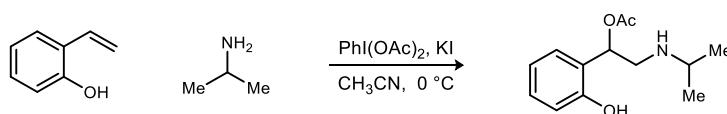


2-(1,2-Bis((3,5-dimethylphenyl)amino)ethyl)phenol (338o). A vial equipped with a stir bar was charged with potassium iodide (60.0 mg, 360 μmol), iodobenzene diacetate (193 mg, 600 μmol), and acetonitrile (3 mL). The aniline (112 μL , 900 μmol) and 2-vinylphenol (36.0 mg, 300 μmol) were added and the resulting mixture was stirred at rt for 18 h. The reaction mixture was then diluted with ethyl acetate and concentrated. Flash column chromatography of the residue (SiO_2 , 5-10-20% ethyl acetate in hexanes) afforded the desired product as a light brown solid (64.3 mg, 60%). Mp 120.0-124.0 $^\circ\text{C}$; $R_f = 0.44$ (20% EtOAc/hexanes); IR (film) 3387, 3023, 2917, 2857 cm^{-1} ; ^1H NMR (400 MHz, CDCl_3) δ 9.91 (br s, 1H), 7.22 (ddd, $J = 7.6, 7.6, 1.6$ Hz, 1H), 7.19 (dd, $J = 8.4, 1.6$ Hz, 1H), 6.93 (ddd, $J = 7.6, 7.6, 1.2$ Hz, 1H), 6.86 (dd, $J = 8.0, 0.8$ Hz, 1H), 6.55 (s, 1H), 6.48 (s, 1H), 6.42 (s, 2H), 6.37 (s, 2H), 4.59 (br s, 1H), 4.48 (dd, $J = 9.6, 4.4$ Hz, 1H), 3.76 (br s, 1H), 3.60 (dd, $J = 13.2, 10.0$ Hz, 1H), 3.46 (dd, $J = 13.2, 4.4$ Hz, 1H), 2.27 (s, 6H), 2.19 (s, 6H); ^{13}C NMR (125 MHz, CDCl_3) ppm 156.9, 147.5, 146.7, 139.1, 138.9, 128.9, 128.0, 124.4, 123.1, 120.9, 120.1, 117.3, 114.6, 111.7, 60.4, 49.2, 21.5, 21.4; HRMS (ESI): Exact mass calcd for $\text{C}_{24}\text{H}_{29}\text{N}_2\text{O}$ $[\text{M}+\text{H}]^+$ 361.2280, found 361.2285.

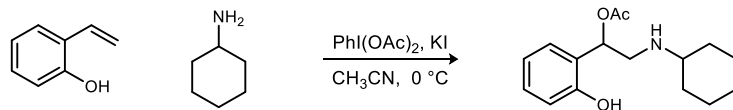


2-(1,2-Bis((4-fluorophenyl)amino)ethyl)phenol (338p). A vial equipped with a stir bar was charged with potassium iodide (60.0 mg, 360 μmol), iodobenzene diacetate (193 mg, 600 μmol), and acetonitrile (3 mL). The aniline (85.0 μL , 900 μmol) and 2-vinylphenol (36.0 mg, 300 μmol) were added and the resulting mixture was stirred at rt for 18 h. The reaction mixture was then diluted with ethyl acetate and concentrated. Flash column chromatography of the residue (SiO_2 , 1-

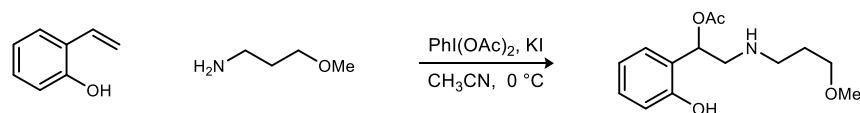
2-5-10-20-50% ethyl acetate in hexanes) afforded the desired product as a dark brown viscous oil (48.1 mg, 47%). $R_f = 0.28$ (20% EtOAc/hexanes); IR (film) 3310, 3040, 2926, 2858 1588, 1510 cm^{-1} ; $^1\text{H NMR}$ (600 MHz, CDCl_3) δ 9.72 (br s, 1H), 7.23 (ddd, $J = 7.8, 7.8, 1.2$ Hz, 1H), 7.16 (dd, $J = 7.2, 1.2$ Hz, 1H), 6.95-6.91 (m, 3H), 6.87-6.84 (m, 3H), 6.74-6.72 (m, 2H), 6.69-6.66 (m, 2H), 4.65 (br s, 1H), 4.44 (dd, $J = 9.6, 4.2$ Hz, 1H), 3.80 (br s, 1H), 3.56 (dd $J = 13.2, 10.2$ Hz, 1H), 3.46 (dd, $J = 13.2, 4.8$ Hz, 1H); $^{13}\text{C NMR}$ (150 MHz, CDCl_3) ppm 158.0 (d, $J = 239.6$ Hz), 156.70, 156.65 (d, $J = 236.9$ Hz), 143.5, 142.7, 129.3, 128.1, 123.7, 120.3, 118.1 (d, $J = 7.5$ Hz), 117.4, 116.0 (d, $J = 22.5$ Hz), 115.8 (d, $J = 22.6$ Hz), 114.8 ($J = 7.5$ Hz), 60.7, 49.8; HRMS (ESI): Exact mass calcd for $\text{C}_{20}\text{H}_{19}\text{F}_2\text{N}_2\text{O}$ $[\text{M}+\text{H}]^+$ 341.1460, found 314.1451.



1-(2-Hydroxyphenyl)-2-(isopropylamino)ethyl acetate (352). A 2-5 mL microwave vial equipped with a stir bar was charged with potassium iodide (60.0 mg, 360 μmol), iodobenzene diacetate (193 mg, 600 μmol), and acetonitrile (3 mL). Isopropylamine (77.0 μL , 900 μmol) and 2-vinylphenol (36.0 mg, 300 μmol) were added and the resulting mixture was stirred at rt for 18 h. The reaction mixture was then diluted with ethyl acetate and concentrated. Flash column chromatography of the residue (SiO_2 , 0.5-1-2-5% methanol in dichloromethane) afforded the desired product as a brown viscous oil (18.2 mg, 26%). $R_f = 0.33$ (50% EtOAc/hexanes); IR (film) 3225, 2972, 2933, 1598 cm^{-1} ; $^1\text{H NMR}$ (600 MHz, CDCl_3) δ 9.23 (br s, 1H), 7.17 (ddd, $J = 8.4, 8.4, 1.2$ Hz, 1H), 7.02 (dd, $J = 7.8, 1.8$ Hz, 1H), 6.88 (dd, $J = 7.8, 0.6$ Hz, 1H), 6.83 (ddd, $J = 7.8, 7.8, 1.2$ Hz, 1H), 6.54 (br s, 1H), 5.00 (d, $J = 8.4$ Hz, 1H), 4.07 (qq, $J = 6.6, 6.6$ Hz, 1H), 3.88 (dd, $J = 15.6, 9.0$ Hz, 1H), 3.24 (dd, $J = 15.0, 1.2$ Hz, 1H), 2.22 (s, 3H), 1.30 (d, $J = 6.6$ Hz, 3H), 1.15 (d, $J = 6.6$ Hz, 3H); $^{13}\text{C NMR}$ (150.9 MHz, CDCl_3) ppm 174.0, 156.2, 129.0, 126.6, 125.3, 119.6, 117.5, 77.6, 50.4, 50.2, 21.8, 21.3, 20.6; HRMS (ESI): Exact mass calcd for $\text{C}_{13}\text{H}_{19}\text{NNaO}_3$ $[\text{M}+\text{Na}]^+$ 260.1263, found 260.1258. HSQC (600 MHz) and HMBC (600 MHz) analyses further confirmed the compound structure.

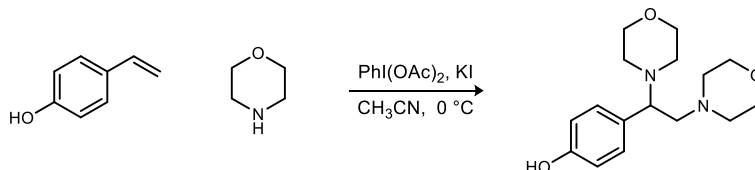


2-(Cyclohexylamino)-1-(2-hydroxyphenyl)ethyl acetate (353). A 2-5 mL microwave vial equipped with a stir bar was charged with potassium iodide (60.0 mg, 360 μmol), iodobenzene diacetate (193 mg, 600 μmol), and acetonitrile (3 mL). Cyclohexylamine (103 μL , 900 μmol) and 2-vinylphenol (36.0 mg, 300 μmol) were added and the resulting mixture was stirred at rt for 20 h. The reaction mixture was then diluted with ethyl acetate and concentrated. Flash column chromatography of the residue (SiO_2 , 25-50-75-100% ethyl acetate in hexanes) afforded the desired product as a gray-brown solid (23.8 mg, 29%). Mp 154.0-158.0 $^\circ\text{C}$; $R_f = 0.45$ (50% EtOAc/hexanes); IR (film) 3126, 2924, 2853, 1570 cm^{-1} ; ^1H NMR (600 MHz, CDCl_3) δ 7.17 (ddd, $J = 9.0, 9.0, 1.8$ Hz, 1H), 7.02 (dd, $J = 7.8, 1.8$ Hz, 1H), 6.87 (d, $J = 7.8$ Hz, 1H), 6.84 (ddd, $J = 7.2, 7.2, 0.6$ Hz, 1H), 4.97 (d, $J = 7.8$ Hz, 1H), 3.91 (dd, $J = 15.0, 8.4$ Hz, 1H), 3.55 (tt, $J = 12.0, 3.6$ Hz, 1H), 3.27 (dd, $J = 15.0, 0.6$ Hz, 1H), 2.21 (s, 3H), 1.94-1.88 (m, 2H), 1.86-1.81 (m, 1H), 1.71-1.64 (m, 2H), 1.52-1.44 (m, 1H), 1.43-1.28 (m, 3H), 1.13-1.05 (m, 1H); ^{13}C NMR (150.9 MHz, CDCl_3) ppm 174.2, 156.2, 128.9, 126.6, 125.3, 119.6, 117.5, 77.6, 59.2, 51.1, 31.8, 31.0, 25.9, 25.6, 25.0, 21.9; HRMS (ESI): Exact mass calcd for $\text{C}_{16}\text{H}_{23}\text{NNaO}_3$ $[\text{M}+\text{Na}]^+$ 300.1576, found 300.1582. HSQC (600 MHz) and HMBC (600 MHz) analyses further confirmed the compound structure.

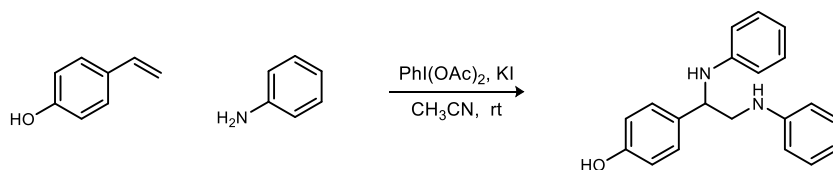


1-(2-Hydroxyphenyl)-2-((3-methoxypropyl)amino)ethyl acetate (354). A 2-5 mL microwave vial equipped with a stir bar was charged with potassium iodide (60.0 mg, 360 μmol), iodobenzene diacetate (193 mg, 600 μmol), and acetonitrile (3 mL). 3-Methoxypropylamine (92.0 μL , 900 μmol) and 2-vinylphenol (36.0 mg, 300 μmol) were added and the resulting mixture was stirred at rt for 18 h. The reaction mixture was then diluted with ethyl acetate and concentrated. Flash column chromatography of the residue (SiO_2 , 25-50-75-100% ethyl acetate in hexanes) afforded the desired product as a light-brown viscous oil (26.5 mg, 33%). $R_f = 0.17$ (50% EtOAc/hexanes); IR (film) 3238, 2928, 1616 cm^{-1} ; ^1H NMR (600 MHz, CDCl_3) δ 7.15 (ddd, $J = 9.0, 9.0, 1.8$ Hz, 1H), 7.07 (dd, $J = 7.2, 1.2$ Hz, 1H), 6.86 (dd, $J = 8.4, 0.6$ Hz, 1H), 6.83 (ddd, $J = 7.8, 7.8, 1.2$ Hz, 1H), 5.15 (dd, $J = 7.8, 2.4$ Hz, 1H), 3.67 (dd, $J = 14.4, 7.8$ Hz, 1H), 3.53 (dd, $J = 14.4, 2.4$ Hz, 1H),

3.38-3.34 (m, 4H), 3.30 (s, 3H), 2.16 (s, 3H), 1.85-1.75 (m, 2H); ^{13}C NMR (150.9 MHz, CDCl_3) ppm 174.0, 155.7, 128.9, 126.4, 125.4, 119.6, 117.2, 74.4, 69.0, 58.6, 55.3, 48.3, 28.6, 21.2; HRMS (ESI): Exact mass calcd for $\text{C}_{14}\text{H}_{21}\text{NNaO}_4$ $[\text{M}+\text{Na}]^+$ 290.1368, found 290.1364. HSQC (600 MHz) and HMBC (600 MHz) analyses further confirmed the compound structure.

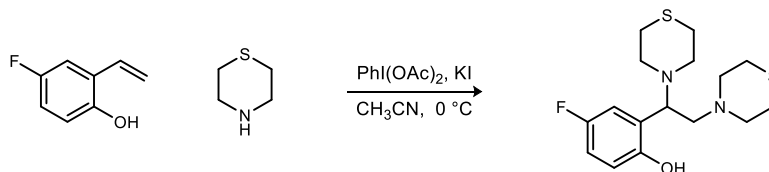


4-(1,2-Dimorpholinoethyl)phenol (340b). Prepared according to the general procedure using morpholine (78.0 μL , 900 μmol) and 4-vinylphenol (36.0 mg, 300 μmol). Flash column chromatography of the residue (SiO_2 , 0.5-1-2-5-10% methanol in dichloromethane) afforded the desired product as a light-yellow viscous oil (51.9 mg, 59%). $R_f = 0.19$ (5% MeOH/DCM); IR (film) 3242 (br), 2959, 2857, 2820, 1613, 1595, 1516 cm^{-1} ; ^1H NMR (400 MHz, CDCl_3) δ 7.07 (d, $J = 8.4$ Hz, 2H), 6.71 (d, $J = 8.4$ Hz, 2H), 6.16 (br s, 1H), 3.73 (br dd, $J = 4.0, 4.0$ Hz, 4H), 3.69 (br dd, $J = 4.8, 4.8$ Hz, 5H), 3.12 (dd, $J = 12.8, 6.8$ Hz, 1H), 2.72 (dd, $J = 13.2, 6.0$ Hz, 1H), 2.62 (m, 4H), 2.52 (m, 4H); ^{13}C NMR (100 MHz, CDCl_3) ppm 155.5, 129.8, 115.2, 66.72, 66.67, 66.5, 61.3, 54.0, 51.0; Exact mass calcd for $\text{C}_{16}\text{H}_{25}\text{N}_2\text{O}_3$ $[\text{M}+\text{H}]^+$ 293.1865, found 293.1879.

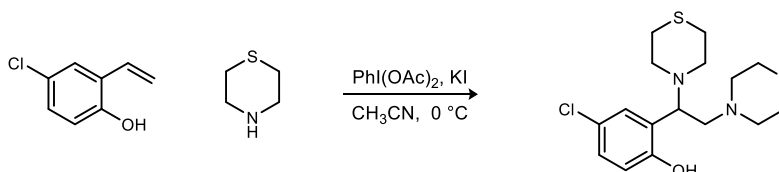


4-(1,2-Bis(phenylamino)ethyl)phenol (340c). A vial equipped with a stir bar was charged with potassium iodide (60.0 mg, 360 μmol), iodobenzene diacetate (193 mg, 600 μmol), and acetonitrile (3 mL). Aniline (82.0 μL , 900 μmol) and 4-vinylphenol (36.0 mg, 300 μmol) were added and the resulting mixture was stirred at rt for 18 h. The reaction mixture was then diluted with ethyl acetate and concentrated. Flash column chromatography of the residue (SiO_2 , 1-2-5-10-20-40% ethyl acetate in hexanes) afforded the desired product as a brown viscous oil (78.0 mg, 85%). $R_f = 0.24$ (20% EtOAc/hexanes); IR (film) 3391, 3051, 3022, 1601, 1503 cm^{-1} ; ^1H NMR (400 MHz, CDCl_3) δ 7.25 (d, $J = 8.4$ Hz, 2H), 7.21 (dd, $J = 8.4, 7.6$ Hz, 2H), 7.12 (dd, $J = 8.4, 7.6$ Hz, 2H), 6.80 (d, $J = 8.4$ Hz, 2H), 6.78 (dd, $J = 7.2$ Hz, 1H), 6.70 (dd, $J = 7.2, 7.2$ Hz, 1H), 6.66 (d, $J = 7.6$ Hz, 2H), 6.57 (d, $J = 8.0$ Hz, 2H), 4.59 (dd, $J = 7.6, 5.2$ Hz, 1H), 4.46 (br s, 2H), 3.47 (dd, $J = 12.4, 4.8$ Hz, 1H), 3.38 (dd, $J = 12.4, 7.6$ Hz, 1H); ^{13}C NMR (150 MHz, CDCl_3) ppm 155.0, 147.8, 147.1, 133.2,

129.4, 129.2, 127.7, 118.2, 117.8, 115.7, 113.7, 113.4, 56.8, 51.0; Exact mass calcd for C₂₀H₂₁N₂O [M+H]⁺ 305.1648, found 305.1645.

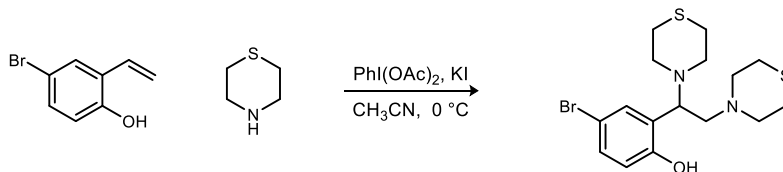


2-(1,2-Dithiomorpholinoethyl)-4-fluorophenol (338q). Prepared according to the general procedure using thiomorpholine (91.0 μ L, 900 μ mol) and 4-fluoro-2-vinylphenol (41.4 mg, 300 μ mol). Flash column chromatography of the residue (SiO₂, 5-10-20-40% ethyl acetate in hexanes) afforded the desired product as a light-yellow solid (85.3 mg, 83%). Mp 72.0-76.0 °C; R_f = 0.38 (20% EtOAc/hexanes); IR (film) 3030(br), 2910, 2813, 1743, 1593 cm⁻¹; ¹H NMR (400 MHz, CDCl₃) δ 11.00 (br s, 1H), 6.87-6.79 (m, 2H), 6.73 (dd, *J* = 8.4, 4.8 Hz, 1H), 3.75 (dd, *J* = 6.0, 6.0 Hz, 1H), 3.09 (dd, *J* = 6.8, 3.2 Hz, 1H), 3.06 (dd, *J* = 6.0, 3.6 Hz, 1H), 2.92-2.86 (m, 3H), 2.77-2.72 (m, 4H), 2.72-2.67 (m, 4H), 2.66-2.62 (m, 5H); ¹³C NMR (150 MHz, CDCl₃) ppm 156.1 (d, ¹J_{FC} = 236.9 Hz), 153.2, 125.8 (d, ³J_{FC} = 7.5 Hz), 117.4, 117.3, 114.9 (d, ²J_{FC} = 16.9 Hz), 64.9, 58.4, 55.6, 51.9, 28.1, 27.9; HRMS (ESI): Exact mass calcd for C₁₆H₂₄FN₂OS₂ [M+H]⁺ 343.1314, found 343.1329.

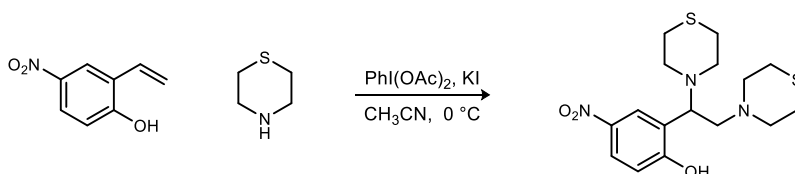


4-Chloro-2-(1,2-dithiomorpholinoethyl)phenol (338r). A vial equipped with a stir bar was charged with potassium iodide (60.0 mg, 360 μ mol), iodobenzene diacetate (290 mg, 900 μ mol), and acetonitrile (3 mL) and was chilled to 0 °C. Thiomorpholine (91.0 μ L, 900 μ mol) and 4-chloro-2-vinylphenol (46.4 mg, 300 μ mol) were added and the resulting mixture was stirred at 0 °C for 18 h. The reaction mixture was then diluted with ethyl acetate and concentrated. Flash column chromatography of the residue (SiO₂, 0.5-1-2-5-10-20-40% ethyl acetate in hexanes) afforded the desired product as a light orange solid (69.1 mg, 64%). Mp 100.0-104.0 °C; R_f = 0.31 (20% EtOAc/hexanes); IR (film) 3030 (br), 2911, 2810, 1742, 1603, 1579 cm⁻¹; ¹H NMR (400 MHz, CDCl₃) δ 11.30 (br s, 1H), 7.10 (dd, *J* = 8.8, 2.4 Hz, 1H), 7.03 (d, *J* = 2.4 Hz, 1H), 6.73 (d, *J* = 8.8 Hz, 1H), 3.72 (dd, *J* = 6.0, 6.0 Hz, 1H), 3.08 (dd, *J* = 7.2, 3.2 Hz, 1H), 3.05 (dd, *J* = 6.4, 3.6 Hz, 1H), 2.91-2.85 (m, 3H), 2.75-2.61 (m, 13H); ¹³C NMR (125 MHz, CDCl₃) ppm 156.0, 128.5,

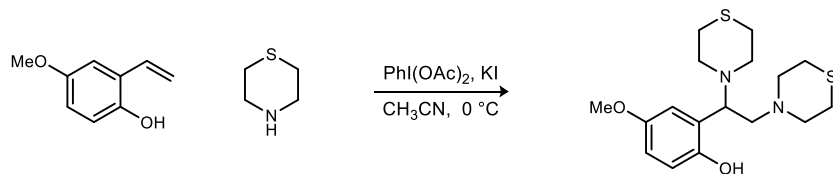
128.3, 126.3, 123.7, 118.0, 65.2, 58.6, 55.6, 52.0, 28.0, 27.9; HRMS (ESI): Exact mass calcd for $C_{16}H_{24}ClN_2OS_2$ $[M+H]^+$ 359.1019, found 359.1033.



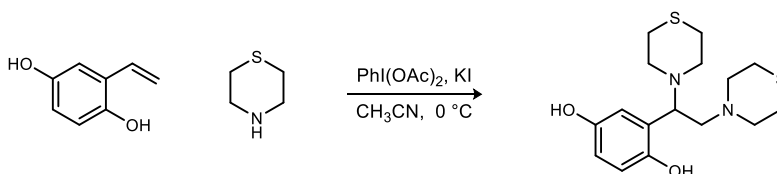
4-Bromo-2-(1,2-dithiomorpholinoethyl)phenol (338s). A vial equipped with a stir bar was charged with potassium iodide (60.0 mg, 360 μ mol), iodobenzene diacetate (290 mg, 900 μ mol), and acetonitrile (3 mL) and was chilled to 0 °C. Thiomorpholine (91.0 μ L, 900 μ mol) and 4-bromo-2-vinylphenol (59.7 mg, 300 μ mol) were added and the resulting mixture was stirred at 0 °C for 18 h. The reaction mixture was then diluted with ethyl acetate and concentrated. Flash column chromatography of the residue (SiO_2 , 0.5-1-2-5-10-20-40% ethyl acetate in hexanes) afforded the desired product as a light yellow solid (85.1 mg, 70%). Mp 105.0-109.0 °C; R_f = 0.31 (20% EtOAc/hexanes); IR (film) 3030 (br), 2911, 2810, 1742, 1600, 1576 cm^{-1} ; 1H NMR (400 MHz, $CDCl_3$) δ 11.29 (br s, 1H), 7.24 (dd, J = 8.4, 2.4 Hz, 1H), 7.17 (d, J = 2.4 Hz, 1H), 6.68 (d, J = 8.4 Hz, 1H), 3.72 (dd, J = 6.4, 6.4 Hz, 1H), 3.09 (dd, J = 6.8, 3.2 Hz, 1H), 3.06 (dd, J = 6.4, 3.6 Hz, 1H), 2.91-2.85 (m, 3H), 2.75-2.61 (m, 13H); ^{13}C NMR (125 MHz, $CDCl_3$) ppm 156.5, 131.5, 131.3, 126.8, 118.6, 110.9, 65.2, 58.6, 55.6, 52.0, 27.99, 27.97; HRMS (ESI): Exact mass calcd for $C_{16}H_{24}BrN_2OS_2$ $[M+H]^+$ 403.0513, found 403.0518.



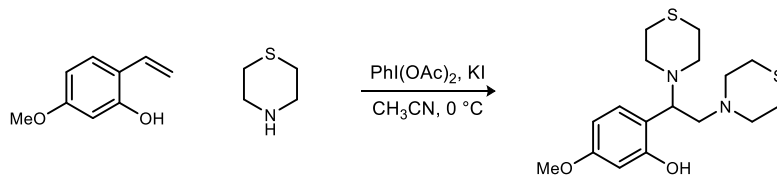
2-(1,2-Dithiomorpholinoethyl)-4-nitrophenol (338t). Prepared according to the general procedure using thiomorpholine (91.0 μ L, 900 μ mol) and 4-nitro-2-vinylphenol (49.5 mg, 300 μ mol). Flash column chromatography of the residue (SiO_2 , 2-5-10-20-40% ethyl acetate in hexanes) afforded the desired product as a viscous yellow oil (55.1 mg, 50%). R_f = 0.10 (20% EtOAc/hexanes); IR (film) 3060 (br), 2910, 2813, 1615, 1586 cm^{-1} ; 1H NMR (400 MHz, $CDCl_3$) δ 8.12 (d, J = 2.8 Hz, 1H), 8.07 (dd, J = 8.8, 2.0 Hz, 1H), 6.83 (d, J = 9.2 Hz, 1H), 3.88 (dd, J = 7.6, 4.8 Hz, 1H), 3.13-3.08 (m, 2H), 2.95-2.89 (m, 3H), 2.87-2.65 (m, 13H); ^{13}C NMR (125 MHz, $CDCl_3$) ppm 164.3, 140.0, 125.2 (2C), 124.7, 117.1, 64.6, 57.7, 55.6, 51.6, 28.0, 27.9; HRMS (ESI): Exact mass calcd for $C_{16}H_{24}N_3O_3S_2$ $[M+H]^+$ 370.1259, found 370.1265.



2-(1,2-Dithiomorpholinoethyl)-4-methoxyphenol (338u). Prepared according to the general procedure using thiomorpholine (91.0 μL , 900 μmol) and 4-methoxy-2-vinylphenol (45.1 mg, 300 μmol). Flash column chromatography of the residue (SiO_2 , 20-40% ethyl acetate in hexanes) afforded the desired product as an off-white solid (57.0 mg, 54%). Mp 114.0-116.0 $^\circ\text{C}$; $R_f = 0.25$ (20% EtOAc/hexanes); IR (film) 2908, 2828, 1492 cm^{-1} ; ^1H NMR (600 MHz, CDCl_3) δ 10.56 (br s, 1H), 6.74-6.70 (m, 2H), 6.64 (d, $J = 2.4$ Hz, 1H), 3.74 (s, 3H), 3.72 (dd, $J = 6.0$ Hz, 1H), 3.08 (dd, $J = 7.8, 3.0$ Hz, 1H), 3.06 (dd, $J = 6.6, 3.0$ Hz, 1H), 2.91-2.86 (m, 3H), 2.77-2.60 (m, 13H); ^{13}C NMR (150 MHz, CDCl_3) ppm 152.5, 150.9, 125.7, 117.0, 114.6, 113.2, 65.4, 59.0, 55.7, 55.6, 52.1, 28.03, 27.97; HRMS (ESI): Exact mass calcd for $\text{C}_{17}\text{H}_{27}\text{N}_2\text{O}_2\text{S}_2$ $[\text{M}+\text{H}]^+$ 355.1514, found 355.1521.

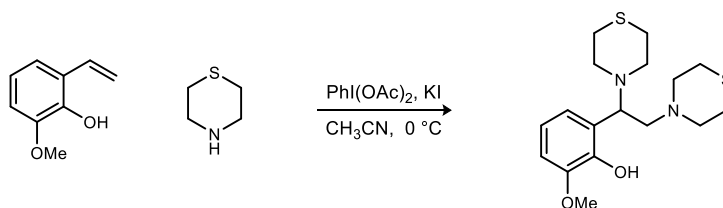


2-(1,2-Dithiomorpholinoethyl)benzene-1,4-diol (338v). Prepared according to the general procedure using thiomorpholine (91.0 μL , 900 μmol) and 2-vinylbenzene-1,4-diol (40.9 mg, 300 μmol). Flash column chromatography of the residue (SiO_2 , 50-75-100% ethyl acetate in hexanes) afforded the desired product as a light-brown viscous oil (23.8 mg, 23%). $R_f = 0.35$ (5% MeOH/DCM); IR (film) 3300 (br), 2911, 2817, 2362, 1731, 1560 cm^{-1} ; ^1H NMR (400 MHz, CDCl_3) δ 6.68 (d, $J = 8.4$ Hz, 1H), 6.64 (dd, $J = 8.8, 2.8$ Hz, 1H), 6.59 (d, $J = 2.8$ Hz, 1H), 3.71 (dd, $J = 6.0, 6.0$ Hz, 1H), 3.07 (ddd, $J = 10.4, 6.4, 3.6$ Hz, 2H), 2.89 (m, 3H), 2.70 (m, 13H); ^{13}C NMR (150 MHz, CDCl_3) ppm 150.8, 148.3, 125.8, 117.3, 115.4, 115.3, 65.2, 59.0, 55.6, 52.1, 28.0, 27.9; Exact mass calcd for $\text{C}_{16}\text{H}_{25}\text{N}_2\text{O}_2\text{S}_2$ $[\text{M}+\text{H}]^+$ 341.1357, found 341.1365.

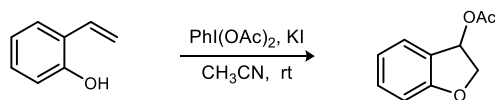


2-(1,2-Dithiomorpholinoethyl)-5-methoxyphenol (338w). Prepared according to the general procedure using thiomorpholine (91.0 μL , 900 μmol) and 5-methoxy-2-vinylphenol (45.1 mg, 300

μmol). The residue was diluted with dichloromethane and filtered through a silica plug with dichloromethane and ethyl acetate and then concentrated. Flash column chromatography of the residue (SiO₂, 1-2-5-10-20-40% ethyl acetate in hexanes) afforded the desired product as a yellow-orange viscous oil (60.2 mg, 57%). *R_f* = 0.25 (40% EtOAc/hexanes); IR (film) 3020 (br), 2911, 2833, 1619, 1587, 1508 cm⁻¹; ¹H NMR (400 MHz, CDCl₃) δ 11.31 (br s, 1H), 6.92 (d, *J* = 8.4 Hz, 1H), 6.38 (d, *J* = 2.4 Hz, 1H), 6.36 (dd, *J* = 8.4, 2.8 Hz, 1H), 3.79-3.73 (m, 1H), 3.76 (s, 3H), 3.10 (dd, *J* = 6.8, 3.2 Hz, 1H), 3.07 (dd, *J* = 6.4, 4.0 Hz, 1H), 2.92-2.83 (m, 3H), 2.76-2.62 (m, 13 H); ¹³C NMR (125 MHz, CDCl₃) ppm 160.3, 158.5, 128.9, 116.9, 105.0, 102.1, 64.9, 58.9, 55.6, 55.1, 51.8, 28.0, 27.9; HRMS (ESI): Exact mass calcd for C₁₇H₂₇N₂O₂S₂ [M+H]⁺ 355.1514, found 355.1528.

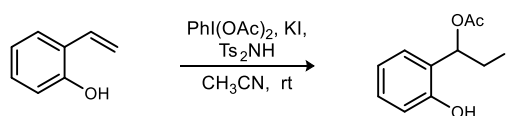


2-(1,2-Dithiomorpholinoethyl)-6-methoxyphenol (338x). Prepared according to the general procedure using thiomorpholine (91.0 μL, 900 μmol) and 2-methoxy-6-vinylphenol (45.1 mg, 300 μmol). Flash column chromatography of the residue (SiO₂, 5-10-20-40-80% ethyl acetate in hexanes) afforded the desired product as an off-white solid (88.7 mg, 83%). Mp 115.0-118.0 °C; *R_f* = 0.10 (20% EtOAc/hexanes); IR (film) 3020 (br), 2908, 2829, 1585 cm⁻¹; ¹H NMR (400 MHz, CDCl₃) δ 9.65 (br s, 1H), 6.79 (dd, *J* = 8.4, 1.6 Hz, 1H), 6.73 (dd, *J* = 7.6, 7.6 Hz, 1H), 6.64 (dd, *J* = 8.0, 1.6 Hz, 1H), 3.85 (s, 3H), 3.82 (dd, *J* = 6.4, 6.4 Hz, 1H), 3.09 (dd, *J* = 6.8, 2.8 Hz, 1H), 3.05 (dd, *J* = 6.4, 3.2 Hz, 1H), 2.94-2.86 (m, 3H), 2.80-2.71 (m, 4H), 2.71-2.65 (m, 5H), 2.65-2.59 (m, 4H); ¹³C NMR (125.8 MHz, CDCl₃) ppm 148.2, 146.6, 125.0, 120.2, 118.6, 110.7, 65.3, 59.3, 55.8, 55.5, 52.1, 28.0, 27.9; HRMS (ESI): Exact mass calcd for C₁₇H₂₇N₂O₂S₂ [M+H]⁺ 355.1514, found 355.1521.

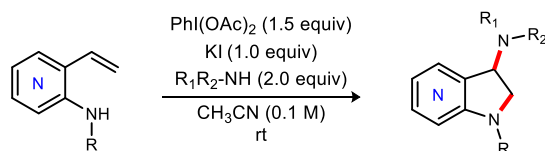


2,3-Dihydrobenzofuran-3-yl acetate (355). A 2-5 mL microwave vial equipped with a stir bar was charged with potassium iodide (60.0 mg, 360 μmol), iodobenzene diacetate (193 mg, 600 μmol), and acetonitrile (3 mL). 2-Vinylphenol (36.0 mg, 300 μmol) was added and the resulting

mixture was stirred at rt for 18 h. The reaction mixture was then diluted with ethyl acetate and concentrated. Flash column chromatography of the residue (SiO₂, 2-20% diethyl ether in hexanes) afforded the desired product as a light yellow transparent viscous oil (36.8 mg, 69%). $R_f = 0.37$ (20% Et₂O/hexanes); IR (film) 3054, 2948, 2884, 1737, 1612, 1600 cm⁻¹; ¹H NMR (400 MHz, CDCl₃) δ 7.45 (dd, $J = 7.6, 0.4$ Hz, 1H), 7.30 (ddd, $J = 8.4, 8.4, 1.2$ Hz, 1H), 6.95 (dd, $J = 7.2, 7.2$ Hz, 1H), 6.90 (d, $J = 8.0$ Hz, 1H), 6.25 (dd, $J = 6.8, 2.4$ Hz, 1H), 4.62 (dd, $J = 11.6, 6.8$ Hz, 1H), 4.51 (dd, $J = 11.2, 2.4$ Hz, 1H), 2.07 (s, 3H); ¹³C NMR (100.6 MHz, CDCl₃) ppm 170.8, 161.0, 131.3, 126.7, 124.3, 121.0, 110.5, 76.0, 74.2, 21.0; HRMS (CI): Exact mass calcd for C₁₀H₁₀O₃ [M]⁺ 178.0624, found 178.0623.

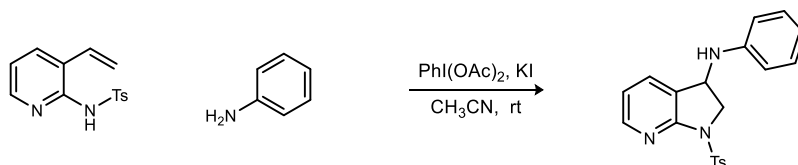


1-(2-hydroxyphenyl)-2-iodoethyl acetate (356). A vial equipped with a stir bar was charged with potassium iodide (60.0 mg, 360 μmol), iodobenzene diacetate (193 mg, 600 μmol), and acetonitrile (3 mL). Bistosylimide (293 mg, 900 μmol) and 2-vinylphenol (36.0 mg, 300 μmol) were added and the resulting mixture was stirred at rt for 18 h. The reaction mixture was then diluted with ethyl acetate and concentrated. Flash column chromatography of the residue (SiO₂, 2-5-10-20-50-100% diethyl ether in hexanes) afforded the desired product as a yellow-orange viscous oil (11.3 mg, 12%). $R_f = 0.76$ (80% Et₂O/hexanes); IR (film) 3396 (br), 2923, 2852, 1719, 1598 cm⁻¹; ¹H NMR (600 MHz, CDCl₃) δ 7.24 (ddd, $J = 9.6, 9.6, 1.8$ Hz, 2H), 6.95 (ddd, $J = 7.2, 7.2, 0.6$ Hz, 1H), 6.87 (d, $J = 8.4$ Hz, 1H), 6.42 (br s, 1H), 6.07 (dd, $J = 9.0, 4.8$ Hz, 1H), 3.65 (dd, $J = 10.2, 9.0$ Hz, 1H), 3.55 (dd, $J = 10.8, 4.8$ Hz, 1H), 2.16 (s, 3H); ¹³C NMR (150.9 MHz, CDCl₃) ppm 171.2, 153.7, 130.4, 126.8, 124.3, 121.1, 117.5, 71.9, 20.9, 5.6; HRMS (ESI): no mass was observed due to decomposition upon multiple submissions.

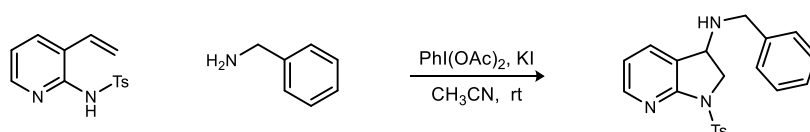


General procedure for Hypervalent Iodine-Mediated Intra/Intermolecular Diamination: To a vial equipped with a stir bar was added PhI(OAc)₂ (72.5 mg, 225 μmol), KI (24.9 mg, 150 μmol), the vinyl aminopyridine (41.2 mg, 150 μmol), and acetonitrile (1.50 mL). The amine (300 μmol) was added and the resulting mixture was allowed to stir at rt for 18 h. The reaction mixture was then diluted with ethyl acetate and concentrated. No reductive workup was used in these studies,

but is recommended for a larger scale. EtOAc was used to transfer the heterogeneous reaction mixture to a larger flask for concentration. After concentration, the resulting residue was then subjected to flash column chromatography.

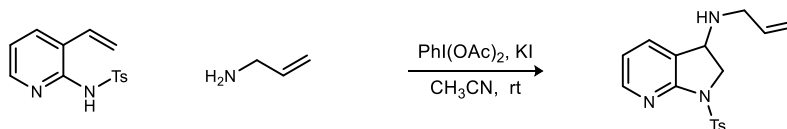


***N*-Phenyl-1-tosyl-2,3-dihydro-1*H*-pyrrolo[2,3-*b*]pyridin-3-amine (521a).** A vial equipped with a stir bar was charged with potassium iodide (33.2 mg, 200 μ mol), iodobenzene diacetate (96.6 mg, 300 μ mol), 4-methyl-*N*-(3-vinylpyridin-2-yl)benzenesulfonamide (55.0 mg, 200 μ mol), and acetonitrile (2 mL). Aniline (36.5 μ L, 400 μ mol) was added and the resulting mixture was stirred at rt for 18 h. The reaction mixture was then diluted with ethyl acetate and concentrated. Flash column chromatography of the residue (SiO₂, 5-10-20-40% ethyl acetate in hexanes) afforded the desired product as a light-brown solid (70.4 mg, 96%). Mp 194.0-196.0 °C; R_f = 0.54 (50% EtOAc/hexanes); IR (film) 3386, 3052, 2924, 2340, 1923, 1601 cm⁻¹; ¹H NMR (600 MHz, CDCl₃) δ 8.31 (dd, J = 5.4, 1.2 Hz, 1H), 7.96 (d, J = 8.4 Hz, 2H), 7.56 (ddd, J = 7.2, 1.2, 1.2 Hz, 1H), 7.27 (d, J = 8.4 Hz, 2H), 7.21 (dd, J = 8.4, 7.2 Hz, 2H), 6.90 (dd, J = 7.8, 5.4 Hz, 1H), 6.81 (dd, J = 7.2, 7.2 Hz, 1H), 6.59 (d, J = 7.2 Hz, 2H), 5.05 (br s, 1H), 4.27 (dd, J = 10.8, 7.8 Hz, 1H), 3.92 (dd, J = 10.8, 4.8 Hz, 1H), 3.76 (br s, 1H), 2.39 (s, 3H); ¹³C NMR (150 MHz, CDCl₃) ppm 155.8, 149.3, 145.5, 144.3, 134.9, 133.9, 129.6, 129.5, 128.1, 124.7, 119.0, 118.4, 113.6, 55.4, 50.9, 21.6; HRMS (ESI): Exact mass calcd for C₂₀H₂₀N₃O₂S [M+H]⁺ 366.1276, found 366.1272.

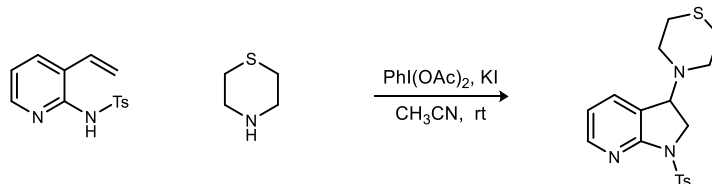


***N*-Benzyl-1-tosyl-2,3-dihydro-1*H*-pyrrolo[2,3-*b*]pyridin-3-amine (521b).** Prepared according to the general procedure using benzylamine (32.8 μ L, 300 μ mol) and 4-methyl-*N*-(3-vinylpyridin-2-yl)benzenesulfonamide (41.2 mg, 150 μ mol). Flash column chromatography of the residue (SiO₂, 10-30-60% ethyl acetate in hexanes) afforded the desired product as an orange viscous oil (41.8 mg, 73%). R_f = 0.28 (50% EtOAc/hexanes); IR (film) 3319, 3060, 3029, 2923, 1597 cm⁻¹; ¹H NMR (400 MHz, CDCl₃) δ 8.18 (dd, J = 5.2, 1.2 Hz, 1H), 7.89 (d, J = 8.0 Hz, 2H), 7.46 (d, J = 7.2 Hz, 1H), 7.27-7.16 (m, 7H), 6.81 (dd, J = 7.2, 4.8 Hz, 1H), 4.23 (dd, J = 8.0, 4.4 Hz, 1H), 4.01 (dd, J = 10.4, 8.0 Hz, 1H), 3.86 (dd, J = 10.8, 4.4 Hz, 1H), 3.72 (s, 2H), 2.28 (s, 3H), 1.57 (br

s, 1H); ^{13}C NMR (100 MHz, CDCl_3) ppm 155.7, 148.6, 144.2, 139.2, 134.9, 133.8, 129.4, 128.5, 128.03, 127.96, 127.3, 125.8, 118.2, 55.1, 54.6, 50.5, 21.5; HRMS (ESI): Exact mass calcd for $\text{C}_{21}\text{H}_{22}\text{N}_3\text{O}_2\text{S}$ $[\text{M}+\text{H}]^+$ 380.1433, found 380.1430.

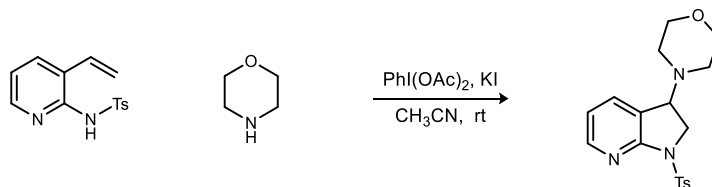


***N*-Allyl-1-tosyl-2,3-dihydro-1*H*-pyrrolo[2,3-*b*]pyridin-3-amine (521c).** Prepared according to the general procedure using allylamine (22.4 μL , 300 μmol) and 4-methyl-*N*-(3-vinylpyridin-2-yl)benzenesulfonamide (41.2 mg, 150 μmol). Flash column chromatography of the residue (SiO_2 , 50-70-90% ethyl acetate in hexanes) afforded the desired product as an orange-brown viscous oil (30.8 mg, 62%). $R_f = 0.12$ (50% EtOAc/hexanes); IR (film) 3317, 3065, 2924, 1596 cm^{-1} ; ^1H NMR (400 MHz, CDCl_3) δ 8.24 (dd, $J = 4.8, 1.2$ Hz, 1H), 7.96 (d, $J = 8.4$ Hz, 2H), 7.54 (d, $J = 6.8$ Hz, 1H), 7.25 (d, $J = 7.6$ Hz, 2H), 6.87 (dd, $J = 7.6, 5.2$ Hz, 1H), 5.86 (dddd, $J = 11.6, 10.4, 6.0, 6.0$ Hz, 1H), 5.20 (dd, $J = 17.2, 1.6$ Hz, 1H), 5.12 (dd, $J = 10.4, 1.2$ Hz, 1H), 4.29 (dd, $J = 8.0, 4.0$ Hz, 1H), 4.06 (dd, $J = 10.8, 8.0$ Hz, 1H), 3.88 (dd, $J = 10.8, 4.4$ Hz, 1H), 3.27 (d, $J = 6.0, 0.8$ Hz, 2H), 2.37 (s, 3H), 1.62 (br s, 1H); ^{13}C NMR (100 MHz, CDCl_3) ppm 155.6, 148.7, 144.2, 135.8, 134.9, 133.8, 129.4, 128.0, 125.7, 118.2, 116.8, 55.1, 54.6, 49.1, 21.5; HRMS (ESI): Exact mass calcd for $\text{C}_{17}\text{H}_{19}\text{N}_3\text{NaO}_2\text{S}$ $[\text{M}+\text{Na}]^+$ 352.1096, found 352.1082.

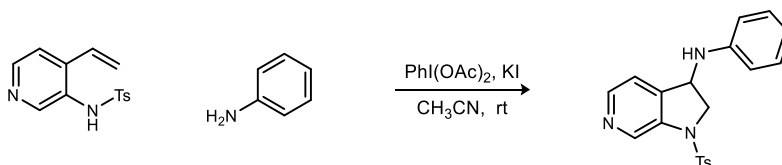


4-(1-Tosyl-2,3-dihydro-1*H*-pyrrolo[2,3-*b*]pyridin-3-yl)thiomorpholine (521d). A vial equipped with a stir bar was charged with potassium iodide (29.9 mg, 180 μmol), iodobenzene diacetate (96.6 mg, 300 μmol), 4-methyl-*N*-(3-vinylpyridin-2-yl)benzenesulfonamide (41.2 mg, 150 μmol), and acetonitrile (1.5 mL). Thiomorpholine (45.3 μL , 450 μmol) was added and the resulting mixture was stirred at rt for 18 h. The reaction mixture was then diluted with ethyl acetate and concentrated. Flash column chromatography of the residue (SiO_2 , 20-50-80% ethyl acetate in hexanes) afforded the desired product as a light-brown solid (21.8 mg, 39%). Mp 182.0-186.0 $^\circ\text{C}$; $R_f = 0.27$ (50% EtOAc/hexanes); IR (film) 3054, 2921, 2821, 1644, 1594 cm^{-1} ; ^1H NMR (400 MHz, CDCl_3) δ 8.27 (dd, $J = 4.8, 1.2$ Hz, 1H), 7.97 (d, $J = 8.4$ Hz, 2H), 7.51 (d, $J = 7.2$ Hz, 1H), 7.26 (d, $J = 8.0$ Hz, 2H), 6.89 (dd, $J = 7.6, 5.2$ Hz, 1H), 4.28 (dd, $J = 9.6, 4.0$ Hz, 1H), 4.12 (dd, J

= 11.2, 4.0 Hz, 1H), 3.86 (dd, $J = 11.2, 9.2$ Hz, 1H), 2.78-2.70 (m, 2H), 2.63-2.53 (m, 6H), 2.38 (s, 3H); ^{13}C NMR (100 MHz, CDCl_3) ppm 156.3, 149.0, 144.3, 135.1, 134.8, 129.5, 128.0, 122.6, 118.1, 62.8, 50.7, 49.0, 28.2, 21.6; HRMS (ESI): Exact mass calcd for $\text{C}_{18}\text{H}_{22}\text{N}_3\text{O}_2\text{S}_2$ $[\text{M}+\text{H}]^+$ 376.1153, found 376.1154.

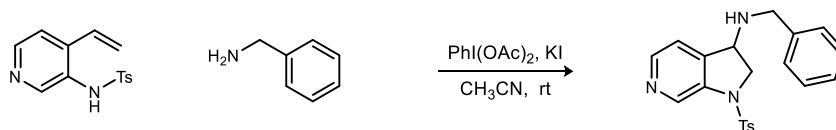


4-(1-Tosyl-2,3-dihydro-1H-pyrrolo[2,3-b]pyridin-3-yl)morpholine (521e). Prepared according to the general procedure using morpholine (26.0 μL , 300 μmol) and 4-methyl-*N*-(3-vinylpyridin-2-yl)benzenesulfonamide (41.2 mg, 150 μmol). Flash column chromatography of the residue (SiO_2 , 50-70-90% ethyl acetate in hexanes) afforded the desired product as a dark-yellow solid (30.8 mg, 57%). Mp 161.0-165.0 $^\circ\text{C}$; $R_f = 0.10$ (50% EtOAc/hexanes); IR (film) 2923, 2854, 1593 cm^{-1} ; ^1H NMR (400 MHz, CDCl_3) δ 8.28 (dd, $J = 5.2, 1.6$ Hz, 1H), 7.95 (d, $J = 8.4$ Hz, 2H), 7.55 (d, $J = 7.2$ Hz, 1H), 7.25 (d, $J = 8.0$ Hz, 2H), 6.91 (dd, $J = 7.2, 5.2$ Hz, 1H), 4.27 (dd, $J = 9.2, 3.6$ Hz, 1H), 4.15 (dd, $J = 11.6, 3.6$ Hz, 1H), 3.83 (dd, $J = 11.2, 9.2$ Hz, 1H), 3.61 (dd, $J = 4.8, 4.8$ Hz, 4H), 2.49-2.44 (m, 2H), 2.37 (s, 3H), 2.31-2.26 (m, 2H); ^{13}C NMR (100 MHz, CDCl_3) ppm 156.3, 149.1, 144.4, 135.2, 134.8, 129.5, 127.9, 122.4, 118.2, 66.8, 61.4, 48.8, 48.4, 21.6; HRMS (ESI): Exact mass calcd for $\text{C}_{18}\text{H}_{22}\text{N}_3\text{O}_3\text{S}$ $[\text{M}+\text{H}]^+$ 360.1382, found 360.1378.

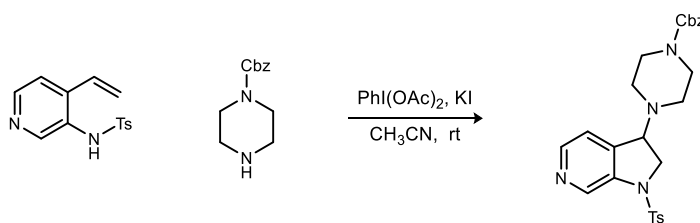


***N*-Phenyl-1-tosyl-2,3-dihydro-1H-pyrrolo[2,3-c]pyridin-3-amine (524a).** A vial equipped with a stir bar was charged with potassium iodide (6.70 mg, 40.5 μmol), iodobenzene diacetate (19.6 mg, 60.7 μmol), the vinyl aminopyridine (11.1 mg, 40.5 μmol), and acetonitrile (405 μL). Aniline (7.40 μL , 80.9 μmol) was added and the resulting mixture was stirred at rt for 18 h. The reaction mixture was then diluted with ethyl acetate and concentrated. Flash column chromatography of the residue (SiO_2 , 5-10-20-40-80% ethyl acetate in hexanes) afforded the desired product as a dark brown viscous oil (1.6 mg, 11%). $R_f = 0.62$ (70% EtOAc/hexanes); IR (film) 3380, 3050, 2922, 2851, 1600 cm^{-1} ; ^1H NMR (400 MHz, CDCl_3) δ 9.02 (s, 1H), 8.35 (d, $J = 4.8$ Hz, 1H), 7.67 (d, $J = 8.4$ Hz, 2H), 7.25 (d, $J = 6.0$ Hz, 2H), 7.20 (m, 3H), 6.81 (dd, $J = 7.2, 7.2$ Hz, 1H), 6.47 (d, $J =$

7.6 Hz, 2H), 4.97 (br m, 1H), 4.16 (dd, $J = 11.6, 8.0$ Hz, 1H), 3.78 (d, $J = 11.6, 4.8$ Hz, 1H), 3.34 (br d, $J = 8.0$ Hz, 1H), 2.41 (s, 3H); ^{13}C NMR (150 MHz, CDCl_3) ppm 145.3, 145.2, 144.8, 140.8, 139.0, 137.4, 133.2, 130.0, 129.6, 127.4, 120.0, 119.2, 113.5, 56.2, 53.3, 21.6; HRMS (ESI): Exact mass calcd for $\text{C}_{20}\text{H}_{20}\text{N}_3\text{O}_2\text{S}$ $[\text{M}+\text{H}]^+$ 366.1276, found 366.1284.

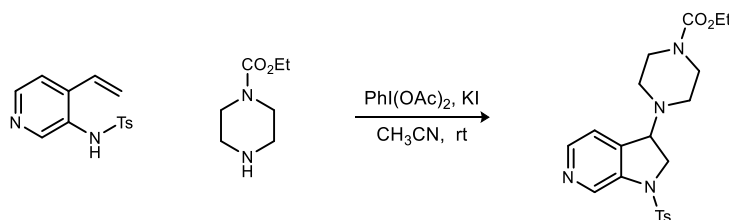


***N*-Benzyl-1-tosyl-2,3-dihydro-1H-pyrrolo[2,3-c]pyridin-3-amine (524b).** A vial equipped with a stir bar was charged with potassium iodide (7.80 mg, 47.0 μmol), iodobenzene diacetate (22.9 mg, 71.0 μmol), 4-methyl-*N*-(4-vinylpyridin-3-yl)benzenesulfonamide (12.9 mg, 47.0 μmol), and acetonitrile (470 μL). Benzylamine (10.3 μL , 94.0 μmol) was added and the resulting mixture was stirred at rt for 18 h. The reaction mixture was then diluted with ethyl acetate and concentrated. Flash column chromatography of the residue (SiO_2 , 40-60-80% ethyl acetate in hexanes) afforded the desired product as a yellow-orange viscous oil (8.60 mg, 48%). $R_f = 0.22$ (70% EtOAc/hexanes); IR (film) 3032, 2924, 2854, 2360, 2341, 1596 cm^{-1} ; ^1H NMR (400 MHz, CDCl_3) δ 8.98 (s, 1H), 8.34 (br d, $J = 4.0$ Hz, 1H), 7.69 (d, $J = 8.4$ Hz, 2H), 7.34-7.18 (m, 8H), 4.23 (dd, $J = 8.0, 4.4$ Hz, 1H), 3.95 (dd, $J = 11.6, 8.0$ Hz, 1H), 3.77 (dd, $J = 11.2, 4.4$ Hz, 1H), 3.66 (s, 2H), 2.30 (s, 3H), 1.53 (br s, 1H); ^{13}C NMR (125 MHz, CDCl_3) ppm 145.1, 144.8, 141.9, 139.0, 138.9, 137.1, 133.2, 129.9, 128.5, 128.0, 127.4, 127.3, 120.1, 57.1, 55.7, 50.7, 21.5; HRMS (ESI): Exact mass calcd for $\text{C}_{21}\text{H}_{22}\text{N}_3\text{O}_2\text{S}$ $[\text{M}+\text{H}]^+$ 380.1433, found 380.1427.



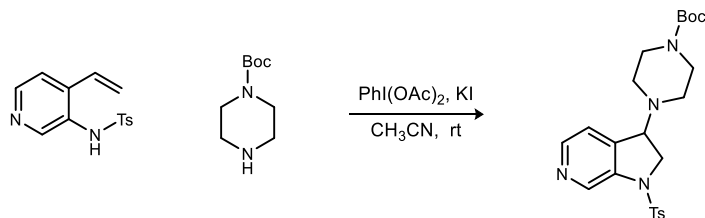
Benzyl 4-(1-tosyl-2,3-dihydro-1H-pyrrolo[2,3-c]pyridin-3-yl)piperazine-1-carboxylate (524c). A vial equipped with a stir bar was charged with potassium iodide (8.3 mg, 50.0 μmol), iodobenzene diacetate (24.2 mg, 75.0 μmol), 4-methyl-*N*-(4-vinylpyridin-3-yl)benzenesulfonamide (13.7 mg, 50.0 μmol), and acetonitrile (500 μL). Benzyl piperazine-1-carboxylate (19.3 μL , 100 μmol) was added and the resulting mixture was stirred at rt for 18 h. The reaction mixture was then diluted with ethyl acetate and concentrated. Flash column chromatography of the residue (SiO_2 , 50-70-90% ethyl acetate in hexanes) afforded the desired

product as a clear viscous oil (15.6 mg, 63%). $R_f = 0.48$ (5% MeOH/DCM); IR (film) 3033, 2925, 2860, 2822, 2360, 2336, 1699 cm^{-1} ; $^1\text{H NMR}$ (400 MHz, CDCl_3) δ 9.00 (br s, 1H), 8.31 (br d, $J = 4.0$ Hz, 1H), 7.73 (d, $J = 8.4$ Hz, 2H), 7.39-7.29 (m, 5H), 7.25 (d, $J = 8.8$ Hz, 2H), 7.16 (d, $J = 4.8$ Hz, 1H), 5.10 (s, 2H), 4.34 (dd, $J = 9.2, 4.0$ Hz, 1H), 3.88 (dd, $J = 11.6, 4.4$ Hz, 1H), 3.71 (dd, $J = 11.6, 9.2$ Hz, 1H), 3.36 (br d, $J = 4.8$ Hz, 4H), 2.35 (s, 3H), 2.29-2.22 (m, 2H), 2.21-2.02 (br m, 2H); $^{13}\text{C NMR}$ (125 MHz, CDCl_3) ppm 155.0, 144.9, 144.6, 139.6, 138.1, 136.5, 136.3, 133.2, 130.0, 128.5, 128.1, 127.9, 127.3, 120.9, 67.2, 63.8, 49.5, 47.8, 43.7, 21.5; HRMS (ESI): Exact mass calcd for $\text{C}_{26}\text{H}_{29}\text{N}_4\text{O}_4\text{S}$ $[\text{M}+\text{H}]^+$ 493.1910, found 493.1901.

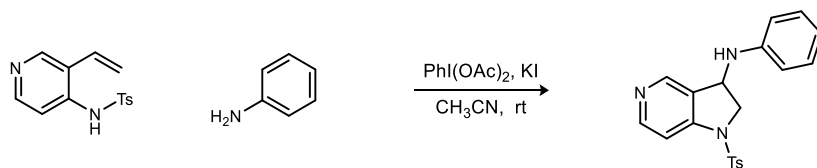


Ethyl 4-(1-tosyl-2,3-dihydro-1H-pyrrolo[2,3-c]pyridin-3-yl)piperazine-1-carboxylate (524d).

A vial equipped with a stir bar was charged with potassium iodide (13.9 mg, 83.8 μmol), iodobenzene diacetate (40.6 mg, 126 μmol), 4-methyl-*N*-(4-vinylpyridin-3-yl)benzenesulfonamide (23.0 mg, 83.8 μmol), and acetonitrile (840 μL). Ethyl 1-piperazinecarboxylate (24.5 μL , 168 μmol) was added and the resulting mixture was stirred at rt for 18 h. The reaction mixture was then diluted with ethyl acetate and concentrated. Flash column chromatography of the residue (SiO_2 , 0.5-1-2-5% methanol in dichloromethane) afforded the desired product as a dark-yellow viscous oil (23.8 mg, 66%). $R_f = 0.52$ (5% MeOH/DCM); IR (film) 3053, 2981, 2931, 2863, 2822, 2763, 1697, 1596 cm^{-1} ; $^1\text{H NMR}$ (400 MHz, CDCl_3) δ 8.99 (s, 1H), 8.31 (d, $J = 4.8$ Hz, 1H), 7.73 (d, $J = 8.4$ Hz, 2H), 7.27 (d, $J = 8.4$ Hz, 2H), 7.17 (d, $J = 4.8$ Hz, 1H), 4.34 (dd, $J = 9.6, 6.6$ Hz, 1H), 4.11 (q, $J = 7.2$ Hz, 2H), 3.89 (dd, $J = 11.6, 4.4$ Hz, 1H), 3.71 (d, $J = 11.6, 9.2$ Hz, 1H), 3.33 (dd, $J = 4.8, 4.8$ Hz, 4H), 2.39 (s, 3H), 2.26 (ddd, $J = 10.4, 4.8, 4.8$ Hz, 2H), 2.19-2.05 (br s, 2H), 1.24 (t, $J = 6.8$ Hz, 3H); $^{13}\text{C NMR}$ (125 MHz, CDCl_3) ppm 155.3, 144.9, 144.6, 139.6, 138.1, 136.3, 133.2, 130.0, 127.3, 120.9, 63.8, 61.4, 49.6, 48.0, 43.6, 21.5, 14.6; HRMS (ESI): Exact mass calcd for $\text{C}_{21}\text{H}_{27}\text{N}_4\text{O}_4\text{S}$ $[\text{M}+\text{H}]^+$ 431.1753, found 431.1750.

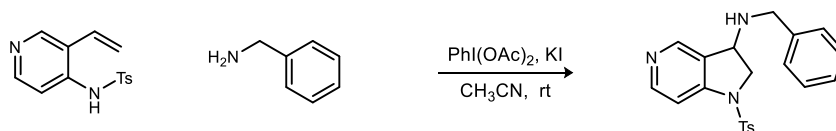


tert-Butyl 4-(1-tosyl-2,3-dihydro-1H-pyrrolo[2,3-c]pyridin-3-yl)piperazine-1-carboxylate (524e). A vial equipped with a stir bar was charged with potassium iodide (8.3 mg, 50.0 μmol), iodobenzene diacetate (24.2 mg, 75.0 μmol), 4-methyl-*N*-(4-vinylpyridin-3-yl)benzenesulfonamide (13.7 mg, 50.0 μmol), and acetonitrile (500 μL). *tert*-Butyl piperazine-1-carboxylate (18.6 mg, 100 μmol) was added and the resulting mixture was stirred at rt for 18 h. The reaction mixture was then diluted with ethyl acetate and concentrated. Flash column chromatography of the residue (SiO_2 , 50-70-90% ethyl acetate in hexanes) afforded the desired product as a light-yellow transparent viscous oil (17.0 mg, 74%). $R_f = 0.22$ (80% EtOAc/Hexanes); IR (film) 2975, 2929, 2861, 2822, 2360, 2337, 1692 cm^{-1} ; ^1H NMR (400 MHz, CDCl_3) δ 8.99 (br s, 1H), 8.31 (br d, $J = 4.8$ Hz, 1H), 7.74 (d, $J = 8.4$ Hz, 2H), 7.27 (d, $J = 8.8$ Hz, 2H), 7.17 (d, $J = 4.8$ Hz, 1H), 4.34 (dd, $J = 9.2, 4.0$ Hz, 1H), 3.90 (dd, $J = 11.6, 4.4$ Hz, 1H), 3.71 (d, $J = 11.6, 9.2$ Hz, 1H), 3.32-3.23 (br m, 4H), 2.39 (s, 3H), 2.28-2.21 (m, 2H), 2.19-2.00 (br m, 2H), 1.43 (s, 9H); ^{13}C NMR (125 MHz, CDCl_3) ppm 154.5, 144.9, 144.6, 139.6, 138.1, 136.3, 133.2, 130.0, 127.4, 120.9, 79.8, 63.8, 49.7, 48.1 (br), 43.8 (br), 28.4, 21.6; HRMS (ESI): Exact mass calcd for $\text{C}_{23}\text{H}_{31}\text{N}_4\text{O}_4\text{S}$ $[\text{M}+\text{H}]^+$ 459.2066, found 459.2056.

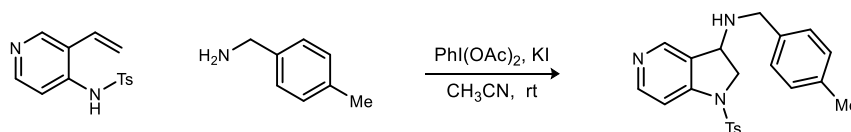


N-Phenyl-1-tosyl-2,3-dihydro-1H-pyrrolo[3,2-c]pyridin-3-amine (527a). A vial equipped with a stir bar was charged with potassium iodide (12.5 mg, 75.0 μmol), iodobenzene diacetate (36.2 mg, 113 μmol), 4-methyl-*N*-(3-vinylpyridin-4-yl)benzenesulfonamide (20.6 mg, 75.0 μmol), and acetonitrile (750 μL). Aniline (13.7 μL , 150 μmol) was added and the resulting mixture was stirred at rt for 18 h. The reaction mixture was then diluted with ethyl acetate and concentrated. Flash column chromatography of the residue (SiO_2 , 0.5-1-2% methanol in dichloromethane) afforded the desired product as a light-brown solid (22.2 mg, 81%). Mp 194.0-196.0 $^\circ\text{C}$; $R_f = 0.52$ (5% MeOH/DCM); IR (film) 3393, 3249, 3106, 3030, 2924, 1600 cm^{-1} ; ^1H NMR (400 MHz, CDCl_3)

δ 8.50 (d, $J = 5.6$ Hz, 1H), 8.47 (s, 1H), 7.69 (d, $J = 8.0$ Hz, 2H), 7.59 (d, $J = 5.6$ Hz, 1H), 7.27 (d, $J = 8.4$ Hz, 2H), 7.20 (dd, $J = 8.4, 7.6$ Hz, 2H), 6.81 (dd, $J = 7.2, 7.2$ Hz, 1H), 6.51 (d, $J = 7.6$ Hz, 2H), 5.07 (br s, 1H), 4.13 (dd, $J = 11.2, 7.6$ Hz, 1H), 3.86 (dd, $J = 11.2, 3.6$ Hz, 1H), 3.57 (br s, 1H), 2.42 (s, 3H); ^{13}C NMR (125 MHz, CDCl_3) ppm 151.2, 149.3, 147.1, 145.3, 145.0, 133.6, 130.1, 129.6, 127.5, 127.2, 119.0, 113.4, 109.3, 56.8, 51.8, 21.6; HRMS (ESI): Exact mass calcd for $\text{C}_{20}\text{H}_{19}\text{N}_3\text{O}_2\text{S}$ [M^+] 365.1192, found 365.1192.

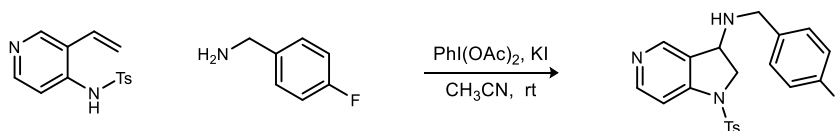


***N*-Benzyl-1-tosyl-2,3-dihydro-1H-pyrrolo[3,2-c]pyridin-3-amine (527b).** A vial equipped with a stir bar was charged with potassium iodide (12.5 mg, 75.0 μmol), iodobenzene diacetate (36.2 mg, 113 μmol), the vinyl aminopyridine (20.6 mg, 75.0 μmol), and acetonitrile (750 μL). Benzylamine (16.4 μL , 150 μmol) was added and the resulting mixture was stirred at rt for 18 h. The reaction mixture was then diluted with ethyl acetate and concentrated. Flash column chromatography of the residue (SiO_2 , 0.5-1-2-5% methanol in dichloromethane) afforded the desired product as a yellow viscous oil (12.3 mg, 43%). $R_f = 0.51$ (5% MeOH/DCM); IR (film) 3027, 2922, 2852, 2359, 2337, 1595, cm^{-1} ; ^1H NMR (400 MHz, CDCl_3) δ 8.46 (br s, 2H), 7.71 (d, $J = 8.4$ Hz, 2H), 7.58 (d, $J = 5.6$ Hz, 1H), 7.34-7.29 (m, 2H), 7.28-7.22 (m, 5H), 4.36 (dd, $J = 8.0, 4.0$ Hz, 1H), 3.93 (dd, $J = 11.2, 8.0$ Hz, 1H), 3.84 (dd, $J = 11.2, 4.0$ Hz, 1H), 3.70 (s, 2H), 2.60 (br s, 1H), 2.34 (s, 3H); ^{13}C NMR (100 MHz, CDCl_3) ppm 150.4, 149.2, 146.6, 145.0, 139.0, 133.5, 130.0, 128.5, 128.0, 127.4, 127.1, 109.2, 56.2, 55.6, 50.4, 21.5; HRMS (ESI): Exact mass calcd for $\text{C}_{21}\text{H}_{22}\text{N}_3\text{O}_2\text{S}$ [$\text{M}+\text{H}$] $^+$ 380.1433, found 380.1416.

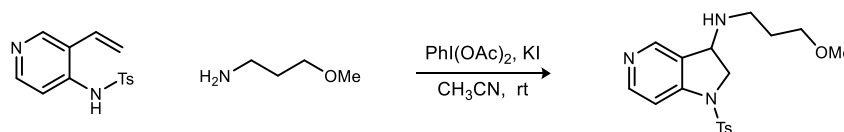


***N*-(4-Methylbenzyl)-1-tosyl-2,3-dihydro-1H-pyrrolo[3,2-c]pyridin-3-amine (527c).** A vial equipped with a stir bar was charged with potassium iodide (12.5 mg, 75.0 μmol), iodobenzene diacetate (36.2 mg, 113 μmol), 4-methyl-*N*-(3-vinylpyridin-4-yl)benzenesulfonamide (20.6 mg, 75.0 μmol), and acetonitrile (750 μL). 4-Methylbenzylamine (19.1 μL , 150 μmol) was added and the resulting mixture was stirred at rt for 18 h. The reaction mixture was then diluted with ethyl acetate and concentrated. Flash column chromatography of the residue (SiO_2 , 0.5-1-2-5% methanol in dichloromethane) afforded the desired product as a clear viscous oil (13.2 mg, 45%).

$R_f = 0.46$ (5% MeOH/DCM); IR (film) 3321, 3028, 2923, 2855, 2732, 1595 cm^{-1} ; ^1H NMR (400 MHz, CDCl_3) δ 8.45 (br s, 2H), 7.71 (d, $J = 8.4$ Hz, 2H), 7.56 (d, $J = 5.2$ Hz, 1H), 7.25 (d, $J = 8.4$ Hz, 2H), 7.13 (s, 4H), 4.34 (dd, $J = 8.0, 3.6$ Hz, 1H), 3.92 (dd, $J = 10.8, 7.6$ Hz, 1H), 3.83 (dd, $J = 11.2, 4.0$ Hz, 1H), 3.66 (s, 2H), 2.35 (s, 3H), 2.33 (s, 3H); ^{13}C NMR (125 MHz, CDCl_3) ppm 150.6, 149.0, 146.8, 144.9, 136.9, 135.9, 133.5, 129.9, 129.1, 128.6, 127.9, 127.1, 109.1, 56.1, 55.5, 50.14, 21.5, 21.0; HRMS (ESI): Exact mass calcd for $\text{C}_{22}\text{H}_{24}\text{N}_3\text{O}_2\text{S}$ $[\text{M}+\text{H}]^+$ 394.1589, found 394.1571.

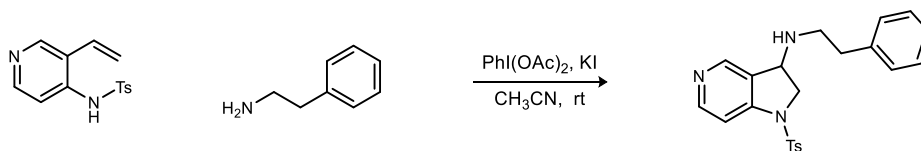


***N*-(4-Fluorobenzyl)-1-tosyl-2,3-dihydro-1H-pyrrolo[3,2-c]pyridin-3-amine (527d).** A vial equipped with a stir bar was charged with potassium iodide (12.5 mg, 75.0 μmol), iodobenzene diacetate (36.2 mg, 113 μmol), 4-methyl-*N*-(3-vinylpyridin-4-yl)benzenesulfonamide (20.6 mg, 75.0 μmol), and acetonitrile (750 μL). 4-Fluorobenzylamine (17.1 μL , 150 μmol) was added and the resulting mixture was stirred at rt for 18 h. The reaction mixture was then diluted with ethyl acetate and concentrated. Flash column chromatography of the residue (SiO_2 , 0.5-1-2-5% methanol in dichloromethane) afforded the desired product as a light-yellow transparent viscous oil (15.3 mg, 51%). $R_f = 0.48$ (5% MeOH/DCM); IR (film) 3256, 3041, 2925, 2853, 2357, 2336, 1596 cm^{-1} ; ^1H NMR (400 MHz, CDCl_3) δ 8.47 (br s, 1H), 8.45 (s, 1H), 7.71 (d, $J = 8.4$ Hz, 2H), 7.57 (d, $J = 5.6$ Hz, 1H), 7.27-7.19 (m, 4H), 6.99 (dd, $J = 8.8, 8.8$ Hz, 2H), 4.34 (dd, $J = 8.0, 3.6$ Hz, 1H), 3.92 (dd, $J = 11.2, 8.0$ Hz, 1H), 3.84 (dd, $J = 11.2, 3.6$ Hz, 1H), 3.67 (s, 2H), 2.35 (s, 3H); ^{13}C NMR (125 MHz, CDCl_3) ppm 162.1 (d, $J = 245.3$ Hz), 150.8, 149.1, 146.9, 145.0, 134.8 (d, $J = 3.0$ Hz), 133.6, 130.0, 129.5 (d, $J = 7.9$ Hz), 128.5, 127.2, 115.3 (d, $J = 21.4$ Hz), 109.2, 56.1, 55.6, 49.6, 21.5; HRMS (ESI): Exact mass calcd for $\text{C}_{21}\text{H}_{18}\text{FN}_3\text{O}_2\text{S}$ $[\text{M}-2\text{H}]^-$ 395.1098, found 395.1085.

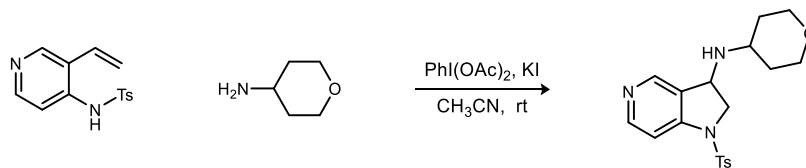


***N*-(3-Methoxypropyl)-1-tosyl-2,3-dihydro-1H-pyrrolo[3,2-c]pyridin-3-amine (527e).** A vial equipped with a stir bar was charged with potassium iodide (12.5 mg, 75.0 μmol), iodobenzene diacetate (36.2 mg, 113 μmol), 4-methyl-*N*-(3-vinylpyridin-4-yl)benzenesulfonamide (20.6 mg, 75.0 μmol), and acetonitrile (750 μL). 3-Methoxypropylamine (15.3 μL , 150 μmol) was added

and the resulting mixture was stirred at rt for 18 h. The reaction mixture was then diluted with ethyl acetate and concentrated. Flash column chromatography of the residue (SiO₂, 0.5-1-2-5% methanol in dichloromethane) afforded the desired product as a light-brown viscous oil (13.0 mg, 48%). *R_f* = 0.29 (5% MeOH/DCM); IR (film) 3249, 3036, 2926, 2873, 1644, 1596 cm⁻¹; ¹H NMR (600 MHz, CDCl₃) δ 8.44 (s, 1H), 8.43 (s, 1H), 7.73 (d, *J* = 7.8 Hz, 2H), 7.54 (d, *J* = 5.4 Hz, 1H), 7.28 (d, *J* = 8.4 Hz, 2H), 4.34 (dd, *J* = 7.8, 3.6 Hz, 1H), 3.91 (dd, *J* = 10.8, 7.8 Hz, 1H), 3.80 (dd, *J* = 10.8, 3.6 Hz, 1H), 3.38 (dd, *J* = 6.0, 6.0 Hz, 2H), 3.29 (s, 3H), 2.66-2.58 (m, 2H), 2.39 (s, 3H), 1.66 (dddd, *J* = 6.6, 6.6, 6.6, 6.6 Hz, 2H); ¹³C NMR (150 MHz, CDCl₃) ppm 150.6, 149.1, 146.8, 144.9, 133.6, 130.0, 128.4, 127.2, 109.0, 71.0, 58.7, 56.3, 56.1, 43.9, 29.9, 21.6; HRMS (ESI): Exact mass calcd for C₁₈H₂₄N₃O₃S [M+H]⁺ 362.1538, found 362.1537.

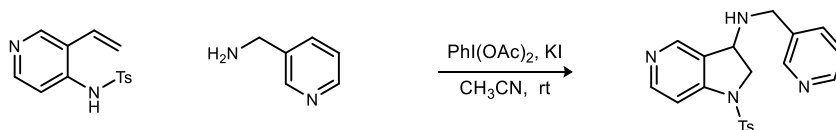


***N*-Phenethyl-1-tosyl-2,3-dihydro-1*H*-pyrrolo[3,2-*c*]pyridin-3-amine (527f).** A vial equipped with a stir bar was charged with potassium iodide (12.5 mg, 75.0 μmol), iodobenzene diacetate (36.2 mg, 113 μmol), 4-methyl-*N*-(3-vinylpyridin-4-yl)benzenesulfonamide (20.6 mg, 75.0 μmol), and acetonitrile (750 μL). Phenethylamine (18.8 μL, 150 μmol) was added and the resulting mixture was stirred at rt for 18 h. The reaction mixture was then diluted with ethyl acetate and concentrated. Flash column chromatography of the residue (SiO₂, 0.5-1-2-5% methanol in dichloromethane) afforded the desired product as an orange viscous oil (14.1 mg, 48%). *R_f* = 0.42 (5% MeOH/DCM); IR (film) 3312, 3028, 2925, 2855, 1637, 1596 cm⁻¹; ¹H NMR (400 MHz, CDCl₃) δ 8.42 (d, *J* = 5.6 Hz, 1H), 8.36 (s, 1H), 7.70 (d, *J* = 8.4 Hz, 2H), 7.54 (d, *J* = 5.6 Hz, 1H), 7.31-7.19 (m, 5H), 7.13 (dd, *J* = 8.4, 1.6 Hz, 2H), 4.36 (dd, *J* = 8.0, 4.0 Hz, 1H), 3.90 (dd, *J* = 11.2, 8.4 Hz, 1H), 3.76 (dd, *J* = 11.2, 4.0 Hz, 1H), 2.83-2.67 (m, 4H), 2.39 (br s, 1H), 2.39 (s, 3H); ¹³C NMR (125 MHz, CDCl₃) ppm 150.5, 149.1, 146.7, 144.9, 139.3, 133.6, 130.0, 128.59, 128.57, 128.3, 127.2, 126.4, 109.0, 56.14, 56.09, 47.4, 36.4, 21.6; HRMS (ESI): Exact mass calcd for C₂₂H₂₄N₃O₂S [M+H]⁺ 394.1587, found 394.1587.



***N*-(Tetrahydro-2*H*-pyran-4-yl)-1-tosyl-2,3-dihydro-1*H*-pyrrolo[3,2-*c*]pyridin-3-amine**

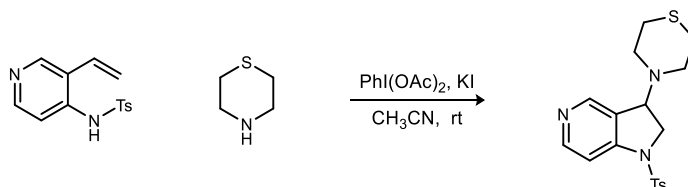
(527g). A vial equipped with a stir bar was charged with potassium iodide (12.5 mg, 75.0 μmol), iodobenzene diacetate (36.2 mg, 113 μmol), 4-methyl-*N*-(3-vinylpyridin-4-yl)benzenesulfonamide (20.6 mg, 75.0 μmol), and acetonitrile (750 μL). 4-Aminotetrahydropyran (15.5 μL , 150 μmol) was added and the resulting mixture was stirred at rt for 18 h. The reaction mixture was then diluted with ethyl acetate and concentrated. Flash column chromatography of the residue (SiO_2 , 0.5-1-2-5-10% methanol in dichloromethane) afforded the desired product as a light-yellow viscous oil (9.20 mg, 33%). $R_f = 0.35$ (5% MeOH/DCM); IR (film) 3299, 3046, 2927, 2850, 1596 cm^{-1} ; ^1H NMR (400 MHz, CDCl_3) δ 8.44 (br d, $J = 5.2$ Hz, 1H), 8.40 (br s, 1H), 7.73 (d, $J = 8.4$ Hz, 2H), 7.55 (d, $J = 5.2$ Hz, 1H), 7.29 (d, $J = 8.0$ Hz, 2H), 4.42 (dd, $J = 8.0, 4.0$ Hz, 1H), 3.95 (dd, $J = 10.8, 7.6$ Hz, 1H), 3.98-3.91 (br m, 2H), 3.74 (dd, $J = 10.8, 4.0$ Hz, 1H), 3.42-3.33 (m, 2H), 2.78 (dddd, $J = 10.0, 3.6, 3.6, 3.6, 3.6$ Hz, 1H), 2.40 (s, 3H), 1.73-1.64 (br m, 2H), 1.49 (br s, 1H), 1.44-1.32 (m, 2H); ^{13}C NMR (100 MHz, CDCl_3) ppm 150.6, 148.9, 146.7, 145.0, 133.6, 130.0, 129.0, 127.2, 109.1, 66.33, 66.30, 57.2, 53.0, 51.3, 33.9, 33.4, 21.6; HRMS (ESI): Exact mass calcd for $\text{C}_{19}\text{H}_{24}\text{N}_3\text{O}_3\text{S}$ $[\text{M}+\text{H}]^+$ 374.1538, found 374.1534.



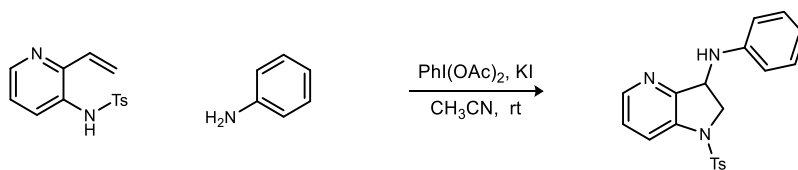
***N*-(Pyridin-3-ylmethyl)-1-tosyl-2,3-dihydro-1*H*-pyrrolo[3,2-*c*]pyridin-3-amine (527h).**

A vial equipped with a stir bar was charged with potassium iodide (39.8 mg, 240 μmol), iodobenzene diacetate (96.6 mg, 300 μmol), 4-methyl-*N*-(3-vinylpyridin-4-yl)benzenesulfonamide (54.8 mg, 200 μmol), and acetonitrile (2 mL). 3-Picolylamine (40.4 μL , 400 μmol) was added and the resulting mixture was stirred at rt for 18 h. The reaction mixture was then diluted with ethyl acetate and concentrated. Flash column chromatography of the residue (SiO_2 , 0.5-1-2-5-10% methanol in dichloromethane) afforded the desired product as a dark-yellow viscous oil (48.4 mg, 64%). $R_f = 0.28$ (5% MeOH/DCM); IR (film) 3030, 2924, 2853, 1595 cm^{-1} ; ^1H NMR (600 MHz, CDCl_3) δ 8.51 (br d, $J = 4.2$ Hz, 1H), 8.49-8.46 (br m, 3H), 7.72 (d, $J = 8.4$ Hz, 2H), 7.61 (d, $J = 7.8$ Hz, 1H), 7.58 (d, $J = 6.0$ Hz, 1H), 7.27-7.23 (m, 3H), 4.36 (dd, $J = 7.8, 3.6$ Hz, 1H), 3.93 (dd, $J = 11.4,$

7.8 Hz, 1H), 3.86 (dd, $J = 11.4, 3.6$ Hz, 1H), 3.70 (s, $J = 2$ H), 2.34 (s, 3H); ^{13}C NMR (150 MHz, CDCl_3) ppm 150.9, 149.5, 149.1, 148.9, 146.9, 145.1, 135.7, 134.5, 133.5, 130.0, 128.2, 127.2, 123.5, 109.3, 56.0, 55.7, 47.7, 21.6; Exact mass calcd for $\text{C}_{20}\text{H}_{21}\text{N}_4\text{O}_2\text{S}$ $[\text{M}+\text{H}]^+$ 381.1385, found 381.1389.

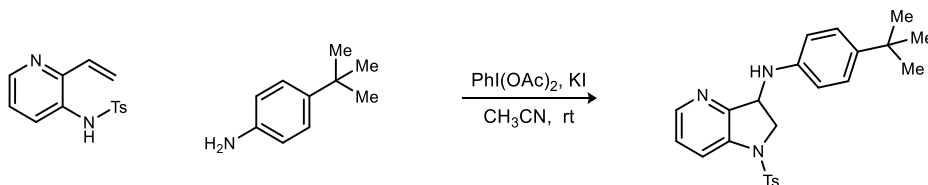


4-(1-Tosyl-2,3-dihydro-1H-pyrrolo[3,2-c]pyridin-3-yl)thiomorpholine (527i). A vial equipped with a stir bar was charged with potassium iodide (12.5 mg, 75.0 μmol), iodobenzene diacetate (36.2 mg, 113 μmol), 4-methyl-*N*-(3-vinylpyridin-4-yl)benzenesulfonamide (20.6 mg, 75.0 μmol), and acetonitrile (750 μL). Thiomorpholine (15.1 μL , 150 μmol) was added and the resulting mixture was stirred at rt for 18 h. The reaction mixture was then diluted with ethyl acetate and concentrated. Flash column chromatography of the residue (SiO_2 , 0.5-1-2-5% methanol in dichloromethane) afforded the desired product as a light-yellow viscous oil (9.60 mg, 34%). $R_f = 0.46$ (5% MeOH/DCM); IR (film) 2922, 2819, 1594 cm^{-1} ; ^1H NMR (400 MHz, CDCl_3) δ 8.45 (br s, 1H), 8.41 (br s, 1H), 7.74 (d, $J = 8.4$ Hz, 2H), 7.57 (d, $J = 5.2$ Hz, 1H), 7.30 (d, $J = 8.0$ Hz, 2H), 4.37 (dd, $J = 9.2, 3.6$ Hz, 1H), 3.95 (dd, $J = 11.6, 4.0$ Hz, 1H), 3.72 (dd, $J = 11.2, 9.0$ Hz, 1H), 2.60-2.41 (m, 8H), 2.40 (s, 3H); ^{13}C NMR (125 MHz, CDCl_3) ppm 150.9, 149.7, 147.7, 145.1, 133.7, 130.0, 127.2, 125.4, 108.5, 63.8, 50.6, 50.0, 28.1, 21.6; HRMS (ESI): Exact mass calcd for $\text{C}_{18}\text{H}_{22}\text{N}_3\text{O}_2\text{S}_2$ $[\text{M}+\text{H}]^+$ 376.1153, found 376.1135.



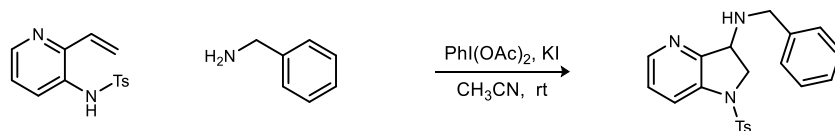
***N*-Phenyl-1-tosyl-2,3-dihydro-1H-pyrrolo[3,2-b]pyridin-3-amine (530a).** Prepared according to the general procedure using aniline (27.3 μL , 300 μmol) and 4-methyl-*N*-(2-vinylpyridin-3-yl)benzenesulfonamide (41.2 mg, 150 μmol). Flash column chromatography of the residue (SiO_2 , 5-10-20-40% ethyl acetate in hexanes) afforded the desired product as a brown viscous oil (38.2 mg, 70%). $R_f = 0.50$ (50% EtOAc/hexanes); IR (film) 3393, 3288, 3053, 3028, 2925, 2872, 1602, 1503 cm^{-1} ; ^1H NMR (400 MHz, CDCl_3) δ 8.25 (dd, $J = 4.8, 1.2$ Hz, 1H), 7.97 (dd, $J = 8.4, 1.2$ Hz, 1H), 7.64 (d, $J = 8.4$ Hz, 2H), 7.25-7.17 (m, 5H), 6.79 (dd, $J = 7.2, 7.2$ Hz, 1H), 6.52 (d, $J = 7.6$

Hz, 2H), 4.84 (dd, $J = 7.6, 5.2$ Hz, 1H), 4.35 (dd, $J = 10.8, 8.0$ Hz, 1H), 3.99 (br s, 1H), 3.74 (dd, $J = 11.2, 5.6$ Hz, 1H), 2.39 (s, 3H); ^{13}C NMR (100 MHz, CDCl_3) ppm 152.1, 146.1, 145.2, 144.8, 136.7, 133.3, 130.0, 129.3, 127.3, 123.9, 122.2, 118.7, 113.4, 56.4, 54.3, 21.6; HRMS (ESI): Exact mass calcd for $\text{C}_{20}\text{H}_{19}\text{N}_3\text{NaO}_2\text{S}$ $[\text{M}+\text{Na}]^+$ 388.1096, found 388.1093.



***N*-(4-(*tert*-Butyl)phenyl)-1-tosyl-2,3-dihydro-1*H*-pyrrolo[3,2-*b*]pyridin-3-amine (530b).**

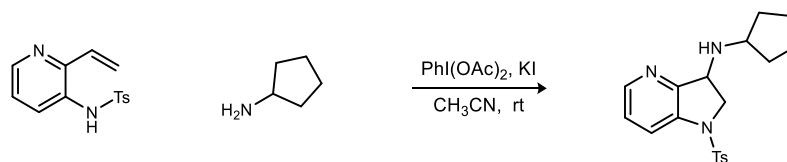
Prepared according to the general procedure using 4-*tert*-butylaniline (47.8 μL , 300 μmol) and 4-methyl-*N*-(2-vinylpyridin-3-yl)benzenesulfonamide (41.2 mg, 150 μmol). Flash column chromatography of the residue (SiO_2 , 5-10-20-40% ethyl acetate in hexanes) afforded the desired product as a dark-brown viscous oil (25.6 mg, 41%, 90% BRSM). $R_f = 0.59$ (50% EtOAc/hexanes); IR (film) 3391, 3060, 2961, 2867, 1614, 1519 cm^{-1} ; ^1H NMR (400 MHz, CDCl_3) δ 8.24 (d, $J = 4.4$ Hz, 1H), 7.95 (d, $J = 8.4$ Hz, 1H), 7.66 (d, $J = 8.4$ Hz, 2H), 7.26-7.21 (m, 5H), 6.50 (d, $J = 8.8$ Hz, 2H), 4.82 (dd, $J = 7.6, 6.0$ Hz, 1H), 4.36 (dd, $J = 11.2, 8.0$ Hz, 1H), 3.98 (br s, 1H), 3.73 (dd, $J = 10.8, 5.6$ Hz, 1H), 2.39 (s, 3H), 1.29 (s, 9H); ^{13}C NMR (100 MHz, CDCl_3) ppm 152.3, 145.1, 144.8, 143.8, 141.6, 136.6, 133.3, 129.9, 127.3, 126.1, 123.8, 122.0, 113.2, 56.6, 54.6, 33.9, 31.5, 21.6; Exact mass calcd for $\text{C}_{24}\text{H}_{27}\text{N}_3\text{NaO}_2\text{S}$ $[\text{M}+\text{Na}]^+$ 444.1722, found 444.1717.



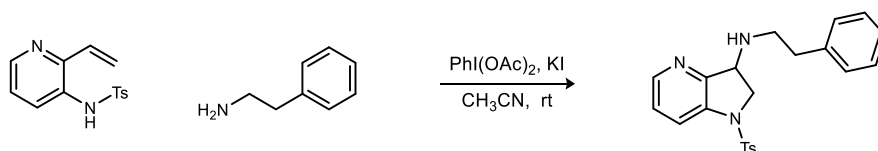
***N*-Benzyl-1-tosyl-2,3-dihydro-1*H*-pyrrolo[3,2-*b*]pyridin-3-amine (530c).**

Prepared according to the general procedure using benzylamine (32.8 μL , 300 μmol) and 4-methyl-*N*-(2-vinylpyridin-3-yl)benzenesulfonamide (41.2 mg, 150 μmol). Flash column chromatography of the residue (SiO_2 , 20-40-60-80% ethyl acetate in hexanes) afforded the desired product as a dark yellow viscous oil (50.2 mg, 88%). $R_f = 0.34$ (50% EtOAc/hexanes); IR (film) 3060, 3026, 2922, 2852, 2338, cm^{-1} ; ^1H NMR (400 MHz, CDCl_3) δ 8.21 (dd, $J = 4.8, 1.2$ Hz, 1H), 7.91 (dd, $J = 8.4, 1.6$ Hz, 1H), 7.66 (d, $J = 8.4$ Hz, 2H), 7.33-7.21 (m, 7H), 7.17 (dd, $J = 8.0, 4.8$ Hz, 1H), 4.25 (dd, $J = 8.4, 5.2$ Hz, 1H), 4.00 (dd, $J = 11.2, 8.4$ Hz, 1H), 3.77 (d, $J = 4.4$ Hz, 2H), 3.70 (dd, $J = 10.8, 4.8$ Hz, 1H), 2.34 (s, 3H), 1.75 (br s, 1H); ^{13}C NMR (100 MHz, CDCl_3) ppm 153.7, 144.8, 144.7, 139.3,

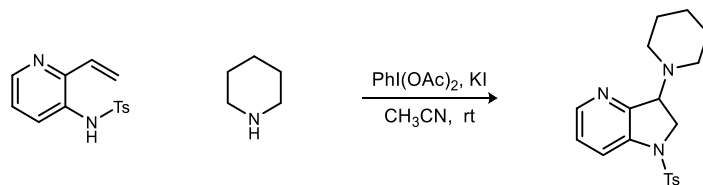
136.5, 133.4, 129.9, 128.4, 128.2, 127.2, 123.3, 121.8, 57.8, 55.3, 51.4, 21.5; HRMS (ESI): Exact mass calcd for $C_{21}H_{21}N_3NaO_2S$ $[M+Na]^+$ 402.1252, found 402.1252.



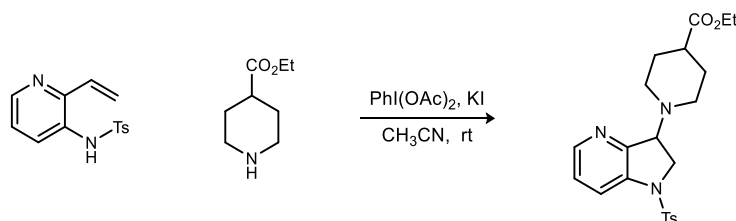
***N*-Cyclopentyl-1-tosyl-2,3-dihydro-1*H*-pyrrolo[3,2-*b*]pyridin-3-amine (530d).** Prepared according to the general procedure using cyclopentylamine (29.6 μ L, 300 μ mol) and 4-methyl-*N*-(2-vinylpyridin-3-yl)benzenesulfonamide (41.2 mg, 150 μ mol). Flash column chromatography of the residue (SiO_2 , 40-60-80-100% ethyl acetate in hexanes) afforded the desired product as a dark-brown viscous oil (31.7 mg, 59%). $R_f = 0.20$ (70% EtOAc/hexanes); IR (film) 2954, 2868, 1594 cm^{-1} ; 1H NMR (400 MHz, $CDCl_3$) δ 8.19 (dd, $J = 4.8, 1.2$ Hz, 1H), 7.88 (dd, $J = 8.4, 1.2$ Hz, 1H), 7.68 (d, $J = 8.0$ Hz, 2H), 7.25 (d, $J = 8.0$ Hz, 2H), 7.15 (dd, $J = 8.4, 4.8$ Hz, 1H), 4.26 (dd, $J = 8.0, 5.6$ Hz, 1H), 4.09 (dd, $J = 10.8, 8.0$ Hz, 1H), 3.69 (dd, $J = 10.8, 5.6$ Hz, 1H), 3.20 (dddd, $J = 6.8, 6.8, 6.8, 6.8$ Hz, 1H), 2.38 (s, 3H), 1.87-1.73 (m, 3H), 1.72-1.62 (m, 2H), 1.57-1.46 (m, 2H), 1.37-1.19 (m, 2H); ^{13}C NMR (100 MHz, $CDCl_3$) ppm 153.1, 144.7, 144.6, 136.5, 133.3, 129.9, 127.3, 123.4, 121.7, 58.4, 57.4, 55.8, 33.2, 32.8, 23.9, 23.7, 21.5; HRMS (ESI): Exact mass calcd for $C_{19}H_{23}N_3NaO_2S$ $[M+Na]^+$ 380.1409, found 380.1415.



***N*-Phenethyl-1-tosyl-2,3-dihydro-1*H*-pyrrolo[3,2-*b*]pyridin-3-amine (530e).** Prepared according to the general procedure using phenethylamine (37.7 μ L, 300 μ mol) and 4-methyl-*N*-(2-vinylpyridin-3-yl)benzenesulfonamide (41.2 mg, 150 μ mol). Flash column chromatography of the residue (SiO_2 , 40-60-80-100% ethyl acetate in hexanes) afforded the desired product as a dark-orange viscous oil (40.4 mg, 68%). $R_f = 0.22$ (70% EtOAc/hexanes); IR (film) 3060, 3026, 2923, 2853, 1595 cm^{-1} ; 1H NMR (400 MHz, $CDCl_3$) δ 8.18 (dd, $J = 4.8, 1.2$ Hz, 1H), 7.89 (dd, $J = 8.4, 1.2$ Hz, 1H), 7.67 (d, $J = 8.4$ Hz, 2H), 7.29-7.13 (m, 8H), 4.26 (dd, $J = 8.4, 5.2$ Hz, 1H), 4.01 (dd, $J = 10.8, 8.4$ Hz, 1H), 3.70 (dd, $J = 11.2, 5.2$ Hz, 1H), 2.93-2.88 (m, 1H), 2.82-2.70 (m, 3H), 2.37 (s, 3H); ^{13}C NMR (100 MHz, $CDCl_3$) ppm 153.3, 144.69, 144.66, 139.4, 136.5, 133.4, 129.9, 128.6, 128.5, 127.3, 126.3, 123.3, 121.6, 58.3, 55.1, 48.4, 36.4, 21.5; HRMS (ESI): Exact mass calcd for $C_{22}H_{23}N_3NaO_2S$ $[M+Na]^+$ 416.1409, found 416.1410.

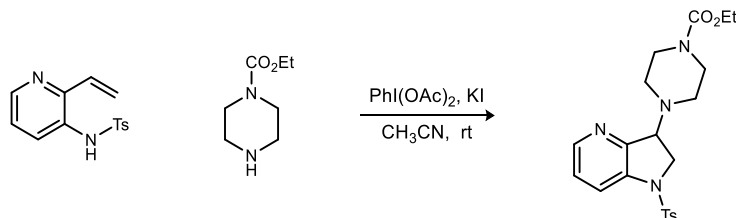


(Piperidin-1-yl)-1-tosyl-2,3-dihydro-1H-pyrrolo[3,2-b]pyridine (530f). Prepared according to the general procedure using piperidine (29.6 μL , 300 μmol) and 4-methyl-*N*-(2-vinylpyridin-3-yl)benzenesulfonamide (41.2 mg, 150 μmol). Flash column chromatography of the residue (SiO_2 , 40-60-80-100% ethyl acetate in hexanes) afforded the desired product as a brown viscous oil (33.7 mg, 63%). $R_f = 0.12$ (50% EtOAc/hexanes); IR (film) 2933, 2853, 1595 cm^{-1} ; ^1H NMR (400 MHz, CDCl_3) δ 8.24 (d, $J = 4.0$ Hz, 1H), 7.94 (d, $J = 8.4$ Hz, 1H), 7.69 (d, $J = 8.4$ Hz, 2H), 7.26 (d, $J = 8.0$ Hz, 2H), 7.17 (dd, $J = 8.4, 4.8$ Hz, 1H), 4.31 (dd, $J = 9.2, 3.6$ Hz, 1H), 4.03 (dd, $J = 12.0, 3.6$ Hz, 1H), 3.76 (dd, $J = 11.6, 9.6$ Hz, 1H), 2.51 (br dd, $J = 5.2, 5.2$ Hz, 2H), 2.37 (s, 3H), 2.19 (br m, 2H), 1.50 (br d, $J = 4.8$ Hz, 4H), 1.35 (br dd, $J = 5.6, 5.6$ Hz, 2H); ^{13}C NMR (100 MHz, CDCl_3) ppm 150.8, 144.8, 144.6, 137.5, 133.3, 129.9, 127.3, 123.4, 120.9, 64.6, 49.6, 49.5, 25.5, 23.9, 21.5; Exact mass calcd for $\text{C}_{19}\text{H}_{23}\text{N}_3\text{NaO}_2\text{S}$ $[\text{M}+\text{Na}]^+$ 380.1409, found 380.1395.

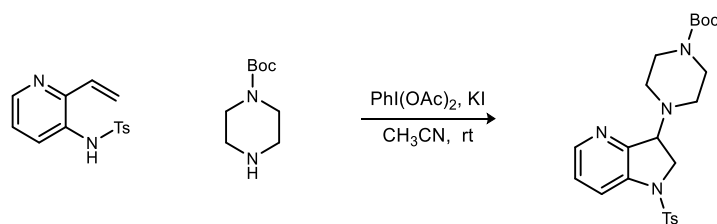


Ethyl 1-(1-tosyl-2,3-dihydro-1H-pyrrolo[3,2-b]pyridin-3-yl)piperidine-4-carboxylate (530g). Prepared according to the general procedure using ethyl isonipecotatate (46.2 μL , 300 μmol) and 4-methyl-*N*-(2-vinylpyridin-3-yl)benzenesulfonamide (41.2 mg, 150 μmol). Flash column chromatography of the residue (SiO_2 , 40-60-80-100% ethyl acetate in hexanes) afforded the desired product as light-brown viscous oil (45.5 mg, 71%). $R_f = 0.17$ (50% EtOAc/hexanes); IR (film) 2947, 2815, 1728, 1592 cm^{-1} ; ^1H NMR (600 MHz, CDCl_3) δ 8.23 (dd, $J = 5.4, 1.8$ Hz, 1H), 7.93 (dd, $J = 8.4, 1.2$ Hz, 1H), 7.68 (d, $J = 8.4$ Hz, 2H), 7.26 (d, $J = 8.4$ Hz, 2H), 7.17 (dd, $J = 8.4, 4.8$ Hz, 1H), 4.27 (dd, $J = 9.6, 4.2$ Hz, 1H), 4.09 (q, $J = 7.2$ Hz, 2H), 3.90 (dd, $J = 11.4, 3.6$ Hz, 1H), 3.76 (dd, $J = 11.4, 9.6$ Hz, 1H), 2.57 (br d, $J = 10.8$ Hz, 1H), 2.50 (br d, $J = 11.4$ Hz, 1H), 2.41-2.36 (m, 1H), 2.38 (s, 3H), 2.16-2.11 (m, 1H), 1.89 (dd, 10.8, 9.0 Hz, 1H), 1.74 (ddd, $J = 14.4, 14.4, 1.8$ Hz, 2H), 1.68-1.58 (m, 2H), 1.21 (t, $J = 7.2$ Hz, 3H); ^{13}C NMR (150 MHz, CDCl_3) ppm 174.8, 151.4, 144.8, 144.6, 137.3, 133.3, 129.9, 127.2, 123.3, 121.0, 64.2, 60.2, 49.8, 48.4

(0.5C), 47.8 (0.5C), 40.9, 28.2 (0.5C), 28.1 (0.5C), 21.5, 14.2; Exact mass calcd for C₂₂H₂₇N₃NaO₄S [M+Na]⁺ 452.1620, found 452.1619.

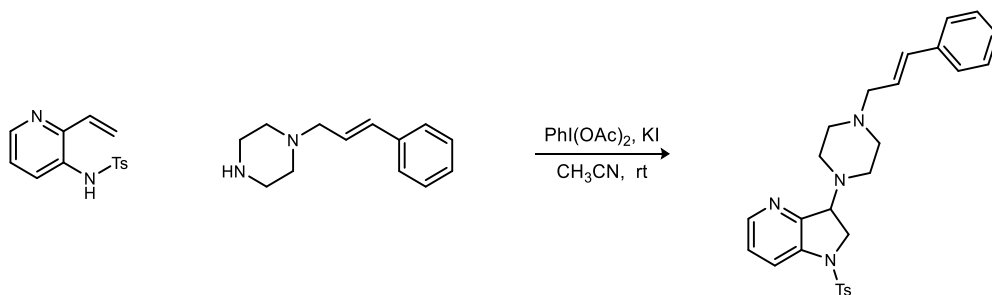


Ethyl 4-(1-(1-tosyl-2,3-dihydro-1H-pyrrolo[3,2-b]pyridin-3-yl)piperazine-1-carboxylate (530h). Prepared according to the general procedure using ethyl 1-piperazinecarboxylate (44.0 μ L, 300 μ mol) and 4-methyl-*N*-(2-vinylpyridin-3-yl)benzenesulfonamide (41.2 mg, 150 μ mol). Flash column chromatography of the residue (SiO₂, 50-75-100% ethyl acetate in hexanes) afforded the desired product as an orange viscous oil (55.6 mg, 86%). R_f = 0.10 (50% EtOAc/hexanes); IR (film) 3062, 2981, 2927, 2861, 2764, 1696, 1594 cm⁻¹; ¹H NMR (400 MHz, CDCl₃) δ 8.24 (dd, J = 4.8, 1.2 Hz, 1H), 7.95 (dd, J = 8.4, 1.2 Hz, 1H), 7.69 (d, J = 8.4 Hz, 2H), 7.27 (d, J = 7.6 Hz, 2H), 7.18 (dd, J = 8.0, 4.8 Hz, 1H), 4.30 (dd, J = 9.2, 3.6 Hz, 1H), 4.09 (q, 7.2 Hz, 2H), 3.90 (dd, J = 12.0, 4.0 Hz, 1H), 3.77 (dd, J = 11.2, 9.2 Hz, 1H), 3.35 (br s, 4H), 2.42 (br s, 2H), 2.39 (s, 3H), 2.19-2.11 (br m, 2H), 1.22 (t, J = 6.8 Hz, 3H); ¹³C NMR (125 MHz, CDCl₃) ppm 155.2, 150.6, 144.9, 144.7, 137.4, 133.2, 129.9, 127.2, 123.6, 121.1, 64.1, 61.3, 49.5, 48.1 (br), 43.4 (br), 21.5, 14.6; Exact mass calcd for C₂₁H₂₆N₄NaO₄S [M+Na]⁺ 453.1572, found 453.1574.



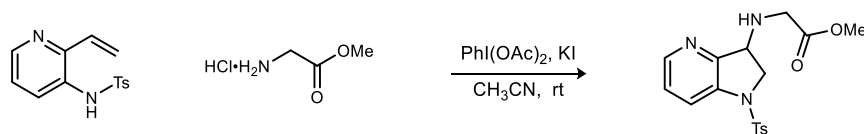
***tert*-Butyl 4-(1-(1-tosyl-2,3-dihydro-1H-pyrrolo[3,2-b]pyridin-3-yl)piperazine-1-carboxylate (530i).** Prepared according to the general procedure using *tert*-butyl piperazine-1-carboxylate (55.9 mg, 300 μ mol) and 4-methyl-*N*-(2-vinylpyridin-3-yl)benzenesulfonamide (41.2 mg, 150 μ mol). Flash column chromatography of the residue (SiO₂, 20-40-60-80% ethyl acetate in hexanes) afforded the desired product as a golden viscous oil (50.8 mg, 74%). R_f = 0.15 (50% EtOAc/hexanes); IR (film) 3384, 3062, 2975, 2930, 2860, 1692, 1591 cm⁻¹; ¹H NMR (600 MHz, CDCl₃) δ 8.24 (dd, J = 4.8, 1.2 Hz, 1H), 7.94 (dd, J = 8.4, 1.2 Hz, 1H), 7.69 (d, J = 8.4 Hz, 2H), 7.27 (d, J = 7.8 Hz, 2H), 7.18 (dd, J = 8.4, 4.8 Hz, 1H), 4.29 (dd, J = 9.0, 3.6 Hz, 1H), 3.90 (dd, J = 11.4, 4.2 Hz, 1H), 3.77 (dd, J = 12.0, 9.6 Hz, 1H), 3.29 (br s, 4H), 2.39

(br s, 2H), 2.39 (s, 3H), 2.14 (br s, 2H), 1.42 (s, 9H); ^{13}C NMR (150 MHz, CDCl_3) ppm 154.5, 150.8, 144.9, 144.7, 137.4, 133.2, 129.9, 127.2, 123.5, 121.1, 79.6, 64.1, 49.6, 48.2 (br), 44.0 (br, 0.5C), 42.9 (br, 0.5C), 28.4, 21.5; Exact mass calcd for $\text{C}_{23}\text{H}_{30}\text{N}_4\text{NaO}_4\text{S}$ $[\text{M}+\text{Na}]^+$ 481.1885, found 481.1903.



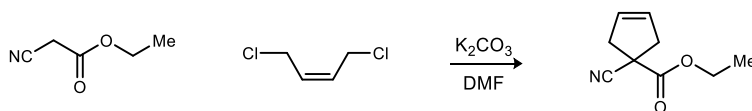
(E)-3-(4-Cinnamylpiperazin-1-yl)-1-tosyl-2,3-dihydro-1H-pyrrolo[3,2-b]pyridine (530j).

Prepared according to the general procedure using *trans*-1-cinnamylpiperazine (60.7 mg, 300 μmol) and 4-methyl-*N*-(2-vinylpyridin-3-yl)benzenesulfonamide (41.2 mg, 150 μmol). Flash column chromatography of the residue (SiO_2 , 0.5-1-2-5-10% methanol in dichloromethane) afforded the desired product as a light-yellow viscous oil (46.7 mg, 66%). $R_f = 0.42$ (5% MeOH/DCM); IR (film) 3026, 2935, 2812, 1673, 1595 cm^{-1} ; ^1H NMR (600 MHz, CDCl_3) δ 8.23 (dd, $J = 4.8, 1.2$ Hz, 1H), 7.93 (dd, $J = 8.4, 1.2$ Hz, 1H), 7.69 (d, $J = 8.4$ Hz, 2H), 7.39-7.20 (m, 7H), 7.16 (dd, $J = 8.4, 5.4$ Hz, 1H), 6.49 (d, $J = 15.6$ Hz, 1H), 6.22 (ddd, $J = 15.0, 6.6, 6.6$ Hz, 1H), 4.31 (dd, $J = 9.0, 3.6$ Hz, 1H), 3.96 (dd, $J = 11.4, 4.2$ Hz, 1H), 3.76 (dd, $J = 11.4, 9.6$ Hz, 1H), 3.13 (br s, 2H), 2.61-2.56 (br m, 2H), 2.53-2.38 (br m, 4H), 2.34 (s, 3H), 2.32-2.26 (br m, 2H); ^{13}C NMR (150 MHz, CDCl_3) ppm 151.1, 144.74, 144.68, 137.3, 136.7, 133.3, 129.9, 128.5, 127.6, 127.3, 126.3, 123.3, 120.9, 63.9, 60.8, 52.9, 49.3, 48.0, 21.5; HRMS (ESI): Exact mass calcd for $\text{C}_{27}\text{H}_{31}\text{N}_4\text{O}_2\text{S}$ $[\text{M}+\text{H}]^+$ 475.2168, found 475.2146.



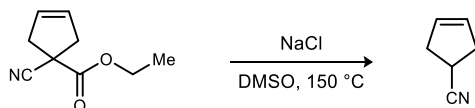
Methyl 2-((1-tosyl-2,3-dihydro-1H-pyrrolo[3,2-b]pyridin-3-yl)amino)acetate (530k). A vial equipped with a stir bar was charged with potassium iodide (24.9 mg, 150 μmol), iodobenzene diacetate (72.5 mg, 225 μmol), 4-methyl-*N*-(2-vinylpyridin-3-yl)benzenesulfonamide (41.2 mg, 150 μmol), and acetonitrile (1.5 mL). Potassium carbonate (41.5 mg, 300 μmol) and glycine methyl ester hydrochloride (37.7 mg, 300 μmol) were added and the resulting mixture was stirred

at rt for 18 h. The reaction mixture was then diluted with ethyl acetate and concentrated. Flash column chromatography of the residue (SiO₂, 50-80-100% ethyl acetate in hexanes) afforded the desired product as an orange viscous oil (33.9 mg, 63%). $R_f = 0.18$ (70% EtOAc/hexanes); IR (film) 3327, 3062, 2951, 2924, 1741, 1594 cm⁻¹; ¹H NMR (400 MHz, CDCl₃) δ 8.19 (dd, $J = 4.8, 1.2$ Hz, 1H), 7.90 (dd, $J = 8.4, 1.2$ Hz, 1H), 7.68 (d, $J = 8.4$ Hz, 2H), 7.26 (d, $J = 8.0$ Hz, 2H), 7.17 (dd, $J = 8.4, 5.2$ Hz, 1H), 4.25 (dd, $J = 8.4, 5.2$ Hz, 1H), 4.03 (dd, $J = 10.8, 8.4$ Hz, 1H), 3.70 (s, 3H), 3.68 (dd, $J = 10.8, 4.8$ Hz, 1H), 3.46 (s, 2H), 2.38 (s, 3H); ¹³C NMR (125 MHz, CDCl₃) ppm 172.1, 153.1, 144.8, 144.7, 136.4, 133.2, 129.9, 127.3, 123.5, 121.6, 57.5, 55.1, 51.9, 48.1, 21.5; Exact mass calcd for C₁₇H₁₉N₃NaO₄S [M+Na]⁺ 384.0994, found 384.0976.

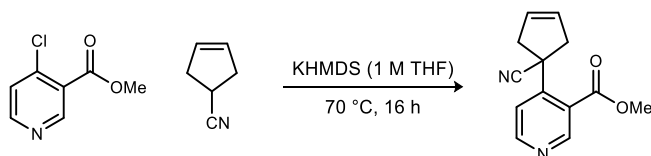


Ethyl 1-cyanocyclopent-3-enecarboxylate (569).²⁵⁷ To a flame dried flask equipped with a stir bar was added K₂CO₃ (11.1 g, 80.0 mmol), ethyl cyanoacetate (2.13 mL, 20.0 mmol), and DMF (20 mL). The resulting mixture was stirred at room temperature followed by the dropwise addition of the dichlorobutene (3.16 mL, 30.0 mmol) in DMF (6 mL). After stirring for 15 hours at room temperature, the reaction mixture was diluted with water and extracted with ether. The combined organic layers were washed with brine, dried (MgSO₄), and concentrated. Flash column chromatography of the residue (SiO₂, 5-20% ethyl acetate in hexanes) afforded the desired product as a clear liquid (3.26 g, 99%). $R_f = 0.25$ (10% EtOAc/hexanes); IR (film) 2986, 2939, 2863, 2245, 1743 cm⁻¹; ¹H NMR (400 MHz, CDCl₃) δ 5.67 (s, 2H), 4.25 (q, $J = 5.6$ Hz, 2H), 3.11 (d, $J = 12.4$ Hz, 2H), 3.02 (d, $J = 12.4$ Hz, 2H), 1.31 (t, $J = 5.6$ Hz, 3H); ¹³C NMR (125.8 MHz, CDCl₃) ppm 169.0, 127.3, 121.0, 62.9, 45.3, 43.8, 13.8; HRMS (ESI) Exact mass calcd for C₉H₁₂NO₂ [M+H]⁺ 166.0863, found 166.0869.

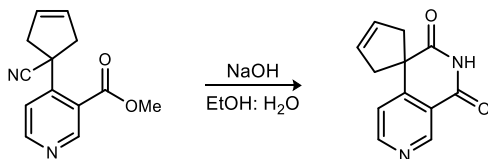
²⁵⁷ Modification of: Hu, H.; Faraldos, J. A.; Coates, R. M. *J. Am. Chem. Soc.* **2009**, *131*, 11998-12006.



Cyclopent-3-enecarbonitrile (565).²⁵⁷ To a flask equipped with a stir bar was added the carboxylate (9.40 g, 56.9 mmol), NaCl (13.3 g, 228 mmol), and DMSO (86 mL) and the resulting suspension was heated to 150 °C for 19 h. The reaction mixture was then cooled to room temperature, diluted with water, and extracted with ether. The combined organic layers were washed with brine, dried (MgSO₄), and concentrated. Vacuum distillation of the crude oil afforded the desired carbonitrile as a clear oil (2.32 g, 44%). The characterization of this compound matched that of literature.²⁵⁷

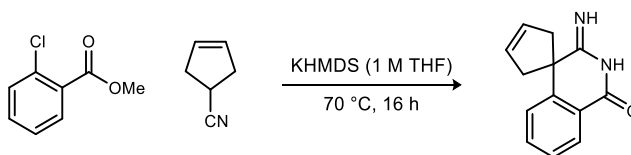


Methyl 4-(1-cyanocyclopent-3-en-1-yl)nicotinate (560). To a flame dried flask equipped with a stir bar was added the methyl nicotinate (1.37 g, 8.00 mmol) and the carbonitrile (497 mg, 5.33 mmol). A condenser was attached, KHMDS (1 M in THF) (8 mL) was added through the condenser, and the resulting mixture was stirred under reflux for 16 hours. The reaction mixture was then cooled to room temperature, poured onto water and extracted with ether. The organic extracts were washed with satd aq NaHCO₃, water, and brine, dried (MgSO₄), and concentrated. Flash column chromatography of the residue (SiO₂, 0.5-2% methanol in dichloromethane) afforded the desired product as a golden-orange viscous oil (515 mg, 42%). $R_f = 0.65$ (5% MeOH/DCM); IR (film) 3440, 3063, 2952, 2857, 2237, 1728, 1586 cm⁻¹; ¹H NMR (400 MHz, CDCl₃) δ 8.94 (s, 1H), 8.70 (d, $J = 5.2$ Hz, 1H), 7.30 (d, $J = 5.2$ Hz, 1H), 5.82 (s, 2H), 4.00 (s, 3H), 3.36 (d, $J = 15.6$ Hz, 2H), 3.13 (d, $J = 15.2$ Hz, 2H); ¹³C NMR (125.8 MHz, CDCl₃) ppm 166.9, 152.6, 151.4, 147.9, 128.1, 126.5, 123.3, 121.0, 52.9, 46.9, 43.6; HRMS (ESI) Exact mass calcd for C₁₃H₁₃N₂O₂ [M+H]⁺ 229.0977, found 229.0972.

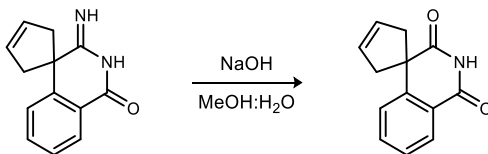


4-(1-Cyanocyclopent-3-en-1-yl)nicotinic acid (571). To a flask equipped with a stir bar was added the ester (79.0 mg, 346 μ mol) and ethanol (6.92 mL). To the solution was added NaOH (138

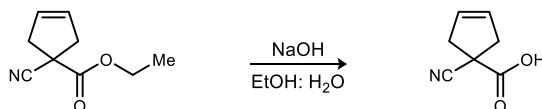
mg, 3.46 mmol) in water (1.73 mL), and the resulting mixture was stirred at room temperature for 48 h. The reaction mixture was acidified to a pH of 2 with 1 M HCl and concentrated to remove ethanol. The residue was diluted with water, extracted with dichloromethane, and the organic extracts were dried (MgSO₄) and concentrated. Flash column chromatography of the residue (SiO₂, 1-5% methanol in dichloromethane) afforded the desired product as a white viscous oil (12.6 mg, 17%). *R_f* = 0.62 (5% MeOH/DCM); IR (film) 2986, 2918, 2698, 1701, 1602 cm⁻¹; ¹H NMR (400 MHz, CDCl₃) δ 9.35 (s, 1H), 8.80 (d, *J* = 5.2 Hz, 1H), 8.24 (br s, 1H), 7.37 (d, *J* = 5.6 Hz, 1H), 5.86 (s, 2H), 3.40 (d, *J* = 14.0 Hz, 2H), 2.77 (d, *J* = 14.0 Hz, 2H); ¹³C NMR (125.8 MHz, CDCl₃) ppm 176.0, 163.0, 155.6, 155.0, 150.1, 128.5, 119.1, 118.3, 50.8, 50.0; (ESI) Exact mass calcd for C₁₂H₁₁N₂O₂ [M+H]⁺ 215.0821, found 215.0812.



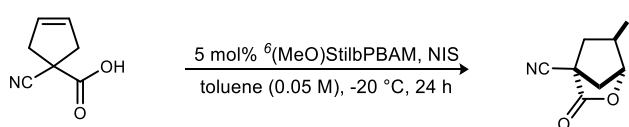
3'-Imino-2',3'-dihydro-1'H-spiro[cyclopent[3]ene-1,4'-isoquinolin]-1'-one (574). To a flame dried flask equipped with a stir bar was added the benzoate (573 μL, 4.00 mmol) and the carbonitrile (248 mg, 2.67 mmol). A condenser was attached, KHMDS (4 mL, 1 M in THF) was added through the condenser, and the resulting mixture was stirred under reflux for 16 hours. The reaction mixture was then cooled to room temperature, poured onto water and extracted with ether. The organic extracts were washed with satd aq NaHCO₃, water, and brine, dried (MgSO₄), and concentrated. Flash column chromatography of the residue (SiO₂, 1-2-5-10-20% methanol in dichloromethane) afforded the isoquinolinone as an off-white viscous oil (22.3 mg, 4%). *R_f* = 0.22 (5% MeOH/DCM); IR (film) 3272, 3005, 1631, 1599, 1509 cm⁻¹; ¹H NMR (400 MHz, CDCl₃) δ 8.18 (dd, *J* = 7.6, 0.8 Hz, 1H), 7.58 (ddd, *J* = 8.0, 8.0, 1.2 Hz, 1H), 7.39 (ddd, *J* = 7.6, 7.6, 0.8 Hz, 1H), 7.32 (d, *J* = 8.0 Hz, 1H), 5.94 (s, 2H), 3.24 (d, *J* = 14.8 Hz, 2H), 2.98 (d, *J* = 14.8 Hz, 2H); ¹³C NMR (125.8 MHz, CDCl₃) ppm 168.3, 147.2, 133.6, 129.6, 127.4, 127.0, 125.0, 124.5, 52.8, 45.9; (ESI) Exact mass calcd for C₁₃H₁₃N₂O [M+H]⁺ 213.1022, found 213.1019.



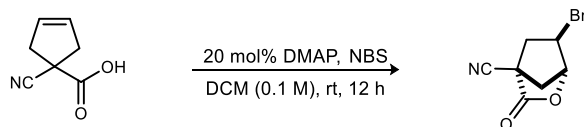
1'H-Spiro[cyclopent[3]ene-1,4'-isoquinoline]-1',3'-(2'H)-dione (575). To a flask equipped with a stir bar was added the isoquinolinone (22.3 mg, 98.1 μmol) and methanol (1.96 mL). To the solution was added NaOH (4.70 mg, 118 μmol) in water (491 μL), and the resulting mixture was stirred at room temperature for 18 h. The reaction mixture was acidified to a pH of 2 with 1 M HCl and concentrated to remove methanol. The residue was diluted with water, extracted with dichloromethane, and the organic extracts were dried (MgSO_4) and concentrated to afford the isoquinolinedione as a white solid (18.3 mg, 88%). Mp 152.0-156.0 $^{\circ}\text{C}$; $R_f = 0.63$ (5% MeOH/DCM); IR (film) 3192, 3079, 2921, 2847, 1708, 1689 cm^{-1} ; ^1H NMR (400 MHz, CDCl_3) δ 8.54 (br s, 1H), 8.18 (dd, $J = 8.4, 1.6$ Hz, 1H), 7.63 (ddd, $J = 9.2, 7.6, 1.2$ Hz, 1H), 7.43 (m, 2H), 5.84 (s, 2H), 3.38 (d, $J = 13.6$ Hz, 2H), 2.78 (d, $J = 13.6$ Hz, 2H); ^{13}C NMR (125.8 MHz, CDCl_3) ppm 177.6, 164.2, 147.9, 135.2, 128.5, 127.9, 127.4, 125.0, 122.5, 51.0, 50.7; (ESI) Exact mass calcd for $\text{C}_{13}\text{H}_{12}\text{NO}_2$ $[\text{M}+\text{H}]^+$ 214.0869, found 214.0834.



1-Cyanocyclopent-3-enecarboxylic acid (576). To a flask equipped with a stir bar was added the cyano carboxylate (1.00 g, 6.05 mmol) and ethanol (121 mL). To the solution was added NaOH (291 mg, 7.26 mmol) in water (30 mL) and the resulting mixture stirred at room temperature for 18 hours. The reaction mixture was then acidified to a pH of 2 with 1 M HCl and concentrated. The residue was diluted with water, extracted with dichloromethane and the organic extracts were dried (MgSO_4) and concentrated to afford the desired acid as an off-white crystalline solid (659 mg, 79%). Mp 68.0-72.0 $^{\circ}\text{C}$; $R_f = 0.15$ (5% MeOH/DCM); IR (film) 3488, 2929, 2604, 2250, 1730, 1629 cm^{-1} ; ^1H NMR (400 MHz, CDCl_3) δ 10.0 (br s, 1H), 5.72 (s, 1H); 3.16 (m, 4H); ^{13}C NMR (125.8 MHz, CDCl_3) ppm 174.5, 127.4, 120.3, 45.1, 44.0; (ESI) Exact mass calcd for $\text{C}_7\text{H}_8\text{NO}_2$ $[\text{M}+\text{H}]^+$ 137.0471, found 137.0473.

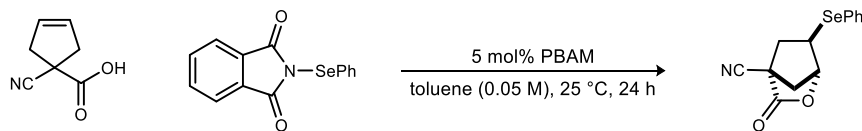


(1R,4S,6R)-6-Iodo-3-oxo-2-oxabicyclo[2.2.1]heptane-4-carbonitrile (577). To a flame dried vial equipped with a stir bar was added ⁶(MeO)StilbPBAM (3.30 mg, 5.00 μ mol), the carboxylic acid (13.7 mg, 100 μ mol) and toluene (2 mL), and the reaction was cooled to -20 °C. NIS (23.4 mg, 104 μ mol) was added and the reaction mixture was stirred without light for 24 h. The mixture was treated with 20% aq sodium thiosulfate (2 mL) and then partitioned between dichloromethane (15 mL) and 3 M NaOH (15 mL). The aqueous layer was extracted twice and the organic layers were combined, dried (MgSO₄), and concentrated. Flash column chromatography (SiO₂, 5-10-20% ethyl acetate in hexanes) yielded the desired lactone as a light-yellow solid (6.3 mg, 24%). The product was determined to be 32% ee by chiral HPLC analysis (Chiralcel OD-H, 10% ⁱPrOH/hexanes, 1 mL/min, $t_r(e_1, \text{minor}) = 26.7$ min, $t_r(e_2, \text{major}) = 31.7$ min). Mp 163.0-165.0 °C; $[\alpha]_D^{20}$ - no optical rotation taken due to low ee; $R_f = 0.74$ (50% EtOAc/hexanes); IR (film) 3014, 2962, 2920, 2364, 2342, 2252, 1786 cm⁻¹; ¹H NMR (400 MHz, CDCl₃) δ 5.03 (d, $J = 1.6$ Hz, 1H), 4.15 (dddd, $J = 7.2, 4.0, 2.0, 0.8$ Hz, 1H), 3.00 (ddd, $J = 14.4, 8.0, 2.0$ Hz, 1H), 2.97 (d, $J = 11.2$ Hz, 1H), 2.77 (ddd, $J = 6.8, 2.4, 2.4$ Hz, 1H), 2.74 (dd, $J = 14.0, 4.4$ Hz, 1H); ¹³C NMR (125.8 MHz, CDCl₃) ppm 168.4, 113.8, 84.3, 44.2, 41.2, 40.5, 12.3; (ESI) Exact mass calcd for C₇H₇INO₂ [M+H]⁺ 263.9516, found 263.9508.

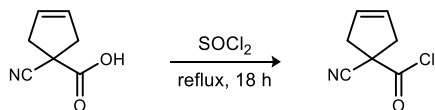


(1R,4S,6R)-6-Bromo-3-oxo-2-oxabicyclo[2.2.1]heptane-4-carbonitrile (580). To a flame dried vial equipped with a stir bar was added DMAP (9.80 mg, 80.0 μ mol), the carboxylic acid (54.9 mg, 400 μ mol) and dichloromethane (4 mL). NIS (23.4 mg, 104 μ mol) was added and the reaction mixture was stirred at room temperature without light for 12 h. The mixture was treated with 20% aq sodium thiosulfate (4 mL) and then partitioned between dichloromethane (30 mL) and 3 M NaOH (30 mL). The aqueous layer was extracted twice and the organic layers were combined, dried (MgSO₄), and concentrated. Flash column chromatography (SiO₂, 5-10-20% ethyl acetate in hexanes) yielded the desired lactone as an off-white solid (16.8 mg, 19%). Mp 162.0-164.0 °C; $R_f = 0.74$ (50% EtOAc/hexanes); IR (film) 2922, 2255, 1787 cm⁻¹; ¹H NMR (400 MHz, CDCl₃) δ

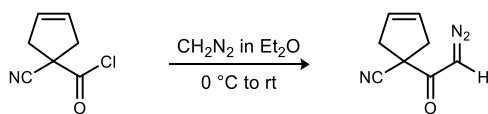
4.98 (d, $J = 0.8$ Hz, 1H), 4.22 (dddd, $J = 7.6, 3.2, 1.6, 1.2$ Hz, 1H), 2.96 (ddd, $J = 14.4, 7.6, 2.0$ Hz, 1H), 2.85 (d, $J = 11.2$ Hz, 1H), 2.73 (ddd, $J = 11.2, 2.0, 2.0$ Hz, 1H), 2.65 (dd, $J = 14.4, 4.0$ Hz, 1H); ^{13}C NMR (125.8 MHz, CDCl_3) ppm 168.2, 113.9, 82.6, 43.1, 41.0, 40.1, 39.7; (ESI) Exact mass calcd for $\text{C}_7\text{H}_7\text{BrNO}_2$ $[\text{M}+\text{H}]^+$ 215.9655, found 215.9658.



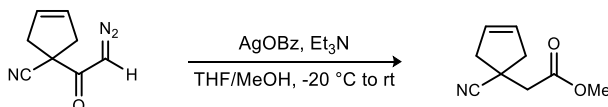
(1R,4S,6R)-3-Oxo-6-(phenylselanyl)-2-oxabicyclo[2.2.1]heptane-4-carbonitrile (582). To a flame dried vial equipped with a stir bar was added PBAM (2.50 mg, 5.00 μmol), the carboxylic acid (13.7 mg, 100 μmol) and toluene (2 mL). NIS (23.4 mg, 104 μmol) was added and the reaction mixture was stirred without light for 24 h at rt. The mixture was treated with 20% aq sodium thiosulfate (2 mL) and then partitioned between dichloromethane (15 mL) and 3 M NaOH (15 mL). The aqueous layer was extracted twice and the organic layers were combined, dried (MgSO_4), and concentrated. Flash column chromatography of the residue (SiO_2 , 5-10% ethyl acetate in hexanes) yielded the desired lactone as a tan solid (7.6 mg, 26%). The product was determined to be 2% ee by chiral HPLC analysis (Chiralcel OD-H, 10% $i\text{PrOH}$ /hexanes, 1 mL/min, $t_r(e_1, \text{minor}) = 28.7$ min, $t_r(e_2, \text{major}) = 38.9$ min). Mp 87.0-91.0 $^\circ\text{C}$; $[\alpha]_D^{20}$ - no optical rotation taken since compound was nearly racemic. $R_f = 0.48$ (50% EtOAc/hexanes); IR (film) 2922, 2852, 2253, 1799 cm^{-1} ; ^1H NMR (400 MHz, CDCl_3) δ 7.57 (d, $J = 6.8$ Hz, 2H), 7.36 (m, 3H), 4.77 (s, 1H), 3.64 (dd, 7.2, 7.2 Hz, 1H), 2.73 (ddd, $J = 14.0, 8.4, 1.2$ Hz, 1H), 2.63 (m, 2H), 2.19 (dd, $J = 13.6, 4.8$ Hz, 1H); ^{13}C NMR (125.8 MHz, CDCl_3) ppm 169.0, 134.5, 129.8, 129.0, 127.5, 114.6, 83.0, 43.2, 41.6, 38.8, 35.7; (ESI) Exact mass calcd for $\text{C}_{13}\text{H}_{11}\text{NNaO}_2\text{Se}$ $[\text{M}+\text{H}]^+$ 315.9853, found 315.9848.



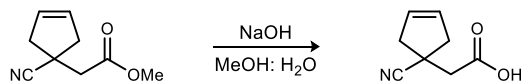
1-Cyanocyclopent-3-ene-1-carbonyl chloride (584). To a flask equipped with a stir bar was added the carboxylic acid (500 mg, 3.65 mmol) and SOCl_2 (7.90 mL, 0.109 mol). The resulting mixture was stirred under reflux for 18 h before being cooled to rt and concentrated. The resulting residue was carried onto the next step quantitatively without any further purification.



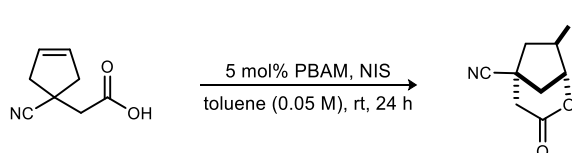
1-(2-Diazoacetyl)cyclopent-3-enecarbonitrile (585). To a flask equipped with a stir bar was added the acid chloride (794 mg, 5.10 mmol). The flask was chilled to 0 °C followed by the addition of CH₂N₂ (35.7 mmol, 1.50 g) in Et₂O and the resulting mixture was warmed to rt and allowed to stir for 18 h. The reaction mixture was then diluted with EtOAc and washed with satd aq NaHCO₃, satd aq NH₄Cl, and brine. The organic layer was dried (MgSO₄), filtered, and concentrated. Flash column chromatography of the residue (SiO₂, 1-2-5-10-20-50% ethyl acetate in hexanes) afforded the desired diazoketone as a non-viscous yellow oil (316 mg, 38%). R_f = 0.60 (50% EtOAc/hexanes); IR (film) 3109, 2925, 2856, 2236, 2118, 1641 cm⁻¹; ¹H NMR (400 MHz, CDCl₃) δ 5.89 (s, 1H), 5.68 (s, 2H), 3.12 (d, *J* = 15.2 Hz, 2H), 2.96 (d, *J* = 14.8 Hz, 2H); ¹³C NMR (125.8 MHz, CDCl₃) ppm 188.0, 127.4, 122.3, 54.6, 48.7, 43.7; (ESI) Exact mass calcd for C₈H₇N₃O [M⁺] 161.0584, found 161.0589.



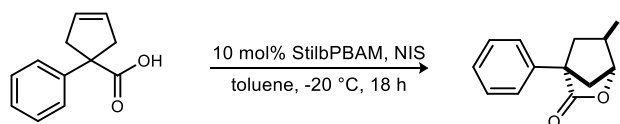
Methyl 2-(1-cyanocyclopent-3-en-1-yl)acetate (586). To a flame-dried flask equipped with a stir bar and wrapped in aluminum foil was added the diazoketone (154 mg, 956 μmol), MeOH (19.3 mL) and anhydrous THF (13.4 mL). The reaction mixture was chilled to -20 °C before a solution of silver benzoate (48.1 mg, 210 μmol) in freshly distilled Et₃N (770 μL, 5.52 mmol) was added. The resulting mixture was warmed to rt and allowed to stir for 6 h. The solvents were evaporated and the residue was taken up in EtOAc. The organic layer was washed with satd aq solutions of NaHCO₃, NH₄Cl and brine, dried (MgSO₄), filtered and concentrated to afford clean product as an orange-brown oil (102 mg, 64%). R_f = 0.27 (20% EtOAc/hexanes); IR (film) 2921, 2852, 2237, 1739 cm⁻¹; ¹H NMR (400 MHz, CDCl₃) δ 5.69 (s, 2H), 3.75 (s, 3H), 3.03 (d, *J* = 14.8 Hz, 2H), 2.71 (s, 2H), 2.62 (d, *J* = 14.8 Hz, 2H); ¹³C NMR (125.8 MHz, CDCl₃) ppm 169.8, 127.9, 124.3, 52.1, 44.5, 42.1, 37.2; (ESI) Exact mass calcd for C₉H₁₁NO₂ [M⁺] 165.0784, found 165.0785.



1-Cyanocyclopent-3-enecarboxylic acid (583). To a flask equipped with a stir bar was added the ester (18.7 mg, 113 μmol) and methanol (2.3 mL). To the solution was added NaOH (5.40 mg, 136 μmol) in water (565 μL) and the resulting mixture stirred at room temperature for 18 hours. The reaction mixture was then acidified to a pH of 2 with 1 M HCl and concentrated. The residue was diluted with water, extracted with dichloromethane and the organic extracts were dried (MgSO_4) and concentrated to afford the desired acid as a light-yellow viscous oil (15.1 mg, 88%). $R_f = 0.31$ (5% MeOH/DCM); IR (film) 3473, 3068, 2925, 2859, 2241, 1718 cm^{-1} ; ^1H NMR (400 MHz, CDCl_3) δ 10.13 (br s, 1H), 5.69 (s, 2H), 3.03 (d, $J = 15.2$ Hz, 2H), 2.78 (s, 2H), 2.62 (d, $J = 14.8$ Hz, 2H); ^{13}C NMR (125.8 MHz, CDCl_3) ppm 175.3, 127.9, 124.1, 44.5, 41.9, 36.9; Exact mass calcd for $\text{C}_8\text{H}_9\text{NO}_2$ [M^+] 151.0628, found 151.0632.



(1R,5S,7R)-7-Iodo-3-oxo-2-oxabicyclo[3.2.1]octane-5-carbonitrile (587). To a flame dried vial equipped with a stir bar was added PBAM (1.00 mg, 2.10 μmol), the carboxylic acid (6.20 mg, 41.0 μmol) and toluene (820 μL). NIS (9.60 mg, 42.7 μmol) was added and the reaction mixture was stirred at rt without light for 24 h. The mixture was treated with 20% aq sodium thiosulfate (2 mL) and then partitioned between dichloromethane (7 mL) and 3 M NaOH (7 mL). The aqueous layer was extracted twice and the organic layers were combined, dried (MgSO_4), and concentrated. Flash column chromatography (SiO_2 , 5-10-20% ethyl acetate in hexanes) yielded the desired lactone as an off-white solid (1.3 mg, 12%). The product was determined to be 4% ee by chiral HPLC analysis (Chiralpak IB, 10% $^i\text{PrOH}$ /hexanes, 1 mL/min, $t_r(e_1, \text{major}) = 47.5$ min, $t_r(e_2, \text{minor}) = 55.8$ min). $[\alpha]_D^{20}$ - no optical rotation taken since compound was nearly racemic; $R_f = 0.24$ (20% EtOAc/hexanes); IR (film) 3464, 2920, 2245, 1741 cm^{-1} ; ^1H NMR (400 MHz, CDCl_3) δ 5.04 (d, $J = 2.4$ Hz, 1H), 4.45 (dddd, $J = 8.0, 8.0, 4.4, 2.4$ Hz, 1H), 3.04 (dd, $J = 18.4, 2.8$ Hz, 1H), 3.02 (dd, $J = 15.6, 1.6$ Hz, 1H), 2.96 (ddd, $J = 13.2, 2.8, 2.8$ Hz, 1H), 2.90-2.82 (m, 2H), 2.43 (d, $J = 13.2$ Hz, 1H); ^{13}C NMR (125.8 MHz, CDCl_3) ppm 164.1, 119.2, 86.5, 48.2, 42.6, 36.3, 35.4, 17.5; Exact mass calcd for $\text{C}_8\text{H}_9\text{INO}_2$ [$\text{M}+\text{H}^+$] 277.9672, found 277.9668.



(1R,4S,6R)-6-Iodo-4-phenyl-2-oxabicyclo[2.2.1]heptan-3-one (596). To a vial equipped with a stir bar was added StilbPBAM (6.00 mg, 10.0 μmol), the carboxylic acid (18.8 mg, 100 μmol) and toluene (2 mL), and the reaction was cooled to -20 °C. NIS (23.4 mg, 104 μmol) was added and the reaction mixture was stirred without light for 24 h. The mixture was treated with 20% aq sodium thiosulfate (2 mL) and then partitioned between dichloromethane (15 mL) and 6 M NaOH (15 mL). The aqueous layer was extracted twice and the organic layers were combined, dried (MgSO_4), and concentrated. Flash column chromatography (SiO_2 , 10% ethyl acetate in hexanes) yielded the desired lactone as a light-yellow solid (9.4 mg, 30%). The product was determined to be 65% ee by chiral HPLC analysis (Chiralpak IA, 10% $i\text{PrOH}$ /hexanes, 1 mL/min, $t_r(e_1, \text{minor}) = 8.8$ min, $t_r(e_2, \text{major}) = 12.8$ min). Mp 54.0-56.0 °C; $[\alpha]_D^{20} -89.0$ (c 0.30, CHCl_3); $R_f = 0.36$ (10% EtOAc/hexanes); IR (film) 3030, 2927, 2860, 1786 cm^{-1} ; ^1H NMR (600 MHz, CDCl_3) δ 7.43-7.34 (m, 5H), 5.05 (d, $J = 1.2$ Hz, 1H), 4.28 (ddd, $J = 6.6, 4.2, 2.4$ Hz, 1H), 2.97 (ddd, $J = 13.8, 7.8, 1.8$ Hz, 1H), 2.90 (d, $J = 10.8$, 1H), 2.72 (dddd, $J = 4.2, 2.4, 2.4, 2.4$ Hz, 1H), 2.62 (dd, $J = 13.8, 4.2$ Hz, 1H); ^{13}C NMR (150.9 MHz, CDCl_3) ppm 176.0, 134.0, 128.7, 128.2, 127.2, 83.3, 56.2, 42.9, 41.1, 16.8; Exact mass calcd for $\text{C}_{12}\text{H}_{12}\text{IO}_2$ $[\text{M}+\text{H}]^+$ 314.9876, found 314.9872.